UNIVERSIDAD POLITÉCNICA DE MADRID
Escuela Técnica Superior de Ingenieros Industriales



Biomimetic design and additive manufacturing strategies for multi-scale and multi-material tissue engineering

DOCTORAL THESIS

Submitted for the degree of Doctor by:

Adrián Martínez Cendrero
Bachelor's degree in Industrial Engineering
Master's degree in Industrial Engineering

Madrid, 2024

UNIVERSIDAD POLITÉCNICA DE MADRID
Escuela Técnica Superior de Ingenieros Industriales

Doctoral Degree in Mechanical Engineering

Biomimetic design and additive manufacturing strategies for multi-scale and multi-material tissue engineering

DOCTORAL THESIS

Submitted for the degree of Doctor by:

Adrián Martínez Cendrero
Bachelor's degree in Industrial Engineering
Master's degree in Industrial Engineering

Under the supervision of:
Prof. Dr. Andrés Díaz Lantada
Associate Professor Ph.D. in Mechanical Engineering

Madrid, 2024

Title: Biomimetic design and additive manufacturing strategies for multi-scale and multi-material tissue engineering

Author: Adrián Martínez Cendrero

Doctoral Programme: Mechanical Engineering, Universidad Politécnica de Madrid (UPM)

Thesis Supervision:

Prof. Dr. Andrés Díaz Lantada

Associate Professor Ph.D. in Mechanical Engineering in UPM

External Reviewers:

Thesis Defense Committee:

Thesis Defense Date:

This PhD thesis has been funded by the European Union's Horizon 2020 Research and Innovation Programme under grant agreement No. 953134 (INKplant project: Ink-based hybrid multi-material fabrication of next generation implants). INKplant's project partners are acknowledged for their inspiring comments, fruitful debates and material-technological support for the technological validation of the thesis research.

I met a traveller from an antique land
Who said: Two vast and trunkless legs of stone
Stand in the desert. Near them, on the sand,
Half sunk, a shattered visage lies, whose frown,
And wrinkled lip, and sneer of cold command,
Tell that its sculptor well those passions read
Which yet survive, stamped on these lifeless things,
The hand that mocked them and the heart that fed.

And on the pedestal these words appear:
"My name is Ozymandias, king of kings:
Look on my works, ye Mighty, and despair!"
Nothing beside remains. Round the decay
Of that colossal wreck, boundless and bare
The lone and level sands stretch far away

- - -

Conocí a un viajero de una tierra antigua
quien dijo: «dos enormes piernas pétreas, sin su tronco
se yerguen en el desierto. A su lado, en la arena,
semihundido, yace un rostro hecho pedazos, cuyo ceño
y mueca en la boca, y desdén de frío dominio,
cuentan que su escultor comprendió bien esas pasiones
las cuales aún sobreviven, grabadas en estos inertes objetos,
a las manos que las tallaron y al corazón que las alimentó.

Y en el pedestal se leen estas palabras:
"Mi nombre es Ozymandias, rey de reyes:
¡Contemplad mis obras, poderosos, y desesperad!"
Nada queda a su lado. Alrededor de la decadencia
de estas colosales ruinas, infinitas y desnudas
se extienden, a lo lejos, las solitarias y llanas arenas».

Ozymandias - Percy Bysshe Shelley

A mi familia, por haberme transmitido los valores del respeto, el inconformismo y la superación.

Acknowledgement

Institutional acknowledgements

I would like to thank the institutions and projects that have made this doctoral thesis possible.

First of all, I would like to thank the Universidad Politécnica de Madrid (UPM), and in particular the Escuela Técnica Superior de Ingenieros Industriales (ETSII) and the research team of the Machine Engineering Division (DIM), without whom the achievement of this doctoral work would not have been possible.

I would like to thank the European project "INKplant: Ink-based multi-material hybrid manufacturing of next generation implants" (Horizon 2020 Programme, Leadership in Industrial and Enabling Technologies, H2020-NMBP-TR-IND-2018-2020 "Biological scaffolds for tissue engineering and repair" call, Grant Agreement: nº 953134), for having contributed by funding part of the work included in this PhD thesis. Special mention goes to the project coordinator, Dr. Elena Guillén, Profactor GmbH (Steyr, Austria).

I would like to thank all members of the European INKplant consortium for their contribution to the achievement of the objectives of this doctoral research: Profactor GmbH (Steyr, Austria), Lithoz GmbH (Vienna, Austria), Luxenergy (Leoben, Austria), Tiger Coatings (Wels, Austria), Johannes Kepler University Institute of Polymer Product Engineering and Institute of Polymer Chemistry (Linz, austria), Ludwig Boltzmann Institute (Vienna, Austria), Medical University of Vienna (Vienna, Austria), Kepler University Hospital (Linz, Austria), BioMed Center Innovation (Bayreuth, Germany), Charité - Universitätsmedizin Berlin (Berlin, Germany), TransTissue Technologies GmbH (Berlin, Germany), Fluidinova (Porto, Portugal), Stratasys (Rehovot, Israel), 3D Matrix Medical Technology (Lyon, France), Elkem Silicones (Lyon France), University Medical Center Utrecht (Utrecht, The Netherlands), Asociación Española de Normalización (Madrid, Spain), Biotechnology Institute (Vitoria, Spain) and the Universidad Politécnica de Madrid (Madrid, Spain).

I would like to thank the applied research company Profactor GmbH (Steyr, Austria) and the Lithoz GmbH company (Vienna, Austria) for hosting me during the two stages of international mobility within the framework of the PhD and the European project INKplant. In particular, I would like to thank my supervisors, Engineer Researcher Michael Kainz (Profactor) and Dr. Serkan Nohut (Lithoz), for their care, attention and consideration during these stages.

I would like to thank the Escuela Técnica Superior de Ingenieros Industriales for having financed part of the international mobility stays during this doctoral period.

Personal acknowledgements

I would like to begin this section by thanking my thesis supervisor, Professor Andrés Díaz Lantada, without whom this document and all that it contains would never have materialised. From the first moment I met Andrés, back in 2017, he awakened in me an interest in biomedical research and everything surrounding the world of additive manufacturing and digital design. Since then, I see in him a reference to whom I try to be like every day, as he manages to bring out and enhance the best in me, having experienced a tremendously enriching growth in recent years, both personally and professionally. Almost 8 years have passed since we embarked on this journey together. The Ubora, INKplant and Biomet4D projects have led us to meet great friends and professionals from all over the world, having lived unimaginable experiences in countries in Africa, Europe and Asia. There are so many experiences and moments that I keep for the memory, that I can only recognise part of the success of my small achievements in your person Andrés. I will always be grateful to you for making me a better person day by day, allowing me to work hand in hand with you and the incredible team we have formed. I can only tell you that I am looking forward to what the future holds.

I would also like to thank all my colleagues at the Universidad Politécnica de Madrid, specifically the team of the Machine Engineering Division, for being there day after day during this whole stage. In particular, I would like to thank my colleagues Rodrigo Zapata, Francisco Franco, Carlos Aguilar, Alejandro de Blas, Javier Segura, Sonia Trujillo and Adrián López for their total availability and willingness to lend a hand, no matter how demanding the task to adddress was. I would also like to thank the teachers and colleagues in the research group, José Luis, Juanma, Javier, Enrique, Julio, Silvia, Pedro and Emilio. To Luis and Rocío, for their support, affection and trust, I cherish the memories I had in Pisa and Kampala. Special mention to Socorro Martín, Soqui, for having to suffer my doctorate due to my numerous European experiences, without ever losing her smile or good manners, despite having buried her in dozens of papers, reports, complaints and other bureaucracies. Thank you Soqui for your concern for my well-being during all this time.

With special affection I would like to thank William Solórzano for having accompanied me inseparably during this doctoral stage. Undoubtedly, one of the best results I have been able to obtain from this process has been that life has put us on the same path, despite the fact that the day we met I underestimated you in many aspects that I will always remember as an amusing anecdote. Thank you William, from the bottom of my heart, for having dedicated so many hours to that hip prosthesis. For trusting me to the point of wanting to found a start-up together. You have been a great support in the achievement of this work, and I can only thank you eternally. I feel proud to have met a person like you, and despite how young you are, you are not aware of what I learn from you day by day, in all aspects of life. You know that in Madrid and in Extremadura you will always have your Spanish family for whatever you need. Furthermore, I owe to you the unbeatable opinion I have of Peru, its people and its culture, to the point that I would never have seen myself involved in a project to digitise and conserve pre-Columbian ceramics. Anyone who knows you well knows that it is impossible not to get involved, seeing the passion and desire you put into it.

Going back to the entrepreneurship, I would like to mention and thank the whole family of the Dental Troyano Laboratory. To Francisco Troyano, María Jesús Ropero, Jorge Troyano and

Santiago Clemente, for opening the doors of their house and putting up with me so many hours swarming and bothering innocently between work and work. Special thanks to Paco, for the effort, dedication and humility that you dedicate to your profession. You are undoubtedly a reference in your sector, respected and admired by all, and those of us who are close to you are lucky enough to know that you are a thousand times better person than a dental technician. Thank you for allowing me to enjoy and learn by leaps and bounds from a humble master, without arrogance or superiority, with the certainty that work well done with perseverance and passion describes good people and great professionals. Proof of this is that I am lucky enough to enjoy Álvaro Troyano, a friend for so many years, a companion on the playing pitch and now a professional partner. In every job, course, congress or talk we give, I cannot help but recognise in Álvaro many of the good qualities of his predecessors, Chus and Paco. Who would have thought that what one day started with a ball rolling would degenerate into engineered scaffolds for tissue engineering, bone regeneration and aesthetic dental restorations. Thank you Álvaro for always being there, without having to ask for it. Thank you for your goodwill and your inexhaustible vocation to help others without expecting anything in return. I can assure you that you are the living reflection of your parents, and I feel a tremendous pride in having you by my side for whatever the future holds. The future of Dental Troyano is secure.

Moving the focus to Central Europe, I would also like to thank all my colleagues from the Austrian companies Profactor and Lithoz, with whom I have been fortunate to share a large part of the year 2023. Thanks to Michael Kainz, Sandra Haas, Hannes Fachberger, Isabel Caetano da Silva, Elena Guillén and all my colleagues at Profactor GmbH for welcoming me as one of them in Steyr and making the hard winter more bearable. I would like to thank Michael for the many hours of effort invested in the development of a never before conceived manufacturing technology, which has been an unprecedented learning experience for me in the field of inkjet technology and non-planar 3D printing. To you Elena, thank you for everything you have done in the INKplant project, helping me as much as you could with my PhD stuff. Thank you for always taking me into account and for your infinite trust, which has given me so much confidence during these three years, contributing enormously to my professional development throughout the project. On the other hand, during my stay at Lithoz, I would like to thank the whole team of the "New Materials" department for welcoming me with open arms from the first moment I entered the Mollardgasse office. So many hours of bouldering in the climbing wall or that adventure in the Alps are memories that have engraved Vienna with a special fondness in my heart. I would like to thank Martin Schwentenwein, Daniel Bomze, Sebastian Geir, Mariana Bergamini and the whole Lithoz team for the love they have shown me, putting all their resources at my disposal to achieve my goals. I especially wanted to highlight Serkan Nohut and Altan Altun, for receiving me and treating me like a friend. Thank you for showing me every detail of everything related to ceramics 3D printing. Besides, you know that if Andrés, because of his Turkish influence, had already awakened in me the interest to visit the cradle of the Ottoman Empire, meeting you has only confirmed it. In short, thanks to all of you who have made Austria a little piece of home for me during these three years. You will always have an Austrian ambassador in Madrid or wherever life takes me.

Of course, I would like to thank my family, to whom I owe everything I have achieved and harvested throughout my life. I have always said that it is well-born to be grateful, and I can do nothing but reflect my thoughts in my actions. I wanted to thank my parents for giving me everything and more than they have ever had. Because in spite of our most difficult moments, we have always had a clear understanding of the reason for making things happen. Thanks to my mother, Lola, for being a source of inspiration, self-improvement and endless work. I have told you many times, I am proud of the human quality that accompanies you, being the bravest and hardest working woman I know. Thanks to my father, Pepe, for instilling in me the values of confidence and independence, without which I could not have developed the personal security so necessary and of which I am especially proud. And above all, thanks to my brother, Guillermo, because without being aware of it, you are the reason for everything. Thanks to you and the education I have received, it was awakened in me the vocation of wanting to leave a better society every day than the one I found. Living so many moments at your side has given me the courage to dedicate my professional future to exploiting the possibilities represented by the synergy between technology and medicine, fighting and working to improve the lives of those most in need.

And finally, I would like to thank my partner, Maria, for taking care of the most complicated part of this whole process. I certainly have the feeling that this stage is coming to an end and you know better than anyone the most bitter side of a PhD. Thank you for being my unconditional support, for being there in so many hard moments of overwhelm, stress or anxiety. Without your presence and your temperance none of this would have been possible. Thank you for making me a better person every day, for giving me the calm and the pause that I often lack, and for walking by my side no matter what comes my way. I feel privileged every second that passes to share each day with you. Thank you from the bottom of my heart.

Agradecimientos

Agradecimientos institucionales

Me gustaría agradecer a las instituciones y proyectos que han hecho esta tesis doctoral posible.

En primer lugar, me gustaría agradecer a la Universidad Politécnica de Madrid (UPM), y en particular a la Escuela Técnica Superior de Ingenieros Industriales (ETSII) y al equipo de investigación de la División de Ingeniería de Máquinas (DIM), sin los cuales la consecución de este trabajo doctoral no hubiese sido posible.

Me gustaría expresar mi agradecimiento al proyecto europeo "INKplant: Ink-based multi-material hybrid manufacturing of next generation implants" (Horizon 2020 Programme, Leadership in Industrial and Enabling Technologies, H2020-NMBP-TR-IND-2018-2020 "Biological scaffolds for tissue engineering and repair" call, Grant Agreement: nº 953134), por haber contribuido financiando parte del trabajo incluido en esta tesis doctoral. Mención especial a la coordinadora del proyecto, la Dra. Elena Guillén, del centro de investigación Profactor GmbH (Steyr, Austria).

Agradezco a todos los miembros del consorcio europeo INKplant, por haber contribuido a la consecución de los objetivos marcados en esta investigación doctoral: Profactor GmbH (Steyr, Austria), Lithoz GmbH (Viena, Austria), Luxenergy (Leoben, Austria), Tiger Coatings (Wels, Austria), Johannes Kepler University Institute of Polymer Product Engineering and Institute of Polymer Chemistry (Linz, austria), Ludwig Boltzmann Institute (Viena, Austria), Medical University of Vienna (Vienna, Austria), Kepler University Hospital (Linz, Austria), BioMed Center Innovation (Bayreuth, Alemania), Charité - Universitätsmedizin Berlin (Berlin, Alemania), TransTissue Technologies GmbH (Berlin, Alemania), Fluidinova (Oporto, Portugal), Stratasys (Rehovot, Israel), 3D Matrix Medical Technology (Lyon, Francia), Elkem Silicones (Lyon Francia), University Medical Center Utrecht (Utrecht, Paises Bajos), Asociación Española de Normalización (Madrid, España), Biotechnology Institute (Vitoria, España) y a la Universidad Politécnica de Madrid (Madrid, España).

Agradezco al centro de investigación Profactor GmbH (Steyr, Austria) y a la empresa Lithoz GmbH (Viena, Austria), por haberme acogido durante las dos etapas de movilidad internacional realizadas en el marco del doctorado y del proyecto europeo INKplant. Agradezco en particular a mis responsables en dichas estancias, al Engineer Researcher Michael Kainz (Profactor) y al Dr. Serkan Nohut (Lithoz), por el cariño, la atención y la consideración mantenida durante estas etapas.

Agradezco a la Escuela Técnica Superior de Ingenieros Industriales por haber financiado parte de las estancias de mobilidad internacional realizadas durante este periodo doctoral.

Agradecimientos personales

Me gustaría comenzar este apartado dando las gracias a mi director de tesis, el profesor Andrés Díaz Lantada, sin el cual este documento y todo lo que en él se recoge nunca se hubiera materializado. Desde el primer momento en que conocí a Andrés, allá por 2017, despertó en mí el interés por la investigación biomédica y todo lo que rodea al mundo de la fabricación aditiva y el diseño digital. Desde entonces, veo en él un referente al que intento parecerme cada día, ya que consigue sacar y potenciar lo mejor de mí, habiendo experimentado estos últimos años un crecimiento tremendamente enriquecedor, tanto a nivel personal como profesiona. Han pasado casi 8 años desde que emprendimos este viaje juntos. Los proyectos Ubora, INKplant y Biomet4D nos han llevado a conocer a grandes amigos y profesionales de todo el mundo, habiendo vivido experiencias inimaginables en países de África, Europa y Asia. Son tantas las experiencias y momentos que guardo para el recuerdo, que sólo puedo reconocer parte del éxito de mis pequeños logros en tu persona Andrés. Siempre te estaré agradecido por hacerme mejor persona día a día, permitiéndome trabajar mano a mano contigo y con el increíble equipo que hemos formado. Sólo puedo decirte que estoy deseando saber qué nos depara el futuro.

También me gustaría dar las gracias a todos mis compañeros de la Universidad Politécnica de Madrid, concretamente al equipo de la División de Ingeniería de Máquinas, por haber estado ahí día tras día durante toda esta etapa. En particular, quiero agradecer a mis compañeros Rodrigo Zapata, Francisco Franco, Carlos Aguilar, Alejandro de Blas, Javier Segura, Sonia Trujillo y Adrián López su total disponibilidad y disposición para echar una mano, sin importar cuan exigente fuese la tarea a realizar. Agradecer también a los profesores y compañeros del grupo de investigación, José Luis, Juanma, Javier, Silvia, Pedro, Julio y Enrique. A Luis y a Rocío, por su apoyo, cariño y confianza, guardo con especial cariño los recuerdos vividos en Pisa y en Kampala. Mención especial a Socorro Martín, Soqui, por tener que sufrir mi doctorado debido a mis numerosas experiencias europeas, sin perder nunca la sonrisa ni las buenas maneras, a pesar de haberla enterrado en decenas de papeles, informes, denuncias y demás burocracias. Gracias Soqui por preocuparte por mi bienestar durante todo este tiempo.

Con especial cariño quiero agradecer a William Solórzano el haberme acompañado inseparablemente durante esta etapa doctoral. Sin duda, uno de los mejores resultados que he podido obtener de este proceso ha sido que la vida nos haya puesto en el mismo camino, a pesar de que el día que nos conocimos te subestimé en muchos aspectos que siempre recordaré como una divertida anécdota. Gracias William de todo corazón por haber dedicado tantas y tantas horas a esa prótesis de cadera. Por confiar en mí hasta el punto de querer emprender juntos. Has sido sin duda un gran apoyo en la consecución de de este trabajo, y sólo puedo darte las gracias eternamente. Me siento orgulloso de haber conocido a una persona como tú, y a pesar de lo joven que eres, no eres consciente de lo que aprendo de ti día a día, en todos los aspectos de la vida. Sabes que en Madrid y en Extremadura siempre tendrás a tu familia española para lo que necesites. Además, a ti te debo la inmejorable opinión que tengo de Perú, de sus gentes y de su cultura, hasta el punto de que nunca me hubiese visto involucrado en un proyecto de digitalización y conservación de cerámica precolombina. Cualquiera que te conozca bien sabe que es imposible no involucrarse, viendo la pasión y las ganas que le pones.

Volviendo al emprendimiento, me gustaría mencionar y agradecer a toda la familia del Laboratorio Dental Troyano. A Francisco Troyano, María Jesús Ropero, Jorge Troyano y Santiago Clemente, por abrirme las puertas de su casa y aguantarme tantas horas pululando y molestando inocentemente entre trabajo y trabajo. Especial agradecimiento a Paco, por el esfuerzo, dedicación y humildad que dedicas a tu profesión. Sin duda eres un referente en tu sector, respetado y admirado por todos, y los que estamos cerca de ti tenemos la suerte de saber que eres mil veces mejor persona que protésico dental. Gracias por permitirte disfrutar y aprender a pasos agigantados de un maestro humilde, sin prepotencia ni altanería, con la certeza de que el trabajo bien hecho con constancia y pasión describe a las buenas personas y a los grandes profesionales. Prueba de ello es que tengo la suerte de disfrutar de Álvaro Troyano, amigo desde hace tantos años, compañero en el terreno de juego y ahora socio en lo profesional. En cada trabajo, curso, congreso o charla que impartimos, no puedo evitar reconocer en Álvaro muchas de las buenas cualidades de sus predecesores, Chus y Paco. Quién nos iba a decir que lo que un día empezó con un balón rodando, degeneraría en andamios de ingeniería de tejidos, regeneración ósea y restauraciones dentales. Gracias Álvaro por estar siempre ahí sin tener que pedirlo. Gracias por tu buena voluntad y tu inagotable vocación de ayudar a los demás sin esperar nada a cambio. Puedo asegurar que eres el vivo reflejo de tus padres, y siento un tremendo orgullo de teneros a mi lado para lo que nos depare el futuro. El futuro de Dental Troyano está asegurado.

Trasladando el foco a Europa central, también me gustaría dar las gracias a todos mis colegas de las empresas austriacas Profactor y Lithoz, con quienes he tenido la suerte de compartir gran parte del año 2023. Gracias a Michael Kainz, Sandra Haas, Hannes Fachberger, Isabel Caetano da Silva, Elena Guillén y a todos mis compañeros de Profactor GmbH por acogerme como uno más en Steyr y hacerme más llevadero el duro invierno. Me gustaría agradecer a Michael las muchas horas de esfuerzo invertidas en el desarrollo de una tecnología de fabricación nunca antes concebida, que ha supuesto para mí una experiencia de aprendizaje sin precedentes en el campo de la tecnología inkjet y la impresión no plana. A ti Elena, gracias por todo lo que has hecho en el proyecto INKplant, ayudándome además en todo lo que has podido con mi doctorado. Gracias por tenerme en cuenta siempre y por tu confianza infinita, que tanta seguridad me ha generado en estos tres años, contribuyendo enormemente en mi desarrollo profesional a lo largo del proyecto. Por otro lado, durante mi estancia en Lithoz, me gustaría dar las gracias a todo el equipo del departamento de "Nuevos Materiales" por acogerme con los brazos abiertos desde el primer momento en que entré en la oficina de Mollardgasse. Tantas horas de escalada en el rocódromo o aquella aventura en los Alpes, son recuerdos que han grabado Viena con un cariño especial en mi corazón. Quiero agradecer a Martin Schwentenwein, Daniel Bomze, Sebastian Geir, Mariana Bergamini y a todo el equipo de Lithoz el cariño que me han demostrado, poniendo todos sus recursos a mi disposición para conseguir los objetivos fijados. Quería destacar especialmente a Serkan Nohut y Altan Altun, por recibirme y tratarme como a un amigo. Gracias por enseñarme cada detalle de todo lo relacionado con la impresión 3D de materiales cerámicos. Además, sabéis que si Andrés, por su influencia turca, ya había despertado en mí el interés por visitar la cuna del Imperio Otomano, conoceros no ha hcho más que confirmarlo. En definitiva, gracias a todos los que me habéis convertido a Austria en un trocito de hogar durante estos tres años. Siempre tendréis un embajador austriaco en Madrid.

Por supuesto, quiero dar las gracias a mi familia, a la que debo todo lo que he conseguido y cosechado durante toda mi vida. Siempre he dicho que es de bien nacidos ser agradecidos, y no puedo hacer otra cosa que reflejar mis pensamientos en mis actos. Quería dar las gracias a mis padres por haberme dado todo y más de lo que han tenido. Porque a pesar de nuestros momentos más difíciles siempre, hemos tenido claro el porqué de las cosas. Gracias a mi madre, Lola, por ser una fuente de inspiración, superación y trabajo sin fin. Te lo he dicho muchas veces, estoy orgulloso de la calidad humana que te acompaña, siendo la mujer más valiente y trabajadora que conozco. Gracias a mi padre, Pepe, por inculcarme los valores de la confianza y la independencia, sin los cuales no podría haber desarrollado la seguridad personal tan necesaria y de la que me siento especialmente orgulloso. Y sobre todo, gracias a mi hermano, Guillermo, porque sin ser consciente de ello, él es la razón de todo. Gracias a mi ti y a la educación que he recibido, despertó en mí la vocación de querer dejar cada día una sociedad un poco mejor que la que encontré. Vivir tantos momentos a tu lado me ha dado el valor de querer dedicar mi futuro profesional a explotar las posibilidades que representa la sinergia entre la tecnología y la medicina, luchando y trabajando por mejorar la vida de los más necesitados.

Y por último, me gustaría dar las gracias a mi compañera, María, por haberse encargado de la parte más complicada de todo este proceso. Ciertamente tengo la sensación de que esta etapa está llegando a su fin y tú conoces mejor que nadie el lado más difícil de un doctorado. Gracias por ser mi apoyo incondicional, por estar ahí en tantos momentos duros de agobio, estrés o ansiedad. Sin tu presencia y tu templanza nada de esto habría sido posible. Gracias por hacerme mejor persona cada día, por darme la calma y la pausa que a menudo me faltan, y por caminar a mi lado venga lo que venga. Me siento privilegiada cada segundo que pasa por compartir cada día cotigo. Gracias de todo corazón.

Abstract

Tissue engineering, as an integral part of regenerative medicine, has a fascinating history and has evolved significantly over time. This field has developed from the field of biomaterials and focuses on the combination of scaffolds, cells and biologically active molecules to create functional tissues. Its main goal is to restore, maintain or improve damaged tissues or entire organs. The first steps towards what we know today as cell culture can be attributed to historical figures such as Paracelsus in the 16th century, who attempted to create human life using a mixture of chemicals, and Rudolf Virchow in the 19th century, who pioneered the cultivation of cells outside the body. However, the development of cell and molecular biology in the 20th century marked the formal beginning of what we know today as tissue engineering and regenerative medicine. Scientists such as Alexis Carrel, who innovated vascular suturing and tissue culture techniques, and Joseph Vacanti and Robert Langer, considered the modern fathers of tissue engineering, played pivotal roles in advancing the field. Their work in creating scaffolds for cell culture ushered in a new era in regenerative medicine.

In particular, tissue engineering has found practical applications in regenerative medicine and in the field of implantology, including the repair of joint injuries, the generation of skin for major burns or the creation of functional organs, such as artificial bladders, among others. These advances have been achieved thanks to a deep understanding of cellular and molecular biology. The present doctoral research focuses on the study of customised tissue scaffold solutions to cover joint pathologies present in lower limbs. Tissue engineering solutions are mainly proposed to cover knee and hip injuries.

Currently, tissue engineering uses scaffolds made of materials such as collagen, hydrogels, nanofibres and biopolymers, meeting criteria of biocompatibility, inertness to the environment, gradual and controlled degradation, adequate porosity and non-toxicity. By applying cell cultures on these scaffolds, it is possible to obtain biologically colonised structures, even going as far as obtaining purely organic implants. Thus, advances in this field have allowed the development of artificial tissues, such as organoids of livers and pancreas, minimum viable portions that emulate part of the physiology, or skin grafts, among others, through techniques such as 3D bioprinting. The generation of these scaffolds generally requires specific porosity for proper cell proliferation, which in turn ensures vascularisation. For this reason, 3D printing represents a promising tool in the sector, as it allows the creation of extremely spatially complex geometries, in part by minimising or even eliminating the post-machining required in conventional manufacturing processes.

This need for new tools and systems to provide new medical breakthroughs is driving the relentless development of technology and materials in the field of 3D printing. Obtaining increasingly sophisticated medical solutions is enabling the study of new pathologies or the paradigm shift of traditional treatments, providing new possibilities that can improve the patient's treatment, intervention or rehabilitation process.

Moreover, new emerging technologies allow the combination of materials, offering the possibility of manufacturing hybrid solutions composed of polymers, biogels, metals or ceramics, among others. This fact, together with the ability to manufacture geometries with a

high degree of difficulty in terms of their spatial distribution and the high degree of product customisation, position this type of technology as a promising alternative capable of replicating the uniqueness that each living organism possesses. Indeed, the human body is very similar between individuals of the species in general, but unique when considering its anatomy in detail and in a particular way. This fact helps to understand the potential of such additive manufacturing technologies in the biomedical field.

Fused filament manufacturing (FFF), stereolithography (SLA) or digital light projection (DLP), inkjet, sintering (SLS) or laser melting (SLM) systems are some of the most common 3D printing technologies in the medical sector. Generally, these technologies are classified according to the origin of the materials they can print. For example, for ceramic lithography manufacturing (LCM), ceramic materials are commonly referred to as ceramic 3D printing, which means that these materials are compatible for this type of system, but others are not. Many of these technologies have versions capable of combining materials, usually from the typology. For example, a multi-material fused filament deposition system can combine different types of polymers. An obvious advantage of these systems is the printing of removable support material, facilitating post-processing of the product and improving its final quality. Other more recent approaches, however, seek to provide functionality to their products by combining different materials from different categories, which in practice allows areas of the same part with different mechanical properties to be obtained, among many other applications.

In relation to this last concept, the European research project no. 953134, **INKplant: Ink-based hybrid multi-material fabrication of next generation implants**, of the European framework programme for research, development and innovation "Horizon 2020", should be presented. This doctoral thesis document has been developed in parallel to the achievement of this project, given the author's professional relationship with it, being part of the design work team of the project at the UPM. Thus, among other objectives, the INKplant project pursues the design, manufacture, evaluation and validation of a new generation of hybrid and biomimetic implants, which through the combination of different materials and technologies allow obtaining multi-scale, multi-functional and multi-material solutions, capable of replicating the conditions existing in the human organism in terms of mechanobiological properties. To this end, it has a consortium of 19 members from 7 mostly European countries. Participants include technology developers, materials developers, research institutes and centres, universities, hospitals and regulatory bodies.

In consecuence, the main objective of the PhD thesis is investigating and validating the synergic applicability of computational modelling tools, rapid prototyping resources and high-performance additive manufacturing technologies for achieving functionally graded, multi-scale and multi-material tissue engineering scaffolds for reconstructing critical sized articular defects involving bone and cartilage. The aim of this methodology is to enable the production of biomimetic implants, being validated through three case studies, and oriented to additive manufacturing processes. To this end, mechanical engineering techniques have been developed and applied to health. By means of finite element simulations and mechanical and biological tests, the behaviour of the proposed solutions has been evaluated. Thus, the

first chapters describe the state of the art and the software tools, 3D printing technologies and materials used to achieve the objectives.

Chapter 4 describes the creation of a library of tissue scaffold structures for tissue engineering applications that has been openly published. The aim is to develop a methodology that promotes repeatability and replicability of the process, following a multi-functional, multi-scale, multi-material approach, which lays the foundation for further work.

Chapter 5 will describe the methods and approaches applied to achieve rapid prototyping strategies. This stage of the work is conceived as a validation of the original idea to check its feasibility. In this way, the first hybrid prototypes are obtained by combining vacuum casting processes in sacrificial moulds obtained by using more conventional 3D printing technologies, such as fused filament manufacturing or systems based on stereolithography principles.

Subsequent chapters culminate the thesis with the study of the 3 articular case studies. Total meniscus implantation is approached by means of 2 different strategies. Depending on the fabrication technologies used, in this case PolyJet and silicon Liquid Deposition Modelling (LDM). Two different concepts will be presented, taking into account the relevant considerations and constraints adapted according to the printing modality.

The osteochondral defect represents an ideal candidate for implementing a multi-material and multi-functional repair, as both bone tissue and cartilage are often affected in this type of pathology. A hybrid and multifunctional implant is therefore proposed for this task, obtained from the combination of materials from different families with different mechanical properties. Using LCM and inkjet technology, a hybrid concept is developed that combines bioactive ceramics for the hard phase of the implant, corresponding to the bone zone, with biodegradable polymers for the soft phase, which recreates cartilage conditions.

For the hip implant, the fabrication of a short stem hip prosthesis is addressed. A new approach to its design, calculation and topological optimisation is described, based on information obtained from finite element mechanical simulations. It is shown that it is possible to lighten an implant with a benefit from the mechanobiological point of view, reducing the effect of stress shielding in the implanted bone area, which results in an improvement in the patient's quality of life and an increase in the longevity of the implant.

Finally, the doctoral thesis closes with a chapter that includes the general conclusions of the work, the new avenues of research that have arisen from this work and the technological scientific impact generated. In conclusion, this doctoral thesis offers an in-depth vision of the new capabilities and possibilities that the development of new design and optimisation methodologies, oriented towards the implementation of high-performance additive manufacturing technologies, can have in the field of tissue engineering and regenerative medicine. The aim is to establish new design flows conceived to obtain tissue scaffolds customised to the patient, as well as innovative topological optimisation processes. All this, while maintaining a multi-scale, multifunctional and multi-material approach that makes it possible to obtain new cutting-edge families of biomimetic implants. This doctoral work aims to highlight the need to enhance and exploit the personalisation of medical solutions for patients in this field of medicine, generating a positive impact on patients' quality of life.

Resumen

La ingeniería de tejidos, como parte integral de la medicina regenerativa, tiene una historia fascinante y ha evolucionado significativamente a lo largo del tiempo. Este ámbito se ha desarrollado a partir del campo de los biomateriales y se enfoca a la combinación de andamios, células y moléculas biológicamente activas para crear tejidos funcionales. Su objetivo principal es restaurar, mantener o mejorar tejidos dañados u órganos completos. Los primeros pasos hacia lo que hoy conocemos como cultivo celular pueden atribuirse a figuras históricas como Paracelso en el siglo XVI, quien intentó crear vida humana utilizando una mezcla de sustancias químicas, y Rudolf Virchow en el siglo XIX, quien fue pionero en el cultivo de células fuera del cuerpo. Sin embargo, el desarrollo de la biología celular y molecular en el siglo XX marcó el inicio formal de lo que hoy conocemos como ingeniería tisular y medicina regenerativa. Científicos como Alexis Carrel, que innovó las técnicas de sutura vascular y cultivo de tejidos, y Joseph Vacanti y Robert Langer, considerados los padres modernos de la ingeniería tisular, desempeñaron papeles fundamentales en el avance de este campo. Su trabajo en la creación de andamiajes para el cultivo celular marcó el comienzo de una nueva era en la medicina regenerativa.

Particularmente, la ingeniería de tejidos ha encontrado aplicaciones prácticas en la medicina regenerativa y en el campo de la implantología, incluyendo la reparación de lesiones articulares, la generación de piel para grandes quemaduras o la creación de órganos funcionales, como vejigas artificiales entre otros. Estos avances han sido alcanzados gracias a un profundo entendimiento de la biología celular y molecular. La presente investigación doctoral se centra en el estudio de soluciones de andamios tisulares personalizados para cubrir patologías articulares presentes en miembros inferiores. Se proponen principalmente soluciones de ingeniería de tejidos para cubrir lesiones de rodilla y cadera.

En la actualidad, la ingeniería de tejidos utiliza andamios fabricados de materiales como colágeno, hidrogeles, nanofibras y biopolímeros, cumpliendo criterios de biocompatibilidad, inertes al medio, degradación gradual y controlada, porosidad adecuada y no toxicidad. Mediante aplicación de cultivos celulares sobre estos andamios es posible obtener estructuras colonizadas biológicamente, llegando a incluso a la obtención de implantes puramente orgánicos. Así, los avances en este campo han permitido el desarrollo de tejidos artificiales, como organoides de hígados y páncreas, porciones mínimas viables que emulan parte de la fisiología, o injertos de piel, entre otros, a través de técnicas como la bioimpresión 3D. La generación de estos andamios requiere por lo general de una porosidad específica para la correcta proliferación celular que a su vez garantice la vascularización. Por este motivo, la impresión 3D representa una herramienta prometedora en el sector, ya que permite la creación de geometrías extremadamente complejas desde el punto de vista espacial, en parte gracias a la minimización o incluso la eliminación de los post-mecanizados necesarios en los procesos de fabricación convencionales.

Esta necesidad de nuevas herramientas y sistemas para proporcionar nuevos avances médicos está ocasionando un incesable desarrollo de tecnología y materiales en el ámbito de la

impresión 3D. La obtención de soluciones médicas cada vez más sofisticadas está permitiendo el estudio de nuevas patologías o el cambio de paradigma de tratamientos tradicionales, aportando nuevas posibilidades que puedan mejorar el proceso de tratamiento, intervención o rehabilitación del paciente.

Además, las nuevas tecnologías emergentes permiten la combinación de materiales, ofreciendo la posibilidad de fabricar soluciones híbridas compuestas por polímeros, biogeles, metales o cerámicos entre otros. Este hecho, unido a la capacidad de fabricar geometrías con un alto grado de dificultad en cuanto a su distribución espacial y el alto grado de personalización del producto, posicionan este tipo de tecnologías como una alternativa prometedora capaz de replicar la singularidad que cada uno de los organismos vivos posee. En efecto, el cuerpo humano es muy similar entre los distintos individuos de la especie con carácter general, pero único si se considera su anatomía al detalle y de manera particular. Este hecho ayuda a entender el potencial que este tipo de tecnologías de fabricación aditiva tiene en el ámbito biomédico.

La fabricación por filamento fundido (FFF), los sistemas de estereolitografía (SLA) o de proyección digital de luz (DLP), de inyección de tinta (inkjet), sinterizado (SLS) o de fusión láser (SLM) son algunas de las tecnologías de impresión 3D más presentes en el sector de la medicina. Generalmente, estas tecnologías se clasifican en función del origen de los materiales que pueden imprimir. Por ejemplo, para fabricación cerámica por litografía (LCM) se suele hablar comúnmente de impresión 3D de materiales cerámicos, lo que significa que estos materiales son compatibles para este tipo de sistema, pero otros no. Muchas de estas tecnologías presentan versiones capaces de combinar materiales, en general provenientes de la tipología. Por ejemplo, un sistema multimaterial de deposición de filamento fundido puede combinar distintos tipos de polímeros. Una ventaja evidente de estos sistemas es la impresión de material de soporte removible, facilitando el postprocesado del producto y mejorando su calidad final. Sin embargo, otros enfoques más recientes, buscan dotar de funcionalidad a sus productos mediante la combinación de distintos materiales, de distintas categorías, lo que en la práctica permite obtener zonas de una misma pieza con diferentes propiedades mecánicas, entre otras muchas aplicaciones.

Con relación a este último concepto, cabe presentar el proyecto de investigación europeo nº 953134, **INKplant: Ink-based hybrid multi-material fabrication of next generation implants**, del programa marco europeo de investigación, desarrollo e innovación "Horizonte 2020". El presente documento de tesis doctoral ha sido desarrollado en paralelo a la consecución de dicho proyecto, dada la situación de vinculación profesional del autor con el mismo, formando parte del equipo de trabajo de diseño del proyecto en la UPM. Así, entre otros objetivos, el proyecto INKplant persigue el diseño, fabricación, evaluación y validación de una nueva generación de implantes híbridos y biomiméticos, que mediante la combinación de distintos materiales y tecnologías permitan la obtención de soluciones multiescala, multifuncionales y multimateriales, capaces de replicar las condiciones existentes en el organismo humano en términos de propiedades mecanobiológicas. Para ello, cuenta con un consorcio de 19 miembros de 7 países mayoritamiente europeos. Entre los participantes se encuentran desarrolladores de tecnología, desarrolladores de materiales, institutos y centros de investigación, universidades, hospitales y organismos de regulación.

Por consiguiene, el objetivo principal de la tesis doctoral es investigar y validar la aplicabilidad sinérgica de las herramientas de modelado computacional, los recursos de prototipado rápido y las tecnologías de fabricación aditiva de alto rendimiento para conseguir andamios de ingeniería tisular multiescala y multimaterial multifuncionales, para reconstruir defectos articulares de tamaño crítico que afecten a hueso y cartílago. La aplicación de dicha metodología persigue la obtención de nuevas vías para la obtención de implantes biomiméticos, siendo validada a través de tres casos de estudio, y orientada a procesos de fabricación aditiva. Para ello, se han desarrollado y aplicado técnicas de la ingeniería mecánica a la salud. Mediante simulaciones de elementos finitos y ensayos mecánicos y biológicos, se han evaluado el comportamiento de las soluciones propuestas. Así, en los primeros capítulos se describen el estado del arte y las herramientas de software, tecnologías de impresión 3D y los materiales empleados para la consecución de los objetivos.

El capítulo 4 recoge la creación de una biblioteca de estructuras de andamios tisulares para aplicaciones de ingeniería de tejidos que ha sido publicada de forma abierta. Se persigue el propósito de desarrollar una metodología que fomente la repetibilidad y la replicabilidad del proceso, siguiendo un enfoque multifuncional, multiescala y multimaterial, que siente las bases del trabajo posterior.

En el capítulo 5 se describirán los métodos y maneras aplicados para la consecución de estrategias de prototipado rápido. Entiéndase esta etapa del trabajo como una validación de la idea original para comprobar su viabilidad. Se obtienen de esta manera los primeros prototipos híbridos combinando procesos colada al vacío en moldes de sacrificio obtenidos mediante el uso de tecnologías de impresión 3D más convencionales, como la fabricación de filamento fundido o sistemas basados en principios de estereolitografía.

Los capítulos posteriores culminan la tesis con el estudio de los 3 casos de estudio articulares. El implante total de menisco se aborda por medio de 2 estrategias diferentes. En función de las tecnologías de fabricación empleadas, en este caso PolyJet y modelado por deposición líquida de silicona. Se presentarán dos conceptos diferentes que contemplan las consideraciones y las limitaciones pertinentes adaptadas en función de la modalidad de impresión.

El defecto osteocondral representa un candidato idóneo para implementar una reparación multimaterial y multifuncional, dado que tanto tejido óseo como el cartílago se suelen ver afectados en este tipo de patología. Se propone por tanto un implante hibrido y multifuncional para esta tarea, obtenido a partir de la combinación de materiales de distintas familias con distintas propiedades mecánicas. Mediante el uso de tecnologían LCM e inkjet se desarrolla un concepto híbrido que combine cerámicas bioactivas para la fase dura del implante, correspondiente a la zona ósea, con polímeros biodegradables para la fase blanda, que recrea las condiciones del cartílago.

En cuanto al implante de cadera, se aborda la fabricación de una prótesis corta de cadera. Se describe una nueva aproximación a su diseño, cálculo y optimización topológica, a partir de información obtenida por medio de simulaciones mecánicas por elementos finitos. Se demuestra que es posible aligerar un implante repercutiendo en un beneficio desde el punto de vista mecanobiológico, reduciendo el efecto de apantallamiento de tensiones en la zona del

hueso implantado, lo que repercute en una mejora en la calidad de vida del paciente y un aumento en la longevidad del implante.

Finalmente, cierra la tesis doctoral el capítulo que recoge las conclusiones generales del trabajo, las nuevas vías de investigación surgidas a partir de este trabajo y el impacto científico tecnológico generado. En conclusión, esta tesis doctoral ofrece una visión profunda de las nuevas capacidades y posibilidades que el desarrollo de nuevas metodologías de diseño y optimización, orientadas a la implementación de tecnologías de fabricación aditiva de altas prestaciones, pueden repercutir en el ámbito de la ingeniería de tejidos y la medicina regenerativa. Se pretende establecer nuevos flujos de diseño concebidos para la obtención de andamios tisulares personalizados al paciente, así como procesos de optimización topológica innovadores. Todo ello, manteniendo un enfoque multiescala, multifuncional y multimaterial que posibilite la obtención de nuevas familias vanguardistas de implantes biomiméticos. El presente trabajo doctoral persigue poner de manifiesto la necesidad de potenciar y explotar la personalización de las soluciones médicas a los pacientes en este ámbito de la medicina, generando un impacto positivo en la calidad de vida de los pacientes.

Table of Contents

1. Introduction 1

1.1. Background 1

1.2. Motivation, objectives and structure 3

1.2.1. Motivation of the PhD thesis 3

1.2.2. Objectives of the PhD thesis 6

1.2.3. Structure of the PhD thesis 9

2. State of the art 11

2.1. Tissue engineering and biofabrication for articular repair 11

2.1.1. Articular injuries overview 11

2.1.2. Tissue engineering and biofabrication for articular repair: current capabilities and challenges 20

2.2. Design and additive manufacturing of biomimetic structures 25

2.2.1. Design approaches for complex bioinspired geometries 25

2.2.2. Additive manufacturing technologies in medicine 30

3. Materials and methods 37

3.1. Design and simulation methods and resources 37

3.1.1. CAD modelling software 37

3.1.2. Finite-element modelling software and topology optimisation resources 39

3.1.3. Slicing software 42

3.2. Prototyping materials and technologies 45

3.2.1. Fused filament fabrication (FFF) technologies and materials 45

3.2.2. Digital light processing (DLP) technologies and materials 49

3.2.3. Vacuum casting system and soft molding technology 51

3.3. High performance additive manufacturing technologies and materials 54

3.3.1. PolyJet additive manufacturing 54

3.3.2. Lithography based Ceramic Manufacturing (LCM) 56

3.3.3. Liquid Deposition Modelling (LDM) 60

4. Development of an open-source library of tissue engineering scaffolds 65

4.1. Geometrical constraints and design requirements 66

4.1.1. Design for additive manufacturing strategy 67

4.2. CAD modelling of the library 69

4.3. Evaluation of properties 75

4.3.1. Library of tissue engineering scaffolds: property charts and design guidelines 75

4.3.2. Fulfillment of FAIR data principles 88

4.4. Conclusions and future proposals 89

4.5. Open-source documentation 90

5. Rapid prototyping route for multi-material tissue engineering scaffolds 93

5.1. Overview of design process for rapid prototyping ... 93
5.2. Design results and discussion ... 95
5.2.1. Computer-aided design of lattices and sacrificial molds with controlled porosities ... 95
5.2.2. Combination of manufacturing processes towards scaffolds with hard and soft phases ... 96
5.2.3. Cell culture processes for preliminary *in vitro* validation ... 99
5.3. Prototyping result and discussion ... 100
5.3.1. Design and manufacturing results for chondral and osteochondral plugs ... 100
5.3.2. Design and manufacturing results for meniscal biomimetic constructs ... 104
5.3.3. Cell culture results for preliminary *in vitro* validation ... 106
5.4. Conclusions and future proposals ... 108
6. Engineering multi-material tissue engineering scaffolds and bioinspired implants for meniscus articular repair ... 109
6.1. Meniscus injury overview ... 109
6.2. PolyJet multi-material meniscal scaffold from a tibial plateau ... 117
6.3. Liquid Deposition Modelling (LDM) meniscal scaffold from patient medical images ... 131
6.4. Conclusions and future proposals ... 142
7. Engineering multi-material tissue engineering scaffolds and bioinspired implants for osteochondral articular repair ... 145
7.1. Osteochondral injury overview ... 145
7.2. Multi-material tissue engineering osteochondral scaffold from regular geometries ... 150
7.3. Multi-material tissue engineering osteochondral scaffold from patient medical images ... 159
7.4. Conclusions and future proposals ... 165
8. Bioinspired topology optimisation of a ceramic short-hip stem ... 167
8.1. Hip joint injury overview ... 167
8.2. Innovative design and optimisation methodology of a ceramic short-hip stem ... 179
8.2.1. Design of a bulk hip prosthesis ... 181
8.2.2. Finite-element model ... 182
8.2.3. Topology optimisation ... 185
8.3. Manufacturing process and results ... 190
8.3.1. Mechanobiological analysis ... 190
8.3.2. Mechanical performance of the optimized implants ... 193
8.3.3. LCM manufacturing process and fabrication of the optimal design ... 195
8.4. Conclusions and future proposals ... 200
9. Main conclusions and future research proposals ... 201
9.1. Main conclusions of the PhD thesis ... 201
9.2. Proposed continuation lines ... 206
9.3. Summary of scientific-technological contributions of the PhD thesis ... 214
References ... 217

List of Figures

Figure 1: INKplant's concept: from medical imaging to optimized patient-specific scaffolds. 6

Figure 2: Current status of joint injuries: aetiology, trigger factors, diagnostic procedures, conventional treatments and new approaches based on TERM. 19

Figure 3: Examples of biomimetic properties of nature used as sources of inspiration in engineering design processes. (a) Shark skin denticles as an example for the development of high-performance swimming suits. (b) Hydrophobic properties of the lotus flower surface. (c) Development of a bee-based micro-robot to evaluate artificial pollination systems. (d) Texture of gecko limbs recreated for the generation of improved adhesive surfaces. Pictures acquired and adapted from "Nature Inspired Architectural Designs: Using Biomimicry as a Design Strategy" (126), "Biomimicry lessons from sharks" (127), "Bio-Inspired Robots and Structures toward Fostering the Modernization of Agriculture" (128), Geckskin website (129) and Stanford News website (130). 29

Figure 4: Diagram illustrating the situation of AMTs in today's medicine: strengths, technologies and materials classification and medical applications. AMTs mentioned according to ISO/ASTM 52900:2021 standard (149). 35

Figure 5: CAD/CAE design and conformal lattice design software used in this PhD. (a) NX 2206 software interface, used for the CAD design of the implants nominal geometries and for the finite-element modelling tasks. (b) nTopology software interface used for the generation of the lattice structures that gives rise to the tissue scaffolds. 43

Figure 6: Slicing software used in this PhD thesis for the use of FFF and DLP additive manufacturing technologies. Bambu Studio (a) and Ultimaker Cura (b) slicer's interfaces used to obtain the G-code files. (c) Chitubox slicer interface used to generate the digital masks. 44

Figure 7: MCP - 004 ST vacuum casting system and prototype of meniscal tissue scaffold casted in silicone. Parts obtained through the implementing of the rapid prototyping strategy described in chapter 5. Vacuum casting system picture acquired and adapted from Aarya Industries (181). 53

Figure 8: FFF technologies used throughout this PhD thesis. (a) Tevo Tornado printer and prototype of printed shin guards for sports practice. (b) Bambu X1 carbon printer with AMS multi-material auxiliary system and surgical guides set designed from porcine anatomy. 3D printer pictures acquired from manufacturers' websites (162, 172) 53

Figure 9: DLP-based LCD technologies used in this research work: (a) Anycubic Photon Mono X printer and prototype surgical guide for single implant positioning as a dental application. (b) Phrozen Sonic Mini 4K printer and fabrication of a dental anatomy as a control model for the production of a restoration. Anatomical models pictures courtesy of Dental Troyano S.L. and 3Dtive S.L. 3D printers pictures acquired and adapted from manufacturers' website (175, 176) 54

Figure 10: LCM printing technology workflow. (a) Design and slicing stage. (b) Printing process. (c) Thermal post-processing stages of debinding and sintering. (d) Final product. Picture acquired from Lithoz GmbH website 59

Figure 11: High performance AMTs used to throughout this PhD thesis. (a) PolyJet technology from Stratasys company. As shown in the diagram, it uses a rotating circular manufacturing platform to which the printer head and the UV emitter are attached. (b) Lithoz LCM technology for printing ceramics. This system is inspired by in-deposit light-curing systems. It also uses a circular platform that receives the light from the emitter at the bottom. (c) Controlled deposition system for silicones and biogels developed by Delta Tower. Images acquired from the manufacturers' websites (186, 189, 195). Diagrams of the technologies obtained from (196, 197, 198). 62

Figure 12: Printed parts using high performance AMTs. (a) Human anatomical model and model of sneakers obtained from the combination of materials combining colours and mechanical properties. (b) Collection of biomedical devices made of ceramic materials. A pommel plate and a graft for bone regeneration in HA 480 (blue colour) and a collection of hand phalanges in ATZ 980 (white colour) can be seen. (c) Heart biomodel and flexible conduit. Pictures acquired and adapted from manufacturers' websites (199, 200, 201). 63

Figure 13: Design for multi-material printability considering varied AMTs: a) Employment of nominal unit cell connection, instead of extended unit cell connection, to avoid printability problems in multi-material lithography based ceramic manufacturing. b) Voxel-based design approach for achieving multi-material and functionally-graded constructs and scaffolds through multi-nozzle inkjet printing or PolyJet -based machines (i.e. Stratasys' Connect systems). c) Pixel-based design approach for textured surfaces to optimize precision according to machines' resolution (i.e. for digital light processing and lithography-based ceramic manufacturing). 69

Figure 14: Example of finite-element model for evaluating the mechanical properties of a tissue engineering scaffold: Evaluation of Young's (compression) modulus. a) Unit cell, mesh, loads and boundary conditions applied for compression study. b) Resulting stress and displacement fields leading to the calculation of compression modulus. 71

Figure 15: Example of finite-element model for evaluating the mechanical properties of a tissue engineering scaffold: Evaluation of shear modulus. a) Unit cell, mesh, loads and boundary conditions applied for shear study. b) Resulting stress and displacement fields leading to the calculation of shear modulus. 72

Figure 16: Example of sensitivity analysis performed to select the adequate mesh size. 73

Figure 17: Example of finite-element model for evaluating the fluidic properties of a tissue engineering scaffold. a) CAD and FEM model with control volume, mesh and boundary conditions. b) Resulting velocity and pressure fields leading to the evaluation of performance. 74

Figure 18: Mechanical properties of scaffolds with woodpile structure. 80

Figure 19: Mechanical properties of different unit cells employed for designing scaffolds. ... 81

Figure 20: Mechanical properties of multi-scale / fractal scaffolds. 83

Figure 21: Exposed surface and relative density for different scaffolds' families. 84

Figure 22: Fluidic performance of different unit cells employed for designing scaffolds. 86

Figure 23: Fluidic performance of scaffolds with woodpile structure. 86

Figure 24: Fluidic performance of multi-scale / fractal scaffolds. 87

Figure 25: Schematic illustration of design steps for lattices and tools for osteochondral plugs. (a) Three reference lattices based on conventional woodpile structures with different porosities. (b) Design of PVA mold including inner lattice connected to mold's walls for improved solubility. Aimed at casting PDMS and achieving porous PDMS lattices or sponges. (c) Longer PVA molds with inner lattice inside and with PLA lattice used as insert. 97

Figure 26: Schematic illustration of design steps for personalized meniscus scaffold and tools. (a) Reference sketches projected upon the upper part of the tibia for design personalization. (b) Layers of radial and circumferential hard networks acting as bone-cartilage interfaces. (c) Design of usual meniscus half-moon and scaffolding lattice by Boolean operations. (d) PVA soluble mold design with hard interfacial insert and inner PVA lattice. 98

Figure 27: Prototypes of scaffolds (and related tools) for chondral and osteochondral repair. (a) PVA molds and PVA molds with PLA inserts prepared for PDMS casting. (b) PDMS lattices or sponges obtained after casting and dissolving the PVA molds in water. (c) Osteochondral plugs with PLA lattice inserts interwoven to PDMS porous scaffolds. 102

Figure 28: Prototypes of functionally graded scaffolds with soft (PDMS) and hard (PLA) phases. (a) Prototypes of different models with insets showing detailed pores in the PDMS sponges, in the PLA lattices and in the interwoven interface. (b) Topographical reconstruction of pores within the PDMS showing the 3D printed layers left by the PVA after being dissolved in water. PDMS pores depend on PVA filament's dimensions. 103

Figure 29: Prototypes of functionally graded scaffolds for meniscal repair with hard and soft phases, both planarly printed and non-planarly printed as personalized options for repair. (a) Basic prototypes with planar hard insert for the hard phase acting as bone-cartilage interface. (b) Example of tools or sacrificial PVA molds: PVA lattice connected to mold's walls (left) and mold closing lid (right) following the computer-aided design from Figure 26d. (c) Advanced prototypes with non-planar insert for the hard phase adapted to the tibia and following the more complex personalized design process of Figure 27. 105

Figure 30: Curved layer fused deposition modelling of PLA inserts for the subchondral region printed upon a PVA bed with the upper surface of the tibia model employed. 106

Figure 31: Biocompatibility of PDMS structures with large (C1), middle-sized (C2) and small pores (C3). a) General cell biocompatibility tested with eluate of construct on MC3T3-E1 cell line related to pure cell culture medium as percentage of control. b) Epifluorescence microscopy images of live/dead (green/red) stained cells seeded on PDMS scaffolds observed from surface side (top view) and cross section (cross view) in the inner region.

Each construct type was biocompatible, facilitated cell attachment and maintenance up to 28 days. Long-term studies are still needed but initial assessment is promising. Reference bar size = 500 μm. Data and pictures provided from Charité - Universitätsmedizin Berlin. Special thanks to Dr. Tilo Dehne. 107

Figure 32: Illustrative diagrams of the meniscus and knee anatomies. (a) Main bones, muscles and tendons involved in knee joint functionality. (b) General view and section view differentiating the meniscal zones, fibers and tissues. (c) Schematic drawing of the meniscus vascularisation in three zones (coronal section). R-R, Red–Red; R-W, Red–White; W-W, White–White. Pictures acquired and adapted from "Use of motion capture in assisted of knee ligament injury diagnosis" (253), "The human meniscus: A review of anatomy, function, injury, and advances in treatment" (248) and "Isolated meniscus injuries in skeletally immature children and adolescents: state of the art" (254). 111

Figure 33: Different categories of meniscal injuries based on their morphology. Longitudinal, (b) radial, (c) oblique, (d) flap and (e) bucket handle tears. Pictures acquired and adapted from Radsource website (252)..... 112

Figure 34: Current medical solutions for total or partial meniscectomy. (a) Collagen disc from Stryker's medical company. (b) Allograft meniscus prior to removal from the tibial plateau. Pictures acquired and adapted from "The collagen meniscus implant" (260) and "Meniscal transplantation: procedures, outcomes, and rehabilitation" (259). 114

Figure 35: Schematic draft summarizing all the meniscus case study clinical requirements. Pictures courtesy of Charité - Universitätsmedizin Berlin and TransTissue Technologies GmbH, members of the EU INKplant consortium. Special thanks to Dr. Tilo Dehne and Dr. Michaela Endres. 117

Figure 36: DFAM process of a meniscus implant adapted to the subchondral anatomy of a patient. (a) Design obtained from the positioning of reference guides that allow the execution of a sweeping operation, joining the respective sections.. (b) Sequence of operations for the generation of the solid body completely adapted to the bone..... 119

Figure 37: Main construction parameters related to the generation of a lattice structure in the nTopology software. (263) (a) Nominal imported volume. (b) Different types of unit cells (cubic simple, gyroid, column elements) applied to the nominal volume. (c) Different spatial configurations (rectangular, cylindrical and spherical) of the cells around the nominal body. (d) Lattice structure with different thickness values implemented on regular sphere. 120

Figure 38: Pore spacing parameter, 'p', for a regular periodic unit cell distribution. 122

Figure 39: Conformal lattice design on nominal volume imported from NX 2206. (a) Imported stl models. (b) Obtaining lattice with spatial distribution of rectangular cell map and simple cubic unit cell using Boolean intersection operation. (c) Corrective operations on discontinuities in the contours of the lattice to guarantee a constant thickness throughout the entire geometry. 123

Figure 40: Design and integration process of the friction-reducing layer and the structural integrity layer in the porous layer. (a) Generative operations of the nominal casing that give

rise to the friction reducing layer. (b) Isometric and section view of the porous layer integrated into the friction-reducing layer. (c) Design and integration of the structural integrity layer on the porous layer. 126

Figure 41: Innovative meniscus scaffold model for tissue engineering applications that meets the requirements outlined in the INKplant project (see Figure 35). (a) Prototype with porous layer with simple cubic unit cell lattice structure. (b) Prototype with porous layer with gyroid unit cell lattice structure. (c) Isometric, front and lateral views of prototype meniscal scaffold completely adapted to the subchondral surface. 127

Figure 42: Design of meniscal scaffold with biomimetic behaviour. (a) Scheme illustrating the position of the lateral and medial menisci on the tibia plateau and section view of their tissue orientations. (b) New biomimetic concept of meniscal scaffold prototype in which the trusses follow radial and circumferential arrangements, imitating the natural distribution. Pictures in (a) acquired and adapted from "Meniscus Repair: From In Vitro Research to Patients" (264). 128

Figure 43: Functionally-graded meniscal tissue scaffolds collection printed using a multi-material PolyJet system from Stratasys. Prototypes printed by Stratasys colleagues in the frame of the INKplant project. Special thanks to Dr. Mariana Pokrass, Dr. Lev Kuno and Lior Zonder. Pictures courtesy of Álvaro Troyano, from 3Dtive S.L. 129

Figure 44: DFAM methodology applied to obtain a batch of meniscal scaffolds to be evaluated during a clinical workshop with animal cadavers organized within the framework of the INKplant project. (a) Design process in NX 2206 to obtain the nominal geometry and conformal lattice design stage in nTopology. (b) Manufacturing process using PolyJet technology by Stratasys coleeagues. (c) Collection of FG meniscal scaffolds to be manipulated during the workshop. Special thanks to the all the colleagues of the European INKplant project who took part in the process: Charité - Universitätsmedizin Berlin, TransTissue Technologies GmbH, Stratasys, Profactor GmbH and JKU Linz Institute of Polymer Product Engineering. 130

Figure 45: Design and implementation process of lattice structure that follows a woodpile pattern on a regular meniscus. (a) Nominal geometries with added flat surface. (b) Generation of the lattice with woodpile layout and application of intersection Boolean operation. (c) Isometric and top view of a variety of meniscal scaffolds with different porosities designed for pore sizes and element diameters of 0.4 , 0.6 and 0.8 mm respectively. 133

Figure 46: Sequence of operations for the implementation of a lattice following a radial and perimeter biomimetic beam layout inspired in the trusses distribution shown in Figure 42a. 135

Figure 47: Meniscus scaffolds prototypes printed by colleagues of Elkem Silicones using a Liquid Deposition Modelling (LDM) system. (a) Meniscal scaffolds with pore size and element diameter of 0.4 and 0.8 mm respectively. (b) Meniscal scaffold with biomimetic arrangement of structure lattice following a woodpile pattern. (c) Cylindrical specimens printed to test porosity with designed pores of 0.4, 0.6, and 0.8 mm respectively. Pictures

courtesy of Elkem Silicones. Special thanks to Dr. Clément Perrinet and Dr. Damien Djian 136

Figure 48: Medical imaging technology used for digitisation of porcine meniscus collection. Pictures courtesy of the INKplant consortium colleagues of Charité - Universitätsmedizin Berlin and TransTissue Technologies GmbH. Special thanks to Dr. Tilo Dehne and Dr. Michaela Endres. 139

Figure 49: Sequence of operations implemented in Siemens NX to obtain the nominal geometry of the meniscus adapted to the patient. Medical image segmentation performed by JKU Linz Institute of Polymer Product Engineering in the frame of the INKplant project, upon which our personalised design procedure is applied. Special thanks to Eng. Disha Tupe. 139

Figure 50: Design process of meniscal scaffolds that follow a lattice distribution with a woodpile pattern. (a) Auxiliary support structures to facilitate scaffold fabrication. (b) Comparisons of scaffolds with lattice structures of circular and square sections respectively. (c) Slicing of the structures shown in b) to highlight the calculation of the trajectories based on the chosen section. (d) Design of hybridized lattices for manufacturing multimaterial scaffold through controlled deposition of PDMS and biogel with cell loading..... 140

Figure 51: Meniscal tissue scaffolds collecion obtained using a rapid prototyping strategy in a multi-material FFF system. (a) Bambu studio, software tool used to generate the G-code. (b) Collection of prototypes obtained from the designs shown in Figure 50. (c) Top view to evaluate the porosity achieved and the correct hybridisation between the two PLA materials used. Pictures courtesy of 3Dtive S.L. and Dental Troyano S.L. Special thanks to Eng. William Solórzano and Álvaro Troyano. 141

Figure 52: Meniscus scaffolds prototypes printed by Elkem Silicones' colleagues from the INKplant project. LDM multi-material system used for this task. (a) Fabrication of porous meniscal scaffold directly printed on the building platform. (b) Fabrication of multi-material hybrid scaffold by combination of Elken PDMS and 3D Matrix Medical Technology biogel with contained cell cargo. Pictures courtesy of Elkem Silicones colleagues. Special thanks to Dr. Clément Perrinet and Dr. Damien Djian. 142

Figure 53: Anatomical diagram of the affected regions in an osteochondral injury. Pictures acquired and adapted from Dr. Riley J. Williams website (270) and "Molecular Signaling Interactions and Transport at the Osteochondral Interface: A Review" (269)..... 146

Figure 54: Current surgical procedures to place an osteochondral insert. (a) Mosaicplasty or autologous osteochondral transplant (AOT), in which case the origin of the implant is the patient's own tissue. (b) Osteochondral allograft transplantation (OCA), in which case the origin of the implant is from a cadaveric donor. Pictures acquired and adapted from "Chondral repair of the knee joint using mosaicplasty" (271) and "Mesenchymal stem cells for subchondral bone marrow lesions: From bench to bedside" (275). 149

Figure 55: Agili-C osteochondral implant, developed by the medical company CartiHeal. Pictures acquired and adapted from CartiHeal website (281) and Medicalbuyer website (282). 150

Figure 56: Figure 35: Schematic draft summarizing the osteochondral case study clinical requirements. Pictures courtesy of Charité - Universitätsmedizin Berlin and TransTissue Technologies GmbH, members of the EU INKplant consortium. Special thanks to Dr. Tilo Dehne and Dr. Michaela Endres..... 151

Figure 57: DFAM methodology applied for the generation of a tissue scaffold for the treatment of osteochondral lesions. (a) Obtaining the porous cylindrical body with a porosity gradient in the Z direction. (b) Generation of the transition layer between the hard and soft phases. 153

Figure 58: DFAM of osteochondral scaffold that integrates the hard phase, belonging to the chondral bone, the soft phase, belonging to the cartilage and the transition membrane, recreating the zone of calcified cartilage. (a) Isometric view of an exploded assembly. (b) Front view of the design where the porosity gradient can be seen. (c) Top-down view of the design where the coincidence of porous channels can be seen in all phases. 154

Figure 59: Ring set design adapted to the vertical walls of the nominal cylinder to bind beam discontinuities. (a)Intersection of circles with multiple diameter values on a pattern of elements distributed on a grid. (b) Isometric view and front view of the updated design with the conformal rings combined. 155

Figure 60: Osteochondral scaffold with circular pore channels and trabeculae with rectangular cross-section. 156

Figure 61: Osteochondral scaffold prototypes manufactured through high performance AMTs. (a) Osteochondral hybrid scaffold printed on a PolyJet system by Stratasys colleagues. Porosity analysis performed. (b) Collection of ceramic specimens printed in an LCM system by Lithoz GmbH colleagues. (c) Osteochonral scaffolds soft phase specimens printed in a DLP system with a biodegradable polymer by Luxenergy colleagues. Pictures courtesy of Stratasys, Lithoz and Luxinergy. 157

Figure 62: (a) Isometric view of the final design of the osteochondral scaffold and exploded view with all layers differentiated. (b) Tissue scaffold solution implantation procedure using press fitting technique. 158

Figure 63: Scaffold prototypes designed and fabricated for evaluation at the clinical INKplant workshop organised with surgeons. (a) Animal knee joint with artificially generated osteochondral defect. The fit of the printed tissue scaffold is checked. (b) Collection of geometries tested during the activity. Pictures courtesy of Charité - Universitätsmedizin Berlin and TransTissue Technologies GmbH. Special thanks to Dr. Tilo Dehne and DR. Michaela Endres. Prototypes printed by Lithoz GmbH and Luxinergy validating the PhD candidate designs. 159

Figure 64: Osteochondral defect generated on the condylar area of a femur of animal origin. Pictures courtesy of Charité - Universitätsmedizin Berlin and TransTissue Technologies GmbH. Special thanks to Dr. Tilo Dehne and Dr. Michaela Endres. 160

Figure 65: Osteochondral prototypes printed in hydroxyapatite and biogel. (a) Collection of scaffolds printed in HA by Lithoz using LCM technology. (b) Soft phase printed by Prpfactor GmbH with biogel using inkjet technology on a 5-axis printer above a hard phase

surface. Pictures courtesy of Lithoz GmbH (a) and Profactor GmbH (b). Especial thanks to Research Engineer Michael Kainz and Dr. Elena Guillen from Profactor GmbH and Dr. Serkan Nohut, Research Engineer Altan Altun and Research Engineer Sebastian Geier from Lithoz. 162

Figure 66: Summary of all design operations implemented in NX 2206 software to obtain the nominal geometry adapted to the patient's anatomy. (a) Imported model obtained by medical segmentation. (b) Delimitation of the defect by means of diameter and depth preset in the surgical planning stage. (c) Generation of a surface adapted to the patient's bone contour to heal the defect. (d) Extrusion of a 2mm thick membrane as cartilage tissue adjacent to the chondral region. Medical images segmentation performed by Research Engineer Disha tupe, from JKU Linz Institute of Polymer Product Engineering. 163

Figure 67: Summary of the operations implemented in nTopology conformal lattice design software. (a) Isometric exploded view of all the layers of the tissue scaffold. (b) Checking of the cell maps in the hard and soft phases to guarantee the alignment of the pores along the structure. (c) Implantation procedure using the press fitting technique with the implant completely adapted to the patient's geometry. (d) Section view showing how the solution adapted to the patient respects the existing anatomical regions compared to the regular cylindrical model. 164

Figure 68: Pathological situation depending on the degree of bone mineralisation. Picture acquired and adapted from "Mechanical basis of bone strength: Influence of bone material, bone structure and muscle action" (287). 167

Figure 69: (a) Bone morphology distinguishing between cortical and trabecular zones of a femoral section. (b) Stress-strain curves of cortical and trabecular bone regions. Pictures acquired and adapted from "Mechanical basis of bone strength: Influence of bone material, bone structure and muscle action" (287) and "Structural optimisation: Biomechanics of the femur" (296). 169

Figure 70: Graph showing the rate of bone remodelling as a function of the existing mechanical stimulus as well as the possible states to which this situation leads. Picture acquired and adapted from "Innovative Design Methodology for Patient-Specific Short Femoral Stems" (302). 170

Figure 71: (a) Most common stresses that lead to hip fractures. (b) Most prevalent areas of the femur that are prone to fracture. Pictures acquired and adapted from "Proximal Femoral Fractures: What the Orthopedic Surgeon Wants to Know" (307) and OrthoInfo website (303). 172

Figure 72: Comparison of healthy hip and tissue associated with osteoarthritis and the appearance of necrotic tissue. Pictures acquired and adapted from Mount Sinai website (314). 173

Figure 73: (a) Representations of partial hip prosthesis (left) and complete hip prosthesis (right). (b) Components present in common hip prosthesis. Pictures acquired and adapted from Dr. Julian Guerra website (315) and OrthoInfo website (303). 174

Figure 74: (a) Classification of short-stem prostheses according to their morphology: I Femoral neck, II Calcar-loading stem, III Calcar-loading stem with lateral flare and IV Shortened tapered stem. (b) Commercial short-stem hip prosthesis from the company DePuy®. Pictures acquired and adapted from "An Update on Cementless Femoral Fixation in Total Hip Arthroplasty" (324) and "Short-stem Designs for Total Hip Arthroplasty: Neck Stabilized Femoral Components" (325). 176

Figure 75: Mechanobiology of the intact femur versus the femur implanted with a hip prosthesis. Picture acquired and adapted from "Biomaterials in Total Hip Joint Replacements: The Evolution of Basic Concepts, Trends, and Current Limitations—A Review" (331). 178

Figure 76: Areas of bone regeneration and bone absorption in the situation of intact femur versus femur implanted with hip prosthesis. Picture acquired and adapted from "Long-Term Bone Remodelling Around 'Legendary' Cementless Femoral Stems" (332). 179

Figure 77: (a) Segmentation of the right femur using 3D Slicer®. (b) Femoral cavity analysis applying elliptical fitting application. (c) Neck and receiving taper design. 182

Figure 78: Boundary conditions. 184

Figure 79: (a) Implant to be optimized. (b) Distance field isocurves. (c) Grip of unit cells. (d) Thickness map. (e) Lattice with a porosity gradient based on distance field. (f) Section view of the implant obtained by Boolean intersection with the lattice. (g) Two solid reinforcement areas: the receiving taper and the base of the stem. (h) Optimized implant and (i) mediolateral section. (j) Quality control of the optimized solid. 186

Figure 80: (a) Original and smoothed stress field. (b) Optimized implants: based on the distance map and using the MPS and WPS criteria with their respective fields. 189

Figure 81: Remodelling curve and regression graph. 190

Figure 82: (a) Medial and lateral side of the proximal femur assessed in the mechanobiological analysis and regression graph of the latero-medial section. Scatter plots (b) of equivalent strain on medial (left) and lateral (right) sides. 192

Figure 83: Equivalent strain field of cortical bone implanted with optimized prostheses based on (a) distance, (b) MPS and (c) WPS fields. 193

Figure 84: WPS field of the (a) bulk prosthesis and of the optimised prostheses based on the (b) distance, (c) MPS and (d) WPS fields. 195

Figure 85: Schematic diagram of the Lithography-based Ceramic Manufacturing (384). Draft courtesy of Lithoz GmbH. 196

Figure 86: (a) Orientation of the hip prosthesis including bi-modal support structure (removed prior to sintering) and green body obtained from LCM. (b) Ceramic model of the optimized implant with the distance and WPS fields and the mediolateral section of the WPS-based stem. (c) View of the post-processed implant assembled with a replica of the patient's cortical and trabecular bone. Pictures courtesy of Lithoz GmbH and 3Dtive S.L. Special thanks to Dr. Serkan Nohut, Eng. Altan Altun, Eng. Sebastian Geier, Eng. William Solórzano and Alvaro Troyano. 199

Figure 87: Methodology based on reverse engineering for the fabrication of personalised implants or medical solutions to the patient. (a) Current methodology acquired and adapted from "Erik Kornfellner. Biomechanics, design and tests of multimaterials for additively manufactured implants. PhD Thesis. 2024. Medical University of Vienna". (b) Innovative design methodology developed in this PhD thesis for the fabrication of biomimetic tissue engineered scaffolds using a multi-scale, multi-material and multi-functional approach framed in the above context. 205

Figure 88: Designs and prototypes of cylindrical specimens with hybridised lattice. (a) Design of a pair of lattices interlaced in space without touching. Special interest in the gaps designed in the connections on the platform to predict shrinkage during heat treatment. (b) Prototypes printed by a combination of hydroxyapatite and tricalcium phosphate. The green body is shown in shades of orange and brown. In bluish and whitish tones the part once sintered. Note the volumetric contraction during the process. Pictures courtesy of Lithoz GmbH. Special thanks to Dr. Serkan Nohut, Eng. Altan Altun and Eng. Sebastian Geier. 207

Figure 89: Cylindrical specimens printed in HA to evaluate the ability to obtain biomimetic grafts for bone regeneration by recreating the morphological properties of cortical and trabecular bone. (a) Specimens printed in multi-material mode. The core of the specimen is made of porous HA by including porogens in the polymeric matrix. The contour is printed in dense HA. (b) Collection of specimens printed in dense HA simulating gradient patterns in order to obtain biomimetic properties. Pictures courtesy of Lithoz GmbH. Special thanks to Dr. Serkan Nohut, Eng. Altan Altun and Eng. Sebastian Geier. 207

Figure 90: Intelligent and conservative dental restoration concept. (a) Innovative approach to the fabrication of a bi-material crown made of two ceramics with different levels of hardness. (b) Traditional approach to the fabrication of a mono-material ceramic crown. (c) Natural tooth sectioned to highlight its morphological features. Special thanks to Dental Troyano S.L. and 3Dtive S.L. 209

Figure 91: Explanatory diagram of the innovative concept presented as a "Trojan horse"... 210

Figure 92: Proposed concept to obtain a solid body of a meniscus from the generation of AI algorithms applied to black and white digital masks in order to automatically generate the curves that best adapt the sections by means of geometric splines. (a) Model obtained by segmentation of medical images. (b) Voxel model, generated from masks obtained in Chitubox. (c) Curve adapted to the voxelated section obtained in a meniscus digital mask, which allows the modification of the contour captured in the reverse engineering process, allowing the shape of the healthy meniscus to be recovered automatically by superimposing all the treated images. 211

Figure 93: Structure based on a cylindrical frame with a cross attached tangentially on both sides. It shows how the contacts applied in CAD design software differ from the geometries obtained in the slincing process, creating errors that affect the multi-material printing process using digital masks. 212

Figure 94: Treatment of masks obtained to debug probability of dead or overlapping pixels to ensure the correct implementation of a multi-material digital 3D printing system. (a) Slicing of the model shown in Figure 93, where problematic pixels (red highlighted) are debugged at the contacts of the cylindrical frame bases. (b) Slice of a multi-material dental crown, shown in Figure 90, where a border of compromised pixels (red highlighted) is observed due to overlapping of both masks. 213

List of Tables

Table 1: Mechanical requirements set for the development of meniscal and osteochondral implant prototypes. Data provided by colleagues from the INKplant consortium clinical team. 45

Table 2: Technical specifications of the FFF Tevo Tornado and Bambu X1 carbon FFF printers acquired from the manufacturer's website (162, 172). 48

Table 3: Mechanical properties of PLA and PVA materials acquired from the manufacturer's website (Smart Materials 3D). (*) The manufacturer does not provide mechanical properties of PVA as its application is intended for the manufacture of support structures. 48

Table 4: Technical specifications of the Anycubic Photon Mono X and Phrozen Sonic Mini 4K printers acquired from the manufacturer's website (174, 175). 50

Table 5: Mechanical properties of Anycubic Eco resin and the INKplant biodegradable polymer (BDP) acquired from the manufacturer's website (174) and from the INKplant documentation respectively 51

Table 6: Technical specifications of the vacuum system acquired from manufacturer's operating instructions document (178) 52

Table 7: Mechanical properties of Easyplat Mold 40 material acquired from the material datasheet (179). 52

Table 8: Mechanical properties of VeroPure and Elastico materials acquired from the Stratasys website (184) 55

Table 9: Technical specifications from the Stratasys J55 3D printer acquired from Stratasys website (185). 56

Table 10: Technical specifications of the LCM printing system CeraFab S65 Medical acquired from Lithoz GmbH website (189) 59

Table 11: Physical properties provided by the manufacturer Lithoz GmbH of the materials hydroxyapatite and alumina toughened zirconia (190, 191). *(*) Ceramic material with a 20 wt% alumina and 80 wt% zirconia composition.* 59

Table 12: Technical specifications of the LDM printing system Delta Tower Fluid MT acquired from Delta Tower website (195). 61

Table 13: Mechanical properties of Silbione™ series provided by Elkem Silicones (194). 61

Table 14: Results from sensitivity analysis 73

Table 15: Summary of geometrical families with selected examples from the open-source library of tissue engineering scaffolds. *Suboptimal technology for printing the selected geometries (other geometries may work better). **Better avoided although printable. Acronyms: FDM – fused deposition modelling, SLA – laser stereolithography, DLP – digital light processing, LCM – lithography based ceramic manufacture, LMM – lithography based

metal manufacture, SLS – selective laser sintering, SLM (PBLF) – selective laser melting / (powder bed laser fusion), 2PP – two photon polymerization. 77

Table 16: Overall porosities values calculated for the meniscal scaffolds batch depicted in Figure 45c. 134

Table 17: Mechanical properties of the cortical and trabecular bone. 184

Table 18: Relationship between distance field values and unit cell thickness. Values not shown in the table are obtained by linear interpolation. 187

Table 19: Relationship between MPS and WPS field and unit cell thickness. Values not shown in the table are obtained by linear interpolation. 188

Table 20: Minimum and maximum WPS values and failure probability of bulk and optimized implants. 194

Table 21: Debinding and sintering of LithaCon ATZ 980 at 1550 °C with a dwelling time of two hours. 198

Abbreviations and Acronyms

AM	Additive Manufacturing
AMTs	Additive Manufacturing Technologies
ACL	Anterior Cruciate Ligament
ACI	Autologous Chondrocyte Implantation
AVN	Avascular Necrosis
BDP	Biodegradable polymer
BJ	Binder Jetting
CT	Computed Tomography
CAD	Computer aided design
CAE	Computer aided engineering
CAM	Computer aided manufacturing
CM	Conditioned Medium
DFAM	Design For Additive Manufacturing
DICOM	Digital Imaging and Communication in medicine
DLP	Digital Ligh Processing
DMD	Digital Micromirror
DIW	Direct Ink Writing
EMA	European Medicines Agency
FDM	Filament Deposition Modelling
FFF	Filament Fused Fabrication
FAIR	Findability, Accessibility, Interoperability and Reusability
FEA	Finite-Element Analysis
FEM	Finite-Element Modelling
FDA	Food and Drug Administration
fMRI	Functional Magnetic Resonance Imaging
FG	Functionally Graded
h-MSC	human Mesenchymal Stem Cell
HA	Hydroxyapatite
ISO	International Organization for Standardization
LCD	Liquid Crystal Display
LDM	Liquid Deposition Modelling
LMM	Lithography based Metal Manufacturing
LCM	Lithography-based Ceramic Manufacturing
MRI	Magnetic Resonance Imaging
MJ	Material Jetting
MACI	Matrix-Assisted Chondrocyte Implantation
MPS	Maximum Principal Stress

MEMS	Micro-Electro-Mechanical systems
NSAIDs	Non-Steroidal Anti-Inflammatory Drugs
N/A	Not available
OBJ	Object
OS	Open-source
OCA	Osteochondral Allograft
OAT	Osteochondral Autologous transplantation
PDGF	Platelet-Derived Growth Factor
PLA	Poly(Lactic Acid)
PLGA	Poly(Lactic-co-Glycolic Acid)
PCL	Polycaprolactone
PDMS	Polydimethylsiloxane
PEG	Polyethylene Glycol
PGA	Polyglycolide
PLY	Polygon
PMMA	Polymethylmethacrylate
PVA	Polyvinyl Alcohol
PBLF	Powder bed laser fusion
SLM	Selective Laser Melting
SLS	Selective Laser Sintering
STL	Standard Tesellation Language
SLA	Stereolithography
TERM	Tissue Engineering and Regenerative Medicine
THA	Total Hip Arthroplasty
TGF-β	Transforming Growth Factor-Beta
TCP	Tricalcium Phosphate
TPMS	Triply Periodical Minimal Surface
2PP	Two-Photon Polymerization
UTS	Ultimate Tensile Strength
UV	Ultraviolet
UPM	Universidad Politécnica de Madrid
WPS	Worst Principal Stress

1. Introduction

1.1. Background

Tissue engineering and regenerative medicine (TERM) are interdisciplinary fields that lie at the intersection of biology, engineering, and medicine, with the primary goal of repairing, replacing, maintaining, or improving the functions of tissues or organs in the human body. These fields have experienced exponential growth in recent decades, thanks to technological advances and a better understanding of biological mechanisms at the cellular and molecular level. This introduction summarizes the origin, historical precursors, foundations, strengths, role of 3D printing, and obstacles associated with tissue engineering and regenerative medicine.

The fascination with tissue and organ regeneration dates back to antiquity, with myths and legends reflecting the human desire for healing and rejuvenation. Stories such as that of the titan Prometheus in Greek mythology, who was punished by the daily regeneration of his liver, are early testimonies to this interest. Furthermore, the legend of Saints Cosmas and Damian, who miraculously performed a leg transplant, indicates an early conceptualisation of regenerative medicine. The development of cell and molecular biology in the 20th century marked the formal beginning of what we know today as tissue engineering and regenerative medicine. Scientists such as Alexis Carrel, who innovated vascular suturing and tissue culture techniques, and Joseph Vacanti and Robert Langer, considered modern pioneers of tissue engineering, played pivotal roles in advancing the field. Their work in creating scaffolds for cell culture ushered in a new era in regenerative medicine.

Tissue engineering is based on three main components: cells, scaffolds and growth factors. Cells can be obtained from the patient (autologous) or from a donor (allogenic) and are essential to repopulate the scaffold and form the desired tissue. Scaffolds provide the three-dimensional structure necessary for cell growth, while growth factors and biochemical signals guide cell differentiation and proliferation towards specific tissue types. Cells are the fundamental building blocks of tissue, and tissues are the basic unit of function in the body. Generally, groups of cells form and secrete their own supporting structures, called the extracellular matrix. This matrix, or scaffold, does more than just serve as a support for cells; it also acts as a relay station for various signalling molecules. Thus, cells receive messages from many sources that become available from the local microenvironment or cell niche. Each signal can initiate a chain of responses that determines what happens to the cell. By understanding how individual cells respond to signals, how they interact with their environment and how they organise themselves into tissues and organisms, researchers have been able to manipulate these processes to heal damaged tissues or even create new ones.

The process often begins with the construction of a scaffold from a wide range of possible sources, from proteins to polymers. Once the scaffolds are created, cells can be introduced with or without a "cocktail" of growth factors. If the environment is right, tissue develops. In some cases, the cells, scaffolds and growth factors are all mixed together at the same time, allowing the tissue to "self-assemble". Another method of creating new tissue uses an existing scaffold. Cells from a donated organ are detached and the remaining collagen scaffold is used to grow new tissue. This process has been used to bioengineer portions of heart, liver, lung and kidney tissues. This approach offers great hope for using the scaffold with human tissue discarded during surgery and combining it with a patient's own cells to make customised organs that are not rejected by the immune system.

Despite its outstanding potentials, tissue engineering plays a relatively small role in the treatment of patients. Supplementary bladders, small arteries, skin grafts, cartilage and even a complete trachea have been implanted in patients, but the procedures are still experimental, and not always succesful. While more complex organ tissues such as heart, lung and liver have been successfully recreated in the laboratory, they are still a long way from being fully reproducible and ready to be implanted in a patient. However, these tissues can be of great use in research, especially in drug development, cosmetics, etc. By using functional human tissue to help select drugs, candidates could accelerate development and provide key tools to facilitate personalised medicine, while saving money and reducing the number of animals used for research. The main strengths of tissue engineering include the ability to customise treatments to the specific needs of individual patients, reducing the risk of immune rejection. In addition, it offers alternatives to organ transplants, with the potential to alleviate donor shortages. Tissue engineering also enables the development of human tissue models in the laboratory, which can be used for disease research and drug screening.

To fulfil their promises, tissue engineering and regenerative medicine face significant challenges. Vascularisation of artificial tissues and organs is one of the most critical obstacles, as without an adequate blood supply, tissues cannot survive and integrate properly into the body. Immune response and the risk of rejection are also major concerns, especially for allogenic cells and tissues. In addition, replication of the structural and functional complexity of native biological tissues remains a considerable technical and scientific challenge. These obstacles require innovative approaches in biomaterial design, bioengineering, and synthetic biology to overcome. In addition, there are significant ethical and regulatory challenges. The regulation of tissue engineering and regenerative medicine products is complex, given their innovative nature and potential for profound impacts on human health. Ethical considerations, including informed consent and fairness in access to advanced therapies, are critical to the responsible integration of these technologies into medical practice.

3D printing has emerged as a revolutionary tool in regenerative medicine, allowing the creation of complex scaffolds that mimic the three-dimensional structure of natural tissues. This technology is bound to contribute to the manufacture of tissues and organs with precise geometries, customised to the needs of the patient. 3D printing has also opened up new avenues in research, allowing the study of the interaction between different cell types in complex structures.

Tissue engineering and regenerative medicine represent fields of research and clinical application with transformative potential. As researchers continue to overcome technical and ethical hurdles, these disciplines promise to revolutionise the treatment of a wide range of diseases and injuries, offering hope for tissue and organ regeneration and repair. Multidisciplinary collaboration between biologists, engineers, clinicians, and regulators is essential to address current and future challenges, facilitating the development of safe, effective, and affordable therapies. As we move forward, it is crucial to maintain an open and ethical dialogue on the impact and implications of these technologies, ensuring that they benefit society in an equitable and fair manner.

1.2. Motivation, objectives and structure

1.2.1. Motivation of the PhD thesis

Tissue engineering is bound to reshape healthcare by providing patients with personalized solutions for repairing and regenerating damaged tissues. The classic approach involves the employment of three-dimensional constructs, named "scaffold", ideally designed to mimic the properties of the extracellular matrix and the features of the cellular microenvironment. Cells from animals, donors or patients are cultured within the scaffolds for *in vitro* or *in vivo* studies and final medical application. Cytokines, chemokines and growth factors are often incorporated to these biohybrid systems, as they play an important role in cell recruitment, activation, proliferation, differentiation and survival. These scaffolds, apart from their mechanical integrity, should be porous for enabling the exchange of nutrients, the elimination of debris and the eventual vascularization of the biohybrid constructs achieved. In the ideal situation, biodegradability is often a requirement, although bioinert or bioactive scaffolds may also play an important role for tissue engineering and regenerative medicine, as implants with properties beyond those available in the medical industry. Currently, in the European Union, scaffolds without cells may be employed as implants with biomimetic features for enhanced performance and are Class III medical devices according to Medical Device Regulation 2017/745. In the case of scaffolds incorporating cells, they are advanced therapy medicinal products . Evolving from tissue engineering, biofabrication aims at employing biomaterials and cells during the manufacturing of biohybrid constructs, instead of having cells colonizing previously manufactured scaffolds.

The potentials of tissue engineering and biofabrication are huge, but clinical translation is still limited to scattered experiences, because both fields are still matter of research and several challenges still need to be overcome. Tissue engineering still needs to adequately integrate designs, materials and processes capable of adequately addressing the multi-material, multi-scale, multi-phase and functionally graded nature of human tissues with increasing biomimetic and biomechanical fidelity. Biofabrication faces the challenge of processing cells together with extremely high-performance materials like ceramics or alloys, which processing usually implies temperatures and pressures unacceptable for living cells within. In both

synergic areas, the repair or regeneration of large sized (or critical sized) defects, those reaching several cm^3, is extremely demanding, as the exchange of gases and nutrients by diffusion mechanisms is not enough and the creation of a functional vasculature is required.

Mechanical engineering plays a crucial role in these fields, probably a more relevant one in the area of tissue engineering, for the relevance of the scaffolding elements. Indeed, technologies of the mechanical engineering realm like additive manufacturing prove essential for achieving the complex-shaped geometries of scaffolds, required for addressing the complexity of life. The computational modelling of these bioinspired structures and their optimisation with biomechanical considerations are also fundamental, as will be discussed.

Summarizing, this PhD thesis is developed with a motivation of contributing to advancing healthcare, through the research and establishment of innovative synergies between design, modelling and manufacturing technologies and the processing of special biomaterials combinations. This is required for fostering a biomechanical approach to the repair and regeneration of a wide set of articular problems and tissues, especially those involving osteochondral defects affecting both bone and cartilage, and those concerning large meniscal, and bone injures.

Context

In agreement with the above, the PhD has been carried out in the context of: 1) the PhD Programme in Mechanical Engineering at Universidad Politécnica de Madrid (UPM), 2) the Product Development Laboratory of the Machines Engineering Division at the ETSI Industriales of UPM, and 3) the European project **"INKplant: Ink-based multi-material hybrid manufacturing of next generation implants"** (Horizon 2020 Programme, Leadership in Industrial and Enabling Technologies, H2020-NMBP-TR-IND-2018-2020 "Biological scaffolds for tissue engineering and repair" call, Grant Agreement: nº 953134), coordinated by Dr. Elena Guillén from Profactor GmbH (Steyr, Austria). This project funded the PhD thesis and two three-month international research stays of the candidate in Profactor GmbH and Lithoz GmbH (Vienna, Austria), as part of the requisites for obtaining the "International PhD Mention" and contributing to different objectives of the INKplant project.

First of all, the PhD Programme in Mechanical Engineering at Universidad Politécnica de Madrid has a research line focused on the frontiers between mechanical engineering and product development, in which the development of biomechanical and medical devices has been a key research topic for more than a decade. Within the Mechanical Engineering Department at Universidad Politécnica de Madrid, the Machines Engineering Division has researched and lectured in these topics for more than 30 years. Starting with courses on biomechanics by professors Bautista, Lafont and Muñoz, progressively the educational connections with biomedical engineering and medical technologies grew, in parallel to the establishment of the research lines of the Product Development Laboratory and the creation at UPM of bachelor's and master's degrees in biomedical engineering, mechanical engineering and industrial engineering adapted to the European Area of Higher Education. Different courses were implemented in these degrees by professors Lafont and Díaz Lantada, to which the rapid design and prototyping of medical devices was incorporated as a topic for project-based learning actions. Another turning point was marked by the participation of professors

Díaz Lantada, Muñoz Guijosa and Chacón in the European project "UBORA: Euro-African Open Biomedical Engineering e-Platform for Innovation through Education", conceived and led by the University of Pisa and professors Ahluwalia and De Maria and developed in collaboration with a remarkable team of European and African universities, through which novel approaches to medical devices innovation and education were implemented and the concept of "open-source medical device" was importantly fostered.

In the UBORA project, the candidate took part, first as trainee during his bachelor's degree thesis, then as mentor during his master's degree thesis, contributed to the UBORA biomedical design schools of Nairobi (2017), Pisa (2018) and Kampala (2019), and became a researcher in the field of additive manufacturing technologies applied to the development of medical devices. This background led to a passion for engineering technologies for health, for promoting open innovation and open science approaches in this challenging and socially impactful industry, and to the consequent application of the candidate for a research position within the European project INKplant, which importantly contributed to framing the objectives of the PhD thesis, as detailed below in a summarized fashion derived from the original project proposal:

"*The vision of INKplant is the fusion/combination of different biomaterials, high resolution additive manufacturing technologies already proven for industrial processes (lithographic ceramic manufacturing, 3D multi-material inkjet printing, digital light processing, among others), and advanced simulation and biological evaluation, to bring new solutions for the design of biomimetic scaffolds which can address the complexity of regenerating different tissues in the human body, and have the potential to reduce healthcare costs by more than 30%*".

Currently, medical implants for tissue repair are manufactured in standard sizes and shapes with the aim of simplifying the production process. Implants that require individual size and shape must be adapted by cutting or shaping in the operating room, or the size of the defect must be adapted to the next possible size of the implant. This is accompanied by additional tissue loss, which can be prevented, if customized implants can be produced. The use of innovative 3D printing technologies and novel inks would enable the manufacturing of individual customized implants, which is key to maximize tissue preservation in the defect area. Recent developments in 3D printing technologies can provide single-material biocompatible implants with the individualized macroscopic shape to fit a patient-specific tissue defect.

However, for real advancement of additive manufacturing to provide solutions to the patient´s individual requirements, there is a need for new biomaterials, technologies and processes that additionally allow the fabrication of multi-material biomimetic scaffolds with appropriate composition and microstructure that induce tissue-specific regeneration and consider the individual variations (see Figure 1). It is not possible to address the complexity in structure and properties of human tissues with a single material or a single-step fabrication process, and the existing applications have come to their limit without clinically-widespread solutions.

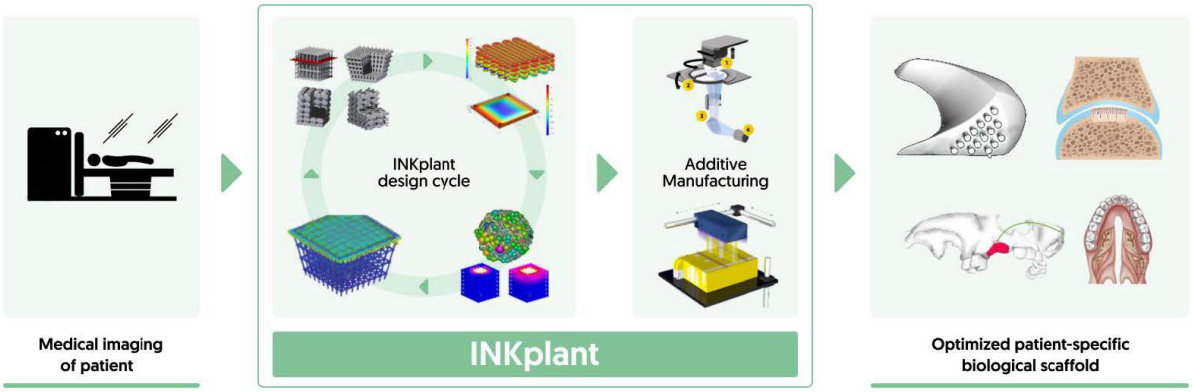


Figure 1: INKplant's concept: from medical imaging to optimized patient-specific scaffolds.

"Achieving the thresholds of complexity and detail at high precision and production capacity, INKplant use cases should provide solutions to two of the most widespread and urgent medical challenges in European health care, bringing an individualized and gender-specific new treatment concept into mass production. Patients suffering from chronic defects of joints (use case 1) and dental tissues (use case 2) have severely decreased life quality and depend continuously on health care. Even if not immediately fatal, these conditions have dramatic side effects and put a strong strain on health care systems, while increasing the risk for further infection. As 22% of the European population will be aged over 65 by the year 2025, rising to almost 30% by 2050, regenerative approaches become more important to sustainably heal and avoid further treatments".

Within INKplant, the role of UPM has been linked to leading the computational modelling work package and developing the global design for additive manufacturing strategy, while remarkably contributing to the materialization of the different conceptual designs of scaffolds and use cases, first as computational models optimized through biomechanical simulations, then as rapid prototypes and functional medical devices by employing various manufacturing routes and synergic additive manufacturing technologies, both low-cost and high-performance. UPM has also managed the open innovation calls within INKplant, providing support to external users of developed materials and technologies in the design of their proposed concepts. In all these tasks the candidate has played a key role, researching and learning in a fascinating field throughout the development of the PhD thesis, whose objectives are detailed in the following section.

1.2.2. Objectives of the PhD thesis

Considering the challenging nature of imitating life and, at the same time, the potential provided by additive manufacturing technologies in this regard, especially when multiple materials are processed together or when high-performance polymers and ceramics are structured in a freeform fashion, this PhD thesis intends to provide innovative methods and solutions for obtaining high-fidelity tissue engineering scaffolds, mainly for articular problems.

In consequence, the main objective of the PhD thesis is:

Investigating and validating the synergic applicability of computational modelling tools, rapid prototyping resources and high-performance additive manufacturing technologies for achieving functionally graded, multi-scale and multi-material tissue engineering scaffolds for reconstructing critical sized articular defects involving bone and cartilage.

Through this investigation, achieve a knowledge-based methodology for the development of personalized and biomimetic prostheses with biomechanical performance.

To achieve the main goals of this PhD thesis, an additional set of specific objectives must be taken into account and methodically tackled, following the inspiring experiences of UPM Product Development Laboratory in the biomedical field and benefiting from the background of the candidate in the development of open-source medical devices and the application of additive manufacturing technologies:

1. Promote multi-material, multi-scale and functionally graded design and manufacturing methods for achieving tissue engineering scaffolds combining ceramics for bony phases and polymers for chondral phases.
2. Explore ways of engineering scaffolds and prostheses based on the use of digital materials, voxelated matter, conformal lattices and topology optimized structures and surfaces for improved biomimicry and advantageous cell-material interactions.
3. Investigate rapid prototyping routes by combining additively manufactured networks, soft molds and casted elastomers for obtaining biomechanical transitions between soft and hard regions of scaffolds for complex tissular restorations.
4. Innovate high performance additive manufacturing technologies, including digital light processing, multi-inkjet printing and lithography-based ceramic manufacturing, for accomplishing large sized patient-matched scaffolding constructs with design-controlled microstructures and surface topographies.
5. Apply the investigated computational modelling techniques, rapid prototyping resources and additive manufacturing technologies for developing artificial constructs for repairing, reconstructing or replacing meniscal, osteochondral and bone defects.
6. Exemplify the progresses achieved by the INKplant project consortium through a collection of prototyped demonstrators designed for optimal additive manufacturing employing the technologies and materials resulting from the research project.
7. Deliver a selection of developments, gathered and generated knowledge and data as open-source medical devices with proper documentation and following FAIR (findability, applicability, interoperability, reusability) data principles as a special contribution to open science in the tissue engineering field.

8. Study and encourage technology transfer pathways for bringing the obtained know-how closer to healthcare professionals, patients and end users in general, including the creation of case studies for educational activities, the development of concrete collaborations with medical doctors and the participation in industrialization actions.

9. Contribute to the short- and long-term viability of INKplant project consortium and to the success of technological and biomedical innovations developed within INKplant, by supporting the strategic planning of new research proposals focused on higher technology research levels, underpinning the establishment of international and intersectoral networks, and helping medical and industrial partners to bring their concepts into life and leverage their achievements.

Apart from the scientific-technological and industrial objectives, the PhD thesis is carried out with necessary fundamental educational objectives, namely: 1) the planning of a career oriented to research, development and innovation, and 2) the acquisition of a wide set of technical abilities and leadership and essential skills. To this end, different educational activities performed should be highlighted:

a. Performing a three-month international research stay in Profactor GmbH, Austrian research company coordinating the INKplant EU project, to work in the team of Dr. Elena Guillen (INKplant coordinator) and contribute to the development and application of 5-axis multi-material inkjet printing in an international and research-oriented environment.

b. Carrying out a three-month international and intersectoral research stay in Lithoz GmbH, Austrian additive manufacturing company and world reference in high-quality lithography-based ceramic manufacturing, to work in the team of Dr. Serkan Nohut and contribute to the printing of topology optimized critical size constructs and to the design for multi-ceramic printing, while experiencing a real industrial teamwork environment.

c. Taking part in different educational actions required by the PhD Programme in Mechanical Engineering at UPM, including courses and seminars focused on the management of bibliographical resources and scientific-technical documentation (30 hours) and courses and seminars oriented to the management of research, development and innovation projects (30 hours).

d. Involvement in hands-on educational actions at UPM, including the training of younger PhD candidates and students developing their final degree theses or their research visits at the Product Development Laboratory, especially as regards design for additive manufacturing and the employment of several additive manufacturing resources.

e. Participation in workshops and seminars in different courses and spring/summer schools at UPM focused on the development of medical devices with invited talks on "design for additive manufacturing" and "medical applications of 3D printing technologies".

f. Engagement in multi-stakeholder dissemination and communication actions aimed at promoting the impacts of the PhD thesis, such as: preparing scientific articles and congress communications, creating visual materials and prototypes for impactful communication, attending to scientific-technological, conferences, events and fairs, participating in open days of departments and laboratories at UPM, visiting potential partners for establishing alliances in medical additive manufacturing, and contributing to preparing deliverables and reporting advances to funding entities like the European Commission.

1.2.3. Structure of the PhD thesis

According to the above, the PhD thesis is structured as follows:

Chapters 1, 2 and 3 are introductory. In chapter 1 the topic has been presented, the objectives of the PhD thesis announced and the document structure described. Chapter 2 delves into the state of the art as regards the current and future tissue engineering and regenerative medicine applications accomplished through the use of additive manufacturing technologies. Chapter 3 summarizes the software tools, materials and additive manufacturing systems employed for the correct development of this research in parallel to the develop of the European INKplant project.

Chapter 4 develops the basis of a new additive manufacturing-oriented design methodology for the generation of tissue engineering scaffolds. Through the creation of a collection of design maps and graphs, it is wished that this library will serve as a tool for designers, as it has been created with multi-scale, multi-material and multi-functional technologies and materials in mind to comply with tissue engineering requirements. Chapter 5 describes a rapid prototyping process strategy in which, through the use of accessible manufacturing technologies (DLP, FFF, vacuum casting), a workflow is established to obtain hybrid scaffolds formed by the combination of polymeric inserts with porous silicone meshes, thanks to a casting process in sacrificial moulds obtained by fused filament printing techniques.

Chapters 6, 7 and 8 exemplifies the generated knowledge and studied methods through a set of 3 case studies of joint injuries: meniscal replacement, osteochondral defect and total hip replacement. Applying everything developed in chapters 4 and 5, bioinspired tissue scaffold designs with a high degree of complexity are presented to illustrate the development of new families of biomimetic implants. Thanks to the combination of materials, making use of technologies at the forefront of additive manufacturing, these new biomedical solutions can be endowed with a biomimetic character. The implementation of porosity gradients or the adaptation of geometric contours to the patient's anatomical structures, as well as the development of topological optimisation processes based on finite-element mechanical testing are some of the strategies described in these chapters.

Finally, chapter 9 summarises the PhD thesis, presenting the main conclusions, the scientific-technological contributions and the generated impact as well as the future lines of research arising from this research.

2. State of the art

2.1. Tissue engineering and biofabrication for articular repair

2.1.1. Articular injuries overview

Articular or joint injuries can be categorized into several categories based on their origin, mechanism of injury, and the type of tissue affected. Understanding these different types is essential for accurate diagnosis and the selection of appropriate treatments.

One of the most typical causes for joint injuries is related with the practising of sports. Injuries that occur in sports often result from a variety of factors including accidents, inadequate training, or overuse of specific joints (1, 2, 3). These injuries encompass a wide array of conditions, including but not limited to sprains and strains, meniscus injuries or anterior cruciate ligament (ACL) injuries. Sprains and strains injuries affect ligaments (sprains) and muscles or tendons (strains) and are quite prevalent among athletes and sports practitioners. For instance, ankle sprains are a frequently occurring sports-related injury (4, 5). Menisci, situated within the knee joint, can suffer tears during sudden and forceful movements, commonly observed in sports like soccer and basketball (6, 7). The ACL, a crucial knee ligament, is frequently prone to injury in sports that involve abrupt changes in direction and jumping (8, 9).

Another category, normally related to older individuals, are degenerative injuries. These pathologies primarily result from the gradual wear and tear experienced over time, with a higher prevalence among elderly. For instance, osteoarthritis, the most prevalent form of arthritis, develops when the protective cartilage at the ends of bones gradually deteriorates (10). This condition frequently impacts the knees, hips, and hands. Moreover, rheumatoid arthritis, an autoimmune disease, can lead to joint pain and deformities. (11)

In the daily routine it is also common to suffer fortuitous accidents that lead to joint injuries. These injuries typically occur as a consequence of substantial external impact or force and can potentially affect any joint within the body. They encompass compound fractures, also known as open fractures (12), characterized by a fractured bone that breaches the skin's surface, and compression injuries, frequently observed in the spine, particularly among older individuals who have osteoporosis (13).

Besides this, some articular pathologies can present a variety of conditions that do not specifically fit into the categories of sports injuries or degenerative issues. Some of these candidates are bursitis, tendonitis, dislocations and subluxations or articular fractures among others. Bursitis involves the inflammation of bursae, which are small sacs filled with fluid that serve as protective cushions between bones and soft tissues (14). Tendonitis refers to the

inflammation or irritation of a tendon, typically brought on by excessive use (15). Dislocations and subluxations describe situations where a bone is displaced from its usual position within a joint (16, 17). Articular fractures specifically affect the surfaces of bones within a joint (18).

As it can be observed, articular injuries are traumatic events or degenerative processes that affect the structure and function of the joints. Understanding the underlying mechanisms and causes of these injuries is essential for proper prevention and treatment. For this purpose, the following paragraphs delve into the factors contributing to joint injuries:

- Biomechanical factors: in the field of biomechanics, factors such as repetitive stress (19) and overloading (20) are crucial in maintaining joint integrity and health. Repetitive stress refers to the cumulative damage that joints can suffer due to repetitive movements in activities like running, jumping, or consistently lifting heavy objects. This type of stress can lead to gradual joint deterioration over time. On the other hand, overloading involves excessive loading on a joint or group of joints, surpassing their shock-absorbing capacity, which is common in contact sports and weightlifting. Both factors can result in joint injuries by compromising the ability of joints to handle forces applied during physical activities.
- Genetic and biochemical factors: some individuals may possess a genetic predisposition to develop specific joint conditions, such as osteoarthritis (21). Genetic markers associated with an elevated risk of these conditions have been identified. Additionally, biochemical alterations in synovial fluid composition or cartilage structure, influenced by various factors, can contribute to joint injuries (22). For instance, a reduction in joint lubrication can lead to increased friction and wear.
- Environmental and lifestyle factors: the development of joint conditions can be influenced by a multitude of factors. Excess body weight and obesity, for instance, place an added mechanical burden on weight-bearing joints, like the knees and hips, thereby heightening the vulnerability to conditions such as osteoarthritis (23, 24). This susceptibility is further compounded by the lack of physical activity, which can lead to muscle weakness, subsequently compromising joint stability and the body's protective mechanisms against injuries. Moreover, certain occupational roles characterized by repetitive movements or substantial weight-bearing tasks can also increase the risk of joint injuries. Similarly, engagement in specific sports and athletic activities may expose individuals to distinct types of joint-related injuries, thus highlighting the intricate interplay of factors contributing to joint health and potential pathologies (25).
- Trauma and accidents: traumatic injuries, such as falls, car accidents, or direct impacts on a joint, can cause immediate damage to joint structures. This includes fractures, sprains, and dislocations (26).
- Autoimmune diseases: some autoimmune diseases, like rheumatoid arthritis, can trigger an abnormal immune response that affects the joints, causing inflammation and joint damage (27).

- Aging: the natural aging process brings about changes in joint structure and function. Cartilage wear and degeneration can heighten the risk of joint injuries, especially in elderly people (28).

Epidemiology and demography

The field of joint injuries epidemiology provides us with valuable insights into the prevalence and occurrence of these conditions in diverse populations. This knowledge is essential for gaining a comprehensive understanding of the disease burden and for shaping effective strategies for both prevention and treatment. Joint injuries, while encountered across all age groups, exhibit distinct patterns in terms of type and frequency. Sports-related injuries tend to be more common among the younger, active populace, particularly in athletes and individuals who regularly partake in physical activities (29, 30). On the other hand, degenerative Injuries, such as osteoarthritis and other forms of arthritis, are prevalent among older individuals. Their occurrence tends to rise with advancing age, and these conditions are often associated with the gradual wear and tear of joints (11).

Regarding age, as mentioned previously, sports-related injuries are more prevalent in younger individuals, whereas degenerative injuries like osteoarthritis primarily afflict the elderly (25, 28). Gender can also affect the appearance of articular injuries. Certain injuries, such as hip fractures, exhibit a higher incidence in women, especially post-menopause due to reduced bone density (31). The occurrence and nature of sports-related injuries may vary between genders due to differences in sports participation and biomechanics (32). Another factor is the professional role or activity that a person occupies in his daily life. Professions involving repetitive motions or heavy lifting may predispose individuals to specific joint injuries (23). For instance, workers in the construction industry may face an elevated risk of knee and shoulder injuries.

Lifestyle factors play a significant role in the development of joint-related conditions. As said before, excess body weight and obesity, for example, contribute to increased mechanical stress on weight-bearing joints, particularly the knees, leading to a heightened susceptibility to conditions such as osteoarthritis (23, 24, 25). In addition to lifestyle, genetic influences have also been identified as pivotal factors in joint health. There is compelling evidence indicating a genetic predisposition to certain joint injuries and conditions, including osteoarthritis, emphasizing the multifaceted nature of these ailments (21). Furthermore, environmental elements should not be overlooked when considering joint health. Access to safe and well-maintained sports facilities, along with adequate training and supervision, can significantly impact the incidence of sports-related injuries (23, 29, 30). These environmental factors, in conjunction with individual lifestyle and genetic predispositions, contribute to the complex interplay that underlies joint health and the potential development of joint-related pathologies. The incidence and prevalence of certain joint injuries are on the rise worldwide. This trend can be attributed to factors like the aging global population, an increasing engagement in sports activities across all age groups, and a growing prevalence of obesity (23, 29, 30).

Diagnosis of articular injuries and conventional treatments

Accurate diagnosis is a fundamental step in the effective management of joint injuries. It allows for the identification of the nature and extent of the injury, subsequently guiding therapeutic decisions. The following delves into the diagnostic techniques employed in the field of joint injuries.

During the diagnostic evaluation of joint-related issues, a comprehensive approach is often undertaken. The initial step involves a meticulous physical examination of the afflicted joint, wherein healthcare professionals employ a range of assessments, including mobility tests, stability evaluations, and the careful observation for indications of inflammation (33, 34). In situations where autoimmune disorders are suspected to be involved in joint pathology, such as in the case of rheumatoid arthritis, blood tests are a crucial component of the diagnostic process (35). These blood tests are designed to identify specific markers that can provide valuable insights into the presence and severity of the autoimmune condition.

Furthermore, synovial fluid analysis represents a critical diagnostic tool, particularly when infections or inflammatory conditions are under consideration (36, 37). This procedure entails the aspiration of synovial fluid from the affected joint, enabling a thorough examination of its composition. The analysis of synovial fluid can yield essential information for accurate diagnosis and the formulation of appropriate treatment strategies. Overall, this multifaceted diagnostic approach is essential in the clinical assessment of joint health and the identification of underlying pathologies.

Diagnostic imaging modalities are essential tools in the assessment of joint injuries and related conditions, offering valuable insights into musculoskeletal health. Radiographs, which are widely employed in clinical practice, provide high-resolution two-dimensional images of bone structures. This imaging technique is instrumental in the identification of fractures, dislocations, and manifestations of joint wear, exemplified by osteoarthritis (38, 39). Magnetic resonance imaging (MRI), on the other hand, represents a sophisticated diagnostic approach that harnesses the power of magnetic fields and radio waves to generate detailed images of joint structures. Notably, MRI excels in capturing intricate details of soft tissues, including ligaments, tendons, and cartilage. Consequently, it plays a pivotal role in the evaluation of soft tissue injuries, with a particular emphasis on conditions like rotator cuff injuries, where the visualization of these structures is paramount (40, 41). Moreover, ultrasound is another valuable imaging technique used for the assessment of joints, primarily focusing on superficial structures such as tendons and bursae. Its real-time capabilities offer dynamic insights, making it a useful tool for guiding procedures like synovial fluid aspiration (37), thereby aiding in the diagnosis and management of joint-related issues (40). Continuous research in the field of medical imaging has led to significant improvements in the accuracy of joint injury diagnosis. More advanced imaging techniques, such as functional magnetic resonance imaging (fMRI), are being developed, capable of providing real-time information on joint function (42). Some other technologies can be listed, like computed tomography (CT), utilized in specific cases where a more detailed visualization of bone structures is required (43). It can be beneficial in preoperative planning. Bone scintigraphy technique is also employed to evaluate blood flow and metabolic activity in joints. It is valuable in diagnosing conditions like septic arthritis (44).

Arthroscopy is a surgical technique that combines diagnosis and treatment. An arthroscope (a thin tube with a camera) is inserted into the joint through a small incision to directly visualize joint structures. This is particularly useful in diagnosing soft tissue injuries and complex joint conditions (45). The management of articular injuries is a broad and diverse field, encompassing the treatment of acute injuries like sprains and fractures, as well as the management of chronic conditions such as osteoarthritis.

Collectively, these diagnostic imaging modalities serve as indispensable assets in the realm of musculoskeletal medicine, enabling clinicians to comprehensively evaluate joint health and pathology.

Among the most common conventional treatments, some of the following can be distinguished depending on the severity of the injury. A suitable treatment plays a crucial role in enhancing joint function and the quality of life for patients. The following describes the most common treatments used in the context of joint injuries:

- Pharmacotherapy: in the management of joint-related discomfort, a variety of therapeutic interventions are employed. Analgesics, such as acetaminophen and nonsteroidal anti-inflammatory drugs (NSAIDs), play a pivotal role in pain alleviation associated with joint injuries. NSAIDs, in addition to their analgesic properties, also possess anti-inflammatory effects, aiding in the reduction of inflammation within the affected joint (46, 47). In instances where severe inflammation is present, corticosteroid injections represent a targeted therapeutic option. These injections are administered directly into the affected joint, providing rapid relief from pain and inflammation (48). Corticosteroids exert their anti-inflammatory effects locally, making them particularly effective for managing acute or severe joint inflammation. Furthermore, in the context of osteoarthritis management, viscosupplementation emerges as a valuable intervention (49, 50). Viscosupplementing substances, such as hyaluronic acid, are administered via injection into the affected joint. This approach aims to enhance joint lubrication, thereby mitigating friction and improving overall joint function. These therapeutic strategies collectively contribute to the comprehensive management of joint-related conditions, offering relief from pain, inflammation, and functional impairment.
- Physical therapy and rehabilitation: physical therapy assumes a pivotal role in the recuperation process following joint injuries, with physical therapists collaborating closely with patients to enhance muscle strength, flexibility, and joint functionality (34). Rehabilitation plans often encompass tailored exercises, treatment modalities like heat or cold therapy, and mobilization techniques, all designed to promote optimal recovery and restore the injured joint to its full potential (51). In situations where surgical intervention becomes necessary, several options are available. In cases of acute injuries such as ligament or tendon ruptures, repair surgery is frequently performed to reestablish the structural integrity of the affected tissue. This surgical approach aims to facilitate the natural healing process and restore the joint to its pre-injury state.

- Surgery: in the realm of orthopedic surgery, several procedures are available to address joint-related issues, each tailored to specific clinical scenarios. Repair surgery represents a viable option for acute injuries characterized by ligament or tendon ruptures, with the primary objective being the restoration of the structural integrity of the damaged tissue . Arthroscopy, as previously mentioned, stands as a minimally invasive surgical technique utilized both for diagnostic and therapeutic purposes. Conducted through small incisions, this procedure employs a specialized instrument known as an arthroscope to visualize and address various joint issues, further minimizing trauma to surrounding tissues (45). On these cases, arthroscopy, serves as an invaluable tool for both diagnosis and treatment, facilitating the visualization and management of various joint pathologies while minimizing surgical trauma and recovery time (45). In cases characterized by severe osteoarthritis or irreversible joint damage, the consideration of joint replacement surgery becomes pertinent (52). Such an intervention has the potential to significantly enhance joint function, alleviate pain, and improve the overall quality of life for individuals affected by debilitating joint conditions. These surgical interventions exemplify the diverse approaches available to address joint-related challenges, offering tailored solutions to meet the unique needs of patients in varying clinical scenarios.
- Supportive therapies: the utilization of orthopaedic devices, including braces, knee braces, or supports, represents a valuable strategy in the effort to stabilize injured joints and mitigate the risk of further trauma. Such devices serve as supportive aids that enhance joint stability, reducing the likelihood of recurrent injuries (53, 54). Patient education assumes a fundamental role in the holistic management of joint injuries. Patients benefit from comprehensive guidance regarding joint protection measures, strategies for averting future injuries, and effective methods for managing chronic pain, fostering a proactive approach to their own well-being. Additionally, lifestyle modifications may be recommended as part of a comprehensive treatment plan (23, 24, 32, 53, 54). For instance, in cases of excess body weight, lifestyle adjustments, such as weight loss interventions, are often advised to alleviate the burden placed on the joints, thereby diminishing mechanical stress and improving joint health.

Nonetheless, despite notable advancements in joint injury management, significant challenges persist within the field. These encompass the imperative to develop more efficacious and minimally invasive therapeutic modalities, as well as addressing concerns regarding treatment accessibility and associated costs. Ongoing research activities in expanding fields like tissue engineering and gene therapy herald transformative changes in the landscape of joint injury management, offering promising prospects for enhanced therapeutic outcomes in the future. The treatment of joint injuries is in constant evolution due to technological innovations that provide more effective and personalized approaches to address these conditions. Below, we delve into the emerging technologies that are transforming the treatment of joint injuries.

Tissue engineering and regenerative therapies

Biological implants have emerged as a promising frontier in the field of joint injury management. Leveraging advancements in tissue engineering, these implants are meticulously designed to either replace or repair damaged joint tissues. Such implants may incorporate stem cells or tissues cultured in vitro, closely replicating the structure and functionality of natural joint tissue. This innovative approach holds substantial potential for regenerating and restoring compromised joint structures, offering renewed hope for individuals grappling with joint-related pathologies (55).

Cell therapies

Cell therapies, particularly stem cell therapy, constitute another area of active research in the search to stimulate the regeneration of injured joint tissues. These therapies harness the regenerative capabilities of cells to facilitate the repair of damaged cartilage and reduce inflammation within the affected joint. The application of cell-based approaches underscores the pursuit of novel and effective strategies for addressing joint-related challenges (56).

Moreover, the strategic use of growth factors, including transforming growth factor-beta (TGF-β) and platelet-derived growth factor (PDGF), plays a pivotal role in promoting tissue repair and collagen formation within the joints (57, 58). These growth factors are instrumental in orchestrating the intricate processes that underlie tissue healing, offering potential therapeutic avenues for enhancing joint health and functionality. In summary, ongoing research in these innovative areas of biological implants, cell therapies, and growth factor applications holds the promise of revolutionizing the landscape of joint injury management and ushering in new and effective treatment modalities.

Nanotechnology in drug delivery

Nanotechnology has led into a new era of precision in drug delivery, revolutionizing the treatment of joint injuries (59, 60). Through the creation of nanomaterials and nanoparticles, this cutting-edge technology offers the capability to load drugs with remarkable efficiency and release them in a controlled manner precisely at the site of the injury. This localized drug delivery approach not only minimizes undesirable side effects but also maximizes the effectiveness of treatment, ensuring that therapeutic agents target the affected joint tissue with unprecedented accuracy.

Furthermore, nanotechnology has also found application in the realm of gene therapy (61), representing a groundbreaking avenue for addressing joint-related conditions. With nanotechnology's assistance, the delivery of gene therapy becomes a feasible endeavour, opening doors to genetic modifications tailored to the specific needs of the joint. By introducing specific genes, this approach has the potential to stimulate tissue regeneration and facilitate the healing process within the injured joint, offering a novel and promising frontier in the field of joint injury management (62). In essence, nanotechnology is poised to reshape the landscape of joint injury treatment by enhancing drug delivery precision and unlocking the potential of gene therapy for tailored interventions.

3D printing technologies

The arrival of 3D printing technology in the biomedical field has ushered in a new era of customization in the development of joint implants and prostheses (63). This cutting-edge approach enables the creation of tailor-made devices that perfectly conform to the patient's unique anatomical structure, thereby enhancing functionality and reducing the risk of implant rejection (64). This level of personalization represents a significant advancement in joint injury management, offering improved outcomes and patient satisfaction (65).

Additionally, 3D printing has also found utility in the creation of anatomical models of joints (66). These models serve as invaluable tools for surgeons, enabling them to meticulously plan procedures with precision. Surgeons can practice complex surgeries on these models before embarking on the actual intervention, enhancing both the safety and effectiveness of surgical procedures. In tandem with 3D printing, ongoing research endeavours are focused on the development of advanced biomaterials designed to closely mimic the properties of natural joint tissues (67). These biomaterials hold the potential to promote cartilage regeneration, offering a promising avenue for the treatment of joint injuries. Furthermore, multimaterial 3D printing enables the combination of diverse materials within a single device, expanding the possibilities for implant design and functionality, providing customized solutions tailored to each patient's specific needs (68). These innovations are transforming regenerative medicine and surgery, opening new frontiers in healthcare.

The scientific research in these emerging technologies is continually evolving, with clinical and preclinical studies providing strong support for their efficacy and safety. Notably, joint tissue engineering research has demonstrated significant improvements in function and pain relief among patients with joint injuries, underscoring the transformative potential of these innovative approaches. However, it is important to acknowledge that these technologies also present challenges. Regulatory approval, accessibility to these advanced therapies, and the ability to produce them on a large scale are critical considerations that must be addressed to fully realize their potential in the treatment of joint injuries. Nevertheless, the ongoing exploration of these groundbreaking advancements holds promise for revolutionizing the landscape of joint injury management and improving the lives of those affected by such conditions.

Challenges and future directions

Despite substantial progress in the realm of joint injury treatment, persistent limitations necessitate continued efforts for improvement. Many existing treatments, such as joint replacements, exhibit limited long-term durability. Given the increasing elderly population, the imperative for solutions capable of withstanding decades of use becomes increasingly significant. Advanced therapies like stem cell therapy (56) and tissue engineering (55) may be financially burdensome and may not always be readily accessible to all patients. Addressing these cost and accessibility issues remains paramount. In certain instances, implants or treatments can provoke adverse immune responses within the body, compromising their efficacy and potentially leading to complications (64). Despite the

customization of 3D-printed implants, there remains a potential for implant rejection or surgical complications in some patients (64).

To surmount these challenges, ongoing research efforts in the domain of joint injuries are continuously evolving, exploring promising avenues for improvement as described before for advanced gene therapy, innovative biomimetic materials, enhanced nanotechnology among others. Continued dedication to research and innovation in these domains is essential to address the existing limitations in joint injury treatment and further enhance patient outcomes.

In summary, joint injuries pose a significant medical challenge affecting a broad population. Advances in tissue engineering, cell therapy, nanotechnology, and 3D printing are transforming how we approach these injuries. However, challenges remain in terms of durability, accessibility, and adverse immune responses. Continuous research is essential to overcome these challenges and provide more effective solutions to patients with joint injuries. As science and technology progress, we may see even more innovative and personalized treatments in the future, significantly improving the quality of life for those suffering from these conditions. Collaboration between scientists, physicians, and the industry is essential to translate these advances into accessible and effective clinical therapies. The field of joint injuries continues to evolve and offers a promising horizon for treatment development of innovative scaffolds for meniscus tissue engineering. This PhD thesis aims to contribute to the related portfolio of methods and solutions.

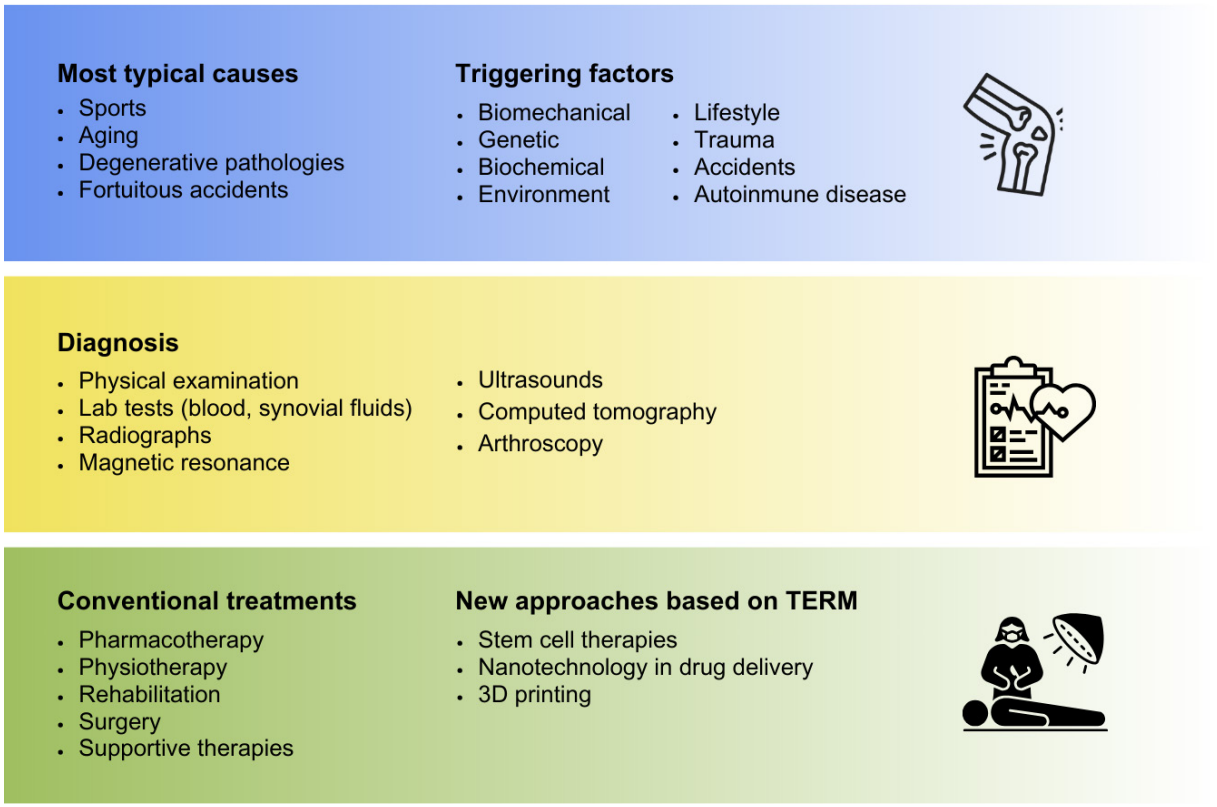


Figure 2: Current status of joint injuries: aetiology, trigger factors, diagnostic procedures, conventional treatments and new approaches based on TERM.

2.1.2. Tissue engineering and biofabrication for articular repair: current capabilities and challenges

Tissue engineering, regenerative medicine and biofabrication pursue the long-held dream of reconstructing or recreating damaged or lost tissues by providing cells with the adequate synthetic biomimetic nano-, micro- and macro-environments to let them deploy their healing potential. To this end, an increased number of combinations of bioinspired geometries, biomaterials, and manufacturing technologies, in many cases assisted by biomolecules, growth factors and drugs, have been researched and developed during the last decades. These efforts have led to literally thousands of artificial cell niches, extracellular matrices and scaffolds for tissue engineering, which act as enhanced implants or as advanced therapy medicinal products that support cells during healing and regeneration (69, 70).

In fact, since the dawn of tissue engineering, scaffolds have played a fundamental role as structural units that support cell attachment, proliferation, and differentiation into relevant tissues (71). Nowadays scaffold-based and scaffold-free strategies coexist and synergies among them have very recently emerged (72). However, tissue engineering is not yet straightforwardly reaching end users, and scaffolds are seldom developed considering diversity, equity and inclusion principles, which puts forward the need for further research linked to their engineering design and sustainable production. Some hurdles in these fields have been previously described (73).

Additive manufacturing technologies (AMTs) have emerged in the last decades, as highly transformative resources, enabling solid freeform fabrication, fostering freedom of design, promoting the personalization of devices and nurturing the world of design with reformulated guiding principles (74). In fact, AMTs have reshaped several industrial fields and, in connection with the "maker movement" or "maker culture" (75), led to the democratization of technology. The geometrical complexity achievable through AMTs, which can be employed for the integration of functionalities, helped to set the foundations of tissue engineering as a field (76, 77). To cite some examples, filament fused fabrication (FFF) or fused deposition modelling (FDM) of polymers and composites (76, 77, 78), selective laser sintering (SLS) and melting (SLM) of alloys (79, 80), laser stereolithography (SLA) and digital light processing (DLP) of photopolymers (81, 82, 83), lithography-based ceramic manufacturing (LCM) (84), or inkjet printing of hydrogels (as precursor of bioprinting) (85), are among the AMTs employed in the last couple of decades to create biomimetic tissue engineering scaffolds.

Arguably, AMTs may also contribute to the societal deployment of tissue engineering solutions, especially if the development principles of open-source (OS) medical devices (86, 87) are applied to the engineering design and sustainable production of scaffolds. Accordingly, open-source tissue engineering scaffolds should be developed making the design and production information available, including blueprints, CAD files, simulation outcomes, standardized maps of properties, G-codes, manufacturing documentation, testing results and usability guidelines. The application of "FAIR" data principles (88) along the development, for promoting the Findability, Accessibility, Interoperability and Reusability of open-source tissue engineering scaffolds would be coherent with their deployment as open-source sanitary

products (89). These approaches could synergize with a progressive development of open standards for tissue engineering, regenerative medicine and biofabrication, which might eventually lead to the harmonization of good practices and regulations for the benefit of patients.

Indeed, tissue engineering, regenerative medicine and biofabrication may benefit from progressively implementing and spreading the use of internationally accepted and applied standards, conceived to support the repeatability, replicability and efficient comparing of research results among researchers and practitioners worldwide (90, 91).

In contrast to most of the medical current solutions, 3D printing allows for the creation of implants tailored to the specific anatomy of each patient, which can improve the fit and functionality of the component. 3D printed implants can be designed to mimic the structure and composition of human anatomy more closely, which could improve their integration and function, by following a biomimetic approach. AMTs enable the use of a wide range of materials, including those that can be bioabsorbable or promote tissue growth. This opens the possibility for the implant to serve as a temporary scaffold, eventually being replaced by regenerated organic tissue. Moreover, the combination of 3D printing with advances in cellular biology and tissue engineering opens the possibility of creating implants that not only replace the damaged area but also promote the regeneration of natural tissue. The increased precision and customization of these implants could potentially reduce recovery time and improve functional outcomes for patients (92).

It is important to note that, although these technologies are highly promising, they are still in the early stages of development and clinical trial. Therefore, their availability and widespread applicability may be limited compared to more established treatment options like collagen implants and allografts.

Tissue engineering scaffolds for articular repair

In general terms, developed scaffolds for tissue engineering applications using 3D printing technologies should possess specific properties and characteristics to be effective and safe. Some of these properties and features include previously mentioned aspects such as the degree of implant customization, a biomimetic behaviour, or biocompatibility, among others. However, in general terms other very relevant properties should be considered when designing a tissue engineering scaffold (60, 69, 70):

- Controlled porosity: it is essential to have extensive control over the implant's porosity to allow the growth of natural tissue into the implant and its integration into the body. To understand the relevancy of this parameter, in the case of the knee joint this porosity also directly influences the distribution of synovial fluid, responsible for lubricating the joint.
- Mechanical performance: they must be strong enough to withstand the loads and stresses associated with the specific anatomical location and function of the tissue they are replacing. Articular regions are complex joints where bones, muscles and cartilage, among others, converge simultaneously. Each of these tissues has different

biomechanical properties, so that the whole structure is capable of functioning globally absorbing loads that converge from many directions, bearing compression, twists, or extensions.

- Controlled degradation: in some cases, it is beneficial for the implant to gradually degrade over time as the natural tissue regenerates, thus obtaining a biohybrid implant.
- Drug delivery technology: in some instances, tissue engineering scaffolds can incorporate controlled drug release systems to promote healing, reduce inflammation, or prevent infections.
- Printing accuracy: precision in 3D printing is crucial to ensure that the implant has the correct dimensions and shape. It is very important to be selectively correct when choosing one type of technology over another to meet our expectations. Tissue engineering often requires a level of precision at a microscopic, even nanometric scale. These facts highlight the importance of implementing design for additive manufacturing (DFAM) strategies, which allow the most relevant aspects associated with the manufacturing system to be considered from the beginning of the process, thus, permitting these technologies to be taken to the limit of their precision.
- Safety and regulation: like any healthcare product or biomedical device, they must comply with the applicable safety and medical regulation standards in the region where they are used.
- Economic viability: manufacturing efficiency and cost must be considered so that these implants are accessible to a wide group of patients.

These characteristics are essential for the success of tissue engineering implants manufactured using 3D printing systems, as they enable the implants to function effectively in the human body and promote the regeneration of damaged or lost tissues. However, not all of them need to be met simultaneously. For example, there may be a case where, for a medical application, it could be interesting to provide the implant with biodegradable properties, while for another pathology, it may be more interesting for the implant to remain in the patient's body providing greater structural integrity. It is important to understand that, depending on the addressed solution, it might have some characteristics prioritized over others, often having to reach a compromise between them. Throughout this work, different case studies illustrate the need to design an implant that requires a very high degree of porosity to allow cell growth and vascularization, but at the same time requires good mechanical behaviour. Generally, obtaining a more porous geometry negatively affects the mechanical properties of our model, so in this case, a compromise solution must be reached that allows both requirements to be satisfied as much as possible.

Complementary to tissue engineering, biofabrication emerges as a pioneering field at the intersection of biomedical engineering, biotechnology, and materials science, characterized by its innovative approach in creating functional tissues and organs using advanced manufacturing techniques. This domain has experienced exponential growth in recent years, driven by significant advances in the understanding of cellular and molecular biology, as well

as by the development of new manufacturing technologies, such as biological 3D printing and self-assembly of nanostructures (93). Biofabrication current state is highlighted by its ability to integrate living cells, biomaterials, and growth factors into three-dimensional constructs that replicate the structural and functional complexity of native biological tissues. This multidisciplinary approach has enabled revolutionary developments in regenerative medicine, offering new strategies for treating degenerative diseases, repairing damaged tissues, and replacing entire organs. Furthermore, bioprinting is opening new horizons in biomedical research, facilitating the creation of in vitro human disease models that are more representative of human physiology compared to traditional model systems (94, 95). This not only enhances understanding of the underlying mechanisms of various pathological conditions but also accelerates the development and evaluation of novel therapies.

This field focuses on the creation of complex biological structures and functional tissues, optimising processes for specific medical applications, including joint regeneration (96). The relationship between biofabrication and tissue engineering in the context of joint repair can be exemplified by the fabrication of scaffold structures for tissue regeneration. Biofabrication offers advanced methods for the production of scaffolds that mimic the architecture and chemical composition of native joint tissues. These scaffolds provide a platform for cell adhesion, growth guidance, and differentiation of cells towards specific phenotypes necessary for joint tissue regeneration. Some 3D printing technologies, such as SLA and FDM, have been used to fabricate scaffolds with precise geometries and controlled porosities. These scaffolds can be designed to replicate the structural complexity of joint tissues, facilitating tissue integration and regeneration. A notable example of biofabrication in joint repair is the use of 3D printing to create poly(lactic acid) (PLA) (97) or poly(lactic-co-glycolic acid) (PLGA) (98) scaffolds that have been successfully implanted in animal models to repair cartilage defects. These studies have shown that biofabricated scaffolds can support cartilage tissue regeneration and improve post-implantation joint function.

Furthermore, the materials and bio-inks used in these applications are essential components in the biofabrication of scaffolds for joint repair applications. The selection of suitable materials is critical to ensure biocompatibility, controlled degradation and adequate mechanical support for tissue regeneration. Recent research has focused on the development of bio-inks containing chondrogenic cells and materials that emulate the extracellular matrix of cartilage, such as hyaluronic acid (99). These advanced bio-inks are designed to promote cell differentiation and maturation of cartilage tissue within the biofabricated scaffold, with the aim of enhancing natural tissue regeneration to improve patient recovery and quality. A relevant field of research in this area is the development of 3D bioprinted scaffolds for articular cartilage regeneration (100). Using bio-inks composed of chondrogenic cells and materials that mimic the extracellular matrix of cartilage, it has been possible to fabricate structures that promote the regeneration of cartilage tissue in animal models.

Furthermore, in parallel to the development of materials and technologies, advanced design and modelling allows the creation of customised tissue structures and the optimisation of scaffolds for specific applications, such as the repair of joint injuries. The use of CAD and

computational simulations helps to design scaffolds that precisely match the anatomy of the joint injury, optimising tissue integration and post-implant functionality.

In the field of tissue engineering, significant challenges are faced ranging from the scalability of biofabrication processes to the inherent complexity of vascularisation of thicker and more complex tissues (101, 102). This issue takes on particular relevance in the context of joint injury repair, where nutritional efficiency and debris removal efficiency are critical factors determining the survival and functionality of regenerated tissue. The integration and long-term survival of biofabricated scaffolds represent a crucial challenge in this environment, where improved vascularisation within regenerated tissues is essential to support cell viability and ensure long-term tissue functionality.

Continued progress in the development of advanced materials and innovation in biofabrication techniques emerge as key elements to address these challenges. Innovation in bio-inks and the development of smart materials capable of responding to biological stimuli are crucial to facilitate the regeneration of complex tissues, including joint repair. These materials must not only promote tissue regeneration but also integrate seamlessly into the biological environment, adapting to the physiological dynamics of the implantation site (103).

Despite significant advances in biofabrication and tissue engineering, especially through the development of 3D bioprinted scaffolds for the repair of joint injuries, important challenges remain. Among these, the need to improve vascularisation and integration of regenerated tissues, as well as the scalability of biofabrication techniques, are of particular importance. Overcoming these obstacles is not trivial and equires a concerted research and development effort. This effort must be focused on continuous innovation of materials and biofabrication techniques, as well as on the development of advanced tissue engineering strategies. Only through a multidisciplinary approach combining biology, chemistry, materials engineering and advanced manufacturing technology it is possible to overcome current and future challenges in joint tissue regeneration, thus opening new horizons in regenerative medicine.

2.2. Design and additive manufacturing of biomimetic structures

2.2.1. Design approaches for complex bioinspired geometries

Design approaches for complex biomimetic geometries require an interdisciplinary convergence of biology, engineering, and technology, especially in the field of additive manufacturing or 3D printing (104, 105). This paradigm focuses on mimicking the structural and functional complexities of biological systems to develop materials and devices with superior or novel capabilities. Biomimetics, by drawing inspiration from nature's evolutionary solutions, offers a vast repertoire of optimised designs that engineers seek to replicate for specific applications, from regenerative medicine to soft robotics. Nature is replete with examples where complex structures perform specific functions with astonishing efficiency and versatility.

Probably the most obvious example of this, the human body, considered a masterpiece of biological evolution, harbours a multitude of structures and systems that have served as a model for the development of biomimetic technologies. A clear example of this is the hierarchical structure of bone, composed of a hydroxyapatite-reinforced collagen matrix that provides both strength and flexibility (106). This optimised design has naturally inspired the development of biomaterials for orthopaedic applications, where the replication of bone microarchitecture facilitates osseointegration and the formation of bone tissue around implants. Furthermore, from a biomechanical point of view, human bones exhibit a porous internal structure optimised to resist forces while minimising weight, a principle applied in the design of lightweight and strong composite materials for orthopaedics and the aerospace industry. The body's joints, which facilitate smooth and efficient movement between bones with minimal friction, have inspired the development of articulated robotic systems and advanced prostheses that mimic the natural dynamics of human movement (107). On the other hand, the skin's ability to heal and regenerate itself has motivated the creation of materials with self-healing capabilities, ranging from smart textiles to protective coatings. From the complexity of its bone architecture to the efficiency of the skin's self-healing mechanisms, each component has inspired innovations in medicine and biotechnology (108). Even the network of neurons and synapses in the human brain, responsible for processing information at astonishing speeds, has been a model for the development of artificial intelligence systems and neural networks that seek to replicate the efficiency of human cognitive processing (109). These biomimetic applications, inspired by the human body, not only reflect the elegance and efficiency of natural biological systems, but also open avenues towards innovative solutions that improve health, technology and the environment.

But it is not only the human organism that has been considered as the sole source of inspiration for the development of applications pursuing a biomimetic approach. On the contrary, the study of living organisms belonging to fauna and flora has led to the discovery of numerous structures and patterns that have been worthy of study.

Fauna, with its extraordinary adaptability and diversity, is an endless source of inspiration for the development of biomimetic structures and properties in science and engineering. Animals have evolved to develop highly specialised physical and behavioural characteristics that allow them to survive and thrive in their respective habitats. For example, shark skin, composed of dermal denticles that reduce water resistance, has inspired the design of high-performance swimming costumes and coatings for boats and aircraft that improve energy efficiency by reducing drag (110). The unique properties of spider web, which combines exceptional strength and flexibility, have prompted research into advanced materials with potential applications in bulletproof vests, sports equipment and medical devices such as sutures (111). In addition, the grasping mechanism of the gecko's legs, which allows these reptiles to climb smooth surfaces without using liquid or sticky adhesives, has led to the development of new adhesion systems that can be reversibly switched on and off, opening up new possibilities in robotics and industrial manufacturing (112). These examples demonstrate how the detailed study of adaptations in wildlife not only reveals fundamental principles of biology, but also offers innovative solutions to technical problems, driving breakthroughs that can transform entire industries and improve everyday life.

Special mention should be made here of entomology. Insect-inspired biomimetic structures represent an infinite source of applicable knowledge for technological and scientific breakthroughs, due to their amazing ability to solve complex problems through simple and efficient solutions. Insects, through millions of years of evolution, have developed unique characteristics adapted to their environments, which engineers and scientists seek to emulate. For example, the beetle exoskeleton, which combines lightness and strength, has inspired the development of advanced composite materials for applications in the aerospace and automotive industries, where weight efficiency is critical (113). Similarly, the wings of Morpho butterflies, whose microscopic structure creates vibrant colours without pigments by refracting light, have motivated the design of new materials for electronic device displays that require vivid colours and energy efficiency (114). In addition, the locomotion principles of insects such as cockroaches, which can navigate difficult terrain with speed and agility, are being applied to the design of search and rescue robots capable of moving in environments that are unstable or dangerous to humans (115). These examples demonstrate how mimicking the adaptive strategies of insects can lead to disruptive innovations in technology, offering sustainable and efficient solutions to contemporary challenges.

Beyond the realm surrounding animals or insects, interesting biomimetic applications can also be found in the study of flora. Flora, with its diversity and evolutionary complexity, offers a vast repertoire of biomimetic structures that have been a source of inspiration for numerous technological innovations. Plants have developed effective solutions to maximise light harvesting, manage water resources, and structure themselves to withstand varied environmental conditions, all of which have been meticulously studied and imitated in the world of engineering and design. An emblematic example is the structure of the dandelion seed, which has inspired the design of airborne drug delivery systems and micro-vehicles that mimic its ability to float efficiently in the air, taking advantage of minimal currents to maximise dispersion (116). Another clear example is that lotus leaf surfaces, known for their superhydrophobic ability to repel water and dirt, have led to the development of self-cleaning

coatings for applications ranging from textiles to solar panels, improving their efficiency and durability by reducing the need for maintenance (117). In addition, the efficiency of tree branching structures, optimised to support loads and distribute resources, has been applied in the structural design of buildings and in the planning of transport and distribution networks, seeking to maximise efficiency while minimising the use of materials (118). These examples underline how the study of flora can lead to significant advances in various areas, providing sustainable and efficient solutions that harmonise with the natural environment.

In addition to the above studies, which focus on the analysis and observation of living beings, biomimetics also encompasses research into other types of subjects, such as micro-organisms, ecosystems and natural phenomena.

Micro-organisms exhibit an astonishing range of biomimetic properties that have fascinated scientists and inspired innovations in various areas of science and technology. These tiny unicellular beings have evolved over millions of years to adapt to a variety of environments and challenges. Their self-repair capabilities, resistance to extreme conditions, and the efficiency with which they can carry out chemical and biological processes have been the subject of study for applications in industry, medicine and biotechnology (119, 120). From the creation of advanced materials inspired by the structure of microbial exoskeletons to the development of new medical treatments based on their defence systems, microorganisms offer a valuable data bank for biomimetic innovation. Their study continues to reveal new perspectives and opportunities to address modern challenges in a sustainable and effective way.

The study of ecosystems offers another rich source of biomimetic inspiration due to the remarkable capabilities and adaptations developed by their component species over millions of years of evolution. These ecosystems harbour a diversity of ingenious solutions to environmental and survival challenges. From the structure of inter-species interaction networks that inspires the design of logistics and communication systems, to the ability of plants to convert sunlight into energy through photosynthesis, which has led to advances in solar technology, ecosystems offer us a vast treasure trove of concepts and strategies that we can apply in a variety of fields (121, 122). By understanding and emulating these natural adaptations, we can develop innovative and sustainable solutions in agriculture, architecture, medicine, engineering and more, thus helping to address some of the most pressing problems facing society and the environment.

The study of natural phenomena provides an inexhaustible source of biomimetic inspiration, as these events unfold as a result of complex physical interactions and processes that often reveal ingenious solutions to challenges in science and technology (123). From analysing weather patterns to improve climate prediction and natural disaster management, to observing how living things adapt to changes in their environment to inspire innovation in robotics and advanced materials, natural phenomena offer a vast field of opportunities for the application of concepts and principles in diverse fields. By understanding and emulating the strategies that nature has perfected over eons, scientists and engineers can develop more efficient, sustainable and environmentally friendly technologies, thus helping to solve complex problems and advance science and innovation.

Translating these biological complexities into practical applications involves design strategies that address both form and function. Biomimetic design is based on a deep understanding of biological principles, followed by the abstraction and application of these principles in the solution of engineering problems. This process begins with the study and analysis of the biological structure of interest, identifying the key features that contribute to its exceptional performance. Additive manufacturing, with its ability to produce complex geometries that would be difficult or impossible to realise with traditional fabrication methods, plays a crucial role in this process. Advanced AMTs, such as stereolithography and selective laser sintering, enable the precise replication of structures with material gradients, controlled porosity, and complex internal geometries, all fundamental characteristics of biological systems (105).

The application of complex biomimetic geometries offers significant advantages in several areas. In tissue engineering, for example, 3D printed structures that mimic the extracellular matrix promote cell adhesion, proliferation, and differentiation, crucial for tissue regeneration. In aerodynamics, designs inspired by the wings of certain insects and birds may lead to the development of more efficient and manoeuvrable drones, capable of withstanding harsh environmental conditions (105, 124, 125).

Despite advances, exact replication of the complexity and functionality of biological systems remains a challenge. The interaction between synthetic materials and biological systems, the replication of the dynamics and adaptive response of biological structures, and the scale of fabrication are areas of intense research. In addition, the sustainability of materials used in additive manufacturing and the environmental impact of these processes are critical considerations for the future development of biomimetic technologies.

In conclusion, the design for additive manufacturing (DFAM) of complex biomimetic geometries is a promising field that benefits from an interdisciplinary approach. The ability to mimic nature's design strategies not only opens up new possibilities in materials and device development but also offers lessons in efficiency and sustainability. As technology advances, the integration of biological complexity into engineering solutions promises to revolutionise numerous industries and improve the quality of life.

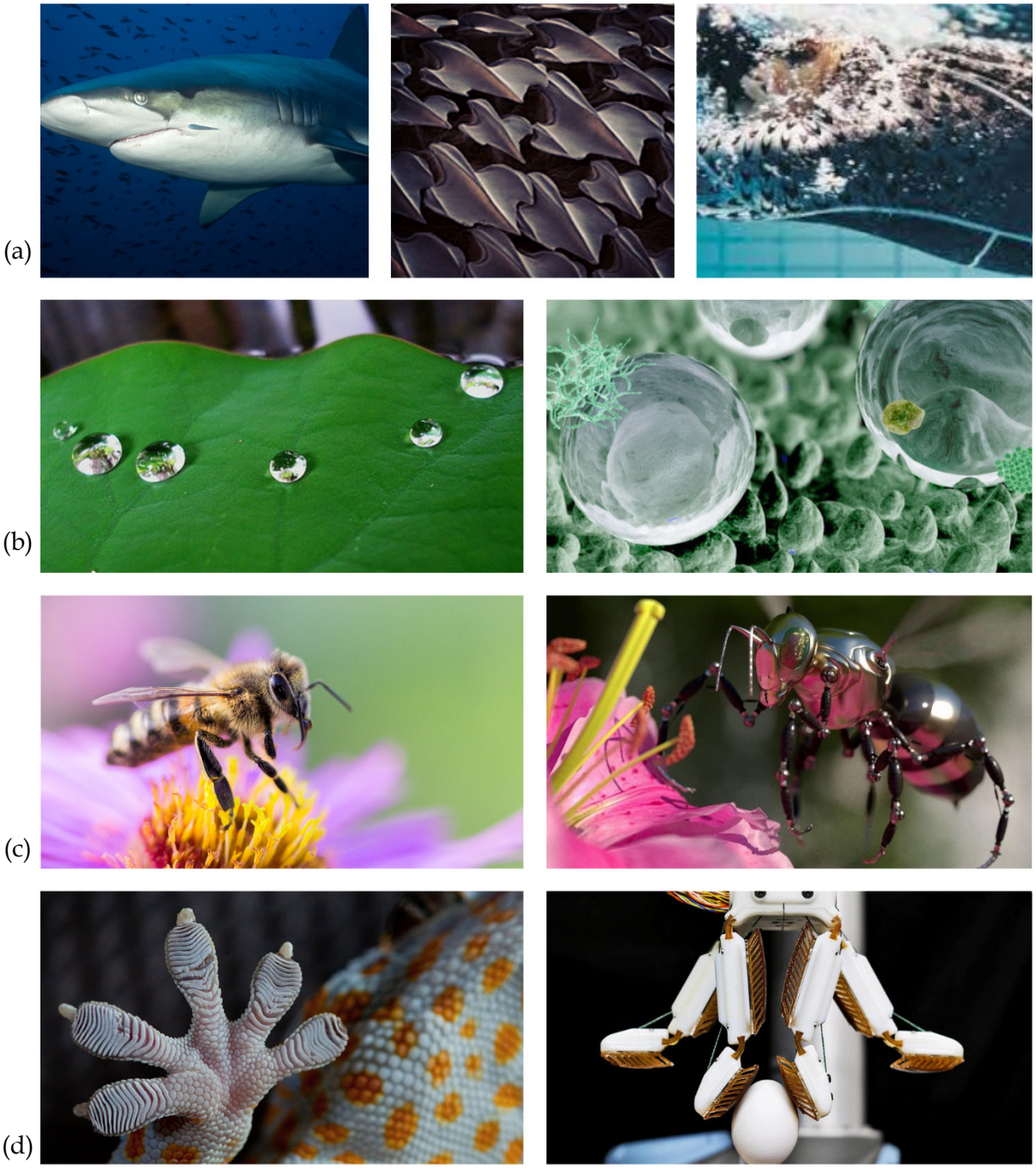


Figure 3: Examples of biomimetic properties of nature used as sources of inspiration in engineering design processes. (a) Shark skin denticles as an example for the development of high-performance swimming suits. (b) Hydrophobic properties of the lotus flower surface. (c) Development of a bee-based micro-robot to evaluate artificial pollination systems. (d) Texture of gecko limbs recreated for the generation of improved adhesive surfaces. Pictures acquired and adapted from "Nature Inspired Architectural Designs: Using Biomimicry as a Design Strategy" (126), "Biomimicry lessons from sharks" (127), "Bio-Inspired Robots and Structures toward Fostering the Modernization of Agriculture" (128), Geckskin website (129) and Stanford News website (130).

2.2.2. Additive manufacturing technologies in medicine

Additive manufacturing (AM) has significantly burst into the medical sphere in recent years, providing an unprecedented horizon of possibilities in tissue engineering and regenerative medicine, surgical planning or the fabrication of customised implants and prostheses among others (131, 132). This technological breakthrough, based on the layering of materials to create three-dimensional objects, has transformed the way we conceive and approach tissue and organ restoration and regeneration in the clinical context. Modern medicine has become increasingly dependent on additive manufacturing technologies to overcome the intricate challenges associated with creating biomimetic structures and customising medical devices. This phenomenon is due to the ability of 3D printing to accurately and rapidly produce biocompatible components that perfectly match patient needs. From the creation of three-dimensional scaffolds that mimic the microarchitecture of natural tissue to the bioprinting of living cells for the construction of functionally relevant tissues, additive manufacturing has proven to be an essential tool in the realisation of significant medical advances.

This thesis aims to investigate in depth the convergence of tissue engineering and additive manufacturing technology in the field of medicine, through the implementation of a biomimetic and personalised design approach. For this purpose, it is firstly introduced the fundamentals of additive manufacturing, its multiple categories and its specific biomedical applications. Ultimately, the challenges and limitations still facing additive manufacturing in the medical field are presented, as well as future directions and trends that may shape the next generation of innovations in medicine and healthcare. This overview aims to provide an introduction to how additive manufacturing technologies are revolutionising medicine, providing a solid context for the exploration of subsequent topics.

To understand its impact on the medical field, it is essential to explore its fundamentals and underlying principles. Additive manufacturing is based on an elementary principle: the construction of three-dimensional objects by adding material. This process differs fundamentally from traditional manufacturing techniques, which often involve the removal of material through cutting or machining processes. In 3D printing, material is deposited in a controlled manner, stacking layer upon layer, allowing the creation of highly customised and complex structures, reducing or even eliminating the need for subsequent post-machining stages on printed parts. Within the medical domain, various additive manufacturing technologies have been adopted to address specific needs. These include stereolithography (SLA) (133) or digital light processing (DLP) (83), where by using an ultraviolet (UV) laser or UV source to polymerised photosensitive liquid resins layer by layer, SLA enables exceptional precision in the creation of anatomical models and tissue scaffolds. In the realm of metal alloys, selective laser melting (SLM) enables the use of a high-energy laser to fuse material powders (79, 83). SLM technology is valuable in the manufacture of customised implants and orthopaedic components that require good mechanical behaviour. Specially related with tissue engineering applications, 3D Bioprinting involves the deposition of bio-inks composed of living cells rather than non-biological materials, enabling the creation of living tissues and organs (93). Generally, these inks are deposited by controlled deposition using a standardized nozzle dispenser. Moreover, some of these technologies have surpass the border of industry

and are truly spread among domestic users. Fused Filament Fabrication (FFF) or Fused Deposition Modelling (FDM) are widely used systems in modelling and prototyping. FFF has been also adapted to medicine for the production of surgical guides and biocompatible scaffolds (76). It is also a technology widely used for the generation of mockups, surgical benches or biomodels used to replicate body anatomies for academic purposes or as working models for training and surgical planning.

In the continuous advancement of additive manufacturing in medicine, new emerging technologies deserve special attention due to their revolutionary potential in tissue engineering and in the implementation of biomimetic applications. They are distinguished among others:

- Lithography Based on Ceramic Manufacturing (LCM): LCM technology is a recent innovation that combines the advantages of 3D printing and advanced ceramics (134, 135, 136). Using a process similar to SLA or DLP systems, but instead of resins, a ceramic paste known as slurry is used, that is polymerised layer by layer through exposure to ultraviolet light. This technique allows the fabrication of high-precision ceramic structures with a wide range of medical applications. In the medical field, LCM has shown promise in the production of customised ceramic implants, such as dental prostheses and artificial joints. Ceramics are known for their biocompatibility, corrosion resistance and durability, making them ideal for biomedical applications. In addition, the ability to manufacture patient-specific ceramic implants can significantly improve quality of life and post-operative recovery.
- 3D nanoprinting: nanoprinting is a technology that enables the creation of nanoscale structures through the precise manipulation of materials in extremely small dimensions. While this technique has been used in a variety of disciplines, its application in medicine has begun to gain attraction in the fabrication of biomimetic devices and drug delivery systems. In the medical field, 3D printing technologies like the Two-Photon Polymerization (2PP) system has been applied to the fabrication of nanometric scaffolds for tissue engineering and biomimetic environments (137, 138). The high degree of precision in fabrication makes this technology a great bet for textured scaffolds, allowing the application or recreation of patterns mimicking natural surfaces in medical solutions. These scaffolds offer a high specific surface area that promotes cell adhesion and growth, which is essential for the regeneration of complex tissues. In addition, 3D nanoprinting is used in the creation of nanoparticles for controlled drug delivery, which improves therapeutic efficacy and reduces side effects.
- 3D printing of biohydrogels: biohydrogel-based 3D printing focuses on the use of biocompatible hydrogel materials for the creation of three-dimensional structures. Hydrogels are polymers with high water holding capacity, making them ideal for replicating the aqueous environment of biological tissues (139, 140). This technology has several relevant medical and biomimetic applications:
    - Bioprinting of living tissues: biohydrogels allow the printing of living cells directly into the material, which facilitates the creation of functional three-

dimensional tissues. This is essential for tissue engineering and the creation of artificial organs (141).

- Biocompatible scaffolds: hydrogels can serve as three-dimensional scaffolds for cell growth and tissue regeneration. These scaffolds provide a favourable environment for cells and can be customised to a patient's needs (142).
- Controlled drug delivery: hydrogels can also incorporate drugs and proteins, allowing for the controlled release of therapeutic substances. This is beneficial in applications such as localised drug delivery and sustained release therapy (143).

Today, biomedical additive manufacturing relies on a selection of materials widely used for the creation of customised medical devices and artificial tissues. These materials, which include biodegradable polymers, hydrogels, advanced ceramics and metal alloys, are noted for their biocompatibility, ability to host living cells, corrosion resistance and durability. These essential properties enable the manufacture of implants, prostheses, tissue regeneration scaffolds and anatomical models with precision and safety, laying the foundation for significant advances in personalised medical care. Many types of polymers, biogels, ceramics and metals can be used when addressing tissue engineering applications. Biodegradable polymers, such as polylactic acid (PLA) and polyglycolide (PGA) (98, 106, 144), are widely used in biomedical additive manufacturing. They are safe, biocompatible and degrade naturally in the body over time. These materials are used in the printing of anatomical models, temporary medical devices and scaffolds for tissue regeneration. Hydrogels are cross-linked polymers with a high water-holding capacity. These materials are ideal for 3D bioprinting, as they can host living cells and provide a three-dimensional tissue-like environment. Hydrogels such as gelatine, alginate and collagen are used in the creation of artificial tissues, organs and scaffolds (99, 143, 145). Also advanced ceramics, such as hydroxyapatite and tricalcium phosphate, are used in the manufacture of dental and orthopaedic implants. These materials are known for their biocompatibility and ability to integrate with bone tissue (146, 147). In permanent implant applications, metal alloys such as titanium and stainless steel are used (64, 79). These materials offer durability, corrosion resistance and the ability to withstand mechanical loads. They are printed using techniques such SLS and FFF.

In addition to this collection, continuous medical and technological advances make it possible to obtain new materials or others developed by combining several of them in order to cover these types of applications. Some of these are described below:

- Customised biomaterials: advances in additive manufacturing are enabling the creation of customised biomaterials for each patient. This could include custom-made orthopaedic implants or specific medical devices to treat unique conditions.
- Bioactive materials: researchers are developing bioactive materials that are not only biocompatible but also interact positively with the human body. These materials could stimulate cell growth, promote angiogenesis and improve implant integration (148).

- Functional hydrogels: functional hydrogels that can release drugs in a controlled manner are used for localised drug delivery applications. This is especially relevant in the treatment of diseases such as cancer and infections (143).
- Nanocomposite materials: the incorporation of nanoparticles into 3D printed materials is enabling improved properties, such as increased strength and drug release capacity. These materials are being investigated in the creation of advanced prostheses and drug delivery systems (60).

In short, materials used in biomedical additive manufacturing are constantly evolving to adapt to clinical and tissue engineering needs. Advances in emerging materials are opening up new possibilities for personalising medical treatments and improving patients' quality of life. The combination of these types of technology with the variety of biomaterials developed positions 3D printing as a very promising technology to address the following applications:

Manufacturing of customised orthopaedic prostheses and implants

Additive manufacturing has also played a key role in the creation of customised implants and orthopaedic prostheses, revolutionising orthopaedic healthcare. Through the use of 3D printing technologies, such as FFF or SLA, customised orthopaedic implants can be manufactured that are perfectly tailored to each patient's unique anatomy. For example, in the case of joint implants, such as hips or knees, high-strength metal alloys such as titanium are used. These implants not only improve mobility and functionality, but also reduce the risk of immunological rejection, as they fit the patient perfectly. Similarly, prosthetic limbs, such as arms or legs, can be precisely designed and manufactured using 3D printing technologies, providing greater comfort and effective restoration of function to amputee patients. These applications exemplify how additive manufacturing is transforming orthopaedic healthcare by providing highly customised and effective solutions that improve patients' quality of life.

Bioprinting dressings for skin tissue regeneration and wound healing

3D bioprinting has emerged as a leading technique for skin regeneration and the treatment of severe burns, highlighting its ability to address these conditions in a highly effective manner. Through the printing of bio-inks composed of dermal cells and extracellular matrix components, the creation of artificial skin that closely mimics both the structure and functions of human skin is achieved. This innovative application offers a highly personalised solution for burn victims, enabling the restoration of the skin barrier in a precise manner and significantly accelerating the healing process. 3D bioprinting thus becomes a key tool in healthcare, demonstrating its potential in improving the quality of life of patients who have suffered severe burns by providing personalised and highly effective treatments.

Tissue engineering and joint repair

Additive manufacturing plays a key role in tissue engineering to address joint injuries and restore functionality to damaged joints. These implants are designed specifically for each patient using MRI and CT, and then 3D printed using technologies such as FDM or SLA and biocompatible materials such as PLA or polyethylene glycol (PEG). The key advantage of this application lies in the ability to provide highly customised solutions that are tailored to each

patient's unique anatomy, accelerating recovery and significantly improving quality of life by restoring function to damaged joints. This technique exemplifies how additive manufacturing is transforming orthopaedic healthcare by addressing joint injuries precisely and effectively.

Modelling functional human organs

Additive manufacturing has significantly advanced the modelling of functional human organs in vitro, representing a significant achievement in regenerative medicine and biomedical research. Using medical imaging data, such as MRI or CT scans, exact replicas of human organs can be created, reproducing their microscopic structures and functions. 3D printing technologies such as bioprinting and stereolithography are used to achieve exceptional precision in the creation of these three-dimensional models. These functional artificial organs are used as valuable tools to research diseases, evaluate treatments and practice surgical procedures before they are performed on real patients. For example, 3D hearts models have been developed that replicate blood circulation and cardiac function, allowing cardiac therapies and medical devices to be tested more accurately. Similarly, 3D kidney models are used to study kidney diseases and evaluate the effectiveness of drugs for treatment. These advances in creating functional human organs in the laboratory are driving biomedical research and the search for more effective therapies for a variety of diseases. Additive manufacturing has become an essential tool for advancing the understanding of human physiology and improving healthcare in general.

Future directions and trends in medical additive manufacturing include significant advances in the development of biomimetic materials that closely mimic the properties and functions of natural tissues, which allows for greater interaction with the body and the promotion of regeneration. In addition, the integration of imaging and diagnostic technologies, such as CT and MRI, with 3D printing technologies should be improved, leading to new working methodologies to improve the planning and customisation of medical procedures.

In conclusion, 3D printing of personalised medicines has the potential to optimise drug therapy, tailoring medicines and treatments to the individual needs of patients, reducing side effects and improving the quality of post-operative care and rehabilitation enabling new advances in minimally invasive surgery, all of it generating a positive impact on the quality of life of patients. Finally, the combination of 3D printing with telemedicine and telesurgery opens new possibilities for remote medical care, especially in remote areas or in emergency situations. These directions and trends represent an exciting future for additive manufacturing in medicine, with the potential to transform healthcare and improve patients' quality of life.

Nevertheless, it is mentioned that the successful implementation of additive manufacturing in medicine faces significant challenges and limitations. Firstly, biocompatibility and safety are key concerns, as it is essential to ensure that the materials used and the printed products are safe for use in the human body and do not trigger adverse reactions. In addition, regulation and medical approval are significant hurdles, as printed medical devices and products must comply with regulations from agencies such as the European Medicines Agency (EMA) or the Food and Drug Administration (FDA) among others. In this aspect, the existence of new standards makes it necessary to include methods or good practices when generating personalized medical devices. Establishing quality and safety standards is essential for proper

implementation in clinical settings. The costs associated with the technology can be prohibitive, including investment in 3D printing equipment and staff training, which poses challenges in terms of accessibility and affordability. The scale of production and manufacturing time must also be addressed, as 3D printing can be a slow process compared to traditional mass production methods.

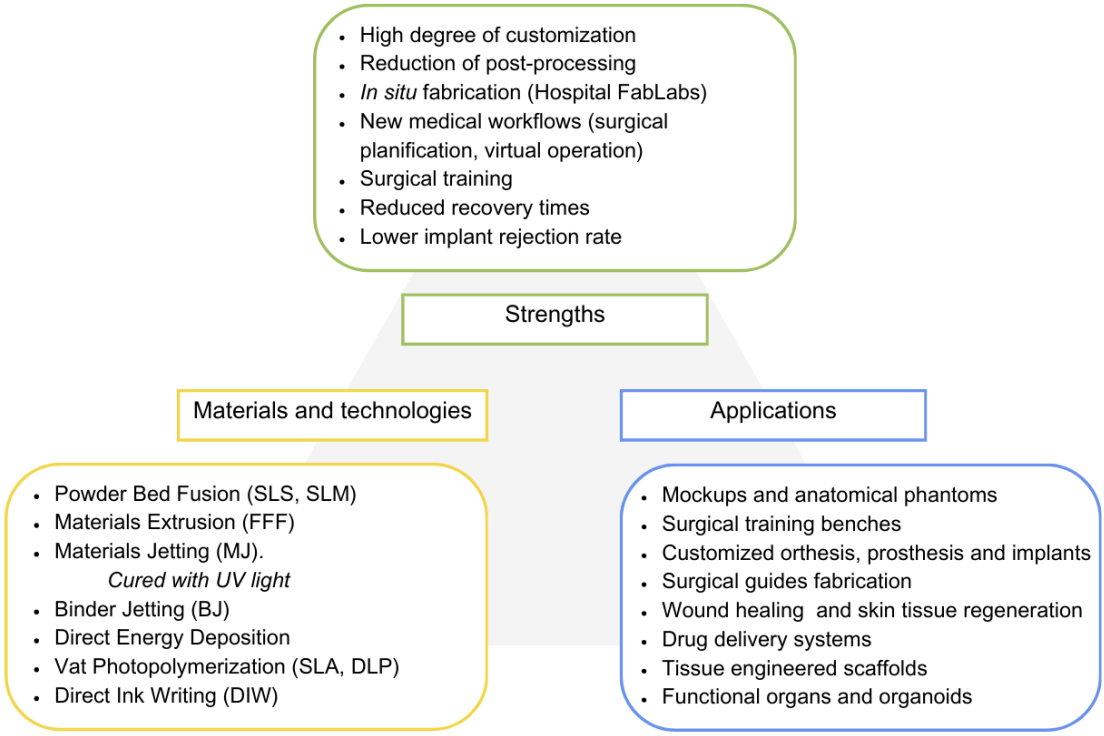


Figure 4: Diagram illustrating the situation of AMTs in today's medicine: strengths, technologies and materials classification and medical applications. AMTs mentioned according to ISO/ASTM 52900:2021 standard (149).

3. Materials and methods

3.1. Design and simulation methods and resources

3.1.1. CAD modelling software

For the correct development of this doctoral research work focused on tissue engineering and the application of 3D printing technologies, the use of computer-aided design (CAD) tools is a fundamental pillar. CAD software enables the conceptualisation, design, and detailed modification of complex three-dimensional structures that will subsequently be materialised by 3D printing. This design capability is especially critical in tissue engineering, where geometric accuracy and customisation are indispensable to replicate the complexity and functionality of biological tissue (150, 151). The use of CAD tools facilitates rapid design iteration, allowing researchers and practitioners to test different configurations and geometries to optimise the mechanical, biological, and biocompatibility properties of artificial tissues. In addition, CAD software is essential for pre-operative planning in clinical applications, enabling the creation of customised implants and brackets that are perfectly tailored to individual patient needs. Notable examples of CAD software used in the field of medicine and 3D printing include AutoCAD, Fusion 360 and Tinkercad from Autodesk company (152) or some others as SolidWorks or Catia, developed by Dassault Systèmes (153). The choice of appropriate software depends on the specific needs of the project, including design complexity, analysis and simulation requirements, and collaboration between teams. In the context of tissue engineering, these CAD tools are not only fundamental to the design and fabrication of biomedical structures, but are also crucial to the advancement of research and clinical applications in this rapidly evolving field.

Moreover, in the field of tissue engineering, the use of computer-aided design (CAD) software in combination with reverse engineering methodologies opens up a range of possibilities for customisation and optimisation of biomedical solutions through 3D printing. Reverse engineering, in this context, involves the process of breaking down an existing biological system or tissue into its fundamental components to understand its structure, function and properties (154, 155). This information is then used to design digital models that can be materialised through 3D printing. The relationship between CAD software, reverse engineering, and 3D printing in tissue engineering manifests itself as follows:

- Real anatomy digitalization: reverse engineering begins with the capture of the geometry and physical characteristics of biological tissues using techniques such as computed tomography (CT) or magnetic resonance imaging (MRI). This data is converted into 3D digital models that serve as the basis for design and manufacturing.

- Modelling and simulation with CAD software: once the anatomy has been digitalized, CAD software allows these digital models to be manipulated, modified and optimised. In the field of biomedical applications, researchers and designers can adjust internal structure, porosity, and surface characteristics to meet specific biomechanical requirements, facilitate integration with existing biological tissue, or promote vascularisation and cell growth.
- Patient-scale customisation: the combination of reverse engineering tools and CAD resources enables the creation of fully customised solutions. Implants, prosthesis or tissue scaffolds can be designed to perfectly match a patient's unique anatomy, improving implant integration and functionality.
- Rapid prototyping and additive manufacturing: with optimised models, 3D printing facilitates the production of rapid prototypes or final fabrication of tissue engineering components. This technology enables the creation of complex structures with a precision and flexibility that would be difficult, if not impossible, to achieve with traditional manufacturing methods.
- Functional and biological evaluation: prior to clinical implementation, products developed through this process can be evaluated in terms of their mechanical properties, biocompatibility, and ability to promote tissue regeneration. This is crucial to ensure that implants or scaffolds will perform as expected once implanted.

This integrated approach not only maximises the potential of 3D printing in creating customised biomedical solutions but also significantly improves the chances of success in tissue engineering applications. By replicating the inherent complexity of biological systems, reverse engineering and CAD software contribute to innovation in the design and manufacture of artificial tissues, organs, and medical devices, marking a breakthrough in the field of regenerative medicine and personalised treatments.

For the completion of this research, NX 2206 (Siemens PLM Solutions) software is chosen as a support tool for the design of the nominal geometries, from which the customised tissue scaffolds are obtained (156). NX 2206 is an advanced computer-aided design (CAD), computer-aided engineering (CAE) and computer-aided manufacturing (CAM) software solution that has the potential to stand out in the field of tissue engineering and custom medical device manufacturing, in part due to its robust reverse engineering module. This module facilitates the creation of accurate digital models from physical data, a crucial capability for the design of implants and medical devices tailored to specific patient needs. In addition, NX also provides a multi-physical simulation environment for biomechanical considerations.

Moreover, in the framework of an international interdisciplinary European project, such as the INKplant project, NX 2206 is a suitable choice as it allows the integration and processing of 3D scan data, obtained through various imaging techniques such as computed tomography (CT) or magnetic resonance imaging (MRI). This is essential for capturing the complex geometry of the patient's tissues or bones, allowing engineers to reconstruct accurate digital models for analysis and modification. In addition, the software offers hybrid modelling capabilities that

combine surfaces and solids, which is especially useful in medical device design. This allows for a seamless transition between modifying imported geometries and creating new ones based on specific design requirements, thus optimising the functionality and biocompatibility of implants. NX 2206 also integrates advanced simulation tools, which, as discussed in subsequent sections, allow the mechanical properties and behaviour under physiological loads of implant designs to be evaluated. This ensures that the devices not only fit anatomically but also meet the biomechanical criteria necessary for successful operation, the results of which can serve as input for topological optimisations based on mechanical behaviour.

Another highlight of Siemens NX in the context of tissue engineering and 3D printing is its ability to import and export a wide variety of file formats. This includes industry standard formats such as step, iges, stl, obj, ply. This versatility is essential for interoperability between consortium members, facilitating collaboration between multidisciplinary teams, enabling the efficient exchange of models between different platforms and specialties, from surgical planning to device design and fabrication. NX 2206 allows designers to work with data from multiple sources and technologies, easily adapting to changing project needs and technological innovations in the field of personalised medicine. It is also understood that the ability to export models in formats optimised for 3D printing (such as stl) is crucial for the manufacture of implants and medical devices. This ensures that models can be directly used by a wide range of 3D printers, spanning different additive manufacturing technologies and materials.

In conclusion, the choice of NX 2206 as a software tool to support the achievement of the objectives targeted in this work is based on the PhD candidate's personal experience in combination with the integrated and flexible environment for the design, analysis, and manufacture of customised implants and medical devices. Its reverse engineering module, together with its capabilities for importing and exporting various formats, positions it as an essential tool in the design and optimisation process of the tissue engineering scaffolds analysed throughout this work, and facilitates the subsequent application of 3D printing technologies to obtain customised solutions.

3.1.2. Finite-element modelling software and topology optimisation resources

Finite-element modelling

Central to this work is the inclusion of finite-element analysis (FEA) or finite-element modelling (FEM) tools to ensure the mechanical and biological viability of tissue scaffolds prior to fabrication and clinical evaluation. This computational approach allows the behaviour of scaffolds under real physiological loads to be simulated and analysed, optimising their design to achieve the desired balance between strength, flexibility, and promotion of cell growth. In terms of mechanical behaviour, FEM allows prediction of how the scaffold will respond to mechanical forces, including stresses, strains, compressions, and torsions encountered in the physiological environment (157, 158). This is crucial to ensure that the structure will maintain its structural integrity and provide the necessary support during the

tissue healing and regeneration process. In addition, finite-element analysis can help optimise implant geometry, including porosity and pore distribution, to balance mechanical strength with the promotion of vascularisation and cellular infiltration. Adequate porosity is essential to facilitate nutrient transport and waste removal, as well as for the integration of the scaffold with the surrounding tissue. The combination of all these capabilities leads to functional scaffolds through custom design. The solutions obtained are adapted to the specific mechanical needs of different anatomical sites and tissue types, taking into account individual variations in patient biomechanics. In addition, the use of fluid simulations helps to evaluate the *in vitro* behaviour of scaffold geometries. They are a very valuable tool when selecting flow rates and pressures for perfusion and allow the analysis of shear stress stimuli on cells as a consequence of the weight of the fluid through the structure, thus allowing the selection of the most optimal arrangements depending on the cell type (157, 158).

Moreover, through advanced modelling techniques, FEM can incorporate aspects of the biological interaction between the scaffold and the surrounding tissue, such as the growth of new tissue and the degradation of the scaffold material. This allows assessment of how these interactions affect the mechanical stability and functionality of the scaffold over time, which is critical when developing tissue engineering applications. FEM can be used to simulate the mechanical environment that cells within the scaffold experience, including the mechanical stimulation that is known to influence cell differentiation and tissue growth. This is crucial for the design of scaffolds that are not only mechanically compatible, but also actively promote functional tissue formation. The simultaneous realisation of this set of mechanobiological requirements leads to the design and achievement of functional solutions capable of fulfilling the tasks of natural tissue.

In the present study, finite-element testing techniques are employed in chapter 4, where a library of tissue engineering scaffolds for which mechanobiological properties, collected in a collection of Ashby maps, have been evaluated. Also, in chapter 4, where an innovative methodology for the design and optimisation of a customized joint implant is presented, for which it is necessary to generate a mechanical simulatuon to evaluate the behaviour of the implant. Furthermore, the combination of FEM and AMTs represents a powerful synergy in tissue engineering. FEM can lead to optimal scaffold design, while 3D printing enables the precise fabrication of these complex structures. This integration ensures that scaffolds not only meet predefined mechanical and biological requirements but can also be produced efficiently and with high fidelity and precision to the original design. Again, Siemens NX 2206 is chosen as the finite-element analysis and simulation tool for this tissue engineering research. The PhD candidate's familiarity with the software allows the advanced capabilities of the programme to be fully exploited from the start of the project. In addition, as mentioned above, NX 2206 integrates a powerful reverse engineering module, which facilitates the creation of accurate digital models from physical data, a critical step in the design of customised implants and medical devices. The combination of the reverse engineering module with the inclusion of a finite-element module, specifically NASTRAN, reinforces NX 2206's position as a complete, multi-disciplinary tool, enabling a variety of tasks to be accomplished in a single environment. NASTRAN is renowned for its accuracy and robustness in simulating complex mechanical behaviour, which is essential for predicting how tissue scaffolds respond under real

physiological conditions. The ability to perform detailed mechanical and thermal analysis within the same software environment used for design and reverse engineering not only optimises workflow but also ensures high consistency and accuracy of results.

In addition, the integration of these functionalities into a single software package reduces the need to transfer data between different programs, minimising the risk of conversion errors and enabling a more integrated approach to the design, analysis, and manufacturing of medical devices. This convergence of capabilities positions Siemens NX 2206 as an outstanding choice for addressing the multidisciplinary challenges inherent in the tissue engineering applications studied in this work, providing a unified platform that supports both innovation and efficiency in the development of advanced medical solutions.

Topology optimisation tool

Regarding topology optimisation and lattice design implementation, for the obtention of the appropriate porosity in the evaluated scaffolds an emerging software tool, nTopology (nTopology, New York, USA), is be used (159). Compared to Siemens NX 2206, although the second is a powerful and versatile tool for engineering design and analysis, in the author's opinion nTopology offers specific advantages in the implementation of lattice structures. While NX 2206 provides an integrated environment for CAD design, reverse engineering and finite-element analysis in the frame of this work, nTopology stands out for its specialised focus on lattice design and topological optimisation. Its interface and tools are specifically designed to facilitate the creation of complex porous structures, allowing for greater customisation and adaptability in the design of tissue scaffolds, reducing time and simplifying the process. This makes it particularly suitable for tissue engineering applications, where design specificity at the microstructural level is crucial for successful implantation and tissue integration. The incorporation of emerging design and optimisation software, such as nTopology, represents a significant advance in the field of tissue engineering, opening new avenues for the creation and optimisation of tissue scaffolds. nTopology is distinguished by its remarkable capabilities to address conformal lattice design applications, which are fundamental in the generation of scaffolds that promote cell growth, vascularisation and tissue integration. Through its innovative approach, nTopology enables advanced manipulation of cell maps, unit cell types and thickness variations, facilitating the creation of geometries that closely mimic the microarchitecture of biological tissues. One of nTopology's key strengths lies in its ability to optimise these geometries more efficiently and with a greater degree of control compared to more conventional software environments. The platform offers specialised tools for fine-tuning the porosity, pore distribution, and mechanical properties of scaffolds, ensuring they meet specific biomechanical requirements while facilitating the optimal environment for cell growth and differentiation. This optimisation capability is critical to designing scaffolds that not only support mechanical loads but also promote desired tissue formation and function (160). The combination of these capabilities makes nTopology an helpful platform for researchers and designers in the field of tissue engineering, providing the tools necessary to explore new frontiers in scaffold design and overcome some of the limitations present in more traditional software.

3.1.3. Slicing software

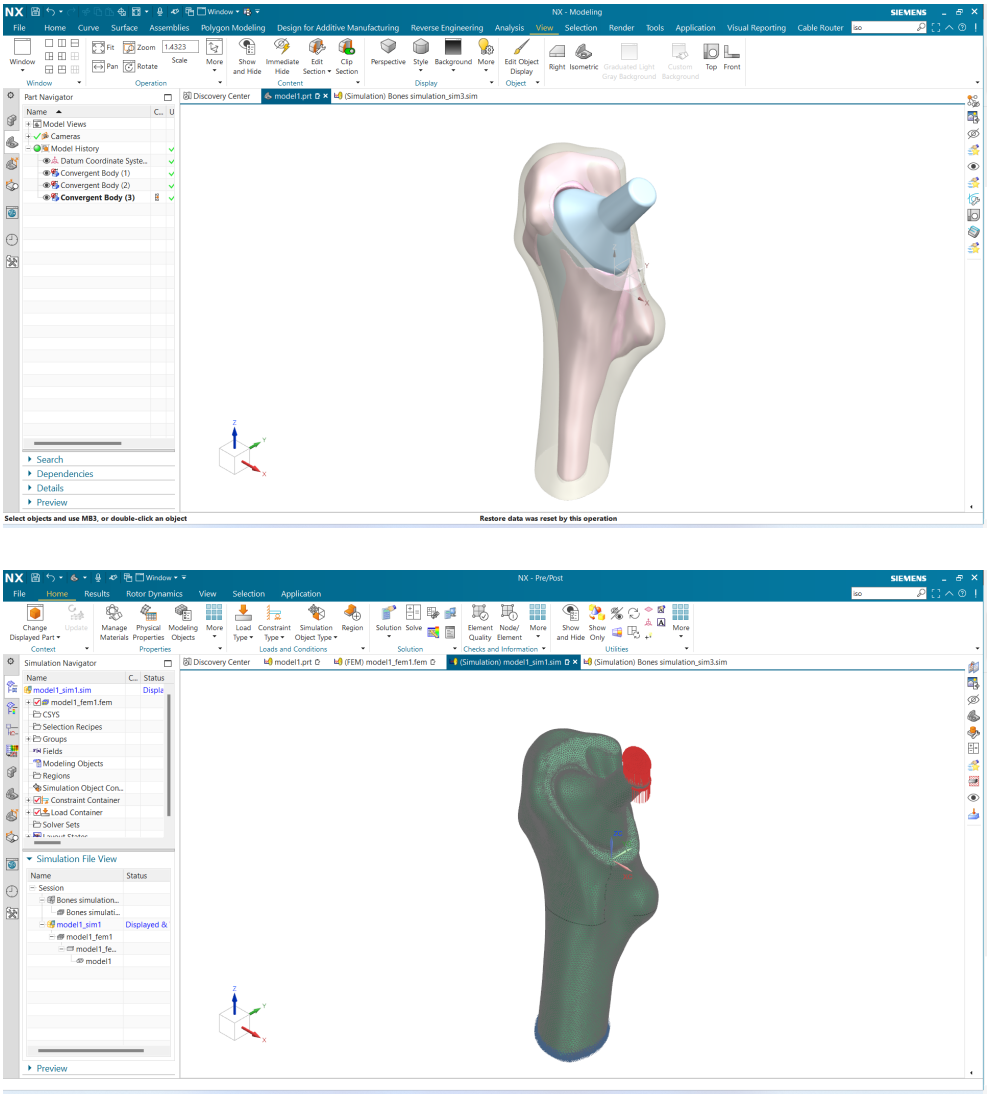
Slicer software is an essential tool in the 3D printing process, acting as an intermediary between the digital design of an object and its physical materialisation through a 3D printer. This type of software takes a three-dimensional model, usually in stl (Stereolithography), obj (Object) or ply (Polygon) format, and divides it (or "slice") into thin horizontal layers that the printer can build sequentially, generating a G-code file for FFF (Fused Filament Fabrication) printers or a series of mask images for photopolymerisation-based technologies such as DLP (Digital Light Processing) or LCD (Liquid Crystal Display).

Slicers for FFF and DLP-LCD differ significantly depending on the printing technologies for which they are designed. On the one hand, FFF slicers include software such as Ultimaker Cura, Prusa Slicer or Bambu Studio. These tools are mainly optimised for FFF printing, where the material is deposited layer by layer by means of a hot extruder head. Among many others, some of the most relevant adjustable parameters in these slicers include layer height, filling, print speed, extrusion temperature and shrinkage, which are critical in determining the quality of the printed object, mechanical strength and dimensional accuracy. The generation of support structures is also a crucial aspect, especially for designs with overhangs or complex geometries.

On the other hand, tools such as Chitubox Lychee or Anycubic Photon Workshop are used to prepare models for printing in DLP or LCD technologies, where light projects images of each layer onto a photosensitive resin, curing it selectively to form the object. Critical parameters here include light exposure per layer, base cure time and layer height, which directly influence detail definition, dimensional accuracy and inter-layer adhesion. The creation of supports also plays an important role, although its focus is on minimising deformation and ensuring proper adhesion of parts to the build platform.

The ability to convert 3D models to different extensions and adjust specific parameters for each printing technology is vital to the flexibility and efficiency of the additive manufacturing process. This not only allows designs to be printable on a wide variety of 3D printers, but also enables the customisation of objects to meet specific performance, aesthetic and functional requirements. In addition, optimising print parameters using software slicers can mean reduced printing times and material usage, as well as improved end-product quality, which are critical for professional, industrial and medical applications. In conclusion, software slicers represent a key part of the 3D printing ecosystem, enabling the smooth transition from digital models to physical objects by properly preparing and adjusting parameters for each specific printing technology. Choosing the right slicer, as well as mastering its capabilities and settings, is essential to maximise the efficiency of additive manufacturing and realise its full innovative potential.

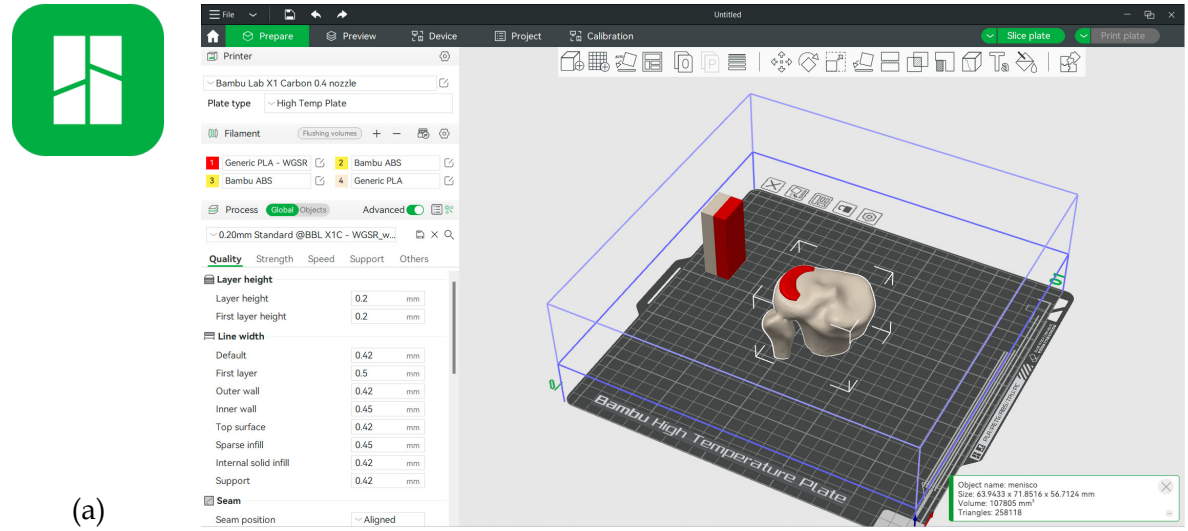
In this work, Ultimaker Cura (161) and Bambu studio (162) slicers have been used to generate the G-code files for FFF printers, which, among other important information, contain the trajectories that the machine takes to deposit the material in a controlled manner and the speeds used. For the generation of the masks necessary to print using LCD technology, the open software Chitubox (163) is used.



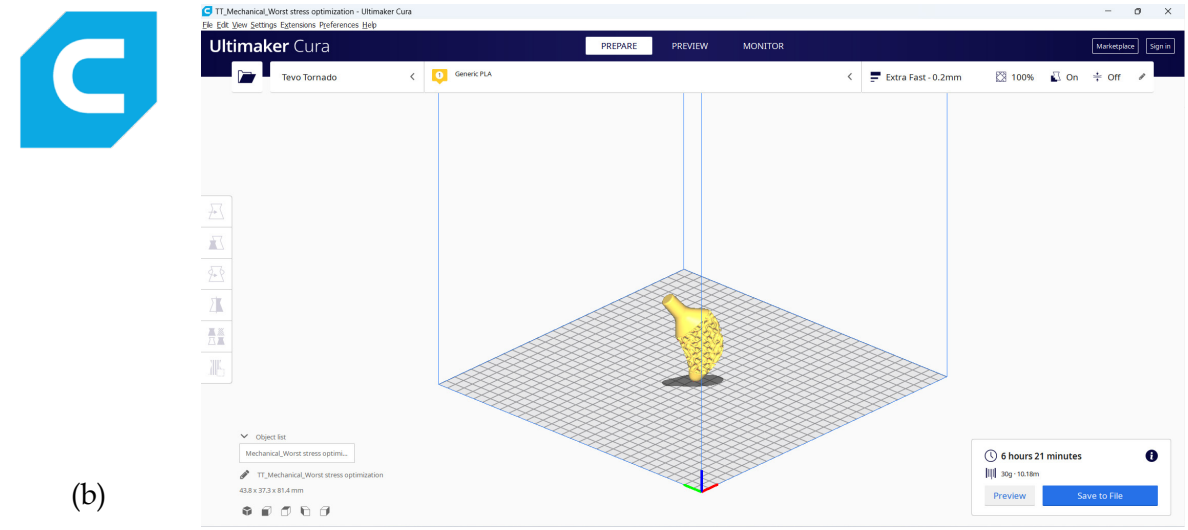
(a)

(b)

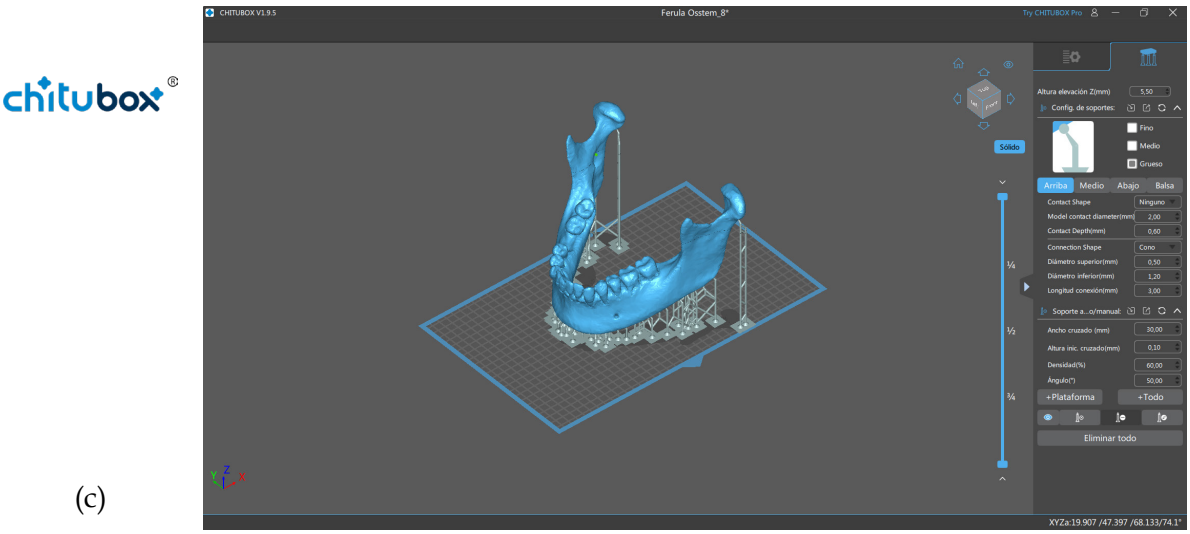
Figure 5: CAD/CAE design and conformal lattice design software used in this PhD. (a) NX 2206 software interface, used for the CAD design of the implants nominal geometries and for the finite-element modelling tasks. (b) nTopology software interface used for the generation of the lattice structures that gives rise to the tissue scaffolds.



(a)



(b)



(c)

Figure 6: Slicing software used in this PhD thesis for the use of FFF and DLP additive manufacturing technologies. Bambu Studio (a) and Ultimaker Cura (b) slicer's interfaces used to obtain the G-code files. (c) Chitubox slicer interface used to generate the digital masks.

3.2. Prototyping materials and technologies

Throughout the following section, the additive manufacturing technologies and materials used during the development of the research work carried out are described. The aim of using these technologies is to validate the manufacturability of complex structures that are capable of providing a biomimetic character that improves current solutions. With regard to the materials used, those that lead to the most reliable printing conditions are chosen, resembling as closely as possible the mechanical requirements of the case studies to be analysed. Table 1 shows some of these mechanical properties established for the study cases of meniscal replacement and osteochondral defect addressed in chapters 6 and 7.

Use case	**Tensile strength (MPa)**	**Compressive Strength (MPa)**	**Shear strength (MPa)**
Meniscus	>19	0.3-10	>14
Osteochondral defect	N/A (*)	6.5-10	N/A

Table 1: Mechanical requirements set for the development of meniscal and osteochondral implant prototypes. Data provided by colleagues from the INKplant consortium clinical team.

(*) N/A: Not Available or Not Addressed

3.2.1. Fused filament fabrication (FFF) technologies and materials

Technologies such as Fused Filament Fabrication (FFF) or Fused Deposition Modelling (FDM), are becoming increasingly common in the medical field, facilitating rapid prototyping methodologies, accessible and versatile among others (76, 78, 164). This AM technique works by extruding thermoplastic materials and instantly stacking them layer by layer to build three-dimensional structures, allowing the creation of complex geometries that would be difficult to achieve with traditional manufacturing methods. Undoubtedly, one of the main advantages of FFF technology is its easy accessibility, derived both from the availability of a wide range of low-cost 3D printers and the simplicity of its operation and maintenance, making this modality one of the most widespread 3D manufacturing technologies worldwide, both in industrial and domestic use. Its wide accessibility has allowed researchers, clinics and hospitals to adopt the technology without the need for large upfront investments, democratising access to advanced manufacturing tools. Today, it is not surprising to find fabrication laboratories (FabLab) included in the organisation charts of hospitals or health clinics. FFF technology is being used in a variety of applications within medicine, such as: the rapid and inexpensive creation of functional prototypes, the creation of new surgical instruments (especially useful in low-resource areas) or the procurement of assistive devices. Additive manufacturing technologies are being widely used in surgical planning procedures and in medical training activities, allowing the creation of exact replicas of specific patient

anatomies from medical images to obtain models that are faithful to the anatomical realities of the patients, from which training benches can be built to train different surgeries. In tissue engineering, these systems are specially used to obtain porous scaffolds to promote cell growth and tissue formation after implantation, especially in the field of bone and cartilage regeneration (71, 77). Furthermore, due to its ability to manufacture parts with relatively large bulk compared to other technologies, FFF is being widely used for the manufacture of patient-designed surgical guides, prostheses, orthoses and temporary implants.

In addition to the above mentioned, it is realised that this technology can use a wide range of materials, as for some applications it may or may not be necessary to ensure their biocompatibility. For example, for the manufacture of a surgical training bench, there is no need to guarantee properties that ensure the biocompatibility of the product, since it is not intended for that purpose. However, this technology is also suitable for the manufacture of biocompatible biomedical solutions. Poly(lactic acid) (PLA), poly(lactic-co-glycolic acid (PLGA) or polycaprolactone (PCL) are some of the most widely used materials, allowing the manufacture of scaffolds with biocompatible and biodegradable properties (98, 144, 165, 166).

When investigating applications, the development of rapid prototyping methodologies based on a design for additive manufacturing (DFAM) approach can have numerous advantages for our study (167, 168, 169). The speed and efficiency of prototyping enables rapid design iteration and prototype production, accelerating the development of customised medical solutions. In addition, the high availability of materials and easy access to technology significantly reduces the costs associated with the development and production of medical devices and tissue engineering scaffolds. Furthermore, the versatility in manufacturing complex geometries enables the creation of medical devices that are perfectly tailored to the needs and individual traits of patients.

In summary, FFF technology has established itself as a valuable tool in the field of biomedicine, offering an accessible and versatile platform for innovation in the design and manufacture of customised medical solutions, from rapid prototypes to implants and functional scaffolds. While it is true that other AM technologies provide a higher degree of precision from a manufacturing point of view, the speed of FFF technology, its accessibility and availability of materials, together with the absence of post-processing in the manufacturing processes, make it one of the ideal tools in the rapid prototyping process of medical solutions.

In chapter 5, this work has addressed a rapid prototyping methodology for obtaining hybridised models of PLA inserts with silicone, emulating the characteristics of the bone and cartilage unions. For this purpose, it was decided to use FFF systems in this work, in particular a Tevo Tornado 3D printer. The extrusion system of this printer was modified by our team, with the aim to enable the deposition of layers in a non-planar way, simulating direct printing on bone. It has been also used the Bambu X1 carbon combo, with the AMS (Automatic Material System) multi-material auxiliary system for the fabrication of polyvinyl alcohol (PVA) sacrificial molds that contain inner PLA inserts.

In this PhD thesis, polymeric materials such as PLA and PVA, two of the most widespread materials, are chosen to make use of FFF technologies and bring them a step beyond towards functionally-graded materials (FGMs) and scaffolds through an innovative prototyping route

(see chapter 5). These materials stand out for their high accessibility, biocompatibility and, in the case of PVA, their remarkable biodegradability, being water soluble. These properties make them ideal candidates for the manufacture of scaffolds in tissue engineering, where the material-tissue interaction should promote regeneration without provoking adverse responses in the organism. It is true that they do not constitute in themselves part of the definitive solutions of this research, as other technologies and materials allow for greater precision and versatility required to meet the clinical objectives, but their properties can lead to an interesting study in the evaluation of the first prototypes manufactured. They serve also as excellent companions to creativity promotion and enhanced communication.

Regarding PLA, it is a thermoplastic polymer derived from renewable resources, such as corn starch or sugar cane, which makes it not only biocompatible but also ecologically sustainable. Its accessibility and ease of processing through FFF technology have made it a standard material in the manufacture of prototypes and end products, including medical applications. PLA is also known for its excellent biodegradability and compatibility with 3D printing processes such as FFF. In tissue engineering, PLA scaffolds offer structural support for cell growth, while degrading at a rate that can be adjusted according to the type of tissue to be regenerated, thanks to the variability in PLA formulations that affect its degradation rate. However, the rate of PLA degradation within the human body can vary depending on several factors, such as the size and shape of the PLA device, as well as the specific environment within the body where the material is located. In general, PLA can degrade slowly within the human body through processes such as hydrolysis, where it is broken down into products that can be metabolised or excreted by the body. This combination of properties makes PLA an exceptional material for the creation of temporary scaffolds that need to disappear once the host tissue has begun its healing or regeneration process.

On the other hand, PVA is a synthetic polymer derived from the polymerisation of vinyl alcohol, known for its transparency and solubility in water. Mainly used as a support material in FFF (Fused Filament Fabrication) or FDM (Fused Deposition Modelling) 3D printing, PVA creates temporary structures that hold the printed parts during the manufacturing process and can be dissolved in water once the printing is complete, leaving the final part without residue. In addition, PVA is considered biocompatible for certain medical and pharmaceutical applications, being used in the manufacture of capsules and tablets, as well as in biomedical applications such as tissue engineering scaffolds and cell culture matrices. Its biodegradability is another remarkable aspect, as it decomposes in aqueous environments under the action of enzymes, although the speed of this process can vary depending on factors such as temperature, pH and the presence of microorganisms, being its degradation slower in terrestrial environments.

The controlled biodegradability of materials such as PLA and PVA is of particular interest, as it allows the introduction of adjustable degradation properties that can be synchronised with the rate of new tissue formation if more complex mathematical models are developed. This means that scaffolds can be designed to provide mechanical support initially, and then degrade at a rate that favours the transfer of mechanical load to the regenerated tissue, thus promoting a natural healing process. These scaffolds can be designed with a specific porous

architecture that facilitates cell adhesion, proliferation, and differentiation, while their biodegradability ensures that the scaffold eventually dissolves, leaving behind a functional regenerated tissue. Therefore, the accessibility and biocompatible properties of PLA and PVA, combined with their processability by FFF technology, make them attractive materials for the creation of customised scaffolds in tissue engineering applications.

In addition, this research introduces an innovative approach by combining both materials, as PVA is used to hybridise PLA solutions with a medical grade PDMS silicone in a way that allows the conditions of a biomimetic bone and cartilage implant to be recreated (165, 170, 171). In chapter 5, it is shown how it is possible to fabricate porous scaffolds in PVA onto which a light-curing material can be cast in a vacuum system. By selectively inserting pre-printed PLA inserts, it is possible to obtain fully hybridised multi-material prototypes after the photopolymerization process of the PDMS and the corresponding water solution of the PVA mould. Smartfil PLA and Smartfil PVA from the Smart Materials 3D catalogue are used throughout the completion of this research.

3D printer	**Tevo Tornado**	**Bambu X1 carbon**
Technology	FFF	FFF
Build volume	300 x 300 x 400 mm^3	256 x 256 x 256 mm^3
Layer resolution (Z)	0.1-0.35 mm	0.1-0.35 mm
Build speed	60-150 mm/s	60 mm/s
Travel speed	250 mm/s	500 mm/s
Multi-material system	No	Yes (AMS system)
Filament diameter	1.75 mm	1.75 mm
Nozzle diameter	400 µm	400 µm
Slicer	Ultimaker Cura *(custom profile)*	Bambu studio

Table 2: Technical specifications of the FFF Tevo Tornado and Bambu X1 carbon FFF printers acquired from the manufacturer's website (162, 172).

Material	**Density (g/cm^3)**	**Tensile strength (MPa)**	**Young Modulus (MPa)**	**Elongation at break (%)**	**Hardness**
PLA	1.24	55.5 (XY) 43.8 (Z)	4635.7 (XY) 3129.8(Z)	1-1.4	85 (D)
PVA (*)	1.23	N/A	N/A	N/A	N/A

Table 3: Mechanical properties of PLA and PVA materials acquired from the manufacturer's website (173). (*) The manufacturer does not provide mechanical properties of PVA as its application is intended for the manufacture of support structures.

3.2.2. Digital light processing (DLP) technologies and materials

Digital light processing (DLP) and liquid crystal display (LCD) 3D printing systems for vat photopolymerisation represent one of the most accurate and accessible digital technologies in the field of additive manufacturing, offering unique capabilities for creating objects with fine details and high precision (83). These technologies use the polymerisation of photosensitive resins to build objects layer by layer. Although they are technologies that require a higher degree of user knowledge, as they request post-processing operations, they have been widely developed and are present, like FFF, in industry and in the domestic sector. In terms of theoretical principles and operation, both technologies, DLP and LCD, share very similar features and are often confused by users. The main difference between the two systems lies in the way UV light is processed (174). Digital Light Processing (DLP) uses a digital projector to cure photosensitive resins, polymerising entire layers of the resin with each exposure. The light from the projector is modulated through thousands of micromirrors, allowing precise control over which areas of the resin layer are cured based on the projected image. This enables the rapid fabrication of layers and thus complete objects with high resolution. On the other hand, 3D printing systems that integrate an LCD panel use a digital display subdivided into micron-order pixels as a mask to selectively expose the photosensitive resin to UV light, curing and solidifying specific layers of the material. Unlike DLP, which uses micromirrors, LCD uses pixels on a screen to block or allow UV light to pass through. This also allows for the creation of detailed objects with high precision, although the uniformity and intensity of light can vary depending on the resolution of the screen.

Today, some of the medical applications addressed by the use of DLP and LCD technologies include the fabrication of anatomical models, the printing of customized surgical guides and splints for the patient, or the generation of temporary implants tailored to the patient. Dental sector is undoubtedly a niche market for this technology, where it has experienced strong growth in recent years (174). Compared to other additive technologies such as FFF or FDM, DLP-LCD systems use smaller manufacturing volumes, but the precision they allow is higher. In comparison, a pixel on an LCD screen can have a square cross-section of a few tenths of a micron (see Table 4), whereas the diameter of commercial FFF extruder nozzles is typically around 8-10 times larger, about 200 to 400 µm generally (see Table 2). For this reason, this technology has become very competitive in the dental sector, given that the required product, teeth, have relatively small dimensions compared to other body anatomies and require a very high level of control of the surface quality.

If DLP-LCD are compared with FFF technologies, a number of advantages can be appreciated, some of them already mentioned, such as higher resolution and precision of the product, improved surface quality and even improved production times, since these systems photopolymerise the layers simultaneously, regardless of the number of models on the impression platform. But certain drawbacks can also be encountered, such as the cost of materials, as photosensitive resins are usually more expensive than the filaments used in FFF; print volume limitations, as already mentioned, the print size is limited by the size of the vat and screen, which may be lower than the build volume capabilities of some FFF printers; and

finally handling and post-processing, as the resins require careful handling due to their potential toxicity and need post-print cleaning and UV curing.

In terms of the materials used, a wide variety of light-curing resins can be found, generally differentiating in the market between: standard resins, used for prototypes and conceptual models; functional resins, which contain specific properties, such as high strength, flexibility, castability; or biomedical or dental grade resins, developed to meet the necessary biocompatibility requirements.

In this PhD research, two materials are used with this type of technology. Firstly, a Photon Mono X printer from Anycubic company is employed for rapid prototyping purposes. The resin used for this task is a commercial variety from the same company (Anycubic ECO resin) (175). It is not a biomedical grade material, but no such certification is necessary as only concepts and designs are intended to be validated. The INKplant project also envisages printing the soft zone of the osteochondral scaffolds, which should have properties similar to those of cartilage, with a biodegradable polymer (BDP) developed by colleagues in the consortium. A Phrozen Sonic Mini 4K printer, from Phrozen company (176), is used to fabricate the first specimens and prototypes when testing this material, following a rapyd prototyping route. It is mentioned that BDP is being tested on a non-medically certified LCD printer as the final concept is not envisioned to be printed with this technology, but expected to be printed with a 5-axis inkjet printer, developed by the Austrian research company, Profactor GmbH. The idea is to be able to directly print polymers, silicones or biogels on scaffolds already manufactured using other technologies, as discussed below. Nevertheless, DLP-LCD printers are truly useful to test this material in early stages of the project as they constitute very accessible and reliable printing systems.

3D printer	**Photon Mono X**	**Phrozen Sonic Mini 4K**
Technology	LCD – based SLA	LCD – based SLA
Light Source (nm)	405	405
Build volume	192 x 120 x 245 mm^3	134 x 75 x 130 mm^3
Lateral resolution (XY)	50 µm	35 µm
Layer resolution (Z)	0.01-0.15 mm	0.01-0.30 mm
Max. printing speed	60 mm/h	-
Slicer	Anycubic Photon Workshop	Chitubox

Table 4: Technical specifications of the Anycubic Photon Mono X and Phrozen Sonic Mini 4K printers acquired from the manufacturer's website (175, 176).

Materials	Tensile strength (MPa)	Compression strength (MPa)	Elongation at break (%)	Shear strength (MPa)	Shore Hardness
Anycubic Eco	40-50 MPa	N/A	8-12	N/A	89 (D)
INKplant BDP	7.83	8.54	35	3.14	N/A

Table 5: Mechanical properties of Anycubic Eco resin and the INKplant biodegradable polymer (BDP) acquired from the manufacturer's website (175) and from the INKplant documentation respectively.

3.2.3. Vacuum casting system and soft molding technology

Vacuum casting is a manufacturing technique that enables the creation of high quality, precision parts through the use of silicone moulds and a casting process in a vacuum environment. This system excels in its ability to produce small to medium runs of components with excellent surface finish and consistent material properties, representing a versatile and efficient option for rapid prototyping and limited production runs. The vacuum casting process begins with the creation of a master model, usually produced using 3D printing or CNC machining techniques. From this model, a silicone mould is produced under vacuum conditions to remove any air bubbles, ensuring that the details of the original model are faithfully reproduced. Once the mould is cured, the casting material is introduced, again under vacuum, to ensure complete infiltration into the mould without defects due to trapped air.

In the medical field, vacuum casting offers a wide range of applications, taking advantage of its ability to work with a variety of biocompatible materials and its flexibility to adapt to complex designs (177). Some notable applications include the manufacture of anatomical models for surgical planning and education, allowing the simulation of specific pathological conditions or complex anatomies for medical training or pre-operative preparation; medical device prototypes, as this technique is ideal for developing functional prototypes, offering a fast and cost-effective route for design iteration and evaluation of functionality, ergonomics and performance; or medical equipment components, allowing the manufacture of customised or replacement parts manufactured quickly and accurately, facilitating the adaptation or improvement of existing equipment (178).

In terms of materials, vacuum casting allows the use of a wide range of polyurethanes and similar resins, which can be selected to mimic the properties of more durable materials such as plastics, rubbers or metals. In medical contexts, priority is given to the use of biocompatible materials that do not produce adverse reactions in contact with the human body or when used in clinical settings. This includes medical grade polyurethanes and silicones that replicate the flexibility and strength of human tissue for anatomical models, or transparent resins for device components that require internal visualisation.

Vacuum casting offers several significant advantages for medical applications as the ability to reproduce fine details and geometric complexities of the original model is crucial for medical

applications where anatomical accuracy is essential. In addition, silicone mould production and vacuum casting are relatively fast processes, allowing for the accelerated development of prototypes or the manufacture of limited series without the need for expensive tooling. The compatibility of this technique with a wide range of materials allows optimal selection according to the specific needs of each medical application, from flexibility to rigidity, transparency or impact resistance. This system is therefore considered to establish itself as an advanced manufacturing technology with considerable potential in the medical field, offering customised, high-quality solutions for the manufacture of anatomical models, medical device prototypes and equipment components. Its combination of precision, speed and material flexibility makes it a valuable tool for innovations in medicine and biomedical engineering.

In chapter 5 of this work, this technology is used to cast an industrial silicone, a commercial PDMS (Easyplat Mold 40), into sacrificial moulds made using FFF technology in PVA material. Casting this silicone under vacuum in the printed moulds significantly helps the material to expand properly at all points of the lattice lattice and aids in the elimination of air bubbles trapped between the trusses.

Vacuum Casting machine	**MCP – 004 ST**
Max. Mold size	650 x 900 x 600 mm^3
Mold max. capacity	5.5 kg
Ultimate vacuum	0.5 mbar

Table 6: Technical specifications of the vacuum system acquired from manufacturer's operating instructions document (179).

Material	**Density (g/cm^3)**	**Tensile strength (MPa)**	**Viscosity (cps)**	**Elongation at break (%)**	**Shore Hardness**
Easyplat Mold 40	1.20	N/A	5000	300	40 (A)

Table 7: Mechanical properties of Easyplat Mold 40 material acquired from the material datasheet (180).

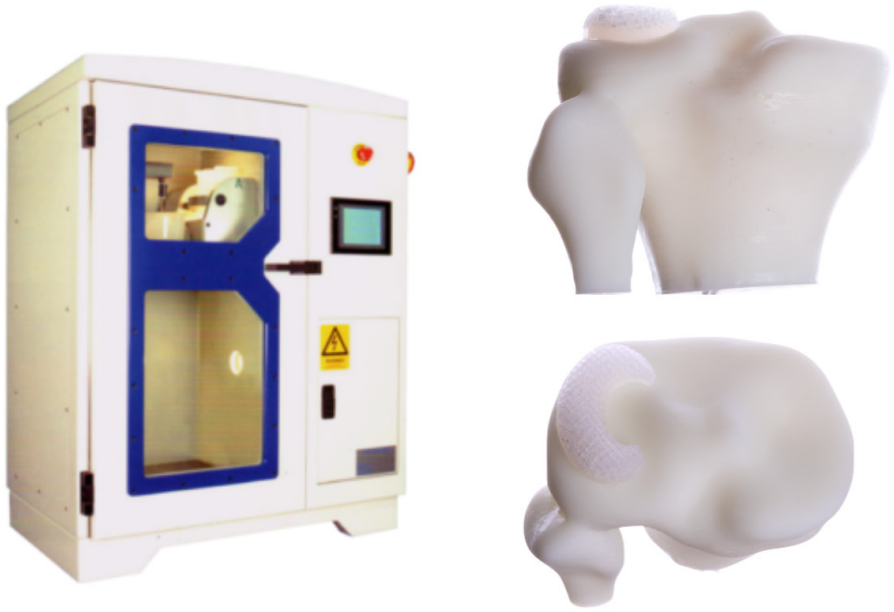


Figure 7: MCP - 004 ST vacuum casting system and prototype of meniscal tissue scaffold casted in silicone. Parts obtained through the implementing of the rapid prototyping strategy described in chapter 5. Vacuum casting system picture acquired and adapted from Aarya Industries (181).

(a)



(b)



Figure 8: FFF technologies used throughout this PhD thesis. (a) Tevo Tornado printer and prototype of printed shin guards for sports practice. (b) Bambu X1 carbon printer with AMS multi-material auxiliary system and surgical guides set designed from porcine anatomy. 3D printer pictures acquired from manufacturers' websites (162, 172).



(a)

(b)

Figure 9: DLP-based LCD technologies used in this research work: (a) Anycubic Photon Mono X printer and prototype surgical guide for single implant positioning as a dental application. (b) Phrozen Sonic Mini 4K printer and fabrication of a dental anatomy as a control model for the production of a restoration. Anatomical models pictures courtesy of Dental Troyano S.L. and 3Dtive S.L. 3D printers pictures acquired and adapted from manufacturers' website (175, 176).

3.3. High performance additive manufacturing technologies and materials

3.3.1. PolyJet additive manufacturing

PolyJet technology is an AM system developed by the Israeli company Stratasys (182). It represents a significant innovation in the field of 3D printing, offering unique capabilities for the creation of prototypes and models with a high degree of detail, precision and versatility in the use of materials. This cutting-edge technology works by depositing nanometric droplets of liquid photopolymers that are immediately cured by ultraviolet light, layer by layer, to build 3D objects. The PolyJet system excels in its ability to print with multiple materials on a single object, allowing the combination of different textures, colours and mechanical properties. The Stratasys J55 printer, used in this research, is an advanced solution that integrates these capabilities into a compact and efficient printer design, ideal for office and design lab environments. This printer combines up to 5 materials plus the support material, making it a

state-of-the-art tool when it comes to prototyping systems. In this work, the materials used to support the research are commercial materials from Stratasys catalogue, in particular Elastico and Vero Vivid. These materials offer flexibility and stiffness behaviour, respectively, allowing users to design and produce parts with varied and specific mechanical properties.

In the medical field, PolyJet technology, and particularly the J55 printer, have significant applications for the fabrication of complex anatomical models (183, 184). This technology is being implemented to manufacture biomodels for surgical planning and medical education, enabling the creation of exact replicas of organs, bones or vascular systems that combine different mechanical properties to simulate reality more accurately. The creation of realistic models aids medical education as well as surgical planning, allowing surgeons to practice and plan procedures on models that closely simulate the reality of human tissue. Through their use, the development of new medical devices benefits greatly from the ability to print prototypes that combine rigidity with elasticity, mimicking the interaction of these devices with human tissue. It is also being implemented in the dental sector for the fabrication of removable structures as temporary complete dentures.

In terms of our research, although the Elastico and Vero Vivid materials are not biomedical grade and therefore not intended for direct implantation or internal clinical applications, their usefulness in the development of scaffolds to replace osteochondral lesions is undeniable in the context of research and prototype targets. The ability to obtain models that combine elastic and rigid properties is particularly advantageous for simulating the biomechanical complexity of the joints and tissues that make up the osteochondral system. These capabilities, as discussed below, facilitate the creation of scaffolds that mimic the structural complexity and mechanical properties of bone and cartilage tissue, allowing for a more accurate design that promotes tissue regeneration. In addition, the printed models can be used for mechanical and biological testing, assessing the interaction between the scaffold and biological tissue without the need for invasive procedures. Some of the properties of these materials and some technical specifications from Stratasys J55 printer are listed in Table 8 and Table 9.

Although the specific materials mentioned are not directly applicable in clinical applications because they are not biomedical grade, PolyJet technology offers an invaluable platform for advancing medical research, developing medical devices and improving treatment strategies for osteochondral injuries. The ability to simulate both bone stiffness and cartilage elasticity in a single model represents a powerful tool for biomedical engineers and healthcare professionals in their efforts to understand and treat complex medical conditions.

Stratasys material	**Tensile strength (MPa)**	**Elongation at break (%)**	**Elastic Modulus (MPa)**	**Tensile tear (kg/cm)**	**Shore Hardness**
VeroPure	40-55	5-20	2200-3000	N/A	83-86 (D)
Elastico	3-5	360-400	N/A	5-7.5	45-50 (A)

Table 8: Mechanical properties of VeroPure and Elastico materials acquired from the Stratasys website (185).

3D printer	**Stratasys J55**
Technology	PolyJet
Building size	140 x 200 x 190 mm^3
Printing Area	Up to 1.174 cm^2
Layer resolution (Z)	Horizontal build layers down to 18 µm
Operating Temperature	Temperature 18 – 25 °C
Operating Humidity	relative humidity 30-70% (non-condensing)
Slicer	GrabCAD print
Lateral resolution (XY) (**) *Deviation from stl dimensions, for one Sigma (67%) of models printed with rigid materials, based on size* *Deviation from stl dimensions, for two Sigma (95%) of models printed with rigid materials, based on size*	 ±150 µm (under 100 mm) ±0.15% of part length (above 100 mm) ±180 µm (under 100 mm) ±0.2% of part length (above 100 mm)

Table 9: Technical specifications from the Stratasys J55 3D printer acquired from Stratasys website (186). *(**) Measured when ambient temperature is 23 °C and relative humidity is 50%.*

3.3.2. Lithography based Ceramic Manufacturing (LCM)

The 3D printing technology known as Lithography-based Ceramic Manufacturing (LCM) represents an advanced frontier in the field of additive manufacturing, particularly in ceramic materials engineering (135, 136, 187, 188). This approach is distinguished primarily by its ability to manufacture ceramic components of high precision and geometric complexity, opening new possibilities in a variety of applications, including regenerative medicine and tissue engineering. LCM is based on similar principles to DLP-LCD imaging systems, using a UV light source to selectively polymerise a photosensitive material containing suspended ceramic particles. The part is built up layer-by-layer, where each layer is solidified by exposure to a specific light pattern, associated with a specific wavelength, which defines the desired geometry. This method allows precise control over the shape of the object, making it possible to create structures with fine details and internal complexities that would be difficult to achieve with traditional manufacturing techniques.

As with DLP systems, LCM uses a UV light source to cure a photosensitive material. However, instead of pure polymers, LCM works with a mixture of polymers and ceramic particles, referred to as a ceramic slurry. This combination allows you to take advantage of the resolution and precision of DLP while integrating the unique properties of the ceramic materials into the final product. After printing, what is known as a 'green body' is obtained. In this state, the

printed product contains polymeric particles combined with ceramics in their microstructure. In order to obtain a ceramic product, it is necessary to remove the polymeric material from the matrix, so the objects require specific thermal post-treatments, which include the removal of the polymer through a debinding and sintering process. During the debinding stage, at a lower temperature than sintering, the polymeric chains are broken, eliminating this material from the part. The product obtained in this intermediate stage is a ceramic product, but particularly it has a very high porosity as all the polymer has been eliminated from the microstructure. It could be imagined as ceramic powder forming a very brittle structure. For this reason, the cycle is completed with a subsequent sintering process, in which the object is heated to higher temperatures than in the debinding stage, causing the densification of the ceramic particles, resulting in a pure ceramic component with superior mechanical and thermal properties. These combined thermal post-treatment stages are associated with a reduction in the volume of the printed part since the polymer component has been removed and the intermediate product has been subsequently densified. For this reason, it is very important to have the capacity to predict in a reliable way the shrinkage of the part throughout the process. This is performed by applying a scale operation at the design stage, so that the final product has the desired dimensions. This fact introduces an extra component of complexity compared to conventional DLP or LCD printing processes, where it is true that in the post-processing and UV curing stage the parts may undergo some dimensional variation, but much less significant than the volumetric shrinkage, which occurs through LCM post-treatment. Moreover, this variation is anisotropic, the shrinkage is found similar in the plane in which the layers are stacked, and therefore parallel to the printer building platform, while in the printing direction, the Z direction, the shrinkage value is different. All these considerations are very relevant when dealing with personalised applications that require an extreme degree of precision, such as the fabrication of scaffolds for tissue engineering.

LCM technology is particularly promising for medical applications that benefit from the properties of ceramic materials, such as their biocompatibility, hardness, and corrosion resistance. These applications include:

- Bone and dental implants: the high biocompatibility and mechanical strength of ceramic materials make them ideal for bone and dental implants.
- Tissue engineering scaffolds: scaffolds made of ceramic materials can be designed with specific porosities that promote osseointegration and cell growth, crucial in bone regeneration.
- Customised medical devices: the ability to create complex shapes enables the fabrication of customised medical devices, such as heart valves or prosthetic components specific to the patient's anatomy.

The main advantage of LCM in the context of medical applications lies in the unique combination of geometric precision and the exceptional properties of ceramic materials. Components manufactured using LCM exhibit high biocompatibility, essential for implantable applications and medical devices; superior mechanical strength, important for loaded implants, such as in orthopaedic applications and joint defects; and they also ensure

chemical and thermal stability, maximising the durability and long-term functionality of implants and medical devices.

In terms of the materials used in LCM, they mainly include resins containing a significant load of ceramic particles. These particles can vary in composition to include oxides such as zirconium (ZrO_2) or alumina (Al_2O_3), among others. Other biomedical grade materials such as hydroxyapatite (HA) and tricalcium phosphate (TCP), which are known to be compatible and biodegradable, are also used. In this work, hydroxyapatite is used for the fabrication of scaffolds for bone regeneration, and alumina toughened zirconia (ATZ) is chosen for the fabrication of a short hip prosthesis by means of an innovative optimisation methodology, as can be seen in chapter 8. Hydroxyapatite is especially valued in tissue engineering because of its compositional and structural similarity to the natural minerals present in human bones and teeth. This similarity promotes excellent integration with bone tissue, facilitating osteoconduction, i.e. the ability to serve as a guide for the growth of new bone tissue around the implant. HA not only supports cell adhesion and proliferation but also stimulates the differentiation of progenitor cells into osteoblasts, which is crucial for the formation of new bone. This intrinsic presence in the human anatomies underlines its biocompatibility and efficacy as an implant material, as it is a component already recognised and accepted by the body. HA is indicated for a wide range of orthopaedic and dental applications and pathologies, including bone regeneration and replacement, dental implants, and tissue engineering and other regenerative medicine applications. Therefore, HA can be used to manufacture medical solutions for fractures, bone defects, or bone loss due to diseases such as osteoporosis, due to its ability to integrate with the surrounding bone and support the growth of natural bone tissue. It is therefore a material of particular interest in the study of tissue engineering and the fabrication of scaffolds. Using LCM technology, these scaffolds can be designed to fit specific bone defects, providing a three-dimensional matrix for cell colonisation and bone tissue regeneration. In the framework of the INKplant project, the material used is hydroxyapatite developed by the Austrian company Lithoz GmbH. Some of its more descriptive properties are listed in Table 10.

On the other hand, ATZ is a composite ceramic that combines aluminium oxide (alumina) with zirconium oxide (zirconia) to improve its mechanical properties and durability. This combination results in a high-performance ceramic material that offers superior mechanical strength, fracture toughness, and stability under physiological conditions. The incorporation of alumina particles in a zirconia matrix not only improves the strength and toughness of the material but also increases its resistance to cracking and wear. This improvement in mechanical properties is crucial for medical applications that require durable and reliable materials. In addition, ATZ exhibits excellent biocompatibility, being inert in the human body and resistant to corrosion in biological environments. Thanks to these characteristics, ATZ has been used to cover various medical applications, taking advantage of its unique combination of hardness, wear resistance, and biocompatibility. Some of these applications include the manufacture of orthopaedic implants, such as artificial hips or knees, where wear resistance and durability are essential for the long-term performance of the implant. It is also commonly used in the dental sector, for the manufacture of dental implants, where ATZ is used to fabricate crowns, bridges, and other implants that require superior aesthetics and good

mechanical strength. In conclusion, ATZ represents an advanced option for the manufacture of implants and medical devices, offering an exceptional combination of mechanical strength, durability and biocompatibility. Its application in regenerative medicine and tissue engineering continues to expand, driven by the growing demand for durable, high-performance medical solutions. This PhD study makes use of this material in chapter 8, where the fabrication of an orthopaedic implant for a customised short hip prosthesis is developed. In this work ceramic slurries developed by the Austrian company Lithoz GmbH have been used, as well as their LCM technology printer, CeraFab S65 Medical. The main characteristics of this technology and material properties are shown in Table 10 and Table 11.

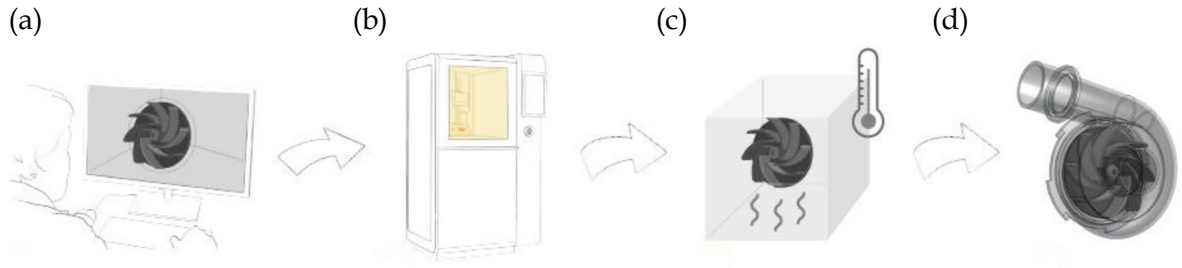


Figure 10: LCM printing technology workflow. (a) Design and slicing stage. (b) Printing process. (c) Thermal post-processing stages of debinding and sintering. (d) Final product. Picture acquired from Lithoz GmbH website .

3D printer	**CeraFab S65 Medical**
Technology	LCM
Building platform	102 x 64 x 320 mm^3
Lateral resolution (XY)	40 µm
Layer resolution (Z)	10-100 µm
Build speed	Up to 150 layers per hour

Table 10: Technical specifications of the LCM printing system CeraFab S65 Medical acquired from Lithoz GmbH website (189).

Material	**Density (g/cm^3)**	**Tensile strength (MPa)**	**Elastic Modulus (GPa)**	**Relative density (%)**
LithaBone HA 480	3.16	115.1	101.7±27.3	92-98
LithaCon ATZ 980 (*)	N/A	2200	220	99

Table 11: Physical properties provided by the manufacturer Lithoz GmbH of the materials hydroxyapatite and alumina toughened zirconia (190, 191). *(*) Ceramic material with a 20 wt% alumina and 80 wt% zirconia composition.*

3.3.3. Liquid Deposition Modelling (LDM)

Throughout this work, for the manufacture of prototypes and models of meniscus scaffolds, Elkem Silicones takes care of the fabrication of the specimens using multi-material LDM AMT developed by Delta Tower GmbH (192). Elkem Silicones (193), as a member of the INKplant consortium, has contributed to this work by implementing an additive manufacturing system based on the principles of extrusion, called Liquid Deposition Modelling (LDM), which makes it possible to print the silicones developed by the company in a combined way. This methodology facilitates the application of a novel range of tailor-made silicone materials, designated as the Silbione™ (194) , for deployment in 3D printing context. It enables the engineering of high-performance components comprised entirely of silicone, featuring intricate geometries and overhangs unattainable through conventional die molds and machining processes, thereby permitting the direct printing of elastomeric parts/objects. This technology represents a significant advance in the biomedical field, offering new possibilities for the creation of complex medical structures and devices by combining various materials in a single manufacturing process. LDM is particularly relevant in the use of silicones, such as biomedical grade polydimethylsiloxane (PDMS) silicone, known for its versatility, biocompatibility and chemical stability, which in this PhD research is evaluated as a candidate material for the fabrication of complete meniscal scaffolds.

Regarding the LDM technology, Elkem's technology is based on an advanced 3D printing system that allows the controlled deposition of multiple materials, including silicones of different mechanical and chemical properties. The process is characterised by its ability to precisely deposit these materials, layer by layer, to form complex structures that can include areas with different flexibilities, transparencies and permeabilities within a single object. Controlled material deposition is achieved through precisely calibrated extrusion, which allow the exact placement of materials according to the specified design. This can be complemented by *in-situ* curing or vulcanisation systems, which solidify the deposited material instantaneously or at a controlled later stage, ensuring the structural integrity and desired properties of the final product. This systems can combine material deposition, like FFF technology, using a dispenser making the role of the extruder regulated by different motors and linear guides to control the displacement, with the ability to dynamically cure the material. Instead of applying UV emission on a fixed tank, this technology mounts an UV source on the printhead that moves in a fixed manner throughout the manufacturing process.

One of the most significant advantages of this technology is the ability to combine silicones with other biodegradable and biocompatible polymers, including those that can be loaded with cells, which is extremely valuable for tissue engineering purposes. This opens the possibility of producing hybrid scaffolds that not only provide the structure and mechanical support needed for tissue engineering but can also integrate specific biological functionalities, such as the controlled release of growth factors or the promotion of cell adhesion.

The hybridisation of PDMS scaffolds with biodegradable polymers offers multiple advantages for TERM applications, as it allows customisation of mechanical and biological properties by creating structures with specific regions designed to maximise mechanical behaviour, as well

as optimised zones for biological interaction with cells and tissues, and incorporates the ability to combine different materials in a scaffold, which facilitates the integration of various functions, such as mechanical support, promotion of cell adhesion and controlled release of bioactives.

Both, PDMS and the biodegradable polymers selected for these applications, are recognised for their biocompatibility, ensuring that the scaffolds are suitable candidates for *in vivo* applications. The combination of materials opens up new avenues for the design of drug delivery systems and cell therapies, taking advantage of the unique properties of each material to optimise release and therapeutic effect. For this reason, the implementation of LDM multi-material technology, especially in combination with biomedical grade PDMS silicones, represents an advanced biofabrication system of great utility, as it offers great potential for the design and production of scaffolds and hybrid medical devices. This technology underlines the potential of 3D printing and additive manufacturing to revolutionise the field of regenerative medicine, promoting the development of more effective and personalised treatments. The 3D printing technical specifications and the material properties are gathered in Table 12 and Table 13.

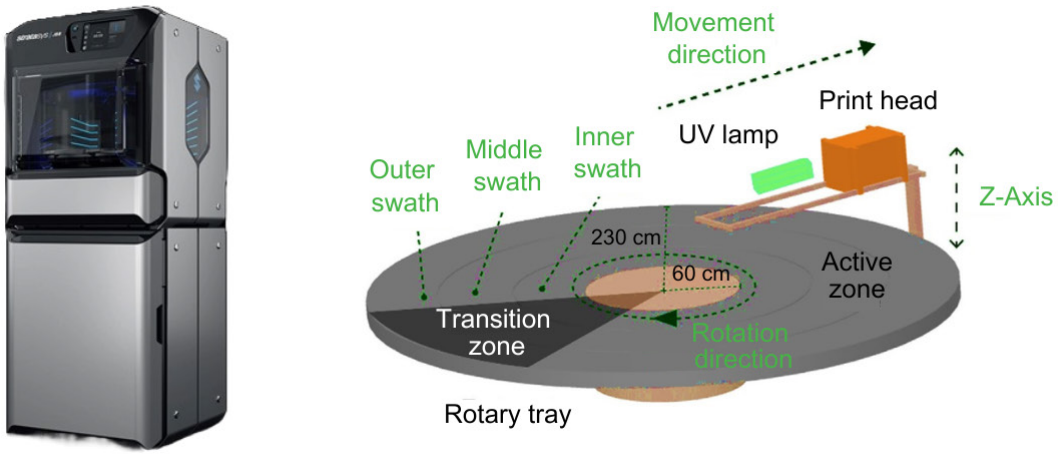
3D printer	**Delta Tower Fluid MT**
Technology	LDM
Tools	Up to 6
Building platform	420 mm diameter x 400 mm height (cylindrical)
Print bed	20 mm thick aluminum bed
Nozzle diameter	0.06 mmto 2mm
Layer resolution	0.03 mm to 2mm

Table 12: Technical specifications of the LDM printing system Delta Tower Fluid MT acquired from Delta Tower website (195).

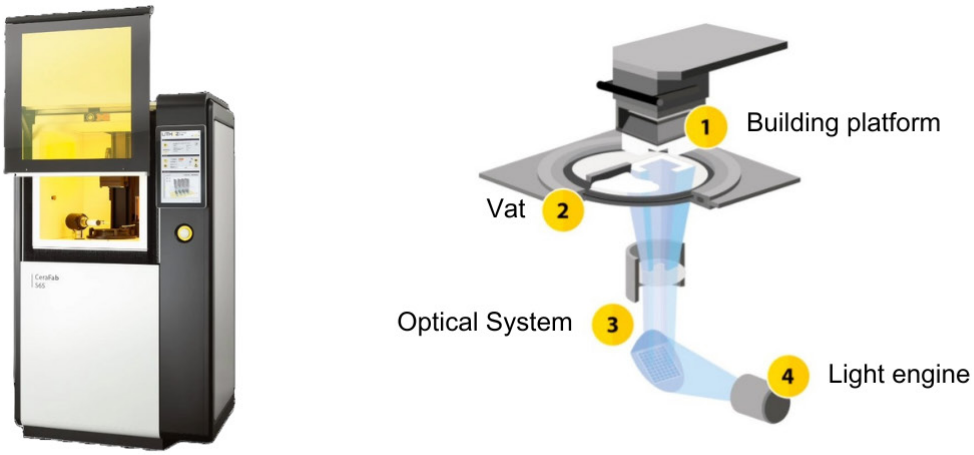
Material	**Density (g/cm^3)**	**Tensile strength (MPa)**	**Elongation at break (%)**	**Tear strength (MPa)**	**Hardness Shore**
Silbione™ series	N/A	6.9-8.9 MPa	470-950	30-40 N/mm	25-70 (A)

Table 13: Mechanical properties of Silbione™ series provided by Elkem Silicones (194).

(a)



(b)



(c)

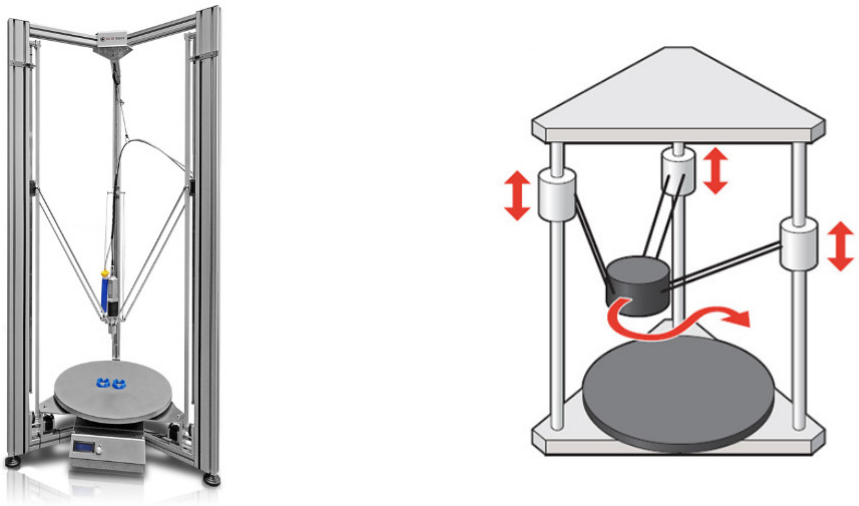


Figure 11: High performance AMTs used to throughout this PhD thesis. (a) PolyJet technology from Stratasys company. As shown in the diagram, it uses a rotating circular manufacturing platform to which the printer head and the UV emitter are attached. (b) Lithoz LCM technology for printing ceramics. This system is inspired by in-deposit light-curing systems. It also uses a circular platform that receives the light from the emitter at the bottom. (c) Controlled deposition system for silicones and biogels developed by Delta Tower. Images acquired from the manufacturers' websites (186, 189, 195). Diagrams of the technologies obtained from (196, 197, 198).



Figure 12: Printed parts using high performance AMTs. (a) Human anatomical model and model of sneakers obtained from the combination of materials combining colours and mechanical properties. (b) Collection of biomedical devices made of ceramic materials. A pommel plate and a graft for bone regeneration in HA 480 (blue colour) and a collection of hand phalanges in ATZ 980 (white colour) can be seen. (c) Heart biomodel and flexible conduit. Pictures acquired and adapted from manufacturers' websites (199, 200, 201).

4. Development of an open-source library of tissue engineering scaffolds[1]

Tissue engineering as a field may benefit from progressively implementing and spreading the use of standards, conceived to support the repeatability, replicability and efficient comparing of research results among experts in the field worldwide. Considering that scaffolds play a fundamental role in many tissue engineering strategies, it would be interesting to count with an internationally accepted set of geometries, acting as a library of lattices, porous materials and scaffolding structures, which could be employed for comparative purposes among materials and manufacturing technologies under development. To this end, an open-source library of tissue engineering scaffolds has been implemented. This library stands out for providing a comprehensive collection of scaffolds blueprints, designed considering the specific features of most additive manufacturing technologies applicable to tissue engineering and biofabrication. Besides, the library has been developed focusing on FAIR data principles along the development, for promoting Findability, Accessibility, Interoperability and Reusability. The scaffolds are shared as open-source (OS) medical devices with the necessary documentation for facilitating their application. Similar initiatives may be synergically integrated towards an ISO standard on tissue engineering scaffolds.

It is necessary to highlight here the inspiring effect of different pioneers of biomedical additive manufacturing and colleagues in the fields of tissue engineering, regenerative medicine and biofabrication. The idea of an accessible computer-aided design library of solutions for these fields is not novel. Seminal studies systematically investigated polyhedral shapes for scaffolds modelling, selected and classified the most suitable ones, implemented the first parametric library of scaffolding structures, demonstrated its utility for personalizing implants and validated it through rapid prototyping resources (202, 203). A study focusing on the interconnectivity of varied types of lattices to obtain complex-shape scaffolds was also conducted one decade ago (204). More recently, the growing interest of additive manufacturing with high performance materials for lightweight design has led to the development of design charts for selection purposes (205, 206), in which lattices, scaffolds and mechanical metamaterials are compared following Ashby graphs (160). In this respect, the most systematic approach, combining computational modelling, simulations, prototyping and testing, has been probably carried out in recent years by Egan's team, in connection to biomedical applications (207, 208, 209), focusing also on the modelling of tissue growth depending on scaffolds' characteristics (210).

However, authors of this study consider that some specific features of the newly presented open-source library of scaffolds are quite remarkable and may complement some of the

[1] A preliminary version of this chapter has been published as "Open-source library of tissue engineering scaffolds". Materials & Design, 223, 111154, 2022, under Creative Commons License (CC 4.0 BY).

aforementioned studies. First, the presented library is designed for additive manufacturing considering most technologies applicable to scaffolds' manufacturing and provides specific designs for enhanced printability employing fused-deposition modelling, inkjet printing, PolyJet technology, selective laser sintering or melting, laser stereolithography, digital light processing, lithography-based ceramic manufacturing or two-photon polymerization, to cite some possibilities. Second, the library counts with specific subsets of scaffolding geometries focused on multi-material and multi-scale or fractal-like solutions, taking into account the biomimetic and biomechanical solutions for complex tissue restorations normally require multi-material and multi-scale approaches, which have become also an essential trend in biomedical AMTs (142, 211, 212). Furthermore, one of the main purposes of this open-source library is testing and pushing the current technological limits of AMTs and related printable materials, for which the dimensions of scaffolds and trusses and the incorporated microstructural and topographical details go beyond the common limits of AMTs and 3D printed scaffolds. Finally, FAIR data principles (88) have guided the implementation of the open-source library, as specifically discussed in section 4.3.2.

4.1. Geometrical constraints and design requirements

The collection of scaffolding geometries is designed with the support of NX 2206 (Siemens PLM Solutions), a computer-aided design and engineering software (CAD-CAE). Solid- and surface-based operations are employed to create trusses, unit elements and building blocks, whose replication and hybridization using matrix, Boolean and recursive tools lead to complex-shape scaffolds with biomimetic features. The simulation capabilities of NX 2206 are applied to the evaluation of performance, including mechanical and fluidic properties, and the creation of design maps, as further described in section 4.2. Other CAD-CAE options, like Catia, Solid Edge, Solid Works, Fusion 360, Inventor, to cite a few, would be also applicable to reach similar results and can be used for expanding the library, as CAD formats are becoming more and more interchangeable. The use of NX 2206 is based on author's personal experience and on the reliable combination of design and modelling resources that it provides.

Considering that the collection is arranged for the manufacturing of scaffolds applying a wide set of AMTs, two slicers are used as supporting CAM tools. First of all, Chitubox v.1.9.4 (ChiTu Systems) is utilized as key reference slicer for digital light projection, stereolithography and LCD printing. In short, the software slices CAD models and generates black and white digital masks that can be used for digitally processing photopolymers and slurries. The printability of multi-material constructs and the impact of mesh quality on the generated masks' resolution can be analyzed thanks to Chitubox, as further analyzed in section 4.2. Together with this slicer, Ultimaker Cura 4.13.1 is employed as state-of-the-art slicer for generating printing paths for fused-deposition modelling, inkjet printing systems and bioprinters, among others. Both of them are user-friendly free slicers that reinforce the open-source approach of the generated collection and help to make 3D printing accessible to users worldwide. Their application is extremely extended and their options for fine-tuning the eventually needed supporting

structures constitute interesting resources for R&D tasks and towards final productivity and sustainability, which is connected to minimizing the volume of printable supports (213).

With these CAD-CAE-CAM resources, five (1-5) main subsets of OS scaffolds are designed, evaluated, optimized and shared as digital libraries through different channels (see 4.3): 1) a collection of unit cells as standard scaffolding geometries; 2) a collection of multi-scale, hierarchical, recursive or fractal-like scaffolds for their biomimetic interest (118, 125); 3) a set of functionally-graded constructs; 4) a set of combinations of the previous geometries to exemplify the versatility and complexity achievable through multi-material additive manufacturing; and 5) an assortment of cell scaffolding textures with systematic variations.

The DFAM strategy, the performance evaluation and the creation of design maps for scaffolds selection purposes are described in the following subsections, before entering in the detailed description of the library of scaffolds with their more relevant properties, which are analyzed in the results section, together with a utility evaluation with different materials and technologies.

4.1.1. Design for additive manufacturing strategy

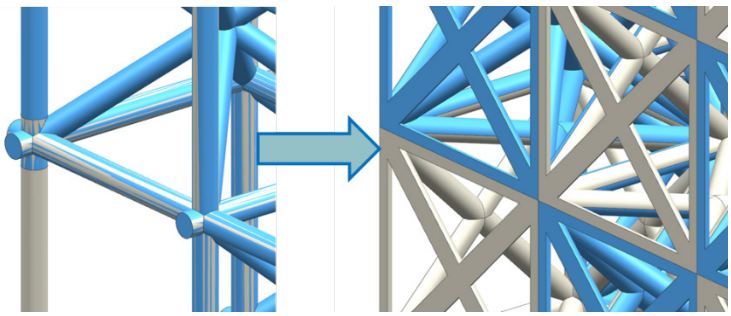
Following (202, 203) good practices from pioneering scaffolding libraries, applicable AMTs are considered for designing the CAD models and achieving optimal performance. The design for additive manufacturing approach, in this study, takes into consideration current limits and expectable mid-term progresses, in terms of precision, resolution and printable materials, of the AMTs most relevant for advancing in tissue engineering and biofabrication. Therefore, the additive photopolymerization of (bio-)photopolymers and ceramic slurries, using digital light processing and lithography-based ceramic manufacturing, and technologies employing bio-inks like, single and multi-nozzle inkjet printing, PolyJet printing and syringe-based bioprinters, are central to this research. To some extent, the features of polymeric and metallic selective laser sintering / melting, laser stereolithography and fused-deposition modelling, as widespread ATMs, are also considered. Two-photon polymerization is also borne in mind, as current gold standard in terms of achievable precision and resolution.

In consequence, the library is constructed to provide enough versatility to challenge the mentioned technologies and to evaluate new biomaterials processable through them. For three-dimensional lattices, with few exceptions, unit cells of 10 x 10 x 10 mm^3 are employed, which provide user-friendly and truly three-dimensional cell culture environments with an overall volume adequate for analyzing their applicability to the treatment of relevant tissue defects. Design for printability leads to selecting cylindric interconnecting (in fact intersecting) struts or trusses to arrange unit cells, whose spatial replication leads to the actual tissue engineering scaffolds. According to the current state-of-the-art and foreseeable advances in terms of precision and resolution, for the mentioned technologies and printable volumes, cross-sectional diameters of 250 µm, 500 µm and 1000 µm are used for the interconnecting elements. Only for the more conventional "woodpile" structures, common of fused deposition modelled scaffolds but also fabricable through additive photopolymerization tools, square cross-sections of 400 µm x 400 µm are chosen, taking account of the dimensions typically

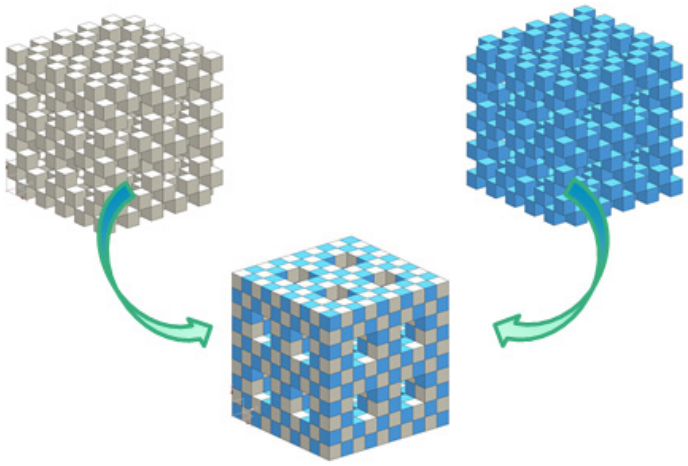
printable with polymeric extruders. Piled cylinders would contact the adjacent cylinders in a single point, while the square cross-sections improve the contact area and structural integrity of such woodpile structures. Normally, the porosity of scaffolds from the library reaches values between a 75% and a 99%, in agreement with recommendations from project's clinicians. Again, the woodpile structures make an exception, reaching lower values of porosity down to a 50%. When dealing with the design for multi-material printing of more complex tissue engineering constructs, and with the design of textures and their incorporation to scaffolds' surfaces, special considerations summarized in Figure 13 are taken.

In short, the nominal unit cells are used, to avoid printability problems. Voxel-based and pixel-based design procedures also help to optimize printability and to reach the technological limits, especially for inkjet and PolyJet processes, for which pixels of 40 x 40 μm^2 to 250 x 250 μm^2 and voxels of 40 x 40 x 40 μm^3 to 250 x 250 x 250 μm^3 are employed, according to the features of technologies available within our team. In any case, the subsets of geometries that compound the library are shared both as directly printable objects (i.e. stl files) and as editable files, including the original NX files, as well as translations to other common CAD software (please see Section 4.3.2). Therefore, future users of the OS library may benefit from the parametric design style followed and hence fine-tune the different geometries to their particular purposes and according to the precision and resolution of the technologies and materials under evaluation.

(a)



(b)



(c)

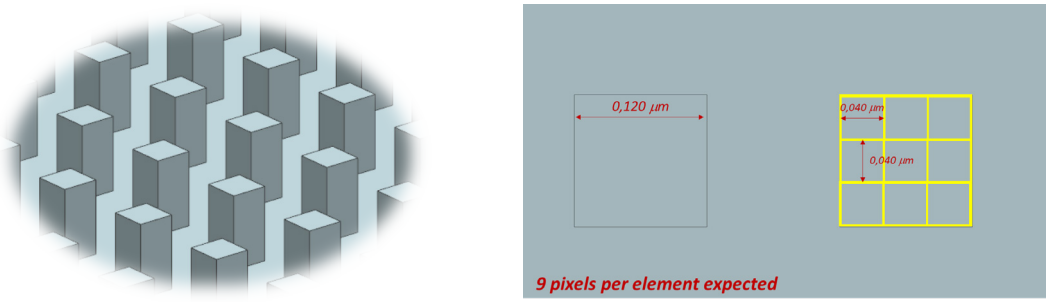


Figure 13: Design for multi-material printability considering varied AMTs: (a) Employment of nominal unit cell connection, instead of extended unit cell connection, to avoid printability problems in multi-material lithography based ceramic manufacturing. (b) Voxel-based design approach for achieving multi-material and functionally-graded constructs and scaffolds through multi-nozzle inkjet printing or PolyJet -based machines (i.e. Stratasys' Connect systems). (c) Pixel-based design approach for textured surfaces to optimize precision according to machines' resolution (i.e. for digital light processing and lithography-based ceramic manufacturing).

4.2. CAD modelling of the library

To facilitate the applicability of the OS scaffolds library and scaffolds selection processes, in fact biomaterials selection processes for tissue engineering and repair, the performance of the geometries from the library is evaluated with the support of finite-element method (FEM) based simulations. These evaluations lead to the creation of design maps related to those from Ashby's methodology (160) and like well-established methods for comparing lattice structures additively manufactured (160, 205, 206, 207, 208, 209). The scaffolds from the library are evaluated following approaches from previous studies (160, 205, 206, 207, 208, 209, 214) with some modifications, as summarized, below and considering relevant geometrical, mechanical and fluidic properties.

Geometrical properties are evaluated with CAD modelling tools for measuring the real surface (Sr) and the real volume (V_r) of the employed lattices. Dividing by the lattice's nominal volume (V_n = L x L x L for cubic unit cells, usually the previously mentioned 10 x 10 x 10 mm^3) allows obtaining the surface to volume ratio (SA:V = S_r/V_n) and the relative density ($\rho_r = V_r / V_n$) of each designed scaffold.

Regarding mechanical properties, relative compression modulus (E_{cr}) and relative shear modulus (G_r) are calculated. For evaluating the compression modulus (E_c) of each scaffold, a vertical force (F along –Z direction) is applied as loading condition in the FEM, which corresponds to an equivalent compression stress (σ_c) equal to F / L^2. Vertical mean displacement (δ) of the scaffold's face, to which the compression load is applied, leads to an equivalent longitudinal deformation (ε_l) equal to δ / L. The division of these quantities leads to the equivalent compression modulus: $E_c = F / (L \cdot \delta)$, which is relativized dividing by the compression modulus of the bulk (E_b) material employed for manufacturing the scaffold: $E_{cr} = E_r / E_b$. A similar procedure applies to the calculation of G_r, but with F and δ along X or Y direction (parallel to the upper face of the scaffold), which leads to $G = F / (L \cdot \delta)$ and $G_r = G$

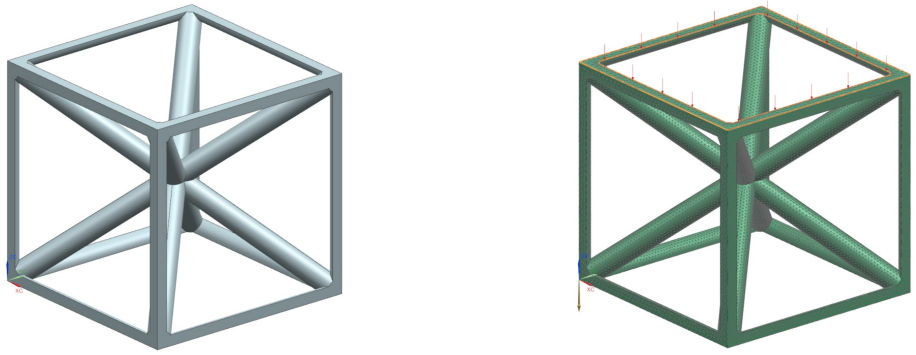
/ G_b with G_b the shear modulus of the bulk material additively processed. The FEM capabilities of Siemens NX 2206 are employed for these calculations.

FEM simulations (for example Figure 14 and Figure 15) are performed as follows: "NX Nastran Structural" solver is used, and the solution is considered linear static (SOL 101). 4-node and 10-node tetrahedral elements are applied for meshing and a sensitivity analysis using progressively smaller elements and the two form functions mentioned is performed (Figure 16 and Table 14). In the end, choosing at least 4 elements along the thickness of scaffolds' trusses leads to stable results. Together with the previously described loads, the faces opposite to those where the loads are applied are fixed. Simulations are performed with compression or shear forces of 10 N, 1 N and 0.1 N, depending on the actual scaffolds' geometries, to stay always in the elastic region, where the linear static solution is applicable.

As regards fluidic properties of the scaffolds, these affect cells' access to nutrients, elimination of debris and may even provide interesting levels of shear forces upon cells, that contribute to their well-being and recreated biomimetic cell culture environments. In connection with the actual mechanical properties of the scaffolds, described above, they are relevant in mechanobiological terms. Previous studies have dealt with the calculation of the permeability of additively manufactured lattices (215, 216, 217), which is connected to the flux vector, to the pressure gradient and to the viscosity of the fluid, according to Darcy's equation.

Here, a similar procedure is applied (Figure 17), although results are presented as pressure drop across the scaffolding geometries as a variable of inlet and outlet velocities, which proves useful for micro-pumping selection purposes and for the evaluation of shear stresses upon cells, as quantity directly related to fluid velocity that affects mechanobiological issues and cellular responses in culture. To summarize the computational fluid dynamics approach, the features of "NX Nastran Thermal-Flow" FEM solver with steady state solution are employed. A control volume is defined by subtracting scaffold's geometry to a channel of 30 x 10 x 10 mm^3 and the obtained geometry is discretized using 4-node and 10-node tetrahedral elements, as described above. Water is applied as material. Inlet and outlet velocities of 0.2 mm/s, 1 mm/s, 3 mm/s and 5 mm/s are used as boundary conditions, hence covering typical values employed for culturing cells with Reynolds numbers well below 2.000 corresponding to laminar flow conditions.

(a)



(b)

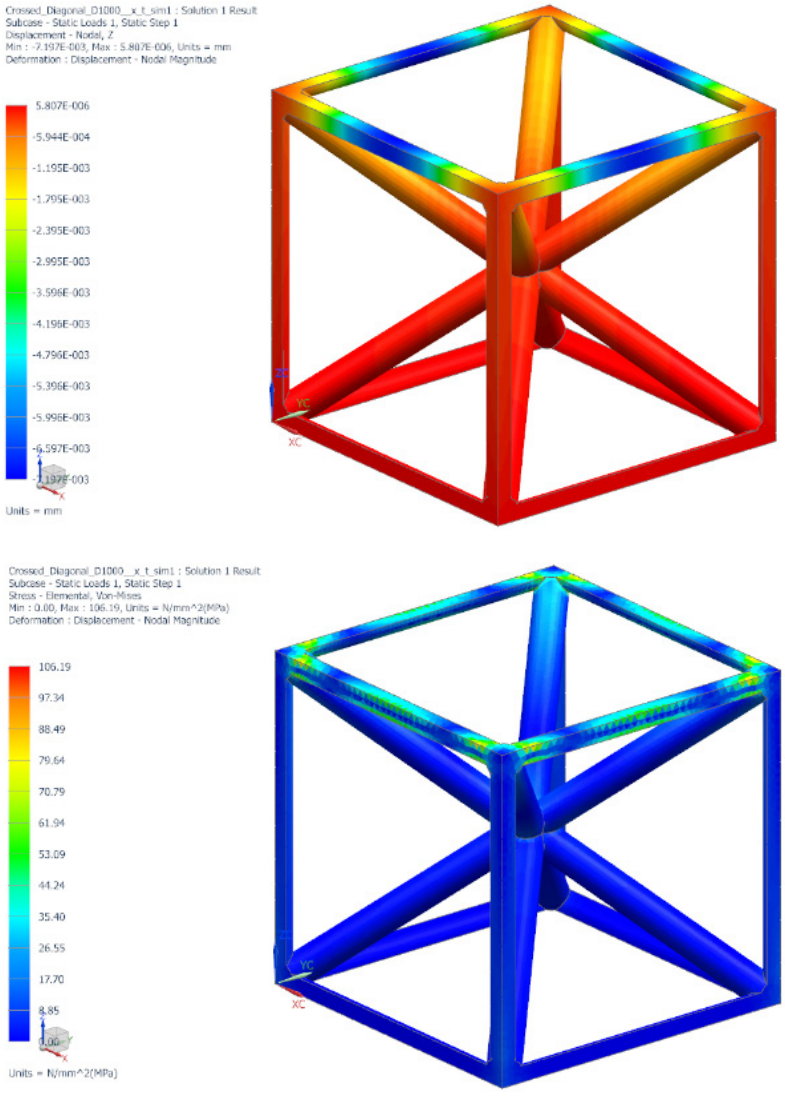
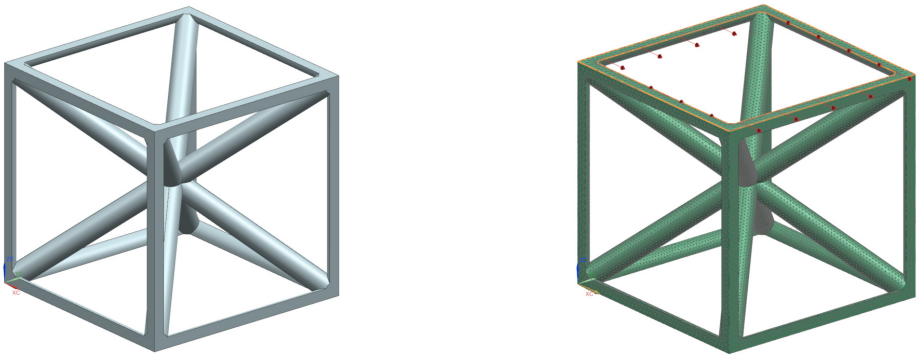


Figure 14: Example of finite-element model for evaluating the mechanical properties of a tissue engineering scaffold: Evaluation of Young's (compression) modulus. (a) Unit cell, mesh, loads and boundary conditions applied for compression study. (b) Resulting stress and displacement fields leading to the calculation of compression modulus.

(a)



(b)

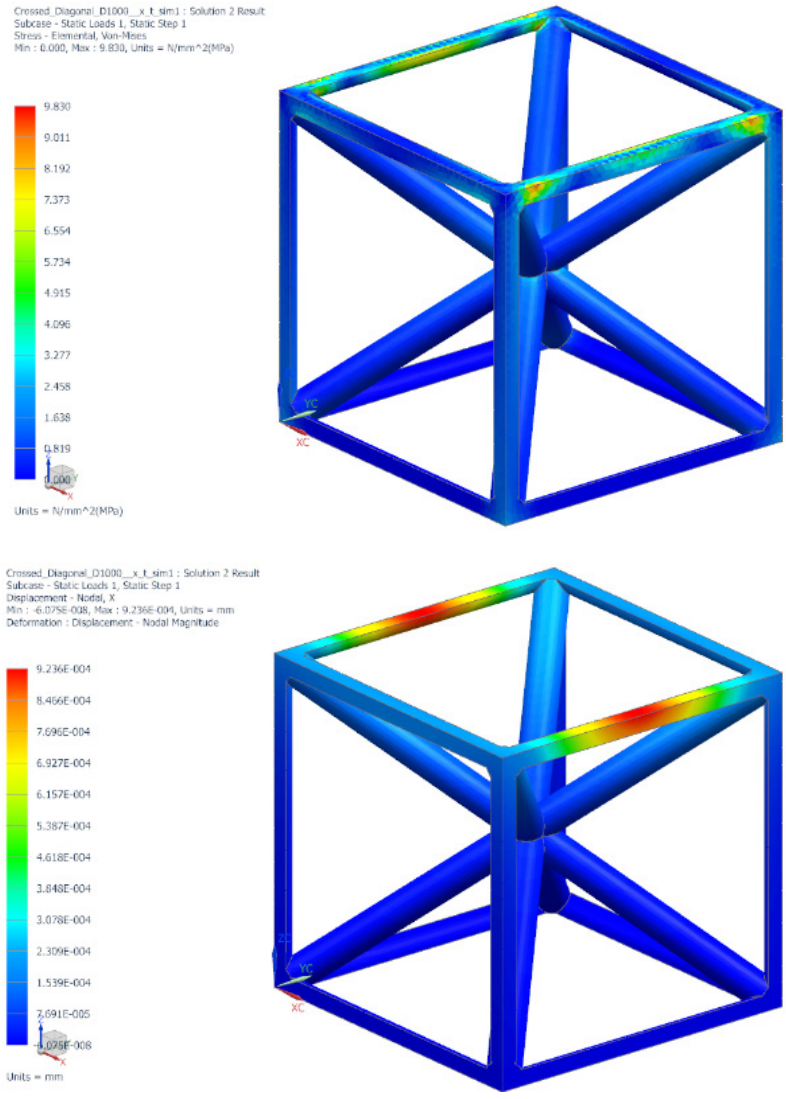


Figure 15: Example of finite-element model for evaluating the mechanical properties of a tissue engineering scaffold: Evaluation of shear modulus. (a) Unit cell, mesh, loads and boundary conditions applied for shear study. (b) Resulting stress and displacement fields leading to the calculation of shear modulus.

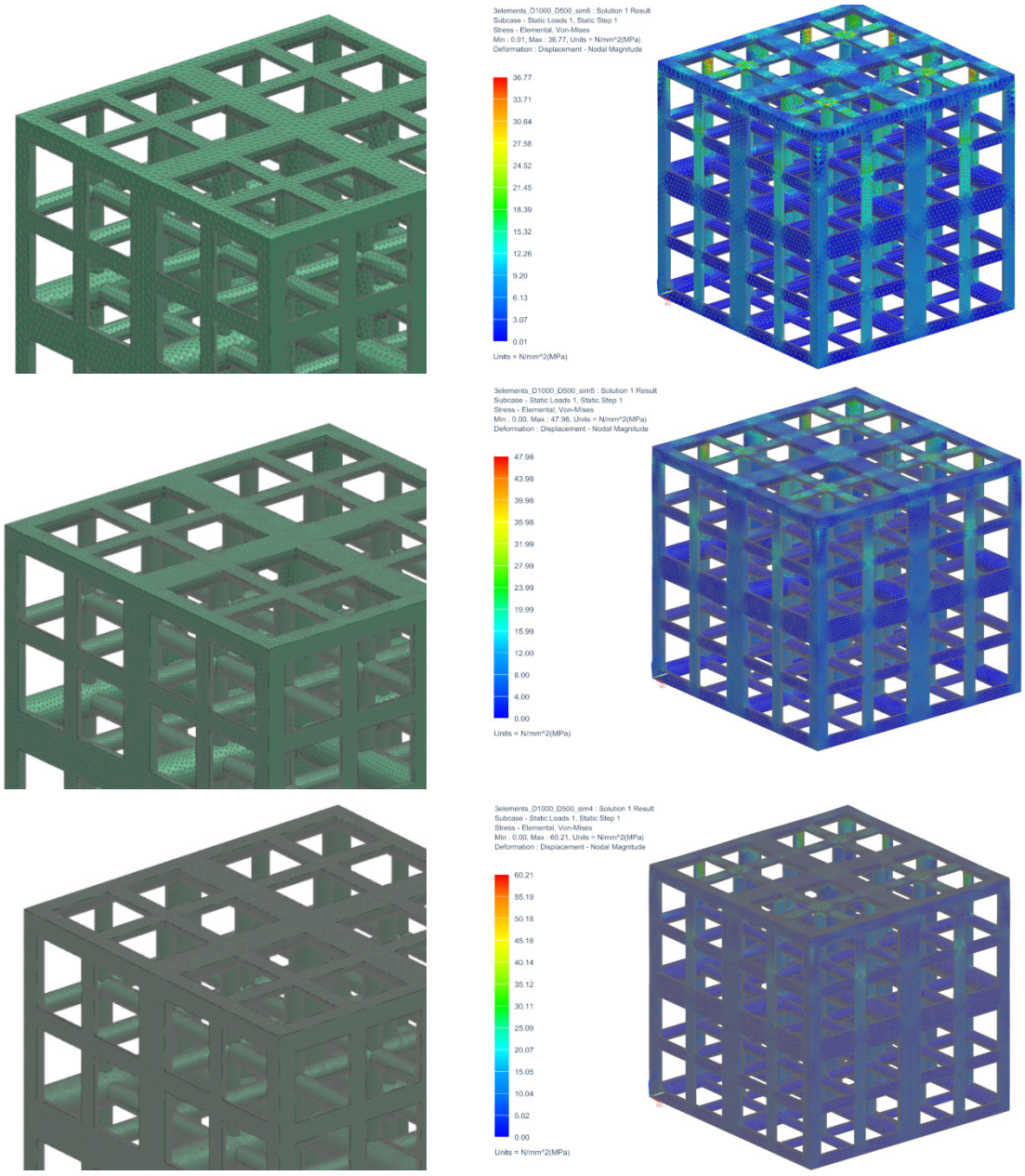


Figure 16: Example of sensitivity analysis performed to select the adequate mesh size.

Form function	Mean element size	Displacement along z (mm)	Max. Stress (Von Mises) (MPa)
Tetra_4	0.25	0.038057	10.7193
	0.125	0.0377248	11.9973
	0.0625	0.0380225	12.9852
Tetra_10	0.5	0.0376422	9.68202
	0.25	0.0380863	10.8424
	0.125	0.0381583	12.1944

Table 14: Results from sensitivity analysis

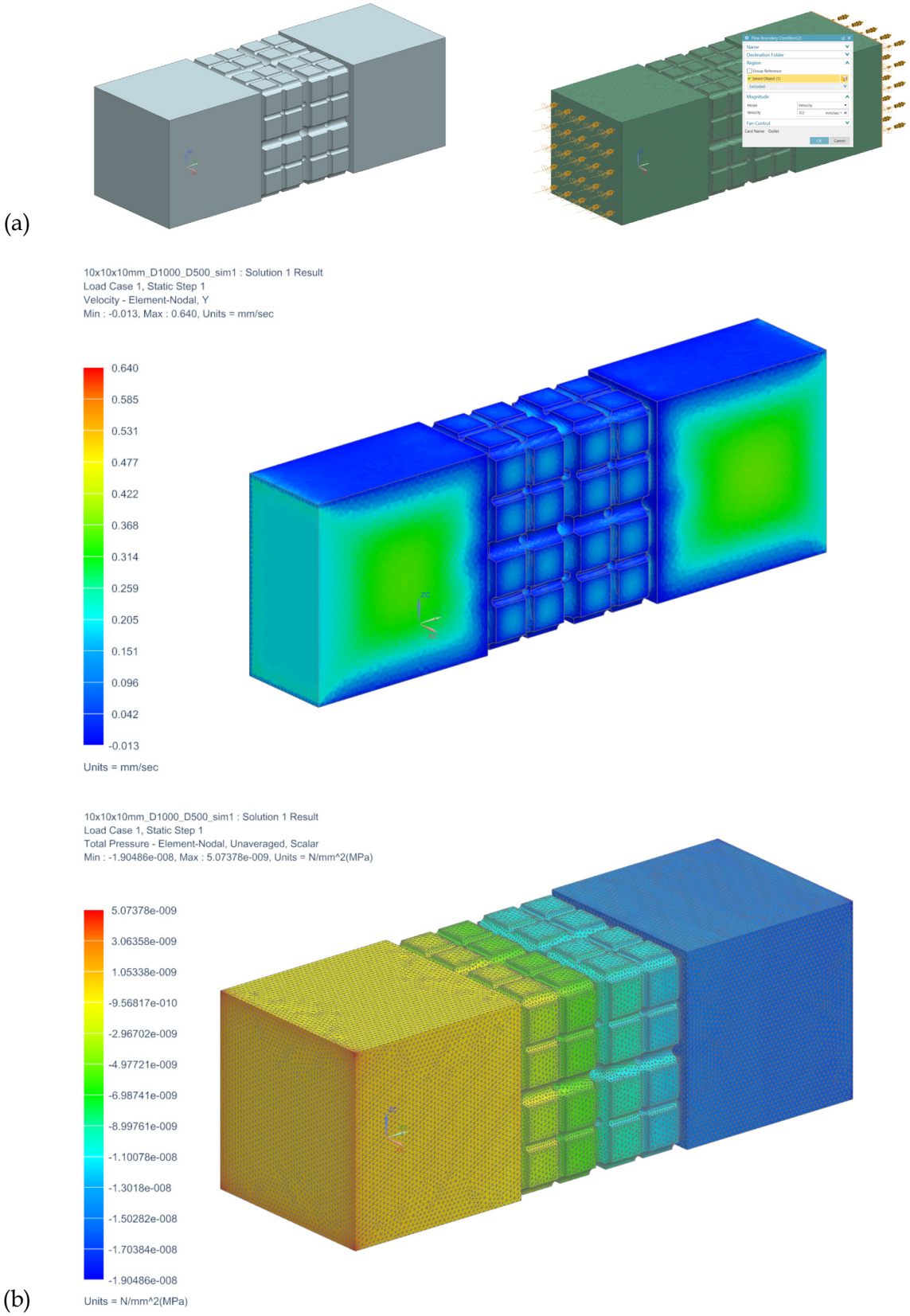


Figure 17: Example of finite-element model for evaluating the fluidic properties of a tissue engineering scaffold. (a) CAD and FEM model with control volume, mesh and boundary conditions. (b) Resulting velocity and pressure fields leading to the evaluation of performance.

4.3. Evaluation of properties

4.3.1. Library of tissue engineering scaffolds: property charts and design guidelines

A total of 24 lattices, divided in "periodic", "woodpile" and "multi-scale" or "fractal" have been included in the library. Periodic ones are based on usual Bravais lattices with applicability in tissue engineering or modifications thereof, including basic cubic structures, cubic face centered geometries, cubic body centered geometries and combined cubic with body and face centered features. Cross-sectional diameters of 250 µm, 500 µm and 1000 µm (further referred to as D250, D500, D1000) are used for the diameters of their trusses, which cover typical cross-sectional dimensions of bone trabeculae and are in agreement with the achievable features with high-performance AMTs. Woodpile structures are designed following well-known examples of scaffolding geometries obtained by fused-deposition modelling, considering trusses with square cross-sections of 400 µm x 400 µm^2, well-adapted to common dimensions of extruded filaments. Multi-scale or fractal structures are achieved by increasing the number of unit cells in the nominal volume of 10 x 10 x 10 mm^3 used for all lattices or by recursive self-similar design operations leading to microlattices within the original periodic lattices.

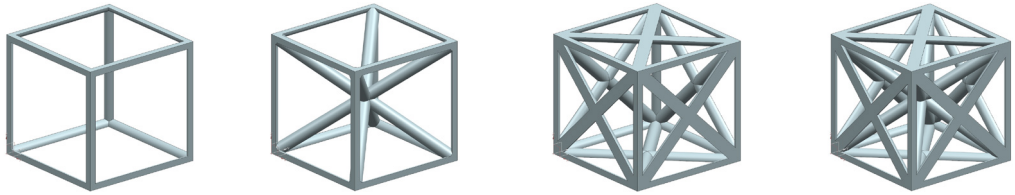
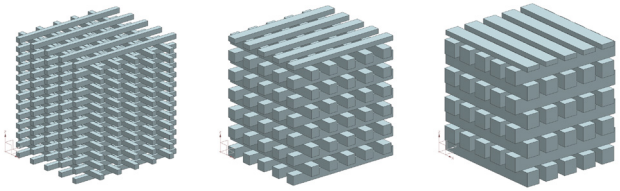
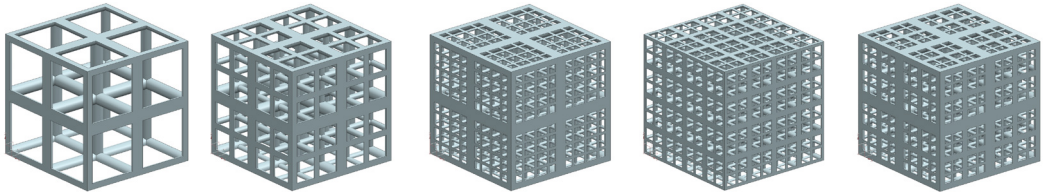
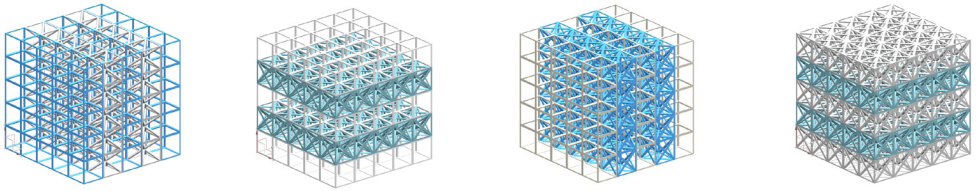
Combinations of the mentioned geometries lead to more complex three-dimensional networks conceived for achieving functional gradients of mechanical properties and for taking benefit of multi-material and multi-scale printing. The possibilities are almost endless, but a selection of 15 geometries is incorporated to the library to illustrate the achievable features. These are complemented with 7 additional voxel-based designs, oriented to multi-nozzle inkjet printing, in which voxels of 250 x 250 x 250 µm^3 and 500 x 500 x 500 µm^3, according to precision of available PolyJet systems are employed.

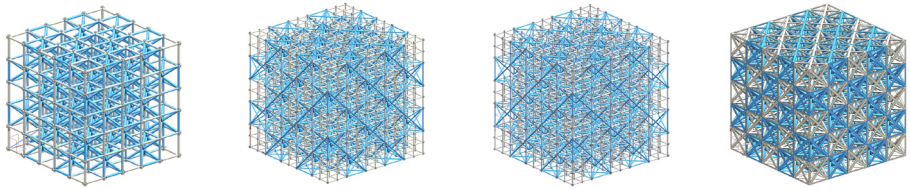
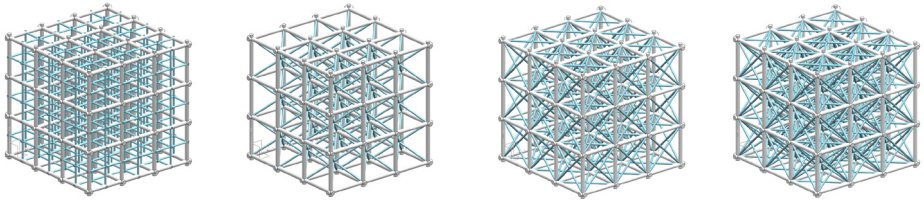
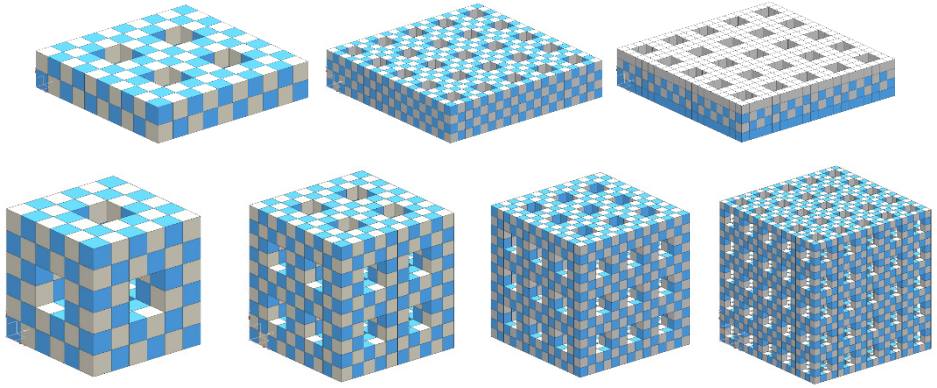
Selected geometries from the library are summarized in Table 15 below, which also highlights the most adequate AMTs for printing the different families of geometries. It can be appreciated that the library provides viable options for almost all types of currently available printing technologies with application in the biomedical field and in the tissue engineering and biofabrication sectors. The most precise designed features try to bring different technologies and materials beyond the current state-of-the-art limits, in terms of precision and resolutions, but feasible solutions for standard and affordable systems are also included. In this way, the library can constitute a versatile supporting collection for all types of researchers in the field, from those more focused on cell-material interactions, to those concentrated on the development of more precise technologies and materials with higher resolution.

Mechanical and fluidic FEM simulations, according to already described methods, lead to the design / characterization maps from Figure 18 to Figure 24. These allow for materials selection tasks and, being normalized by the bulk material's properties employed the simulations, the actual performance of printable materials can be predicted and fine-tuned for enhanced biomechanical performance, depending on the actual mechanical properties of the tissues being repaired. The fluidic maps help with pump selection tasks for dynamic cell culture in

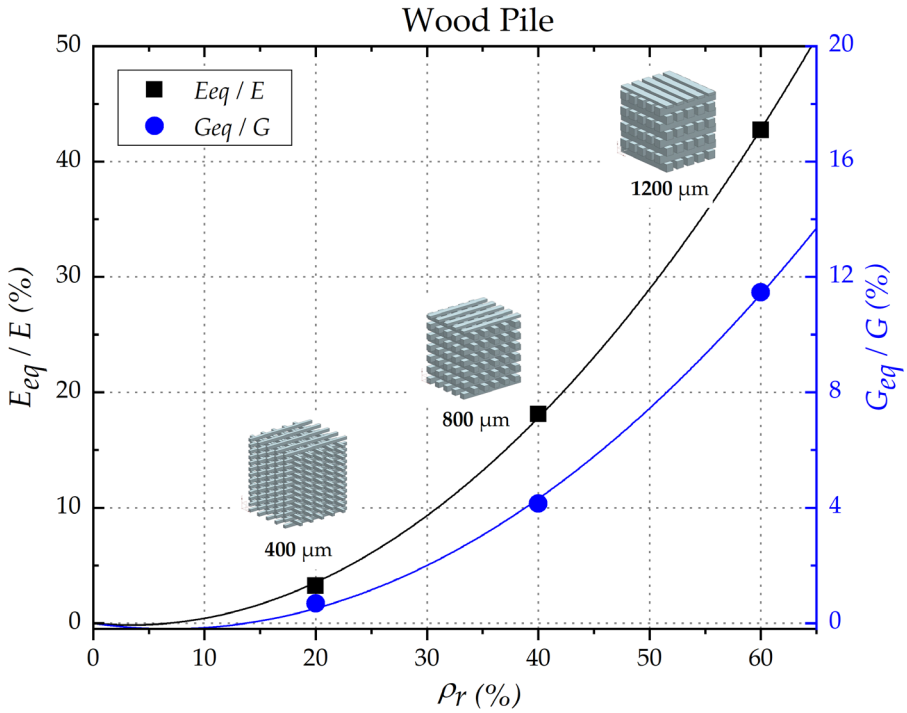
bioreactors. Properties including relative Young's (compression) modulus (E_r), relative shear modulus (G_r), E_r/G_r ratio, relative density (ρ_r), exposed surface (S_r), and pressure drop across the scaffolds for different fluid speeds are reported for all mono-material samples of the library. According to already mentioned Ashby and Egan's methodologies, these maps support the selection of unit cells, to be subsequently applied to the actual implants' geometries, either using Boolean and other common CAD tools or by applying conformal lattice design methods. In the end, biomimetic and biomechanical implant design personalization are fostered.

Table 15: Summary of geometrical families with selected examples from the open-source library of tissue engineering scaffolds. *Suboptimal technology for printing the selected geometries (other geometries may work better). **Better avoided although printable. Acronyms: FDM – fused deposition modelling, SLA – laser stereolithography, DLP – digital light processing, LCM – lithography based ceramic manufacture, LMM – lithography based metal manufacture, SLS – selective laser sintering, SLM (PBLF) – selective laser melting / (powder bed laser fusion), 2PP – two photon polymerization.

Materials	**Geometries**	**Selected images as examples from the OS library**	**Applicable technologies**
Mono-material scaffolds	Periodic unit cells or lattices		SLA, DLP, 2PP, LCM, LMM, inkjet printing*, SLS*, SLS*, SLM*, FDM**, bioprinting**
	Woodpile structures		FDM, bioprinting, inkjet printing, SLA*, DLP*, LCM*, LMM*, SLS*, SLS, SLM*, 2PP**
	Multi-scale / fractal lattices		SLA, DLP, 2PP, LCM, LMM, inkjet printing, SLS*, SLS*, SLM*, FDM**, bioprinting**
Multi-material (MM) scaffolds	Combined lattices for graded designs		Bimaterial LCM, multi-nozzle inkjet printing*, MM SLS*, MM SLM*, MM FDM**, MM bioprinting**

Multi-material (MM) scaffolds	Combined unit cells with the same scale		Bimaterial LCM, DLP with movable vats, multi-nozzle inkjet printing*, MM SLS*, MM SLM*, MM FDM**, MM bioprinting**
	Combined unit cells at different scales		Bimaterial LCM, DLP with movable vats, multi-nozzle inkjet printing*, MM SLS*, MM SLM*, MM FDM**, MM bioprinting**
	Pixel- or voxel-based designs		Multi-nozzle inkjet printing, bimaterial LCM, MM bioprinting(*), MM SLS*, MM SLM*, MM FDM**, DLP with movable vats

Visual inspection of the characterization maps below helps to verify that, in general, denser networks lead to higher mechanical moduli. As previously mentioned, current OS library from tissue engineering scaffolds works with higher porosity ranges than lattices employed in other studies for lightweight design enabled through additive manufacturing. Here, scaffolds move in the porosity range of 75% to almost 99% (except for the denser woodpile structures), hence the typical values obtained for E_r and G_r are usually lower than a 10%, in many cases lower than a 1%, for most geometries of the library. The manufacture of designed geometries employing a wide set of printable materials, from polydimethylsiloxane (PDMS), bioinks, hydrogels and photopolymers, to alumina, zirconia, tricalcium phosphate and hydroxyapatite, to cite some examples, can cover the whole mechanical property range of literally all human tissues. Among remarkable results from the design maps, it is interesting to mention the impact of employing multi-scale and fractal designs for increasing both mechanical properties and exposed surface and surface to volume ratios. Its impact on pressure drop across the scaffolds is also relevant, which should be considered for pump selection purposes and may affect access to nutrients and elimination of debris. However, this shadowing effect is less important than in more common woodpile structures with similar mechanical performance, which puts forward the interest of biomimetic fractal-like designs.



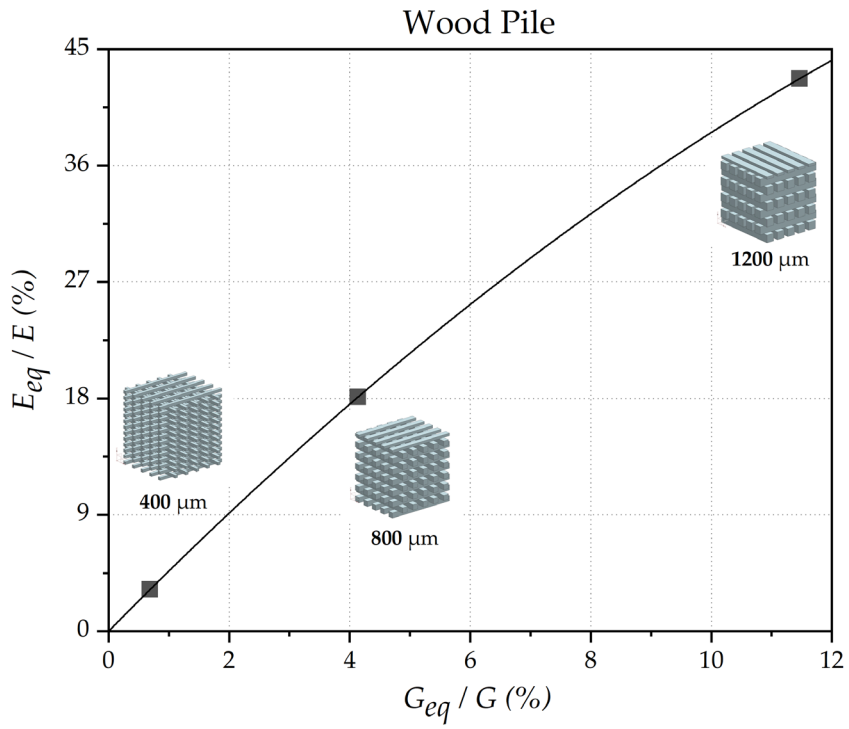
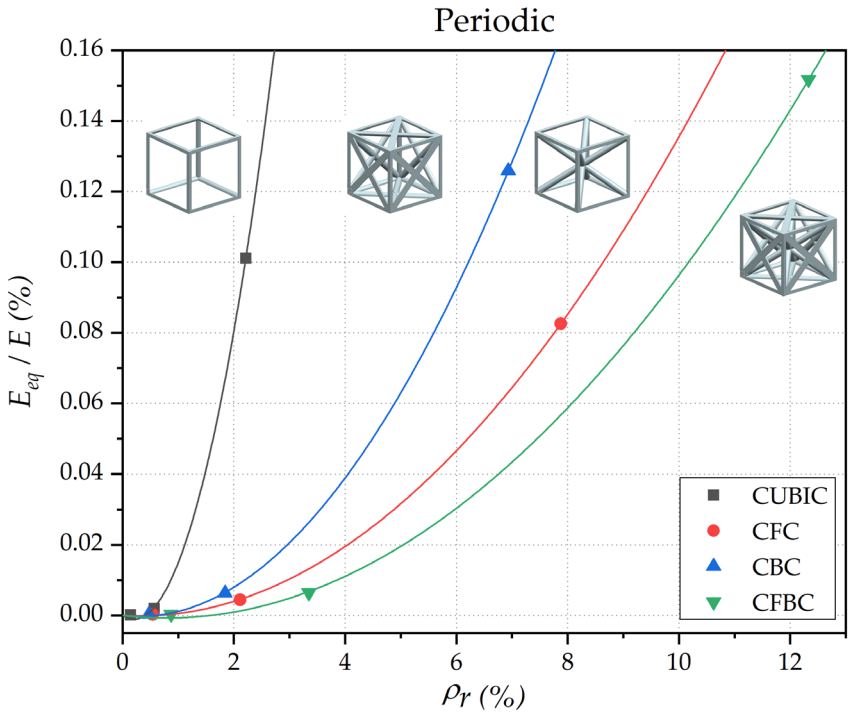


Figure 18: Mechanical properties of scaffolds with woodpile structure.



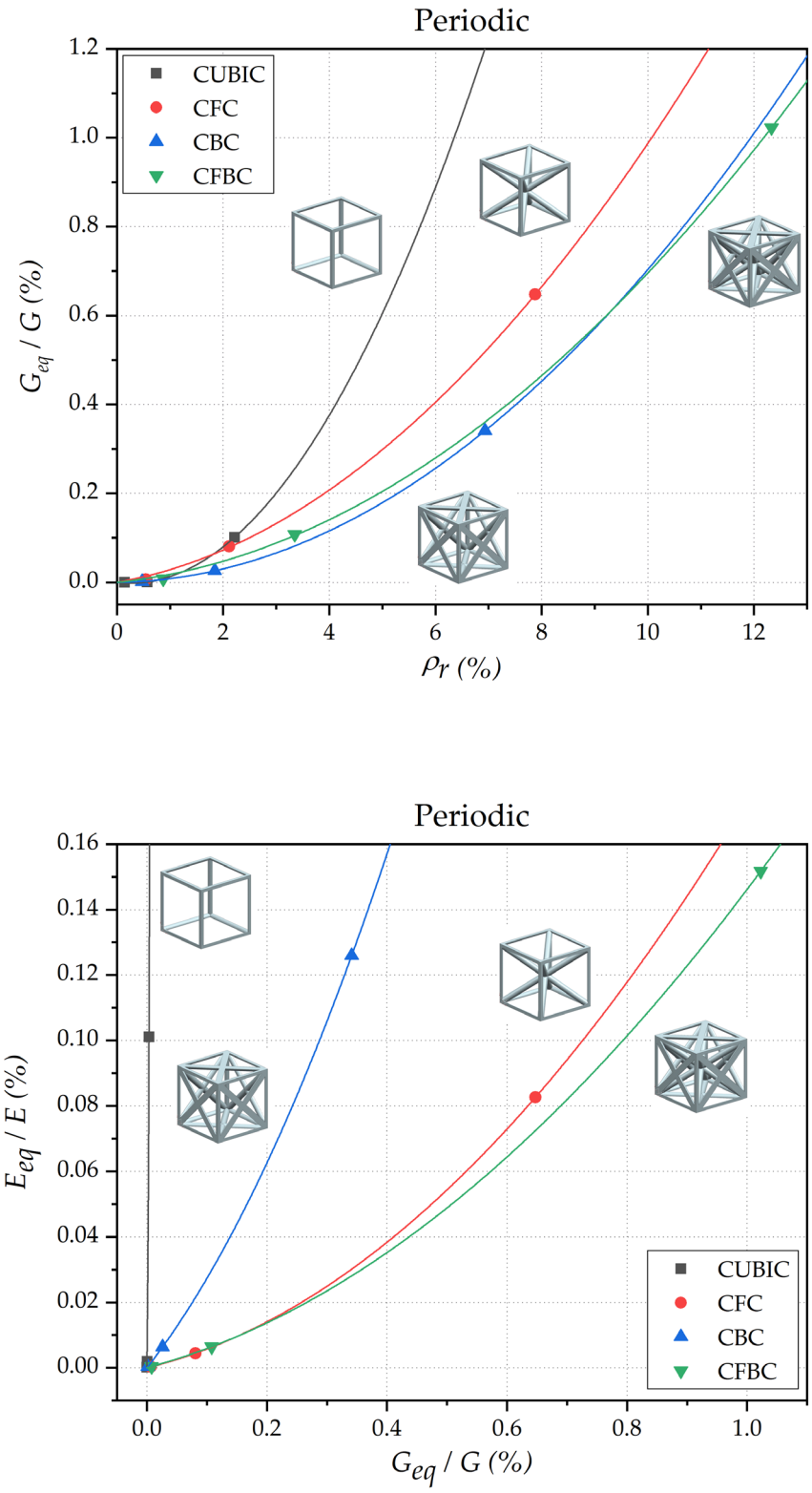
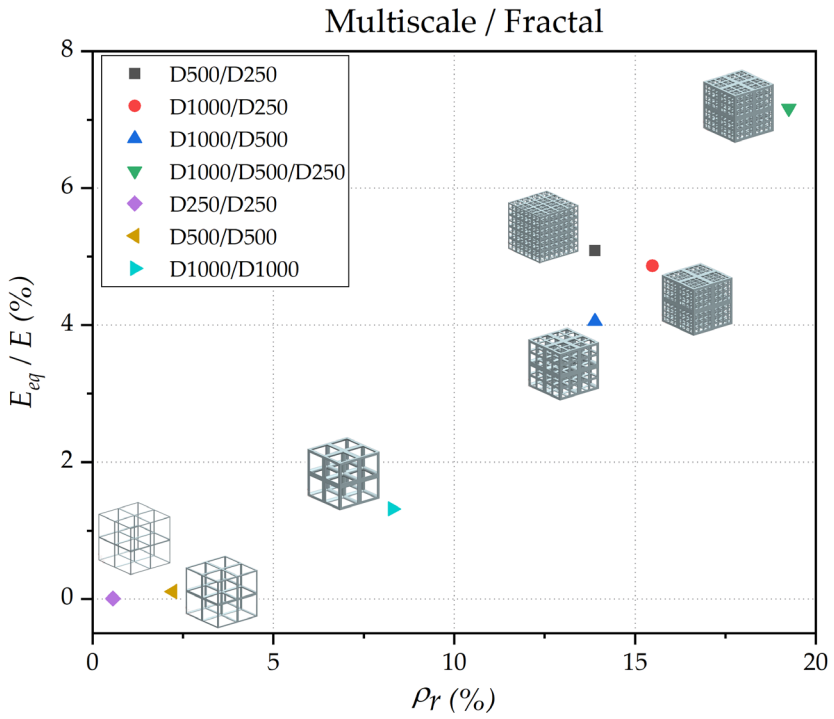
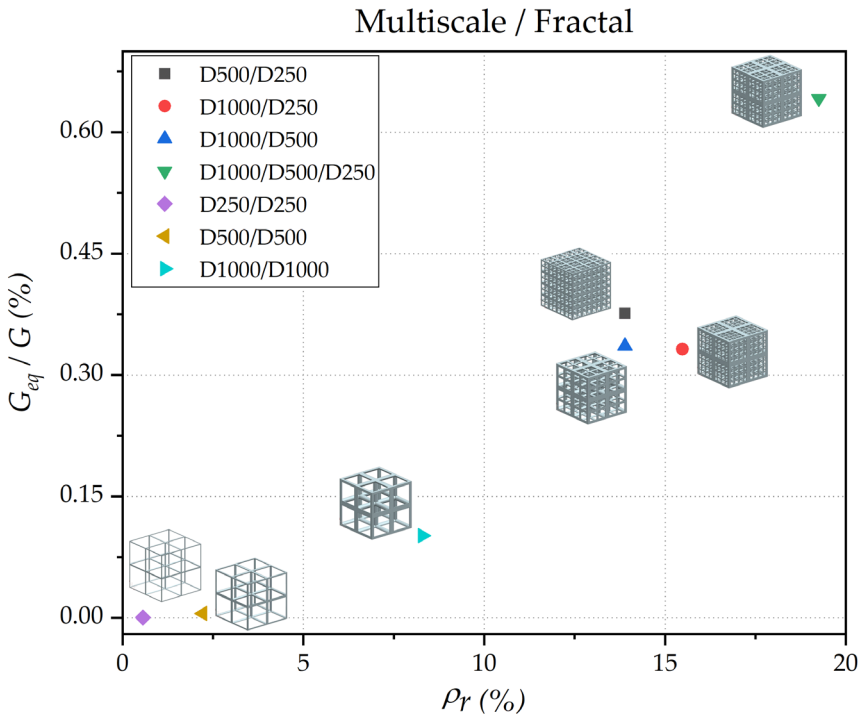


Figure 19: Mechanical properties of different unit cells employed for designing scaffolds.


Multiscale / Fractal
D500/D250
D1000/D250
D1000/D500
D1000/D500/D250
D250/D250
D500/D500
D1000/D1000
E_{eq} / E (%)
ρ_r (%)
0
2
4
6
8
0
5
10
15
20


Multiscale / Fractal
D500/D250
D1000/D250
D1000/D500
D1000/D500/D250
D250/D250
D500/D500
D1000/D1000
G_{eq} / G (%)
ρ_r (%)
0.00
0.15
0.30
0.45
0.60
0
5
10
15
20

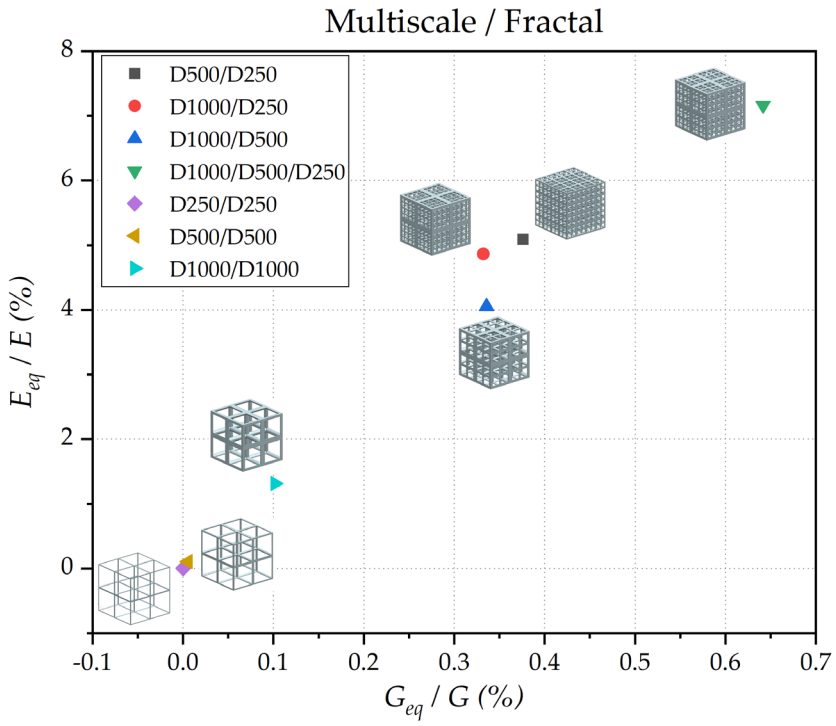
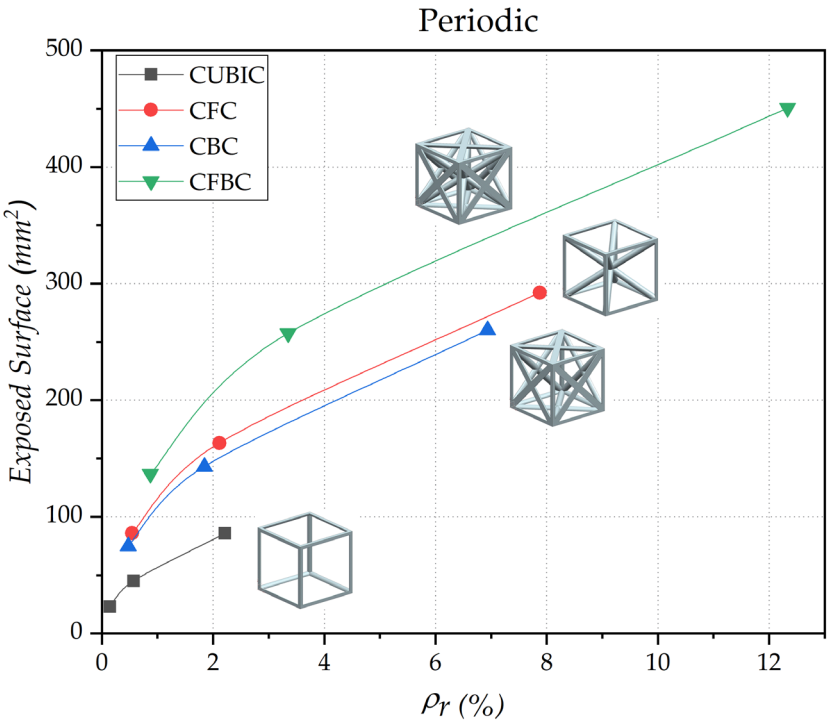


Figure 20: Mechanical properties of multi-scale / fractal scaffolds.



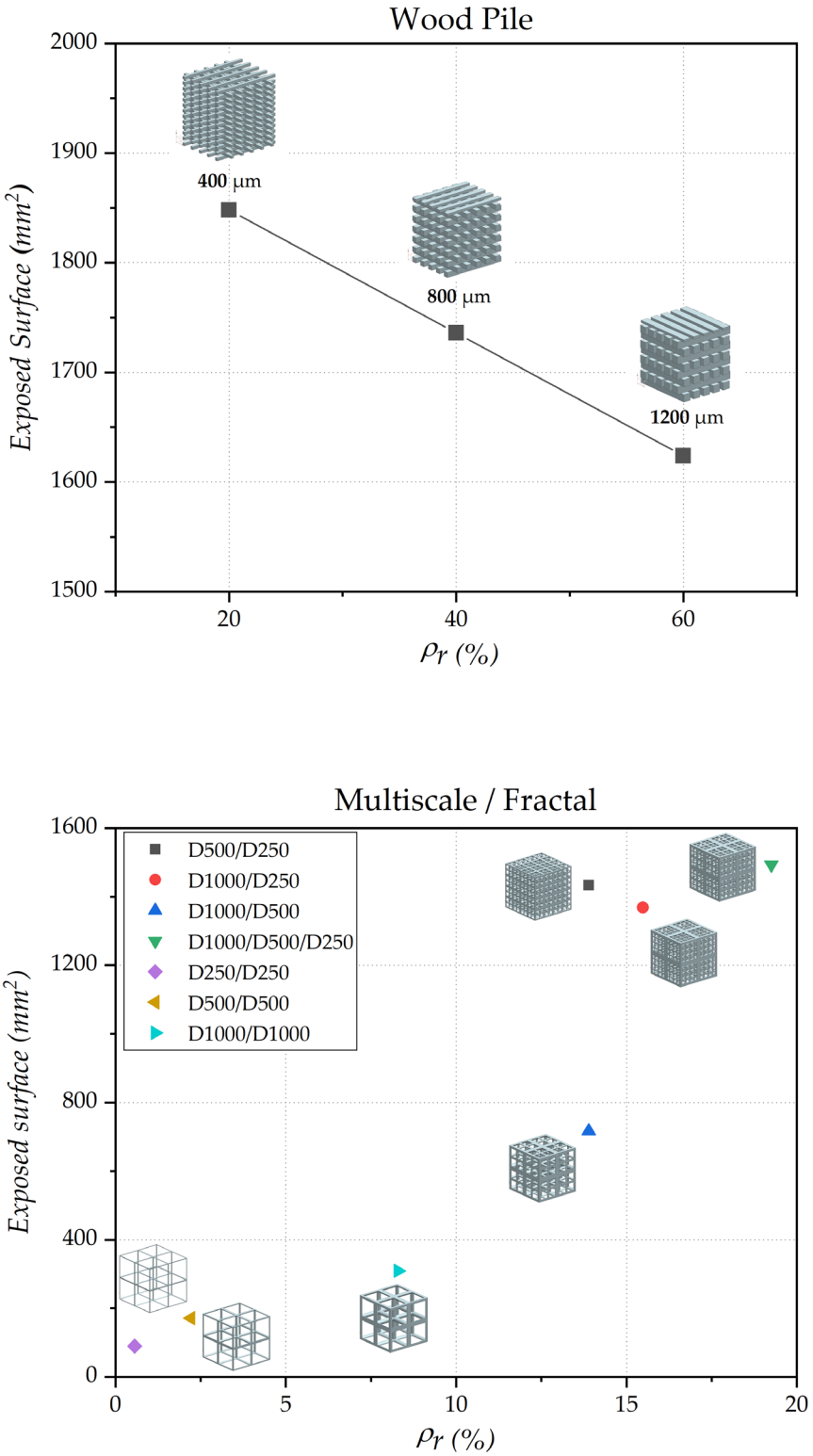
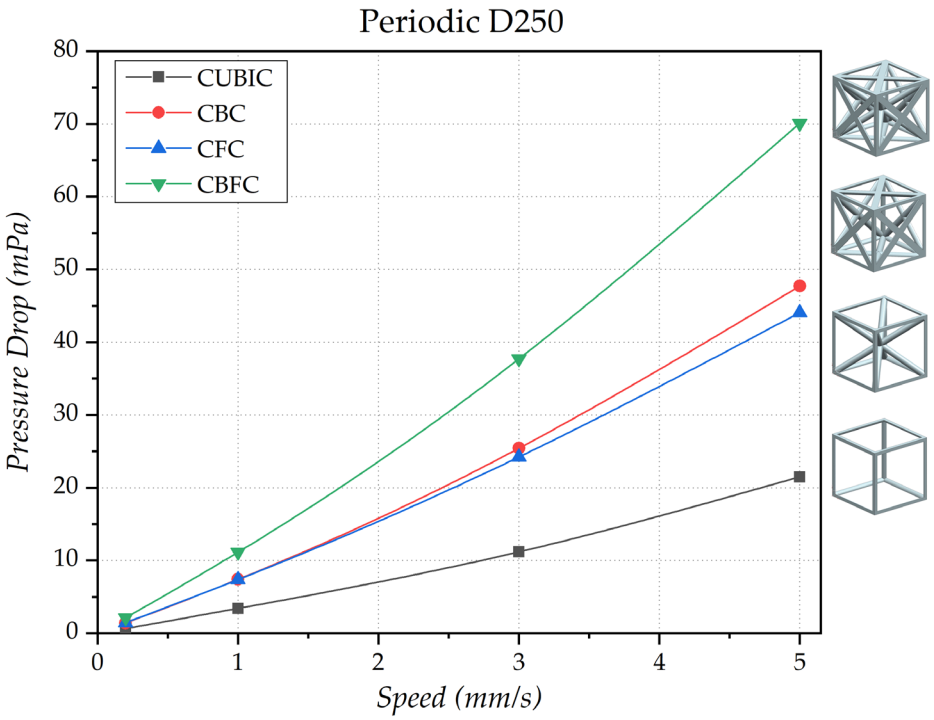
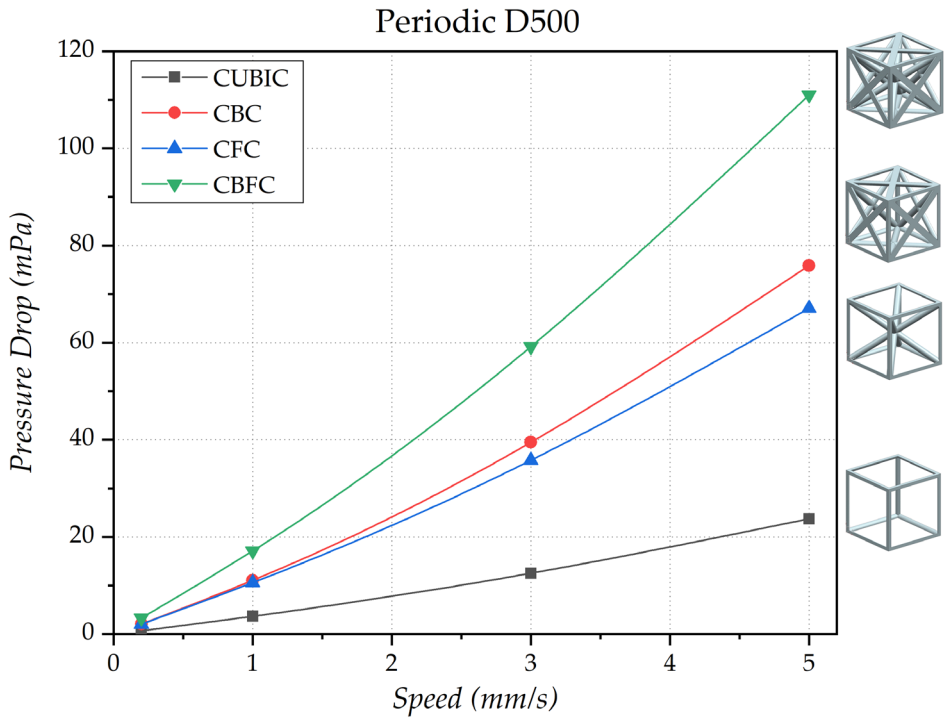


Figure 21: Exposed surface and relative density for different scaffolds' families.


Periodic D250
CUBIC
CBC
CFC
CBFC
Pressure Drop (mPa)
Speed (mm/s)
0
10
20
30
40
50
60
70
80
0
1
2
3
4
5


Periodic D500
CUBIC
CBC
CFC
CBFC
Pressure Drop (mPa)
Speed (mm/s)
0
20
40
60
80
100
120
0
1
2
3
4
5

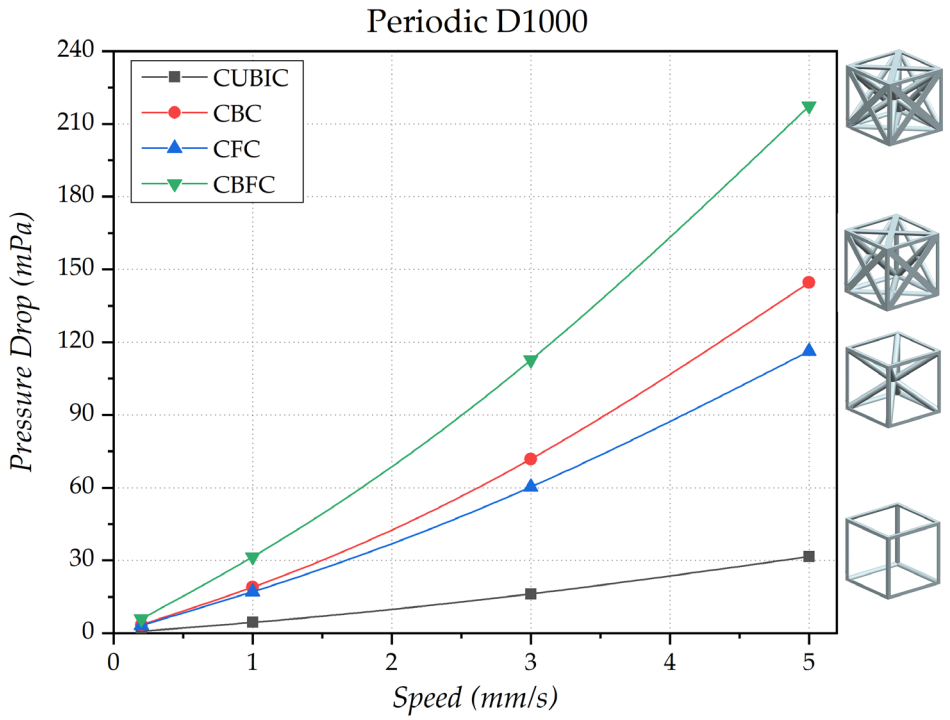


Figure 22: Fluidic performance of different unit cells employed for designing scaffolds.

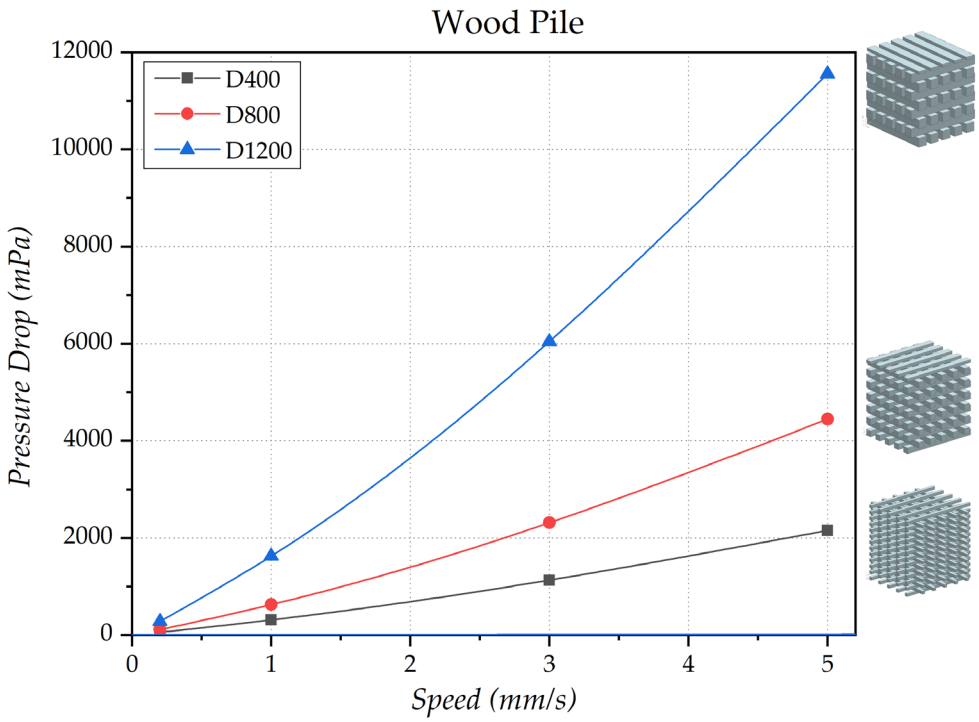


Figure 23: Fluidic performance of scaffolds with woodpile structure.

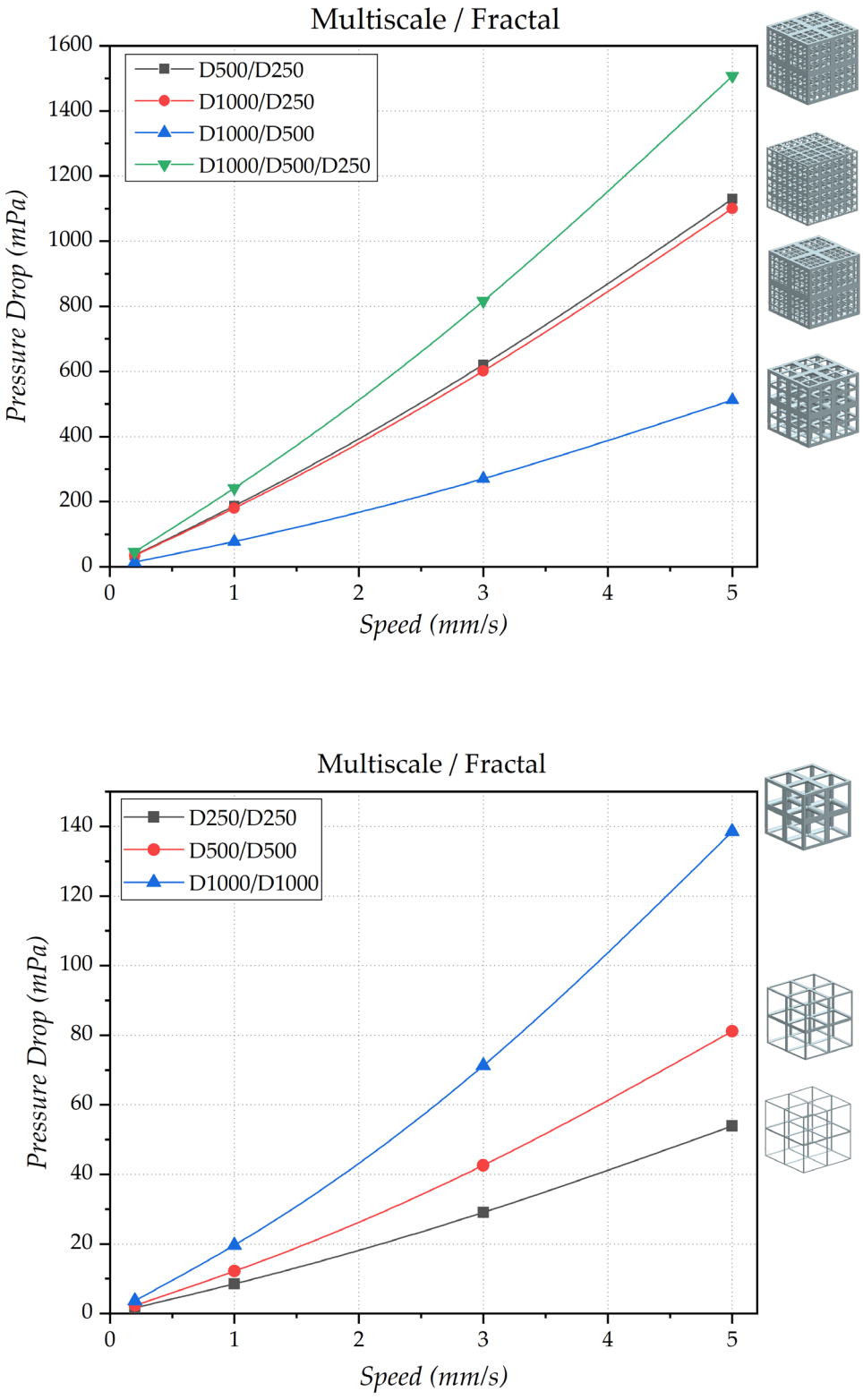


Figure 24: Fluidic performance of multi-scale / fractal scaffolds.

4.3.2. Fulfillment of FAIR data principles

To our knowledge, presented open-source library of scaffolding structures is the first one developed, documented and shared with FAIR data principles (88) in mind, as previously cited, which may constitute an interesting breakthrough towards standardization harmonization and accessibility in the tissue engineering field. Subsections below describe how findability, accessibility, interoperability and reusability are addressed.

Findability

Different ways to enhance the findability of the OS library of scaffolds are conceived. Together with sharing the library through widespread open online repositories with reliable search engines, as further described below (links in Section 4.5), the dissemination of present document and the communication measurements of ongoing projects will, arguably, contribute to making the library popular among practitioners and researchers in the field. When documenting in the selected repositories, different keywords and hashtags are used, including: tissue engineering, tissue engineering scaffolds, cell culture, regenerative medicine, biofabrication, bioprinting, open-source medical devices, implants, to cite some of them.

Accessibility

The OS library of scaffolds and related design maps and characterization data are made accessible through different online co-creation and open-science environments (Section 4.5), including: a) Thingiverse (https://www.thingiverse.com/), known for its connection to the maker movement and for being the key platform for sharing printable objects; b) Zenodo (https://zenodo.org/), a general-purpose open-access repository, developed under the European OpenAIRE program and operated by CERN, focused on open-science and making research and research data accessible; and c) UBORA (https://platform.ubora-biomedical.org/), a sort of "Wikipedia" aimed at fostering open-source medical devices and making them accessible, through which a community of c.a. 1000 medical technology developers from more than 40 countries collaborate. In all these environments, the OS library is freely accessible and the different scaffolds and geometries, together with their documentation, are downloadable. Besides, colleagues in the field, wishing to contribute and enlarge the shared resources and scaffolds, may join the team of developers within UBORA or Zenodo, which is expected to lead to future research collaborations.

Interoperability

A common limitation of CAD models shared through online environments is that the preferred format is stl, which is adequate for printing purposes, but suboptimal for redesign tasks, as normally the stl files are difficult or impossible to edit. In order to foster interoperability, together with the stl files, other CAD formats are also included in the online repositories that make the library accessible. Firstly, the original NX 2206 designs in editable prt or asm formats are provided, so that users can take benefit from the parametric design style employed. Secondly, for users of alternative CAD programmes, common formats like catpart or catproduct (for Catia v.5), ipt or iam (for Inventor), par or asm (for Solid Edge), and sldprt or sldasm (Solid Works), among others, are being incorporated to the library for additional

interoperability. Finally, an alternative to stl, as neutral file format, will be also provided by sharing stp or step files as well, trying to minimize data quality degradation.

Reusability

Together with the format considerations presented above, which also contribute to an adequate reusability, it is necessary to systematically document the shared CAD models and make such documentation accessible. The presented nomenclatures, design maps and manufacturing considerations from previous subsections are aimed at promoting the repeatability and peer-review of presented results, which in turn is expected to facilitate a more straightforward reusability of the designed scaffolds. A remarkable feature of sharing scaffold's unit cells is that they can be reused in state-of-the-art CAD programmes for performing matrix-based and Boolean operations for medical device design purposes. Furthermore, unit cells can be incorporated to topology optimisation software, with which conformal lattice design procedures may be performed for enhanced biomechanical performance of achieved solutions.

Finally, reusability is enabled thanks to the OS library being shared through a Creative Commons license (https://creativecommons.org/). In agreement with the definition of open-source medical devices, for this library a Creative Commons Attribution 4.0 International (CC BY 4.0) license applies. This means that users are free to: "share: copy and redistribute the material in any medium or format; adapt remix, transform, and build upon the material, for any purpose, even commercially; with the condition that proper attribution: appropriate credit to the developers and providing a link to the original license and files, is given". In this regard, "explicit attribution to the team of developers and acknowledgement to the funding received from the European Union's Horizon 2020 research and innovation programme, under grant agreement No. 953134", is asked to users of the library.

4.4. Conclusions and future proposals

Present chapter introduces one of the most relevant collections of tissue engineering scaffolds currently available. It has been developed following design for additive manufacturing strategies, includes systematic variations of parameters and is extensively documented with characterization maps, which facilitates the applicability of geometries and both materials and printing technology selection tasks. Besides, to PhD candidate best knowledge, it constitutes the first open-source library of tissue engineering scaffolds implemented with FAIR data principles in mind and shared as a collection of open-source geometries, including blueprints (CAD files in different formats) and design / characterization documentation, through remarkable open-science networks and co-creation environments like Thingiverse, UBORA and Zenodo. Designed scaffolds include periodic and functionally-graded (FG) lattices, as well as more advanced multi-scale, fractal and multi-material constructs, according to the complex geometries and materials-technologies' combinations required for emulating the intricate cellular microenvironments present in human tissues.

Together with porous geometries, networks and lattices, a collection of microtextured test probes is included for enabling cell-material interaction studies focusing on understanding the relationship between surface topography and cell fate. Their applicability to patterning the surfaces of 3D lattices, which is also illustrated through a set of microtextured scaffolds, increases the degree of versatility and utility of the developed open-source library. In addition, such extremely fine details are useful for analyzing the precision of printing technologies and the resolution of printable materials, as also happens with the multi-scale, fractal and multi-material designs. The OS library has already proven highly effective and practical for systematically and comparably evaluating the performance and limits of materials and technologies currently under development within INKplant EU project.

4.5. Open-source documentation

The open-source library of tissue engineering scaffolds and microtextured test probes and lattices is shared through the following co-creation and open-science environments:

Thingiverse, website dedicated to the sharing of user-created digital design files, widely used by the DIY technology and Maker communities:

- Thingiverse's homesite:

https://www.thingiverse.com/

- Open-source library of tissue engineering scaffolds:

https://www.thingiverse.com/thing:5333296

- Open-source library of microtextured geometries for studying cell-material interactions:

https://www.thingiverse.com/thing:5333456

UBORA platform, a universal "Wikipedia" of OSMDs:

- UBORA's homesite:

https://platform.ubora-biomedical.org/

- Open-source library of tissue engineering scaffolds:

https://platform.ubora-biomedical.org/projects/ba58012c-897b-487e-b8bd-3f7ffe0095e9

- Open-source library of microtextured geometries for studying cell-material interactions:

https://platform.ubora-biomedical.org/projects/17fe248a-d564-44c6-b8ba-e31cfc97b748

ZENODO general-purpose open-access repository developed under the European OpenAIRE program and operated by CERN:

- ZENODO's homesite:

https://zenodo.org/

- Open-source library of tissue engineering scaffolds:

https://zenodo.org/record/6387574#.YkGd5OdBxPY

- Open-source library of microtextured geometries for studying cell-material interactions:

https://zenodo.org/record/6387580#.YkGfGedBxPY

5. Rapid prototyping route for multi-material tissue engineering scaffolds

5.1. Overview of design process for rapid prototyping

The graded nature of human tissues asks for functional scaffolds with gradients of properties capable of biomimetically repairing injured or deteriorated tissues. These functionally graded (FG) tissue engineering scaffolds are of special relevance for promoting the personalized treatment of articular pathologies and osteochondral defects and, despite the multiple research directions explored, no solution is yet perfect. In this study an innovative approach for engineering design-controlled and FG scaffolds is presented. It stands out for combining hard-phase 3D printed lattices and soft-phase PDMS sponges or networks. The developed procedure is illustrated through two case studies: one dealing with the creation of PDMS and PDMS-PLA constructs, as chondral and osteochondral plugs; another focused on the prototyping of personalized PDMS-PLA/resin constructs, as scaffolds for the tissue engineering or repair of the meniscus. Promising potentials for the tissue engineering of complex-shaped and large-size osteochondral and meniscal defects are discussed, and a systematic description of future research directions is included.

Functionally graded scaffolds are becoming mainstream in tissue engineering, since most human tissues and organs are too complex to be restored with a single synthetic material or monolithic implant once damaged. More than a decade ago, pioneering studies dealing with FG-scaffolds reported the applicability of rapid prototyping and additive manufacturing technologies, such as fused-deposition modelling, 3D fiber deposition, inkjet printing or selective laser sintering, for achieving the complex geometries required for these graded constructs (218, 219, 220). Since then, most additive manufacturing technologies capable of processing biomedical polymers, ceramics, alloys and biomaterials have been applied to prototyping FG-scaffolds.

Currently, two main strategies for achieving the desired gradients coexist, one based on mono-material manufacturing of scaffolding geometries designed with gradients, the other based on multi-material combinations for producing scaffolds. Both strategies can be combined for additional versatility. As regards mono-material solutions, graded pore sizes or lattices with varying truss thicknesses can be straightforwardly achieved with CAD modelling resources and employed for mechanobiological studies (221). The use of triply periodic minimal surfaces (TPMS) with thickness variations has been also reported (222, 223). More recently, different additive manufacturing technologies for geometrically graded alloys and scaffolds have been reviewed (224). Concerning multi-material options, polymer-polymer composite scaffolds have been also reviewed (225) and the use of coatings and fillers is also a remarkable option towards FG-scaffolds (226). Stacked, bilayered, trilayered or multi-layered combinations of

materials are also an option, like trilayered combinations of CaP, cryogel and hydrogel for osteochondral repair (227). Recent advances combining both main strategies open the path towards digital biomaterials, with improved control of composition and properties at every point of the scaffolding construct (212).

Articular injures and osteochondral defects can clearly benefit from FG-scaffolds, due to the need for dealing with the repair and regeneration of various involved tissues with very relevant differences of mechanical properties and biochemical composition. The potentials of 3D printing, bioprinting and electrospinning for achieving adequate scaffolds with gradients of properties for osteochondral repair has been previously analyzed (228). Biomimetic bi-phasic and multi-phasic scaffolds have been also reported, as potential solutions for repairing cartilage lesions of the knee, in which soft cartilage over hard subchondral bone with a calcified cartilage interface in-between should be emulated (229). Bilayered gene-activated osteochondral scaffolds, with a plasmid TGF-β1-activated chitosan-gelatin scaffold (chondrogenic layer) and a plasmid BMP-2-activated hydroxyapatite/chitosan-gelatin scaffold (osteogenic layer), put forward the beneficial combination of biomimetic multi-phasic scaffolds, spatially controlled gene delivery and mesenchymal stem cells (230).

Some years ago, our team described the functionalization of composite scaffolds using human mesenchymal stem cell (h-MSC) conditioned medium (CM) for improving scaffold's response and a combination of titanium for the hard osteogenic phase and polydimethylsiloxane (PDMS) for the soft chondrogenic phase (231). The titanium lattice was geometrically graded and obtained additively and used as insert within a mold, in which PDMS with porogens (sugar grains) was casted. After leaching, a porous PDMS network or sponge was obtained. However, porogens may lead to irregular uncontrolled structures with suboptimal mechanical properties and with eventual remaining debris from the pore generators (170), which cannot always escape from the scaffold if the network of porogens is not fully connected. Depending on the actual nature of particles acting as porogens, this may have unwanted effects for cells in culture and for scaffolds' viability.

In consequence, to achieve PDMS components with complex design-controlled shapes, the use of design-controlled sacrificial molds may be preferred (216). In connection to this, sacrificial templates designed using minimal surfaces have been described (232), as well as different sacrificial processes and templates from the micro-electro-mechanical systems (MEMS) and microfluidics fields, some of them involving the use of water-soluble poly(vinyl alcohol) (PVA) (171, 233). Other techniques, previously reviewed for the promotion of vascularization, including bioprinting with fugitive inks or the use of temporal inserts, may be also applicable for complex-shaped PDMS elements with porous or hollow regions (234).

In this study an innovative approach for engineering design-controlled and functionally graded scaffolds, combining hard-phase 3D printed lattices and soft-phase PDMS sponges or networks, is presented. According to our experience, sacrificial templates employed as inserts, within a mold prepared for casting, cannot be always completely washed-away after PDMS casting and polymerization. Normally a thin PDMS layer that engulfs the whole insert is formed, hence preventing washing with water or the appropriate solvent. Hence, in this approach, modified PVA lattices are integrated with the actual mold's walls for facile

dissolution in water. The actual freeform design of these molds and their printing with PVA enable the incorporation of hard inserts and the casting of PDMS. The obtained constructs (PVA molds-lattices, hard inserts and casted PDMS) after water immersion and PVA washing lead to interwoven instead of stacked multi-material scaffolds with hard and soft phases. Geometries are controlled from the design stage, which enables the use of both planar and non-planar inserts, depending on the final purpose of the scaffolds, respectively, in vitro test probes or personalized repairs. The developed procedure is illustrated through two case studies: one dealing with the creation of PDMS and PDMS-PLA constructs, as chondral and osteochondral plugs; another focused on the prototyping of personalized PDMS-PLA/resin constructs, as scaffolds for the tissue engineering or repair of the meniscus. Promising potentials for the tissue engineering of complex-shaped and large-size osteochondral and meniscal defects are discussed, and a systematic description of future research directions for enhanced results is included. Before presenting the main research results and analyzing them, next section deals with the materials and methods employed for this work.

5.2. Design results and discussion

5.2.1. Computer-aided design of lattices and sacrificial molds with controlled porosities

Scaffolds and sacrificial molds with controlled porosities are designed with the support of NX 2206 (Siemens Digital Industries) as main computer-aided design (CAD) resource employed along this study. A design for additive manufacturing strategy (DFAM) is employed (235). In short, considering that both the sacrificial molds for obtaining the soft phases and the lattices used as inserts for the hard phases would be 3D printed by FDM, different independent lattices, as well as lattices connected to molds' walls, are designed considering the employable extrusion nozzle (400 μm of diameter).

Figure 25 presents a schematic illustration of design steps for lattices and tools for osteochondral plugs. Figure 25a shows three reference lattices based on conventional woodpile structures with different porosities are designed as basic test probes. As can be appreciated, variations of porosities are achieved by modifying the distance (d) between printed lines. Besides, Figure 25b illustrates the design of a simple water-soluble PVA mold including an inner lattice connected to mold's walls for improved solubility. These molds are aimed at casting PDMS and achieving porous PDMS lattices or sponges.

A further redesign step leads to the process of Figure 25c, which shows a longer PVA mold with inner lattice inside and with PLA lattice used as insert. Lateral openings help to limit the level of casted PDMS, in order to achieve the desired interwoven structure and final scaffolding structures with three main regions: a) chondral based on porous PDMS, b) interface or subchondral based on interwoven PDMS and PLA, and c) hard or osteogenic region based on PLA lattices.

Figure 26 presents a schematic illustration of design steps for personalized meniscus scaffold and tools. Figure 26a and Figure 26b show different reference sketches projected upon the upper part of the tibia for design personalization and layers of radial and circumferential hard networks acting as bone-cartilage interfaces. Once the reference sketches and subchondral layers are defined, Figure 26c illustrates the design of the usual meniscus half-moon and scaffolding lattice by application of state-of-the-art CAD modelling and Boolean operations. Finally, Figure 26b shows the design of a water-soluble PVA mold (including an inner PVA lattice), to which the hard interfacial subchondral insert is incorporated.

Summarizing, a rapid prototyping and rapid tooling process is planned. Both final components and tools (molds) are designed for FDM printing. Personalization is achievable, as virtually shown in the processes of Figure 26, for which a reference tibia model directly downloaded from Thingiverse (236) has been used as geometrical input. Specific materials, printing technologies and their combinations for manufacturing the desired FG-scaffolds are described below.

5.2.2. Combination of manufacturing processes towards scaffolds with hard and soft phases

PLA filament is used for the manufacture of hard inserts for the bony phase or for the subchondral bone of the osteochondral plugs and meniscus constructs. Water-soluble PVA filament is employed for the creation of sacrificial molds with inner lattices and PLA is used for permanent insert and lattices, both purchased from Smart Materials 3D. A dual extruder fused filament fabrication system (Tevo Tornado) is used for printing purposes. For the personalized meniscus case study, in which non-planar subchondral networks/inserts are employed, mock-up rigid prototypes are manufactured by LCD based on digital light processing system with an Anycubic Photon Mono X machine using a UV photocurable grey resin also from Anycubic.

Once designed, the components and tools are sliced using Cura software for fused deposition modelling purposes and Chitubox for digital light processing. Manufacturing is then carried out by FFF for soluble molds and inserts and digital light processing for the non-planar insert mock-up for the meniscus case study. Prototyped PVA tools, with and without incorporated PLA inserts, are prepared for PDMS casting. A bi-component PDMS (Easyplat Mold 40) is prepared, casted at room temperature and standard atmospheric conditions, and left overnight for complete polymerization. Water-immersion for 48 hours leads to completed dissolution of the PVA molds and, hence, to porous PDMS structures and to sandwiched prototypes of porous PDMS interwoven with PLA lattices or resin inserts. A final rinsing with water and drying with pressurized air leads to the final PDMS sponges and PDMS-PLA scaffolding structures.

The design steps are schematically presented in the following figures. Figure 25 illustrates the reference lattices based on woodpile structures and the osteochondral bimaterial plugs or constructs, achievable by rapid prototyping and tooling. Besides, Figure 26 illustrates the personalized design process for the meniscus scaffold and related rapid tools and inserts. In

their current state, these constructs are not conceived for medical use in real patients, but prove useful for in vitro studies aimed at exploring tissue engineering-based alternatives to standard therapies, as further discussed in section 5.3.

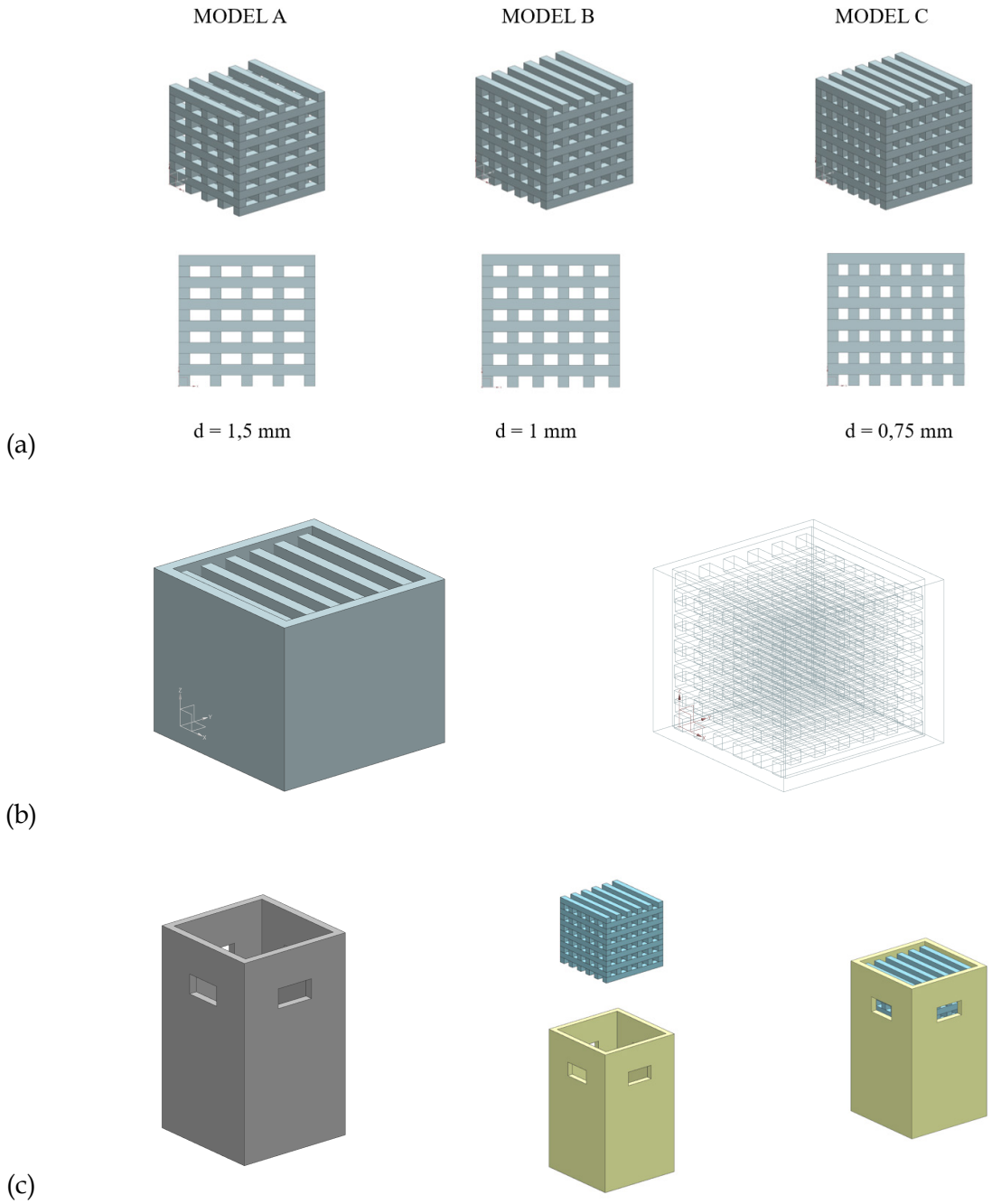


Figure 25: Schematic illustration of design steps for lattices and tools for osteochondral plugs. (a) Three reference lattices based on conventional woodpile structures with different porosities. (b) Design of PVA mold including inner lattice connected to mold's walls for improved solubility. Aimed at casting PDMS and achieving porous PDMS lattices or sponges. (c) Longer PVA molds with inner lattice inside and with PLA lattice used as insert.

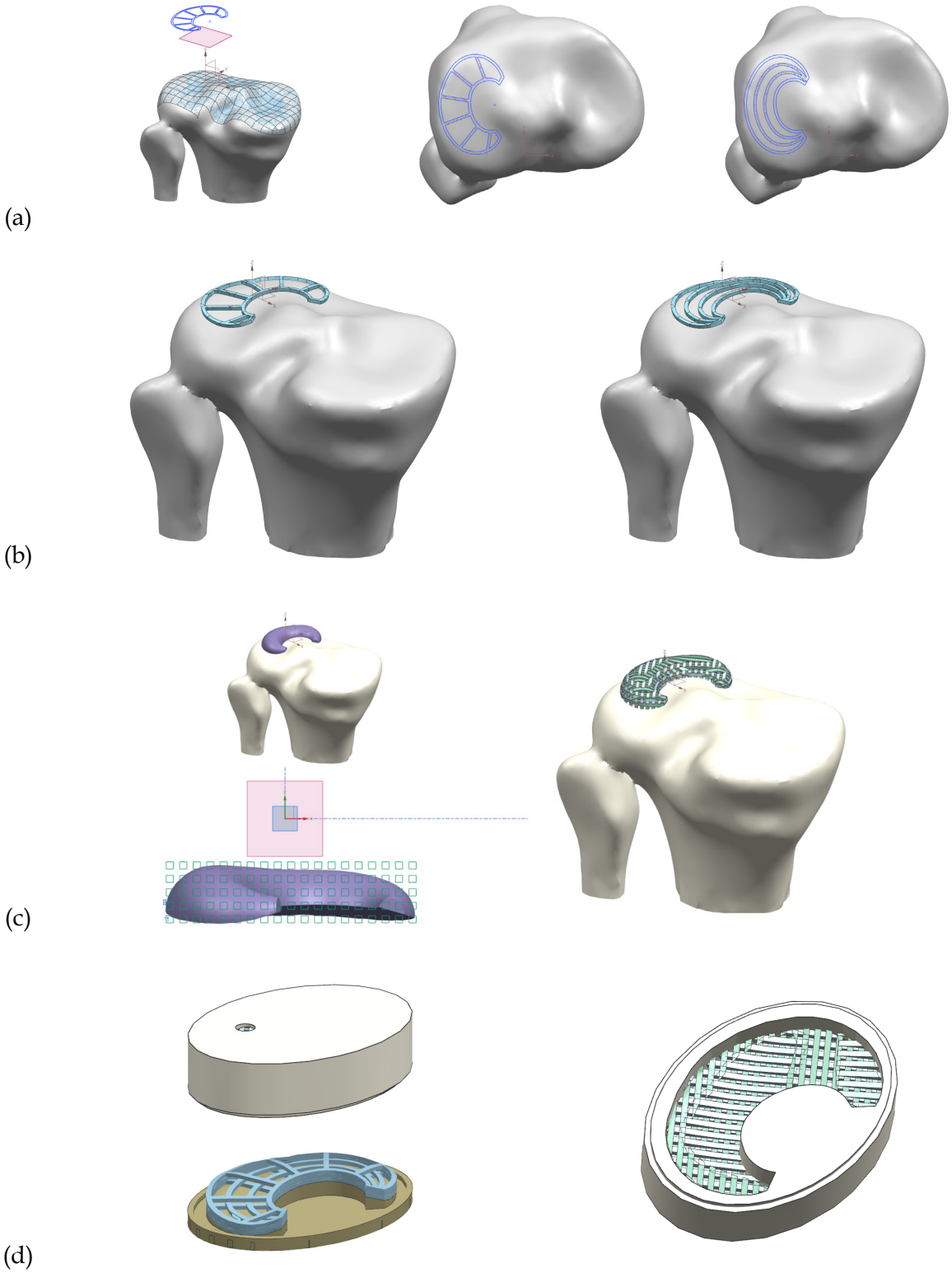


Figure 26: Schematic illustration of design steps for personalized meniscus scaffold and tools. (a) Reference sketches projected upon the upper part of the tibia for design personalization. (b) Layers of radial and circumferential hard networks acting as bone-cartilage interfaces. (c) Design of usual meniscus half-moon and scaffolding lattice by Boolean operations. (d) PVA soluble mold design with hard interfacial insert and inner PVA lattice.

5.2.3. Cell culture processes for preliminary *in vitro* validation

In this section, the PhD candidate would like to thank the Charité Universitätsmedizin Berlin for their contribution. In particular, special thanks to Dr. Tilo Dehne for carrying out the cell study presented below.

Porous PDMS circular test probes (10 mm in height and 6 mm in diameter) obtained by casting in sacrificial PVA molds with inner lattices, following the same design and manufacturing strategy described for the chondral/soft regions of the already described case studies, are employed. Three different pore densities were evaluated, for which 10 replicas of each kind of cylindrical lattices were obtained.

Cell culture and seeding of constructs

The murine cell line MSC3T3-E1 (ACC 210, German collection of microorganism and cell culture GmbH) was used to test biocompatibility of the printed PDMS material. According to the supplier's recommendation the cells were propagated in cell culture medium consisting of alpha minimum essential medium with ribo- and deoxyribonucleosides (α-MEM, GIBCO) supplemented with 10% fetal calf serum, 4 mM L-alanyl-glutamine, 100 U/mL penicillin and 100 g/mL streptomycin (all from Merck). Cells were plated at a density of 2-5 $x10^3$ cells/cm^2, and medium was changed after 72 h. At 90% confluence, cells were detached with 0.05% trypsin/EDTA and sub-cultured at least three times until use. For testing cell compatibility of dissolvable products of the material MC3T3-E1 cells were seeded to 96-well plate with a density of 5,000 cells per well and maintained under standard cell culture conditions (37°C, 5% CO_2, 99% humidity).

For the seeding of constructs a custom-made vessel was used as filling aid. The inner geometry corresponds to the outer dimension of the PDMS-constructs. In addition, a conduit was incorporated the design, that allows the escape of excess liquid when cylinders were compressed for loading. 150 µl of 10 x 10^6 cell/mL cell suspension in culture medium was pipetted into the filling aid. The cylinders were inserted with their porous structure ahead. Load was applied on cylinder's basement part by sterile pipette tip to compress pores and displace air. Immediate load removal enabled relaxing the pores to be filled with the cell suspension. The cell-laden constructs were removed from the filling aid, placed in 24-well standing on the base compartment, and incubated under cell culture condition to allow cell attachment. After 3 hours the upright standing constructs were completely covered with cell culture medium and maintained up to 28 days with media exchange twice a week.

Biocompatibility studies

For testing biocompatibility of non-seeded constructs eluates of each construct type were prepared. The sample was placed in 24-well plate (Corning) and completely immersed with 1 mL cell culture medium and incubated for 24 h under continuous rock shaking in cell culture incubator at (37°C, 5% CO_2, 99% humidity). Control medium was incubated without a sample. 100 µL of prepared eluate was added to a 96-well, that was seeded for 24 h before. After 24 h incubation under cell culture conditions, eluate was removed, and cell were washed with PBS. Metabolic activity was tested with cell culture medium supplemented with 10 % (v/v) CCK8

reagent (Merck). After 2 h, absorbance at 450 nm and 650 nm was recorded with a spectrophotometer (Synergy HT, Biotek instruments). The absorbance difference (450 nm-650 nm) corrected by a blank was related to the control medium a presented a percentage viability.

Cell-seeded constructs were washed with phosphate buffered saline (Merck) and stained with 3 µg/mL fluorescein diacetate (both Sigma-Aldrich) for 15 min and 0,1 mg/mL propidium iodide for 2 min (both Sigma-Aldrich, dissolved in PBS).

For microscopy, an Olympus CKX41 combined with a reflected fluorescence microscopy system was used (Olympus, Hamburg, Germany). The staining results were photo-documented using the ProgRes® speed XT core5 camera and ProgRes® CapturePro 2.10 software (both Jenoptik, Jena, Germany).

5.3. Prototyping result and discussion

5.3.1. Design and manufacturing results for chondral and osteochondral plugs

Designs and prototypes are obtained and presented in increasing order of complexity and biomechanical fidelity. First, a set of PVA molds with internal PVA lattices is achieved (Figure 27a: yellowish samples) and used to cast PDMS. Water immersion for around 48 hours in a 200 ml glass, with slight agitation and change of water every 8 hours leads to the PVA being completely washed away and to the PDMS sponges shown in Figure 27b. In second place, multimaterial constructs are created. To this end, the first PVA molds with inner PVA lattices are modified, extending their lateral walls in vertical direction, which allows the inclusion of inserts obtained with other materials for the harder phases (subchondral and bone regions). Here, PLA inserts are used (green elements in Figure 25a). The modified molds count with lateral openings that control the height of casted PDMS and define the end of the central interfacial region, in which PLA and PDMS coexist. Casting and water immersion following the procedure explained above, leads to the FG multi-material scaffolds or osteochondral plugs of Figure 25c.

Among interesting aspects to consider for design purposes, it is important to highlight the following. The external geometry of the PDMS sponges is defined by the walls of the PVA mold and the pore sizes achieved are controlled by the thickness of PVA trusses employed as inserts, which can be considered for achieving gradients of porosity, pore morphology and pore distribution. An option for obtaining such gradients is playing with the thickness of PVA trusses; another approach is to modify the distance between fused deposition modelled trusses, an option applied in this study to the PLA lattices (models A, B, C from Figure 25a). Atmospheric casting within open molds leads always to a planar upper surface of casted PDMS, corresponding either to an external surface in the single PDMS lattices (Figure 27b), or to an inner interfacial region in the PLA-PDMS constructs (Figure 27c). This can be corrected towards increased geometrical versatility and degree of personalization by employing closed

molds, with a true three-dimensional freedom of design for the molds' walls and morphologies of inserts, as further analyzed in Section 5.3.2 when dealing with the scaffolds for the tissue engineering of meniscus.

Detailed views and microscopies (Opto-electronic DSX100, Olympus) of the achieved PLA-PDMS osteochondral plugs are included in Figure 28, which helps to analyze the quality of a procedure, through which FG polymeric scaffolds are obtained. Figure 28a presents prototypes of different models (A, B, C) with different porosities of the PLA inserts that correspond to the designs from Figure Figure 25a. As previously mentioned, the variation of porosity in the hard PLA phases is achieved by employing variations of spacing between printed PLA trusses. Insets from Figure 28a show detailed pores in the PDMS sponges, in the PLA lattices and in the interwoven interface. In addition, Figure 28b presents a topographical reconstruction of pores within the PDMS showing the 3D printed layers left by the PVA after being dissolved in water. PDMS pores depend on PVA filament's dimensions and thickness of PVA printed trusses. A wavy surface can be appreciated in the topographical reconstructions, which derives from the layer-by-layer FDM process. In any case, these surface irregularities do not seem to affect cells adhesion or colonization in a negative way and probably contribute to creating an adequate microenvironment (see Section 5.3.3).

Remarkably affordable resources and materials are employed in the presented strategy for achieving FG scaffolds, which could be potentially obtained in a low-cost "FabLab". Besides, the process stands out for being straightforwardly implementable and versatile. Indeed, an extremely varied portfolio of materials can be potentially processed in a similar way as presented here for PLA and PDMS using PVA sacrificial molds. Several types of castable bioelastomers and all kinds of 3D printable inserts including polymers, ceramics and alloys should be considered.

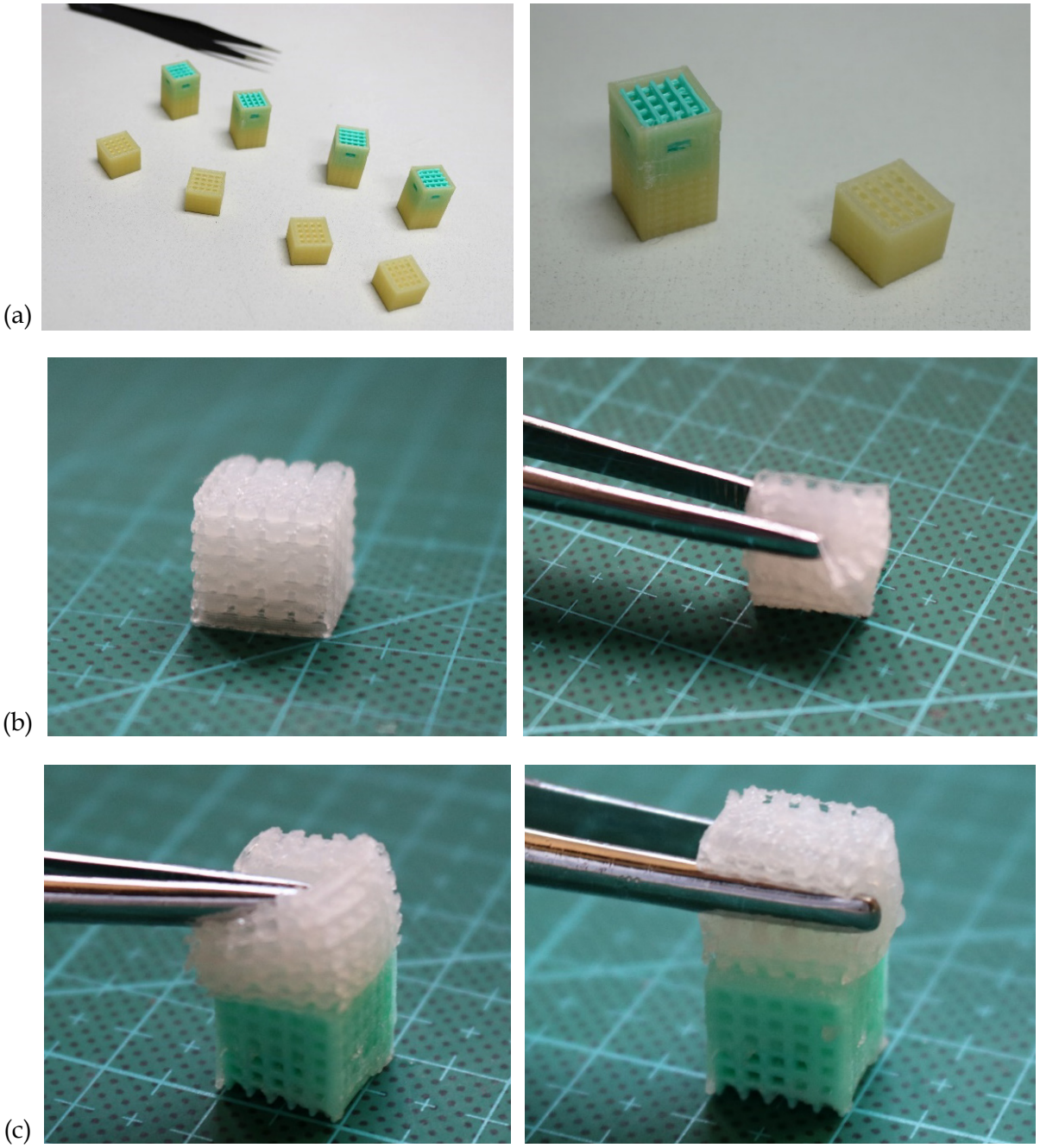


Figure 27: Prototypes of scaffolds (and related tools) for chondral and osteochondral repair. (a) PVA molds and PVA molds with PLA inserts prepared for PDMS casting. (b) PDMS lattices or sponges obtained after casting and dissolving the PVA molds in water. (c) Osteochondral plugs with PLA lattice inserts interwoven to PDMS porous scaffolds.

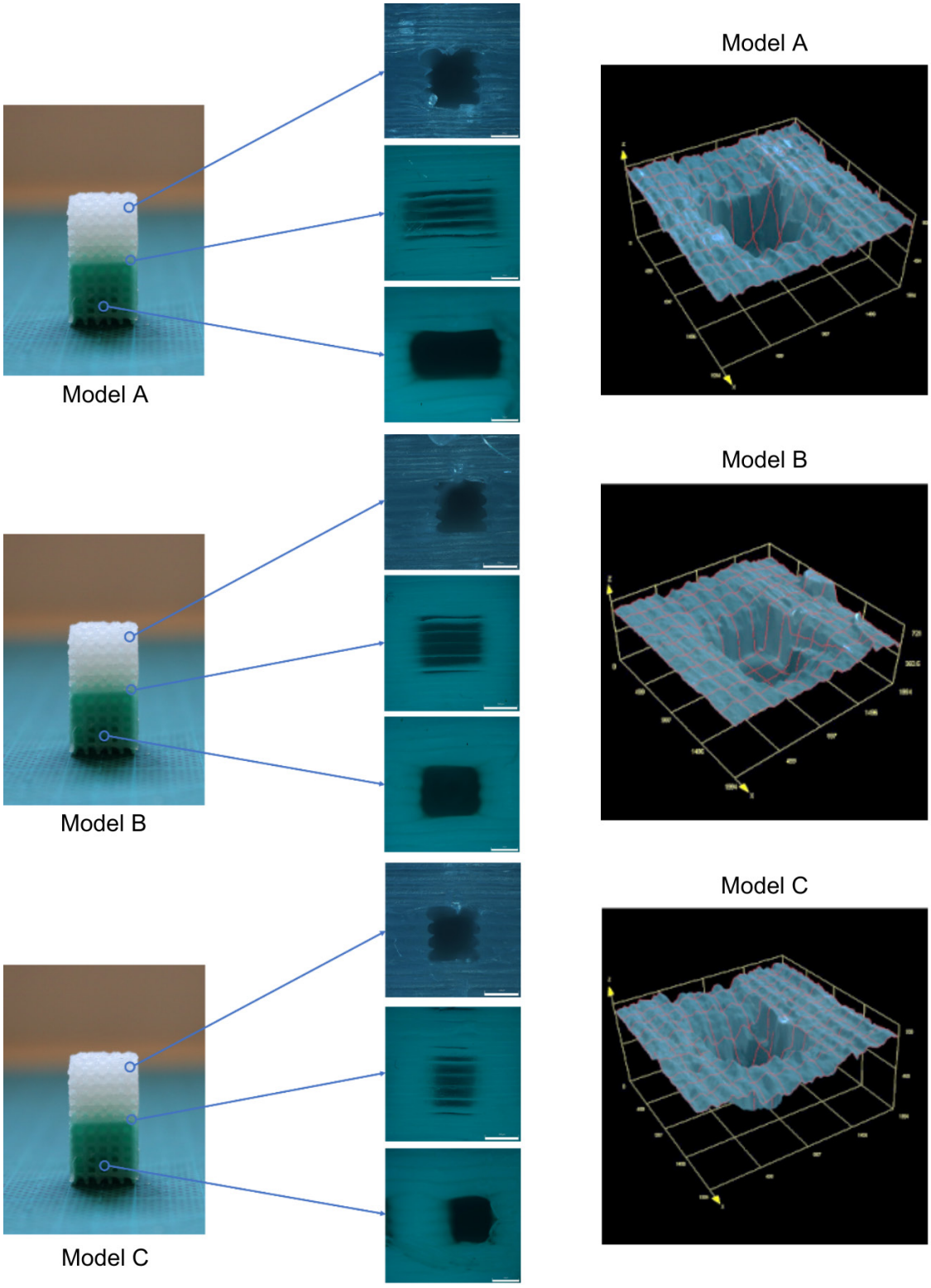


Figure 28: Prototypes of functionally graded scaffolds with soft (PDMS) and hard (PLA) phases. (a) Prototypes of different models with insets showing detailed pores in the PDMS sponges, in the PLA lattices and in the interwoven interface. (b) Topographical reconstruction of pores within the PDMS showing the 3D printed layers left by the PVA after being dissolved in water. PDMS pores depend on PVA filament's dimensions.

5.3.2. Design and manufacturing results for meniscal biomimetic constructs

Next step in the strategy of increasing complexity deals with the achievement of more three-dimensionally complex constructs, as compared with the results presented in Section 5.3.1. Here a whole meniscus with its subchondral region is selected as conceptual case study, to illustrate the procedure and its potentials for design personalization and for repairing complex and multi-phase articular injuries. Again, the increasing complexity approach divides the case study in basic and more advanced prototypes of FG scaffolds, as explained further on.

First of all, almost the same procedure of Section 5.3.1 is applied but with a modified half-moon geometry mimicking that of the meniscus. Through this, the set of prototypes from Figure 29a is obtained. These prototypes count with planar PLA networks interwoven to porous PDMS sponges with continuously varying cross-sections. The PDMS sponges act as soft phases for cartilage repair and the PLA lattices as hard phases for the subchondral regions of the bone-cartilage interfaces. These "croissant"-like scaffolds may be considered as biomimetic test probes imitating the typical half-moon shape of human meniscus. Their utility is remarkable, not just considering future approaches towards real patients, but already in the current conceptual prototyping state of Figure 29a. Among possible quite direct applications, it is important to highlight their possible employment as: 1) standardizable test probes for studying knee injuries and their repairability through tissue engineering strategies; 2) models for surgical planning and training; or 3) in vitro scaffolds for drug testing purposes or for a better understanding of degenerative diseases affecting cartilage, to cite a few options.

A quite higher degree of complexity and personalization is achieved in a second set of design and prototyping experiments, which are schematically illustrated in Figure 29b and Figure 29c. For this set of rapid prototypes, as advanced, a tibia model is selected from Makerbot Thingiverse's repository (thing: 1030467) (236) and a personalized design and manufacturing approach is applied, as already schematically illustrated in Figure 27c. Figure 29b provides an example of tools –sacrificial PVA molds– showing the PVA lattice connected to mold's walls (left) and the mold closing lid (right), manufactured by FDM following the computer-aided design from Figure 26d. The actual FG scaffolds are shown in Figure 29c, which shows the advanced prototypes with non-planar insert for the hard phase adapted to the tibia and following the more complex personalized design process of Figure 27.

In this case a resin insert as mock-up is employed but it is perfectly possible to employ PLA inserts designed and printed in a personalized way, adequately resembling the non-planar geometry of the tibia, but resorting to curved-layer fused deposition modelling processes (237, 238, 239, 240) with slight modifications. Such approach is presented in Figure 30, which includes printed PLA inserts for the meniscal constructs manufactured directly depositing layers upon the upper surface of the same tibia employed as printing bed. The printing bed, manufactured in PVA is again water-soluble and liberates the insert after printing just by water immersion. Figure 29c shows how the constructs perfectly adapt to the employed anatomical model, validating the personalized design approach.

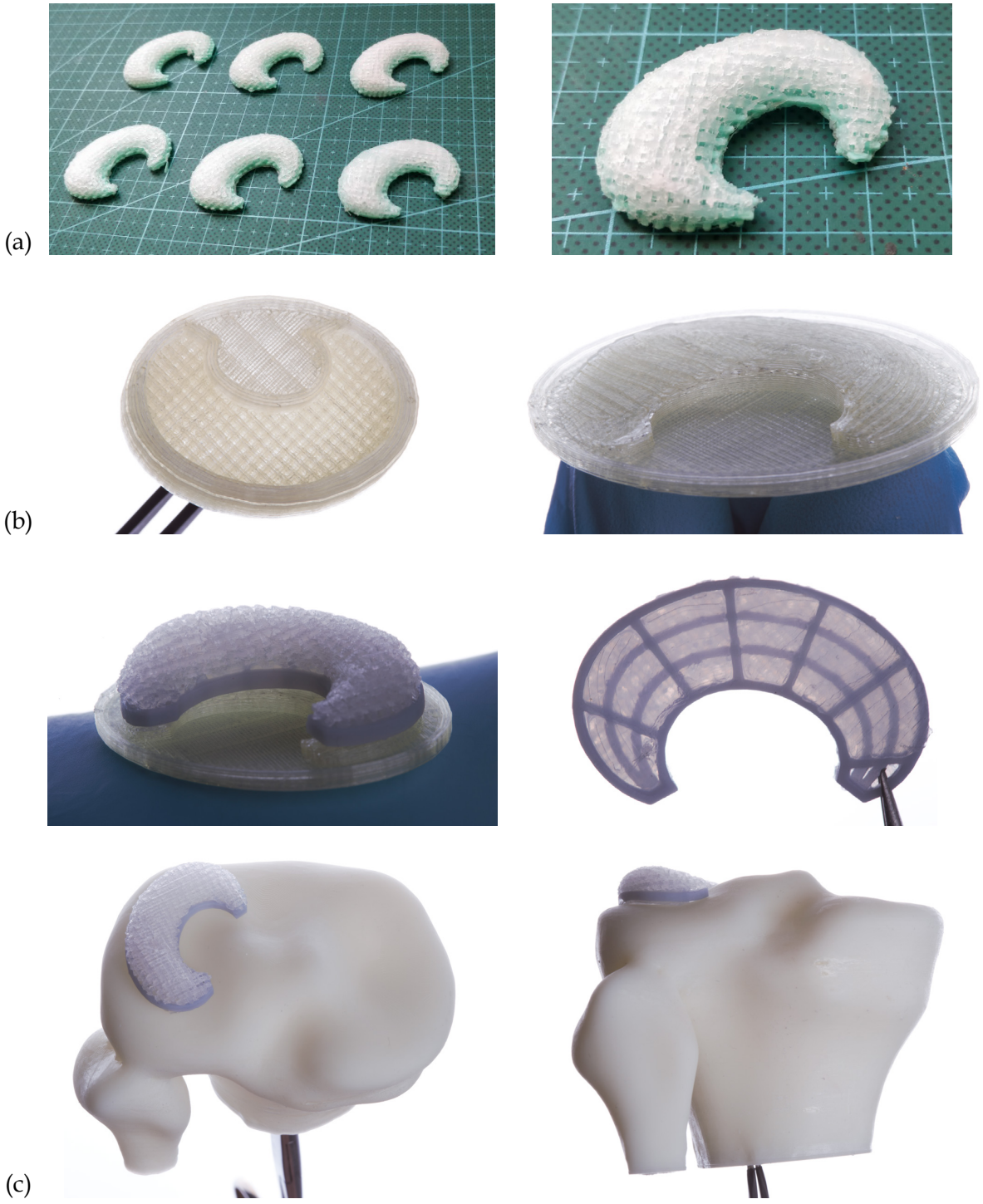


Figure 29: Prototypes of functionally graded scaffolds for meniscal repair with hard and soft phases, both planarly printed and non-planarly printed as personalized options for repair. (a) Basic prototypes with planar hard insert for the hard phase acting as bone-cartilage interface. (b) Example of tools or sacrificial PVA molds: PVA lattice connected to mold's walls (left) and mold closing lid (right) following the computer-aided design from Figure 26d. (c) Advanced prototypes with non-planar insert for the hard phase adapted to the tibia and following the more complex personalized design process of Figure 27.

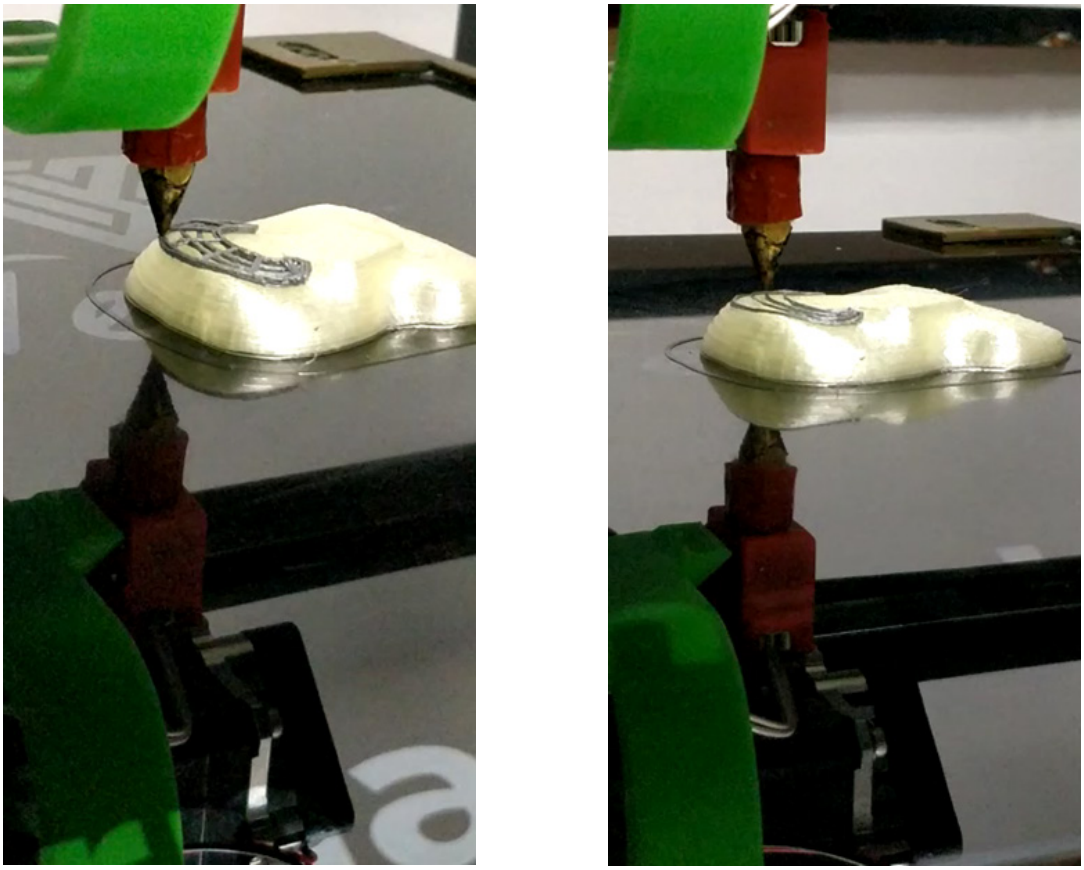


Figure 30: Curved layer fused deposition modelling of PLA inserts for the subchondral region printed upon a PVA bed with the upper surface of the tibia model employed.

Interestingly, any biomaterial printable by technologies including: selective laser sintering, powder bed laser fusion, lithography-based ceramic manufacturing, inkjet printing, bioprinting, fused deposition modelling, digital light processing or stereolithography, among others, could be employed, as insert within the sacrificial molds, and hence hybridized with the design-controlled porous PDMS networks to achieve FG scaffolds for complex-shaped articular repairs involving different tissues.

Results from cell culture trials are detailed and discussed in the following Section 5.3.3. Such preliminary in vitro validations help to analyze the potentials of the solutions described and to put forward relevant research directions for progressively approaching end users, either tissue engineering researchers, drug developers, surgeons, or patients.

5.3.3. Cell culture results for preliminary *in vitro* validation

Figure 31 below summarizes the biocompatibility studies performed employing PDMS structures with large (C1), middle-sized (C2) and small pores (C3), corresponding to morphologies A, B, C from Figure 25a.

Figure 31a presents the general cell biocompatibility tested with eluate of construct on MC3T3-E1 cell line related to pure cell culture medium as percentage of control. Remarkable values,

even beyond 100% for C1 and C3 types of constructs, and close to 100% for C2 type, are found, which puts forward the interest of the PDMS employed and of the scaffolds obtained for in vitro studies linked to tissue engineering.

Besides, Figure 31b presents a set of epifluorescence microscopy images of live/dead (green/red) stained cells seeded on PDMS scaffolds observed from surface side (top view) and cross section in the inner regions (cross view, cutting edge of bisected cylinder) of the different constructs. All types of constructs were found to be biocompatible and facilitated cell attachment and maintenance up to 28 days, which is a promising value for in vitro tissue engineering studies. Interestingly, after 28 days, the scaffolds are covered with a larger number of cells than after day 1, showing surfaces populated with cell colonies in good metabolic condition after almost one month in culture.

Results are considered promising since PDMS is intrinsically high hydrophobic and tends to render surfaces incompatible for prolonged cell adhesion and proliferation. Plasma activation and protein coating have been found beneficial but short-lived and polydopamine coatings have been applied to stabilize adhesion up to 2 weeks (241). In our case, a combination of the described good practices for cell culture and the surface topography obtained upon the PDMS after the dissolution of the 3D printed PVA molds may be responsible for higher cell-surface affinity, enhanced adhesion, and long-term stability.

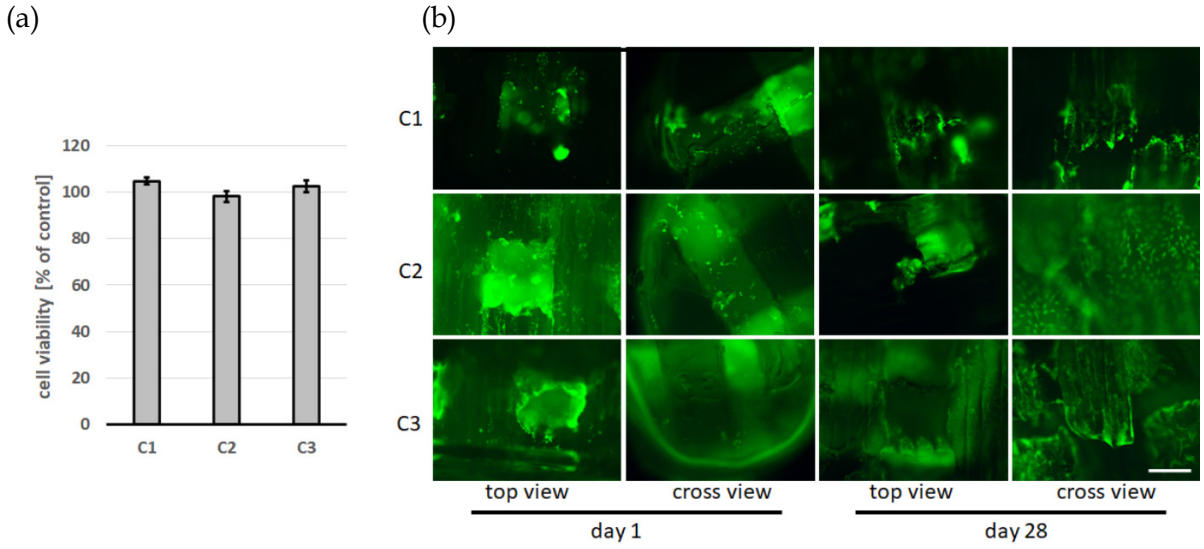


Figure 31: Biocompatibility of PDMS structures with large (C1), middle-sized (C2) and small pores (C3). a) General cell biocompatibility tested with eluate of construct on MC3T3-E1 cell line related to pure cell culture medium as percentage of control. b) Epifluorescence microscopy images of live/dead (green/red) stained cells seeded on PDMS scaffolds observed from surface side (top view) and cross section (cross view) in the inner region. Each construct type was biocompatible, facilitated cell attachment and maintenance up to 28 days. Long-term studies are still needed but initial assessment is promising. Reference bar size = 500 µm. Data and pictures provided from Charité - Universitätsmedizin Berlin. Special thanks to Dr. Tilo Dehne.

5.4. Conclusions and future proposals

A promising approach towards complex-shaped osteochondral and meniscal repair has been presented. It evolves from experiences linked to the creation of multi-material functionally graded scaffolds but reshaping the use of sacrificial inserts, which being connected to molds' walls facilitate solubility. In addition, the employment of complex-shaped inserts and the freeform design of the sacrificial molds leads to biomimetic multi-material constructs with potential applications for several articular problems, especially the more challenging ones involving large-sized defects affecting different tissues. The process has been illustrated through different prototyping sets applied to two case studies: osteochondral plugs and meniscal constructs. The described strategy stands out for its versatility and affordability, which has direct application for in vitro studies, for surgical planning or training, and for standardization activities. The rapid prototyping approach could even prove useful for educational purposes, such as developing hands-on activities for introductory courses to tissue engineering and biofabrication.

Large-scale and complex-shaped repairs involving hard and soft tissues require FG scaffolds and the presented examples seem promising contributions to this field, according to the explained straightforward manufacturability, degree of personalization and versatility of the presented methods. Towards the future, other inserts with mechanical properties closer to those of bone, as alternative to the PLA ones, could be studied. Ceramics like tricalcium phosphate or hydroxyapatite, now processable through lithography-based ceramic manufacturing, and the more common laser sintered or melted titanium alloys seem good candidates for future studies.

At the same time, the laser stereolithography or the digital light processing of biophotoelastomers and water-soluble resins may, respectively, constitute alternative materials for the chondral lattices and for the sacrificial molds. The emergent development of technologies capable of 3D printing PDMS and other bioelastomers (242, 243) can be also an option for achieving design-controlled PDMS lattices without resorting to sacrificial molds, although their hybridization with the lattices corresponding to the harder phases should be explored.

Another continuation line is linked to achieving more complex constructs, involving an increasing number of materials and phases towards enhanced biomimicry. The use of multi-nozzle fused deposition modelling or resorting to multi-nozzle inkjet printing, through which both water-soluble and non-soluble materials could be combined in single constructs-tools could help enhance the permeability between phases and reach a higher control of achievable gradients. In this way, truly digital and even living materials (244, 245, 246, 247) but with the porosities required for tissue engineering scaffolds could be obtained.

6. Engineering multi-material tissue engineering scaffolds and bioinspired implants for meniscus articular repair

6.1. Meniscus injury overview

Meniscal injuries are among the most common orthopaedic conditions, with an aetiology ranging from traumatic mechanisms in young individuals to degenerative processes in older populations. These pathologies constitute a significant proportion of all knee injuries. It is estimated that meniscal orthopaedic surgeries account for approximately 10 to 20% of all knee injuries (248), though this range may vary based on population and context (such as specific sports or age groups). In the broader spectrum of joint injuries, which includes injuries to shoulders, elbows, hips, and ankles, meniscal injuries still represent a notable fraction. However, the specific prevalence compared to all joint injuries varies widely, depending on factors such as age, level of physical activity, and participation in sports (248, 249).

Prevalence by age and gender

Statistics indicate significant variations in the incidence of meniscal injuries by both age and gender. In the younger population, particularly individuals between 20 and 30 years of age, these injuries are predominantly traumatic and are more frequently observed in males, given their higher participation in high-impact sports. It is estimated that up to 60% to 70% of meniscal injuries in this demographic are sports related (248, 249, 250).

In contrast, in the population over 50 years of age, meniscal injuries are mostly of a degenerative nature. In this group, the incidence is more evenly distributed between men and women, reflecting the contribution of age-related degenerative factors. Studies have shown that up to 30% of the population over 50 years of age exhibit some degree of meniscal degeneration (251).

Meniscus anatomy and most frequent types of injuries

The menisci are fibrocartilaginous structures shaped like the letter "C" with concave upper surfaces that match the contours of the femoral condyles and flat undersides that correspond to their respective interfaces with the tibial plateau. The lateral meniscus exhibits a symmetrical C-shape, while the medial meniscus has a more crescentic form, primarily due to the consistently larger size of the posterior horn compared to the anterior one. Notably, the medial meniscus is firmly attached to the joint capsule, which limits its mobility and renders it more susceptible to injury. This difference in capsular attachment is one of the factors contributing to the heightened vulnerability of the medial meniscus. Figure 32 depicts a schematic overview of the knee joint anatomy.

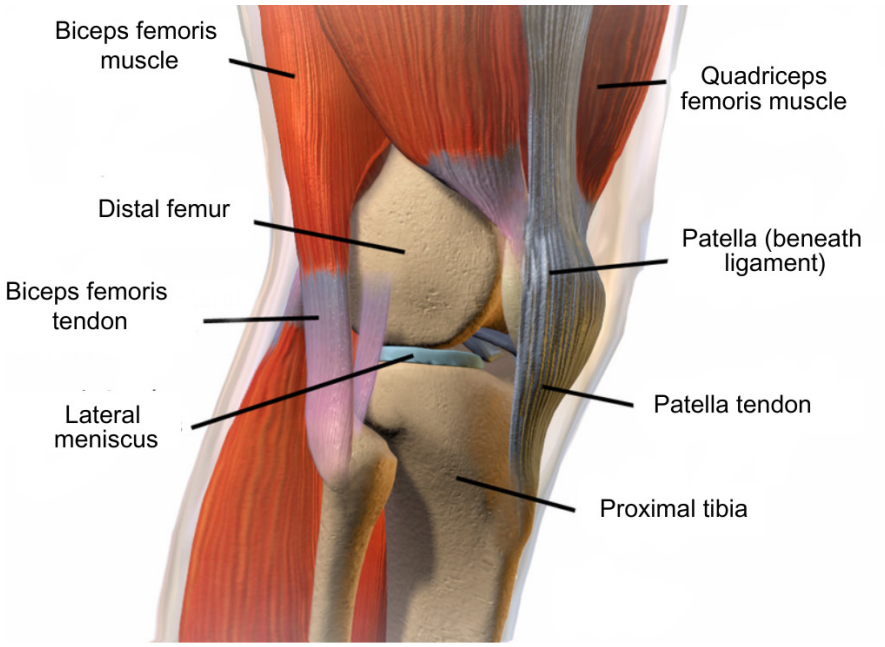
In adults, the vascular supply of the meniscus is limited to its periphery. This peripheral region, often referred to as the "red zone", constitutes approximately 15% of the outer meniscus (248, 249, 252). It is worth noting that tears occurring within the red zone of the meniscus have a higher likelihood of healing compared to those in the avascular "white zone". Tears that are situated within or in contact with the red zone are also more amenable to meniscal repair. However, it's important to mention that standard MRI images do not currently provide signal intensity distinctions between the red and white zones of the menisci.

The meniscus play key roles in the knee: they absorb impacts, provide cushioning, and distribute loading forces, thereby protecting the knee's articular cartilage. They generate joint stability, enhancing the congruence between the femur and the tibia, contributing to the stability of the joint, and have a lubricating function, facilitating the distribution of synovial fluid, which lubricates and nourishes the articular cartilage.

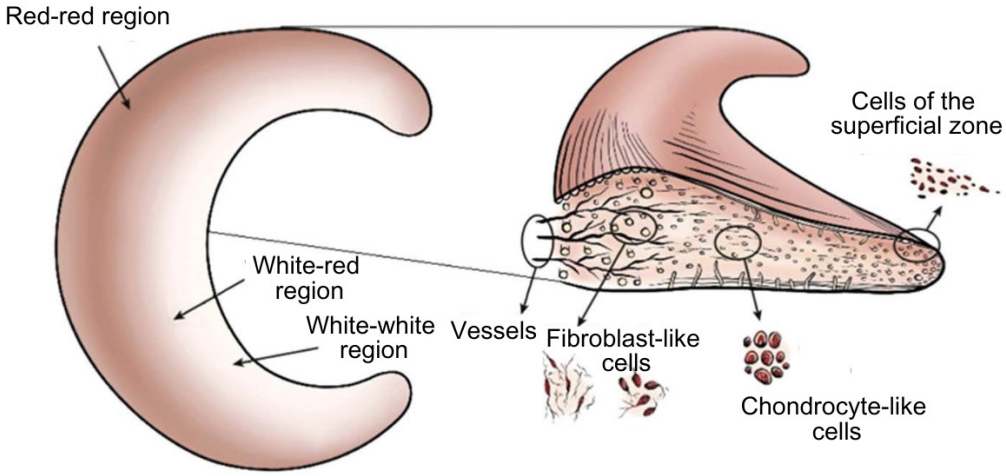
Prevalence of different types of meniscal injuries

Meniscal tears can be classified into different configurations within the realm of scientific analysis, which include horizontal, longitudinal, radial, oblique (often referred to as a parrot-beak tear), and complex or degenerative patterns (248, 249, 252). Horizontal tears, representing the most prevalent meniscal tear pattern, exhibit parallel alignment to the tibial plateau, effectively dividing the meniscus into upper and lower segments. Both longitudinal and radial tears may appear as vertical on MRI. However, longitudinal tears extend in a parallel manner to the c-shaped circumference of the meniscus, whereas radial tears are oriented perpendicularly to the meniscal circumference. An oblique tear, often likened to a "parrot-beak" tear due to its resemblance to a parrot's beak shape, combines elements of both radial and longitudinal tears. These tears are characterized by their perpendicular orientation to the free edge of the meniscus, but they also exhibit a curvature that causes a portion of the tear to align parallel to the c-shaped fibers of the meniscus. Numerous variations in meniscal tear patterns have been assigned specific names to acknowledge their distinct characteristics. One of the most well-known of these is the 'bucket-handle tear'. Bucket-handle tears are essentially a subtype of longitudinal tears, where the inner rim of the tear becomes displaced, creating a configuration reminiscent of a bucket's handle. However, even when found in isolation, they hold significant clinical relevance, as the displaced meniscal fragment often leads to knee locking, causing considerable symptoms and loss of functionality. A "flap tear" is a descriptive term that refers to a situation where the meniscus tears with either superior or inferior displacement, usually in a predominantly horizontal pattern, and then the upper or lower component of the torn meniscus becomes moved from its site of origin. Complex degenerative meniscus tears, encompassing approximately 30% of all such injuries, and commonly they are not easy to classify according to a morphological pattern. Predominantly occurring in adults, with men showing a higher incidence in their early forties and women in their sixties. Their development might be sudden or gradual, with or without preceding trauma. Associated frequently with other joint degenerative changes, these complex tears often lack the capacity for natural repair and are typically resistant to surgical correction. These tears are most common at the medial meniscal body. Arthroscopic treatment is typically required for adequate symptom relief in patients with displaced meniscal flap tears (248, 249).

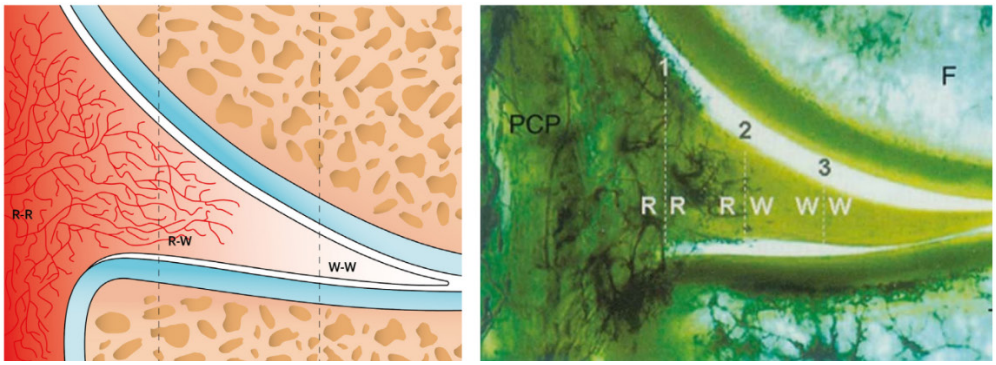
In addition to morphological categorization of meniscal tears, it is crucial to provide precise information about their location.



(a)



(b)



(c)

Figure 32: Illustrative diagrams of the meniscus and knee anatomies. (a) Main bones, muscles and tendons involved in knee joint functionality. (b) General view and section view differentiating the meniscal zones, fibers and tissues. (c) Schematic drawing of the meniscus vascularisation in three zones (coronal section). R-R, Red–Red; R-W, Red–White; W-W, White–White. Pictures acquired and adapted from "Use of motion capture in assisted of knee ligament injury diagnosis" (253), "The

human meniscus: A review of anatomy, function, injury, and advances in treatment" (248) and "Isolated meniscus injuries in skeletally immature children and adolescents: state of the art" (254).

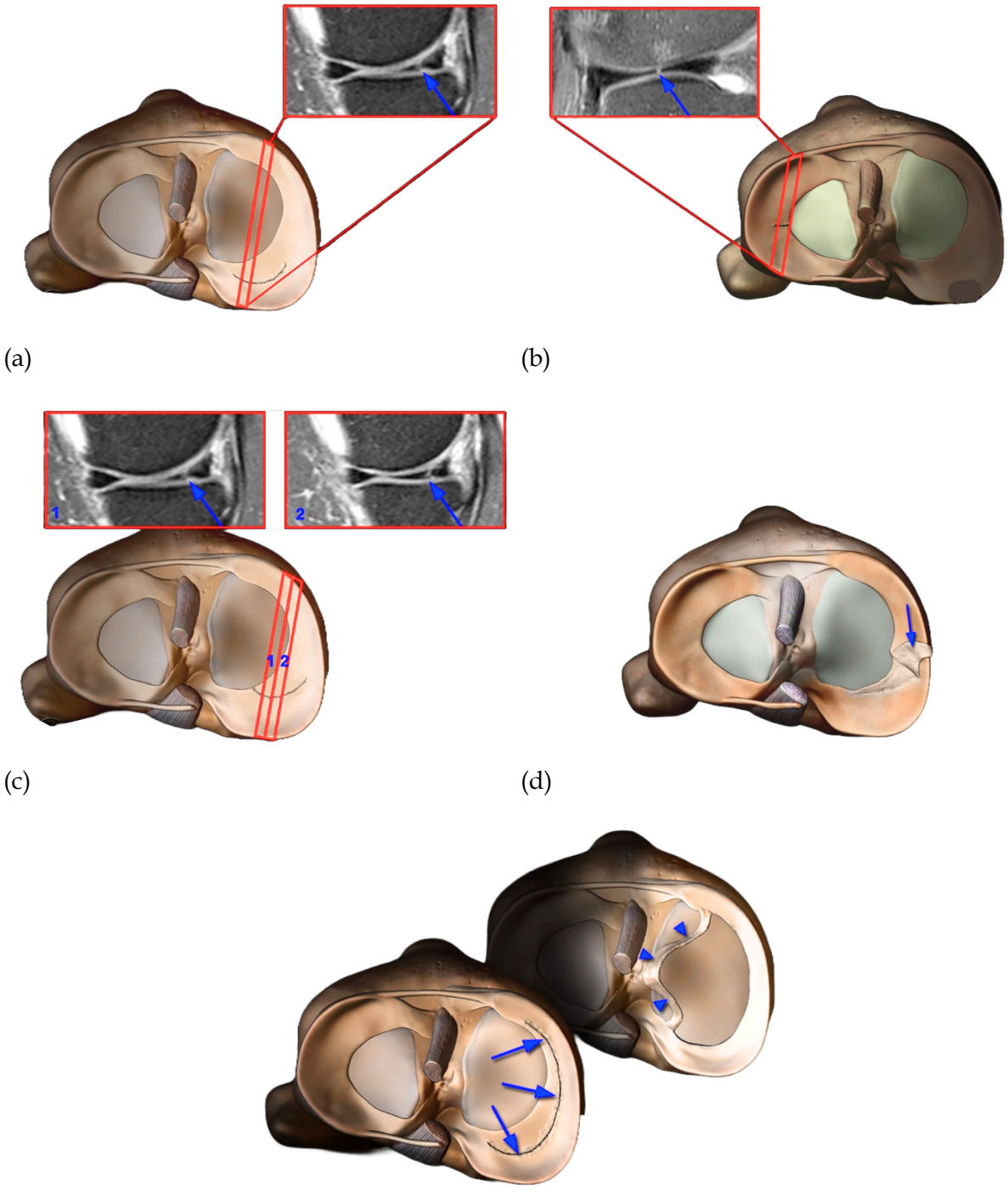


Figure 33: Different categories of meniscal injuries based on their morphology. Longitudinal, (b) radial, (c) oblique, (d) flap and (e) bucket handle tears. Pictures acquired and adapted from Radsource website (252).

Diagnosis, conventional treatments, and existing market solutions

The diagnosis of a meniscal injury begins with a thorough physical examination, where the physician assesses the patient's medical history and symptoms, followed by a visual inspection and palpation of the knee to detect swelling, tenderness, and deformities. Specific tests, such as McMurray's test and Apley's test (249), involve manipulating the knee in different positions to identify pain or clicking sounds, indicative of a possible meniscal injury.

In addition to physical examination, imaging techniques play a crucial role. Although X-rays do not directly show the menisci, they are useful for ruling out other causes of knee pain such fractures. MRI is essential, being the most accurate technique for visualizing meniscal injuries, as it provides detailed images of the menisci and surrounding structures. In some cases, ultrasound (255) may offer a real-time assessment of the meniscus, and in specific situations, MR arthrography, combining MRI and injected contrast, can be used to enhance visualization of the knee's internal structures (248). This integrated approach of clinical evaluation and imaging diagnosis is fundamental for accurately identifying meniscal injuries, allowing for more informed and patient-specific treatment planning.

As for the treatment of meniscal injuries, it has evolved significantly, with an approach that varies depending on the severity of the injury, the patient's age, and their activity level among other factors. Conventional treatments start with non-surgical methods, such as RICE (Rest, Ice, Compression, and Elevation) therapy (255), pain relievers and anti-inflammatory drugs, and physiotherapy to improve mobility and strengthen the muscles supporting the knee. When conservative treatment is not sufficient, surgical options are considered. Meniscectomy, which involves the removal of damaged tissue, has been a common approach (248, 249, 256). However, given the importance of the meniscus in protecting articular cartilage and preventing arthritis, current techniques tend to preserve as much meniscal tissue as possible. Meniscal repair, where the torn meniscus is sutured, is preferred whenever the injury allows, especially in tears in the "red zone" where vascularization is adequate for healing.

In addition to traditional treatments, new technologies and products have emerged in the medical market. Hyaluronic acid injections (257), known for their capacity to lubricate and cushion the joint, offer pain relief for some people with meniscal injuries. There are also advancements in tissue engineering and the use of meniscal implants, providing additional options for those with complex or degenerative injuries.

In today's market, meniscal implants represent an innovative solution for complete meniscus replacement, especially in patients with irreparable injuries or advanced degeneration. These implants, designed to mimic the functionality of the natural meniscus, offer new hope in restoring mobility and alleviating pain, preserving the integrity of the knee, and delaying the onset of osteoarthritis. The choice of implants and their application depend on a detailed assessment of each case, considering factors previously described such as the patient's age, activity level, and extent of the injury. With the constant evolution of technologies in tissue engineering and biomaterials, these meniscal implants are emerging as a promising solution in the field of orthopaedics and sports medicine.

Currently, the primary solution for the complete replacement of a damaged or degenerated meniscus is the meniscal implant. There are two main types of meniscal implants:

- Collagen meniscal implants (258): these implants are designed to replace damaged meniscal tissue. Made from collagen, a protein naturally present in the body's tissues, these implants seek to provide structural and functional support similar to the natural meniscus. They are particularly useful in cases where a significant part of the meniscus has been removed, and the patient is experiencing symptoms such as pain or instability in the knee. However, from a constructive point of view, they present a constant triangular section developed by revolution along an axis, thus offering practically no customization to the patient (see Figure 34).
- Meniscal allografts: these are transplants of meniscal tissue from a cadaver donor (259). A meniscal allograft is an option for patients whose meniscus has been severely damaged or previously removed and who are experiencing knee problems as a result of meniscus loss. These transplants aim to restore the normal functionality of the knee and prevent or delay the development of osteoarthritis. However, as with collagen meniscal implants, the degree of customisation of the solution is almost non-existent, as the implant comes from an external donor, whose joint anatomies have similar but not identical features to those of the patient.

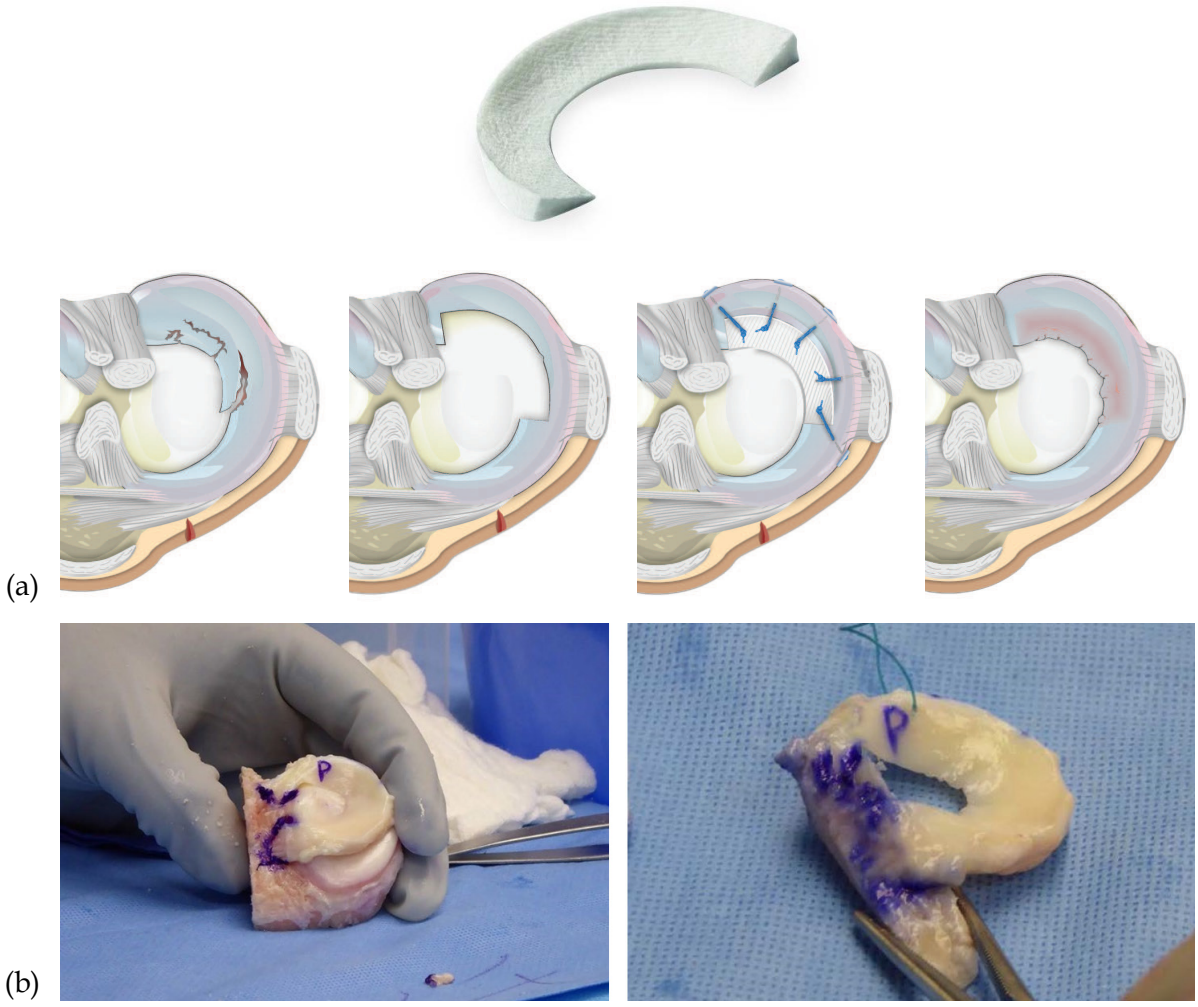


Figure 34: Current medical solutions for total or partial meniscectomy. (a) Collagen disc from Stryker's medical company. (b) Allograft meniscus prior to removal from the tibial plateau. Pictures acquired

and adapted from "The collagen meniscus implant" (260) and "Meniscal transplantation: procedures, outcomes, and rehabilitation" (259).

It is important to note that the choice between a collagen implant and a meniscal allograft depends on several factors, including the amount of meniscal tissue that has been lost or damaged and the availability of finding a suitable cadaveric donor. Additionally, the viability of these treatments can be influenced by the surgeon's skill, and patient preferences.

Due to various socioeconomic factors, such as the growing global population, the increased societal participation in sports activities or the aging of the global population, the trend of joint injuries is expected to rise, which forecasts growth in the meniscal implant market (248, 249, 250). These facts, combined with continuous advancements in biomedical technology, have contributed to the emergence of potentially competitive new solutions, such as meniscal implants obtained from AMTs (261). The design and production of these implants are mainly based on tissue engineering applications, emerging as a promising alternative to collagen implants and allografts. For these reasons, 3D printing has emerged as a cutting-edge tool for the design and manufacture of scaffolds for meniscal repair, with relevance due to its ability to customize the implant geometry using biocompatible and biodegradable materials. The selection of materials such as poly(lactic acid) (PLA), polyglycolic acid (PGA), collagen and fibrin gel are based on the need to ensure biocompatibility and mechanical properties analogous to those of natural meniscal tissue (262). These devices must possess a controlled porous structure that facilitates cell adhesion, promoting the diffusion of nutrients and oxygen, and ensuring the efficient removal of waste products. The configuration and shape of the scaffolds must be precisely tailored to the meniscal anatomy and the specific tear in each patient. In addition, the incorporation of growth factors or bioactive substances in the scaffold matrix can boost tissue regeneration, accelerating the recovery process. Prior to their clinical application, it is essential to subject the scaffolds to rigorous in vitro and in vivo evaluations, in accordance with biomedical safety regulations and standards, to verify their biocompatibility, safety and efficacy.

The continuous emergence of new 3D printing systems and the ongoing development of the technology, combined with the potential benefits that the generation of scaffolds developed for tissue engineering provides an interesting area for study and research.

Throughout the following chapter, this research aims to develop an innovative design for additive manufacturing (DFAM) methodology capable of providing patient-specific tissue engineering functionally-graded (FG) scaffolds by implementing a multi-scale and multi-material approach. At all times, the intention is to provide FG solutions by implementing biomimetic capabilities observed in the human anatomy. For this reason, by prioritising the manufacturability oh these implants, characteristics inherent to the generation of scaffolds such as porosity and the degree of personalisation to the patient are studied with greater precision.

Figure 35 depicts a series of construction characteristics indicated by the INKplant project clinical team. Throughout all the progress of the INKplant project, these concepts have been considered as main requirements to fulfil in order to reach the fixed targets. It must be

considered as a proof of concept, where not all the aspects have been deeply described. From this point, depending on the AMT and materials chosen to address each case of study, modifications are implemented with the final objective of validating the manufacturability of the meniscal scaffold.

On the draft, it can be distinguished three different zones with related features that the implant must fulfil simultaneously.

- Porous layer: this layer provides a dual function, as it maintains the ideal porosity to allow cell colonization, allowing tissue regeneration and simultaneously, it allows the lubrication and cushioning of the joint, allowing vascularization and the transmission of synovial fluid during joint compressions. Moreover, it should ideally have an internal porosity close to 85%.
- Friction-reducing layer: this layer acts as a protective case or shell that, as far as possible, shields the porous core of the implant, made out from a softer material, from external mechanical actions by mitigating or reducing friction during joint operation. It should also be porous to not to prevent the dispersion of synovial fluid across the joint.
- Structural integrity layer: integrated membrane into the porous layer. The primary function of this membrane must be to provide the implant with better mechanical properties in a certain region so that surgeons can leverage it if there is a need to suture the implant during surgery.

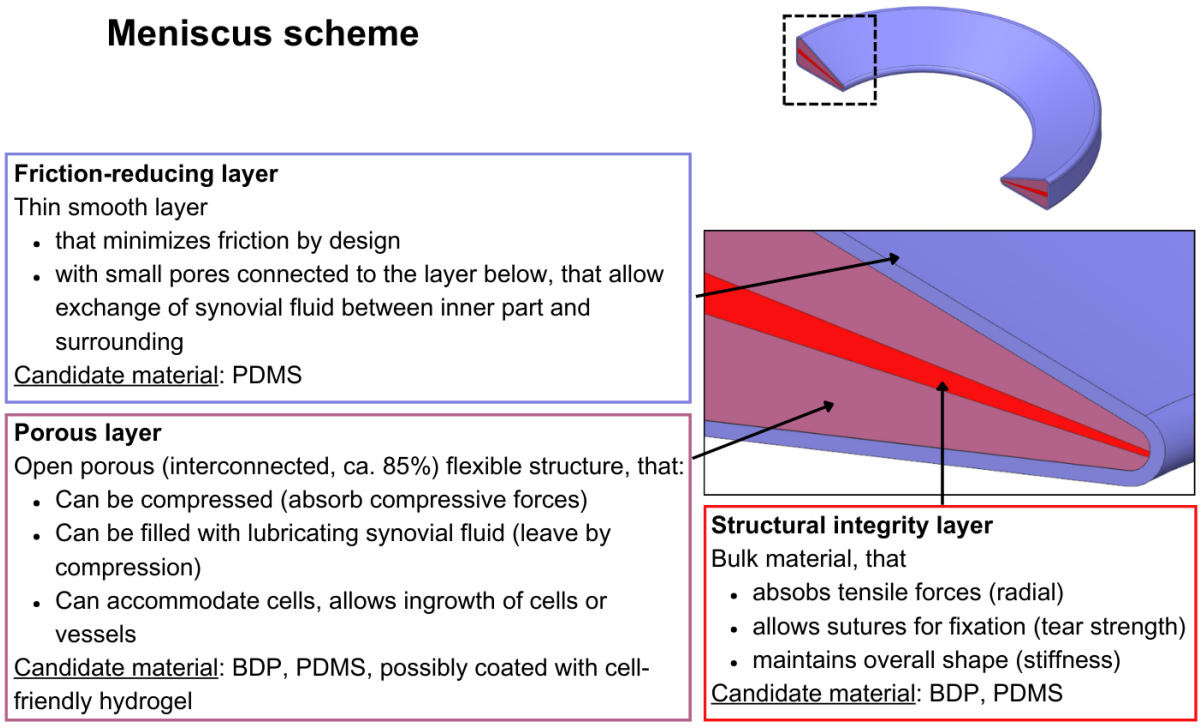


Figure 35: Schematic draft summarizing all the meniscus case study clinical requirements. Pictures courtesy of Charité - Universitätsmedizin Berlin and TransTissue Technologies GmbH, members of the EU INKplant consortium. Special thanks to Dr. Tilo Dehne and Dr. Michaela Endres.

In addition to the mentioned requirements, biological performance, mechanical properties and implant longevity, must be also evaluated. However, this work is not included in this research as it has been carried out for other colleagues of the INKplant consortium.

Back to the design, two types of multi-material technologies are assesed regarding the manufacturing stage. For prototyping purposes, digital 3D printing technologies are used, specifically the PolyJet system from Stratasys company. No medical grade materials are used for this task, only standard commercial ones: Vero Vivid and Elastico, from Stratasys commercial catalogue. It would be taken in advantage the capability of this technology to print structurally complicated geometries even through a reliable combinations of materials. On the other hand, the Elkem LDM printing system will be used to fabricate a silicone meniscal scaffold. In this case, a medical grade PDMS is used, which is deposited in a controlled manner through the implementation of LDM technology, as described in section 3.3.3.

To analyze the most possible scenarios, a reverse engineering-based workflow is followed, where the starting information is obtained in two alternative ways: first, the meniscal scaffold are designed directly over the patient's tibial plateau. This is decided because it may be cases where the meniscus is so damaged that a medical image does not provide much information. It should be noted that in this situation, the meniscus of the other leg could be taken as an anatomical reference by calculating its mirror image. However, this is only possible if at least one of the menisci is in optimal health conditions. Alternatively, the starting information is obtained through patient medical images segmentation, thus generating the stl models from evidence obtained by means of MRI. The meniscus of this second case of study belongs to a porcine cadaver, known to possess anatomical similarities with the human meniscus. Throughout the INKplant project, clinical workshops have been celebrated where surgeons and medical professionals have tested these solutions, simulating real surgeries on these porcine cadavers. For this reason, it was decided to evaluate the implant on an animal model and not on a human one.

6.2. PolyJet multi-material meniscal scaffold from a tibial plateau

Throughout the following chapter, the corresponding design steps are discussed to obtain a scaffold demostrator that complies with the properties listed in Figure 35. Emphasis is placed on the more relevant aspects to consider generating a reliable DFAM strategy. Finally, the evaluation of the printed demonstrators is addressed.

Again, by following a reverse engineering approach, first step is to properly acquire the starting information from real anatomical models. Then, a tibia stl model is used as starting point. It has been downloaded from, Thingiverse, an open-source collaboration platform (236).

This anatomical region of interest must be conveniently captured and processed. For a research case of study an extracted bone from a cadaver can be used, but for the implementation of this methodology in daily practice it must be guaranteed the minimum invasiveness in the patient, preserving its integrity. For this reason, the main method to obtain an anatomy from a patient is through medical images segmentation.

Figure 36a depicts the tibia bone that is employed as reference for the meniscus nominal body generation. For this purpose, NX 2206 is used as the main CAD/CAE resource employed along this PhD thesis. The design only addresses for one of the two menisci of the knee, in this case, the lateral meniscus. As this methodology is presented as a universal workflow for customized meniscal implants generation, it must be replicable by following the same operations in any patient or joint. Thus, the medial meniscus could be obtained exactly by applying the same strategy.

To generate the volume of the implant, a design based on reference guides is proposed. These elements serve as auxiliar elements for generating the solid body through sweeping operations. Figure 36b illustrates the described process, where the curves representing the section guides are shown. Throughout the different operations, a free-form contour has been delimited and projected onto the bone surface of the tibia from an axial view. This contour was defined freely by the author, suggesting that for the design of such medical solutions, the experience of a medical expert is highly valuable. Since this research aims to validate a prototype, no considerations from the literature regarding the optimal volume or most appropriate spatial distribution of the implant have been followed. Only a geometry that mimics meniscal tissue and is fully supported on the tibia are envisioned.

Regarding reference guides delimitation, a center point has been arbitrarily established that allows drawing radii along the entire meniscus 'C-shape' contour. It is mentioned at this point that it can be used as many guides as deemed to obtain a reliable meniscus nominal geometry.

Consequently, Figure 36b illustrates the lateral meniscus nominal volume generated. It can be observed in the different views how this body is completely adapted to the patient's tibial plateau, perfectly fitting the surface of the subchondral bone. This highlights the singularity of the implant, having obtained a personalized solution for the patient.

Next step is to implement all the requested information collected in Figure 35 to generate the tissue engineering scaffold. For this task, nTopology, a specialized software tool in lattice implementation, is used. In the field of medicine, the emergence of new software tools has enabled the semi-automatic acquisition of porous geometries by implementing these lattice structures on solid bodies or nominal volumes. With respect to tissue engineering, these factors have made it possible to design more simplified complex, porous, repetitive, and adaptable geometries, which can be tailored easily in terms of lattice-related parameters.

Therefore, as it was chosen Siemens NX 2206 to obtain the nominal volume of the implant due to its powerful reverse engineering module, it is subsequently used nTopology, a software developed to work with lattice structures among other functionalities, for the implementation of the desired porosity and the generation of the biomimetic FG scaffold.

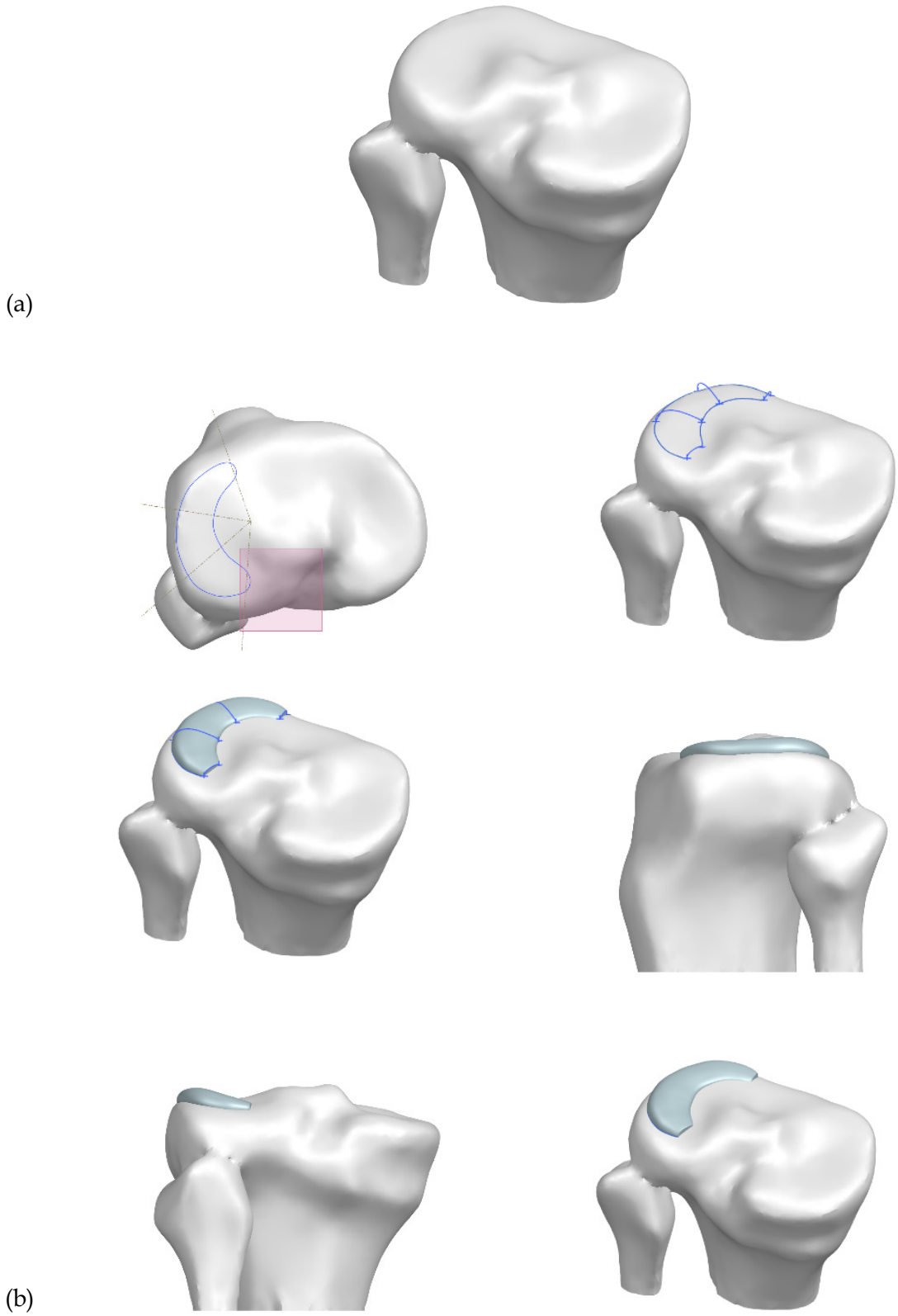


Figure 36: DFAM process of a meniscus implant adapted to the subchondral anatomy of a patient. (a) Design obtained from the positioning of reference guides that allow the execution of a sweeping operation, joining the respective sections.. (b) Sequence of operations for the generation of the solid body completely adapted to the bone.

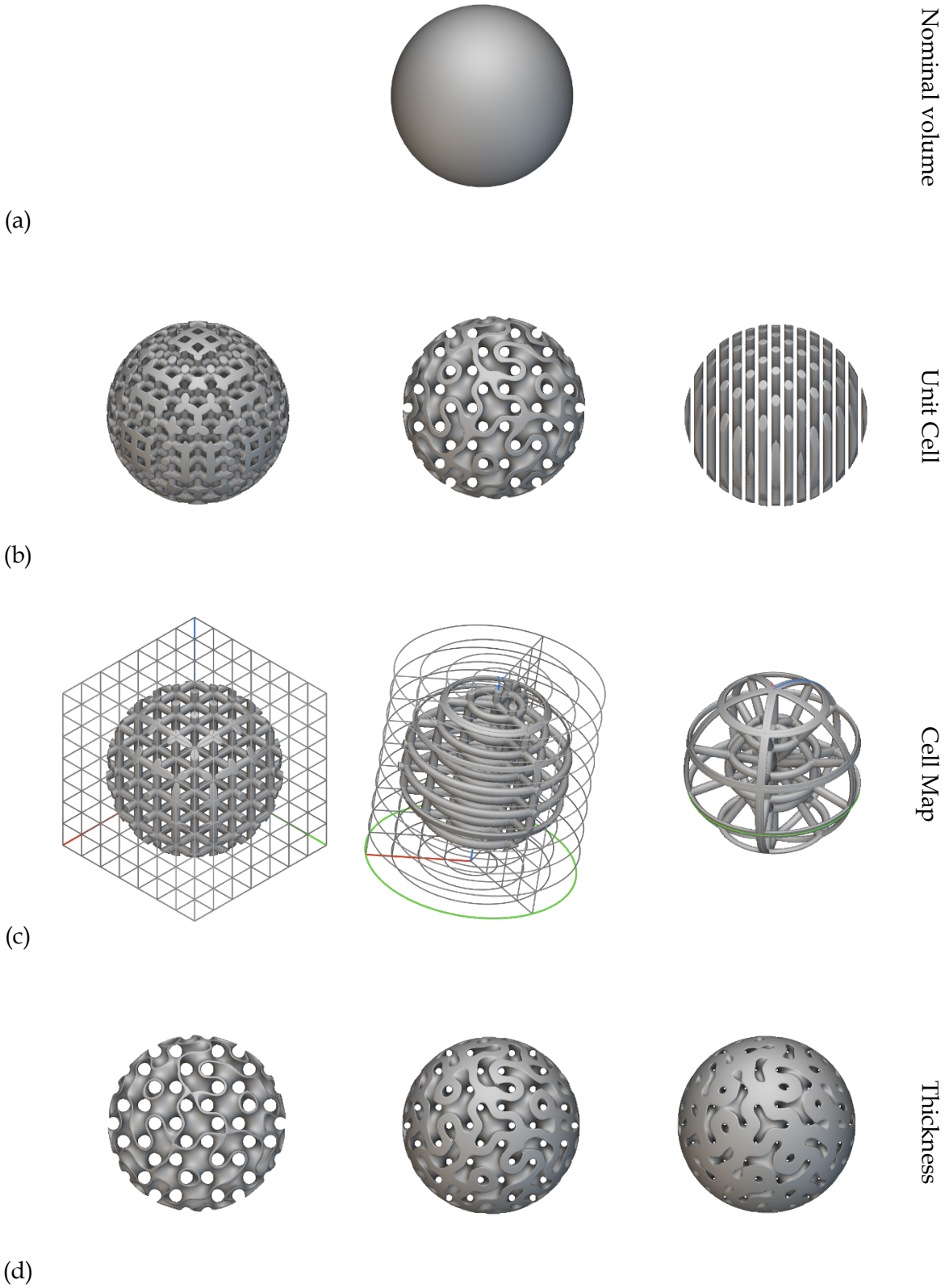


Figure 37: Main construction parameters related to the generation of a lattice structure in the nTopology software. (263) (a) Nominal imported volume. (b) Different types of unit cells (cubic simple, gyroid, column elements) applied to the nominal volume. (c) Different spatial configurations (rectangular, cylindrical and spherical) of the cells around the nominal body. (d) Lattice structure with different thickness values implemented on regular sphere.

When applying a lattice geometry on a nominal volume, there are several factors that must be evaluated as they affect to each other's. To understand how a lattice structure is implemented some of the most relevant parameters that affect the material distribution are explained (263):

- Unit cell: this is the type of unit cell to be selected. It represents the smallest divisible volume, which is repeated as many times in space as the subdivisions of the nominal body are presented in the 'cell map'. It can be used to reproduce along a volume, in the 3D realm, or on a surface. The unit cell can be composed of elements belonging to different types of periodic networks commonly found in literature. Lattices like the TPMS gyroids, or structures replicated in Bravais networks, as the simple cubic, are some examples. Additionally, it is also possible to map any type of element, regular or custom, for a distribution assigned in the cell map, such as geometric shapes (cubes, cones, spheres, etc.).
- Cell map: this controls the distribution of the unit cells throughout the nominal model. Basically, the cell map divides the nominal body into subelements following different rules. These subdivisions can be all geometrically identical or not. Mostly, the cell map can follow a rectangular distribution (subdivision of the prismatic solid encompassing the nominal body, with its faces parallel to the Cartesian planes), cylindrical (cylinder encompassing the nominal body given a radius and a height), spherical (sphere encompassing the nominal body given a radius) or customized (it is possible to generate customized cell distribution maps).
- Thickness: the thickness value, generally in millimetres for tissue engineering applications, that is implemented into the elements of the unit cell. It can be a wall thickness value, as in the case of the gyroid, or beam diameter, as in the case of graphic cells like the centred cubic.

By modifying these three fundamental parameters, control of porosity can be tuned, obtaining a semi-automated process. In Figure 37, the porosity determination across a nominal sphere with a 10 mm radius is shown, based on the set up of the previously described parameters. It is shown how the unit cell choice affects the geometric shape. From left to right, there are examples of simple cubic, gyroid, and a repetitive pattern of columns as unit cells. Regarding the cell map, different configurations are illustrated based on rectangular, cylindrical, or spherical distribution. Lastly, the influence of wall thickness is demonstrated in this case for a gyroid unit cell, observing an increasingly dense geometry as a function of increasing wall thickness.

Once having these concepts explained, it is proceeded to the implementation of these features properly to obtain our scaffolding.

Resuming the meniscus implant design, a rectangular cell map distribution is implemented over the nominal prism that encompasses the meniscus. The dimensions of the unit cells are 1.4 x 1.4 x 1.4 mm^3, belonging to the simple cubic periodic unit cell type, as it is one of the lattices that leads to higher porosities, as demonstrated in chapter 4. On the other hand, the applied beam thickness is 0.6 mm. Once the trusses thickness and the nominal dimensions of

the unit cell have been determined, the pore spacing dimensional length is indirectly established, in case of applying a regular distribution.

In Figure 38, it can be observed an isolated simple cubic unit cell, integrated into its the cell map. As can be seen, the "p" parameter, which linearly represents the amplitude of the pore from its cross-sectional view for each regular cell, can be calculated as the difference between the dimension of the unit cell and the thickness of each beam.

Thus, particularizing for this case, we can easily calculate our porosity as:

$$p = Unit\ Cell\ Dimension - Pore\ spacing = 1.4mm - 0.6mm = 0.8mm \quad (1)$$

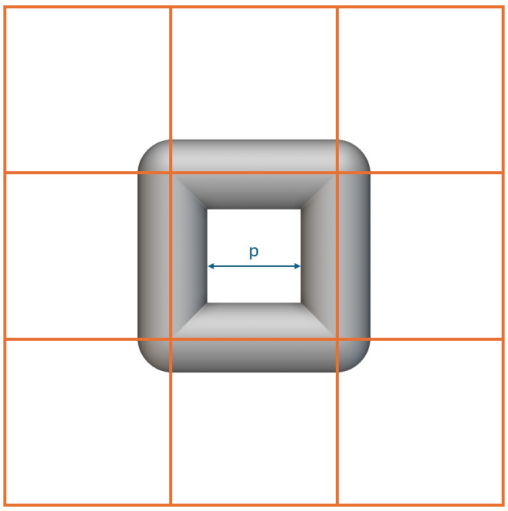


Figure 38: Pore spacing parameter, 'p', for a regular periodic unit cell distribution.

This value is of extreme significance, as when addressing tissue engineering applications through 3D printing systems, two porosities must be considered simultaneously: the overall porosity of the implant, calculated as the volume of material occupied divided by the total available volume, and the pore size, represented in Figure 38, which is fundamental to validate implant manufacturability. In tissue engineering applications, where a very high level of precision is required to replicate pores in the range of micrometres, the pore spacing is closely linked to the manufacturing limits of the technology, as an excessively small pore size can lead to errors during the manufacturing process, thereby preventing the piece from achieving a reliable functionality. In addition, many manufacturing processes, such as the PolyJet technology, require the use of support structures that must be removed in a post-processing step. The pore size therefore, affects the correct removal of the support material, which generally is a process of dissolution in water and mechanical shaking. As the material is distributed throughout the geometry, the applied porosity influences the water to reach all points of the geometry, dissolving the auxiliary material and facilitating its evacuation. Therefore, one must be selective when choosing a technology that provides the necessary precision, repeatability, and reliability to reproduce such accurate details. It is also advisable

to make this choice before the start of the design process, as many considerations should be taken during this stage to facilitate and improve the printing process as much as possible. Hence, the relevance of implementing strategies and methods based on DFAM approaches.

Next, the following lattice structure is implemented on the nominal body of the implant, obtaining a scaffold for tissue engineering. A Boolean intersection operation is applied in the process, resulting in our targeted geometry.

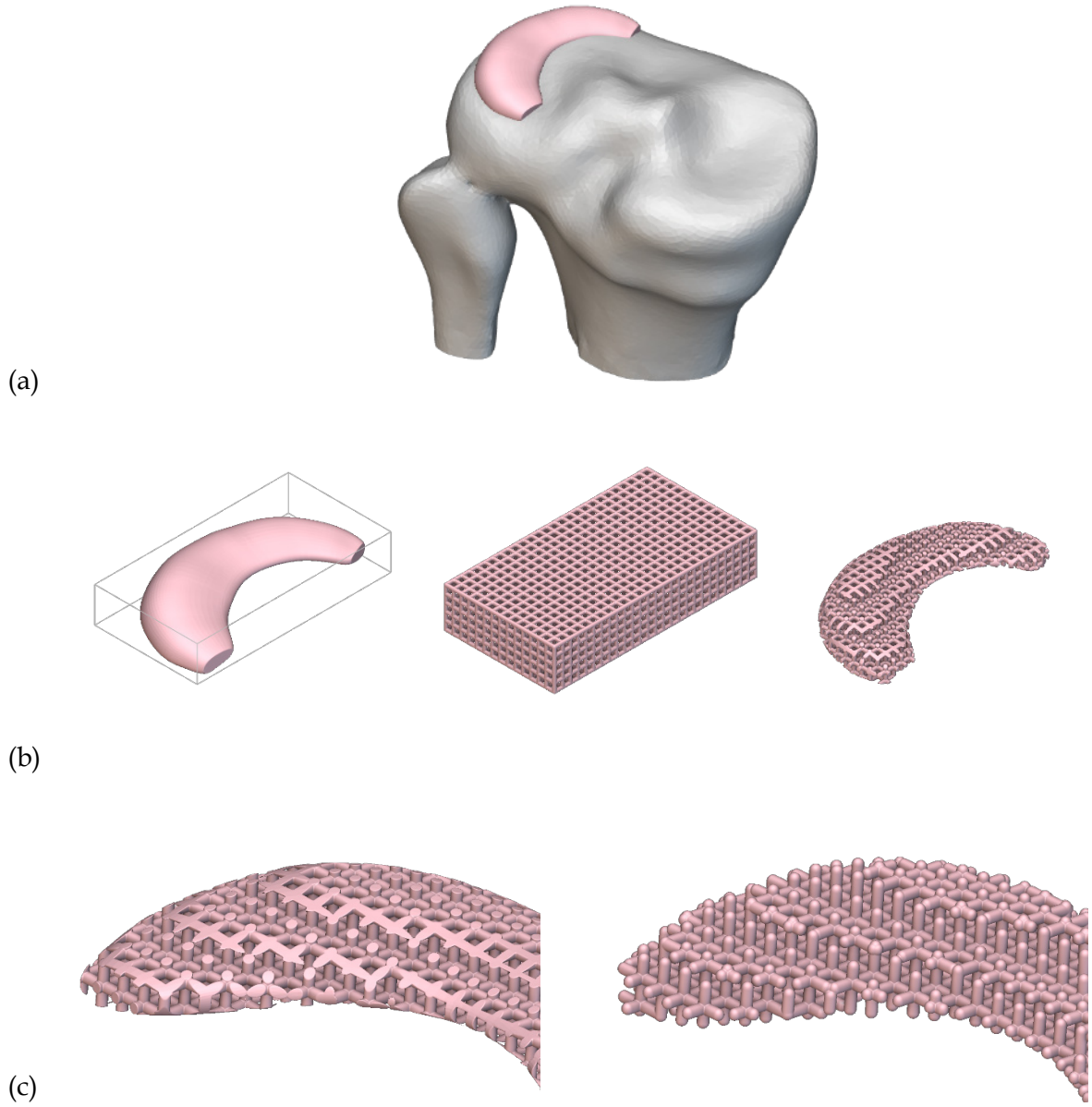


Figure 39: Conformal lattice design on nominal volume imported from NX 2206. (a) Imported stl models. (b) Obtaining lattice with spatial distribution of rectangular cell map and simple cubic unit cell using Boolean intersection operation. (c) Corrective operations on discontinuities in the contours of the lattice to guarantee a constant thickness throughout the entire geometry.

As can be observed in Figure 39c, upon applying a Boolean intersection operation, the resulting geometry loses its regularity and repeatability in its contour, leading to incomplete unit cells along the borders of the nominal body. This occurrence can potentially incur to complications since, a priori, it cannot be determined the state of each and every one of these intersected cells, which may result in regions where infinitesimal thicknesses occur due to the mathematical software calculation. These controversial thicknesses could potentially hinder the manufacturing process in later stages, since they could be values that are below the threshold that can be manufactured by selected system. Figure 39c illustrates this situation and demonstrates how it can be rectified using the appropriate tools. Henceforth, it is of paramount importance to exercise absolute control over such details to ensure, at least as much as possible, so unexpected incidents can ve avoided during the printing process. In this case, by means of operations on the contours of the lattice, an existing minimum thickness threshold can be set up, which the designer must ensure to be reliable during the production.

At this point, the porous layer is ready. Then, next step is to generate the friction-reducing layer envisioned in Figure 35. This layer can be conceptualized as a surface coating, which, like the previous layer, must possess a certain level of porosity. The design process is very similar to that applied for the porous layer, with the particularity that, while previously it has been implemented a standard rectangular cell map distribution to endow the volumetric porosity, currently creating a conformal membrane on the meniscus surface requires generating a custom cell division map. Figure 40a shows how this new distribution is faithfully developed throughout the nominal volume, so that the new spatial distributions are completely independent of each other, not being periodically replicable in space to obtain the initial meniscus. In this manner, it is possible to extract a stl sheet from the nominal solid, and to generate a map from it that allows us to govern the spatial distribution of the friction-reducing layer trusses.

It must be noted that, throughout the entire process nominal contours of the meniscus geometry have not been altered. This can potentially lead to future design challenges in case that the same surface is used to generate both, the porous layer and the friction-reducing membrane that surrounds it, simultaneously. Following this strategy, material confluences are likely to occur at certain points along the border between these two regions. Therefore, to design a reliable friction-reducing layer, that does not lead to complications during the manufacturing phase, it is advisable to first apply an offset operation to the nominal geometry, thereby separating both spaces to prevent potential overlap. Additionally, it is recommended to apply an offset value similar to the desired thickness of the membrane. As illustrated in Figure 40a, this sectional view clearly identifies the nominal volume used for generating the porous layer, as well as the nominal volume shaped like a shell, which serves as the starting point for generating the surface membrane.

Once all regions have been delineated, it is possible to proceed with the generation of the membrane. By implementing a new spatial configuration controlled by the cell map, along with an element thickness of 0.8 mm, the expected outcome is achieved as shown in Figure 40b.

To conclude the design, the only remaining step is to incorporate the structural integrity layer within the porous region. As mentioned earlier, this layer is designed to reinforce the core of the implant, with the goal of creating stronger zones that can be sutured during surgery to attach the model to the patient healthy tissue. To achieve this, it is decided to introduce a thin section of material into the implant structure that runs along the entire profile of the meniscus. As depicted in Figure 40c, it becomes evident that it is necessary to perforate this layer; otherwise, it would isolate the porous layer into two disconnected halves in vertical direction, thus preventing the flow of synovial fluid and limiting cell growth.

Through a Boolean subtraction operation, the material portion of the porous layer that spatially intersects with the structural integrity layer is removed. Thanks to the design process followed, the material can be provided with the desired functionality even using single-material technologies, given that the structural integrity layer acts as a reinforcement of the core of the implant, thus presenting more optimal conditions for suturing during insertion. surgery than the porous layer. However, two different stl files can be generated to proceed with the printing of both layers in different materials, which have different mechanical properties.

Finally, a schematic of the ultimate prototype can be observed in Figure 41a, where all the concepts outlined in the draft provided in Figure 35 have been incorporated.

Once the design is finalized and the workflow that relates the different layers of our concept has been established, it is relatively easy to obtain scaffolds with different porosities that present different unit cell configurations and spatial distributions. Note in Figure 41b that both, porous layer and friction reducing layer have been modified. These features have been implemented just by clicking and selecting different unit cell options and cell maps subdivision. Thus, this new approach enables to tune lattice characteristics such as thickness or porosity in a very simple way.

Additionally, please note in Figure 41c the high level of customization of the tissue engineering scaffold, which is fully adapted to the patient's bone anatomy regardless of the determined thickness values or the chosen cell types, since it has been designed from nominal volumes fully adapted to the initial tibia anatomy.

To maximise the biomimetic qualities that the meniscal scaffold may possess, a series of operations are implemented in order to redistribute the trabeculae spatially so that they are arranged along the meniscus, imitating the natural distribution of the tissues. The aim is to properly modify the distribution cell map to replicate the cubic cell along the nominal geometry of the implant, with a personalized configuration. Figure 42a, illustrates the fibers distribution along the meniscal anatomy (264). Therefore, by properly modifying the cell map layout, it is possible to alter the porous layer trusses, in such a way that they can mimic the distribution of meniscal fibers depicted in Figure 42a. It must be understood that the implementation of this custom cell map entails the loss of the spatial repeatability of the unit cells, meaning that pore spacing is no longer a constant value for each cell, but rather a gradient of increasing porosity is now applied in a radial direction. This phenomenon is depicted in Figure 42b where smaller pores are in the inner zone of the scaffold while larger spaces are situated in the red zone region.

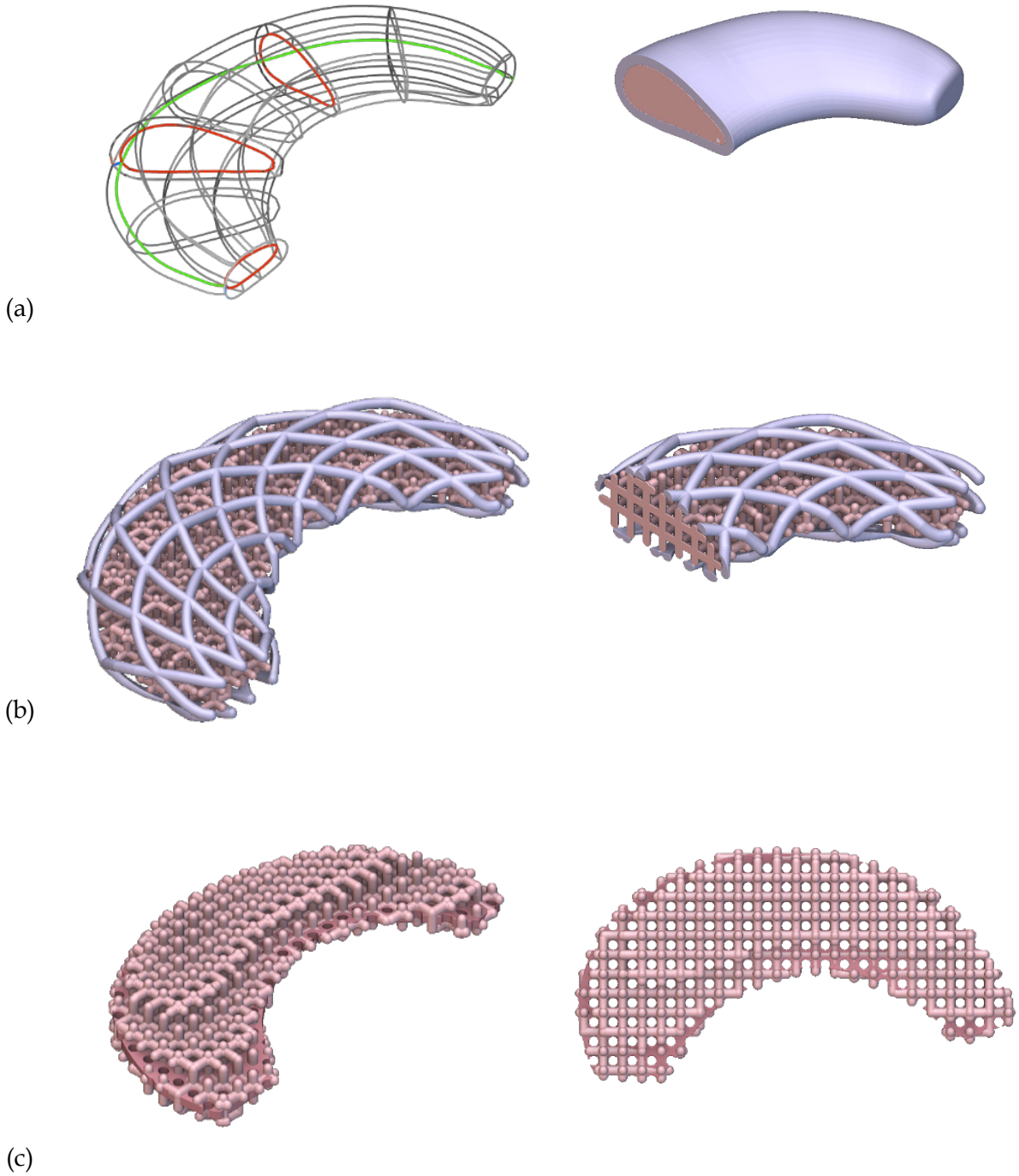


Figure 40: Design and integration process of the friction-reducing layer and the structural integrity layer in the porous layer. (a) Generative operations of the nominal casing that give rise to the friction reducing layer. (b) Isometric and section view of the porous layer integrated into the friction-reducing layer. (c) Design and integration of the structural integrity layer on the porous layer.

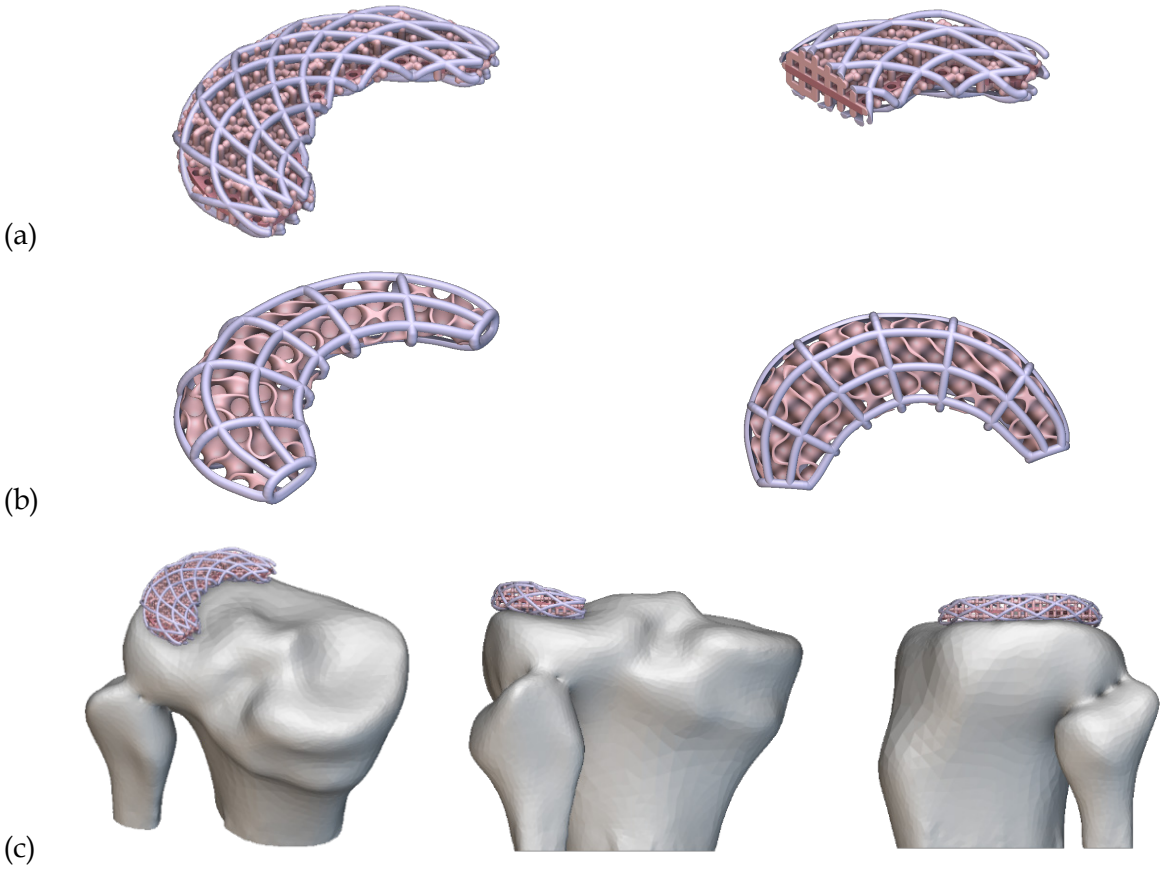


Figure 41: Innovative meniscus scaffold model for tissue engineering applications that meets the requirements outlined in the INKplant project (see Figure 35). (a) Prototype with porous layer with simple cubic unit cell lattice structure. (b) Prototype with porous layer with gyroid unit cell lattice structure. (c) Isometric, front and lateral views of prototype meniscal scaffold completely adapted to the subchondral surface.

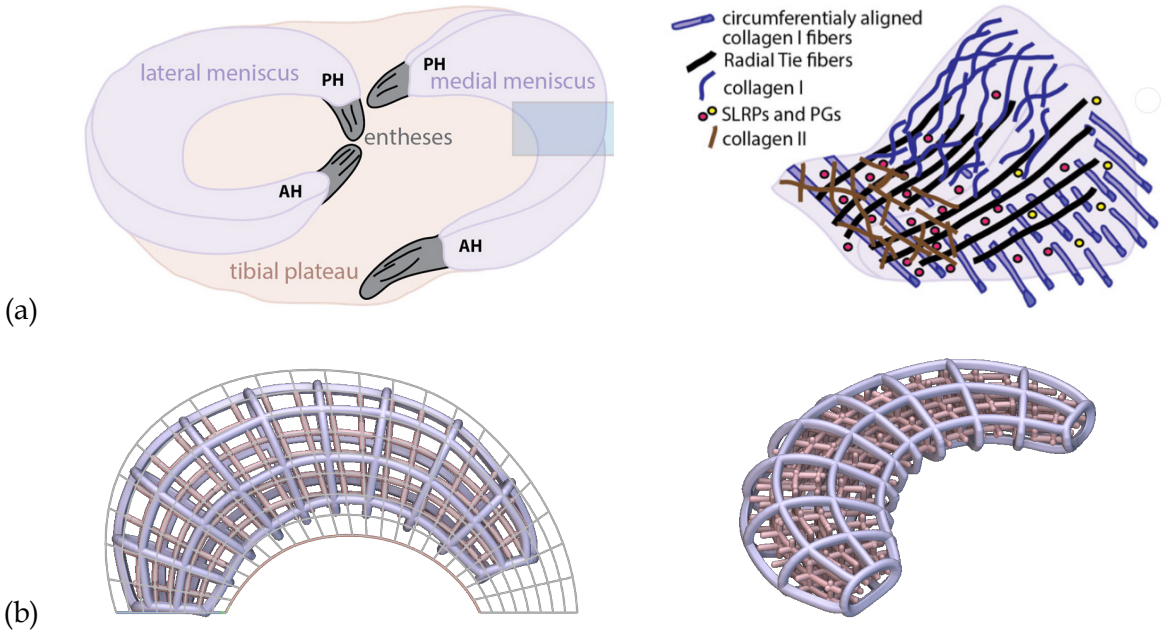


Figure 42: Innovative meniscus scaffold model for tissue engineering applications that meets the requirements outlined in the INKplant project (see Figure 35). (a) Prototype with porous layer with simple cubic unit cell lattice structure. (b) Prototype with porous layer with gyroid unit cell lattice structure. (c) Isometric, front and lateral views of prototype meniscal scaffold completely adapted to the subchondral surface.

Figure 42: Design of meniscal scaffold with biomimetic behaviour. (a) Scheme illustrating the position of the lateral and medial menisci on the tibia plateau and section view of their tissue orientations. (b) New biomimetic concept of meniscal scaffold prototype in which the trusses follow radial and circumferential arrangements, imitating the natural distribution. Pictures in (a) acquired and adapted from "Meniscus Repair: From In Vitro Research to Patients" (264).

Finally, after offering a variety of possible configurations to obtain tissue engineering scaffolds for the restoration of complete menisci, the next step is to evaluate the manufacturability of the designs. For this purpose, the designed models are printed using PolyJet technology, in particular the Stratasys J55 Prime printer. Different materials from Stratasys' commercial catalogue, which have different mechanical properties, are combined in order to evaluate the integration of all these concepts in a single part from a constructive point of view. The prototype collection is shown at Figure 43.

It should be remembered that the sole purpose of using PolyJet technology in the manufacture of these prototypes is to make it possible to obtain a complex prototype that allows all the defined structural requirements to be included. Furthermore, the combination of the Elastico and Vero materials allows the behaviour of the implant to be recreated by selectively providing it with flexible and rigid zones.

In addition to the already designed prototypes, a batch of meniscus scaffolds generated from animal medical images was printed for evaluation by medical professionals. In this way, the described methodology is validated as it has been applied for this real case of study, in which the corresponding operations of image acquisition, medical image segmentation, generation of the anatomical stl models, generation of the nominal geometries and lattice generation have been implemented. Thus, in the framework of the INKplant project, this clinical workshop activity was organised with qualified surgeons, used to deal with this type of articular injuries and these surgical replacements. The main goal of this event was to get the opinions of experienced medical professionals who will ultimately assess the feasibility of this solution. Figure 44 collects the whole process that includes designing the conformal nominal geometry, implementing the lattice structure to obtain the desired porosity and manufacturing the model to get the final result.

Thus, the repeatability of this DFAM methodology for personalised meniscus scaffolds is proven.



Figure 43: Functionally-graded meniscal tissue scaffolds collection printed using a multi-material PolyJet system from Stratasys. Prototypes printed by Stratasys colleagues in the frame of the INKplant project. Special thanks to Dr. Mariana Pokrass, Dr. Lev Kuno and Lior Zonder. Pictures courtesy of Álvaro Troyano, from 3Dtive S.L.

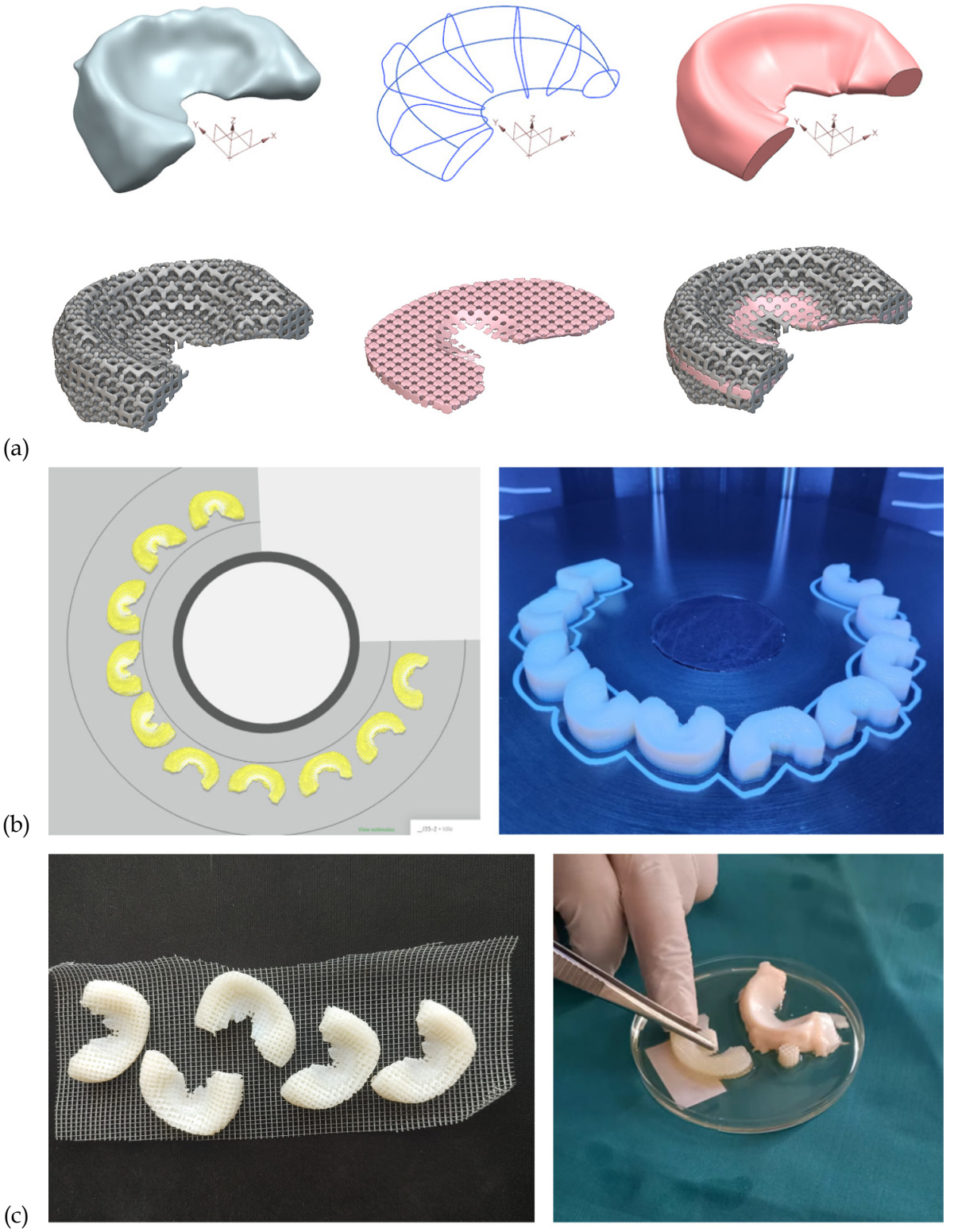


Figure 44: DFAM methodology applied to obtain a batch of meniscal scaffolds to be evaluated during a clinical workshop with animal cadavers organized within the framework of the INKplant project. (a) Design process in NX 2206 to obtain the nominal geometry and conformal lattice design stage in nTopology. (b) Manufacturing process using PolyJet technology by Stratasys coleeagues. (c) Collection of FG meniscal scaffolds to be manipulated during the workshop. Special thanks to the all the colleagues of the European INKplant project who took part in the process: Charité - Universitätsmedizin Berlin, TransTissue Technologies GmbH, Stratasys, Profactor GmbH and JKU Linz Institute of Polymer Product Engineering.

6.3. Liquid Deposition Modelling (LDM) meniscal scaffold from patient medical images

In the previous section, an innovative DFAM methodology has been described in order to obtain a pioneering prototype that included all the clinical requirements stated by the INKplant clinical team colleagues. In order to be able to manufacture a part with such a level of detail and complexity, it has been used a versatile multi-material additive manufacturing technology that facilitated the safe combination of materials, resulting in a FG tissue engineering scaffold. However, from an applicability point of view, the whole process is reduced to a concept presentation, as the materials used lack a health licence and cannot be used for medical purposes yet.

Therefore, in the subsequent chapter, a further exploration is conducted on the employed methodology for the design of the meniscus scaffold for tissue engineering, but this time it is oriented to extrusion-based or deposition additive systems. The main objective is to fabricate a customized meniscus implant utilizing advanced 3D bioprinting technology, employing PDMS, a medical graded silicone, in combination with a cell-loaded biogel. Throughout the process, the most relevant considerations to be highlighted, given that the technology used on this occasion differs in many respects. Building upon the foundations described in the preceding section, this segment initiates with a model obtained from medical imaging of a porcine knee joint.

The printing process is carried out by Elkem Silicones company using an LDM multi-material printing system, characterized by its capability in the controlled deposition of silicones and biogels. The material selected for this purpose is biomedical-grade silicone, PDMS, as delineated in Section 3.3, from the Silbione™ series (194). A comparative analysis with digital 3D printing technologies highlights a significant increase in complexity in fabricating a porous implant using extrusion or deposition-based systems. By using this type of AMT, it is very complex to obtain a prototype like the one shown in Figure 43 as it is highly challenging in terms of constructive capabilities. For this reason, the research focus in obtaining porous scaffolds by implementing "woodpile" patterns, obtained by successive depositions of the traces horizontally and parallel to each other. It should be noted that, while inkjet-based systems such as the PolyJet technology contain multiple nozzles capable of depositing particles on a nanometre scale, this bioprinting system uses a dispenser with a nozzle tip in the order of hundreds of µm, which places its range in terms of precision on a micrometre scale. Given the precision required to obtain these tissue engineering scaffolds, where pore sizes are usually close to the millimetre, the use of this technology means pushing its functionality close to the limit, considering that theoretically it is not possible to guarantee the fabrication of any element whose thickness is below the nozzle diameter. For this reason, it is especially important to take care of all these single details, which may seem not to create any conflict at early stages of the design process but they may lead into unforeseen difficulties at successive phases. Implementing a DFAM is essential in order to identify all of these relevant aspects that can facilitate the printing process.

To simplify the process, this section excludes the friction-reducing layer that surrounds the porous layer, as depicted in Figure 35. The focus is solely on evaluating the feasibility of generating a lattice structure within a nominal body, aiming to provide it with the appropriate porosity for tissue engineering applications, thereby enabling its production using the aforementioned technologies.

Before starting the design for the customization of the scaffold structure, it is decided to perform a series of porosity tests to establish a safe working range, so the manufacturability of the scaffolds is performed securely in the prototyping process. For these tests, a flat face is included on the lower surface of the nominal meniscus obtained in the previous section. This operation is performed by extracting the surface of interest, the one in contact with the subchondral bone, and extruding it consequently. Siemens NX 2206 is used as this stage. The presence of a flat surface on the model facilitates the manufacturing process and saves time and material, since it allows the absence of support material, being able to print the complete model directly over the printing platform. However, this approach sacrifices customization, as the implant no longer conforms adequately to the patient's tibia. The primary aim of these preliminary tests is to create a simplified scaffold geometry that can be quickly manufactured.

To obtain the collection of samples with different porosities, the beam thickness parameters and the nominal dimensions of the cell map shall be modified. Thus, each lattice implemented on the nominal geometry must have a pore size equivalent to the thickness of its trusses. Values of 0.4, 0.6 and 0.8 mm respectively are used for this study. Figure 45a showcases an updated meniscus design tailored to the patient's geometry, easily modified with an extruded flatten face on its underside. The nominal geometry is imported into nTopology, where the scaffolds collection with variable porosity is obtained by modifying the construction parameters of the scaffolding. Figure 45b illustrates the sequence of operations corresponding to the process. Once again, a rectangular configuration of the cell map is used, but this time cubic cells are not periodically replicated on it. This fact is conditioned by the complexity of manufacturing vertical pillars such as those integrated into the cubic cell through a material deposition process. Understanding the complexity of printing a 0.8 mm diameter using a 0.4 mm dispenser. The deposition of material would be practically punctual, which, added to the successive stacking, would result in a weakening of the structure. Instead, to obtain the necessary porosity, it is implemented a configuration of horizontal elements that are stacked on top of each other following a wood pile pattern. The orientations of these columnar groups are aligned with the cartesian X and Y axes. This arrangement results in a lattice comprised of beams stacked in perpendicular directions, alternating in succession to envelop the entire nominal volume. It is critical to note that these beams are designed to stack above one another without intersection, maintaining tangency in the Z-direction, while avoiding intersection in the X- and Y- axis. Achieving this overlapped configuration is straightforward: one lattice set is displaced over the other along the Z-axis by a distance equivalent to its beam thickness, so this relationship can be established within this parametric workflow, allowing the porosity to be updated by correctly determining the parameters.

Ultimately, the porous scaffold, precisely tailored to the meniscus geometry, was derived through a Boolean intersection operation. As intended, Figure 45c showcases a series of

meniscal scaffolds, each exhibiting varied porosities. These models were derived by systematically altering the thickness parameters and the spatial distribution within the cell map configuration. Pore sizes and beam diameters of 0.4, 0.6, and 0.8 mm have been implemented respectively.

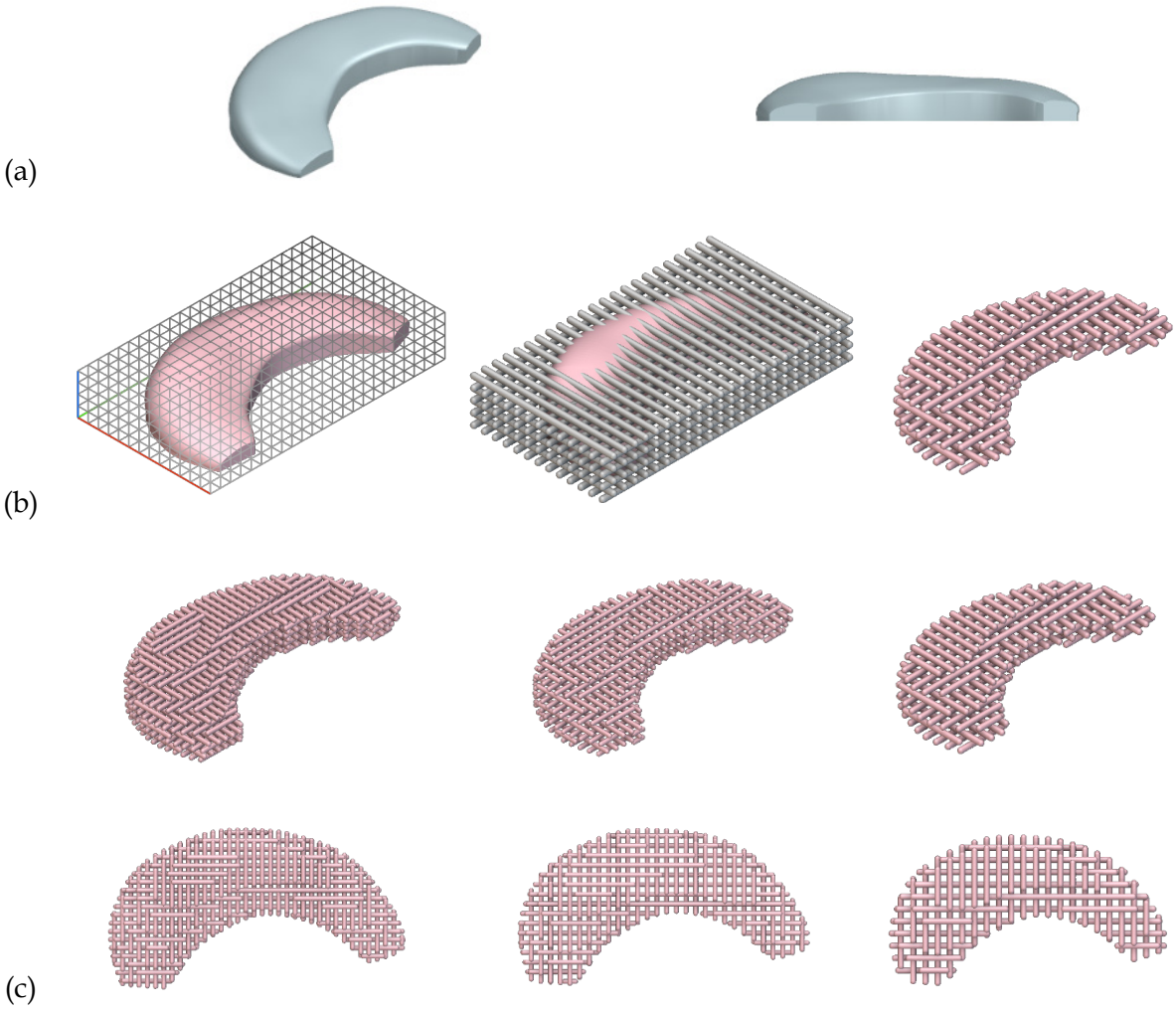


Figure 45: Design and implementation process of lattice structure that follows a woodpile pattern on a regular meniscus. (a) Nominal geometries with added flat surface. (b) Generation of the lattice with woodpile layout and application of intersection Boolean operation. (c) Isometric and top view of a variety of meniscal scaffolds with different porosities designed for pore sizes and element diameters of 0.4 , 0.6 and 0.8 mm respectively.

Once the designs are ready, they are printed to evaluate the ability to generate different ranges of porosity on the same nominal geometry based on a beam thickness and spatial distribution. Delving into the technical aspects of the manufacturing process, it is essential to recognize that the beam diameter significantly influences the choice of the deposition tool. For instance, in the fabrication of meniscus scaffold with a lattice configuration of 0.8mm thickness elements, it is advisable to employ a commercial dispenser with a 0.4 mm inner diameter. This allows for at least two perimeters for each layer of the element. Conversely, for beam diameters of 0.4

mm and 0.6 mm, a dispenser with a commercial diameter of 0.2 mm is recommended, yielding 2 and 3 perimeters respectively. It is imperative to note that these values concern to the production per layer, specifically addressing the material volume in the XY plane parallel to the printing platform.

The height of each element is determined by a parameter known as "layer height", which dictates the number of layers required to accurately reproduce the intended geometry. In this study, a layer height of 0.2 mm was established, ensuring compatibility with all designed prototypes, and facilitating precise layer calculation in the slicing software for G-code generation. It is important to emphasize that in 3D printing, the value of layer height need not exactly divide the height of any given element. Slicing software is adept at approximating parameters to find optimal solutions. Nevertheless, given the precision demanded in this application, an error margin of 25% to 50% due to an additional or missing layer is considered significant, particularly when dealing with layers of 0.2 mm thickness and elements ranging from 0.4 to 0.8 mm in diameter. Thus, with a layer height of 0.2 mm, beam elements with diameters of 0.4, 0.6, and 0.8 mm are constructed made from 2, 3, and 4 layers, respectively. The outcomes of the printing process for the models with 0.4 and 0.8 mm beam diameters are illustrated in Figure 47a.

As mentioned, the precision achieved in the fabrication of these structures is notably lower compared to the use of PolyJet technology. In addition to evaluating the pore size, a calculation of the overall porosity of the implant was performed. To do this, the following relationship is expressed as the amount of free volume between the total volume available. This results in the division of the volume value obtained in the lattice structure divided by the nominal total volume of the meniscus, expressed as a percentage. Theoretically, the overall density of these three candidates should be the same, with a value of 50% porosity for each of them, since both the thickness of the struts and the pore size are assigned the same value, so that the nominal space is equally distributed between pore channels and trusses. However, this is not the case, tending to generate parts with a porosity slightly higher than 50% (see Table 16). As mentioned earlier in this chapter, the irregularities produced in the contours by the Boolean operation applied generate unit cells that are not complete but intersected. This fact directly affects the global porosity value, determining this value according to its distribution along the contours of the nominal body.

$$Porosity\ (\%) = \frac{Nominal\ Volume - Lattice\ Volume}{Nominal\ Volume} \cdot 100 \qquad (2)$$

	Nominal Geometry	**Φ 0.4mm**	**Φ 0.6mm**	**Φ 0.8mm**
Volume (cm^3)	1.482	0.597	0.654	0.583
Porosity (%)	0	59.7	55.9	60.7

Table 16: Overall porosities values calculated for the meniscal scaffolds batch depicted in Figure 45c.

After evaluating the obtained quality in relation to the pore size in the printing process, as well as comparing the global porosities to which the maintenance of a thickness value equal to the separation of trabeculae leads, it is concluded that the ideal candidate must possess a thickness value of 0.8 mm with the beams separated by the same distance value.

This chapter also deals with the biomimetic implant capabilities, wherein the trusses follow a radial and perimetral arrangement, as illustrated in Figure 42a. To achieve this trabecular arrangement, a series of procedures like those previously described were employed. By correctly modifying the cell map configuration, this biomimetic distribution of the material can be achieved. Similar to the model depicted in Figure 42b it is necessary to account for the loss of spatial repeatability for the unit cell pattern, thereby inducing a gradient in porosity. This gradient manifests as a decrease in pore size towards the inner zone and an increase towards the outer direction.

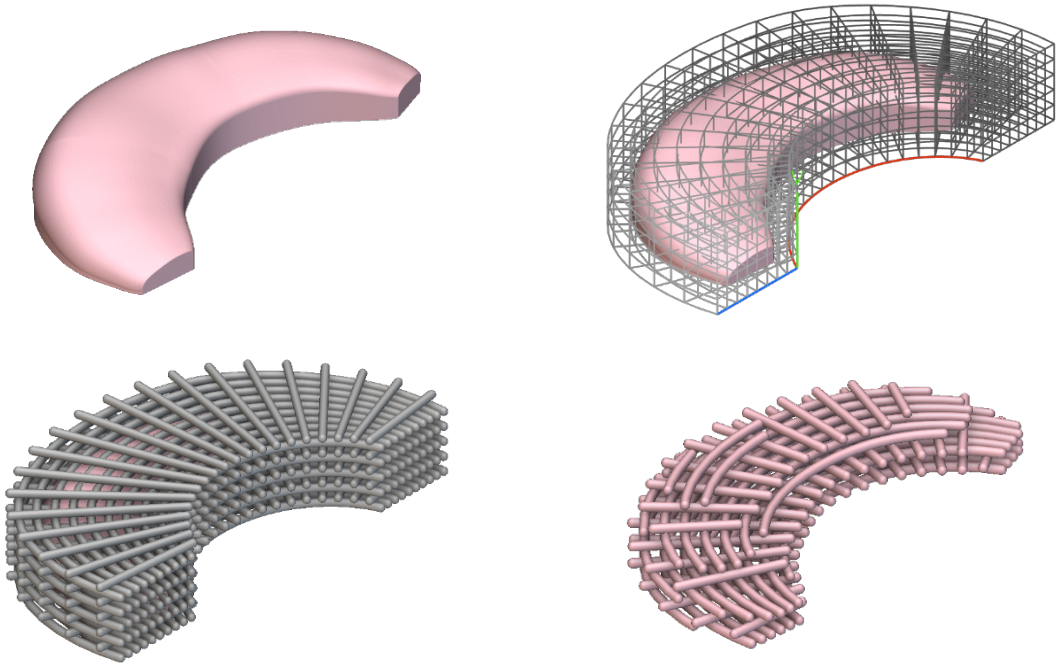
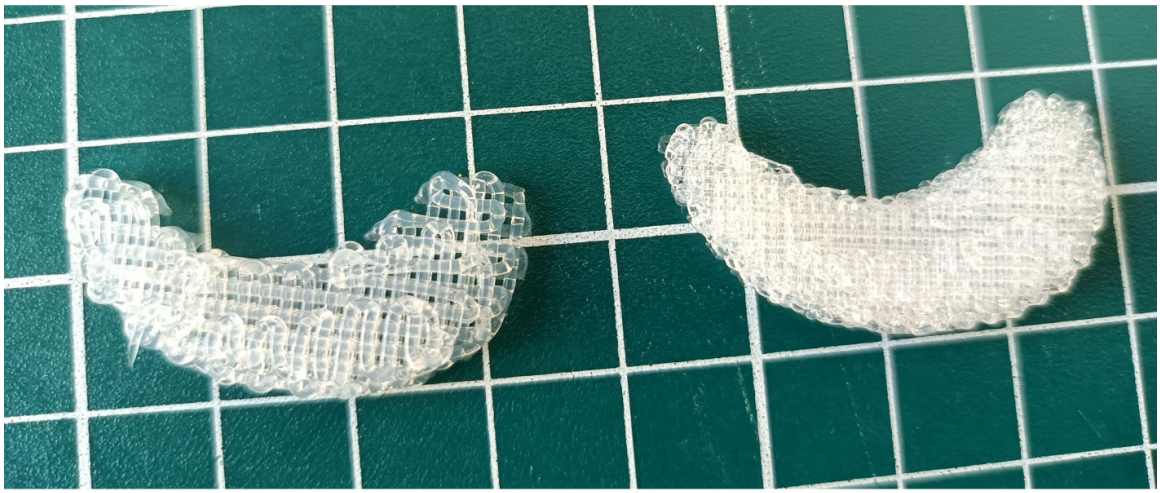


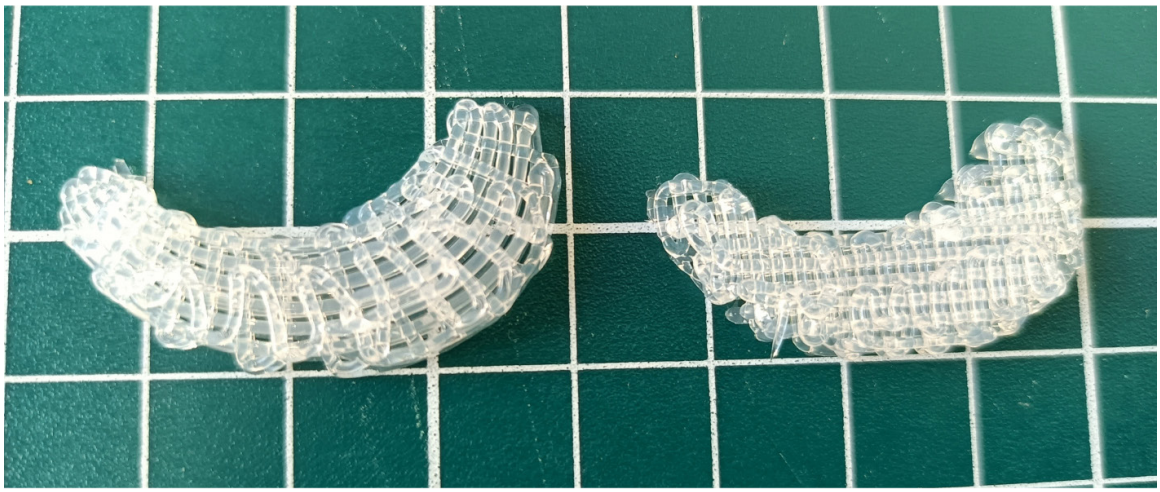
Figure 46: Sequence of operations for the implementation of a lattice following a radial and perimeter biomimetic beam layout inspired in the trusses distribution shown in Figure 42a.

The prototypes fabricated from these designs are displayed in Figure 47b. Visually, it is clear that the surface quality of these solutions may pose certain complications if willing to obtain complex porous geometries with vertical trusses. For this reason, it is decided not to include the friction-reducing layer for this approach.

(a)



(b)



(c)



Figure 47: Meniscus scaffolds prototypes printed by colleagues of Elkem Silicones using a Liquid Deposition Modelling (LDM) system. (a) Meniscal scaffolds with pore size and element diameter of 0.4 and 0.8 mm respectively. (b) Meniscal scaffold with biomimetic arrangement of structure lattice following a woodpile pattern. (c) Cylindrical specimens printed to test porosity with designed pores of 0.4, 0.6, and 0.8 mm respectively. Pictures courtesy of Elkem Silicones. Special thanks to Dr. Clément Perrinet and Dr. Damien Djian .

Once the working range values for pore size and element diameter have been determined, it is presented the design process for a patient specific solution that follows a woodpile pattern. Beside this, this time the nominal implant volume is obtained by means of medical image segmentation. The meniscus used for this case of study belongs from a porcine cadaver. Within the framework of the INKplant project, a collection of 10 meniscal specimens was obtained and used as the object of study. Artificial defects are applied to each of these specimens in such a way that they were useful as a case study where different meniscus tears are represented. In this reverse engineering process, a healthy, defect-free porcine meniscus was digitized using MRI. Subsequent segmentation of the data medical image facilitated the generation of the stl model.

Figure 48 exhibits the medical equipment utilized for scanning, alongside the scanned collection of porcine menisci. Upon acquisition of the medical images and subsequent segmentation and generation of stl files by the colleagues of Charité - Universitätsmedizin Berlin, TransTissue Technologies GmbH and JKU Linz Institute of Polymer Product, the design operations are implemented. To define the nominal geometry of the lateral and medial menisci, reference guides were strategically positioned. These guides, derived from intersecting the meniscus models with a series of radially arranged planes relative to an arbitrary center, facilitate a sweeping operation. By sweeping the respective auxiliar sections garnered from this operation, a solid geometry tailored to the specific meniscus is formed. Notably, this approach, initially based on a healthy meniscus, affords the flexibility to rectify any superficial defect. This is accomplished by modifying the contours of the guides, allowing for the correction of potential lesions. The precision of this operation is directly proportional to the number of guides implemented across the entire section of the stl model. The accuracy of the process can be checked by visually evaluating the overlapping of the generated solid body (gray colour) from the initial stl (blue colour).

Subsequent to importing the nominal geometries into nTopology, the corresponding lattice structures were set up. It is imperative to remember that the beams in the porous layer must maintain a thickness of 0.8 mm, with equivalent pore sizes. Furthermore, the creation of a customised implant at this stage imposes the absence of planar faces along the nominal volume. Therefore, an additional model is proposed to function as a customised support structure, incorporating a flat face on its lower surface. This design facilitates scaffold printing on a customised bed, especially in scenarios where suitable support structures cannot be applied within the manufacturing software (see Figure 50a).

To accommodate printing requirements and address the technical limitations of the system, a modification was made to the lattice structure. The trabeculae's cross-sectional shape was altered from circular to square. This adjustment aids in generating more optimized trajectories in the G-code file. For a 0.8 x 0.8 mm^2 square section element, intended for printing with a 0.4 mm dispenser at a layer height of 0.2 mm, the strategy involved selecting 2 perimeters and 4 stacked layers in Z direction for each element. The comparison between these two configurations can be seen in Figure 50b. By calculating the trajectories described in the manufacturing process in the Ultimaker Cura slicer, this fact can be evidenced (see Figure 50c). It demonstrates that in the left model, where the cross-section remains consistent along the Z-

axis due to its square shape, a distribution of two perimeters is observed for each element within the lattice. In contrast, this uniformity is not achievable with circular configurations, as their thickness varies along the Z-axis.

After having solved this aspect, the customised design of a porous scaffold for meniscus restoration is concluded. However, as mentioned previously, only the porous layer has been replicated. To advance towards a more innovative implant, the pursuit of a FG solution can be addressed from a muti-material approach. Utilizing the capabilities of the LDM multi-material system, which can handle up to five materials plus support material, a thin portion of the already applied lattice structure can be isolated with the aim of having it printed with a more robust biomedical-grade silicone. Automatically this fact introduces an integral structural layer concept, delineating areas within the same implant that possess distinct mechanical properties.

In addition, this prototype was used to explore new possibilities in terms of manufacturing. In controlled deposition 3D printing technologies like this, due to the absence of photopolymerization systems or other stimuli potentially detrimental to cell proliferation, this technology is considered optimal for evaluating the feasibility of fabricating an implant through PDMS deposition hybridised with another biogel that contain a cellular charge throughout its entire volume. To undertake this task, it was necessary to generate the stl of the negative lattice cavities, theoretically representing air-filled voids. These stl files were produced using Boolean subtraction operations, contrasting the porous implant with the nominal volume of the meniscus. This approach indirectly yields a new lattice, complementary to the preexisting one, such that the combination of both reconstructs the initial nominal space. Figure 50d illustrates this process, showcasing how by assembling two meniscal lattices, the complete volume can be generated. Lastly, Figure 51 and Figure 52 displays the printed prototypes for the validation of the designs.



Figure 48: Medical imaging technology used for digitisation of porcine meniscus collection. Pictures courtesy of the INKplant consortium colleagues of Charité - Universitätsmedizin Berlin and TransTissue Technologies GmbH. Special thanks to Dr. Tilo Dehne and Dr. Michaela Endres.

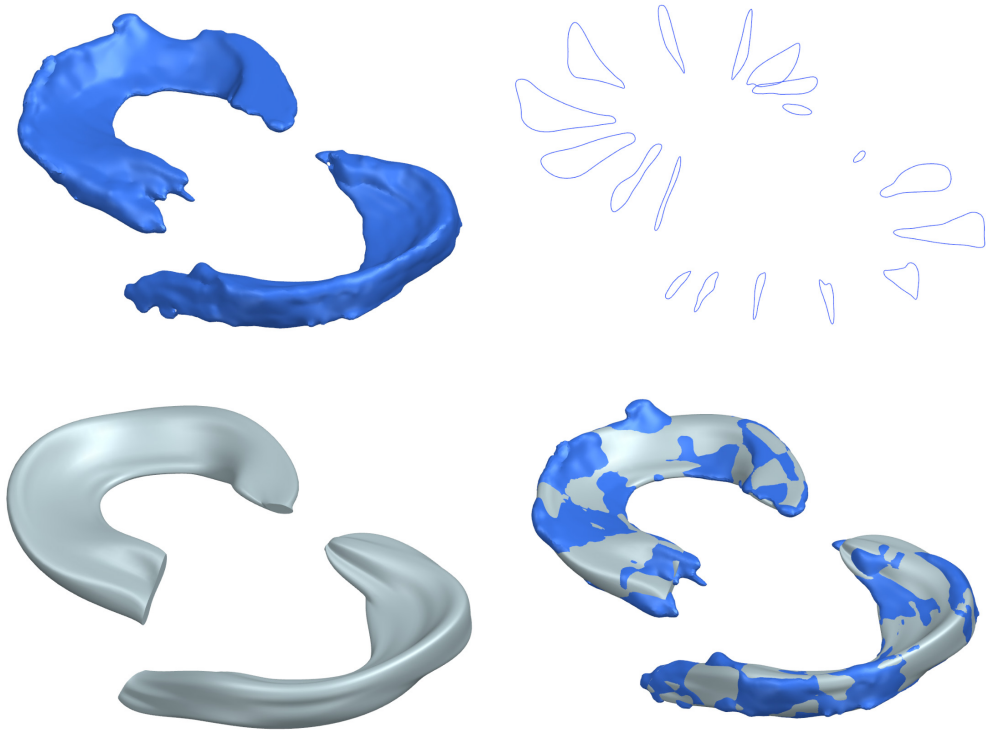


Figure 49: Sequence of operations implemented in Siemens NX to obtain the nominal geometry of the meniscus adapted to the patient. Medical image segmentation performed by JKU Linz Institute of Polymer Product Engineering in the frame of the INKplant project, upon which our personalised design procedure is applied. Special thanks to Eng. Disha Tupe.

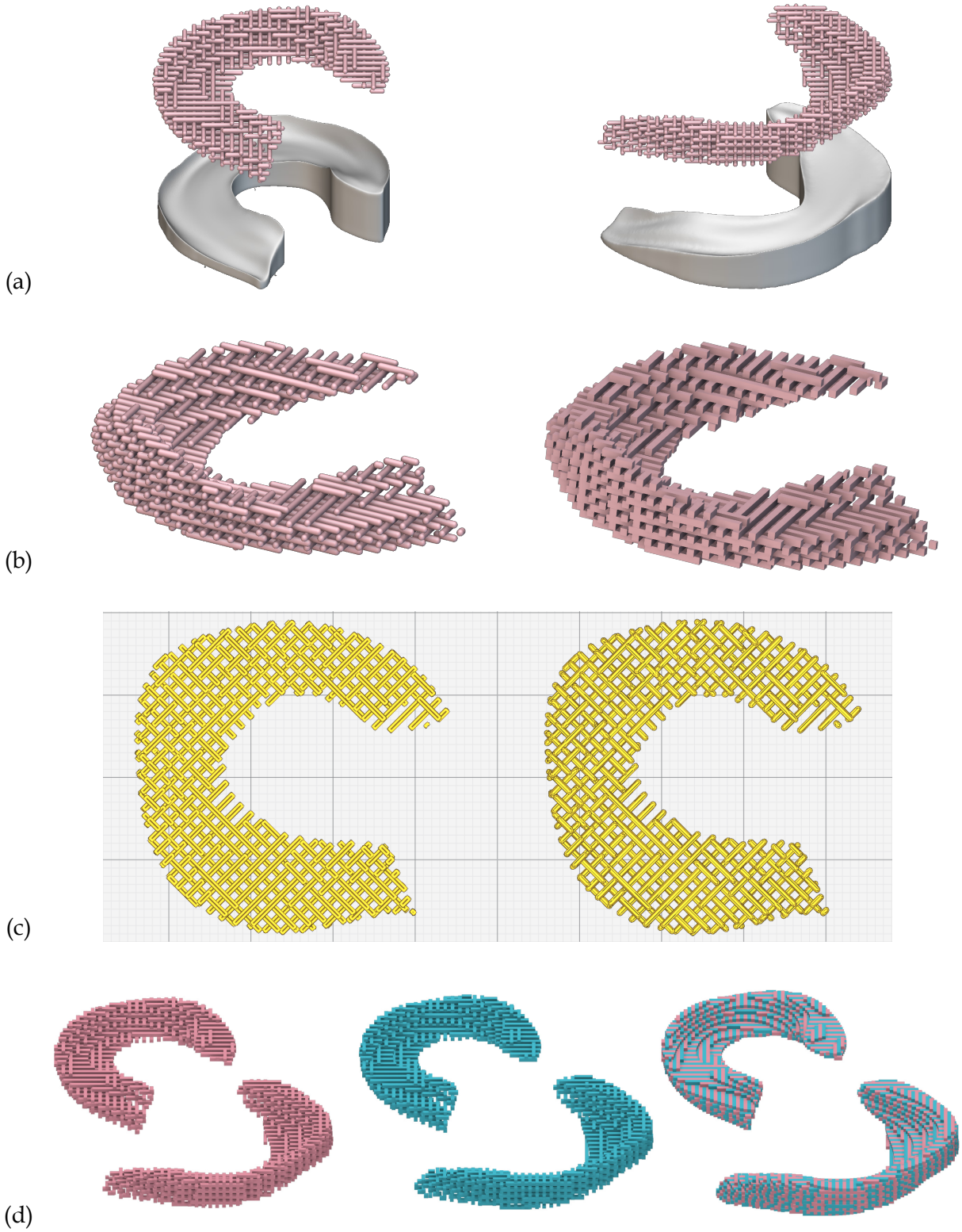
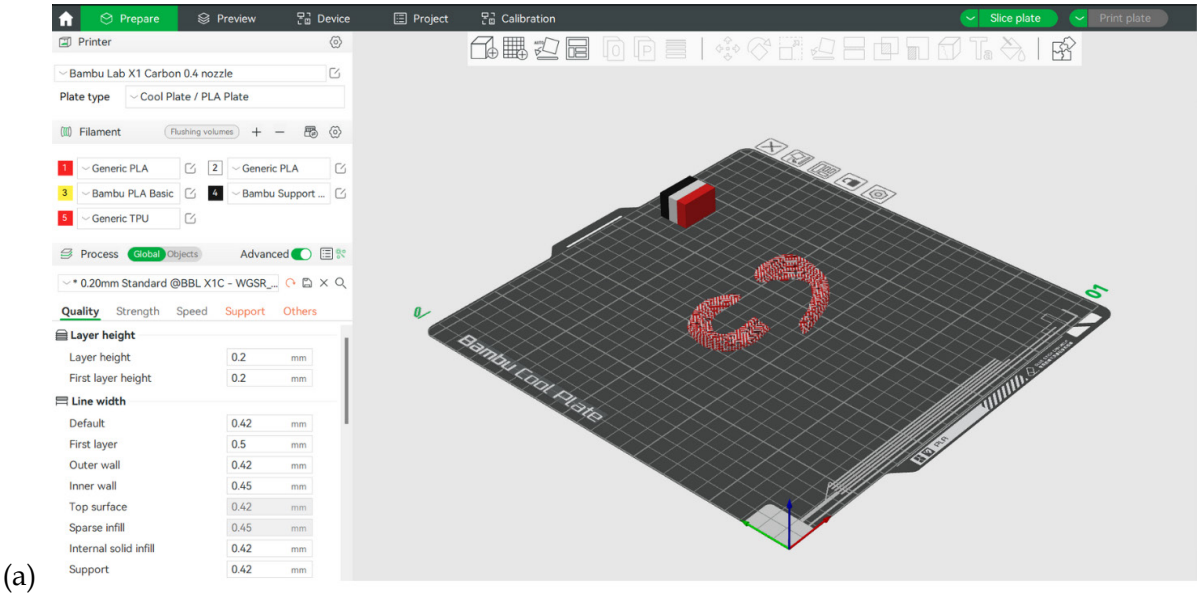


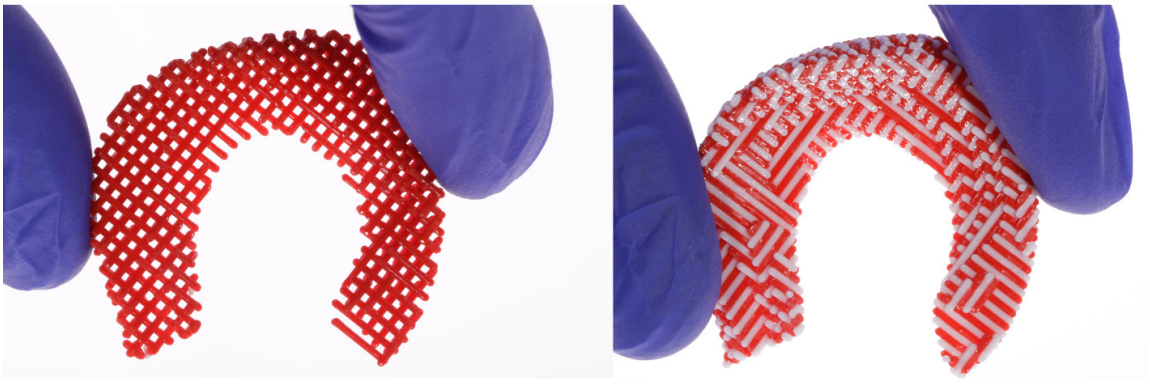
Figure 50: Design process of meniscal scaffolds that follow a lattice distribution with a woodpile pattern. (a) Auxiliary support structures to facilitate scaffold fabrication. (b) Comparisons of scaffolds with lattice structures of circular and square sections respectively. (c) Slicing of the structures shown in b) to highlight the calculation of the trajectories based on the chosen section. (d) Design of hybridized lattices for manufacturing multimaterial scaffold through controlled deposition of PDMS and biogel with cell loading.



(a)



(b)



(c)

Figure 51: Meniscal tissue scaffolds collecion obtained using a rapid prototyping strategy in a multi-material FFF system. (a) Bambu studio, software tool used to generate the G-code. (b) Collection of prototypes obtained from the designs shown in Figure 50. (c) Top view to evaluate the porosity achieved and the correct hybridisation between the two PLA materials used. Pictures courtesy of 3Dtive S.L. and Dental Troyano S.L. Special thanks to Eng. William Solórzano and Álvaro Troyano.

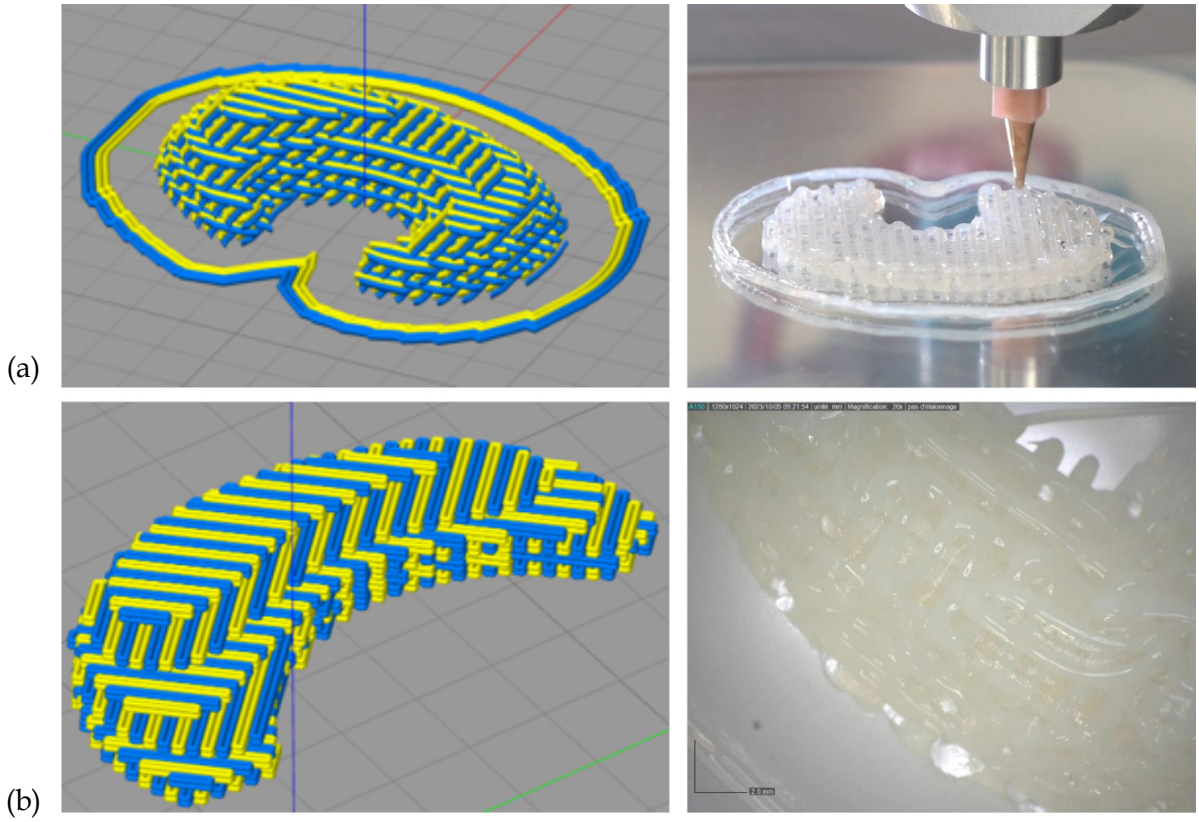


Figure 52: Meniscus scaffolds prototypes printed by Elkem Silicones' colleagues from the INKplant project. LDM multi-material system used for this task. (a) Fabrication of porous meniscal scaffold directly printed on the building platform. (b) Fabrication of multi-material hybrid scaffold by combination of Elken PDMS and 3D Matrix Medical Technology biogel with contained cell cargo. Pictures courtesy of Elkem Silicones colleagues. Special thanks to Dr. Clément Perrinet and Dr. Damien Djian.

6.4. Conclusions and future proposals

The analysis in this chapter indicates that digital additive manufacturing technologies, operating from voxelated materials, offer virtually unlimited freedom in the shaping of complex geometries. The versatility of these systems, combined with the ability to print multiple materials, is an extremely promising tool for the research and manufacture of more complex tissue engineering scaffolds. The application of these technologies can result in significant improvements in key tissue engineering properties such as porosity, vascularisation and mechanical behaviour, among other aspects. However, it is crucial to carry out research and development aimed at obtaining certifiable biocompatible materials and flows. This is further complicated by the need to develop sacrificial materials that act as auxiliary support elements, which must be adequately removable, and their residual remains in the matrix must be inert to possible cellular interactions, thus ensuring biocompatibility.

On the other hand, biofabrication technologies using extrusion or controlled deposition of polymers, biogels or silicones represent a promising avenue, especially because of the ability to obtain porous scaffolds with an incorporated cellular load. This development opens up new

research opportunities, even raising the possibility of future in situ deposition of scaffold structures during surgical procedures. However, at present, these technologies face important constructional limitations, especially with regard to the fabrication of lattice lattices possessing point vertical pillars (e.g. single cubic, face-centred cubic, body-centred cubic lattices). New manufacturing methodologies, such as the development of slicers for the generation of non-planar 3D printing paths can be a turning point for the realisation of new applications.

Finally, having obtained promising results using the custom design methodology for the fabrication of tissue engineered scaffolds, it is crucial to mention that all generated prototypes represent full meniscal replacement implants. Therefore, the need to integrate all relevant concepts (such as the porous layer, the friction reduction layer and the structural integrity layer) to develop a reduced meniscal implant specifically designed to replace only the damaged tissue, which is the most common situation in most meniscal injuries, is evident. This consideration underlines the importance of evaluating the developed prototypes with the surrounding meniscal tissue, an aspect that has so far not been addressed and remains as future research topic.

7. Engineering multi-material tissue engineering scaffolds and bioinspired implants for osteochondral articular repair

7.1. Osteochondral injury overview

Osteochondral lesions present a multifaceted challenge in orthopaedics, impacting both the subchondral bone and the articular cartilage (265, 266). These conditions are presented by damage to multiple tissues, the cartilage covering joint surfaces and the bone to which it is connected, frequently leading to significant discomfort and reduced mobility in patients. The aetiology of these lesions varies, encompassing acute traumas such as direct impacts or rotational injuries to the joint, as well as degenerative diseases like osteoarthritis (267, 268). Predominantly occurring in load-bearing joints, including the knee, ankle, and to a lesser degree, the hip, osteochondral defects are prevalent in young, physically active individuals, particularly those engaged in high-impact sports. Nevertheless, they can also occur in individuals of any age due to accidents or degenerative conditions. Common symptoms of these injuries include pain in the joint, swelling, and occasionally, joint locking or instability. Typically, physical activity exacerbates the pain, while rest provides relief.

Figure 53 illustrates a schematic representation of the anatomical structures involved in such injuries (269). Each highlighted component is critical for joint function and integrity, composed of distinct tissue types, leading to highly specialized areas. These regions of the joint are described briefly as they are referred repeatedly in the following chapter.

- Articular surface: the outermost layer of articular cartilage, facilitating smooth articulation of joint surfaces during movement.
- Superficial zone: this cartilage layer houses cells that secrete lubricating proteins, vital for reducing friction in joint movements.
- Transitional or middle zone: serving as an interface between the superficial and deep zones, this layer offers a progressive shift in cartilage composition and firmness.
- Deep zone: comprising vertically aligned cartilage cells, this zone is instrumental in shock absorption within the joints.
- Tidemark: this line signifies the transition from articular cartilage to calcified cartilage, indicating a shift to a more mineralized cartilage composition.
- Calcified cartilage: providing a firm link between the articular cartilage and the subchondral bone plate.

- Cement line: this boundary line is crucial for the adhesion between the calcified cartilage and the subchondral bone.
- Subchondral bone plate: a dense bone layer that supports the mechanical function of the articular cartilage.
- Subarticular spongiosa: made of trabecular bone, it aids in shock absorption and load distribution across the joint.
- Artery, vein, and nerve: these components are essential for providing nourishment, sensation, and overall health to the joint.

In this draft, the knee joint has been specifically considered, as it is the case of study in this work.

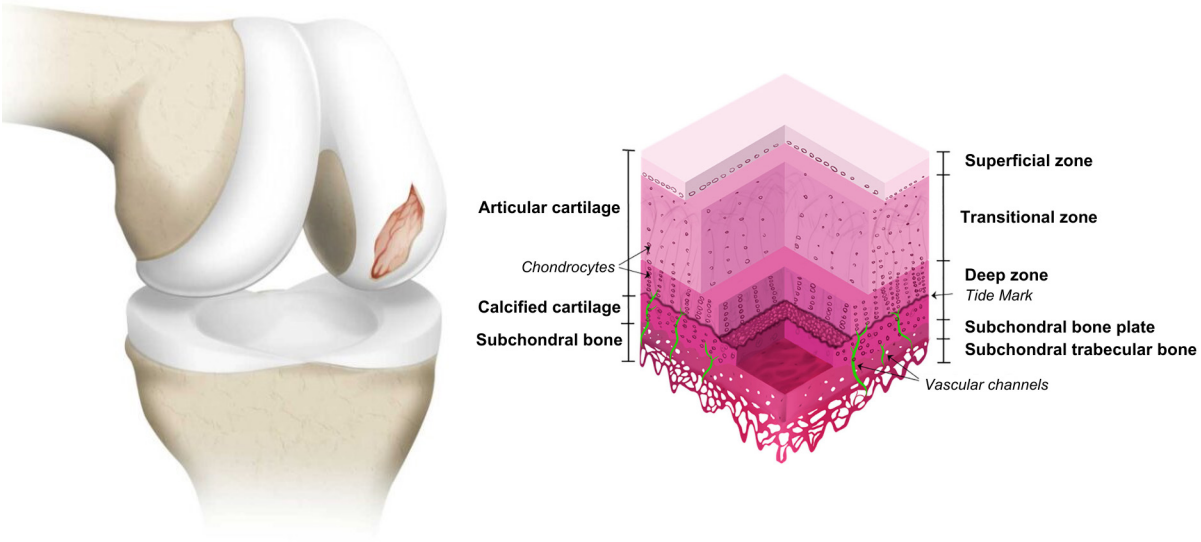


Figure 53: Anatomical diagram of the affected regions in an osteochondral injury. Pictures acquired and adapted from Dr. Riley J. Williams website (270) and "Molecular Signaling Interactions and Transport at the Osteochondral Interface: A Review" (269).

Osteochondral lesions can compromise one or more of these structures, affecting the joint's integrity and functionality. Addressing these lesions requires precise diagnostic and therapeutic strategies to effectively restore joint biomechanics.

The diagnostic process for an osteochondral lesion typically involves a comprehensive approach that integrates patient medical history, physical examination, and advanced imaging techniques. Initially, patients might report symptoms such as joint pain, swelling, and mechanical issues like clicking, locking, or instability. These symptoms can arise following a traumatic event or gradually develop in the context of degenerative diseases. A detailed clinical examination is critical for diagnosing these injuries. During this examination, the clinician assesses for joint line tenderness, evaluates the range of motion, checks for swelling,

and investigates any signs of joint instability. Specific evaluation, like the McMurray test (249) used to detect meniscal tears, can also provoke symptoms indicative of osteochondral lesions.

In cases where an injury is suspected, diagnostic imaging plays a pivotal role in determining the injury's extent. Radiographs are typically the initial imaging method employed to evaluate joint integrity and rule out other bone-related pathologies, such as fractures. However, early-stage osteochondral lesions may not be visible on radiographs due to their inability to effectively visualize soft tissues like cartilage. In contrast, MRI is an essential diagnostic tool for these lesions, offering comprehensive images of both bone and soft tissues, including cartilage. MRI can delineate the lesion's size, depth, and stability, along with associated bone marrow edema and cyst formation (267, 268).

In orthopaedics and traumatology, treating osteochondral lesions presents an ongoing challenge, especially with larger and deeper lesions. Traditional treatment strategies may involve a mix of surgical and conservative methods. Osteochondral lesions can be addressed through various transplantation techniques, each with specific indications and limitations. This includes some of the techniques described below:

- Autologous osteochondral transplantation (AOT) or mosaicplasty (271, 272): in this process, small cylinders of bone and cartilage are harvested from a non-critical load-bearing area of the patient, such as the knee's periphery. These grafts are then implanted into the osteochondral defect. The term 'mosaicplasty' stems from the mosaic-like pattern formed by placing multiple cylindrical grafts closely together. Figure 54a illustrates an osteochondral lesion where, post removal of the damaged tissue, the resultant cavity has been filled with these small cylinders sourced from less load-bearing areas of the patient's joint.
- Osteochondral allograft transplantation (OCA): this method is akin to mosaicplasty but utilizes grafts from cadaveric donors instead of the patient's own tissues (273). OCA is particularly beneficial for extensive defects or situations where the patient lacks sufficient healthy tissue for autologous grafting (see Figure 54b).
- Microfracture technique: this alternative approach avoids tissue implantation. The procedure involves creating multiple small perforations, or microfractures, in the subchondral bone at the site of the lesion (274). This controlled injury stimulates the formation of a blood clot, leading to the migration of stem cells capable of differentiating into cartilage-like tissue.

The selection of the appropriate treatment modality for such defects depends on various factors, including the patient's age, functional demands, lesion size and depth, and any coexisting conditions. Contemporary advancements in technology and biomaterials are fostering the development of novel approaches for treating osteochondral lesions, particularly severe ones involving concurrent bone and cartilage damage. Noteworthy among these are:

- Collagen matrix with bone marrow concentrate: this technique involves applying a collagen matrix as a scaffold combined with bone marrow concentrate (275). This provides a rich environment of mesenchymal stem cells and growth factors, promoting the regeneration of cartilage and subchondral bone.

- Cell implants: these involve the grafting of laboratory-cultured cells, such as in autologous chondrocyte implantation (ACI) or matrix-induced chondrocyte implantation (MACI). This approach is similar to mosaicplasty but unique in that the grafts undergo extracorporeal treatment before implantation. Two variations exist (276, 277):
    - Autologous chondrocyte implantation (ACI): in this method, healthy cartilage is biopsied from the patient and sent to a laboratory where chondrocytes are cultured and proliferated. These expanded chondrocytes are then implanted back into the defect, typically under a periosteal flap or collagen membrane.
    - Matrix autologous chondrocyte implantation (MACI): an advancement of ACI, this technique involves culturing autologous chondrocytes within a three-dimensional matrix, which is then implanted into the lesion. The matrix aids in securing the cells and may enhance integration with adjacent tissues.

These therapies, however, are more invasive as they necessitate two procedures: a biopsy to harvest healthy tissue, followed by a second procedure for implantation. Overall, these strategies aim to restore the articular surface with tissue closely resembling the original cartilage in mechanical and biochemical properties.

One of the most significant advancements in this domain involves the use of AMTs to create biomedical scaffolds. These scaffolds are engineered to replicate the structure and composition of bone and cartilage tissues, serving as a platform for cellular regeneration and growth (265, 266). The customization afforded by 3D printing is particularly valuable, allowing for scaffolds tailored to the precise dimensions and geometry of each patient's defect. In contrast to autologous transplantation or mosaicplasty, 3D printed scaffolds eliminate the need to harvest healthy tissue from another body part. Furthermore, compared to allogenic transplantation, the fabrication of these scaffolds reduces dependence on available cadaveric tissue. Additionally, these scaffolds can be designed to biodegrade over time, ideally leaving behind only the newly regenerated tissue, potentially offering a more natural and less invasive integration compared to traditional treatment. Presently, there is a wide spectrum of materials (278, 279, 280) under investigation for crafting these structures. These include biodegradable polymers like poly(lactic acid) (PLA), polyglycolic acid (PGA), and polycaprolactone (PCL); bioactive ceramics such as calcium phosphate (CaP) and hydroxyapatite (HA); and natural materials like collagen, a primary component of natural cartilage, or hyaluronic acid, prevalent in the extracellular matrix. This diversity of materials, coupled with the advent of new multi-material printing systems, heralds the creation of new integrated solutions capable of producing multifunctional scaffolds. Additionally, the realm of 3D printed scaffolds for osteochondral defect repair is exploring bioprinting technologies, which involve depositing living cells directly into the scaffold during printing, and the development of materials that incorporate growth factor-enhancing properties essential for tissue regeneration.

These advancements mark the next frontier in treatments for joint injuries, potentially enhancing clinical outcomes and reducing the morbidity associated with traditional surgical techniques. The field of osteochondral lesion treatment remains a source of research and development, striving to improve functional outcomes and life quality for patients. The

complexity of osteochondral lesions and their significant impact on patient well-being make the pursuit of effective treatments a dynamic research area. Tissue engineering, in particular, holds promise for more effective and lasting solutions compared to conventional methods, potentially enabling the complete restoration of damaged joints. Integrating traditional surgical methods with cutting-edge technologies like 3D printing and tissue engineering is poised to significantly advance available treatment options, offering more personalized and effective remedies for repairing bone and cartilage damage.

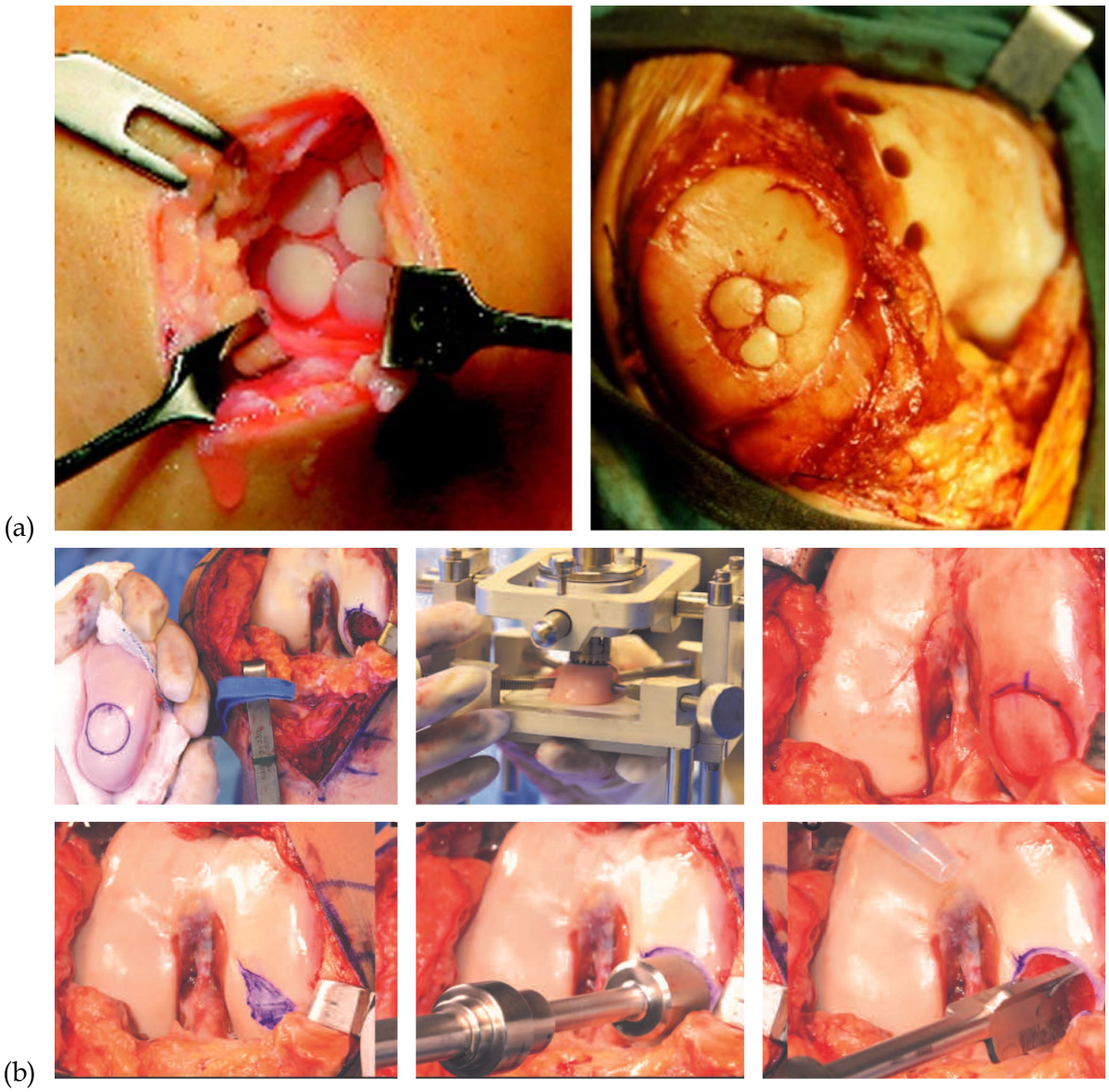


Figure 54: Current surgical procedures to place an osteochondral insert. (a) Mosaicplasty or autologous osteochondral transplant (AOT), in which case the origin of the implant is the patient's own tissue. (b) Osteochondral allograft transplantation (OCA), in which case the origin of the implant is from a cadaveric donor. Pictures acquired and adapted from "Chondral repair of the knee joint using mosaicplasty" (271) and "Mesenchymal stem cells for subchondral bone marrow lesions: From bench to bedside" (275).



Figure 55: Agili-C osteochondral implant, developed by the medical company CartiHeal. Pictures acquired and adapted from CartiHeal website (281) and Medicalbuyer website (282).

The following section delves into the development of an innovative design methodology aimed at replicating the tissue properties of regions affected by such pathologies. The goal is to design, manufacture, evaluate, and validate innovative, patient-customized solutions, exploiting the potentials of 3D printing technologies. Figure 55, shows a contemporary commercial medical solution for osteochondral defect repair (283, 284, 285). The flexibility and versatility provided by AMTs enable us, in the subsequent section, to harness product customization extensively. Additionally, these technologies afford a heightened level of control over scaffold porosity, a crucial aspect in facilitating tissue regeneration. This capability to tailor both, the physical structure and the functional properties of scaffolds, underscores the significant potential of 3D printing in advancing medical solutions for joint repair.

7.2. Multi-material tissue engineering osteochondral scaffold from regular geometries

The following section presents a study that aims to develop an innovative DFAM methodology for the generation of FG and biomimetic osteochondral tissue engineering scaffolds. Through the combination of biomedical materials and the implementation of cutting-edge 3D printing technologies, the aim is to manufacture an integrative solution obtained through a multi-scale, multi-material and multi-functional approach. To this end, the manufacturability of different 3D printing technologies is evaluated to produce tissue engineered scaffolds with micrometre-scale porosity applied throughout the geometry.

As depicted in Figure 54, osteochondral defects can simultaneously affect both meniscal and bone tissues, each possessing distinct biomechanical and biological properties. As mentioned, an intermediary zone, the calcified cartilage area, serves as a transition between these two tissues. This gradient in properties necessitates a multi-functional solution capable of restoring the conditions of all damaged tissues. Consequently, part of the scaffold is designed to meet the stipulated requirements of the cartilage, termed the “soft phase”, while another region addresses the bone structure capabilities, known as the “hard phase”. Individualized designs

for each scaffold zone ensures optimal construction characteristics for the different areas. Differentiating the design of these phases is crucial due to the distinct manufacturing technologies required for each.

To fabricate the hard phase, LCM is employed, replicating bone-like conditions. For the soft phase, inkjet, PolyJet , and DLP-LCD polymeric systems are used. Candidate material for the for the ceramic hard phase is hydroxyapatite. One of the objectives is to develop an implant that allows cell colonization, so the materials used to manufacture the final solution must have biocompatible and biodegradable properties.

The combination of different materials through varied manufacturing technologies necessitates their eventual marriage to form a hybrid implant. Several possibilities are considered to fulfil this task: one involves the manufacture of each phase separately by implementing parallel workflows. Once the scaffolds are printed, they can be assembled or joint by applying some adhesive material or treatment on the interface. Another scenario explores the possibility of integrating printing systems and materials, allowing the printing of the soft phase directly onto a pre-manufactured ceramic scaffold, thereby integrating both tasks into a sequenced workflow. This approach aims to streamline the fabrication process while ensuring the structural and functional integrity of the resulting hybrid implant.

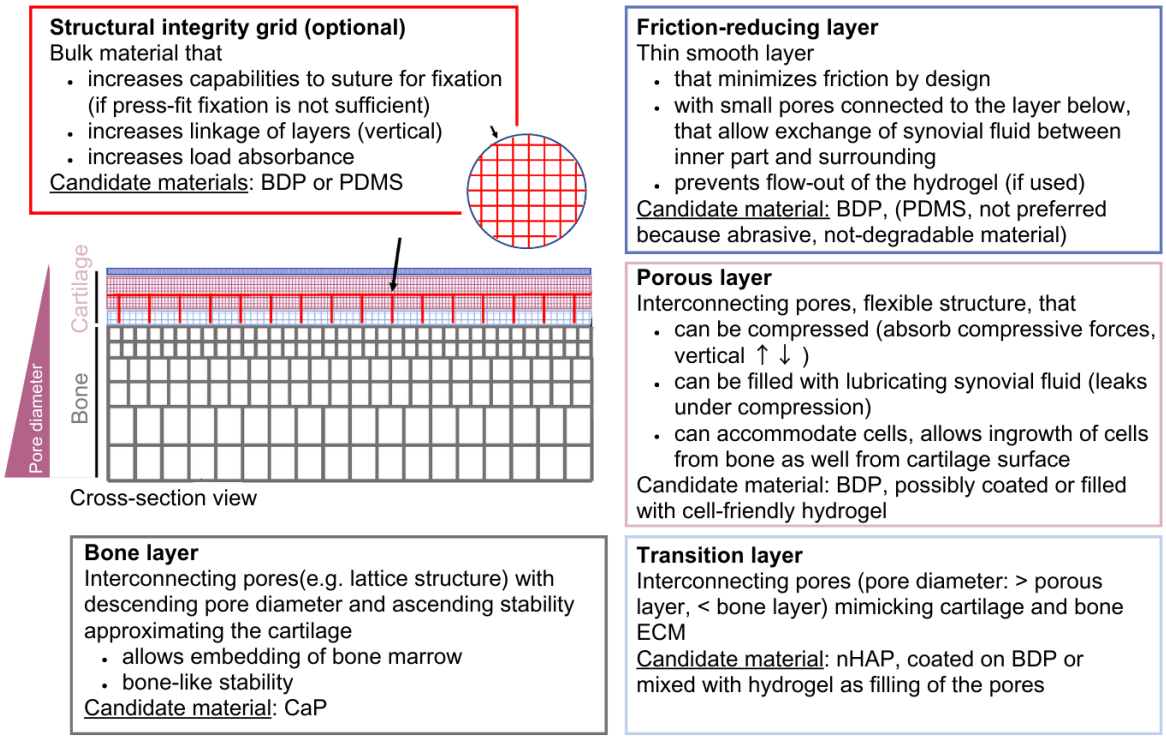


Figure 56: Figure 35: Schematic draft summarizing the osteochondral case study clinical requirements. Pictures courtesy of Charité - Universitätsmedizin Berlin and TransTissue Technologies GmbH, members of the EU INKplant consortium. Special thanks to Dr. Tilo Dehne and Dr. Michaela Endres.

On the other hand, regarding the functional requirements of the implant, a scheme identifying the following zones is presented in Figure 56. This scheme has been provided by the clinical

team of the INKplant project from the Charité medical institution. Thus, the following information is collected:

- Bone layer: layer intended to recreate the hard phase of the implant. It must have an integral porosity so that it is interconnected throughout its nominal volume. In addition, it must apply an increasing gradient of pore size as it moves away from the cartilaginous zone.
- Transition layer: it must reproduce the cementation line and the calcified cartilage zone. A priori it is presented as a transition zone of both phases.
- Porous layer: it represents the soft phase, belonging to the cartilaginous tissue. The pores in this region should be equal or less than those of the implant in the hard phase.
- Friction-reducing layer: upper layer destined to be in contact during the functional exercise of the joint. It is decided to include it in the concept to try to protect the lower porous structures.
- Structural integrity grid: conceived as some type of optional system to facilitate suturing during surgery. It is not represented as a mandatory layer since these types of implants are usually placed by adjustment and do not usually require suturing.

To integrate all these characteristics in the same system, the design stage initiates from regular shapes mimicking available commercial solutions, that resemble cylindrical geometries. During surgery, the implantation of the scaffold is performed by means of a press-fit fixation technique, so the cylindrical nominal geometry is a good candidate for the placement of the scaffold, as it possesses vertical walls extruded from a circular section and therefor lack of corners.

Thus, the design process starts with a nominal cylinder with 15 mm in diameter and heigh. The following operations are implemented in nTopology. It is important to emphasize that this methodology does not foresee obtaining a catalogue of implants with standardized measures by overall size, pore spacing, etc. Taking advantage of the degree of customization provided by AMTs, the following workflow is proposed in which each pathology should be evaluated and diagnosed individually, stablishing a surgical planning study, which concludes with the obtaining of a customized implant for the patient through the application of this methodology.

Next, a lattice structure is applied on the generated cylinder. This geometry is determined by a rectangular cell map, whose nominal volumes in this case are 2 x 2 x 2 mm^3. As for the beam diameter, a thickness gradient is applied in increasing direction with the Z-axis, as collected in the design draft from Figure 56.

The applied porosity gradient varies from 0.8 mm to 1.2 mm. Since the nominal dimensions of the unit cells are 2 mm per side, the pore size is calculated by the difference of these values. Thus, the pores located in the lower levels of the scaffold have a porosity of 1.2 mm, while the pores located in the zone belonging to the soft phase have a porosity of 0.8 mm. The applied thickness transition over time follows a linear behaviour as a function of the Z height of the specimen (see Figure 57a).

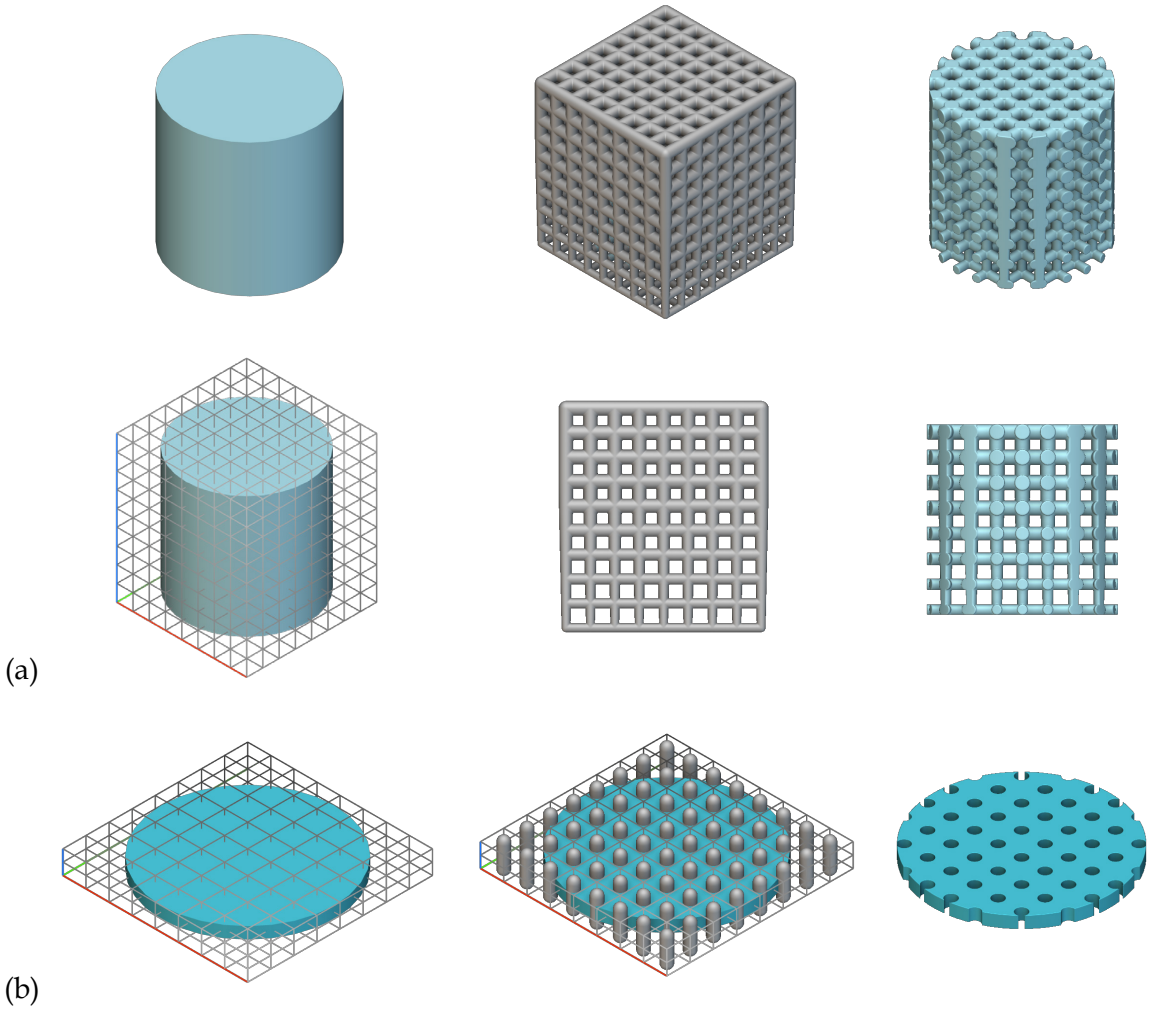


Figure 57: DFAM methodology applied for the generation of a tissue scaffold for the treatment of osteochondral lesions. (a) Obtaining the porous cylindrical body with a porosity gradient in the Z direction. (b) Generation of the transition layer between the hard and soft phases.

Next, the transition layer is included, which delimits the hard phase from the soft phase and therefore it connects the cartilage region from the bone area. From the scheme shown in Figure 53, it can be understood that this layer resembles de "cement line" area. As this transition layer geometrically delimits both tissues, this region is used as a platform with a larger exposed surface to either increase the area in case of printing on it, or to increase the contact surface in case both solutions are married and assembled together. To obtain such geometry, a thin section of the cylinder is isolated at a certain height and perforated by implementing a distribution of columnar elements. It is strictly necessary that both, the bone phase and the hard phase, are in contact and intercommunicated, so that material transfer can occur between both environments, facilitating tissue generation and the properties gradient from cartilage to subchondral tissues.

Figure 57b depicts the sequence of applications performed, taking as starting point a section of the nominal cylinder of 1mm thickness, located at an elevation of 10 mm above the scaffold base. The lattice distribution of column elements is also implemented. These holes must be

coincident with the cell map used for the porous layer generation, thus guaranteeing the alignment of the vertical channels of both phases and their direct communication. Through a Boolean subtraction between the initial porous geometry and the obtained transition layer, it can be created the space where the transition layer is placed.

The first design configuration is shown in Figure 58. This concept divides the scaffold into three distinct regions: it can be seen the upper region for the soft phase in pink colour; the transition layer, representing the calcified cartilage area in dark blue colour, and the hard phase for the bone zone, in a soft blue tone. From this point onwards, these colours are used to identify the correspondent tissues. The scaffold arrangement proves transverse porosity across its entire volume, incorporating the transition membrane as a reinforcement structure. Crucially, the scaffold's design does not impede interconnectivity between zones, it even presents pores channels in the vertical walls of the cylinder, something which, as can be seen in the Figure 55, is not included in most of the commercial solution.

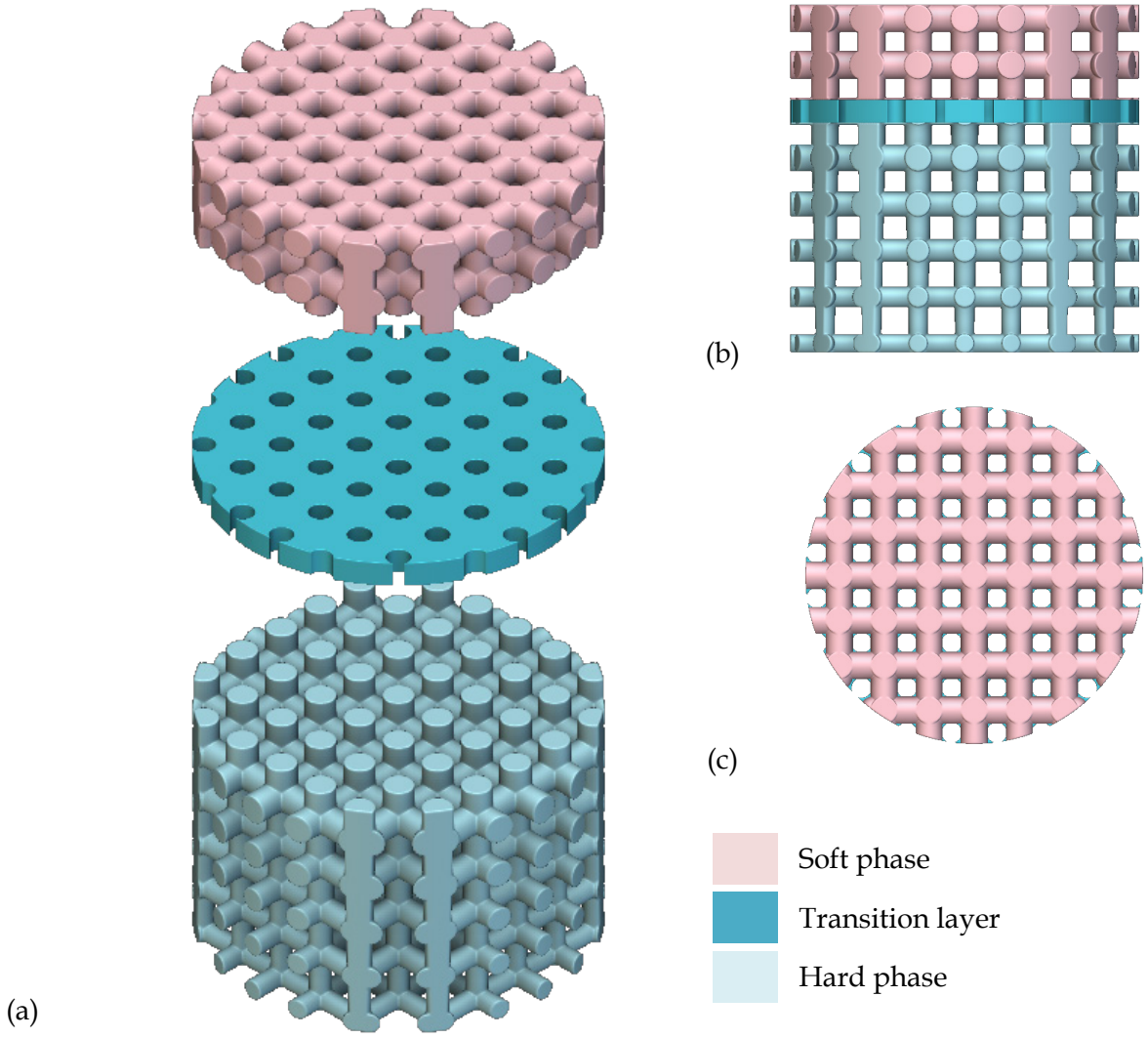


Figure 58: DFAM of osteochondral scaffold that integrates the hard phase, belonging to the chondral bone, the soft phase, belonging to the cartilage and the transition membrane, recreating the zone of calcified cartilage. (a) Isometric view of an exploded assembly. (b) Front view of the design where the porosity gradient can be seen. (c) Top-down view of the design where the coincidence of porous channels can be seen in all phases.

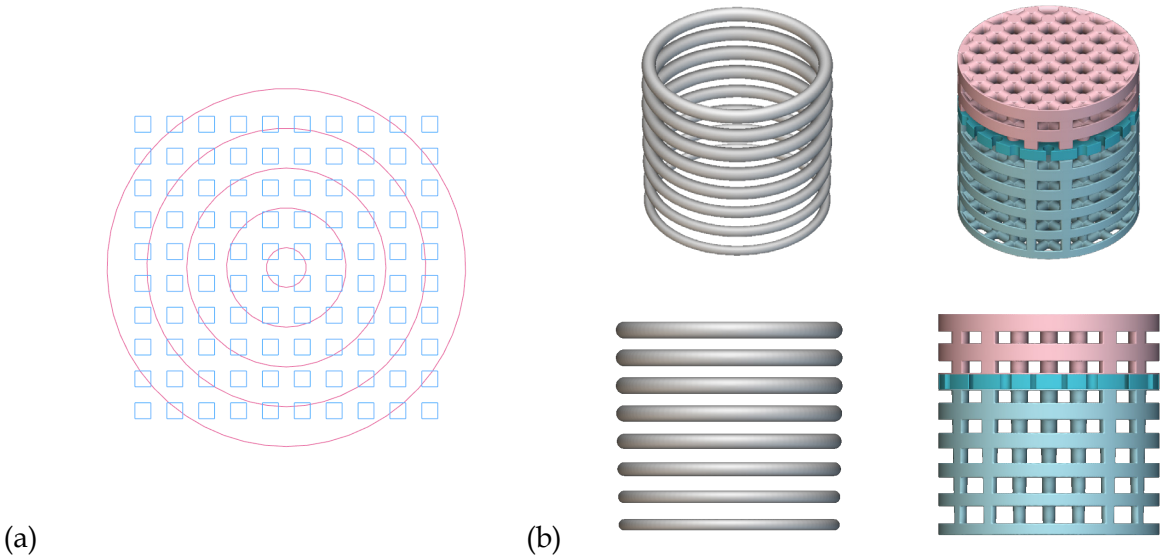


Figure 59: Ring set design adapted to the vertical walls of the nominal cylinder to bind beam discontinuities. (a)Intersection of circles with multiple diameter values on a pattern of elements distributed on a grid. (b) Isometric view and front view of the updated design with the conformal rings combined.

An alternative corrective action could involve adjusting the diameter of the nominal geometry or reconfiguring the cell map. Yet, following this methodology cylindrical nominal values for height and diameter are predetermined during surgical planning stage, trying to ensure minimal invasiveness and adequate removal of damaged tissue. Altering these dimensions in following stages of the workflow could lead to either excessive removal of healthy tissue or inadequate excision of damaged tissue, potentially compromising treatment success.

Then, a third option is presented. If acting at the design stage, continuity of all vertical wall perimeters can be guaranteed by grouping them into a set of annular geometries. This mixed solution maintains porosity in all volume directions, slightly increasing peripheral material distribution. By implementing this action, lateral porosity is preserved. As illustrated in Figure 59b, by incorporating an array of conformal rings adapted to the lattice geometry, all the perimetral discontinuities are rectified. Additionally, the diameter of these rings must comply with the beam diameter at each Z level, resulting in a gradient where the rings thickness increase in Z direction (Figure 59b). In the final concept, these rings intersect the nominal geometry, creating semi-sections that lead to a flat surface on all the cylinder's vertical walls. Again, it is recalled that in order to address the design of this case of study, the selected unit cell type for the lattice implementation is a simple cubic type. Its selection is based on being the cell type that leads to the highest overall porosity among those evaluated, as seen in Section 4.3.1, and due to its simplicity in design. It also enables the choice of larger beam diameters, that facilitated manufacturability without leading to too low porosity structures.

Moreover, as observed in previous figures, a simple cubic distribution leads to pore channels with rectangular sections, creating sharp angles at the horizontal and vertical beams connections. As recalled, this research pursues the generation, of a scaffold prototype to restore osteochondral lesions through cellular regeneration and promotion. From the

literature, it is known that cells have a predisposition to colonize geometries with smooth surfaces rather than those with very sharp edges (265, 280, 286). For this reason, to have both options, the negative geometry of the generated scaffold is also obtained, indirectly producing a new model with a trabecular distribution of rectangular beam sections and circular porous channels. Note that, while the simple cubic cell was previously named as a candidate for achieving very light geometries, calculating its inverse geometry relative to a nominal volume leads to a much more voluminous solution. Figure 60, shows the alternative scaffold, where these circular pore channels and rectangular beam sections can be observed.

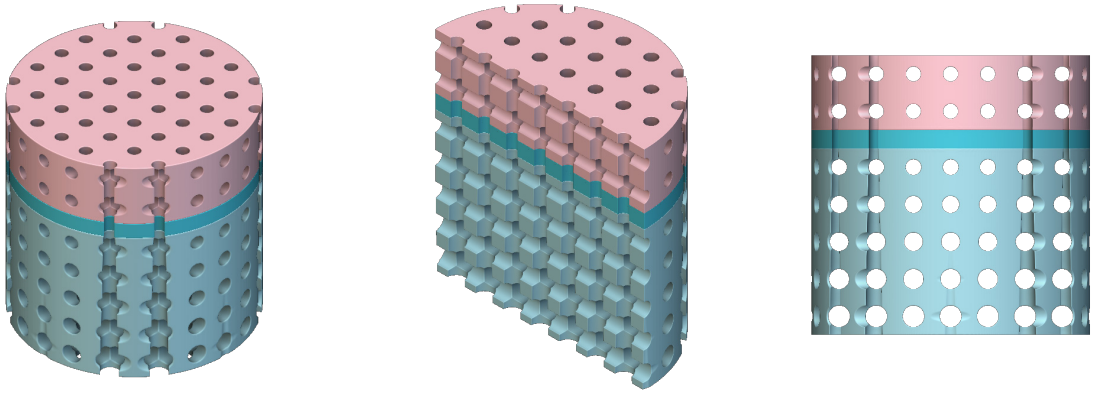


Figure 60: Osteochondral scaffold with circular pore channels and trabeculae with rectangular cross-section.

After evaluating the results obtained from the printed samples, a range of working porosities is established, varying between 0.8 – 1.2 mm for the hard phase and 0.5 - 0.8 mm for the soft phase.

As the overall thickness for the total cartilage layer region cannot be greater than 2 mm per the indications of the clinical team, the difficulty of implementing a lattice structure in such a small space is evident. For this reason, the chosen cell distribution is 0.5 mm for both element diameter and pore size. The nominal cell dimensions are 1 x 1 x 1 mm^3.

On the other hand, as far as the hard phase is concerned, a porosity gradient ranging from 1.2 mm pore size in the lower zone to 0.8 mm in the upper zone is still implemented. This time, in order to align the pores belonging to both phases, a cell map with dimensions 2 x 2 x 2 mm^3 is implemented, so that the pore ratio between the soft and hard phase is 2:1 respectively. This can be observed in Figure 62a. Nevertheless, the highest available communication between the two zones is guaranteed, allowing the tissue development between the two environments.

Figure 62 schematizes the process of implant placement after the removal of damaged tissue in the lesion. Finally, to analyse the potential of these scaffolds, a batch of samples was printed with the aim of having them evaluated during the celebration of a medical workshop organised in the framework of the INKplant project. This activity brought together surgeons and other health professionals with the aim of manipulating, testing and implanting these

tissue engineering scaffolds. In this workshop, osteochondral defects were artificially created on animal joints in to simulate as realistic as possible a surgery using the developed solutions. Figure 63 shows some of the prototypes made for this event and their implantation in an animal cadaver bone.

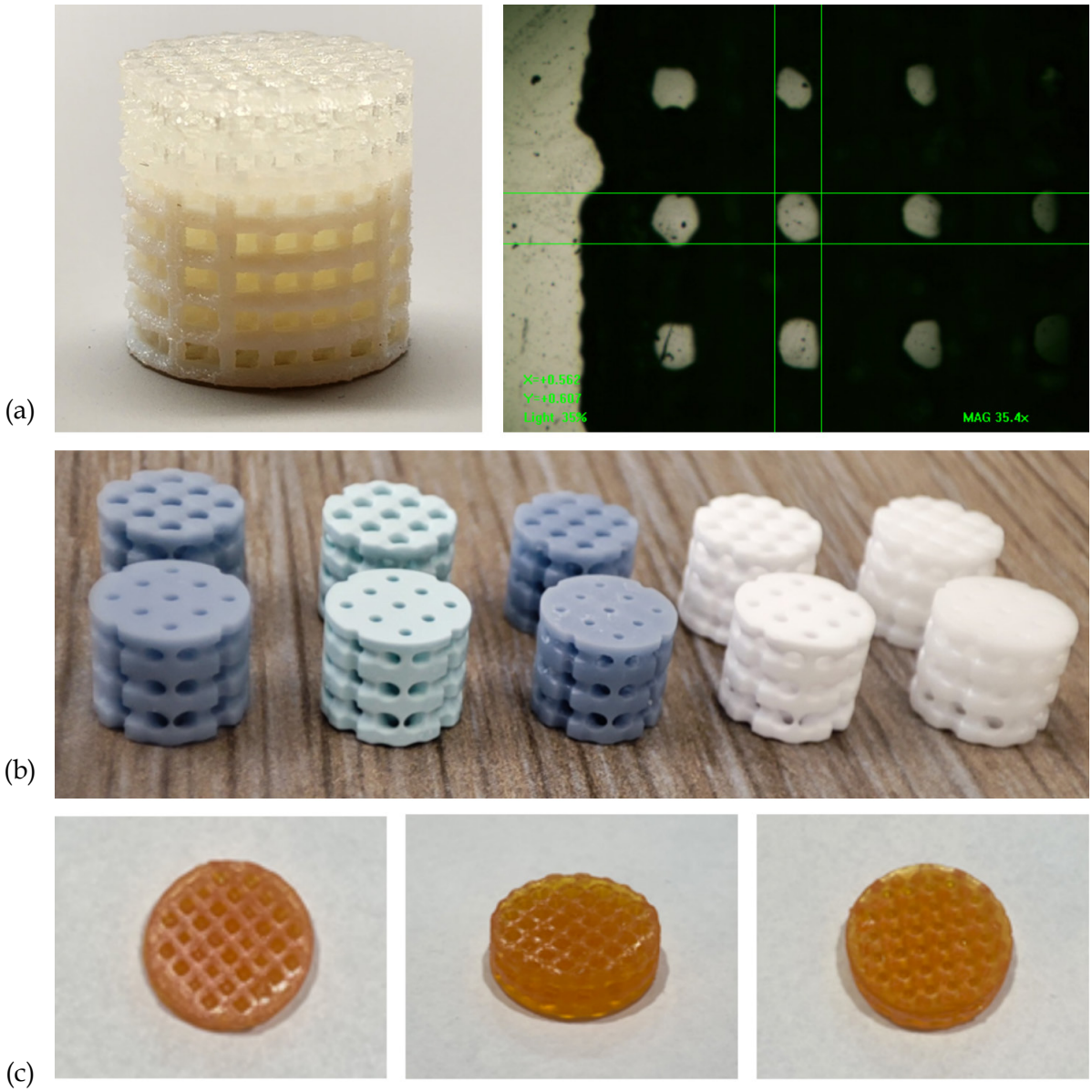
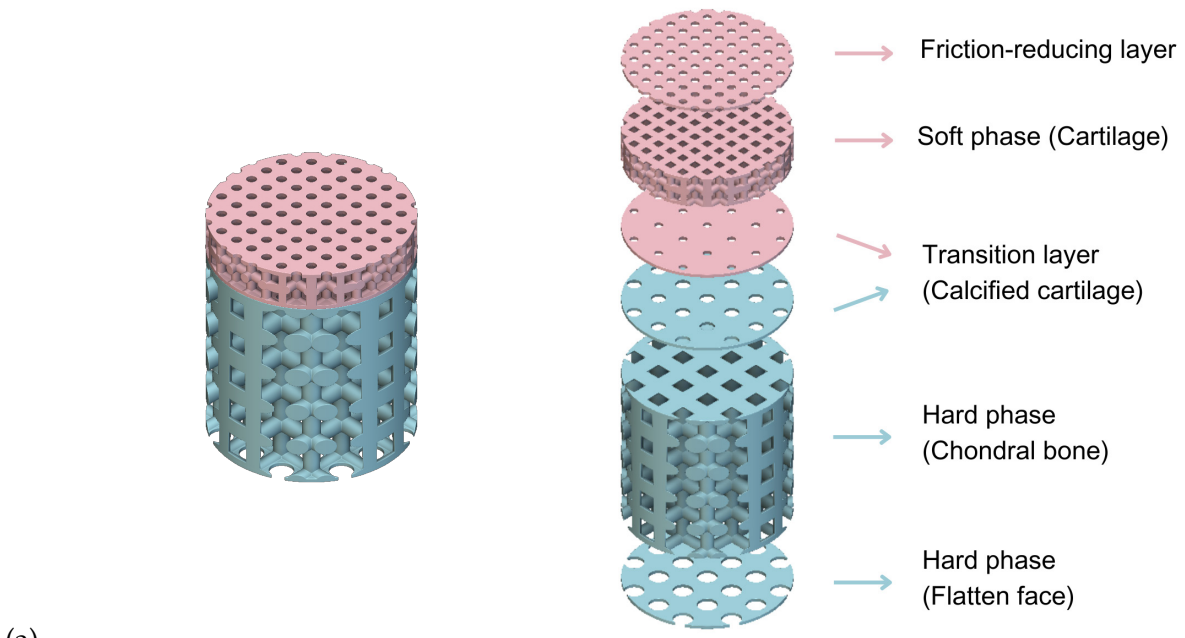
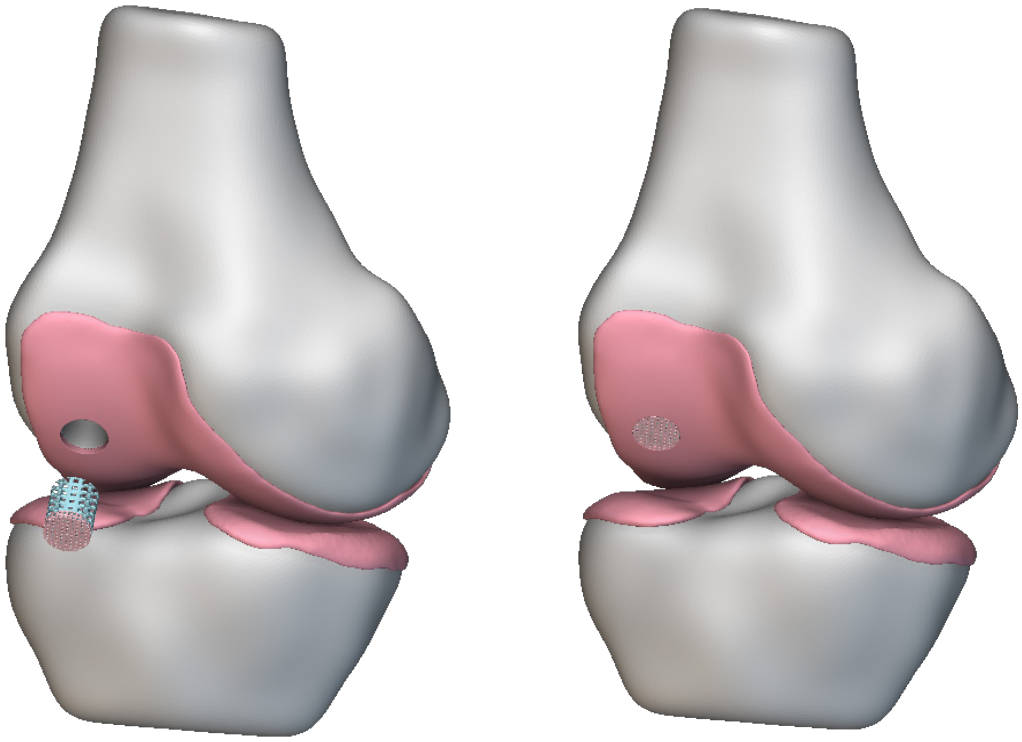


Figure 61: Osteochondral scaffold prototypes manufactured through high performance AMTs. (a) Osteochondral hybrid scaffold printed on a PolyJet system by Stratasys colleagues. Porosity analysis performed. (b) Collection of ceramic specimens printed in an LCM system by Lithoz GmbH colleagues. (c) Osteochonral scaffolds soft phase specimens printed in a DLP system with a biodegradable polymer by Luxenergy colleagues. Pictures courtesy of Stratasys, Lithoz and Luxinergy.



(a)



(b)

Figure 62: (a) Isometric view of the final design of the osteochondral scaffold and exploded view with all layers differentiated. (b) Tissue scaffold solution implantation procedure using press fitting technique.

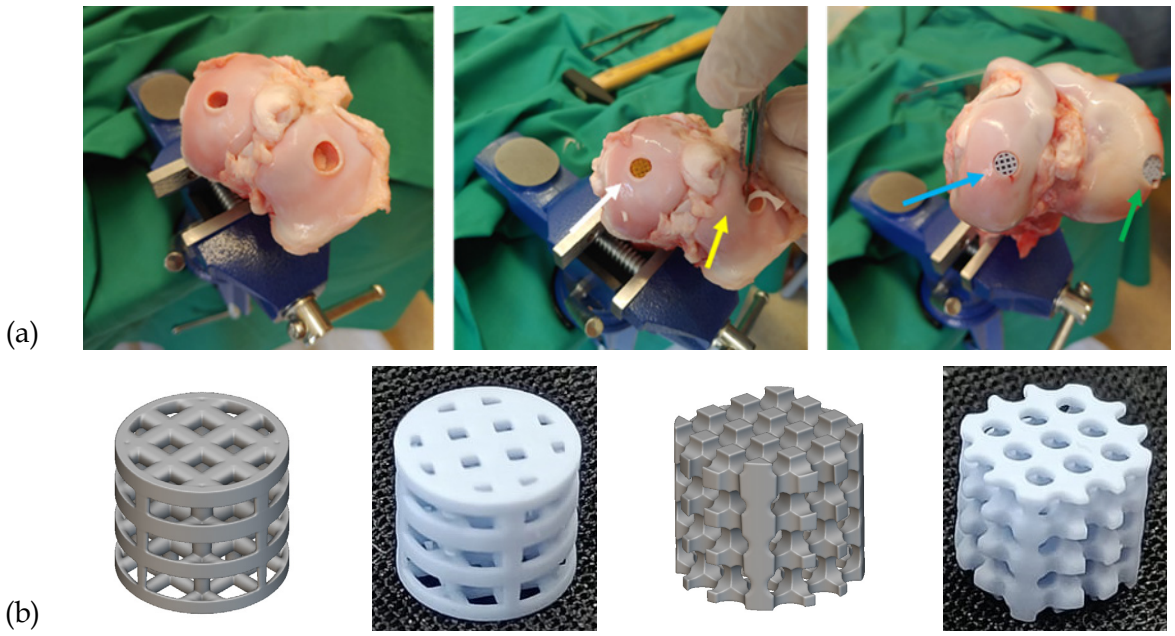


Figure 63: Scaffold prototypes designed and fabricated for evaluation at the clinical INKplant workshop organised with surgeons. (a) Animal knee joint with artificially generated osteochondral defect. The fit of the printed tissue scaffold is checked. (b) Collection of geometries tested during the activity. Pictures courtesy of Charité - Universitätsmedizin Berlin and TransTissue Technologies GmbH. Special thanks to Dr. Tilo Dehne and DR. Michaela Endres. Prototypes printed by Lithoz GmbH and Luxinergy validating the PhD candidate designs.

7.3. Multi-material tissue engineering osteochondral scaffold from patient medical images

In the previous section, an innovative concept of a tissue engineering scaffold was introduced, which, through the hybridization of materials during the manufacturing process, aims to provide a multifunctional solution capable of simultaneously satisfying the operational conditions of both cartilage and bone.

However, all these constructive features have been applied to a regular cylindrical geometry, that lacks any degree of customisation beyond fitting over the incision drilled in a patient's bone. To provide the solution with a higher degree of customization, a new implant is designed completely adapted to the patient's subchondral anatomy. To carry out this task, all the requirements applied in the previous chapter on a cylindrical nominal geometry are now implemented on a geometry obtained from patient medical images.

To initiate this study, a real anatomy from a porcine knee joint is evaluated. An artificial defect was created on this healthy knee through drilling. The stl model of the damaged tissue, differentiated into soft or cartilage tissue and hard or bone tissue, is obtained from medical images segmentation acquired from MRI. The equipment used for this task was shown in Figure 48. The capture, segmentation, and generation of the initial stl models are delegated to colleagues from JKU Linz Institute of Polymer Product Engineering, as member institution of the INKplant consortium. Figure 64 shows the joint under study, where the performed drilling

is visible, creating an artificial defect with a cylindrical geometry. The generated defect is properly evaluated, having approximate dimensions of 10mm in both diameter and depth. However, it should be understood that this information is only available in the case of an extracorporeal analysis, where the defect has been artificially created and can be measured out of the body. In a real articular injury diagnostic process, this information can only be obtained from the segmentation of the captured medical images. It is on these images that surgical planning is based, and it is the surgeon or any other medical professional who should estimate the scaffold diameter and depth. However, this is not entirely accurate, as being a patient-adapted solution, it is no longer a regular cylinder defined by a diameter and height, but now the cylindrical area related to the soft phase is defined by the subchondral bone profile. This means that this information must be obtained by applying the methodology based on reverse engineering operations validated in this study.

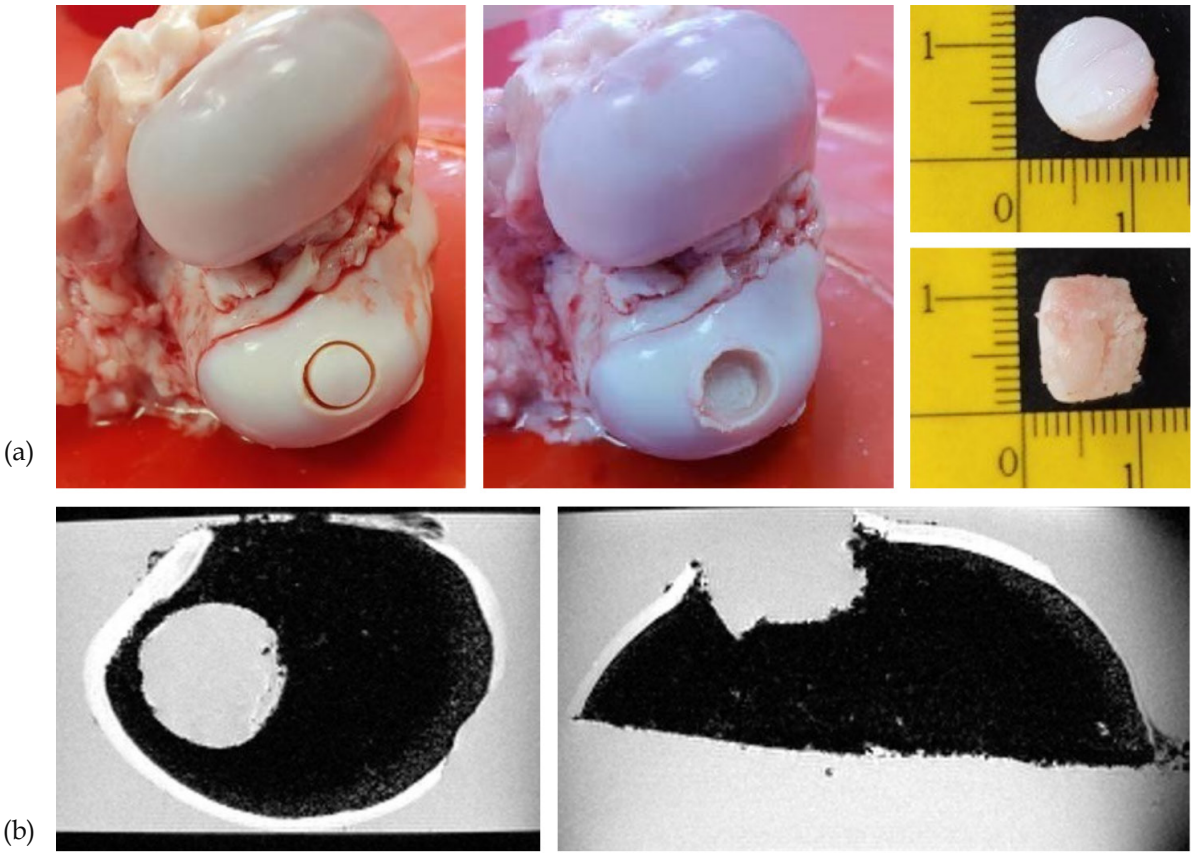


Figure 64: Osteochondral defect generated on the condylar area of a femur of animal origin. Pictures courtesy of Charité - Universitätsmedizin Berlin and TransTissue Technologies GmbH. Special thanks to Dr. Tilo Dehne and Dr. Michaela Endres.

From the images obtained in the MRI, the bone area can be distinguished in dark colour and the cartilage in a lighter colour (see Figure 64). In these cross-sections, the magnitude of the lesion is analysed, planning how much material should be removed during surgery, and estimating the nominal volume for the tissue engineering scaffold.

Once the stl files are generated, they are imported into the Siemens NX CAD software. In this CAD tool, the nominal geometry is developed, upon which it implements all the requirements linked to the lattice. The first step is to simulate the hole that is created during surgery to remove all surrounding damaged tissue. It is understood that although a patient-specific solution is being designed, only the border contours of the subchondral tissue and cartilage are exclusively recreated. To ensure the implant fits correctly during surgery, it is necessary to adjust the contact walls perpendicularly to the damaged surface. For this reason, a cylindrical volume extrusion operation is carried out, leading to vertical walls with a circular section, thus avoiding the emergence of corners or unwanted angles. During the implementation of these types of operations, work is done directly on the bone upper perimeter, as it is understood that the cartilage must be supported in this area. Therefore, the entire nominal area related to the soft phase is indirectly obtained from the bone region just by applying a thickness operation above the bone volume. Once the implant depth is calculated, the contours defining the drilling perforation are isolated. This creates a solid body bounded by the previously established depth on the bottom and the bone contours of the joint on the top, all following a cylindrical arrangement. Again, by using reference guides as auxiliar elements, it is possible to close the defect according to the patient's anatomy, thus providing an assembled volume on the system.

After closing the defect, a nominal geometry associated with the hard phase of the implant is obtained, based on a cylindrical geometry whose top face is adapted to the patient's bone contour. From this upper surface, a thickness operation of 2 mm in Z direction is applied to generate the soft phase, which perfectly and tangentially fit the bone.

Figure 66 describes all the process. It can be seen how the nominal volume associated with the meniscus slightly protrudes in some contours. This is because the operation applied to generate the soft phase contains a constant value, which is not true in natural cartilage, where the thickness can vary along the joint, specially in a subject with a pathology, even leading to the absence of tissue due to wear. There are various ways in which a variable thickness could be implemented based on criteria previously established by the PhD candidate but understand that this geometry serves as a starting point for the lattice implementation, defining its upper and lower limits, variable thickness is not desirable if to achieve a homogeneously distributed pore distribution over the subchondral zone.

At this point, the generation of the implicit volume of the implant solution is concluded. Next, following the previously developed methodology, all the requirements collected in our approach are implemented. Thus, following the step-by-step workflow, two individual lattice structures are implemented on both volumes. Their respective membranes are also placed accordingly (see Figure 67a).

In this design stage, compared to the previously explained steps, it's important to highlight the need for an additional step to ensure the alignment of pores between the two phases. In this case, on the hard phase, a cell distribution following a rectangular map pattern is re-implemented. However, this is not the case for the soft phase, which, being a geometry adapted to the bone, requires a customized cell map if the pores are to follow channels parallel to the contours of the nominal volume. Figure 67b illustrates this particularity.

Finally, the design of the developed concept for tissue engineering scaffolds for osteochondral restorations adapted to a patient is displayed. In Figure 67c it can be seen how, despite being a completely patient-specific design, the scaffold implantation process follows the same philosophy as the current approach. Thus, by applying a press-fit technique, the porous scaffold is inserted into the incision made during surgery. In addition to the combination of materials with different biomechanical properties, the biomimetic character of the solution is highlighted as the soft phase follows the profile of the cartilage along the entire subchondral surface, as can be seen in Figure 67d. This provides for better tissue generation, delineating the anatomical regions described in the Figure 53 in a more realistic way. To conclude, prototypes are fabricated to validate the model, yielding the following results.

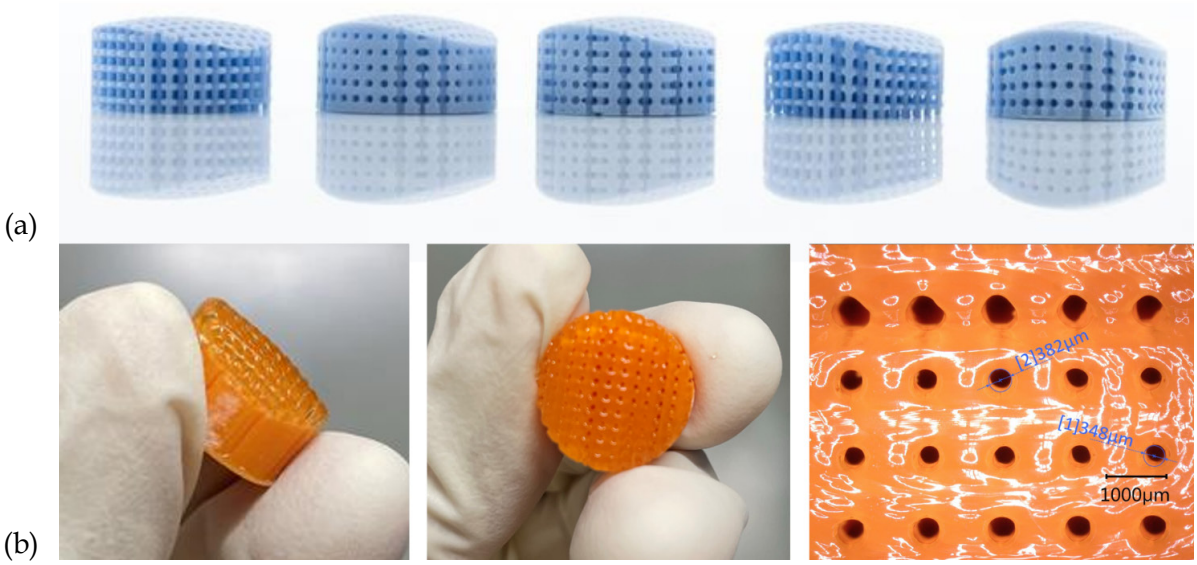


Figure 65: Osteochondral prototypes printed in hydroxyapatite and biogel. (a) Collection of scaffolds printed in HA by Lithoz using LCM technology. (b) Soft phase printed by Prpfactor GmbH with biogel using inkjet technology on a 5-axis printer above a hard phase surface. Pictures courtesy of Lithoz GmbH (a) and Profactor GmbH (b). Especial thanks to Research Engineer Michael Kainz and Dr. Elena Guillen from Profactor GmbH and Dr. Serkan Nohut, Research Engineer Altan Altun and Research Engineer Sebastian Geier from Lithoz.

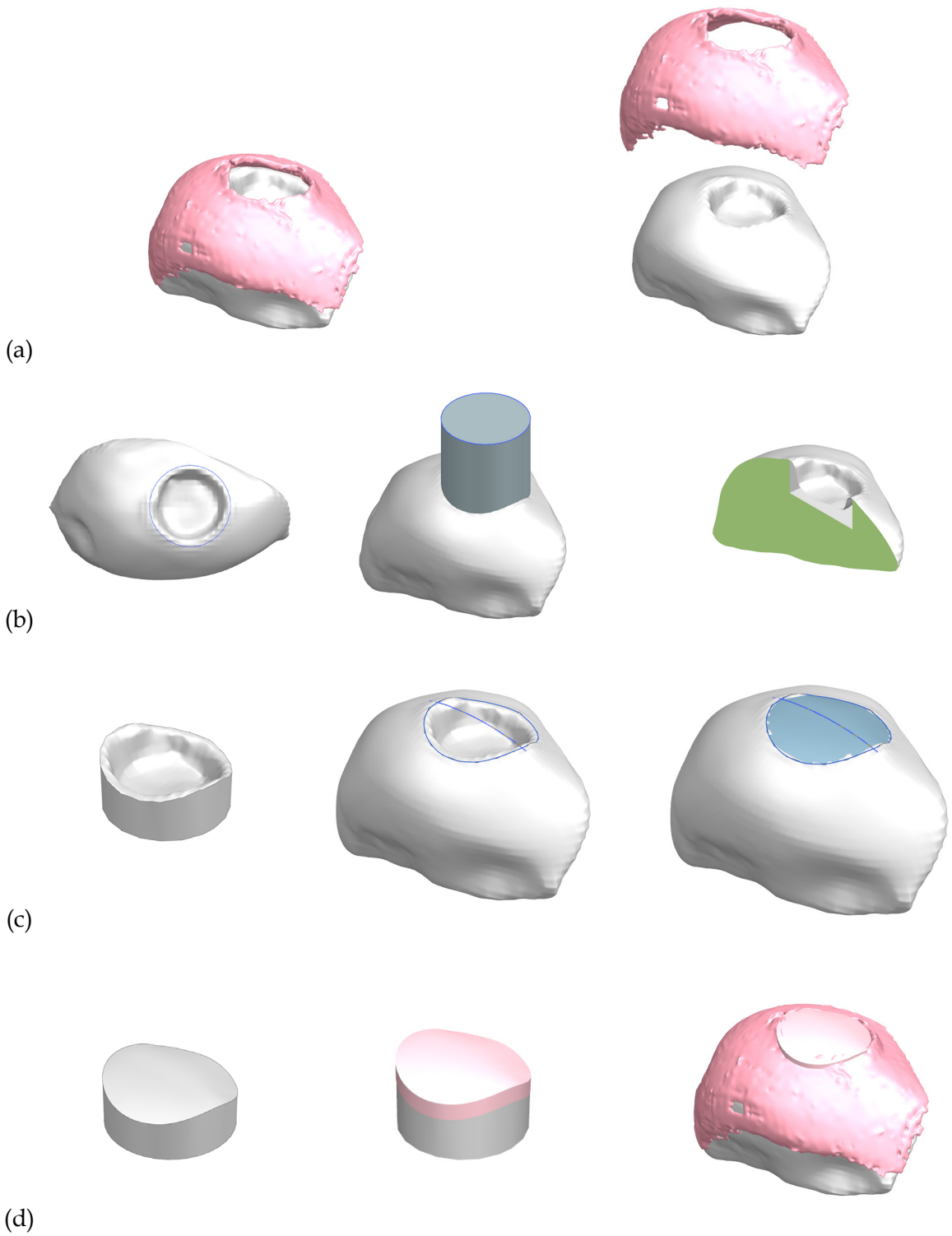


Figure 66: Summary of all design operations implemented in NX 2206 software to obtain the nominal geometry adapted to the patient's anatomy. (a) Imported model obtained by medical segmentation. (b) Delimitation of the defect by means of diameter and depth preset in the surgical planning stage. (c) Generation of a surface adapted to the patient's bone contour to heal the defect. (d) Extrusion of a 2mm thick membrane as cartilage tissue adjacent to the chondral region. Medical images segmentation performed by Research Engineer Disha tupe, from JKU Linz Institute of Polymer Product Engineering.

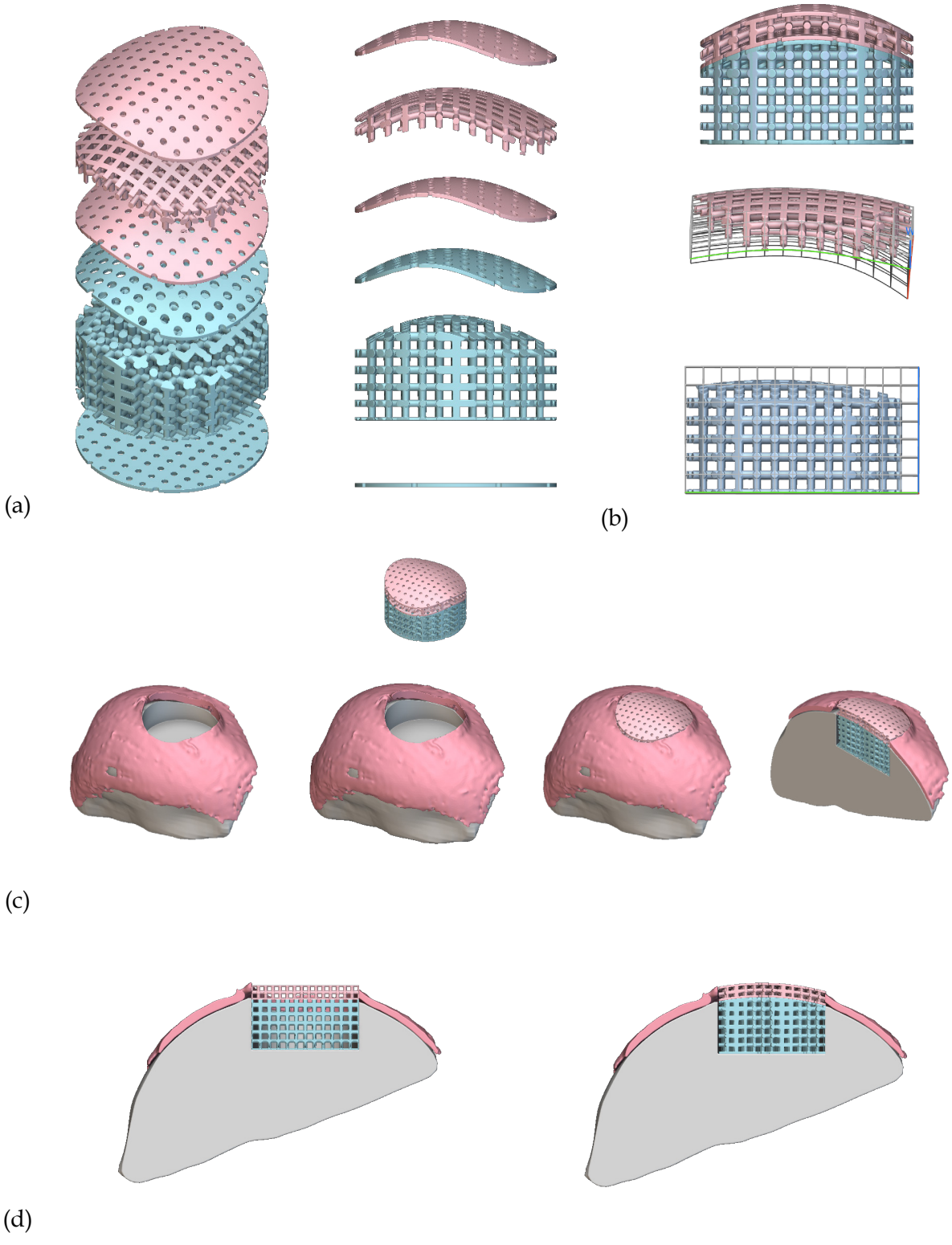


Figure 67: Summary of the operations implemented in nTopology conformal lattice design software. (a) Isometric exploded view of all the layers of the tissue scaffold. (b) Checking of the cell maps in the hard and soft phases to guarantee the alignment of the pores along the structure. (c) Implantation procedure using the press fitting technique with the implant completely adapted to the patient's geometry. (d) Section view showing how the solution adapted to the patient respects the existing anatomical regions compared to the regular cylindrical model.

7.4. Conclusions and future proposals

The constant search for functional and biomimetic solutions leads to the development of combined technologies and processes for the creation of innovative implants. As seen in this work, significant progress in multi-material and multi-functional hybrid implants can be addressed through the ability to print a soft biomaterial onto a bioactive ceramic substrate in a controlled manner, thus obtaining tissue hard and soft phases. Throughout this work, the evaluation of this emerging practices has been possible thank to the development of advanced additive manufacturing systems, such as the 5-axis inkjet printing machine developed by Profactor GmbH as part of the INKplant project.

However, progress in new technologies requires the simultaneous development of software tools, materials, among others. In particular regarding software tools, a change in the approach to generating the digital masks that enable controlled material deposition is essential. The non-planar deposition of material means that the generated layers do not maintain a constant value in the Z-coordinate for each layer, so the slicing programs must be adapted to generate the masks using new procedures. For this new digital mask generation approach, it is proposed to investigate the use of isoparametric that can be mapped onto the target surfaces in order to extract the special information for the correct material deposition. This scope requires at some point the conversion of information between 2D and 3D space, as it is needed to include a 3D surface into a black and white pixel image. It is crucial to understand that non-planar deposition implies that each point of the contained image has associated X, Y and Z spatial coordinates, unlike the traditional fabrication approach where layers are stacked at a constant Z distance so this value was irrelevant for this purpose.

Finally, regarding the proposed methodology to obtain customised customised scaffolds, it is necessary to further integrate it into the whole chain of the reverse engineering process. For example, in the surgical planning stage, the pre-procedure determination of an implant diameter and depth requires the inclusion in the approach of the design and fabrication of surgical guides that ensure the proper removal of damaged tissue by the surgeon and the precise positioning of the implant during surgery. This fact, in addition to the development of the new methodologies themselves, implies the training of professionals in these new flows, which entails a learning process. Therefore, all these aspects derived from the development of new techniques must be analysed and addressed jointly with all the actors involved in the process.

8. Bioinspired topology optimisation of a ceramic short-hip stem

8.1. Hip joint injury overview

Bone morphology and hip joint anatomy

Bone is a dynamic tissue with organic and inorganic components including hydroxyapatite (HA), collagen, small amounts of proteoglycans, non-collagenous proteins and water. Their composition strongly influences their mechanical behaviour and fracture resistance. In particular, the degree of mineralisation and porosity determine the quality of the bone material and thus its response to loading. Bone quality influences its ability to resist deformation (stiffness), absorb stress (elasticity) and energy (toughness) before failure (287). The degree of mineralisation or bone mass density is a property that affects bone fracture likelihood. HA and amorphous phosphate crystals, inorganic components, provide the bone with stiffness and compressive strength, and organic components provide its tensile properties. Excessive mineralisation does not lead to augmented bone strength but, on the contrary, to increase stiffness, decreases ductility and, therefore, increases risk of fracture as in osteopetrosis. Conversely, poor mineralisation also decreases mechanical strength, as in osteoporosis (see Figure 68).

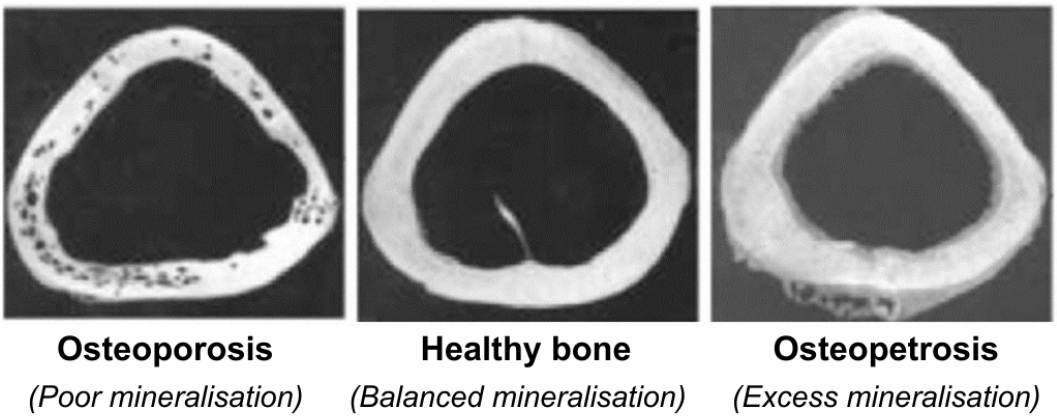


Figure 68: Pathological situation depending on the degree of bone mineralisation. Picture acquired and adapted from "Mechanical basis of bone strength: Influence of bone material, bone structure and muscle action" (287).

It is therefore understood that the degree of mineralisation is directly proportional to the bony tissue stiffness, which is quantified by Young's modulus, and inversely proportional to its

ductility (287). Such properties give rise to relevant characteristics related to the fulfilment of the following functions (288, 289):enabling locomotion, providing rigid support and sites for muscle action, providing a protective shield for internal organs and bone marrow, acting as an ionic backup for the maintenance of mineral homeostasis, acting as an endocrine organ that regulates metabolism and maintains an acid-base balance, and providing an environment for haematopoiesis within the medullary spaces. In addition, its mechanical properties are the result of a compromise between the need for stiffness, to reduce stress and achieve more efficient kinematics; and the need for sufficient ductility, to absorb impact, reduce the risk of fracture and minimise skeletal weight. It differs from engineered materials because it is not inert, on the contrary, it undergoes substantial changes in structure, shape and composition depending on the mechanical and physiological environment, based on a process known as bone remodelling (290). Bone adaptability allows for effective repair that prevents fractures. However, fractures are still quite common and are often caused by the sudden onset of loading that exceeds the bone tolerance or by cyclic loading activity that accumulates damage at a rate that cannot be repaired, causing a decrease in bone stiffness and strength until failure occurs at a much lower intensity (290).

Bone fractures prediction and prevention are important topics in orthopaedics due to their high frequency, surgical complications and socio-economic impact. For example, the number of hip fractures worldwide was estimated to be 1.66 million in 1990 and is expected to increase to 6 million by 2050 (291).

In terms of morphology, bone tissue is heterogeneous in a macroscopic scale, porous and anisotropic. Although porosity can vary continuously from 5 to 95%, most bone tissues have very low or high porosity. Consequently, a distinction is usually made between two types of bony anatomies: cortical and trabecular (292).

- Trabecular or cancellous bone has a porosity of 50-95% and is usually found in cuboidal bones, flat bones and at the ends of long bones. The pores are interconnected and filled with marrow (tissue composed of blood vessels, nerves and various types of cells whose main function is to produce the basic blood cells). Its bone matrix has a variable reticular shape, resembling a composition of very thin interlocking plates and rods called trabeculae, with a thickness of about 200 μm (292). Cancellous bone derives its main mechanical benefit from its architecture, which provides structural support without increasing the weight of all bone tissue. Due to its location within the medullary cavity, it is not an efficient weight-bearing structure by itself. Its most relevant mechanical function is to channel the withstood stresses into the stronger and more massive cortical bone. Due to the high interconnection, it provides a series of rods that can reinforce the bone, similar to the way the bracing of the Eiffel Tower makes it a stable and strong structure (293).
- Cortical bone, also called compact bone, is found as the main component of the shafts or diaphysis of the limbs long and short bones, also surrounding the cancellous bone of the vertebral body and at the ends (or metaphysis) of long bones. Its porosity is approximately 3-5%, although it can vary depending on several factors, such age or osteoporotic changes in the skeleton. Its high density makes this tissue homogeneous

and very though. Their main function is to provide both support and protection, which prevents them from being easily broken or splintered; therefore, cortical regions are suitable for withstanding axial, bending and torsional stresses efficiently (293, 294).

Morphological differences between cortical and trabecular bone entail important biomechanical implications. Cortical bone has a higher elastic modulus in comparison with trabecular one, so its stress-strain curve is steeper. This implies that cortical area is capable of supporting a higher degree of load per area with a lower deformation rate. In addition, due to its low porosity it has a high compressive strength which contributes to the bone mechanical behaviour. On the other hand, trabecular has a lower Young's modulus due to its higher porosity which biomechanically is represented in a more flattened curve. This fact means that, in comparison with cortical regions, its compressive strength is lower, but possesses a higher strain rate, which leads to greater flexibility (se Figure 69) (287, 295).

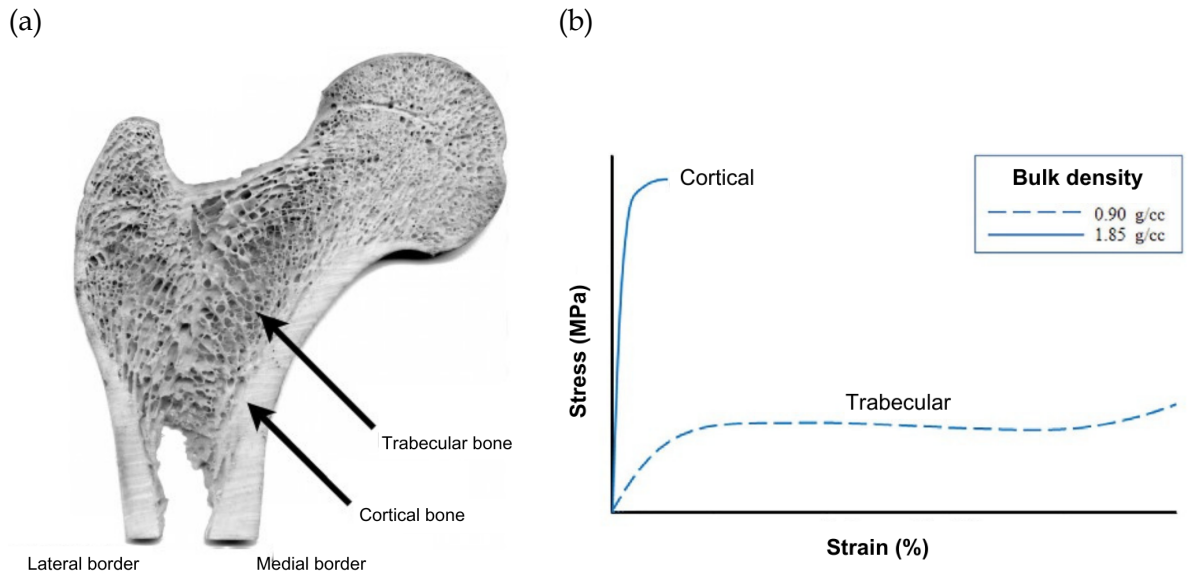


Figure 69: (a) Bone morphology distinguishing between cortical and trabecular zones of a femoral section. (b) Stress-strain curves of cortical and trabecular bone regions. Pictures acquired and adapted from "Mechanical basis of bone strength: Influence of bone material, bone structure and muscle action" (287) and "Structural optimisation: Biomechanics of the femur" (296).

In addition to the above, bone tissue is a material that is constantly renewed to maintain its stability and integrity and it is also adapted to the particular mechanical environment in which it performs, in order to obtain maximum stiffness with minimum weight (297).This process is known as bone remodelling or adaptation and involves sequential osteoclast-mediated bone resorption and osteoblast-mediated bone formation in the same location. Through this mechanism, the skeleton is capable of self-adapting to its mechanical environment and results in bone matrix replacement and repair of localised defects (298, 299). The bone adaptation to mechanical stimuli, as one of the causes of the bone remodelling process, is referred as Wolff's law (300) or bone formation's law. This equation suggests that bone density changes ($d\rho_{app}/dt$) in response to variations in bone functional forces. Despite this, Frost (301)

introduced the idea of the mechanostat. The principles of the mechanostat claim that bone adapts towards a target deformation, similar to a thermostat that regulates heating and cooling towards a target temperature. According to the mechanostat, if the bone experiences a deformation greater than the desired, a bone counter-action takes place (continuous creation), which brings the deformation rate back to the balanced situation. Whereas, if the bone undergoes a lower deformation, bone resorption occurs, which causes a higher deformation to revert the imbalance. Frost also proposed a dead zone for the mechanostat, similar to that which allows a thermostat to maintain the temperature between two values, only regulating heating or cooling when the temperature goes out of range.

Therefore, based on the definitions of Wolff (300) and Frost (301) , bone atrophy or osteoporosis occurs when bones are subjected to insufficient mechanical stimuli, with bone resorption predominating, while hypertrophy or osteopetrosis appears when they are subjected to excessive stimuli, with bone formation predominating. This behaviour is shown in the bone remodelling curve (Figure 70), which graphically summarises the idea of Frost's mechanostat. It can be seen a threshold of equilibrium between resorption and formation called the "dead or lazy zone" where bone density is maintained balanced, and outside this conditions the phenomena of osteoporosis and osteopetrosis occur.

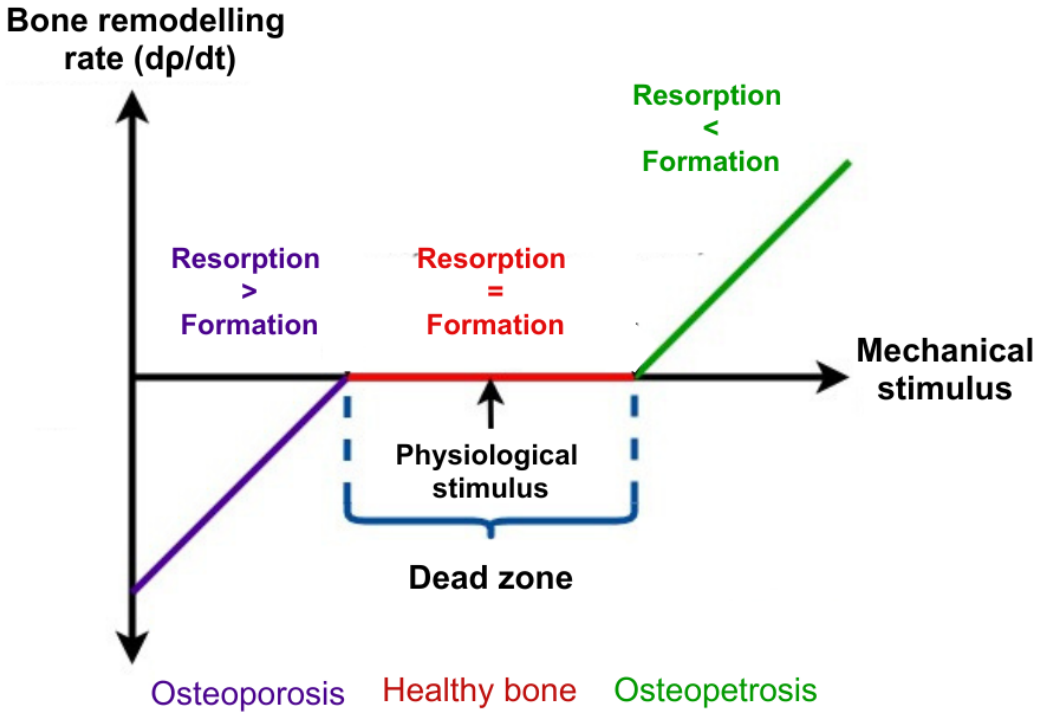


Figure 70: Graph showing the rate of bone remodelling as a function of the existing mechanical stimulus as well as the possible states to which this situation leads. Picture acquired and adapted from "Innovative Design Methodology for Patient-Specific Short Femoral Stems" (302).

Hip joint injuries aetiology and most common causes

Most hip fractures occur in older patients whose bones have been weakened by osteoporosis; in these patients, even a simple twisting or tripping injury can cause a fracture, or in some

cases, the bone may be so weak that the fracture occurs spontaneously while walking or standing. When a hip fracture occurs in a young patient, it is usually the result of a high-energy impact, such as a fall from a ladder or a collision with a vehicle (303). A fracture of the proximal femur or hip fracture is a break in the upper part of the femur. Fractures can be very painful. For this reason, prompt surgical treatment is recommended, usually requiring a multidisciplinary approach including underlying medical conditions and appropriate surgical fixation, early mobilisation and rehabilitation to ensure recovery of functional mobility (304). Delays in surgical treatment are associated with increased complication and mortality rates (304, 305). Suboptimal treatment of hip fractures can lead to debilitating complications such as avascular necrosis (AVN), fracture non-union or malunion, or failure of fixation elements. Therefore, early detection and classification of hip fractures are essential to guide appropriate treatment. A hip fracture can cause injury to one of four areas of the upper femur (Figure 71b):

- Head of the femur.
- Neck of the femur. The area of the femur below the femoral head.
- Intertrochanteric area. The area below the femoral neck and above the long part or shaft of the femur. It is called intertrochanteric because it is marked by the greater and lesser trochanter.
- Subtrochanteric area. The upper part of the femur below the greater and lesser trochanters.

Intertrochanteric and neck of femur fractures are the most common types of hip fracture. Femoral head fractures are extremely rare and are usually the result of a high-velocity event (303). Specifically, this section focus on understanding femoral neck and femoral head fractures because they are related to hip replacement. Femoral neck fractures constitute stress or repeated impact fractures originate in this region. Those that occur from repetitive excessive bone overloading are known as fatigue fractures, while fractures that occur from normal loading of an abnormally weakened bone are known as failure fractures. Stress fractures occur when axial microtrauma accumulated in the head is transmitted to the femoral neck, whereby fatigue of the normally strong and compensatory gluteus medius muscle subjects the neck to excessive bending forces (Figure 71a) (306, 307).

Although femoral neck fatigue fractures are uncommon in the population, they should be suspected in patients complaining of traumatic or atraumatic hip pain, especially in young, physically active patients such as elite athletes, long-distance runners or military recruits (308). Insufficiency fractures occur more frequently in elderly osteoporotic patients, often without a unique traumatic injury (308).

The prevalence, common mechanisms of injury, classification and treatment of femoral neck fractures depend on the patient's age and initial functional status (304, 309). Adults are generally considered elderly if they are older than 70-75 years and as young elderly or young if they are younger than 65-70 years, qualified by estimated physiological age or functional status (309).

(a) (b)

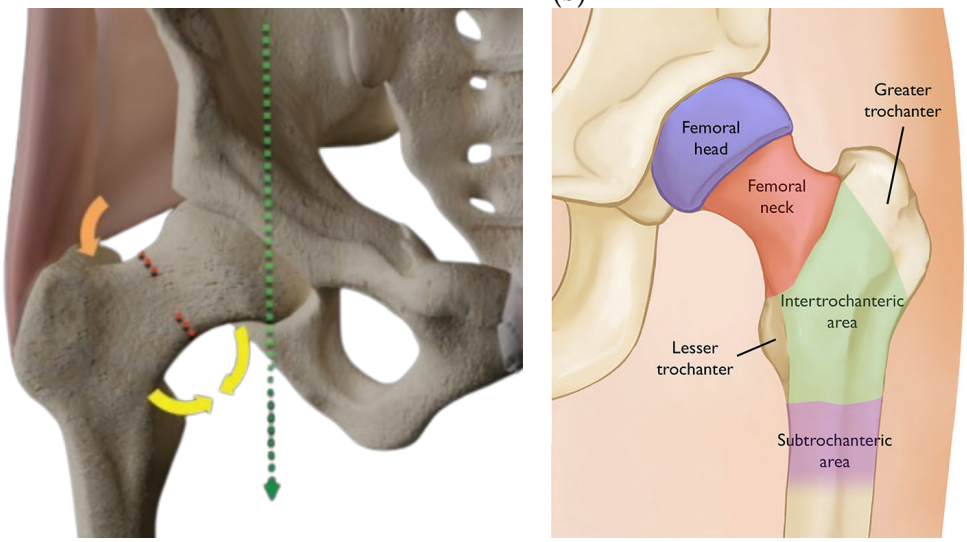


Figure 71: (a) Most common stresses that lead to hip fractures. (b) Most prevalent areas of the femur that are prone to fracture. Pictures acquired and adapted from "Proximal Femoral Fractures: What the Orthopedic Surgeon Wants to Know" (307) and OrthoInfo website (303).

Hip arthroplasty or hip replacement

Total hip arthroplasty (THA), also called hip joint replacement or hip replacement, is a surgical procedure in which all or part of the hip joint is replaced using an artificial device (prosthesis) to restore joint motion (299).The hip joint can be damaged due to fracture of the femoral neck or femoral head and diseases such as (310):

- Osteoarthritis: Commonly known as wear-and-tear arthritis or osteoarthritis, osteoarthritis damages the articular cartilage that covers the ends of bones and helps joints move smoothly (Figure 72).
- Rheumatoid arthritis: Caused by an overactive immune system, it produces a type of inflammation that can erode cartilage and sometimes the underlying bone, resulting in damaged and deformed joints.
- Osteonecrosis or avascular necrosis (AVN): If insufficient blood is supplied to the hip joint, as can occur in the case of dislocation or fracture, the bone may fracture or collapse (Figure 72).

The most common conditions that may require a femoral prosthesis are osteoarthritis and femoral neck fracture. Also, tumours in the hip joint, inability to work, sleep or move due to pain may require joint replacement. This pathology is typical of elderly people, however, the rate of fractures in people under 40 years of age has increased due to the practice of various sports (299).

Hip arthroplasty was one of the greatest advances in orthopaedic surgery in the 20th century and contributes to improving the quality of life of patients by reducing pain and restoring mobility. In the medical field, two types of hip arthroplasty are commonly performed (299). A partial hip replacement, or hemiarthroplasty, is the replacement of only the patient's femoral

head. Therefore, the new prosthetic femoral head (acetabular cup) rotates within the natural bony socket. The natural socket is lined with hyaline or articular cartilage that acts as a lubricant (decreases friction), a shock absorber and helps distribute stress more evenly within the bone. In general, this cartilage does not remain healthy when it is moved against an artificial surface in place of the articular cartilage of the femoral head, this can lead to the breakdown of the hip cartilage and produce pain. Total hip replacement involves replacing the femoral head and implanting a prosthetic shell with a plastic liner into the natural socket. With this procedure, the prosthetic femoral head is moved into a prosthetic socket (311).

Each procedure has advantages and disadvantages, but as a general rule, the best results for longevity and consistent pain relief are achieved with a total hip replacement. Historically, femoral neck fractures left patients crippled or even caused death due to lack of mobility and all its associated complications. During the 1960s, partial hip replacement was introduced. For the first time, doctors were able to replace a broken femoral head with an artificial one. This was a dramatic breakthrough that saved countless lives and greatly improved mobility and quality of life for many. Although it was a major leap in hip replacement surgery, most patients did not have a perfect outcome, as they experienced pain due to the prosthesis not being stable within the femur or the new head wearing down the articular cartilage (311).

In some cases, due to pain and lack of stability, revision surgery is necessary: this term is used when a previously replaced hip joint is replaced. Almost 10% of all operations undergo revision surgery. The risk of revision surgery is extremely high, especially for elderly patients, and complications include cardiac and pulmonary problems and even death (312, 313). In turn, the first hip arthroplasty is known as primary surgery.

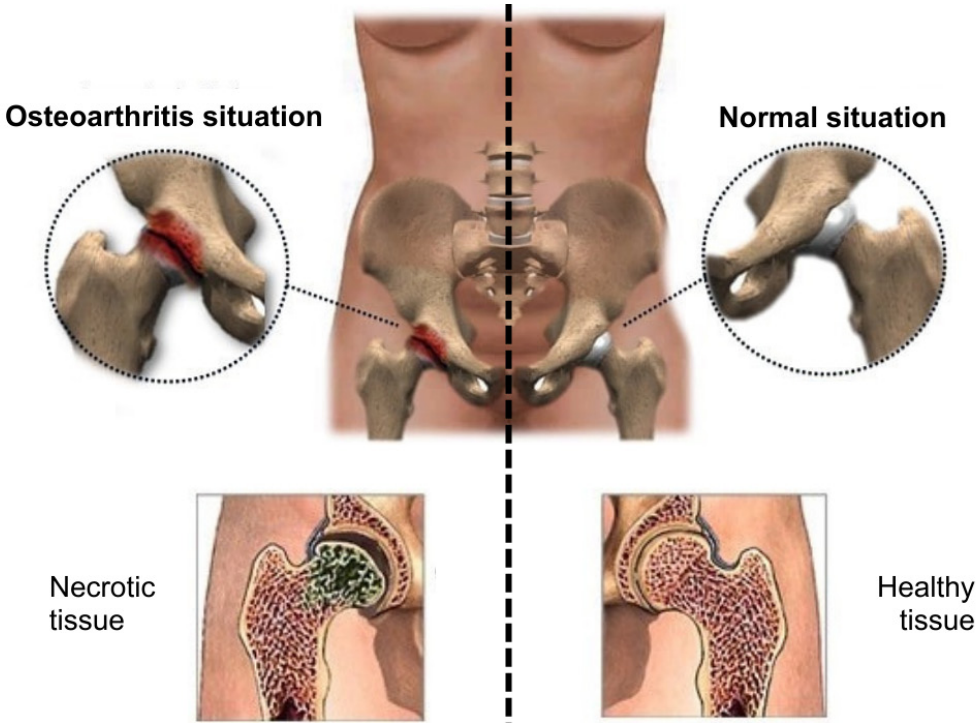


Figure 72: Comparison of healthy hip and tissue associated with osteoarthritis and the appearance of necrotic tissue. Pictures acquired and adapted from Mount Sinai website (314).

(a) (b)

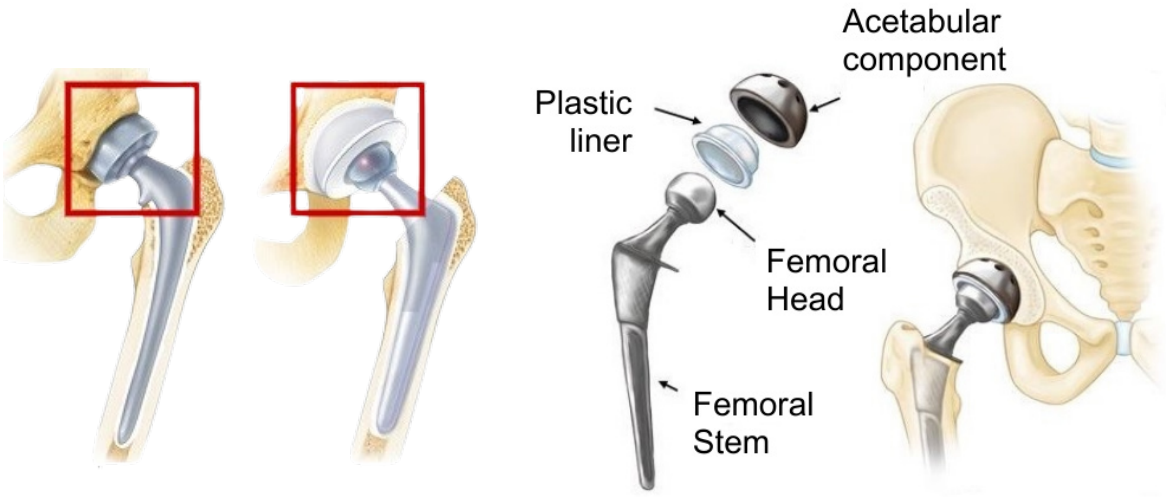


Figure 73: (a) Representations of partial hip prosthesis (left) and complete hip prosthesis (right). (b) Components present in common hip prosthesis. Pictures acquired and adapted from Dr. Julian Guerra website (315) and OrthoInfo website (303).

Current medical solutions for total hip replacement (THA)

The femoral prosthesis, also called a hip prosthesis, is a mechanical implant that replaces the hip joint primarily for two typical situations: to reduce pain and improve joint mobility due to progressive wear and tear caused by osteoarthritis or in cases of fracture of the femoral neck due to trauma or osteoporosis (299). The hip prosthesis consists of a stem, a ball joint, an insert and an acetabular cup (Figure 73b). In hip arthroplasty, a femoral prosthesis is implanted by cutting the damaged femoral head and removing the trabecular bone of the femur to insert a stem into the femoral socket. The upper part of the stem is connected to a ball joint that replaces the damaged femoral head. If it is a total replacement, the articular cartilage of the hip is replaced by a cup called a acetabular cup that allows attachment to the ball-joint, however, a spacer called an insert is placed between the two components to prevent excessive friction in the artificial joint. The femoral stem in turn is composed of: rod, neck and receiving cone. The rod is an elongated wedge that is fixed to the shaft of the femur to give stability to the prosthesis, the neck is the element that replaces the femoral neck, and the receiving cone allows the connection of the stem to the articulating sphere.

Regarding fixation, there are two types of femoral prostheses: cemented and uncemented.

- Cemented prostheses. These are prostheses in which the stem is attached to the bone by means of a surgical cement called polymethylmethacrylate (PMMA). The cement is injected into the previously prepared femoral canal and the stem is inserted by the surgeon in the correct position, therefore, the surgeon must have sufficient expertise in the placement of this type of implant. The cemented prosthesis is recommended for elderly patients (over 65 years of age) with osteoarthritis of the hip, osteoporosis and poor bone quality; since it does not have the capacity for biological adherence required

by the cementless prosthesis, failure would be imminent (299). Loosening of this type of implant occurs due to loosening of the cement due to its degradation, which in turn causes the release of PMMA particles into the blood that cause vasodilatation (316). Consequently, its use is not recommended in patients with low cardiovascular reserve because adverse clinical responses such as hypoxia, hypotension, arrhythmias, increased peripheral vascular resistance and in extreme cases cardiac arrest have been reported (317, 318).

- Cementless prostheses. This type of implant has a porous surface finish that attempts to simulate bone porosity, so that the bone grows around it and adheres naturally, i.e. bone and implant integrate (osseointegration). Usually, HA coatings are used to promote bone growth, which stimulates osteogenesis, integrating both elements quickly and effectively (299). It has the advantage of being a more natural fixation than that provided by cement, but its success depends on the patient's preconditions. This type of implant is recommended for patients under 65 years of age, as their bone quality is adequate and therefore has a high capacity to adhere to the implant. One of the main disadvantages of this type of stem, compared to cemented implants, is that they require a long recovery period, since the prosthesis must be fixed by bone growth (299).

Overall, both cementless and cemented hip prostheses provide patients with effective long-term relief if the surgical procedure is correct. Cementless fixation of femoral prosthetic components is the procedure of choice for many surgeons, although a certain percentage may fail in the long term, resulting in events that alter periprosthetic bone turnover. Conventional stems (Figure 73), which are the most commonly used commercially, invade the femoral shaft and transmit stresses to that region. Because their insertion requires removal of trabecular bone and bone marrow, a change in the transmission of mechanical stimuli occurs and leads to devascularisation of the endosteum, which may result in long-term AVN (319). As a result of the effects caused by conventional stems, new concepts in implant design have emerged in an attempt to decrease the aforementioned disturbances, which is the purpose of short stems (319).

Short stems were designed as an alternative to conventional stems to preserve proximal femoral bone stock and are therefore often indicated in primary CTA. Although there is no universally accepted limit for short stems, some have suggested a length equal to or less than 120 mm, which approximates the junction between the metaphysis and proximal diaphysis (320). Shor stems classification includes:

- Femoral neck (Figure 74a I): these stems only have fixation at the femoral neck, and are therefore used when a fracture occurs and the femoral neck remains intact. Their primary stability is through compression of the cancellous bone. Variable clinical results have been reported, as the surgical procedure is demanding and prone to suboptimal positioning, with different indications for surgery in relation to age, bone quality and abnormal anatomy.

- Calcar-loading stem (Figure 74a II): these are collared stems, which can reach as far as the junction between the metaphysis and the proximal diaphysis. They achieve fixation in the calcar and the proximal cortical bone. The aim is not to scrape the cancellous bone, but to incise the metaphyseal bone to obtain cortical contact in the loading region. By preserving the femoral neck, this stem provides rotational stability. Despite increased proximal loading, stress shielding may occur at the greater trochanter.
- Calcar-loading stem with lateral flare (Figure 74a III): as the name suggests, these stems have a lateral flare that achieves fixation in the lateral and medial cortical bone, allowing load distribution in the proximal femur resembling physiological stress distribution. Logroscino et al (321) demonstrated that the stem reproduced physiological load distribution in the femur without signs of shielding 1 year postoperatively, thus showing excellent osseointegration. Multiple studies have further demonstrated that a short metaphyseal-fitting femoral component can achieve stable fixation despite lacking diaphyseal fixation (145, 322, 323).
- Shortened tapered stem (Figure 74a IV): these stems are similar to conventional proximal tapered tapered stems, but with a shorter distal taper to avoid stress shielding, which often extends only to the proximal aspect of the diaphysis. These shanks were designed for proximal stress transfer.

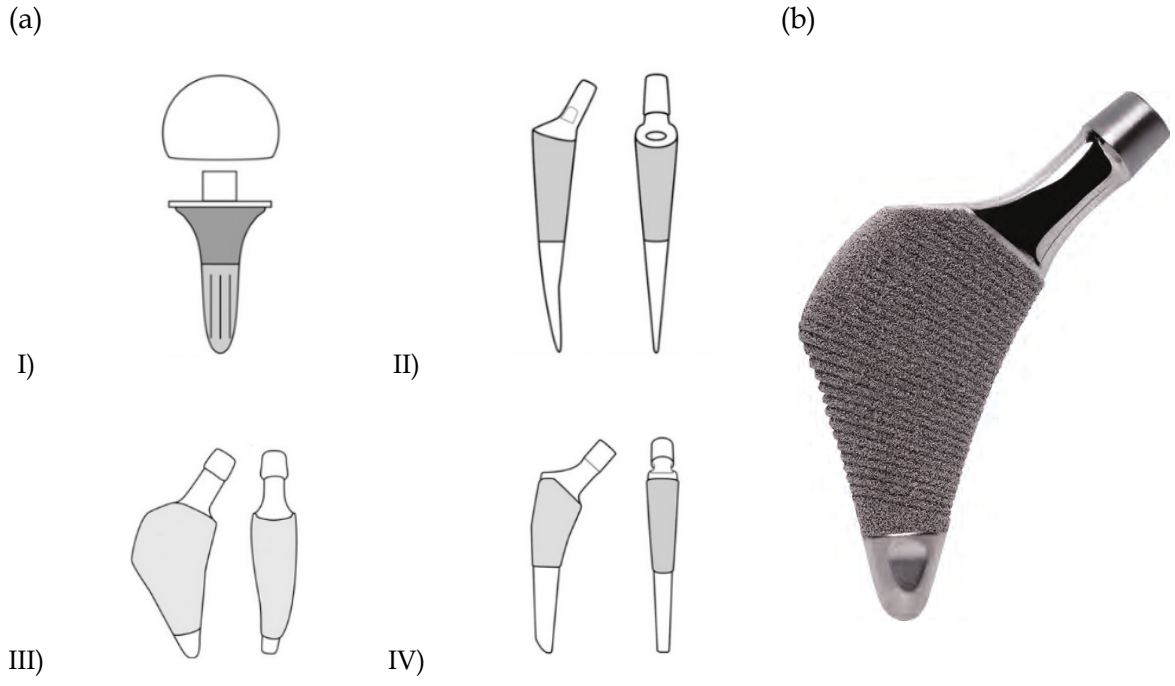


Figure 74: (a) Classification of short-stem prostheses according to their morphology: I Femoral neck, II Calcar-loading stem, III Calcar-loading stem with lateral flare and IV Shortened tapered stem. (b) Commercial short-stem hip prosthesis from the company DePuy®. Pictures acquired and adapted from "An Update on Cementless Femoral Fixation in Total Hip Arthroplasty" (324) and "Short-stem Designs for Total Hip Arthroplasty: Neck Stabilized Femoral Components" (325).

Of these 4 types of short stems, the most widely used and best performing in follow-up studies is the calcar loading stem with lateral flaring (320, 326, 327). The design of this implant is attributed to Nicola and Francesco Santori in 1993. However, it was not until 2006 (145) that they perfected the design technique and showed the scientific community the excellent short-term clinical results. Nevertheless, the DePuy® company, in agreement with the Santori brothers, began to produce the implant as standard under the trade name DePuy Proxima™ hip (Figure 74b).

Mechanobiology

The femur undergoes cycles of bone replacement maintaining its structure by balancing osteoclastic (resorption) and osteoblastic (formation) action. This occurs because it is continually exposed to mechanical stimuli that allow for proper remodelling. However, according to Wolff's law, increased loading leads to an increase in bone mass and reduction leads to its loss. The ideal stem should restore the physiological load transfer of the femur, unfortunately, after insertion of the prosthesis, the load pattern is modified. Consequently, the natural response of bone to the conventional stem is proximal bone resorption and distal bone formation (Figure 75) (328), due to which the phenomenon of stress shielding (SS) arises, causing bone mass to decrease and resulting in loosening or failure of the implant.

The short- and long-term stability of cementless implants is strongly determined by the load transfer between the implant and the bone tissue. Shielding in the femur occurs when part of the loads are taken up by the stem and prevented from going to the bone. Normally the femur carries the external load itself, being transmitted through the neck from the head to the diaphysis. When a stiffer stem is inserted into the canal, it shares the load with the bone. Originally, the load is supported by the bone alone, but now it is supported by the implant and the bone. As a result, the femur is subjected to less stress and is therefore protected against stress. Consequently, the upper part of the femur is less loaded and the distal end is overloaded (Figure 75) (292).

Shielding reduces implant support and increases the risk of loosening. The effects of implant loosening and micro-displacement of the prosthesis relative to the femur can cause difficulties for patients when performing daily activities. If this situation is prolonged, it can cause a lot of pain and revision surgery is likely to be performed, however, the bone surrounding the removed femoral component has less bone stock; therefore, the new implant must be longer and thicker to stabilise in the femur. However, stress shielding can occur again, so this phenomenon must be eliminated(292).

Shielding is defined radiographically by the appearance of proximal femoral bone loss and bone formation distally (Figure 76) (329). Mechanically, Joshi et al (330) quantified it as the difference between bone strain before (σ_{int}) and after THA (σ_{imp}) relative to the strain of the intact femur:

$$SS = \frac{\sigma_{int} - \sigma_{imp}}{\sigma_{int}} \quad (3)$$

It is important to understand that each stem design leads to a specific change in the loading pattern that leads to adaptive bone remodelling. However, there are two types of bone remodelling: physiological and iatrogenic. Physiological is related to natural bone aging, i.e. it is an age-related bone change; iatrogenic, on the other hand, is related to bone changes caused by the implant. Nothing can be done to prevent physiological remodelling, however, iatrogenic remodelling depends on the surgical technique, the design and the level of activity during the recovery time. For this reason, proper femoral stem design helps to prevent this type of remodelling that contributes to implant loosening, periprosthetic fractures and complicates revision surgeries (329).

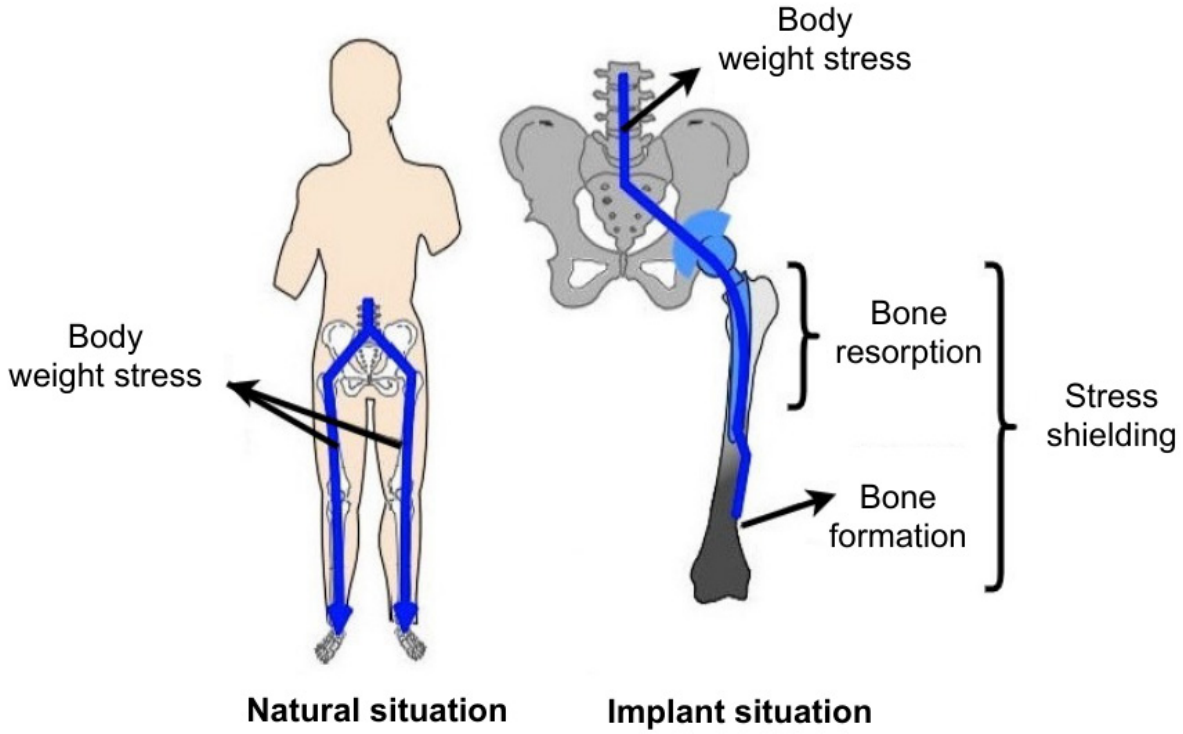


Figure 75: Mechanobiology of the intact femur versus the femur implanted with a hip prosthesis. Picture acquired and adapted from "Biomaterials in Total Hip Joint Replacements: The Evolution of Basic Concepts, Trends, and Current Limitations—A Review" (331).

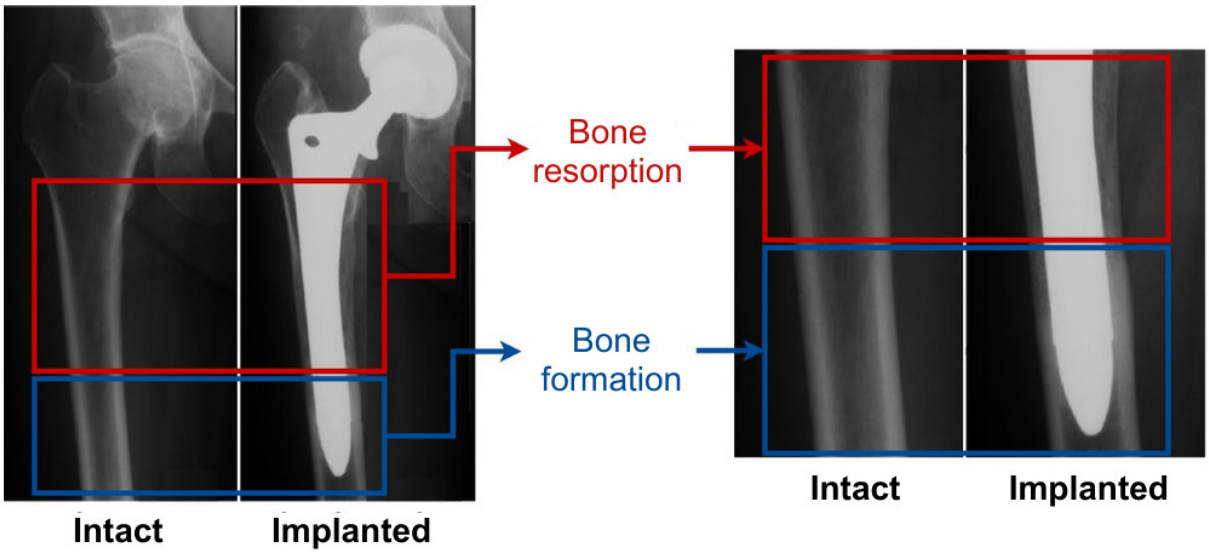


Figure 76: Areas of bone regeneration and bone absorption in the situation of intact femur versus femur implanted with hip prosthesis. Picture acquired and adapted from "Long-Term Bone Remodelling Around 'Legendary' Cementless Femoral Stems" (332).

8.2. Innovative design and optimisation methodology of a ceramic short-hip stem

Bioinspired or biomimetic design strategies of medical implants with enhanced biomechanical performance often lead to porous structures or lightweight lattice-based geometries with functional gradients of density and mechanical properties (333, 334, 335). These gradients of porosity and intricate structures are especially common in next generation implants for bone repair and reconstruction and in tissue engineering scaffolds and biofabricated constructs for articular restoration (336, 337, 338). Although these lightweight structures for biomedical purposes can be achieved by traditional manufacturing processes like casting (339, 340), foaming (341), molding with porogens (342), brazing, soldering, sintering, or adhesive bonding (343), among other options, it is necessary to acknowledge the radical transformation brought to biomedical manufacturing by additive manufacturing technologies (AMTs) and the freedom of design they are already enabling (344, 345). Indeed, the complexity of biological structures can be -to some extent- mimicked from the design stage and materialized by high-precision industrial additive manufacturing technologies, following "3D matter made to order" and even "voxelated design" approaches (344, 345, 346). However, it is necessary to further research in straightforward design and innovative additive manufacturing (AM) methods for lightweight bioinspired implants, especially as regards the expansion of the portfolio of usable materials and the creation of massive implants, beyond the more common proof-of-concept scaffold probes for in vitro testing (347).

As regards additively manufactured articular implants, currently the most extended option is the layered manufacturing of stainless steels and Ti alloys (322, 323) through selective laser melting, electron beam melting and powder bed laser fusion (PBLF), although other metallic biomaterials, such as Ni-Ti (348), Mg (349), Zn (350) or Co-Cr (351) alloys, are also processable

with similar methods. Other techniques like wire arc AM (352), metal binder jetting (353) and fused deposition modelling (164) are applicable in some cases. At present PBLF is well established and helping to promote metallic metamaterials and multi-scale metallic components for medical purposes (354, 355). However, metallic implants, either additively or subtractively manufactured using biomimetic designs, can release ions from their surfaces, cause undesired chemical reactions, may be subject to oxidative or galvanic corrosion, and are known for causing stress-shielding and bone resorption in the long term (356).

A shift to ceramic materials for bone replacement and articular implants seems to be a very promising move, as this study aims to demonstrate. In fact, ceramic materials for bone replacement have been studied for decades (357, 358), although their impact might have been limited, until recent, by the lack of competitive additively manufacturing technologies capable of controlling the geometries of ceramic implants from the design stage and fostering bioinspired designs. Nowadays different additive manufacturing technologies, each with various configurations, allow for processing ceramic materials (359), including: indirect powder bed fusion, sheet lamination of ceramic tapes, ceramic material extrusion, direct inkjet printing, binder jetting, vat photopolymerization or lithography-based ceramic manufacturing (LCM), direct powder bed fusion, directed energy deposition, among others.

Currently, the most transformative option for additive ceramic processing is lithography-based ceramic manufacturing, which stands out for the large portfolio of processable ceramic materials, including functional or smart ceramics, for the achievable resolution, for the attainable full density after sintering, and for the possibility of combining different ceramic slurries during the construction, in order to achieve biceramic components, as explained further on and illustrated by different references pioneering studies.

As already presented, LCM is a VAT photopolymerization procedure and relies on the layered digital light processing of ceramic slurries. These slurries, counting with a polymeric matrix (a photosensitive resin) and including high content of ceramic particles, are photopolymerized through digital masks in a layer-by-layer fashion, the photopolymer binding the ceramic particles together. The obtained "green part" is subsequently debinded and sintered to reach a fully ceramic object (134, 135, 360). LCM has proven highly effective for processing several types of bioceramics, including bioinert ceramics like alumina (134) and zirconia (361) and bioactive ceramics like hydroxyapatite (146, 362, 363), tricalcium phosphate (147) and bioactive glass (84, 148). Its medical applications are promising due to the geometrical complexity achievable, the filigrane structures reachable, the final biological and biomechanical properties, and some interesting tribological responses (364). Different examples of conceptual medical devices obtained with LCM include monolithic labs- and organs-on-chips (365), functionally graded scaffolds (366), lattices and metamaterials for cell culture trials (187, 367) and dental replacements (136, 368), to cite a few.

Nevertheless, most examples of LCM-based medical devices concepts are still quite limited in mass and size, usually ranging from 1 to 5 cm^3, as the most common application are still the creation of small-sized bone grafts, cellular structures, tissue engineering scaffolds and test probes for in vitro studies. LCM is extremely appropriate for these scaffolding structures, normally based on lattices and porous structures with very thin walls (c.a. 0.4 mm to 0.8 mm

of thickness and with small gradients). However, working with designs for massive components is more challenging, due to the large contractions during debinding and sintering that may lead to inner cracks and warping, if the design and printing are not adequately planned.

In this study the lithography-based ceramic manufacturing of massive implants for bone replacement is addressed. Topology optimisation is employed to obtain lightweight designs with adequate transitions from bulk to porous regions. These optimized topologies prevent mechanical problems during lithography-based ceramic manufacturing and subsequent sintering, and lead to structurally successful devices. The process is illustrated through the design of a short-stem for a human hip prosthesis, which is topology optimized using geometry-based and stress-based methods to reach two different designs oriented to additive manufacturing. Both are adequately manufactured employing LCM, for assessing their viability and analyzing current challenges and future potentials. The case studies designed and manufactured constitute quite singular examples of large-sized and massive implants achieved by LCM, whose remarkable features for healthcare innovation are once again demonstrated. The study finalizes with a systematically gathered set of good practices for successful design and LCM of large-sized massive implants and with a selection of future research directions towards even more complex multi-scale and multi-material implants.

8.2.1. Design of a bulk hip prosthesis

The design of the bulk implant is based on a virtual model of the proximal femur created by segmentation using 3D Slicer 5.4.0 of the "TCGA-VP-A878" CT scan (369), available from the open access library "The Cancer Imaging Archive" (Figure 77a). An elliptical cross-section is chosen for its effectiveness in distributing stresses along the implant shaft (370). A dedicated web application is used to determine the ellipse that would best fit the femoral cavity while respecting its anatomical boundaries. Oblique sections are taken to mimic the lateral aspect of the proximal femur down to the lesser trochanter. Each section thus obtained is analysed using the aforementioned application to derive the corresponding sections of the implant (Figure 77b). However, to ensure the suitability of the implant for insertion into the cavity formed after the osteotomy, the guidelines of (302) are followed. These guidelines recommend that the section of the implant is defined as the intersection of the fitting curve with the curves of the successive projections, i.e. the curve from each plane is projected onto the next. The final shape of the hip stem is achieved by interpolating these curves.

In addition, the design of the receiving taper and the implant neck is aimed at preserving the patient's physiological range of motion. This is achieved by quantifying anatomical parameters such as neck-shaft angle, anteversion and offset. While a full femoral reconstruction is normally required to assess these parameters, the methodology outlined in (302) allows their determination using the proximal femoral reconstruction and the elliptical fitting application. A plane is created approximately at the centre of the femoral head and a circumference of 12 mm in diameter is drawn. A second plane with a circumference of 14 mm is drawn at a distance of 20 mm. The interpolation of these circumferences formed the 12/14 model receiving taper (Figure 77c), which is commonly used in European femoral stems (371).

The stem and taper are then interpolated to construct the implant neck, and the sharp edges of the implant are rounded to reduce the risk of tissue damage (Figure 77c). The entire design process is performed by importing the cortical and trabecular bone reconstructions into NX 2206.

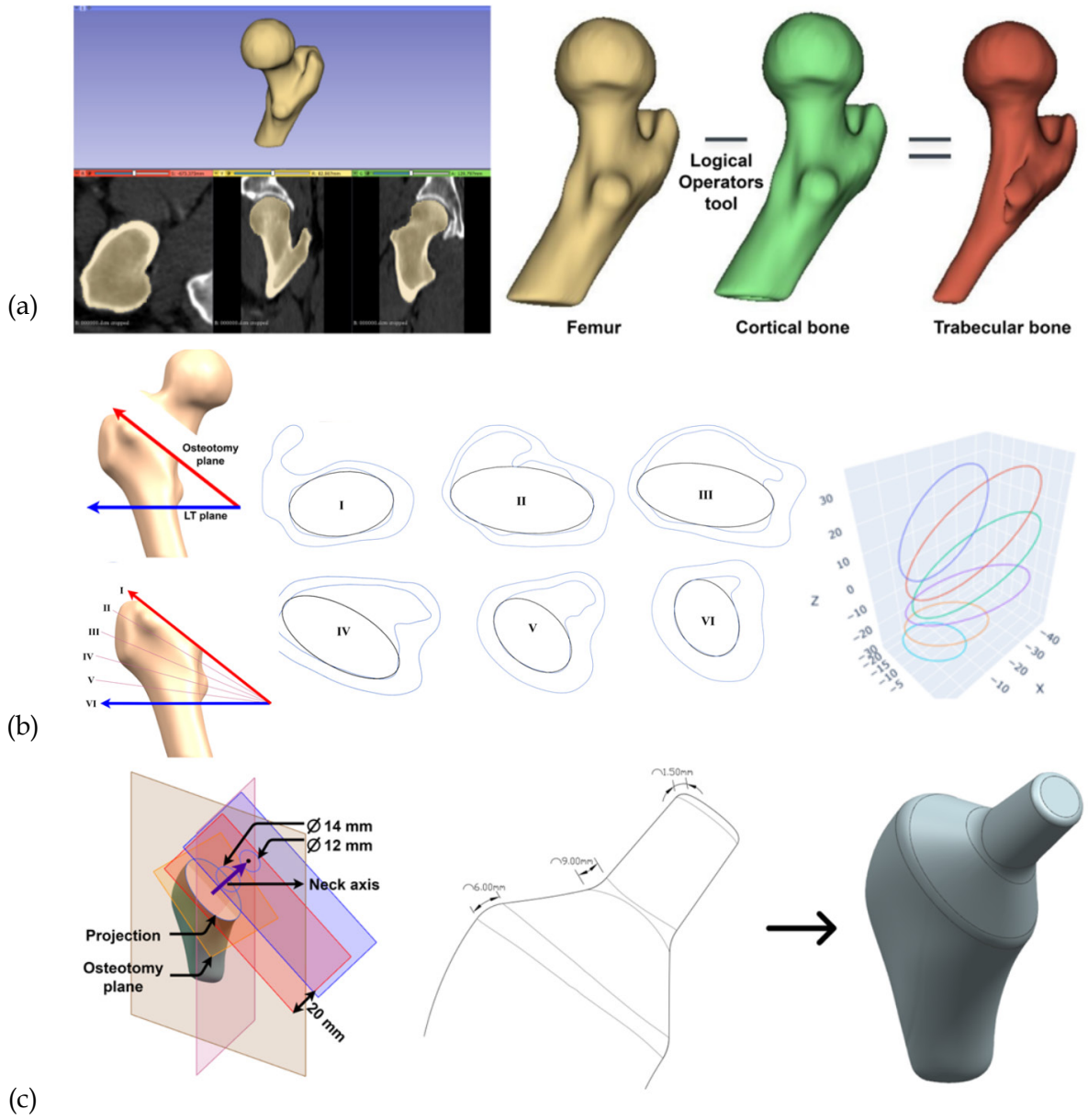


Figure 77: (a) Segmentation of the right femur using 3D Slicer®. (b) Femoral cavity analysis applying elliptical fitting application. (c) Neck and receiving taper design.

8.2.2. Finite-element model

One of the main challenges in conventional hip implant design is the stress/strain shielding phenomenon, which results in increased bone growth in the proximal region and reduced

bone mass in the distal region. While short hip implants mitigate this effect, the high stiffness of their material perpetuates the problem. Consequently, the modern approach focuses on reducing stiffness through topological optimisation of the implant structure, effectively minimising shielding and improving both the mechanical and biological stability.

As mentioned before, finite-element modelling (FEM) serves as a key tool for *in silico* evaluation of the mechanobiological performance of implant designs, using computed tomography data to exploit the correlation between the Hounsfield unit and the mechanical properties of cortical and trabecular bone. In addition, the use of an appropriate failure theory is essential to assess the mechanical integrity of the implant, which is crucial for optimisation to avoid solutions that may lead to premature implant failure due to excessively low stiffness. Following the methodology outlined in (302), this study quantifies the mechanical properties of trabecular and cortical bone using the average Hounsfield unit and presents the results in Table 17. The chosen implant material, LithaCon ATZ 980 - an alumina toughened zirconia supplied by Lithoz GmbH - has a Young's modulus of 220 GPa, compressive strength of 2200 MPa and Poisson's ratio of 0.27.

The FEA is performed using NX together with the Nastran solver, generating two different models: an intact femur and a femur with an implant. The intact femur model includes only the cortical and trabecular bones, while the implanted model includes the osteotomised bones and the tailored stem. Once the material properties had been defined, the models were subjected to ISO loading conditions, a widely accepted standard for evaluating hip implants (372). This standard is considered more effective than physiological loading because it simulates an axial load applied to the femoral neck, a region prone to fracture (302, 373). An axial load of -2300 N is applied to either the acetabular region or the flat surface of the implant, fixing the bases of both the cortical and trabecular bone (Figure 78). This simulation strategy allows a direct examination of the stress/strain shield and a thorough evaluation of the implant mechanical behaviour.

A convergence analysis using p-method and h-method, with an admissible error of 2%, is performed to select the optimum element size and type. This ensured accuracy of results and computational efficiency, with cortical and trabecular bone meshed using 0.8 mm elements and the stem meshed using 0.2 mm elements, all employing the CTETRA 4 element. As bone remodelling occurs predominantly during osseointegration (374), mesh integration is achieved using the surface-to-surface bonding technique.

Properties	Cortical bone	Trabecular bone
HU (-)	1458	779
E_x (MPa)	9140.76	5363.09
E_y (MPa)		
E_z (MPa)	15234.61	
G_{xy} (MPa)	3264.56	2062.73
G_{yz} (MPa)	3808.65	
G_{zx} (MPa)		
v_{xy} (MPa)	0.4	0.3
v_{yz} (MPa)	0.25	
v_{zx} (MPa)		

Table 17: Mechanical properties of the cortical and trabecular bone.

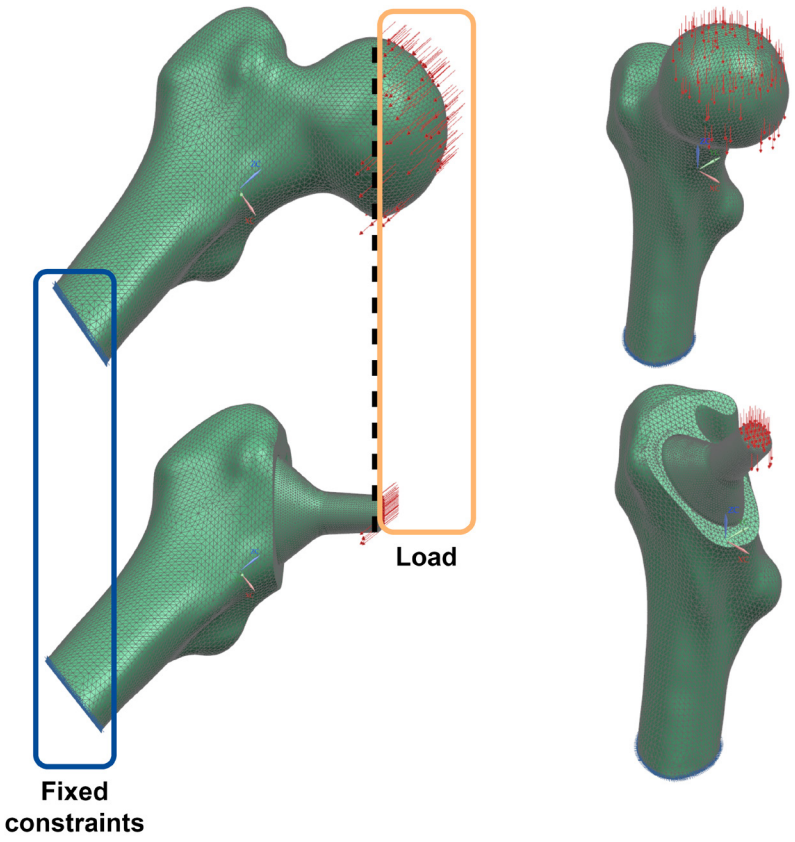


Figure 78: Boundary conditions.

8.2.3. Topology optimisation

The primary goal of optimisation, particularly for hip implants, is to achieve structural lightweighting while maintaining critical mechanical functionalities. This reduction in structural weight leads to a reduction in stiffness, which in turn should minimise stress shielding effects by bringing the modulus of elasticity of the implant closer to that of natural bone. However, the assessment of material strength remains critical, particularly for ceramics, which are known to have lower tensile strength compared to their compressive resistance. In addition, the constraints imposed by the manufacturing process must also be considered.

The process of topological optimisation is aided by nTopology, which can address both geometric optimisation and optimisation of the mechanical response of the implant. This is achieved by applying the field-driven design methodology provided by the software. This innovative approach allows any physical parameter, including geometry, simulation results, experimental data and more, to be defined as a field. The use of this methodology enables the intricate creation of complex structures with precise control over porosity throughout the design, ensuring an optimal balance between structural integrity and biological compatibility.

Geometric-based method

The optimisation of the implant geometry (Figure 79a) is based on the distance field analysis, which calculates the shortest distance from any point on the implant to its outer surface. For better understanding, the generation of a cross-section of the implant allows the visualization of isocurves, marking points that are equidistant from the surface (see Figure 79b). This method makes it feasible to associate distance measurements with specific thicknesses in desired areas, allowing precise control of the thickness of the porous structure within the optimized implant. Such meticulous control is essential for design for additive manufacturing (DFAM) and is particularly critical in the LCM process because it involves several key stages, including the heat treatment of the green body - the state of the material after photopolymerization with ceramic particles - where the management of maximum and minimum thicknesses is crucial.

The cellular structure chosen for optimisation is the gyroid, a natured-inspired triply periodic minimal surface (TPMS), characterised by smoothness, continuity and zero mean curvature throughout (375). Unlike strut-based topologies, the gyroid surface not only minimises stress concentration at local points, but also excels as a heat exchanger (376) and biomimetic scaffold (377). This provides significant structural and mechanical advantages over conventional designs, increasing design and manufacturing flexibility, such as improved oxygen and nutrient transport to bone cells (375, 377). Meanwhile, sheet-based TPMS structures mimic natural bone architecture with remarkable biocompatibility, comparisons between sheet-based and strut-based gyroids show that the former retains isotropic behaviour and superior energy absorption capacity, even when produced by additive manufacturing processes (378). Therefore, the sheet-based gyroid is preferred in the optimisation process due to these attributes.

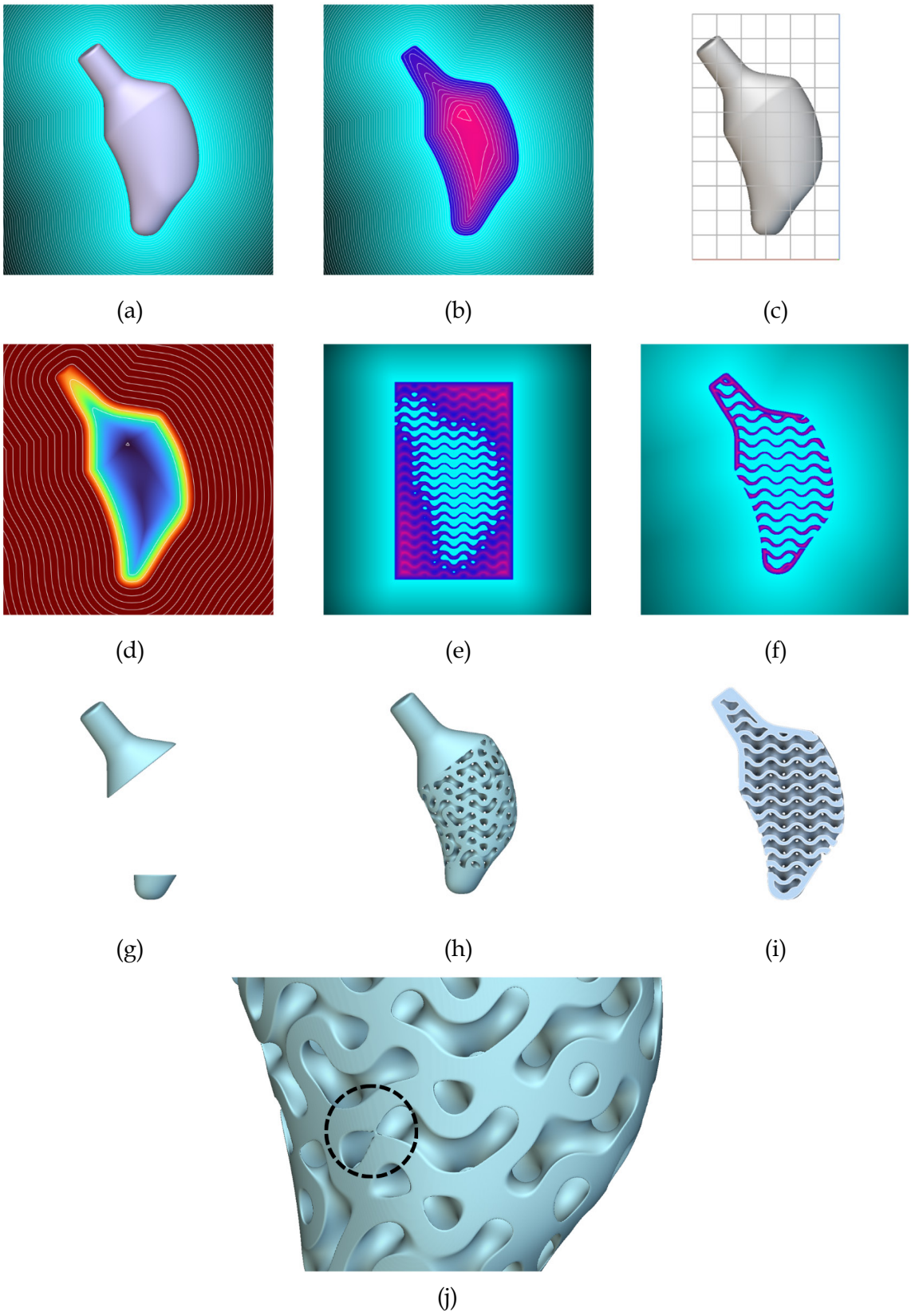


Figure 79: (a) Implant to be optimized. (b) Distance field isocurves. (c) Grip of unit cells. (d) Thickness map. (e) Lattice with a porosity gradient based on distance field. (f) Section view of the implant obtained by Boolean intersection with the lattice. (g) Two solid reinforcement areas: the receiving

taper and the base of the stem. (h) Optimized implant and (i) mediolateral section. (j) Quality control of the optimized solid.

To create the grid, a map of unit cells is developed to encapsulate the implant (Figure 79c), where each cell measures 10 x 10 x 10 mm^3 and its thickness varies according to the distance field. LCM technology indicates that the thickness of the implant regions should not exceed 8 mm, and this restriction is used to determine the thickness of each cell based on the distance field values detailed in Table 18. Linear interpolation is used for intermediate field values. Figure 78d shows the thickness map for the implant-integrated grid, where blue indicates the minimum thickness and red indicates the maximum one, ensuring a gradual thickness transition from the outer to the inner surface. With these specifications, a grid of variable thickness is achieved (Figure 79e). The final shape of the implant is obtained by the Boolean operation of intersection between the solid implant and the grid (Figure 79f), thus achieving the desired material reduction with a defined thickness gradient.

Distance field (mm)	Thickness (mm)
0	3.0
-3.8	2.0
-7.6	1.5
-11.35	1.0

Table 18: Relationship between distance field values and unit cell thickness. Values not shown in the table are obtained by linear interpolation.

In addition, to optimize the mechanical behaviour of the implant and improve its implantability by the orthopaedic surgeon, two solid reinforcement zones of 2 mm thickness are integrated in the receiving taper and at the base of the stem (Figure 79g), which are connected to the grid structure by a Boolean addition operation (Figure 79h and i). It is essential to evaluate the contours of the optimized solid in order to avoid printing problems caused by excessively thin thicknesses (Figure 79j). In the final stage, when preparing the stl model for printing, a minimum element size is selected to match the smallest manufacturable thickness, in this case 400 µm, to ensure the structural integrity of the implant. This security threshold is set as it represents 10 times the minimum print size, which corresponds to the pixel section of the printer that is described in the following section.

Stress-based method

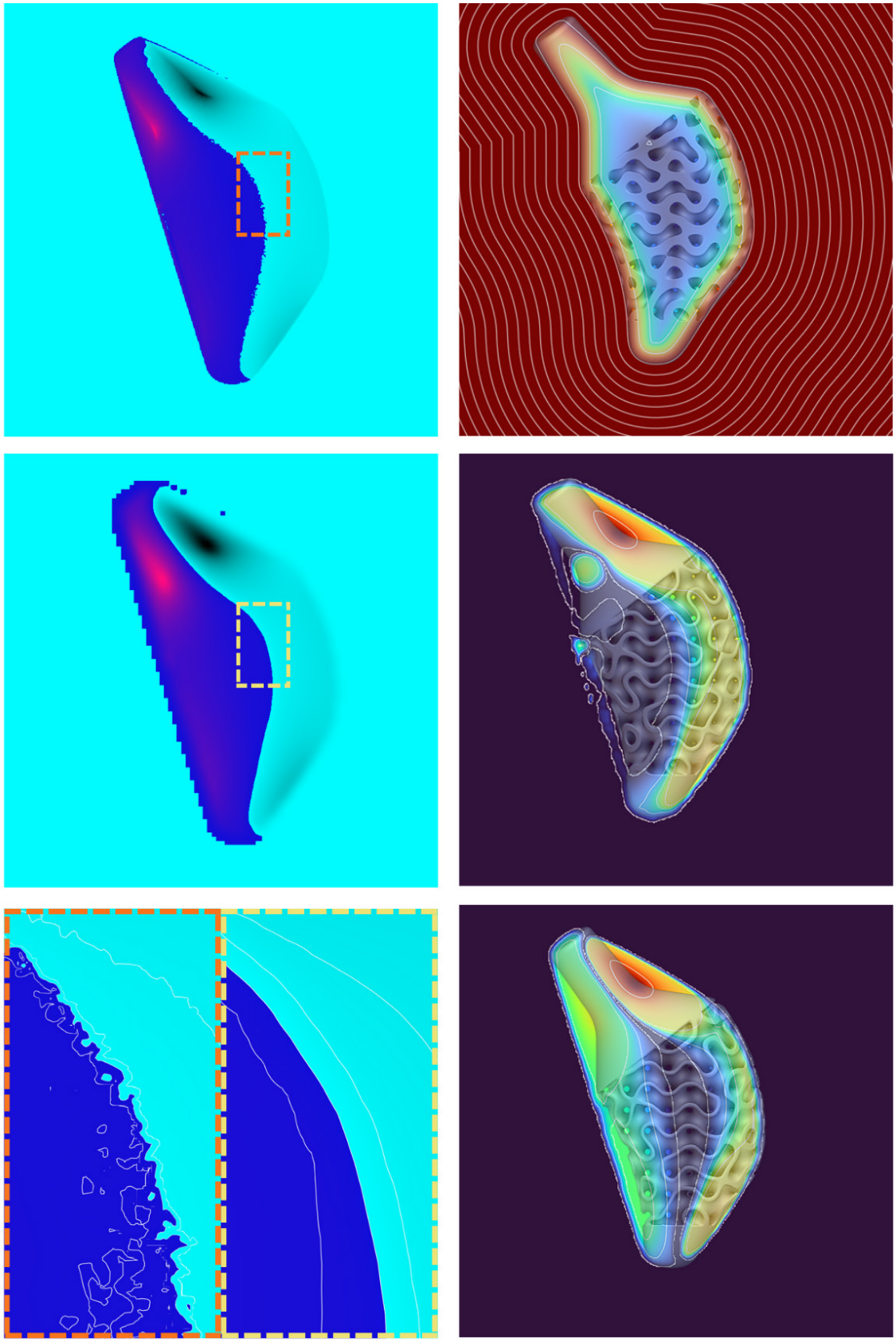
The mechanical optimisation of orthopaedic implants is a comprehensive process based on the careful analysis of the results of computer simulations, as described in the finite-element modelling section. This analysis focuses on the interaction between the implant and the osteotomised cortical and trabecular bone. Ceramic materials, characterised by their fragility and limited tensile strength, require rigorous evaluation to assess their failure potential. To this end, the Maximum Principal Stress (MPS) criterion is used to identify the critical junctions susceptible to failure under tensile forces (379). In addition, Worst Principal Stress (WPS)

analysis is incorporated to achieve a differentiated optimisation that considers the intrinsic differences between tensile and compressive zones. This method involves the calculation of the maximum absolute values of principal stresses, while preserving their original sign, allowing a clear distinction to be made between compressive and tensile stresses. This distinction is essential for the implant design, as it allows the use of variable thicknesses to meet the specific requirements of each zone. As a result, areas subject to tension are designed with greater thickness than areas subject to compression. This approach culminates in the development of two implant prototypes: one optimized according to the MPS criterion and the other according to the WPS criterion (Figure 80b). A key challenge in this process is the treatment of distortions at the boundary between positive and negative stress values (Figure 80a), a phenomenon attributed to the triangulation process inherent in finite-element meshing. Such distortions can lead to unwanted oscillations in the thickness of the optimized implant. To overcome this problem, the stress fields are refined by smoothing, followed by an exhaustive analysis of the revised maximum, minimum and 25th, 50th and 75th percentile values across both MPS and WPS. This meticulous analysis is then integrated with the specified thicknesses to further optimize the design of the implant (see Table 19).

MPS value (MPa)	**WPS value (MPa)**	**Thickness (mm)**
79.97	79.97	4.0
6.50	7.96	3.0
3.26	5.78	2.0
0.70	3.61	1.5
0	0	1.5
-0.13	-3.63	1.5
-0.64	-9.20	2.0
-1.64	-17.34	2.5
-7.50	-104.65	3.5

Table 19: Relationship between MPS and WPS field and unit cell thickness. Values not shown in the table are obtained by linear interpolation.

The final stage, similar to geometric optimisation, is to design an implant with a lattice structure. However, in this case, the thickness of both the shell of the receiving taper and the distal part of the stem are meticulously adjusted based on the stress analysis, with variations ranging from 2 to 1 mm. This comprehensive strategy ensures that the implants are not only mechanically optimized, but also tailored to specific biomechanical requirements based on extensive simulation data. This holistic approach underlines the central role of advanced simulation techniques in the design and optimisation of orthopaedic implants, ensuring their efficacy and patient-specific adaptability.



(a) (b)

Figure 80: (a) Original and smoothed stress field. (b) Optimized implants: based on the distance map and using the MPS and WPS criteria with their respective fields.

8.3. Manufacturing process and results

8.3.1. Mechanobiological analysis

Topological optimisation of custom hip implants is essential to counteract the stress shielding problem that arises because implants are much stiffer than bone, typically 7 to 9 times stiffer. Lightweighting the implant can reduce its stiffness, but care must be taken not to compromise its mechanical strength, especially in ceramic implants which are more susceptible to tensile stress. It is therefore essential to assess the bone response (mechanobiological) and the performance of the implant before deciding on the final design to be materialised with LCM.

Stress shielding can lead to unwanted iatrogenic bone remodelling. Osteocytes sense changes in mechanical loading and respond by releasing chemical signals that can lead to bone formation or resorption. If the mechanical stimulus is less than usual, bone mass is lost; if it is greater, new bone is formed, but this does not necessarily make the bone stronger and can weaken it. This can lead to problems such as aseptic loosening, periprosthetic fractures and the need for revision surgery. However, there is a range of stimuli, known as the 'dead zone', where changes in bone density after implantation are negligible. Implant design aims to stay within this threshold to avoid negative effects on the bone.

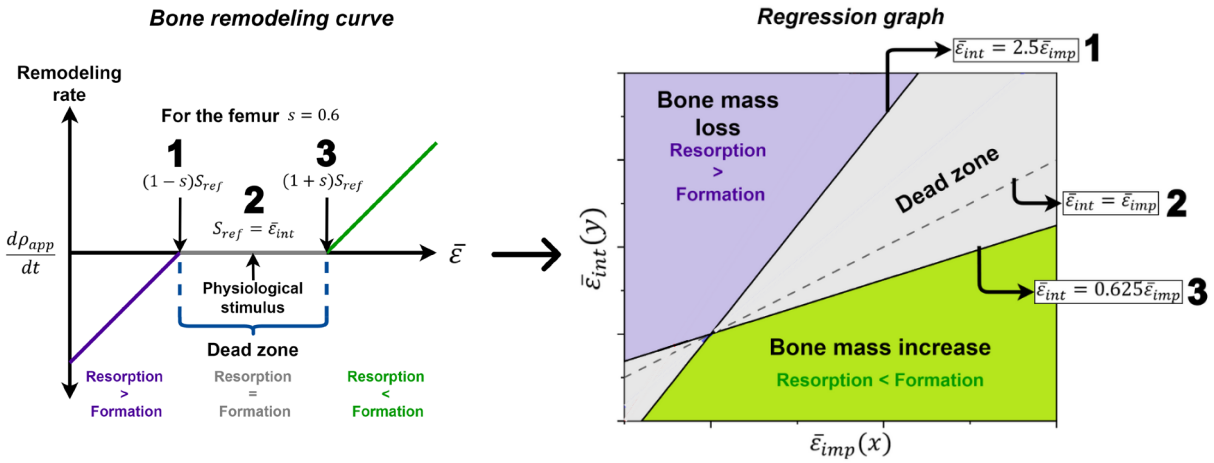
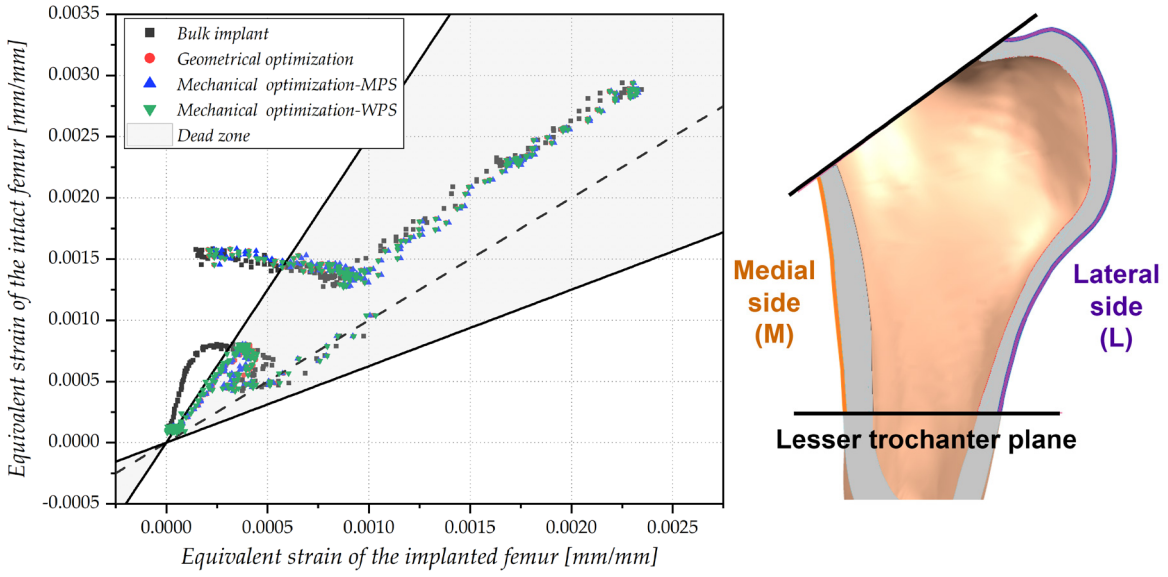


Figure 81: Remodelling curve and regression graph.

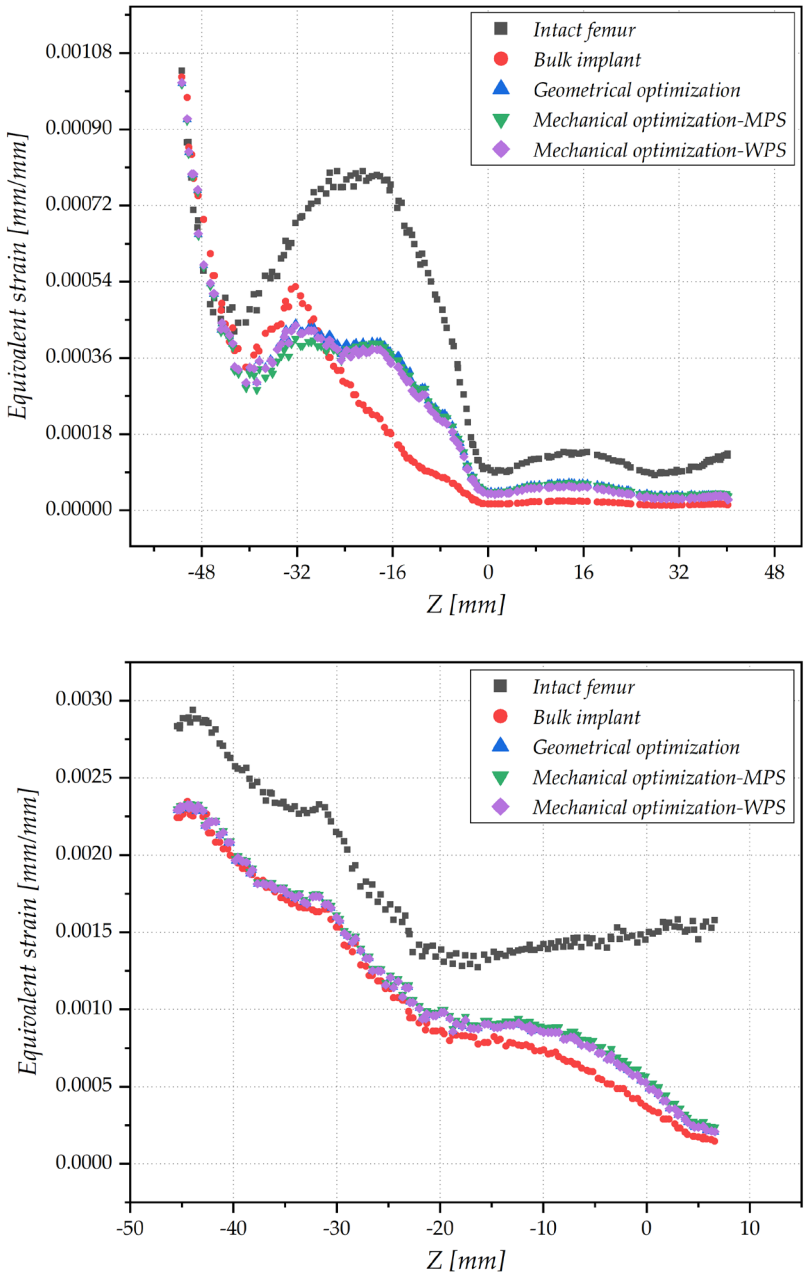
Mikic and Carter (380) demonstrated that equivalent strain is an effective mechanical indicator for modelling bone remodelling by summarising the multi-axial state of strains obtained from both in vivo and in vitro studies using strain gauges. This measure is expressed mathematically as the norm of the strain tensor, resulting in a positive scalar value that is easy to interpret and does not vary with direction. In addition, research by Turner et al. (381) in clinical trials with hip replacement patients showed that variations of up to 40% in equivalent strain can stabilize the implant and reduce bone remodelling. Solórzano-Requejo et al. (302) proposed a simple method to assess the biomechanical performance of hip implants by plotting the information from the bone remodelling curve on a Cartesian graph, where the X-

axis represents the equivalent deformation after implantation and the Y-axis represents the physiological equivalent deformation, thus facilitating the analysis of the effect of optimisation on induced bone remodelling (Figure 81).

This approach allows the effect of optimisation on iatrogenic bone remodelling to be evaluated through *in silico* studies based on the finite-element method with different optimised implant designs. The specific area of interest is the latero-medial section (Figure 82a), which is particularly sensitive to bone remodelling due to the loss of the femoral neck, which transfers the load from the acetabulum directly to the femur. The results indicate that a non-optimized implant could cause a significant loss of bone mass in the femur, whereas optimisation significantly improves implant performance by placing most of the femur in the dead zone (Figure 82a). However, it is crucial to examine the medial and lateral regions separately (Figure 82b). The graphs show that in the medial region the optimisation improves the behaviour of the implant, bringing it closer to the natural physiological stimulus of the intact femur, but in the lateral region this behaviour deviates from a certain point due to the absence of the femoral neck. This phenomenon indicates that the remodelling in this area is a direct result of the osteotomy, and it is suggested that changing the implant design to a stemless implant could correct this problem by providing adequate loading to the affected area.



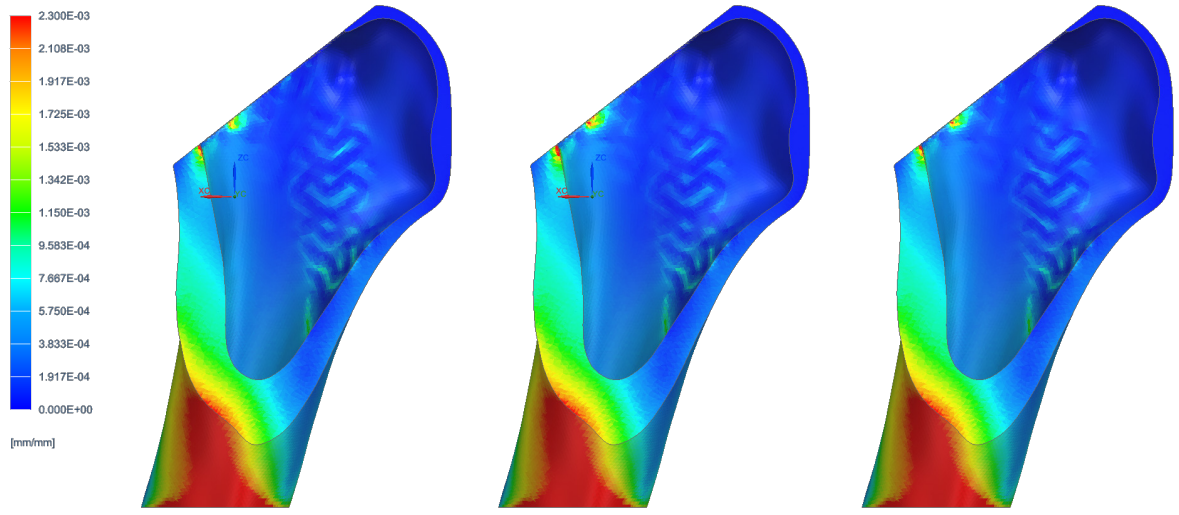
(a)



(b)

Figure 82: (a) Medial and lateral side of the proximal femur assessed in the mechanobiological analysis and regression graph of the latero-medial section. Scatter plots (b) of equivalent strain on medial (left) and lateral (right) sides.

It is concluded that, from a mechanobiological point of view, comparing the response of the cortical bone (Figure 83), the three implants studied behave very similarly, as they all have an equivalent modulus of elasticity due to the same 50% porosity. However, their mechanical performance varies depending on the distribution of materials along the implant. Further research has shown that gyroid-based scaffolds promote greater bone formation than conventional strut-based scaffolds due to their high permeability and curvature profile (377). Therefore, incorporating this mesh into a solid hip prosthesis design could significantly improve osseointegration and the long-term success of the device.



(a) (b) (c)

Figure 83: Equivalent strain field of cortical bone implanted with optimized prostheses based on (a) distance, (b) MPS and (c) WPS fields.

8.3.2. Mechanical performance of the optimized implants

Mechanobiological analysis makes it possible to evaluate the mechanical performance and predict the failure probability of the three optimisations, allowing the best one to be selected. Weilbull's theory (382), based on the concept of the weakest link, is used to mathematically describe the strength distribution of the LithaCon ATZ 980 material. This theory relates the mechanical load to the probability of failure by means of two parameters: the strength at which the probability of failure is 63.2% (σ_0), and the Weibull modulus (m), which indicates the homogeneity of the distribution of defects in the material.

By analysing the Ultimate Tensile Strength (UTS) distribution obtained from three-point bending tests of 28 specimens, the values of strength and Weibull modulus are set at 689 MPa and 15, respectively. Substituting σ for the maximum value of the WPS in equation (4), which coincides with the maximum value of the MPS, gives the values shown in Table 20: Minimum and maximum WPS values and failure probability of bulk and optimized implants.. When comparing the failure probabilities between the optimized implants, it is observed that the WPS optimized implant has the lowest failure probability. This is because this metric incorporates the principal compression values, which are often ignored in other optimisation methods. The use of the gyroid structure as the unit cell for the lattice, which is characterised by a uniform stress distribution, justifies the inclusion of a mechanical stimulus that includes both tension and compression (383). This allows the designer to create a structure with thickness gradient adapted to the specific needs of each zone. Therefore, in the process of topological optimisation of any implant, it is crucial to choose the mechanical stimulus that best matches the properties of the selected unit cell, thus ensuring that the final implant exhibits homogeneous behaviour.

$$F = 1 - exp\left\{-\left(\sigma/\sigma_0\right)^m\right\} \quad (4)$$

	Bulk implant	**Geometrical optimisation**	**MPS optimisation**	**WPS optimisation**
Minimum WPS (MPa)	-154.45	-341.35	-477.72	-334.26
Maximum WPS (MPa)	118.49	205.08	238.11	172.48
Failure probability (-)	3.4E-12	1.28E-8	1.2E-7	9.5E-10

Table 20: Minimum and maximum WPS values and failure probability of bulk and optimized implants.

The inspection of the implants' WPS field (Figure 84a) reveals the need for optimisation. In the bulk stem, areas that do not contribute mechanically are identified, and in the geometrically optimized one there are certain external thicknesses that are not subjected to loading. This suggests that the material in these areas can be redistributed to improve mechanical performance, following the optimisation logic based on stress field analysis. Additionally, the field indicates that the gyroid structure distributes the stresses more efficiently, balancing the tensile and compressive areas within it, that justifies the inclusion of a mechanical stimulus that includes both tension and compression (383). This allows the designer to create a structure with thickness gradient adapted to the specific needs of each zone. Therefore, in the process of topological optimisation of any implant, it is crucial to choose the mechanical stimulus that best matches the properties of the selected unit cell, thus ensuring that the final implant exhibits homogeneous behaviour.

When comparing the optimized implants using stress field, it is observed that the WPS based structure achieves a significant reduction in the areas under overload (Figure 84d). The analysis of the maximum and minimum WPS values shows that the lowest values correspond to the optimisation performed with the WPS stress criterion and compared to the bulk implant, there was an increment in stress of 45.6% in tension and 116.4% in compression. This approach highlights how the most effective alternative for the optimisation of personalized hip implants is to use the WPS as a mechanical stimulus, ensuring a more balanced stress distribution and improving the functionality and durability of the implant.

Despite this increase, the compressive stress in the optimized implant remains well below the critical limit (2200 MPa), eliminating any concern of failure for this reason. It is important to note that this analysis is based on ISO load, which is designed to simulate extreme failure conditions in hip implants. However, under normal conditions, physiological loads on the femur are triaxial and mechanically less demanding. In addition, muscle action, from the

iliotibial band and the vastus lateralis-gluteus medius complex, compensates for lateral stress. Therefore, it is expected that the implant will perform adequately under physiological conditions without problems due to the applied forces.

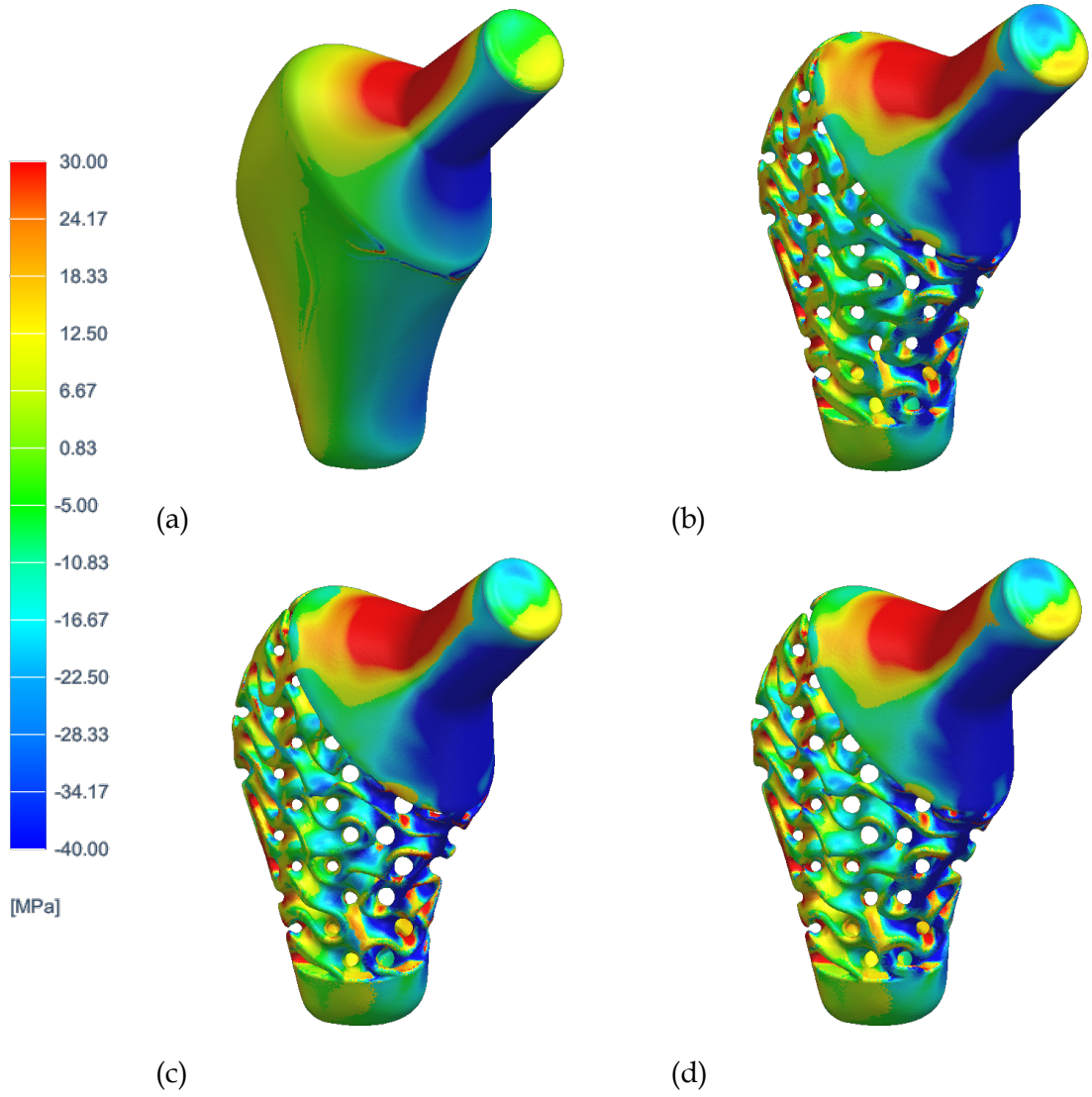


Figure 84: WPS field of the (a) bulk prosthesis and of the optimised prostheses based on the (b) distance, (c) MPS and (d) WPS fields.

8.3.3. LCM manufacturing process and fabrication of the optimal design

Due to the precision required for the optimized implant, a custom medical device, the chosen manufacturing process is LCM. This process utilizes layer-by-layer curing of a photosensitive ceramic suspension. The photopolymer in this process acts as a binder between the ceramic particles, enabling the creation of the optimized implant with fewer supports compared to powder metal melting. The implant is initially produced as a green body, which must undergo further processing such as debinding and sintering to achieve a higher relative density. These additional steps involve debinding, where the binder undergoes thermal decomposition, followed by sintering to form a compact ceramic part.

For the green body fabrication, LithaCon ATZ 980 material is used, supplied by Lithoz GmbH. This material consists of 20% alumina and 80% zirconia, resulting in a composite with superior fracture and abrasion resistance, hardness, and excellent biocompatibility. The manufacturing process utilizes the CeraFab S65 Medical 3D printer (Lithoz GmbH, Austria).

The LCM technology is accessible to the market through Lithoz GmbH with the 3D printing system CeraFab. Three-dimensional structures are virtually dissected into layers by the CeraFab-DP software. The component manufacturing is then carried out through selective exposure of these layers and the resulting photopolymerization in the slurry.

The construction of the printer (see Figure 85) includes a rotating and tilting tray with a translucent bottom. This tray is filled with the photosensitive ceramic suspension. The application of the thin suspension layer is done using a doctor blade and the rotational movement of the tray. The light source is located beneath the tray, and the radiation from the light source is directed onto the bottom of the tray through optics, a DMD chip (digital micromirror device). The build platform is positioned above the tray and moves step by step along the Z-axis during the building process at distances corresponding to the layer thickness—typically between 10 and 100 µm. The build platform has dimensions of 102 x 64 x 320 mm^3, and printing can be done with a resolution of 40 µm along the XY plane.

The mechanobiological analysis and the evaluation of the mechanical performance of the implants show that optimisation based on the WPS criterion is the most favourable alternative. Therefore, it is decided to produce the implant using the techniques described in the manufacturing process section. Due to the shrinkage that the material undergoes during the heat treatment after manufacturing, an adjustment is made to the dimensions of the original part, scaling it by 1.24 and 1.27 in the XY and YZ planes respectively.

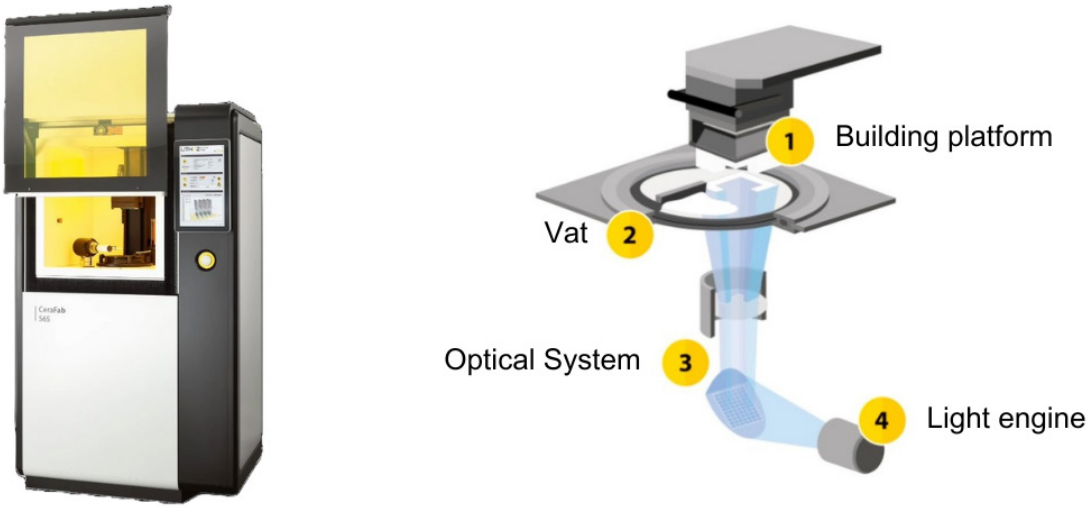


Figure 85: Schematic diagram of the Lithography-based Ceramic Manufacturing (384). Draft courtesy of Lithoz GmbH.

The chosen manufacturing technique requires the implementation of supports to hold the structure on the printing platform (Figure 86a). Although this could be a challenge, the presence of reinforced areas on the receiving taper and the base of the stem facilitates the placement of the supports. The receiving taper is preferred to minimize the need for supports as it is the smallest part and serves as the base for the growth of the entire structure. In addition, complementary supports are designed with a conical end to facilitate their removal without damaging the material, thus preventing warping. The orientation of the part, aligned with the femoral shaft, distributes the load effectively, reducing the risk of catastrophic failure.

Once the green body is obtained, it is post-processed by debinding and sintering, as described in Table 21, to achieve a high relative density implant, close to 99%. Figure 86a shows the green body, where it is possible to observe the tessellation of the stl file used to manufacture the part. Due to the geometric complexity of the part, the initial stl file contained an excessive number of triangles, which made it difficult to process. Consequently, it was decided to simplify the tessellation by reducing the density of the triangles to make the file lighter and easier to manipulate. The final piece, after post-processing, shows how the sintering process significantly reduces the visual effect of the tessellation, as shown in Figure 86b.

A comparison between the theoretical weight of the implant, estimated at 86g, and the actual weight of 88g shows a minimal discrepancy of 2%. To validate the implant, a three-dimensional model of the bone, both cortical and trabecular, was fabricated from the segmented data using polymer resin. Figure 86c shows the assembly, confirming correct implantability and accurate implant dimensions. This process verified that the stem met the design specifications and had no post-processing cracking problems. This success is attributed to the thermal properties of the Gyroid structure, which favours efficient heat dissipation without internal stresses and, thanks to its high exposed surface, facilitates the release of CO_2 resulting from the decomposition of the polymeric binder of the ceramic particles.

To analyse the internal structure of the implant, a latero-medial cut was made in the stl file. This was manufactured using the process described above, with its flat surface positioned directly on the build platform. This method confirmed that the optimisation achieved closely replicated the porosity distribution observed in the human femur, with thicker outer and inner walls, mimicking the cortical and trabecular regions (Figure 86b). This design facilitates the transport of oxygen and nutrients to the bone cells and promotes osseointegration. According to the authors, this implant is not only the largest structure manufactured with LCM technology, but also the first short hip stem produced with this innovative technique.

Heating time (h)	Heating time (hh:mm)	Heating rate (K/min)	Temperature (°C)	Dwell time (h)
0	0	0	30	0
1,50	01:30	0,50	75	2,00
0,50	00:30	0,50	90	2,17
1,96	01:57	0,17	110	2,33
2,08	02:05	0,08	120	5,83
6,67	06:40	0,10	160	10,50
2,08	02:05	0,16	180	7,00
4,17	04:10	0,16	220	7,00
8,33	08:20	0,16	300	7,00
2,08	02:05	0,20	325	2,00
8,75	08:45	0,20	430	6,00
1,00	00:59	1,17	500	0,00
1,00	00:59	1,67	600	0,00
6,49	06:29	1,67	1250	0,00
1,50	01:30	3,33	1550	2,00
-8,44	15:30	3,00	30,00	
			Total time	*110 h (4,6 days)*

Table 21: Debinding and sintering of LithaCon ATZ 980 at 1550 °C with a dwelling time of two hours.

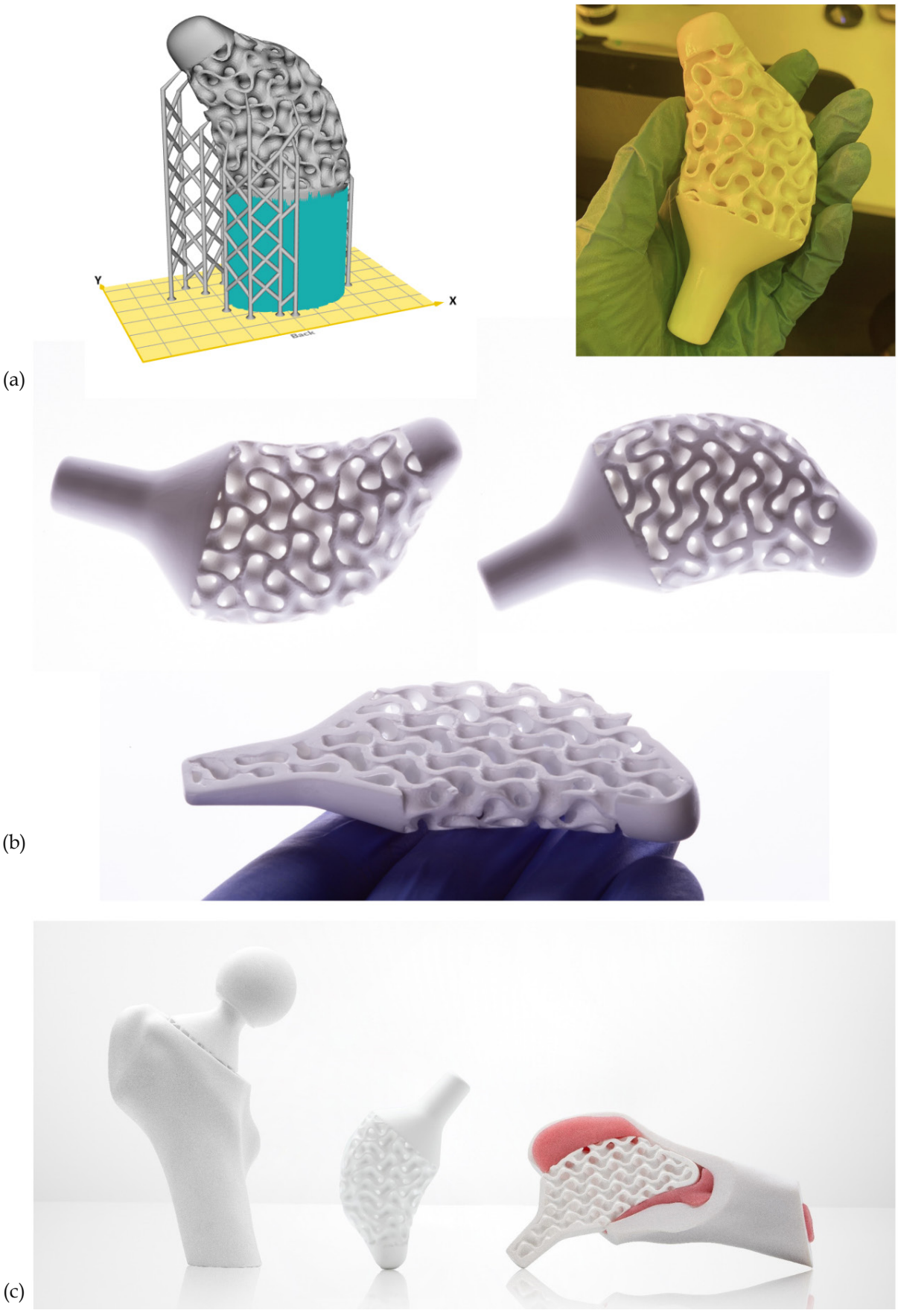


Figure 86: (a) Orientation of the hip prosthesis including bi-modal support structure (removed prior to sintering) and green body obtained from LCM. (b) Ceramic model of the optimized implant with the

distance and WPS fields and the mediolateral section of the WPS-based stem. (c) View of the post-processed implant assembled with a replica of the patient's cortical and trabecular bone. Pictures courtesy of Lithoz GmbH and 3Dtive S.L. Special thanks to Dr. Serkan Nohut, Eng. Altan Altun, Eng. Sebastian Geier, Eng. William Solórzano and Alvaro Troyano.

8.4. Conclusions and future proposals

From the point of view of design and topological optimisation, the choice of the gyroid as the unit cell in this work is due to the fact that it is a bio-inspired grid that manages to mimic the trabecular and cortical regions of human bone, through the variation in thicknesses thanks to the implemented porosity gradient. From the constructive point of view, as it is a TPMS cell, the spatial continuity of the gyroid when replicated minimises the need to place supports for its impression, being of special importance the analysis of the contours of the implant.

Regarding the biomechanical analysis, the optimisation process reduces the stiffness of the implant and consequently reduces the shielding, making it more similar to the desired physiological situation. However, due to the surgical procedure and the consequent loss of the femoral neck, the lateral part of the femur undergoes the most remodelling. This phenomenon is unavoidable as it is an intrinsic factor of the surgery. However, the optimised prototype is shown to mitigate iatrogenic remodelling compared to the solid implant.

Regarding the manufacturing process and the thermal post-treatment, the implementation of the gyroid in the lattice structure favours the heat transfer allowing the evacuation of the products originated as a consequence of the degradation of the polymeric matrix in the debinding stage, favouring especially the evacuation of CO_2 along the whole structure. During the sintering stage, it minimises the thermal stress caused by the deification of the ceramic, avoiding the appearance of cracks or fractures during the shrinkage of the piece.

Additionally, obtaining a porous geometry throughout its volume favours bone growth, mitigates the need for revision surgery and opens up new possibilities to improve its implantability through systems that contain drugs within the pores, avoiding infections after surgery that cause septic loosening.

9. Main conclusions and future research proposals

9.1. Main conclusions of the PhD thesis

During the PhD thesis development, in parallel to the three years of the INKplant project, the planned specific objectives have been achieved. Some challenges remain but at the same time several lines of action have progressed far beyond the initial expectations.

1. Multi-material, multi-scale and functionally graded design and manufacturing methods for achieving tissue engineering scaffolds combining ceramics for bony phases and polymers for chondral phases have been developed, tested and exemplified through several case studies linked to real medical problems with the ambition of promoting these approaches in the field of tissue engineering. Examples of application include: bone and cartilage scaffolds for in vitro studies, novel designs and materials combinations for meniscal reconstruction, plugs for osteochondral defects with chondral, subchondral and bony phases and bone prostheses.
2. New ways of engineering scaffolds and prostheses based on the use of digital materials, voxelated matter, conformal lattices and topology optimized structures and surfaces for improved biomimicry and advantageous cell-material interactions have been explored. This has led to unique combinations of metamaterials and metasurfaces as novel concepts for the tissue engineering field, validated through their application to the design of prostheses with controlled topology and topography and subsequent prototyping.
3. Rapid prototyping routes for concept screening have been established and their impact on creativity promotion in large-scale international projects has been tested. Proceeding by combining filament fused fabrication or digital light processed networks, soft molds and casted elastomers, interesting biomechanical transitions between soft and hard regions of scaffolds for complex tissular restorations have been demonstrated.
4. Several high-performance additive manufacturing technologies, including digital light processing, 5-axis multi-inkjet printing and lithography-based ceramic manufacturing, as a complement to the ones used for rapid prototyping, have been employed and explored for accomplishing large sized patient-matched scaffolding constructs with design-controlled microstructures and surface textures. Desings developed within the PhD thesis and international stays in materials and technology developers' sites have allowed for a methodical evaluation of printability, resolution and repeatability of complex-shaped bioinspired scaffolding structures and cell culture platforms.

5. Synergic computational modelling techniques, rapid prototyping resources and additive manufacturing technologies have been integrated and applied for developing prototypes of artificial constructs for repairing, reconstructing or replacing meniscal, osteochondral and bone defects. Selected models have been used within INKplant consortium, by several partners, for evaluating the resolution of materials and technologies, for mechanical testing to verify their biomechanical performance, for in vitro testing with cells linked to biocompatibility evaluations, and for ex vivo trials with surgeons aimed at usability evaluation.
6. A collection of prototyped demonstrators, designed for optimal additive manufacturing employing the materials and technologies developed within INKplant, has been obtained, manufactured from designs developed by the candidate derived from concepts discussed with materials scientists, technology developers, healthcare professionals, including surgeons, and experts from medical devices companies. Besides, the demonstrators have proved excellent communication resources, within the consortium and for interacting with end users, society and project officers and evaluators.
7. To the candidate's best knowledge, the most comprehensive libraries of tissue engineering scaffolds and surface textures for biomedical applications has been designed, documented and delivered to the public, as open-source concepts for medical devices with proper documentation and following FAIR data principles. These collections constitute very special contributions to open science in the field of tissue engineering.
8. Technology transfer has been fostered through different actions:
    - First, the candidate has supported open-innovation actions within INKplant, especially within a multinational intersectoral collaboration established among the University of Piura, Lithoz GmbH and UPM aimed at reinventing short stem hip prostheses. The computational modelling of a set of topology-optimized short stem hip prostheses, validated through novel simulation strategies and manufactured by lithography-based ceramic manufacturing, has led to extremely large sized ceramic components with controlled microstructures. These ceramic demonstrators have been showcased in remarkable events like Formnext, AM Ceramics and M3D+it. The keys of the design, optimisation and manufacturing processes have been described and submitted for publication.
    - Second, the obtained know-how and an alliance with Dental Troyano S.L. has derived into the foundation of 3Dtive, a company focused on supporting dental professionals with the implementation of computational modelling and additive manufacturing as part of their daily workflow for healthcare personalization.
9. Throughout the PhD thesis development, the candidate has taken part in several dissemination and communication actions, which have contributed to the visibility and

impact of the INKplant project, as well as supported the training of the candidate in several professional skills, beyond the purely scientific-technical ones. The international research stays performed in research (Profactor) and industrial (Lithoz) partners have been also a source of learning and cross-fertilization among academia and industry, which proves especially relevant in engineering PhD theses.

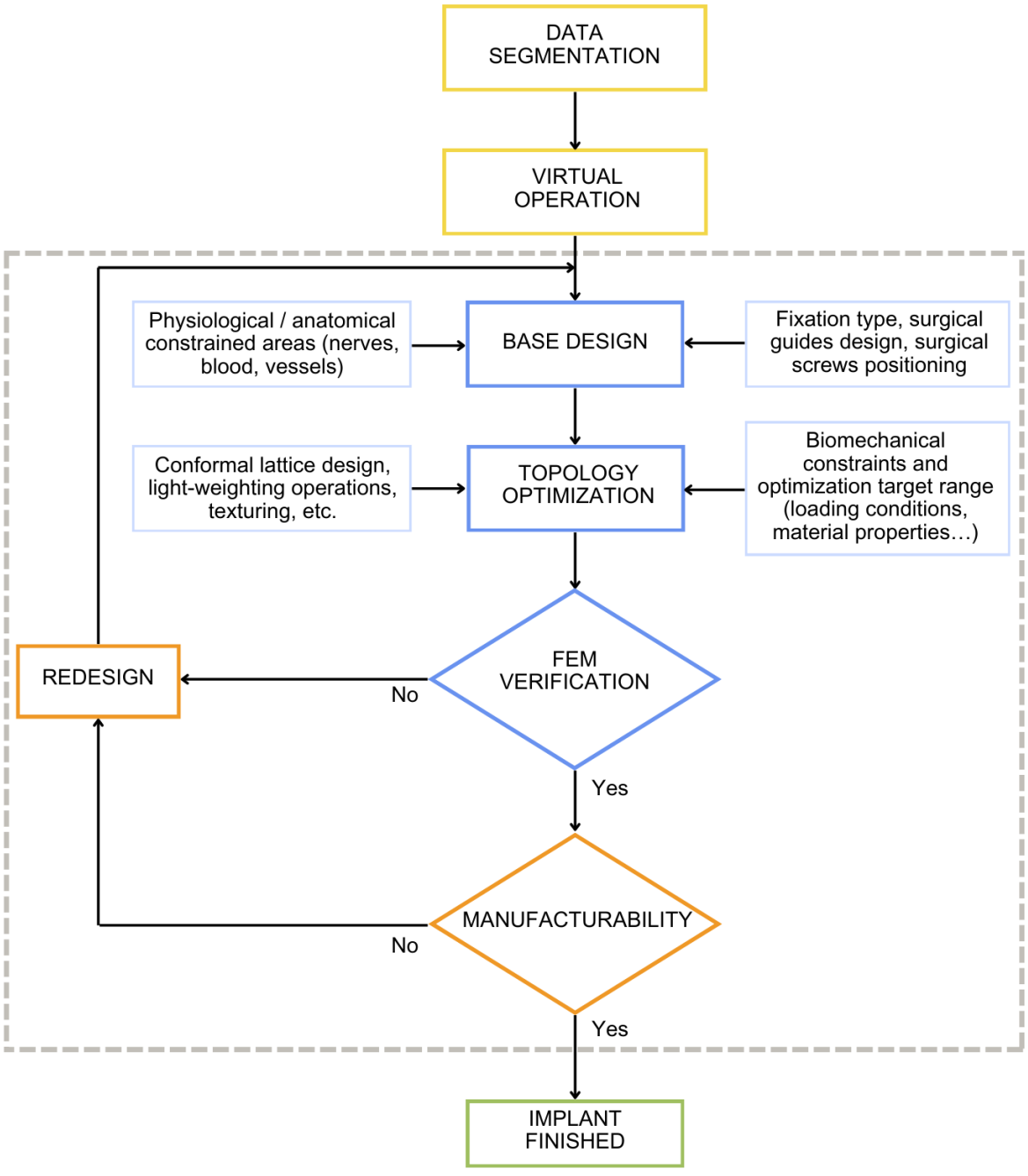
Through the consecution of the aforementioned specific objectives of the PhD thesis, **the general methodological objective has been also attained, leading to an innovative systematic approach for engineering knowledge-based multi-material, multi-scale, functionally graded and personalized tissue engineering scaffolds for repairing or reconstructing critical sized defects affecting bones, cartilage and articular joints.** The proposed development process is schematically presented in Figure 87.

Personally, the PhD has been an unprecedented learning process in my professional life. Despite coming from a previous European project as relevant as the Ubora project, which awakened in me an interest in research and synergy between the fields of medicine and engineering, the INKplant project has managed to put into value everything I have learned in recent years and reinforce the idea of the potential that this AMTs, when used properly, can have on people's quality of life. Proof of this is that in parallel to my doctoral studies I decided to take the step of becoming an entrepreneur, so I founded 3Dtive, which aims to develop biomedical solutions using additive manufacturing systems in the dental and medical sectors.

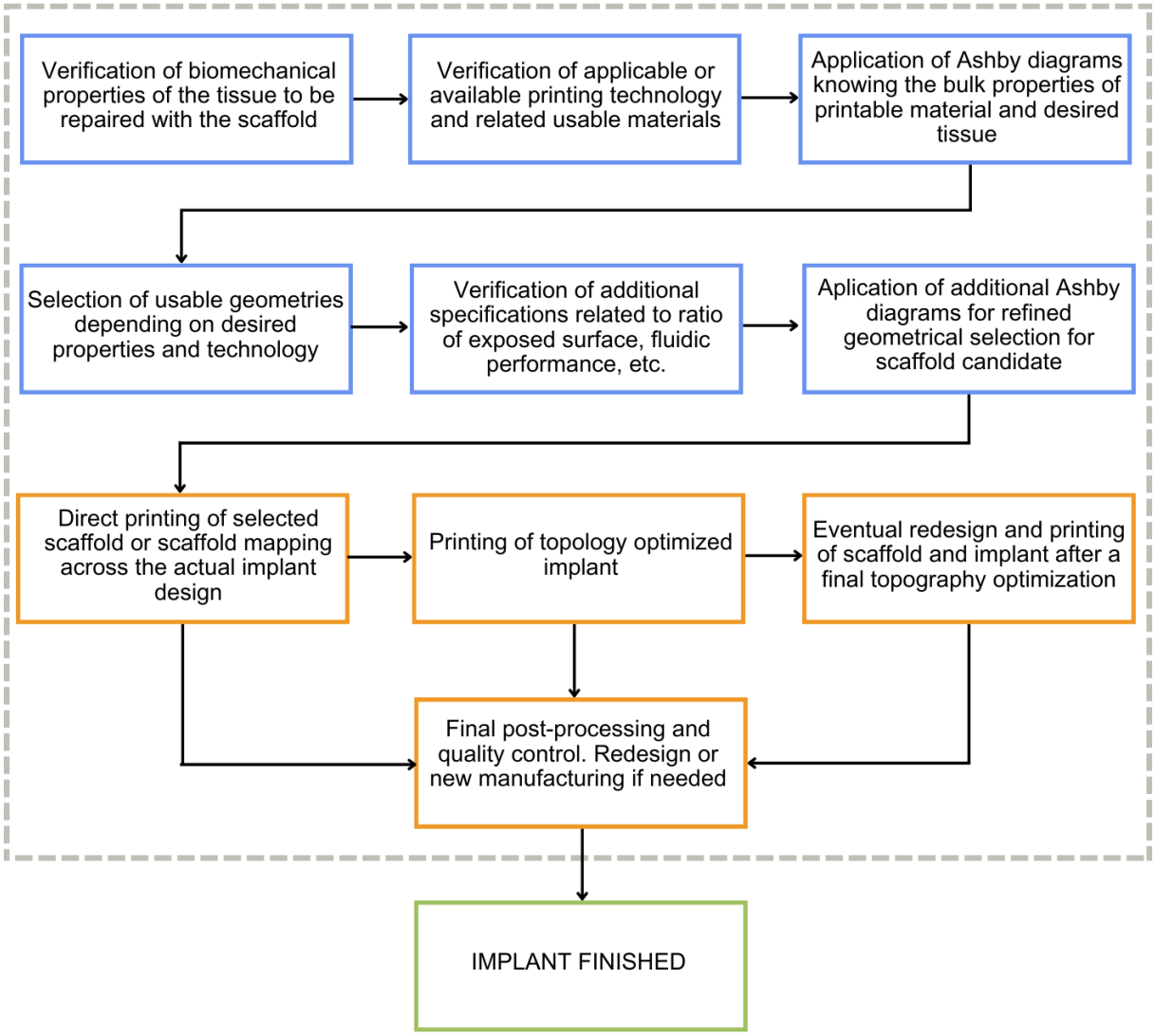
Being part of the EU INKplant project has allowed me to develop freely in achieving the objectives set out in my doctoral work. Having had access to such good professionals in medicine, materials development, additive technology and education has been of extreme professional benefit. Until now, in my career, I had mostly been exposed only to more accessible 3D printing technologies, such as fused filament fabrication systems or stereolithography equipment. I also focused my bachelor and master thesis on the design and rapid prototyping of splints and orthoses, mostly extracorporeal devices. It is understood that, in terms of materials, until I joined INKplant I had mainly worked with polymers and resins. For this reason, for an engineer with a passion for AMTs, having had the possibility of getting access to such cutting-edge systems and see what I have been able to chieve, already fulfils all my personal objectives set at the beginning of this stage. Seeing first-hand how it is possible to replicate geometries and patterns present in our organism, with the instant benefit that this can have on the healthcare system, has made me realise the need for today's medicine to focus on the patient specific solutions, and to promote by all possible means the personalisation of diagnosis also in the field of implantology and the design of biomedical devices. Of course, this whole process involves an implicit development of new ways of design and optimisation, made possible by the emergence of new and increasingly specialised software tools.

Having been able to validate my design work in the manufacture of prototypes using multi-material inkjet systems, LCM and LDM technologies or the development of a 5-axis inkjet printer, are moments in my professional career that I will remember with deep affection and pride. Even more important has been the realisation that thanks to my training and the work and effort I have put in over the last few years, I can rise to the occasion. With all of the above, from a personal perspective, I would argue that one of the most evident conclusions of this

work is based on reaffirming that I am in the place I have to be, researching the topics I want to research, and learning every day from great professionals who, in my opinion, will mark the future of regenerative medicine through the development of materials and additive manufacturing technology systems.



(a)



(b)

Figure 87: Methodology based on reverse engineering for the fabrication of personalised implants or medical solutions to the patient. (a) Current methodology acquired and adapted from "Erik Kornfellner. Biomechanics, design and tests of multimaterials for additively manufactured implants. PhD Thesis. 2024. Medical University of Vienna". (b) Innovative design methodology developed in this PhD thesis for the fabrication of biomimetic tissue engineered scaffolds using a multi-scale, multi-material and multi-functional approach framed in the above context.

9.2. Proposed continuation lines

A PhD thesis should always open new research lines for a future dedicated to research and innovation, in this case in the crossroads of mechanical engineering, biomedical technologies and healthcare. The knowledge acquired has led to new research questions, unsolved challenges and a set of continuation lines for the short- and long-term, explained below. They deal with additional innovations in manufacturing technologies, design strategies for additive manufacturing and personalized medicine, novel materials and structures for medical devices and technology transfer to society.

Among these directions, in which the candidate has already started to work, it is important to highlight the following:

1) Multi-material ceramic printing for complex bone regeneration

During the three-month period of research stay performed in Lithoz, special designs of interwoven tissue engineering scaffolds combining two ceramic phases were prototyped and tested (Figure 88). Among the most interesting challenges to achieve these multi-ceramic constructs, it is necessary to highlight the fact that different ceramic slurries employed sinter at different temperatures and have differential contractions during the debinding and sintering processes that may cause failure in complex-shaped components. Further research linked to the simulation of the sintering process and the dynamics and interactions among these different ceramic materials of interwoven networks is required for optimal results, following preliminary simulations and studies performed by UPM in collaboration with Lithoz within the INKplant project. As can be seen in Figure 88a, thanks to the application of advanced simulations capable of predicting the different shrinkage rate of the ceramics, it is possible at the design stage to apply an offset operation as a correction that generates a certain gap between the trusses connections of the two lattices so that, after subjecting the green body to the thermal process, the final adjustment is as obtained.

From this idea, a collection of hydroxyapatite-printed cylindrical specimens was developed combining a fully dense outer ring with an inner lattice lattice to which a porosity gradient was applied in radial direction (Figure 89). The idea is to validate the possibility of generating biomimetic bone inserts capable of recreating the geometric porosity of trabecular and cortical bone anatomies. As can be seen in Figure 89b, there is a change in the shade of the hydroxyapatite from the fully dense outer zone to the porous inner zone. This phenomenon is due to the addition of porogens in the inner zone that are eliminated during the post heat treatment stage, a process developed by Lithoz GmbH that is of great scientific interest, as it opens up the possibility of combining a porosity obtained from the CAD design with a porosity obtained from the material's own microstructure, on a much smaller scale. Given that hydroxyapatite is considered a biodegradable material, these tools open up the possibility of developing methods to control the degradation rate of the implant much more precisely.

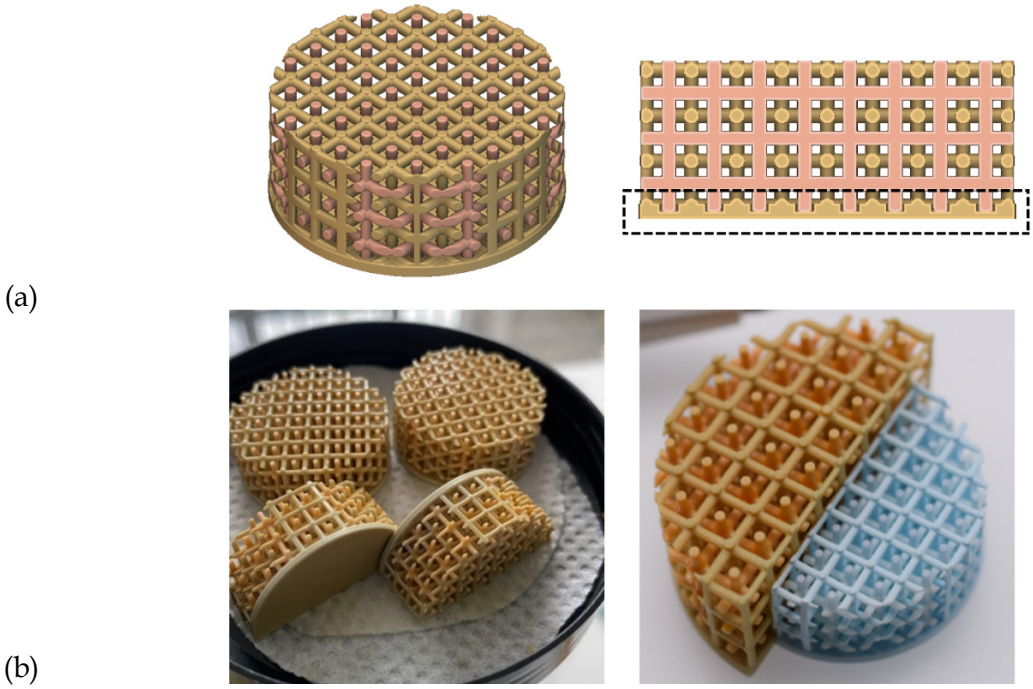


Figure 88: Designs and prototypes of cylindrical specimens with hybridised lattice. (a) Design of a pair of lattices interlaced in space without touching. Special interest in the gaps designed in the connections on the platform to predict shrinkage during heat treatment. (b) Prototypes printed by a combination of hydroxyapatite and tricalcium phosphate. The green body is shown in shades of orange and brown. In bluish and whitish tones the part once sintered. Note the volumetric contraction during the process. Pictures courtesy of Lithoz GmbH. Special thanks to Dr. Serkan Nohut, Eng. Altan Altun and Eng. Sebastian Geier.

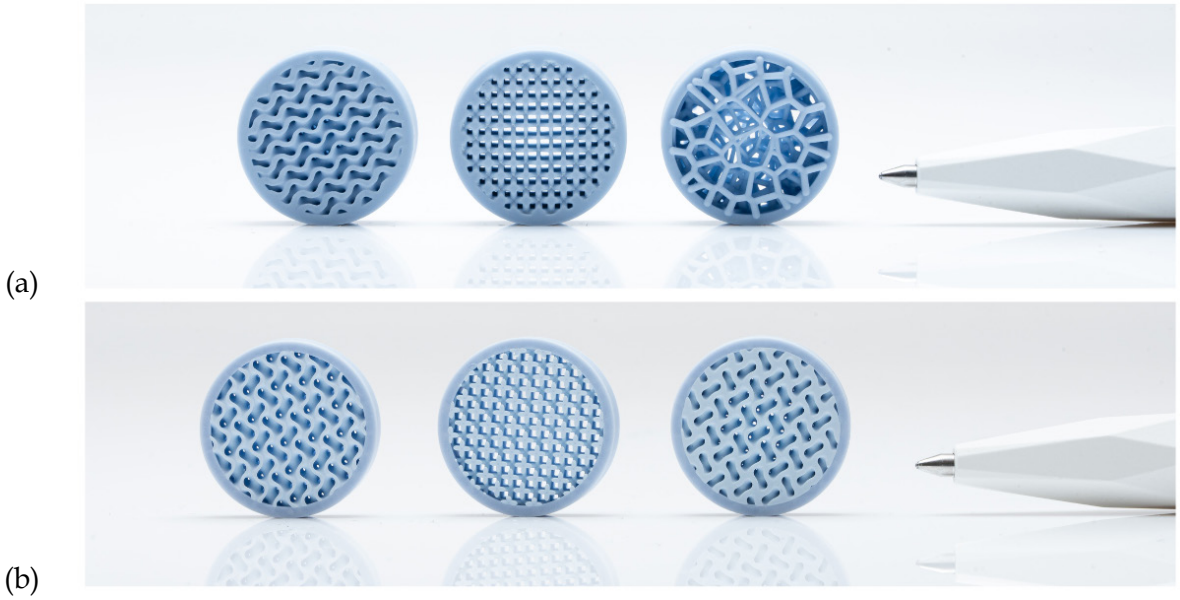


Figure 89: Cylindrical specimens printed in HA to evaluate the ability to obtain biomimetic grafts for bone regeneration by recreating the morphological properties of cortical and trabecular bone. (a) Specimens printed in multi-material mode. The core of the specimen is made of porous HA by including porogens in the polymeric matrix. The contour is printed in dense HA. (b) Collection of specimens printed in dense HA simulating gradient patterns in order to obtain biomimetic properties. Pictures courtesy of Lithoz GmbH. Special thanks to Dr. Serkan Nohut, Eng. Altan Altun and Eng. Sebastian Geier.

2) Multi-Material ceramic printing for smart and preservative dental restorartion

Dental wear poses a significant challenge in contemporary dentistry, impacting a considerable portion of the global population. This phenomenon, characterized by the gradual loss of dental tissue, is influenced by various multifaceted causes, with bruxism being one of the primary and most common. Bruxism, often associated with stress and anxiety, involves involuntary clenching or grinding of the teeth, exerting continuous pressure on dental surfaces. This harmful habit results in premature enamel wear, weakening dental structure and affecting both functionality and aesthetics. The discrepancy in hardness between current dental restorative materials and the natural tissues of teeth poses significant challenges in treating dental wear. Traditional restorations like porcelain, ceramic crowns or veneers have a hardness greater than that of natural dental tissues, especially enamel. This results in a considerable difference in mechanical behaviour between the restoration and the surrounding natural tooth. This hardness discrepancy can lead to long-term issues. For instance, when biting or chewing, harder restorations may subject natural teeth to uneven stress, increasing the probabilities of fractures, microcracks, or accelerating wear on adjacent teeth. Moreover, the mismatch in terms of thermal expansion can create microleakages, allowing bacteria entry and raising the risk of cavities or dental sensitivity.

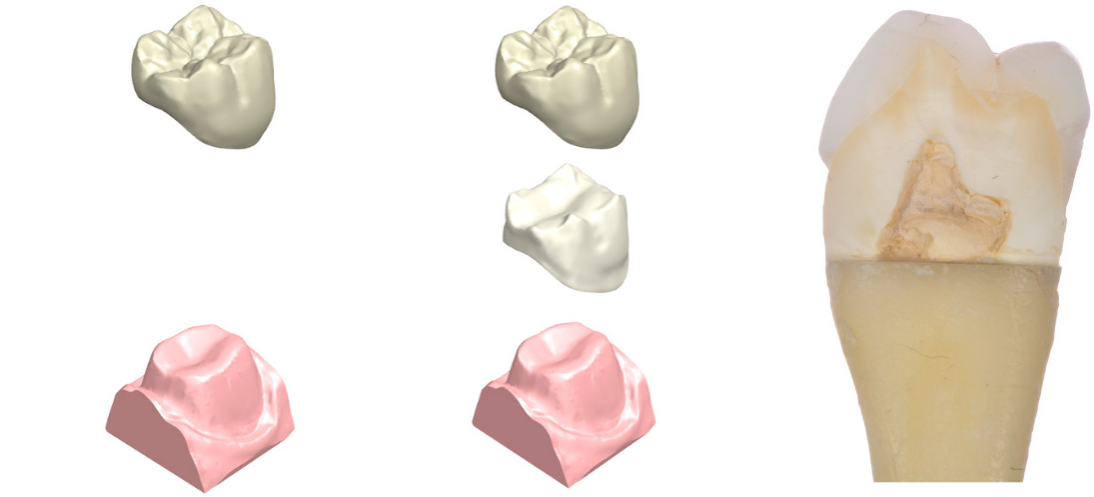
Hence, it's intriguing to seek solutions that closely mimic the properties of natural dental tissues. 3D printing offers notable opportunities in this regard. By developing personalized restorations using 3D printing with materials that better imitate the hardness and mechanical response of natural dental tissues, the disparity in mechanical behaviour can be reduced. These specific materials and customized design could contribute to a more physiological force distribution during chewing, minimizing stress on natural teeth and as a consequence decrease complications such as fracture or excessive wear, enhancing durability and preserving their long-term structural integrity of dental restorations.

The adoption of multimaterial solutions through Lithography-based Ceramic technologies to address dental wear offers significant advantages, especially when using materials with hardness closer to natural tooth structures. The use of tricalcium phosphate or hydroxyapatite, with lower hardness compared to zirconia or lithium disilicate, provides more conservative restorations that are compatible with the patient' original dental structure. Comparatively, the Young's modulus of materials like zirconia and lithium disilicate ranges between 200-240 GPa, significantly surpassing the values of dentin (18-20 GPa) and enamel (120-130 GPa) (385). Conversely, tricalcium phosphate has a Young's modulus of approximately 6 GPa (386), and hydroxyapatite around 80 GPa, approaching the mechanical properties of dentin and enamel more closely. The implementation of these lower-hardness materials offers significant advantages. They reduce stress on natural teeth during chewing by presenting mechanical compatibility closer to dental structure. Additionally, being more similar in terms of hardness and mechanical behaviour, they decrease the risk of fractures or accelerated wear on adjacent teeth.

3D printing technology facilitates the fabrication of multimaterial restorations, enabling the precise combination of these materials with different hardness levels into a single structure. This provides a personalized restoration tailored to the specific needs of the patient,

preserving the integrity of natural teeth, and enhancing the long-term durability of the restorations.

Henceforth, the adoption of multimaterial 3D printing technologies to combine traditional materials like zirconia or lithium disilicate with novel biomedical compounds such as hydroxyapatite or tricalcium phosphate holds promise in significantly mitigating dental wear. By merging these materials, the aim is to achieve a biomimetic restoration that more closely mimics the mechanical properties of natural teeth, thus reducing short and long-term wear and damage. The inclusion of hydroxyapatite or tricalcium phosphate, with hardness closer to dentin and enamel, within 3D-printed prosthetic structures, brings notable benefits. This material combination allows for a more balanced distribution of forces during chewing, minimizing stress on natural teeth. By better aligning with the mechanical properties of the tooth, the likelihood of accelerated wear or fractures is reduced. Furthermore, integrating these new materials with a biomimetic design into dental crowns may lead to better integration with natural tissues, potentially promoting tissue regeneration and reducing the likelihood of bacterial infiltration. This would not only preserve the original dental structure but could also enhance the longevity and functionality, providing greater comfort and durability for patients.



(a) (b) (c)

Figure 90: Intelligent and conservative dental restoration concept. (a) Innovative approach to the fabrication of a bi-material crown made of two ceramics with different levels of hardness. (b) Traditional approach to the fabrication of a mono-material ceramic crown. (c) Natural tooth sectioned to highlight its morphological features. Special thanks to Dental Troyano S.L. and 3Dtive S.L.

3) Promotion of minimal invasion for treating critical size defects

Approaching patients, results like those linked to the topology-optimized short stem hip prostheses are promising and constitute innovative solutions for enhanced biomechanics and biomimicry. However, being large-sized prostheses, their implantation is still highly invasive, as happens with state-of-the-art articular prostheses in general. At the same time, usual tissue engineering scaffolds are just independent porous materials units normally employed for in vitro studies or for the repair of small sized defects. A hybrid approach is conceived at the Product Development Laboratory of UPM, through which specially designed independent scaffolding units become the building blocks for large-sized constructs. Design features supporting mechanical interlocking and self-assembly provide a desired primary stability, while the reduced volume of the scaffolding units allows for minimal invasion and adequate placing within a shape-morphing biodegradable elastomer, previously inserted in a reduced fashion and expanded within the patient for creating a working volume, acting as a kind of "Trojan horse" (see Figure 91).

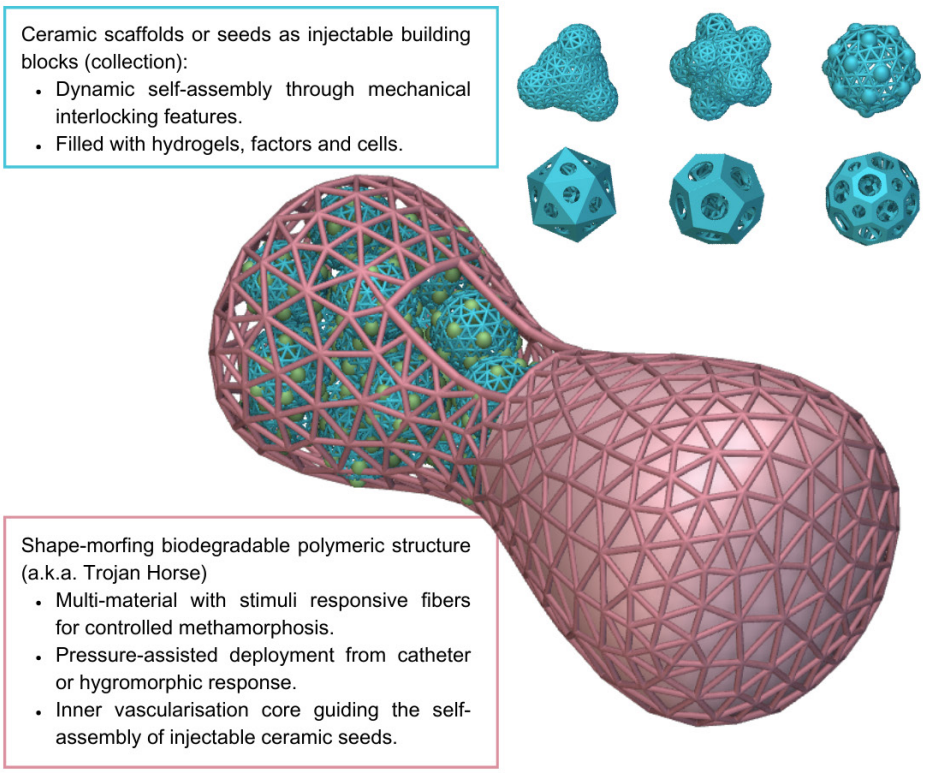


Figure 91: Explanatory diagram of the innovative concept presented as a "Trojan horse".

4) Automated design of high-performance tissue engineering scaffolds

Minimizing human errors in the design of personalized medical implants for their additive manufacturing is important for optimal results. Sources of error include imaging errors when employing computed tomography or magnetic resonance imaging, segmentation errors when selecting the relevant portions of tissues subsequently employed for designing the personalized prostheses in a patient-matched way, format conversion errors when reconstructing from DICOM (digital imaging and

communication in medicine) to stl (standard tessellation language) files, design errors when adapting CAD models to the reconstructed body geometries, and processing or post-processing errors during the materialization of the designs. Working towards the automatization of the medical imaging manipulation procedures and computational designs processes, for which the employment of computational algorithms and artificial intelligence methods seems promising. Initial experiences with semi-automated design procedures for obtaining medical implants from patients images have been already initiated, as exemplified in Figure 92.

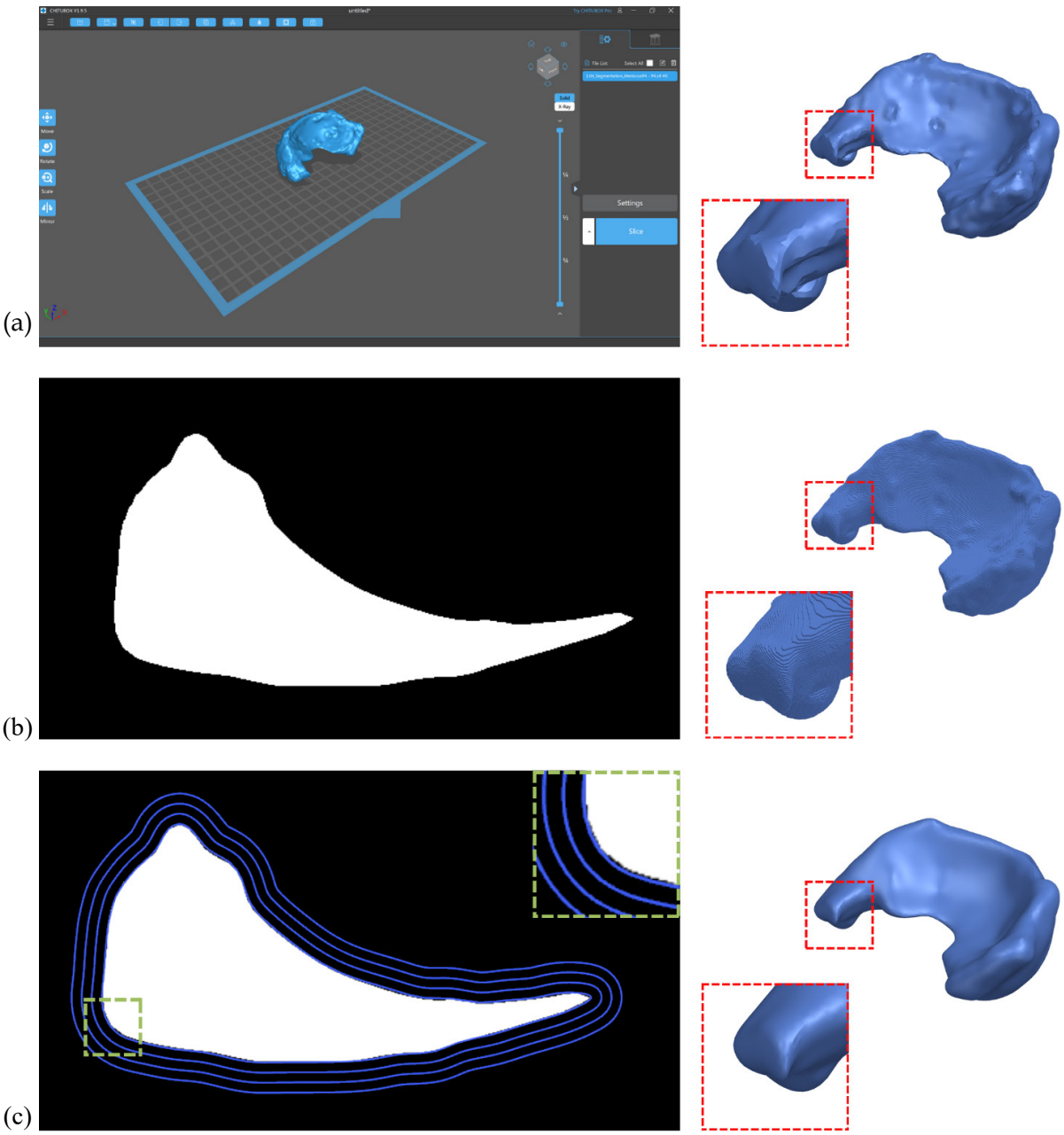


Figure 92: Proposed concept to obtain a solid body of a meniscus from the generation of AI algorithms applied to black and white digital masks in order to automatically generate the curves that best adapt the sections by means of geometric splines. (a) Model obtained by segmentation of medical images. (b) Voxel model, generated from masks obtained in Chitubox. (c) Curve adapted to the voxelated section obtained in a meniscus digital mask, which allows the modification of the contour captured in the reverse engineering process, allowing the shape of the healthy meniscus to be recovered automatically by superimposing all the treated images.

5) Quality promotion in additive manufacturing supported by artificial intelligence

Apart from minimizing human errors, artificial intelligence is emerging as a set of algorithms and procedures that can importantly contribute to enhancing the additive processing of materials and the quality of results in all types of additive manufacturing technologies, which constitutes another relevant proposed research direction. In fact, as regards the additive manufacturing of multi-ceramic components employing multi-vat lithography-based ceramic manufacturing, some initial results have been already achieved, as schematically presented in Figure 94. The detected problem is that multi-material slicers for digital light processing or lithographic procedures in general, when slicing multi-material CAD models stored as assemblies of .stl files, provide black and white networks of pixels that respectively represent unexposed and exposed regions of the processable layers (masks). The transition from the soft surfaces of CAD models, in a first step to the tessellated .stl files, and in a second step to the pixelated masks, tends to generate mismatches in the boundaries among the different materials to be processed. This leads to overexposed regions and underexposed regions, which in turn create shape distortions and weak regions affecting the interfaces between the multiple materials in a critical way. Through automated inspection of the generated masks and searching along the interfaces, the coincident and lacking pixels can be automatically corrected, as intially achieved during INKplant through the development of a dedicated plug-in in collaboration between the candidate and Eng. William Solórzano.

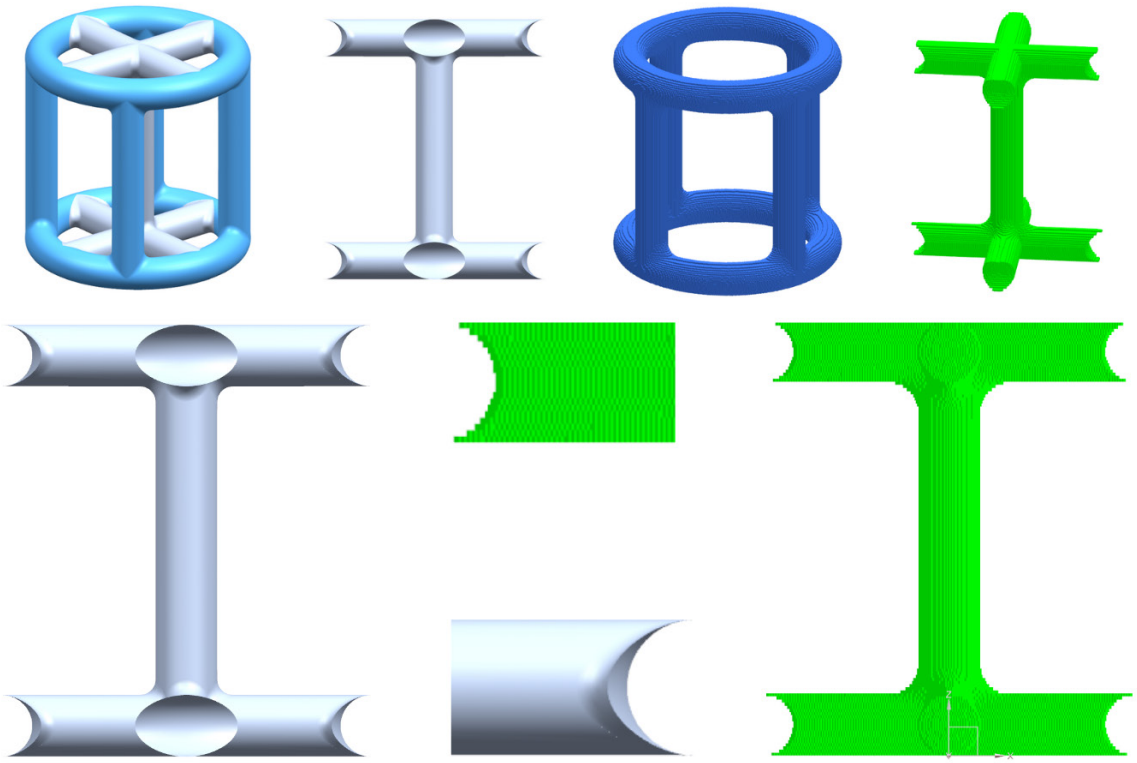
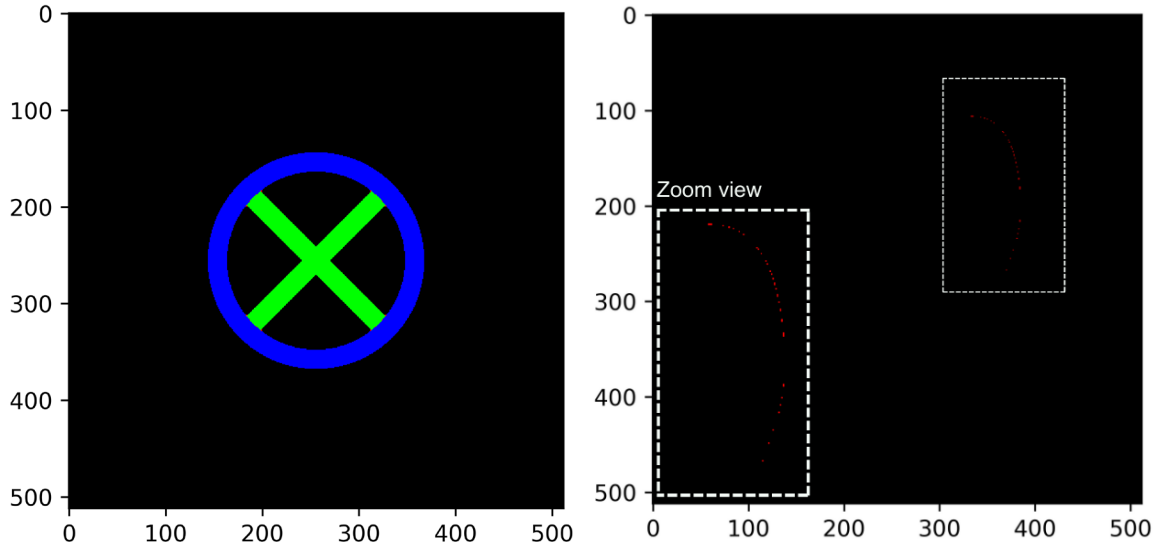
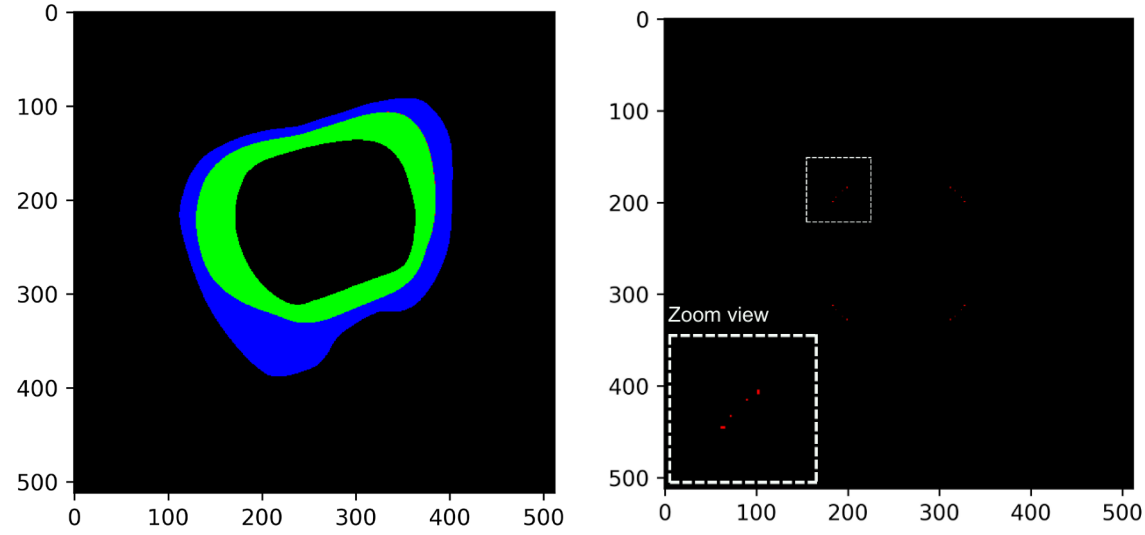


Figure 93: Structure based on a cylindrical frame with a cross attached tangentially on both sides. It shows how the contacts applied in CAD design software differ from the geometries obtained in the slincing process, creating errors that affect the multi-material printing process using digital masks.



(a)



(b)

Figure 94: Treatment of masks obtained to debug probability of dead or overlapping pixels to ensure the correct implementation of a multi-material digital 3D printing system. (a) Slicing of the model shown in Figure 93, where problematic pixels (red highlighted) are debugged at the contacts of the cylindrical frame bases. (b) Slice of a multi-material dental crown, shown in Figure 90, where a border of compromised pixels (red highlighted) is observed due to overlapping of both masks.

6) In vivo validations, certification and technological transfer to society

The main challenges of the PhD thesis, as corresponds to research performed within UPM's Mechanical Engineering Doctoral Programme, have been linked to engineering design and production technologies. As already mentioned, advances achieved include: innovative design approaches, novel modelling and optimisation strategies, enhanced prototyping and manufacturing methods, and the synergic application of all these progresses to the materialization of a comprehensive collection of tissue engineering scaffolds and implants with interesting multi-material, multi-scale and functionally graded structures. In vitro studies

with selected scaffolds have been performed by different partners of the INKplant consortium, but in vivo trials, required for evaluating the safety and efficacy of the proposed solutions are still pending.

Towards the future, either within a possible INKplant 2.0 project or through multi-lateral collaborations across UPM, 3Dtive and different partners of INKplant consortium, including materials and technology developers, healthcare professionals, social sciences and regulatory experts and companies with experience in medical device certification, it is expected to reach in vivo validations, certification and production of selected solutions. According to the project's roadmap, meniscal implants and osteochondral plugs should reach patients by 2030, which provides a highly motivating research avenue for the candidate.

9.3. Summary of scientific-technological contributions of the PhD thesis

Articles in scientific journals

1. Solórzano Requejo, W.; **Martínez Cendrero, A**.; Nohut, S; Altun, A.A.; Ojeda, C.; Schwentenwein, M.; Díaz Lantada, A.- **"Lithography based ceramic manufacturing of topology optimized short stem hip prosthesis"**. Submitted to "Additive Manufacturing", February 2024. Resulting from INKplant's open-innovation action leading to an international transectoral collaboration among the University of Piura, Lithoz GmbH and Universidad Politécnica de Madrid.
2. **Martínez Cendrero, A**.; Dehne, T.; Sittinger, M.; Díaz Lantada, A..- **"Engineering design-controlled interwoven multi-material scaffolds combining hard and soft phases".** Preprint in Research Square, February 2023.
3. **Martínez Cendrero, A**.; Franco Martínez, F.; Requejo, W.G.S.; Díaz Lantada, A..- **"Open-source library of tissue engineering scaffolds"**. Materials & Design, 223, 111154, 2022. Indexed in Journal Citation Reports. Q1, IF: 8.400, position 65/344 in category: "Materials Science, Multidisciplinary".
4. Franco Martínez, F.; Grasl, C.; Kornfellner, E.; Vostatek, M.; **Martínez Cendrero, A**.; Moscato, F.; Díaz Lantada, A..- **"Hybrid design and prototyping of metamaterials and metasurfaces".** Virtual and Physical Prototyping 2022, 17, 1031-1046. Indexed in Journal Citation Reports. Q1, IF: 10.600, position 6/50 in category: "Engineering, Manufacturing".
5. **Martínez Cendrero, A**.; Fortunato, G.M.; Muñoz-Guijosa, J.M.; De Maria, C.; Díaz Lantada, A..- **"Benefits of non-planar printing strategies towards eco-efficient 3D printing".** Sustainability, 13(4), 1599, 2021. Indexed in Journal Citation Reports.
6. Muñoz Guijosa, J.M.; Zapata Martínez, R.; **Martínez Cendrero, A**.; Díaz Lantada, A..- **"Rapid prototyping of personalized articular orthoses by lamination of composite**

materials upon 3D printed molds". Materials, 13(4), 939, 2020. Indexed in Journal Citation Reports.

Publications in proceedings from scientific conferences and participation in congresses

7. Lantada, A.; **Martínez Cendrero, A**.; Martínez, F.; Martínez, R.; Vega, C.; Solórzano-Requejo, W. and Blas De Miguel, A. (2024). "**Bioinspired Design and Manufacturing Strategies for next Generation Medical Implants: Trends and Challenges**". In Proceedings of the 17th International Joint Conference on Biomedical Engineering Systems and Technologies - Volume 1, ISBN 978-989-758-688-0, ISSN 2184-4305, pages 42-53.
8. **Martínez Cendrero, A..- "Multimaterial additive manufacturing for articular articular tissue engineering".** AM Ceramics, Vienna, September 27th – 28th, 2023.
9. Molina Aldareguia, J.; Aguilar Vega, C.; Zapata Martínez, R.; Li, M.; Contreras, O.; Peña Juan, D.; Solórzano Requejo, W.; **Martínez Cendrero, A**.; Díaz Lantada, A..- **"Impresión 4D empleando polímeros y aleaciones con memoria de forma para una nueva generación de dispositivos médicos inteligentes".** XV Congreso Iberoamericano de Ingeniería Mecánica, Madrid, November 22nd – 24th, 2022.
10. Solórzano Requejo, W.; **Martínez Cendrero, A**.; Aguilar Vega, C.; Zapata Martínez, R.; Ojeda, C.; Díaz Lantada, A..- **"Diseño de dispositivos médicos personalizados asistido por inteligencia artificial y métodos numéricos: aplicación a prótesis articulares".** XV Congreso Iberoamericano de Ingeniería Mecánica, November 22nd – 24th, 2022.
11. **Martínez Cendrero, A..- "Open-source tissue engineering scaffolds for evaluating multi-scale and multi-material printing".** International Conference on Biofabrication, Montecatini Terme, September 25th – 28th, 2022.

Books and book chapters

12. Tuesta Guzmán, J.; Solórzano Requejo, W.; **Martínez Cendrero, A**.; Zapata Martínez, R.; Ojeda Díaz, C.; Díaz Lantada, A..- **"Key enabling design and manufacturing technologies for open-source medical devices".** In: "Biomedical engineering for a sustainable development", Book of the "XLI Annual School of the Italian National Bioengineering Group", Grupo Nazionale di Bioingegneria, Patròn, 2022. ISBN: 9788855535700.
13. Díaz Lantada, A., Solórzano, W., **Martínez Cendrero, A**., Zapata Martínez, R., Ojeda, C., Munoz-Guijosa, J.M.- **"Methods and technologies for the personalized design of open-source medical devices"**. In: Ahluwalia, A., De Maria, C., Díaz Lantada, A. (eds).- "Engineering open-Source medical devices". Springer, Cham, 2022.

Generated open-source resources (license CC 4.0 BY)

Works in Thingiverse makers' environment: **"Open-source library of tissue engineering scaffolds"**:

https://www.thingiverse.com/thing:5333296

Works in Thingiverse makers' environment: **"Open-source library of microtextured geometries for studying cell-material interactions":**

https://www.thingiverse.com/thing:5333456

14. Works in UBORA e-platform: "Open-source library of tissue engineering scaffolds": *https://platform.ubora-biomedical.org/projects/ba58012c897b-487e-b8bd-3f7ffe0095e9*
15. Works in UBORA e-platform: **"Open-source library of microtextured geometries for studying cell-material interactions":**

    https://platform.ubora-biomedical.org/projects/17fe248ad564-44c6-b8ba-e31cfc97b748
16. Works in Zenodo repository: **"Open-source library of tissue engineering scaffolds":**

    https://zenodo.org/record/6387574#.YkGd5OdBxPY
17. Works in Zenodo repository: **"Open-source library of microtextured geometries for studying cell-material interactions"**:

    https://zenodo.org/record/6387580#.YkGfGedBxPY

Technological contributions during research stays

18. Research stay in Profactor GmbH research company: Contribution to the development of a 5-axis multi-material inkjet printer and its validation employing non-planar printing strategies for enhanced quality of innovative medical devices. Under the supervision of Dr. Elena Guillén and Research Engineer Michael Kainz. From 14th of November 2022 to 16th of February 2023.
19. Research stay in Lithoz GmbH: Contribution to the printing of large sized topology optimized ceramic implants and to the additive manufacturing of multi-ceramic tissue engineering scaffolds. Under the supervision of Dr. Serkan Nohut and Eng. Altan Altun. From 1st of March 2023 to 31st of May 2023.

References

1. MAFFULLI, N., et al. Sport Injuries: A Review of Outcomes. *British Medical Bulletin*, 2010, vol. 97, no. 1 [viewed 1/22/2024]. pp. 47-80. Available from: https://doi.org/10.1093/bmb/ldq026 ISSN 0007-1420. DOI 10.1093/bmb/ldq026.

2. DAVIES, M.A.M., et al. Serious Sports-Related Injury in England and Wales from 2012-2017: A Study Protocol. *Injury Epidemiology*, 2020, vol. 7, no. 1. pp. 14. Available from: https://doi.org/10.1186/s40621-020-00243-4 ISSN 2197-1714. DOI 10.1186/s40621-020-00243-4.

3. AICALE, R., TARANTINO, D. and MAFFULLI, N. Overuse Injuries in Sport: A Comprehensive Overview. *Journal of Orthopaedic Surgery and Research*, 2018, vol. 13, no. 1. pp. 309. Available from: https://doi.org/10.1186/s13018-018-1017-5 ISSN 1749-799X. DOI 10.1186/s13018-018-1017-5.

4. CHEN, E.T., BORG-STEIN, J. and MCINNIS, K.C. Ankle Sprains: Evaluation, Rehabilitation, and Prevention. *Current Sports Medicine Reports*, Jun, 2019, vol. 18, no. 6. pp. 217-223 ISSN 1537-8918; 1537-890X. DOI 10.1249/JSR.0000000000000603.

5. VUURBERG, G., et al. Diagnosis, Treatment and Prevention of Ankle Sprains: Update of an Evidence-Based Clinical Guideline. *British Journal of Sports Medicine*, 20180307, Aug, 2018, vol. 52, no. 15. pp. 956-098106. Epub 2018 Mar 7 ISSN 1473-0480; 0306-3674. DOI 10.1136/bjsports-2017-098106.

6. SHERMAN, S.L., et al. Meniscus Injuries: A Review of Rehabilitation and Return to Play. *Clinics in Sports Medicine*, Jan, 2020, vol. 39, no. 1. pp. 165-183 ISSN 1556-228X; 0278-5919. DOI 10.1016/j.csm.2019.08.004.

7. BHAN, K. Meniscal Tears: Current Understanding, Diagnosis, and Management. *Cureus*, 20200613, Jun 13, 2020, vol. 12, no. 6. pp. e8590 ISSN 2168-8184; 2168-8184; 2168-8184. DOI 10.7759/cureus.8590.

8. GLATTKE, K.E., TUMMALA, S.V. and CHHABRA, A. Anterior Cruciate Ligament Reconstruction Recovery and Rehabilitation: A Systematic Review. *The Journal of Bone and Joint Surgery.American Volume*, 20211221, Apr 20, 2022, vol. 104, no. 8. pp. 739-754 ISSN 1535-1386; 0021-9355. DOI 10.2106/JBJS.21.00688.

9. ARUNDALE, A.J.H., SILVERS-GRANELLI, H.J. and MYKLEBUST, G. ACL Injury Prevention: Where have we Come from and Where are we Going?. *Journal of Orthopaedic Research : Official Publication of the Orthopaedic Research Society*, 20210511, Jan, 2022, vol. 40, no. 1. pp. 43-54 ISSN 1554-527X; 0736-0266. DOI 10.1002/jor.25058.

10. ABRAMOFF, B. and CALDERA, F.E. Osteoarthritis: Pathology, Diagnosis, and Treatment Options. *The Medical Clinics of North America*, 20191218, Mar, 2020, vol. 104, no. 2. pp. 293-311 ISSN 1557-9859; 0025-7125. DOI 10.1016/j.mcna.2019.10.007.

11. FUSCO, M., et al. Degenerative Joint Diseases and Neuroinflammation. *Pain Practice : The Official Journal of World Institute of Pain*, 20170210, Apr, 2017, vol. 17, no. 4. pp. 522-532 ISSN 1533-2500; 1530-7085. DOI 10.1111/papr.12551.

12. SANDEAN, D. Open Fractures - what is the Evidence, and how can we Improve?. *The Archives of Bone and Joint Surgery*, Sep, 2021, vol. 9, no. 5. pp. 559-566 ISSN 2345-4644; 2345-461X; 2345-461X. DOI 10.22038/abjs.2020.53120.2637.

13. IMAMUDEEN, N., et al. Management of Osteoporosis and Spinal Fractures: Contemporary Guidelines and Evolving Paradigms. *Clinical Medicine & Research*, 20220427, Jun, 2022, vol. 20, no. 2. pp. 95-106 ISSN 1554-6179; 1539-4182; 1539-4182. DOI 10.3121/cmr.2021.1612.

14. RASMUSSEN, K.-.E. and FANØ, N. Trochanteric Bursitis: Treatment by Corticosteroid Injection. *Scandinavian Journal of Rheumatology*, 1985, vol. 14, no. 4. pp. 417-420. Available from: https://doi.org/10.3109/03009748509102047 ISSN 0300-9742. DOI 10.3109/03009748509102047.

15. WILSON, J.J. and BEST, T.M. Common Overuse Tendon Problems: A Review and Recommendations for Treatment. *American Family Physician*, Sep 1, 2005, vol. 72, no. 5. pp. 811-818 ISSN 0002-838X; 0002-838X.

16. DUPLANTIER, N.L., et al. Hip Dislocation Or Subluxation After Hip Arthroscopy: A Systematic Review. *Arthroscopy: The Journal of Arthroscopic & Related Surgery*, 2016, vol. 32, no. 7. pp. 1428-1434. Available from: https://www.sciencedirect.com/science/article/pii/S0749806316001079 ISSN 0749-8063. DOI 10.1016/j.arthro.2016.01.056.

17. HINDLE, P., DAVIDSON, E.K., BIANT, L.C. and COURT-BROWN, C.M. Appendicular Joint Dislocations. *Injury*, 2013, vol. 44, no. 8. pp. 1022-1027. Available from: https://www.sciencedirect.com/science/article/pii/S0020138313000752 ISSN 0020-1383. DOI 10.1016/j.injury.2013.01.043.

18. HAHN, D.M. Current Principles of Treatment in the Clinical Practice of Articular Fractures. *Clinical Orthopaedics and Related Research®*, 2004, vol. 423. Available from: https://journals.lww.com/clinorthop/fulltext/2004/06000/current_principles_of_treatment_in_the_clinical.5.aspx ISSN 0009-921X.

19. HELLIWELL, P.S. and TAYLOR, W.J. Repetitive Strain Injury. *Postgraduate Medical Journal*, 2004, vol. 80, no. 946 [viewed 1/22/2024]. pp. 438-443. Available from: https://doi.org/10.1136/pgmj.2003.012591 ISSN 0032-5473. DOI 10.1136/pgmj.2003.012591.

20. LIEBENSON, C. Functional Problems Associated with the knee—Part One: Sources of Biomechancial Overload. *Journal of Bodywork and Movement Therapies*, 2006, vol. 10, no. 4. pp. 306-311.

21. MADRY, H., LUYTEN, F.P. and FACCHINI, A. Biological Aspects of Early Osteoarthritis. *Knee Surgery, Sports Traumatology, Arthroscopy*, 2012, vol. 20. pp. 407-422.

22. GUILAK, F., et al. The Role of Biomechanics and Inflammation in Cartilage Injury and Repair. *Clinical Orthopaedics and Related Research®*, 2004, vol. 423. Available from: https://journals.lww.com/clinorthop/fulltext/2004/06000/the_role_of_biomechanics_and_inflammation_in.4.aspx ISSN 0009-921X.

23. RICHMOND, S.A., et al. Are Joint Injury, Sport Activity, Physical Activity, Obesity, Or Occupational Activities Predictors for Osteoarthritis? A Systematic Review. *Journal of Orthopaedic & Sports Physical Therapy*, 2013, vol. 43, no. 8. pp. 515-B19.

24. BERENBAUM, F., WALLACE, I.J., LIEBERMAN, D.E. and FELSON, D.T. Modern-Day Environmental Factors in the Pathogenesis of Osteoarthritis. *Nature Reviews Rheumatology*, 2018, vol. 14, no. 11. pp. 674-681.

25. SIEŃKO-AWIERIANÓW, E. and CHUDECKA, M. Risk of Injury in Physically Active Students: Associated Factors and Quality of Life Aspects. *International Journal of Environmental Research and Public Health*, 2020, vol. 17, no. 7. pp. 2564.

26. TERESIŃSKI, G. Forensic medicine of the lower extremity: Human identification and trauma analysis of the thigh, leg, and footSpringer, 2005 *Injuries of the Thigh, Knee, and Ankle as Reconstructive Factors in Road Traffic Accidents*, pp. 311-342.

27. OSTROWSKA, M., et al. Cartilage and Bone Damage in Rheumatoid Arthritis. *Reumatologia/Rheumatology*, 2018, vol. 56, no. 2. pp. 111-120.

28. MARTIN, J.A. and BUCKWALTER, J.A. Articular Cartilage Aging and Degeneration. *Sports Medicine and Arthroscopy Review*, 1996, vol. 4, no. 3. pp. 263-275.

29. COLEMAN, S.H., et al. The Epidemiology of Hip and Groin Injuries in Professional Baseball Players. *Am J Orthop*, 2016, vol. 45, no. 3. pp. 168-175.

30. JACKSON, T.J., STARKEY, C., MCELHINEY, D. and DOMB, B.G. Epidemiology of Hip Injuries in the National Basketball Association: A 24-Year Overview. *Orthopaedic Journal of Sports Medicine*, 2013, vol. 1, no. 3. pp. 2325967113499130.

31. LOU, C., et al. Menopause is Associated with Articular Cartilage Degeneration: A Clinical Study of Knee Joint in 860 Women. *Menopause*, 2016, vol. 23, no. 11. pp. 1239-1246.

32. RØTTERUD, J.H., et al. Effect of Gender and Sports on the Risk of Full-Thickness Articular Cartilage Lesions in Anterior Cruciate Ligament–injured Knees: A Nationwide Cohort Study from Sweden and Norway of 15 783 Patients. *The American Journal of Sports Medicine*, 2011, vol. 39, no. 7. pp. 1387-1394.

33. ORLANDO JÚNIOR, N., LEÃO, M.G.d.S. and OLIVEIRA, N.H.C.d. Diagnosis of Knee Injuries: Comparison of the Physical Examination and Magnetic Resonance Imaging with the Findings from Arthroscopy. *Revista Brasileira De Ortopedia*, 2015, vol. 50. pp. 712-719.

34. MALANGA, G.A., ANDRUS, S., NADLER, S.F. and MCLEAN, J. Physical Examination of the Knee: A Review of the Original Test Description and Scientific Validity of Common Orthopedic Tests. *Archives of Physical Medicine and Rehabilitation*, 2003, vol. 84, no. 4. pp. 592-

603. Available from: https://www.sciencedirect.com/science/article/pii/S000399930204844X ISSN 0003-9993. DOI 10.1053/apmr.2003.50026.

35. SAILAJA, A.K. An overall Review on Rheumatoid Arthritis. *Journal of Current Pharma Research*, 2014, vol. 4, no. 2. pp. 1138.

36. DENTON, J. Synovial Fluid Analysis in the Diagnosis of Joint Disease. *Diagnostic Histopathology*, 2012, vol. 18, no. 4. pp. 159-168.

37. F. Forsberg, et al. *Ultrasound Triggered Microbubble Destruction for Disrupting Biofilms in Synovial Fluid.* , 2020 ISBN 1948-5719. DOI 10.1109/IUS46767.2020.9251545.

38. HAYASHI, D., ROEMER, F.W., JARRAYA, M. and GUERMAZI, A. Imaging of Osteoarthritis. *Geriatric Imaging*, 2013. pp. 93-121.

39. VASHISHTHA, A. and KUMAR ACHARYA, A. An Overview of Medical Imaging Techniques for Knee Osteoarthritis Disease. *Biomedical and Pharmacology Journal*, 2021, vol. 14, no. 2. pp. 903-919.

40. LEE, S.C., WILLIAMS, D. and ENDO, Y. The Repaired Rotator Cuff: MRI and Ultrasound Evaluation. *Current Reviews in Musculoskeletal Medicine*, 2018, vol. 11. pp. 92-101.

41. THOMAZEAU, H., et al. Prediction of Rotator Cuff Repair Results by Magnetic Resonance Imaging. *Clinical Orthopaedics and Related Research (1976-2007)*, 1997, vol. 344. pp. 275-283.

42. KAPRELI, E., et al. Anterior Cruciate Ligament Deficiency Causes Brain Plasticity: A Functional MRI Study. *The American Journal of Sports Medicine*, 2009, vol. 37, no. 12. pp. 2419-2426.

43. NEWBERG, A.H. Computed Tomography of Joint Injuries. *Radiologic Clinics of North America*, 1990, vol. 28, no. 2. pp. 445-460. Available from: https://www.sciencedirect.com/science/article/pii/S0033838922009046 ISSN 0033-8389. DOI 10.1016/S0033-8389(22)00904-6.

44. SWAYNE, L.C., DORSKY, S., CARUANA, V. and KAPLAN, I.L. Septic Arthritis of a Lumbar Facet Joint: Detection with Bone SPECT Imaging. *Journal of Nuclear Medicine*, 1989, vol. 30, no. 8. pp. 1408-1411.

45. DEHAVEN, K.E. and COLLINS, H.R. Diagnosis of Internal Derangements of the Knee. the Role of Arthroscopy. *Jbjs*, 1975, vol. 57, no. 6. pp. 802-810.

46. WEILER, J.M. Medical Modifiers of Sports Injury: The use of Nonsteroidal Antiinflammatory Drugs (NSAIDs) in Sports Soft-Tissue Injury. *Clinics in Sports Medicine*, 1992, vol. 11, no. 3. pp. 625-644.

47. STOVITZ, S.D. and JOHNSON, R.J. NSAIDs and Musculoskeletal Treatment: What is the Clinical Evidence?. *The Physician and Sportsmedicine*, 2003, vol. 31, no. 1. pp. 35-52.

48. FREDBERG, U. Local Corticosteroid Injection in Sport: Review of Literature and Guidelines for Treatment. *Scandinavian Journal of Medicine & Science in Sports*, 1997, vol. 7, no. 3. pp. 131-139.

49. RUTJES, A.W., et al. Viscosupplementation for Osteoarthritis of the Knee: A Systematic Review and Meta-Analysis. *Annals of Internal Medicine*, 2012, vol. 157, no. 3. pp. 180-191.

50. BELLAMY, N., et al. Viscosupplementation for the Treatment of Osteoarthritis of the Knee. *Cochrane Database of Systematic Reviews*, 2006, no. 2.

51. MINOR, M.A. and SANFORD, M.K. The Role of Physical Therapy and Physical Modalities in Pain Management. *Rheumatic Disease Clinics of North America*, 1999, vol. 25, no. 1. pp. 233-248.

52. DIEPPE, P., LIM, K. and LOHMANDER, S. Who should have Knee Joint Replacement Surgery for Osteoarthritis?. *International Journal of Rheumatic Diseases*, 2011, vol. 14, no. 2. pp. 175-180.

53. KOLLER-HODAC, A., LEONARDO, D., WALPEN, S. and FELDER, D. *Knee Orthopaedic Device how Robotic Technology can Improve Outcome in Knee Rehabilitation*. IEEE, 2011.

54. DAVIDSON, J.R., KERWIN, S.C. and MILLIS, D.L. Rehabilitation for the Orthopedic Patient. *Veterinary Clinics: Small Animal Practice*, 2005, vol. 35, no. 6. pp. 1357-1388.

55. SALGADO, A.J., et al. Tissue Engineering and Regenerative Medicine: Past, Present, and Future. *International Review of Neurobiology*, 2013, vol. 108. pp. 1-33.

56. USAS, A. and HUARD, J. Muscle-Derived Stem Cells for Tissue Engineering and Regenerative Therapy. *Biomaterials*, 2007, vol. 28, no. 36. pp. 5401-5406.

57. BETSHOLTZ, C., KARLSSON, L. and LINDAHL, P. Developmental Roles of Platelet-derived Growth Factors. *Bioessays*, 2001, vol. 23, no. 6. pp. 494-507.

58. HOSGOOD, G. Wound Healing: The Role of Platelet-derived Growth Factor and Transforming Growth Factor Beta. *Veterinary Surgery*, 1993, vol. 22, no. 6. pp. 490-495.

59. PARK, K. Facing the Truth about Nanotechnology in Drug Delivery. *ACS Nano*, 2013, vol. 7, no. 9. pp. 7442-7447.

60. FAROKHZAD, O.C. and LANGER, R. Impact of Nanotechnology on Drug Delivery. *ACS Nano*, 2009, vol. 3, no. 1. pp. 16-20.

61. LABHASETWAR, V. Nanotechnology for Drug and Gene Therapy: The Importance of Understanding Molecular Mechanisms of Delivery. *Current Opinion in Biotechnology*, 2005, vol. 16, no. 6. pp. 674-680.

62. NOUR, S., BOLANDI, B. and IMANI, R. Nanoengineering in musculoskeletal regenerationElsevier, 2020 *Nanotechnology in Gene Therapy for Musculoskeletal Regeneration*, pp. 105-136.

63. ZEMA, L., MELOCCHI, A., MARONI, A. and GAZZANIGA, A. Three-Dimensional Printing of Medicinal Products and the Challenge of Personalized Therapy. *Journal of Pharmaceutical Sciences*, 2017, vol. 106, no. 7. pp. 1697-1705.

64. MITRA, I., et al. 3D Printing in Alloy Design to Improve Biocompatibility in Metallic Implants. *Materials Today*, 2021, vol. 45. pp. 20-34. Available from: https://www.sciencedirect.com/science/article/pii/S136970212030448X ISSN 1369-7021. DOI 10.1016/j.mattod.2020.11.021.

65. CHIA, H.N. and WU, B.M. Recent Advances in 3D Printing of Biomaterials. *Journal of Biological Engineering*, 2015, vol. 9, no. 1. pp. 1-14.

66. RUIZ, O.G. and DHAHER, Y. Multi-Color and Multi-Material 3D Printing of Knee Joint Models. *3D Printing in Medicine*, 2021, vol. 7, no. 1. pp. 1-16.

67. PATI, F., et al. Biomimetic 3D Tissue Printing for Soft Tissue Regeneration. *Biomaterials*, 2015, vol. 62. pp. 164-175.

68. PUTRA, N.E., et al. Multi-Material Additive Manufacturing Technologies for Ti-, mg-, and Fe-Based Biomaterials for Bone Substitution. *Acta Biomaterialia*, 2020, vol. 109. pp. 1-20. Available from: https://www.sciencedirect.com/science/article/pii/S1742706120301781 ISSN 1742-7061. DOI 10.1016/j.actbio.2020.03.037.

69. LANGER, R. and VACANTI, J.P. Tissue Engineering. *Science (New York, N.Y.)*, May 14, 1993, vol. 260, no. 5110. pp. 920-926 ISSN 0036-8075; 0036-8075. DOI 10.1126/science.8493529.

70. LANZA, R., LANGER, R., VACANTI, J.P. and ATALA, A. *Principles of Tissue Engineering*. Academic press, 2020.

71. HUTMACHER, D.W. Scaffolds in Tissue Engineering Bone and Cartilage. *Biomaterials*, Dec, 2000, vol. 21, no. 24. pp. 2529-2543 ISSN 0142-9612; 0142-9612. DOI 10.1016/s0142-9612(00)00121-6.

72. OVSIANIKOV, A., KHADEMHOSSEINI, A. and MIRONOV, V. The Synergy of Scaffold-Based and Scaffold-Free Tissue Engineering Strategies. *Trends in Biotechnology*, 20180220, Apr, 2018, vol. 36, no. 4. pp. 348-357 ISSN 1879-3096; 0167-7799. DOI 10.1016/j.tibtech.2018.01.005.

73. LEASK, F. and TERZIC, A. Regenerative Outlook: Offering Global Solutions for Equitable Care. *Regenerative Medicine*, 20201127, Nov, 2020, vol. 15, no. 11. pp. 2249-2252 ISSN 1746-076X; 1746-0751. DOI 10.2217/rme-2020-0177.

74. NATIONAL ACADEMY, o.E. *Frontiers of Engineering: Reports on Leading-Edge Engineering from the 2011 Symposium*. Washington, DC: The National Academies Press, 2012 Available from: https://nap.nationalacademies.org/catalog/13274/frontiers-of-engineering-reports-on-leading-edge-engineering-from-the ISBN 978-0-309-22143-6. DOI 10.17226/13274.

75. *Maker Culture*. -02-14T16:25:24Z, 2024 [viewed Feb 15, 2024]. Available from:https://en.wikipedia.org/w/index.php?title=Maker_culture&oldid=1207356440.

76. ZEIN, I., HUTMACHER, D.W., TAN, K.C. and TEOH, S.H. Fused Deposition Modeling of Novel Scaffold Architectures for Tissue Engineering Applications. *Biomaterials*, Feb, 2002, vol. 23, no. 4. pp. 1169-1185 ISSN 0142-9612; 0142-9612. DOI 10.1016/s0142-9612(01)00232-0.

77. HUTMACHER, D.W. Scaffold Design and Fabrication Technologies for Engineering Tissues--State of the Art and Future Perspectives. *Journal of Biomaterials Science.Polymer Edition*, 2001, vol. 12, no. 1. pp. 107-124 ISSN 0920-5063; 0920-5063. DOI 10.1163/156856201744489.

78. KALITA, S., BOSE, S., HOSICK, H. and BANDYOPADHYAY, A. Development of Controlled Porosity Polymer-Ceramic Composite Scaffolds Via Fused Deposition Modeling. *Materials Science and Engineering: C*, 2003, vol. 23. pp. 611-620 DOI 10.1016/S0928-4931(03)00052-3.

79. LIU, F., LEE, R., LIN, W. and LIAO, Y. Selective Laser Sintering of Bio-Metal Scaffold. *Procedia CIRP*, 2013, vol. 5. pp. 83-87. Available from: https://www.sciencedirect.com/science/article/pii/S2212827113000188 ISSN 2212-8271. DOI 10.1016/j.procir.2013.01.017.

80. WARNKE, P.H., et al. Rapid Prototyping: Porous Titanium Alloy Scaffolds Produced by Selective Laser Melting for Bone Tissue Engineering. *Tissue Engineering.Part C, Methods*, Jun, 2009, vol. 15, no. 2. pp. 115-124 ISSN 1937-3392; 1937-3384. DOI 10.1089/ten.tec.2008.0288.

81. MELCHELS, F.P.W., FEIJEN, J. and GRIJPMA, D.W. A Poly(D,L-Lactide) Resin for the Preparation of Tissue Engineering Scaffolds by Stereolithography. *Biomaterials*, 20090429, Aug, 2009, vol. 30, no. 23-24. pp. 3801-3809 ISSN 1878-5905; 0142-9612. DOI 10.1016/j.biomaterials.2009.03.055.

82. GAUVIN, R., et al. Microfabrication of Complex Porous Tissue Engineering Scaffolds using 3D Projection Stereolithography. *Biomaterials*, 20120225, May, 2012, vol. 33, no. 15. pp. 3824-3834 ISSN 1878-5905; 0142-9612; 0142-9612. DOI 10.1016/j.biomaterials.2012.01.048.

83. DEAN, D., et al. Continuous Digital Light Processing (cDLP): Highly Accurate Additive Manufacturing of Tissue Engineered Bone Scaffolds. *Virtual and Physical Prototyping*, 20120412, Mar 1, 2012, vol. 7, no. 1. pp. 13-24 ISSN 1745-2759; 1745-2767; 1745-2759. DOI 10.1080/17452759.2012.673152.

84. TESAVIBUL, P., et al. Processing of 45S5 Bioglass (R) by Lithography-Based Additive Manufacturing. *Materials Letters*, 2012, vol. 74. pp. 81-84 DOI 10.1016/j.matlet.2012.01.019.

85. BOLAND, T., XU, T., DAMON, B. and CUI, X. Application of Inkjet Printing to Tissue Engineering. *Biotechnology Journal*, Sep, 2006, vol. 1, no. 9. pp. 910-917 ISSN 1860-7314; 1860-6768. DOI 10.1002/biot.200600081.

86. DE MARIA, C., et al. Clinical Engineering Handbook (Second Edition) E. IADANZA ed., Academic Press, 2020 *Chapter 2 - Open-Source Medical Devices: Healthcare Solutions for Low-, Middle-, and High-Resource Settings*, pp. 7-14. Available from: https://www.sciencedirect.com/science/article/pii/B978012813467200002X ISBN 9780128134672. DOI 10.1016/B978-0-12-813467-2.00002-X.

87. AHLUWALIA, A., DE MARIA, C. and DIAZ LANTADA, A. The Kahawa Declaration: A Manifesto for the Democratization of Medical Technology. *Global Health Innovation*, 2018, vol. 1, no. 1. Available from: https://journals.uct.ac.za/index.php/GHI/article/view/507 DOI 10.15641/ghi.v1i1.507.

88. WILKINSON, M.D., et al. The FAIR Guiding Principles for Scientific Data Management and Stewardship. *Scientific Data*, 2016, vol. 3, no. 1. pp. 160018. Available from: https://doi.org/10.1038/sdata.2016.18 ISSN 2052-4463. DOI 10.1038/sdata.2016.18.

89. AHLUWALIA, A., DE MARIA, C. and DIAZ LANTADA, A. *Engineering Open-Source Medical Devices.* , 2022 ISBN 978-3-030-79363-0. DOI 10.1007/978-3-030-79363-0.

90. MARCHIORI, G., BERNI, M., BOI, M. and FILARDO, G. Cartilage Mechanical Tests: Evolution of Current Standards for Cartilage Repair and Tissue Engineering. A Literature Review. *Clinical Biomechanics*, 2019, vol. 68. pp. 58-72. Available from: https://www.sciencedirect.com/science/article/pii/S0268003318304534 ISSN 0268-0033. DOI 10.1016/j.clinbiomech.2019.05.019.

91. KAMOLZ, L.P., LUMENTA, D.B., KITZINGER, H.B. and FREY, M. Tissue Engineering for Cutaneous Wounds: An Overview of Current Standards and Possibilities. *European Surgery*, 2008, vol. 40, no. 1. pp. 19-26 DOI 10.1007/s10353-008-0380-6.

92. WILLIAMS, D. Benefit and Risk in Tissue Engineering. *Materials Today*, 2004, vol. 7, no. 5. pp. 24-29. Available from: https://www.sciencedirect.com/science/article/pii/S1369702104002329 ISSN 1369-7021. DOI 10.1016/S1369-7021(04)00232-9.

93. PATRA, S. and YOUNG, V. A Review of 3D Printing Techniques and the Future in Biofabrication of Bioprinted Tissue. *Cell Biochemistry and Biophysics*, 2016, vol. 74, no. 2. pp. 93-98. Available from: https://doi.org/10.1007/s12013-016-0730-0 ISSN 1559-0283. DOI 10.1007/s12013-016-0730-0.

94. KNOWLTON, S., YENILMEZ, B. and TASOGLU, S. Towards Single-Step Biofabrication of Organs on a Chip Via 3D Printing. *Trends in Biotechnology*, 2016, vol. 34, no. 9. pp. 685-688 DOI https://doi.org/10.1016/j.tibtech.2016.06.005.

95. KYLE, S. 3D Printing of Bacteria: The Next Frontier in Biofabrication. *Trends in Biotechnology*, 2018, vol. 36, no. 4. pp. 340-341 DOI https://doi.org/10.1016/j.tibtech.2018.01.010.

96. PEDDE, R.D., et al. Emerging Biofabrication Strategies for Engineering Complex Tissue Constructs. *Advanced Materials*, 2017, vol. 29, no. 19. pp. 1606061. Available from: https://doi.org/10.1002/adma.201606061 ISSN 0935-9648. DOI 10.1002/adma.201606061.

97. ZHOU, X., et al. Fabrication of Polylactic Acid (PLA)-Based Porous Scaffold through the Combination of Traditional Bio-Fabrication and 3D Printing Technology for Bone Regeneration. *Colloids and Surfaces B: Biointerfaces*, 2021, vol. 197. pp. 111420. Available from: https://www.sciencedirect.com/science/article/pii/S0927776520307761 ISSN 0927-7765. DOI 10.1016/j.colsurfb.2020.111420.

98. GUO, T., et al. 3D Printing PLGA: A Quantitative Examination of the Effects of Polymer Composition and Printing Parameters on Print Resolution. *Biofabrication*, 2017, vol. 9, no. 2.

pp. 024101. Available from: https://dx.doi.org/10.1088/1758-5090/aa6370 ISSN 1758-5090. DOI 10.1088/1758-5090/aa6370.

99. KIRILLOVA, A., et al. 4D Biofabrication using Shape-Morphing Hydrogels. *Advanced Materials*, 2017, vol. 29, no. 46. pp. 1703443. Available from: https://doi.org/10.1002/adma.201703443 ISSN 0935-9648. DOI 10.1002/adma.201703443.

100. ONOFRILLO, C., et al. Biofabrication of Human Articular Cartilage: A Path Towards the Development of a Clinical Treatment. *Biofabrication*, 2018, vol. 10, no. 4. pp. 045006. Available from: https://dx.doi.org/10.1088/1758-5090/aad8d9 ISSN 1758-5090. DOI 10.1088/1758-5090/aad8d9.

101. NOVOSEL, E.C., KLEINHANS, C. and KLUGER, P.J. Vascularization is the Key Challenge in Tissue Engineering. *Advanced Drug Delivery Reviews*, 2011, vol. 63, no. 4. pp. 300-311. Available from: https://www.sciencedirect.com/science/article/pii/S0169409X11000470 ISSN 0169-409X. DOI 10.1016/j.addr.2011.03.004.

102. ROUWKEMA, J., RIVRON, N.C. and VAN BLITTERSWIJK, C.A. Vascularization in Tissue Engineering. *Trends in Biotechnology*, 2008, vol. 26, no. 8. pp. 434-441 DOI https://doi.org/10.1016/j.tibtech.2008.04.009.

103. IKADA, Y. Challenges in Tissue Engineering. *Journal of the Royal Society Interface*, 2006, vol. 3, no. 10. pp. 589-601 DOI https://doi.org/10.1098/rsif.2006.0124.

104. YANG, Y., et al. Recent Progress in Biomimetic Additive Manufacturing Technology: From Materials to Functional Structures. *Advanced Materials*, 2018, vol. 30, no. 36. pp. 1706539. Available from: https://doi.org/10.1002/adma.201706539 ISSN 0935-9648. DOI 10.1002/adma.201706539.

105. DU PLESSIS, A., et al. Beautiful and Functional: A Review of Biomimetic Design in Additive Manufacturing. *Additive Manufacturing*, 2019, vol. 27. pp. 408-427. Available from: https://www.sciencedirect.com/science/article/pii/S2214860419302611 ISSN 2214-8604. DOI 10.1016/j.addma.2019.03.033.

106. LIAO, S.S., CUI, F.Z., ZHANG, W. and FENG, Q.L. Hierarchically Biomimetic Bone Scaffold Materials: Nano-HA/Collagen/PLA Composite. *Journal of Biomedical Materials Research.Part B, Applied Biomaterials*, May 15, 2004, vol. 69, no. 2. pp. 158-165 ISSN 1552-4973; 1552-4973. DOI 10.1002/jbm.b.20035.

107. A. Chu, H. Kazerooni and A. Zoss. *On the Biomimetic Design of the Berkeley Lower Extremity Exoskeleton (BLEEX).* , 2005 ISBN 1050-4729. DOI 10.1109/ROBOT.2005.1570789.

108. ZHOU, F., et al. Rapid Printing of Bio-Inspired 3D Tissue Constructs for Skin Regeneration. *Biomaterials*, 2020, vol. 258. pp. 120287. Available from: https://www.sciencedirect.com/science/article/pii/S0142961220305330 ISSN 0142-9612. DOI 10.1016/j.biomaterials.2020.120287.

109. T. Levi, et al. Development and Applications of Biomimetic Neuronal Networks Toward BrainMorphic Artificial Intelligence. *IEEE Transactions on Circuits and Systems II: Express Briefs*, 2018, vol. 65, no. 5. pp. 577-581 ISSN 1558-3791. DOI 10.1109/TCSII.2018.2824827.

110. WEN, L., WEAVER, J.C. and LAUDER, G.V. Biomimetic Shark Skin: Design, Fabrication and Hydrodynamic Function. *Journal of Experimental Biology*, 2014, vol. 217, no. 10 [viewed 2/17/2024]. pp. 1656-1666. Available from: https://doi.org/10.1242/jeb.097097 ISSN 0022-0949. DOI 10.1242/jeb.097097.

111. AGNARSSON, I., DHINOJWALA, A., SAHNI, V. and BLACKLEDGE, T.A. Spider Silk as a Novel High Performance Biomimetic Muscle Driven by Humidity. *Journal of Experimental Biology*, 2009, vol. 212, no. 13 [viewed 2/17/2024]. pp. 1990-1994. Available from: https://doi.org/10.1242/jeb.028282 ISSN 0022-0949. DOI 10.1242/jeb.028282.

112. CARLO, M. and METIN, S. A Biomimetic Climbing Robot Based on the Gecko. *Journal of Bionic Engineering*, 2006, vol. 3, no. 3. pp. 115-125. Available from: https://www.sciencedirect.com/science/article/pii/S1672652906600152 ISSN 1672-6529. DOI 10.1016/S1672-6529(06)60015-2.

113. LEE, N., et al. Microstructure and Nanomechanical Properties of the Exoskeleton of an Ironclad Beetle (Zopherus Haldemani). *Bioinspiration & Biomimetics*, 2021, vol. 16, no. 3. pp. 036005. Available from: https://dx.doi.org/10.1088/1748-3190/abe27b ISSN 1748-3190; 1748-3182. DOI 10.1088/1748-3190/abe27b.

114. DIDARI, A. and MENGÜÇ, M.P. A Biomimicry Design for Nanoscale Radiative Cooling Applications Inspired by Morpho Didius Butterfly. *Scientific Reports*, 2018, vol. 8, no. 1. pp. 16891. Available from: https://doi.org/10.1038/s41598-018-35082-3 ISSN 2045-2322. DOI 10.1038/s41598-018-35082-3.

115. JAYARAM, K. and FULL, R.J. Cockroaches Traverse Crevices, Crawl Rapidly in Confined Spaces, and Inspire a Soft, Legged Robot. *Proceedings of the National Academy of Sciences*, 2016, vol. 113, no. 8. pp. E950-E957. Available from: https://doi.org/10.1073/pnas.1514591113 DOI 10.1073/pnas.1514591113.

116. WANG, J., et al. Shape Matters: Morphologically Biomimetic Particles for Improved Drug Delivery. *Chemical Engineering Journal*, 2021, vol. 410. pp. 127849. Available from: https://www.sciencedirect.com/science/article/pii/S1385894720339681 ISSN 1385-8947. DOI 10.1016/j.cej.2020.127849.

117. COLLINS, C.M. and SAFIUDDIN, M. Lotus-Leaf-Inspired Biomimetic Coatings: Different Types, Key Properties, and Applications in Infrastructures. *Infrastructures*, 2022, vol. 7, no. 4 ISSN 2412-3811. DOI 10.3390/infrastructures7040046.

118. MANDELBROT, B.B. and MANDELBROT, B.B. *The Fractal Geometry of Nature*. WH freeman New York, 1982.

119. WANGPRASEURT, D., YOU, S., SUN, Y. and CHEN, S. Biomimetic 3D Living Materials Powered by Microorganisms. *Trends in Biotechnology*, 2022, vol. 40, no. 7. pp. 843-857. Available from: https://doi.org/10.1016/j.tibtech.2022.01.003 ISSN 0167-7799. DOI 10.1016/j.tibtech.2022.01.003.

120. SIMONSON, A.W., et al. Pathogen-Specific Antimicrobials Engineered De Novo through Membrane-Protein Biomimicry. *Nature Biomedical Engineering*, 2021, vol. 5, no. 5. pp.

467-480. Available from: https://doi.org/10.1038/s41551-020-00665-x ISSN 2157-846X. DOI 10.1038/s41551-020-00665-x.

121. GARCIA-HOLGUERA, M., CLARK, O.G., SPRECHER, A. and GASKIN, S. Ecosystem Biomimetics for Resource use Optimization in Buildings. *Building Research & Information*, 2016, vol. 44, no. 3. pp. 263-278. Available from: https://doi.org/10.1080/09613218.2015.1052315 ISSN 0961-3218. DOI 10.1080/09613218.2015.1052315.

122. STOJANOVIC, M. Biomimicry in Agriculture: Is the Ecological System-Design Model the Future Agricultural Paradigm?. *Journal of Agricultural and Environmental Ethics*, 2019, vol. 32, no. 5. pp. 789-804. Available from: https://doi.org/10.1007/s10806-017-9702-7 ISSN 1573-322X. DOI 10.1007/s10806-017-9702-7.

123. BLOK, V. and GREMMEN, B. Ecological Innovation: Biomimicry as a New Way of Thinking and Acting Ecologically. *Journal of Agricultural and Environmental Ethics*, 2016, vol. 29, no. 2. pp. 203-217. Available from: https://doi.org/10.1007/s10806-015-9596-1 ISSN 1573-322X. DOI 10.1007/s10806-015-9596-1.

124. FRANCO MARTÍNEZ, F. *Artificial Intelligence Aided Design of Microstructured Surfaces for Tribology and Biointerfaces Engineering*. Universidad Politécnica de Madrid, 2023 DOI https://doi.org/10.20868/UPM.thesis.77158.

125. DÍAZ LANTADA, A., PAREJA SÁNCHEZ, B., GÓMEZ MURILLO, C. and URBIETA SOTILLO, J. Fractals in Tissue Engineering: Toward Biomimetic Cell-Culture Matrices, Microsystems and Microstructured Implants. *Expert Review of Medical Devices*, 20130823, Sep, 2013, vol. 10, no. 5. pp. 629-648 ISSN 1745-2422; 1743-4440. DOI 10.1586/17434440.2013.827506.

126. KARABETÇA, A. *AIOC'15 Nature Inspired Architectural Designs: Using Biomimicry as a Design Strategy.* , 2015.

127. Rob Lichty. *Column - Biomimicry Lessons from Sharks.* -11-10T05:26:32-04:00, 2011 [viewed Feb 12, 2024]. Available from:https://medtechintelligence.com/column/meddesign-biomimcry-lessons-from-sharks/.

128. KONDOYANNI, M., et al. Bio-Inspired Robots and Structures Toward Fostering the Modernization of Agriculture. *Biomimetics*, 2022, vol. 7, no. 2 ISSN 2313-7673. DOI 10.3390/biomimetics7020069.

129. *Geckskin™ is a New Super-Adhesive Based on the Mechanics of Gecko Feet.* [viewed Feb 18, 2024]. Available from:https://geckskin.umass.edu/.

130. S. UNIVERSITY and Taylor Kubota. *A Robotic Hand with a Gecko-Inspired Grip.* -12-15T11:00:36-08:00, 2021 [viewed Feb 12, 2024]. Available from:https://news.stanford.edu/2021/12/15/robotic-hand-gecko-inspired-grip/.

131. CULMONE, C., SMIT, G. and BREEDVELD, P. Additive Manufacturing of Medical Instruments: A State-of-the-Art Review. *Additive Manufacturing*, 2019, vol. 27. pp. 461-473.

Available from: https://www.sciencedirect.com/science/article/pii/S2214860418308911 ISSN 2214-8604. DOI 10.1016/j.addma.2019.03.015.

132. SALMI, M. Additive Manufacturing Processes in Medical Applications. *Materials*, 2021, vol. 14, no. 1 ISSN 1996-1944. DOI 10.3390/ma14010191.

133. MONDSCHEIN, R.J., et al. Polymer Structure-Property Requirements for Stereolithographic 3D Printing of Soft Tissue Engineering Scaffolds. *Biomaterials*, 2017, vol. 140. pp. 170-188. Available from: https://www.sciencedirect.com/science/article/pii/S014296121730399X ISSN 0142-9612. DOI 10.1016/j.biomaterials.2017.06.005.

134. NOHUT, S., et al. Lithography-Based Additive Manufacturing of Porosity Graded Alumina. *Additive Manufacturing Letters*, 2022, vol. 3. pp. 100060. Available from: https://www.sciencedirect.com/science/article/pii/S2772369022000342 ISSN 2772-3690. DOI 10.1016/j.addlet.2022.100060.

135. SCHWENTENWEIN, M., SCHNEIDER, P. and HOMA, J. *Lithography-Based Ceramic Manufacturing: A Novel Technique for Additive Manufacturing of High-Performance Ceramics.* , 2014 DOI 10.4028/www.scientific.net/AST.88.60.

136. HARTMANN, M., PFAFFINGER, M. and STAMPFL, J. *Lithography-Based Ceramic Manufacturing (LCM) for Dental Applications.* , 2018 DOI 10.4028/www.scientific.net/MSF.939.95.

137. RAIMONDI, M.T., et al. Two-Photon Laser Polymerization: From Fundamentals to Biomedical Application in Tissue Engineering and Regenerative Medicine. *Journal of Applied Biomaterials & Functional Materials*, 2012, vol. 10, no. 1. pp. 56-66. Available from: https://doi.org/10.5301/JABFM.2012.9278 ISSN 2280-8000. DOI 10.5301/JABFM.2012.9278.

138. NGUYEN, A.K. and NARAYAN, R.J. Two-Photon Polymerization for Biological Applications. *Materials Today*, 2017, vol. 20, no. 6. pp. 314-322. Available from: https://www.sciencedirect.com/science/article/pii/S1369702117303917 ISSN 1369-7021. DOI 10.1016/j.mattod.2017.06.004.

139. MURPHY, S.V., SKARDAL, A. and ATALA, A. Evaluation of Hydrogels for Bio-Printing Applications. *Journal of Biomedical Materials Research Part A*, 2013, vol. 101A, no. 1. pp. 272-284. Available from: https://doi.org/10.1002/jbm.a.34326 ISSN 1549-3296. DOI 10.1002/jbm.a.34326.

140. LI, H., TAN, C. and LI, L. Review of 3D Printable Hydrogels and Constructs. *Materials & Design*, 2018, vol. 159. pp. 20-38. Available from: https://www.sciencedirect.com/science/article/pii/S0264127518306385 ISSN 0264-1275. DOI 10.1016/j.matdes.2018.08.023.

141. MURPHY, S.V. and ATALA, A. 3D Bioprinting of Tissues and Organs. *Nature Biotechnology*, 2014, vol. 32, no. 8. pp. 773-785. Available from: https://doi.org/10.1038/nbt.2958 ISSN 1546-1696. DOI 10.1038/nbt.2958.

142. DILOKSUMPAN, P., et al. Combining Multi-Scale 3D Printing Technologies to Engineer Reinforced Hydrogel-Ceramic Interfaces. *Biofabrication*, 20200219, Feb 19, 2020, vol. 12, no. 2. pp. 025014-5090/ab69d9 ISSN 1758-5090; 1758-5082; 1758-5082. DOI 10.1088/1758-5090/ab69d9.

143. ABASALIZADEH, F., et al. Alginate-Based Hydrogels as Drug Delivery Vehicles in Cancer Treatment and their Applications in Wound Dressing and 3D Bioprinting. *Journal of Biological Engineering*, 2020, vol. 14, no. 1. pp. 8. Available from: https://doi.org/10.1186/s13036-020-0227-7 ISSN 1754-1611. DOI 10.1186/s13036-020-0227-7.

144. BAPTISTA, R. and GUEDES, M. Morphological and Mechanical Characterization of 3D Printed PLA Scaffolds with Controlled Porosity for Trabecular Bone Tissue Replacement. *Materials Science & Engineering.C, Materials for Biological Applications*, 20200918, Jan, 2021, vol. 118. pp. 111528 ISSN 1873-0191; 0928-4931. DOI 10.1016/j.msec.2020.111528.

145. VIGUET-CARRIN, S., GARNERO, P. and DELMAS, P.D. The Role of Collagen in Bone Strength. *Osteoporosis International : A Journal Established as Result of Cooperation between the European Foundation for Osteoporosis and the National Osteoporosis Foundation of the USA*, 20051209, 2006, vol. 17, no. 3. pp. 319-336 ISSN 0937-941X; 0937-941X. DOI 10.1007/s00198-005-2035-9.

146. MARTINEZ, J.S., et al. High Resolution DLP Stereolithography to Fabricate Biocompatible Hydroxyapatite Structures that Support Osteogenesis. *PloS One*, 20220808, Aug 8, 2022, vol. 17, no. 8. pp. e0272283 ISSN 1932-6203; 1932-6203. DOI 10.1371/journal.pone.0272283.

147. PFAFFINGER, M., HARTMANN, M., SCHWENTENWEIN, M. and STAMPFL, J. Stabilization of Tricalcium Phosphate Slurries Against Sedimentation for Stereolithographic Additive Manufacturing and Influence on the Final Mechanical Properties. *International Journal of Applied Ceramic Technology*, 2017, vol. 14 DOI 10.1111/ijac.12664.

148. BAINO, F., et al. Making Foam-Like Bioactive Glass Scaffolds by Vat Photopolymerization. *Open Ceramics*, 2023, vol. 15. pp. 100392. Available from: https://www.sciencedirect.com/science/article/pii/S2666539523000640 ISSN 2666-5395. DOI 10.1016/j.oceram.2023.100392.

149. *ISO/ASTM 52900:2021(En), Additive Manufacturing — General Principles — Fundamentals and Vocabulary*. [viewed Feb 20, 2024]. Available from: https://www.iso.org/obp/ui/#iso:std:iso-astm:52900:ed-2:v1:en.

150. GIANNITELLI, S.M., ACCOTO, D., TROMBETTA, M. and RAINER, A. Current Trends in the Design of Scaffolds for Computer-Aided Tissue Engineering. *Acta Biomaterialia*, 2014, vol. 10, no. 2. pp. 580-594. Available from: https://www.sciencedirect.com/science/article/pii/S1742706113005412 ISSN 1742-7061. DOI 10.1016/j.actbio.2013.10.024.

151. SUN, W., DARLING, A., STARLY, B. and NAM, J. Computer-Aided Tissue Engineering: Overview, Scope and Challenges. *Biotechnology and Applied Biochemistry*, 2004, vol. 39, no. 1. pp. 29-47. Available from: https://doi.org/10.1042/BA20030108 ISSN 0885-4513. DOI 10.1042/BA20030108.

152. *Autodesk Empowers Innovators Everywhere to make the New Possible.* [viewed Feb 17, 2024]. Available from:https://www.autodesk.com/.

153. *Dassault Systèmes.* 2022-04-28T11:26:32+0000, 2022-04-28T11:26:32+0000 [viewed Feb 17, 2024]. Available from:https://www.3ds.com/.

154. LIN, Y., WANG, C. and DAI, K. Reverse Engineering in CAD Model Reconstruction of Customized Artificial Joint. *Medical Engineering & Physics*, 2005, vol. 27, no. 2. pp. 189-193. Available from: https://www.sciencedirect.com/science/article/pii/S1350453304001729 ISSN 1350-4533. DOI 10.1016/j.medengphy.2004.09.006.

155. R. Racasan, D. Popescu, C. Neamtu and M. Dragomir. *Integrating the Concept of Reverse Engineering in Medical Applications.* , 2010 ISBN null. DOI 10.1109/AQTR.2010.5520710.

156. *Design, Manufacturing & Lifecycle Management | Siemens.* [viewed Feb 17, 2024]. Available from:https://plm.sw.siemens.com/en-US/.

157. OLIVARES, A.L., MARSAL, È, PLANELL, J.A. and LACROIX, D. Finite Element Study of Scaffold Architecture Design and Culture Conditions for Tissue Engineering. *Biomaterials*, 2009, vol. 30, no. 30. pp. 6142-6149. Available from: https://www.sciencedirect.com/science/article/pii/S0142961209007777 ISSN 0142-9612. DOI 10.1016/j.biomaterials.2009.07.041.

158. MARTÍNEZ CENDRERO, A., FRANCO MARTÍNEZ, F., SOLÓRZANO REQUEJO, W.G. and DÍAZ LANTADA, A. Open-Source Library of Tissue Engineering Scaffolds. *Materials & Design*, 2022, vol. 223. pp. 111154. Available from: https://www.sciencedirect.com/science/article/pii/S0264127522007766 ISSN 0264-1275. DOI 10.1016/j.matdes.2022.111154.

159. *Next-Gen Engineering Design Software: nTop (Formerly nTopology).* [viewed Feb 17, 2024]. Available from:https://www.ntop.com/.

160. ASHBY, M.F. and CEBON, D. Materials Selection in Mechanical Design. *Le Journal De Physique IV*, 1993, vol. 3, no. C7. pp. C7-9 DOI 10.1051/jp4:1993701.

161. *UltiMaker Cura.* [viewed Feb 17, 2024]. Available from:https://ultimaker.com/software/ultimaker-cura/.

162. *Bambu Studio.* Available from:https://bambulab.com/en/download/studio.

163. *CHITUBOX / All-in-One SLA/DLP/LCD Slicer / 3D Printing Preprocessing Software-.* [viewed Feb 17, 2024]. Available from:https://www.chitubox.com/en/index.

164. LIU, B., WANG, Y., LIN, Z. and ZHANG, T. *Creating Metal Parts by Fused Deposition Modeling and Sintering.* , 2019 DOI 10.1016/j.matlet.2019.127252.

165. GRÉMARE, A., et al. Characterization of Printed PLA Scaffolds for Bone Tissue Engineering. *Journal of Biomedical Materials Research.Part A*, 20171120, Apr, 2018, vol. 106, no. 4. pp. 887-894 ISSN 1552-4965; 1549-3296. DOI 10.1002/jbm.a.36289.

166. SOUFIVAND, A.A., ABOLFATHI, N., HASHEMI, A. and LEE, S.J. The Effect of 3D Printing on the Morphological and Mechanical Properties of Polycaprolactone Filament and Scaffold. *Polymers for Advanced Technologies*, 2020, vol. 31, no. 5. pp. 1038-1046. Available from: https://doi.org/10.1002/pat.4838 ISSN 1042-7147. DOI 10.1002/pat.4838.

167. HIEU, L.C., et al. Medical Rapid Prototyping Applications and Methods. *Assembly Automation*, 2005, vol. 25, no. 4. pp. 284-292. Available from: https://doi.org/10.1108/01445150510626415 ISSN 0144-5154. DOI 10.1108/01445150510626415.

168. GIBSON, I., et al. The use of Rapid Prototyping to Assist Medical Applications. *Rapid Prototyping Journal*, 2006, vol. 12, no. 1. pp. 53-58. Available from: https://doi.org/10.1108/13552540610637273 ISSN 1355-2546. DOI 10.1108/13552540610637273.

169. ZADPOOR, A.A. Design for Additive Bio-Manufacturing: From Patient-Specific Medical Devices to Rationally Designed Meta-Biomaterials. *International Journal of Molecular Sciences*, 2017, vol. 18, no. 8 ISSN 1422-0067. DOI 10.3390/ijms18081607.

170. MOHANTY, S., et al. *Fabrication of Scalable and Structured Tissue Engineering Scaffolds using Water Dissolvable Sacrificial 3D Printed Moulds.* , 2015 Available from: https://www.sciencedirect.com/science/article/pii/S092849311530134X ISBN 0928-4931. DOI 10.1016/j.msec.2015.06.002.

171. DAHLBERG, T., et al. 3D Printed Water-Soluble Scaffolds for Rapid Production of PDMS Micro-Fluidic Flow Chambers. *Scientific Reports*, 20180220, Feb 20, 2018, vol. 8, no. 1. pp. 3372-w ISSN 2045-2322; 2045-2322. DOI 10.1038/s41598-018-21638-w.

172. *Offical Tevo 3D Printer Store | TEVOUP 3D Printer Store.* [viewed Feb 18, 2024]. Available from:https://tevoup.com/.

173. Smart Materials. *Smart Materials Catalogue.* [viewed Feb 26, 2024]. Available from:https://www.smartmaterials3d.com/upload/catalogo-online/catalogo-espanol-2023.pdf.

174. TSOLAKIS, I.A., et al. Comparison in Terms of Accuracy between DLP and LCD Printing Technology for Dental Model Printing. *Dentistry Journal*, 2022, vol. 10, no. 10 ISSN 2304-6767. DOI 10.3390/dj10100181.

175. *ANYCUBIC Official Website | Innovative Desktop 3D Printer Manufacturer.* [viewed Feb 17, 2024]. Available from:https://store.anycubic.com/.

176. *Phrozen Technology ⁄Desktop LCD 3D Printer ⁄High Resolution.* [viewed Feb 17, 2024]. Available from:https://phrozen3d.com/.

177. SEITZ, H., et al. Rapid Prototyping Models for Surgical Planning with Hard and Soft Tissue Representation. *International Congress Series*, 2004, vol. 1268. pp. 567-572. Available from: https://www.sciencedirect.com/science/article/pii/S0531513104005680 ISSN 0531-5131. DOI 10.1016/j.ics.2004.03.139.

178. CHEE KAI, C., et al. Facial Prosthetic Model Fabrication using Rapid Prototyping Tools. *Integrated Manufacturing Systems*, 2000, vol. 11, no. 1. pp. 42-53. Available from: https://doi.org/10.1108/09576060010303668 ISSN 0957-6061. DOI 10.1108/09576060010303668.

179. HEK GmbH. *MCP 004 ST - Technical Data.*

180. FEROCA, S.A. *Silicona Easyplat Mold-40 Datasheet.*

181. *Vacuum Casting.* [viewed Feb 18, 2024]. Available from:https://aaryaindustries.in/index.php/vacuum-casting/.

182. *Stratasys - Industrial 3D Printing Manufacturers.* [viewed Feb 17, 2024]. Available from:https://www.stratasys.com/en/.

183. KOZIOR, T., et al. Analysis of Metrological Quality and Mechanical Properties of Models Manufactured with Photo-Curing PolyJet Matrix Technology for Medical Applications. *Polymers*, 2022, vol. 14, no. 3 ISSN 2073-4360. DOI 10.3390/polym14030408.

184. AREFIN, A.M.E., KHATRI, N.R., KULKARNI, N. and EGAN, P.F. Polymer 3D Printing Review: Materials, Process, and Design Strategies for Medical Applications. *Polymers*, 2021, vol. 13, no. 9 ISSN 2073-4360. DOI 10.3390/polym13091499.

185. *Stratasys PolyJet Materials.* [viewed Feb 18, 2024]. Available from:https://www.stratasys.com/en/materials/materials-catalog/polyjet-materials/.

186. *Industrial, Commercial, & Professional 3D Printers.* [viewed Feb 18, 2024]. Available from:https://www.stratasys.com/en/3d-printers/printer-catalog/?q=J5&filter=PolyJet&s=true.

187. DIAZ LANTADA, A., et al. *Lithography-Based Ceramic Manufacture (LCM) of Auxetic Structures: Present Capabilities and Challenges.* , 2016.

188. ALTUN, A.A., et al. Additive Manufacturing of Lunar Regolith Structures. *Open Ceramics*, 2021, vol. 5. pp. 100058. Available from: https://www.sciencedirect.com/science/article/pii/S2666539521000043 ISSN 2666-5395. DOI 10.1016/j.oceram.2021.100058.

189. A. ELT. *Ceramic 3D Printer: CeraFab S65 Medical.* -05-09T23:50:17, 2022 [viewed Feb 18, 2024]. Available from:https://lithoz.com/en/3d-printer/cerafab-system-medical/.

190. S. ROMSTORFER. *Ceramic Material: LithaCon ATZ 980.* -03-27T17:41:58, 2023 [viewed Feb 18, 2024]. Available from:https://lithoz.com/en/materials/lithacon-atz-980/.

191. A. ELT. *Ceramic Material: LithaBone HA 480.* -09-21T09:41:58, 2022 [viewed Feb 18, 2024]. Available from:https://lithoz.com/en/materials/lithabone-ha-480/.

192. *HOME En.* [viewed Feb 18, 2024]. Available from:https://deltatower.ch/en/home-2/.

193. *Elkem.* [viewed Feb 17, 2024]. Available from:https://www.elkem.com/.

194. *Silbione™ : Silicone Products for Human Health.* [viewed Feb 17, 2024]. Available from:https://www.elkem.com/products/silicones/silbione/.

195. *Delta Tower FLuid 3D Printer.* [viewed Feb 18, 2024]. Available from:https://deltatower.ch/en/fluid-2/.

196. T. EINHAUER. *LCM Technology.* -04-15T11:58:26, 2022 [viewed Feb 19, 2024]. Available from:https://lithoz.com/en/technology/lcm-technology/.

197. M. AASVIK. *Building a Large Kossel Delta Printer – Pt. 1: Parts and Planning.* [viewed Feb 19, 2024]. Available from:https://www.norwegiancreations.com/2017/01/building-a-large-kossel-delta-printer-pt-1-parts-and-planning/.

198. GOLHIN, A.P., et al. Effects of Accelerated Aging on the Appearance and Mechanical Performance of Materials Jetting Products. *Materials & Design*, 2023, vol. 228. pp. 111863. Available from: https://www.sciencedirect.com/science/article/pii/S0264127523002782 ISSN 0264-1275. DOI 10.1016/j.matdes.2023.111863.

199. *3D Printed Parts & Medical Training Aids | Healthcare.* [viewed Feb 19, 2024]. Available from:https://www.elkem.com/markets/healthcare/3d-printed-parts-medical-training-aids/.

200. I. ZITKOVA. *Ceramic 3D Printing: Medical.* -03-10T11:19:42, 2022 [viewed Feb 19, 2024]. Available from:https://lithoz.com/en/applications/medical/.

201. *PolyJet 3D Printed Parts on Demand | Stratasys Direct.* [viewed Feb 19, 2024]. Available from:https://www.stratasys.com/en/stratasysdirect/technologies/3d-printing/polyjet/.

202. CHEAH, C.M., CHUA, C.K., LEONG, K.F. and CHUA, S.W. Development of a Tissue Engineering Scaffold Structure Library for Rapid Prototyping. Part 1: Investigation and Classification. *The International Journal of Advanced Manufacturing Technology*, 2003, vol. 21, no. 4. pp. 291-301. Available from: https://doi.org/10.1007/s001700300034 ISSN 1433-3015. DOI 10.1007/s001700300034.

203. CHEAH, C.M., CHUA, C.K., LEONG, K.F. and CHUA, S.W. Development of a Tissue Engineering Scaffold Structure Library for Rapid Prototyping. Part 2: Parametric Library and Assembly Program. *The International Journal of Advanced Manufacturing Technology*, 2003, vol. 21. pp. 302-312 DOI 10.1007/s001700300035.

204. CHANTARAPANICH, N., et al. Scaffold Library for Tissue Engineering: A Geometric Evaluation. *Computational and Mathematical Methods in Medicine*, 2012, vol. 2012. pp. 407805 DOI 10.1155/2012/407805.

205. DONG, L., DESHPANDE, V.S. and WADLEY, H.N.G. Mechanical Response of Ti-6Al-4V Octet-Truss Lattice Structures. *International Journal of Solids and Structures*, 2015, vol. 60 DOI 10.1016/j.ijsolstr.2015.02.020.

206. ZHANG, Z., et al. Bamboo-Inspired, Simulation-Guided Design and 3D Printing of Light-Weight and High-Strength Mechanical Metamaterials. *Applied Materials Today*, 2021, vol. 26. pp. 101268 DOI 10.1016/j.apmt.2021.101268.

207. EGAN, P.F., et al. Computationally Designed Lattices with Tuned Properties for Tissue Engineering using 3D Printing. *PloS One*, 20170810, Aug 10, 2017, vol. 12, no. 8. pp. e0182902 ISSN 1932-6203; 1932-6203. DOI 10.1371/journal.pone.0182902.

208. EGAN, P.F., BAUER, I., SHEA, K. and FERGUSON, S.J. Mechanics of Three-Dimensional Printed Lattices for Biomedical Devices. *Journal of Mechanical Design*, 2019, vol.

141, no. 3. Available from: https://doi.org/10.1115/1.4042213 ISSN 1050-0472. DOI 10.1115/1.4042213.

209. BRIGUIET, G. and EGAN, P.F. *Structure, Process, and Material Influences for 3D Printed Lattices Designed with Mixed Unit Cells.* , 2020 Available from: https://doi.org/10.1115/DETC2020-22575 DOI 10.1115/DETC2020-22575.

210. EGAN, P.F., SHEA, K.A. and FERGUSON, S.J. Simulated Tissue Growth for 3D Printed Scaffolds. *Biomechanics and Modeling in Mechanobiology*, 20180606, Oct, 2018, vol. 17, no. 5. pp. 1481-1495 ISSN 1617-7940; 1617-7940. DOI 10.1007/s10237-018-1040-9.

211. CAMPBELL, J., et al. Multimaterial and Multiscale Three-Dimensional Bioprinter. *Journal of Nanotechnology in Engineering and Medicine*, 2015, vol. 6 DOI 10.1115/1.4031230.

212. LI, C., OUYANG, L., ARMSTRONG, J.P.K. and STEVENS, M.M. Advances in the Fabrication of Biomaterials for Gradient Tissue Engineering. *Trends in Biotechnology*, 20200707, Feb, 2021, vol. 39, no. 2. pp. 150-164 ISSN 1879-3096; 0167-7799. DOI 10.1016/j.tibtech.2020.06.005.

213. DIAZ LANTADA, A., DE BLAS ROMERO, A., ISASI, Á and BELLIDO, D. Design and Performance Assessment of Innovative Eco-Efficient Support Structures for Additive Manufacturing by Photopolymerization: Eco-Efficient Supports for Additive Manufacturing. *Journal of Industrial Ecology*, 2017, vol. 21 DOI 10.1111/jiec.12660.

214. DÍAZ LANTADA, A., et al. Tissue Engineering Scaffolds for Bone Repair: General Aspects. *Microsystems for Enhanced Control of Cell Behavior: Fundamentals, Design and Manufacturing Strategies, Applications and Challenges*, 2016. pp. 269-285.

215. DIAS, M.R., FERNANDES, P.R., GUEDES, J.M. and HOLLISTER, S.J. Permeability Analysis of Scaffolds for Bone Tissue Engineering. *Journal of Biomechanics*, 20120224, Apr 5, 2012, vol. 45, no. 6. pp. 938-944 ISSN 1873-2380; 0021-9290. DOI 10.1016/j.jbiomech.2012.01.019.

216. MONTAZERIAN, H., et al. Permeability and Mechanical Properties of Gradient Porous PDMS Scaffolds Fabricated by 3D-Printed Sacrificial Templates Designed with Minimal Surfaces. *Acta Biomaterialia*, 20190625, Sep 15, 2019, vol. 96. pp. 149-160 ISSN 1878-7568; 1742-7061. DOI 10.1016/j.actbio.2019.06.040.

217. MAHAMMOD, B., BARUA, E., DEOGHARE, A. and PANDEY, K. Permeability Quantification of Porous Polymer Scaffold for Bone Tissue Engineering. *Materials Today: Proceedings*, 2020, vol. 22. pp. 1687-1693 DOI 10.1016/j.matpr.2020.02.186.

218. LEONG, K.F., CHUA, C.K., SUDARMADJI, N. and YEONG, W.Y. Engineering Functionally Graded Tissue Engineering Scaffolds. *Journal of the Mechanical Behavior of Biomedical Materials*, 20071117, Apr, 2008, vol. 1, no. 2. pp. 140-152 ISSN 1878-0180; 1878-0180. DOI 10.1016/j.jmbbm.2007.11.002.

219. SUDARMADJI, N., et al. Investigation of the Mechanical Properties and Porosity Relationships in Selective Laser-Sintered Polyhedral for Functionally Graded Scaffolds. *Acta*

Biomaterialia, 20100929, Feb, 2011, vol. 7, no. 2. pp. 530-537 ISSN 1878-7568; 1742-7061. DOI 10.1016/j.actbio.2010.09.024.

220. CHUA, C.K., et al. *Process Flow for Designing Functionally Graded Tissue Engineering Scaffolds.* , 2010 ISBN 978-0-415-87307-9. DOI 10.1201/9780203859476.ch6.

221. BOCCACCIO, A., et al. Geometry Design Optimization of Functionally Graded Scaffolds for Bone Tissue Engineering: A Mechanobiological Approach. *PloS One*, 20160115, Jan 15, 2016, vol. 11, no. 1. pp. e0146935 ISSN 1932-6203; 1932-6203. DOI 10.1371/journal.pone.0146935.

222. ZHOU, X., JIN, Y. and DU, J. Functionally Graded Scaffolds with Programmable Pore Size Distribution Based on Triply Periodic Minimal Surface Fabricated by Selective Laser Melting. *Materials (Basel, Switzerland)*, 20201109, Nov 9, 2020, vol. 13, no. 21. pp. 5046. doi: 10.3390/ma13215046 ISSN 1996-1944; 1996-1944; 1996-1944. DOI 10.3390/ma13215046.

223. LIU, F., et al. Functionally Graded Porous Scaffolds in Multiple Patterns: New Design Method, Physical and Mechanical Properties. *Materials & Design*, 2018, vol. 160 DOI 10.1016/j.matdes.2018.09.053.

224. SHI, H., et al. Functional Gradient Metallic Biomaterials: Techniques, Current Scenery, and Future Prospects in the Biomedical Field. *Frontiers in Bioengineering and Biotechnology*, 20210118, Jan 18, 2021, vol. 8. pp. 616845 ISSN 2296-4185; 2296-4185; 2296-4185. DOI 10.3389/fbioe.2020.616845.

225. SCAFFARO, R., et al. Development of Polymeric Functionally Graded Scaffolds: A Brief Review. *Journal of Applied Biomaterials & Functional Materials*, 20170426, Apr 26, 2017, vol. 15, no. 2. pp. e107-e121 ISSN 2280-8000; 2280-8000. DOI 10.5301/jabfm.5000332.

226. DIXIT, K., RAICHUR, A. and SINHA, N. Polymer-Coated and Nanofiber-Reinforced Functionally Graded Bioactive Glass Scaffolds Fabricated using Additive Manufacturing. *IEEE Transactions on Nanobioscience*, 20220630, Jul, 2022, vol. 21, no. 3. pp. 380-386 ISSN 1558-2639; 1536-1241. DOI 10.1109/TNB.2021.3083278.

227. KANG, H., ZENG, Y. and VARGHESE, S. Functionally Graded Multilayer Scaffolds for in Vivo Osteochondral Tissue Engineering. *Acta Biomaterialia*, 20180719, Sep 15, 2018, vol. 78. pp. 365-377 ISSN 1878-7568; 1742-7061; 1742-7061. DOI 10.1016/j.actbio.2018.07.039.

228. LONGLEY, R., FERREIRA, A.M. and GENTILE, P. Recent Approaches to the Manufacturing of Biomimetic Multi-Phasic Scaffolds for Osteochondral Regeneration. *International Journal of Molecular Sciences*, 20180613, Jun 13, 2018, vol. 19, no. 6. pp. 1755. doi: 10.3390/ijms19061755 ISSN 1422-0067; 1422-0067. DOI 10.3390/ijms19061755.

229. ZHANG, T., et al. Biomimetic Design and Fabrication of Multilayered Osteochondral Scaffolds by Low-Temperature Deposition Manufacturing and Thermal-Induced Phase-Separation Techniques. *Biofabrication*, 20170523, May 23, 2017, vol. 9, no. 2. pp. 025021-5090/aa7078 ISSN 1758-5090; 1758-5082. DOI 10.1088/1758-5090/aa7078.

230. CHEN, J., et al. Simultaneous Regeneration of Articular Cartilage and Subchondral Bone in Vivo using MSCs Induced by a Spatially Controlled Gene Delivery System in Bilayered

Integrated Scaffolds. *Biomaterials*, 20110413, Jul, 2011, vol. 32, no. 21. pp. 4793-4805 ISSN 1878-5905; 0142-9612. DOI 10.1016/j.biomaterials.2011.03.041.

231. DÍAZ LANTADA, A., ALARCÓN INIESTA, H. and GARCÍA-RUÍZ, J.P. Composite Scaffolds for Osteochondral Repair obtained by Combination of Additive Manufacturing, Leaching Processes and hMSC-CM Functionalization. *Materials Science & Engineering.C, Materials for Biological Applications*, 20151008, Feb, 2016, vol. 59. pp. 218-227 ISSN 1873-0191; 0928-4931. DOI 10.1016/j.msec.2015.10.015.

232. HILLMERING F. KARLSSON, J., et al. Fabrication and Transfer of Fragile 3D PDMS Microstructures. *Journal of Micromechanics and Microengineering - J MICROMECHANIC MICROENGINEER*, 2012, vol. 22 DOI 10.1088/0960-1317/22/8/085009.

233. MORSS CLYNE, A., SWAMINATHAN, S. and DÍAZ LANTADA, A. Biofabrication Strategies for Creating Microvascular Complexity. *Biofabrication*, 20190418, Apr 18, 2019, vol. 11, no. 3. pp. 032001-5090/ab0621 ISSN 1758-5090; 1758-5082; 1758-5082. DOI 10.1088/1758-5090/ab0621.

234. GONZÁLEZ-RIVERA, J., et al. Structural and Thermoanalytical Characterization of 3D Porous PDMS Foam Materials: The Effect of Impurities Derived from a Sugar Templating Process. *Polymers*, 2018, vol. 10, no. 6 ISSN 2073-4360. DOI 10.3390/polym10060616.

235. THOMPSON, M.K., et al. *Design for Additive Manufacturing: Trends, Opportunities, Considerations, and Constraints.* , 2016 Available from: https://www.scopus.com/inward/record.uri?eid=2-s2.0-84977624453&doi=10.1016%2fj.cirp.2016.05.004&partnerID=40&md5=2542eb7173f3b7794cd56085056949ce Scopus. DOI 10.1016/j.cirp.2016.05.004.

236. *Human Tibia and Fibula by Hatchmemory.* [viewed Feb 15, 2024]. Available from:https://www.thingiverse.com/thing:1030467.

237. CHAKRABORTY, D., REDDY, B. and CHOUDHURY, A. Extruder Path Generation for Curved Layer Fused Deposition Modeling. *Computer-Aided Design*, 2008, vol. 40. pp. 235-243 DOI 10.1016/j.cad.2007.10.014.

238. Gibson, O. Diegel and S. Singamneni and B. Huang and I. *Curved Layer Fused Deposition Modeling in Conductive Polymer Additive Manufacturing.* , 2011.

239. AHLERS, D., WASSERFALL, F., HENDRICH, N. and ZHANG, J. *3D Printing of Nonplanar Layers for Smooth Surface Generation.* , 2019 DOI 10.13140/RG.2.2.34888.26881.

240. CENDRERO, A.M., et al. *Benefits of Non-Planar Printing Strategies Towards Eco-Efficient 3D Printing.* , 2021 ISBN 2071-1050. DOI 10.3390/su13041599.

241. CHUAH, Y.J., et al. Simple Surface Engineering of Polydimethylsiloxane with Polydopamine for Stabilized Mesenchymal Stem Cell Adhesion and Multipotency. *Scientific Reports*, 20151209, Dec 9, 2015, vol. 5. pp. 18162 ISSN 2045-2322; 2045-2322. DOI 10.1038/srep18162.

242. OZBOLAT, V., et al. 3D Printing of PDMS Improves its Mechanical and Cell Adhesion Properties. *ACS Biomaterials Science & Engineering*, 20180108, Feb 12, 2018, vol. 4, no. 2. pp. 682-693 ISSN 2373-9878; 2373-9878. DOI 10.1021/acsbiomaterials.7b00646.

243. DAVOODI, E., et al. Extrusion and Microfluidic-Based Bioprinting to Fabricate Biomimetic Tissues and Organs. *Advanced Materials Technologies*, 20200526, Aug, 2020, vol. 5, no. 8. pp. 1901044. doi: 10.1002/admt.201901044. Epub 2020 May 26 ISSN 2365-709X. DOI 10.1002/admt.201901044.

244. FENG, J., et al. A Review of the Design Methods of Complex Topology Structures for 3D Printing. *Visual Computing for Industry, Biomedicine, and Art*, 20180905, Sep 5, 2018, vol. 1, no. 1. pp. 5-3 ISSN 2524-4442; 2096-496X; 2524-4442. DOI 10.1186/s42492-018-0004-3.

245. BADER, B., et al. Making Data Matter: Voxel Printing for the Digital Fabrication of Data Across Scales and Domains. *Science Advances*, 2018, vol. 4, no. 5. pp. eaas8652. Available from: https://doi.org/10.1126/sciadv.aas8652 DOI 10.1126/sciadv.aas8652.

246. SKYLAR-SCOTT, M.A., MUELLER, J., VISSER, C.W. and LEWIS, J.A. Voxelated Soft Matter Via Multimaterial Multinozzle 3D Printing. *Nature*, 20191113, Nov, 2019, vol. 575, no. 7782. pp. 330-335 ISSN 1476-4687; 0028-0836. DOI 10.1038/s41586-019-1736-8.

247. SMITH, R., et al. *Hybrid Living Materials: Digital Design and Fabrication of 3D Multimaterial Structures with Programmable Biohybrid Surfaces.* , 2019 DOI 10.1002/adfm.201907401.

248. FOX, A.J.S., et al. The Human Meniscus: A Review of Anatomy, Function, Injury, and Advances in Treatment. *Clinical Anatomy*, 2015, vol. 28, no. 2. pp. 269-287. Available from: https://doi.org/10.1002/ca.22456 ISSN 0897-3806. DOI 10.1002/ca.22456.

249. LUVSANNYAM, E., et al. Meniscus Tear: Pathology, Incidence, and Management. *Cureus*, 20220518, May 18, 2022, vol. 14, no. 5. pp. e25121 ISSN 2168-8184; 2168-8184; 2168-8184. DOI 10.7759/cureus.25121.

250. DROSOS, G.I. and POZO, J.L. The Causes and Mechanisms of Meniscal Injuries in the Sporting and Non-Sporting Environment in an Unselected Population. *The Knee*, 2004, vol. 11, no. 2. pp. 143-149. Available from: https://www.sciencedirect.com/science/article/pii/S0968016003001054 ISSN 0968-0160. DOI 10.1016/S0968-0160(03)00105-4.

251. BUCHBINDER, R., IAN, A.H. and SPROWSON, A. Management of Degenerative Meniscal Tears and the Role of Surgery. *Br J Sports Med*, 2016, vol. 50, no. 22. pp. 1413. Available from: http://bjsm.bmj.com/content/50/22/1413.abstract DOI 10.1136/bmj.h2212.

252. M.D. MARK AWH. *Meniscal Tear Patterns.* -02-01T19:38:32+00:00, 2008 [viewed Jan 24, 2024]. Available from:https://radsource.us/meniscal-tear-patterns/.

253. BEDNARSKI, R. and BIELAK, A. Use of Motion Capture in Assisted of Knee Ligament Injury Diagnosis, 2018.

254. VINAGRE, G., CRUZ, F., ALKHELAIFI, K. and D'HOOGHE, P. *Isolated Meniscus Injuries in Skeletally Immature Children and Adolescents: State of the Art.* Elsevier BV, -05-23, 2021 ISBN 2059-7754. DOI 10.1136/jisakos-2020-000496.

255. MUCHÉ, J.A. Efficacy of Therapeutic Ultrasound Treatment of a Meniscus Tear in a Severely Disabled Patient: A Case report11No Commercial Party having a Direct Financial Interest in the Results of the Research Supporting this Article has Or Will Confer a Benefit upon the Author(s) Or upon any Organization with which the Author(s) is/are Associated. *Archives of Physical Medicine and Rehabilitation*, 2003, vol. 84, no. 10. pp. 1558-1559. Available from: https://www.sciencedirect.com/science/article/pii/S0003999303003150 ISSN 0003-9993. DOI 10.1016/S0003-9993(03)00315-0.

256. PAXTON, E.S., STOCK, M.V. and BROPHY, R.H. Meniscal Repair Versus Partial Meniscectomy: A Systematic Review Comparing Reoperation Rates and Clinical Outcomes. *Arthroscopy: The Journal of Arthroscopic & Related Surgery*, 2011, vol. 27, no. 9. pp. 1275-1288. Available from: https://www.sciencedirect.com/science/article/pii/S0749806311004129 ISSN 0749-8063. DOI 10.1016/j.arthro.2011.03.088.

257. BERTON, A., et al. Quantitative Evaluation of Meniscal Healing Process of Degenerative Meniscus Lesions Treated with Hyaluronic Acid: A Clinical and MRI Study. *Journal of Clinical Medicine*, 2020, vol. 9, no. 7 ISSN 2077-0383. DOI 10.3390/jcm9072280.

258. BUMA, P., VAN TIENEN, T. and VETH, R.P. The Collagen Meniscus Implant. *Expert Review of Medical Devices*, 2007, vol. 4, no. 4. pp. 507-516. Available from: https://doi.org/10.1586/17434440.4.4.507 ISSN 1743-4440. DOI 10.1586/17434440.4.4.507.

259. YOUNG, J., TUDOR, F., MAHMOUD, A. and MYERS, P. Meniscal Transplantation: Procedures, Outcomes, and Rehabilitation. *Orthopedic Research and Reviews*, 20170515, May 15, 2017, vol. 9. pp. 35-43 ISSN 1179-1462; 1179-1462. DOI 10.2147/ORR.S94378.

260. Stryker. The Collagen Meniscus Implant [viewed Feb 19, 2024]. Available from: https://www.stryker.com/content/dam/stryker/sports-medicine/products/collagenmeniscusimplant/resources/CMI%20surgical%20technique%20guide.pdf.

261. ZHANG, Z., et al. *Role of Scaffold Mean Pore Size in Meniscus Regeneration.* Elsevier BV, -07-29, 2016 ISBN 1742-7061. DOI 10.1016/j.actbio.2016.07.050.

262. LUIS, E., et al. 3D Printed Silicone Meniscus Implants: Influence of the 3D Printing Process on Properties of Silicone Implants. *Polymers*, 2020, vol. 12, no. 9 ISSN 2073-4360. DOI 10.3390/polym12092136.

263. *How to Create a Periodic Lattice.* [viewed Feb 17, 2024]. Available from:https://support.ntop.com/hc/en-us/articles/360050828294-How-to-create-a-periodic-lattice.

264. VIGNES, H., CONZATTI, G., HUA, G. and BENKIRANE-JESSEL, N. Meniscus Repair: From in Vitro Research to Patients. *Organoids*, 2022, vol. 1, no. 2. pp. 134 ISSN 2674-1172. DOI 10.3390/organoids1020010.

265. MARTIN, I., et al. Osteochondral Tissue Engineering. *Journal of Biomechanics*, 2007, vol. 40, no. 4. pp. 750-765. Available from:

https://www.sciencedirect.com/science/article/pii/S0021929006000960 ISSN 0021-9290. DOI 10.1016/j.jbiomech.2006.03.008.

266. NUKAVARAPU, S.P. and DORCEMUS, D.L. Osteochondral Tissue Engineering: Current Strategies and Challenges. *Biotechnology Advances*, 2013, vol. 31, no. 5. pp. 706-721. Available from: https://www.sciencedirect.com/science/article/pii/S0734975012001899 ISSN 0734-9750. DOI 10.1016/j.biotechadv.2012.11.004.

267. FARMER, J.M., MARTIN, D.F., BOLES, C.A. and CURL, W.W. CHONDRAL AND OSTEOCHONDRAL INJURIES: Diagnosis and Management. *Clinics in Sports Medicine*, 2001, vol. 20, no. 2. pp. 299-320. Available from: https://www.sciencedirect.com/science/article/pii/S0278591905703082 ISSN 0278-5919. DOI 10.1016/S0278-5919(05)70308-2.

268. SANDERS, R.K. and CRIM, J.R. Osteochondral Injuries. *Seminars in Ultrasound, CT and MRI*, 2001, vol. 22, no. 4. pp. 352-370. Available from: https://www.sciencedirect.com/science/article/pii/S0887217101900265 ISSN 0887-2171. DOI 10.1016/S0887-2171(01)90026-5.

269. OLIVEIRA SILVA, M., GREGORY, J.L., ANSARI, N. and STOK, K.S. Molecular Signaling Interactions and Transport at the Osteochondral Interface: A Review. *Frontiers in Cell and Developmental Biology*, 2020, vol. 8. Available from: https://www.frontiersin.org/articles/10.3389/fcell.2020.00750 ISSN 2296-634X.

270. Chondral Injury | Chondral Lesion | Chondral Defect | Orthopedic Knee Specialist | Manhattan, Brooklyn, New York City NY. -11-09T20:34:43+00:00, 2020 [viewed Feb 18, 2024]. Available from: https://rileywilliamsmd.com/chondral-injury-defect-lesion-manhattan-new-york-city-ny/.

271. ROBERT, H. Chondral Repair of the Knee Joint using Mosaicplasty. *Orthopaedics & Traumatology, Surgery & Research : OTSR*, 20110523, Jun, 2011, vol. 97, no. 4. pp. 418-429 ISSN 1877-0568; 1877-0568. DOI 10.1016/j.otsr.2011.04.001.

272. MUELLNER, T., KNOPP, A., LUDVIGSEN, T.C. and ENGEBRETSEN, L. Failed Autologous Chondrocyte Implantation. *Am J Sports Med*, 2001, vol. 29, no. 4. pp. 516-519. Available from: https://doi.org/10.1177/03635465010290042301 ISSN 0363-5465. DOI 10.1177/03635465010290042301.

273. CHAHAL, J., et al. Outcomes of Osteochondral Allograft Transplantation in the Knee. *Arthroscopy: The Journal of Arthroscopic & Related Surgery*, 2013, vol. 29, no. 3. pp. 575-588. Available from: https://www.sciencedirect.com/science/article/pii/S0749806312018932 ISSN 0749-8063. DOI 10.1016/j.arthro.2012.12.002.

274. SLEDGE, S.L. Microfracture Techniques in the Treatment of Osteochondral Injuries. *Clinics in Sports Medicine*, 2001, vol. 20, no. 2. pp. 365-378. Available from: https://www.sciencedirect.com/science/article/pii/S0278591905703112 ISSN 0278-5919. DOI 10.1016/S0278-5919(05)70311-2.

275. PASCULLI, R.M., et al. Mesenchymal Stem Cells for Subchondral Bone Marrow Lesions: From Bench to Bedside. *Bone Reports*, 20221021, Oct 21, 2022, vol. 17. pp. 101630 ISSN 2352-1872; 2352-1872; 2352-1872. DOI 10.1016/j.bonr.2022.101630.

276. JAISWAL, P.K., et al. Two to Three Year Follow-Up Results of Autologous Chondrocyte Implantation (Aci) Versus Matrix-Induced Autologous Chondrocyte Implantation (Maci) for Osteochondral Defects of the Knee. *Orthopaedic Proceedings*, 2009, vol. 91-B. pp. 84. Available from: https://doi.org/10.1302/0301-620X.91BSUPP_I.0910084a DOI 10.1302/0301-620X.91BSUPP_I.0910084a.

277. BARTLETT, W., et al. Autologous Chondrocyte Implantation Versus Matrix-Induced Autologous Chondrocyte Implantation for Osteochondral Defects of the Knee. *The Journal of Bone & Joint Surgery British Volume*, 2005, vol. 87-B, no. 5. pp. 640-645. Available from: https://doi.org/10.1302/0301-620X.87B5.15905 DOI 10.1302/0301-620X.87B5.15905.

278. YOUSEFI, A., HOQUE, M.E., PRASAD, R.G.S.V. and UTH, N. Current Strategies in Multiphasic Scaffold Design for Osteochondral Tissue Engineering: A Review. *Journal of Biomedical Materials Research Part A*, 2015, vol. 103, no. 7. pp. 2460-2481. Available from: https://doi.org/10.1002/jbm.a.35356 ISSN 1549-3296. DOI 10.1002/jbm.a.35356.

279. TAMPIERI, A., et al. Design of Graded Biomimetic Osteochondral Composite Scaffolds. *Biomaterials*, 2008, vol. 29, no. 26. pp. 3539-3546. Available from: https://www.sciencedirect.com/science/article/pii/S0142961208003542 ISSN 0142-9612. DOI 10.1016/j.biomaterials.2008.05.008.

280. DENG, C., CHANG, J. and WU, C. Bioactive Scaffolds for Osteochondral Regeneration. *Journal of Orthopaedic Translation*, 2019, vol. 17. pp. 15-25. Available from: https://www.sciencedirect.com/science/article/pii/S2214031X18301700 ISSN 2214-031X. DOI 10.1016/j.jot.2018.11.006.

281. *Agili-C™*. [viewed Feb 19, 2024]. Available from:https://www.cartiheal.com/agili-c/.

282. *FDA Approves CartiHeal's Agili-C Implant*. -04-01T02:54:01+00:00, 2022 [viewed Feb 19, 2024]. Available from:https://www.medicalbuyer.co.in/fda-approves-cartiheals-agili-c-implant/.

283. DROBNIČ, M., et al. Treatment of Hallux Rigidus by a Novel Bi-Phasic Aragonite-Based Implant: Results of a Two Year Multi-Centre Clinical Trial. *International Orthopaedics*, 2021, vol. 45, no. 4. pp. 1033-1041. Available from: https://doi.org/10.1007/s00264-020-04872-8 ISSN 1432-5195. DOI 10.1007/s00264-020-04872-8.

284. KON, E., et al. Osteochondral Regeneration using a Novel Aragonite-Hyaluronate Bi-Phasic Scaffold in a Goat Model. *Knee Surgery, Sports Traumatology, Arthroscopy : Official Journal of the ESSKA*, 20130312, Jun, 2014, vol. 22, no. 6. pp. 1452-1464 ISSN 1433-7347; 0942-2056. DOI 10.1007/s00167-013-2467-2.

285. CHUBINSKAYA, S., et al. Agili-C Implant Promotes the Regenerative Capacity of Articular Cartilage Defects in an Ex Vivo Model. *Knee Surgery, Sports Traumatology, Arthroscopy*, 2019, vol. 27, no. 6. pp. 1953-1964. Available from: https://doi.org/10.1007/s00167-018-5263-1 ISSN 1433-7347. DOI 10.1007/s00167-018-5263-1.

286. JACOB, G., SHIMOMURA, K. and NAKAMURA, N. Osteochondral Injury, Management and Tissue Engineering Approaches. *Frontiers in Cell and Developmental Biology*, 20201104, Nov 4, 2020, vol. 8. pp. 580868 ISSN 2296-634X; 2296-634X; 2296-634X. DOI 10.3389/fcell.2020.580868.

287. HART, N.H., et al. Mechanical Basis of Bone Strength: Influence of Bone Material, Bone Structure and Muscle Action. *Journal of Musculoskeletal & Neuronal Interactions*, Sep 1, 2017, vol. 17, no. 3. pp. 114-139 ISSN 1108-7161; 1108-7161.

288. TAICHMAN, R.S. Blood and Bone: Two Tissues Whose Fates are Intertwined to Create the Hematopoietic Stem-Cell Niche. *Blood*, 20041207, Apr 1, 2005, vol. 105, no. 7. pp. 2631-2639 ISSN 0006-4971; 0006-4971. DOI 10.1182/blood-2004-06-2480.

289. CLARKE, B. Normal Bone Anatomy and Physiology. *Clinical Journal of the American Society of Nephrology : CJASN*, Nov, 2008, vol. 3 Suppl 3, no. Suppl 3. pp. 131 ISSN 1555-905X; 1555-9041; 1555-9041. DOI 10.2215/CJN.04151206.

290. DOBLARÉ, M., GARCÍA, J.M. and GÓMEZ, M.J. Modelling Bone Tissue Fracture and Healing: A Review. *Engineering Fracture Mechanics*, 2004, vol. 71, no. 13. pp. 1809-1840. Available from: https://www.sciencedirect.com/science/article/pii/S0013794403002510 ISSN 0013-7944. DOI 10.1016/j.engfracmech.2003.08.003.

291. COOPER, C., CAMPION, G. and MELTON, L.J.3. Hip Fractures in the Elderly: A World-Wide Projection. *Osteoporosis International : A Journal Established as Result of Cooperation between the European Foundation for Osteoporosis and the National Osteoporosis Foundation of the USA*, Nov, 1992, vol. 2, no. 6. pp. 285-289 ISSN 0937-941X; 0937-941X. DOI 10.1007/BF01623184.

292. MARTIN, R.B., BURR, D.B., SHARKEY, N.A. and FYHRIE, D.P. *Skeletal Tissue Mechanics*. Springer, 1998.

293. BURR, D.B. Basic and Applied Bone Biology (Second Edition) D.B. BURR and M.R. ALLEN eds., Academic Press, 2019 *Chapter 1 - Bone Morphology and Organization*, pp. 3-26. Available from: https://www.sciencedirect.com/science/article/pii/B9780128132593000014 ISBN 9780128132593. DOI 10.1016/B978-0-12-813259-3.00001-4.

294. AZNAR, J.M.G. No Title. *Modelos De Remodelación Ósea.Análisis Numérico Y Aplicaciones Al Diseño De Fijaciones De Fracturas Del Fémur Proximal*, 1999.

295. CAEIRO, J.R., GONZÃ¡LEZ, P. and GUEDE, D. Biomecánica Y Hueso (Y II): Ensayos En Los Distintos Niveles Jerárquicos Del Hueso Y Técnicas Alternativas Para La Determinación De La Resistencia Ósea. *Revista De Osteoporosis Y Metabolismo Mineral*, 2013, vol. 5, no. 2. pp. 99-108.

296. PHILLIPS, A. Structural Optimisation: Biomechanics of the Femur. *Proceedings of the ICE - Engineering and Computational Mechanics*, 2011, vol. 165 DOI 10.1680/eacm.10.00032.

297. KLIKA, V., et al. A Coupled Mechano-Biochemical Model for Bone Adaptation. *Journal of Mathematical Biology*, 20131112, Dec, 2014, vol. 69, no. 6-7. pp. 1383-1429 ISSN 1432-1416; 0303-6812. DOI 10.1007/s00285-013-0736-9.

298. ALLEN, M.R. and BURR, D.B. Basic and Applied Bone Biology (Second Edition) D.B. BURR and M.R. ALLEN eds., Academic Press, 2019 *Chapter 5 - Bone Growth, Modeling, and Remodeling*, pp. 85-100. Available from: https://www.sciencedirect.com/science/article/pii/B9780128132593000051 ISBN 9780128132593. DOI 10.1016/B978-0-12-813259-3.00005-1.

299. Carlos Jahel Ojeda Díaz. *Estudio De La Influencia De Estabilidad Primaria En El Diseño De Vástagos De Prótesis Femorales Personalizadas: Aplicación a Paciente Específico.* Ing. Mecánico por la Universidad Nacional de Ingeniería-Perú ed. Universidad Politécnica de Madrid, Mayo, 2009 [viewed Feb 15, 2024]. Available from: https://oa.upm.es/1797/1/CARLOS_JAHEL_OJEDA_DIAZB.pdf.

300. WOLFF, J. Das Gesetz Der Transformation Der Knochen. *DMW-Deutsche Medizinische Wochenschrift*, 1893, vol. 19, no. 47. pp. 1222-1224.

301. FROST, H.M. Bone's Mechanostat: A 2003 Update. *The Anatomical Record Part a: Discoveries in Molecular, Cellular, and Evolutionary Biology: An Official Publication of the American Association of Anatomists*, 2003, vol. 275, no. 2. pp. 1081-1101.

302. SOLÓRZANO-REQUEJO, W., OJEDA, C. and DÍAZ LANTADA, A. Innovative Design Methodology for Patient-Specific Short Femoral Stems. *Materials*, -01-07, 2022, vol. 15, no. 2 ISSN 1996-1944.

303. *Hip Fractures - OrthoInfo - AAOS.* November, 2020 [viewed Feb 15, 2024]. Available from:https://www.orthoinfo.org/en/diseases--conditions/hip-fractures/.

304. ZUCKERMAN, J.D., MD. Hip Fracture. *The New England Journal of Medicine*, 1996, vol. 334, no. 23. pp. 1519-1525. Available from: https://www.proquest.com/scholarly-journals/hip-fracture/docview/223971211/se-2?accountid=14712 https://ingenio.upm.es/openurl/34UPM/34UPM_services_page??url_ver=Z39.88-2004&rft_val_fmt=info:ofi/fmt:kev:mtx:journal&genre=article&sid=ProQ:ProQ%253Ahealthcompleteshell&atitle=Hip+fracture&title=The+New+England+Journal+of+Medicine&issn=00284793&date=1996-06-06&volume=334&issue=23&spage=1519&au=Zuckerman%252C+Joseph+D%252C+MD&isbn=&jtitle=The+New+England+Journal+of+Medicine&btitle=&rft_id=info:eric/8618608&rft_id=info:doi/ ProQuest Central, Research Library. ISSN 00284793. DOI 10.1056/NEJM199606063342307.

305. GRIGORYAN, K.V., JAVEDAN, H. and RUDOLPH, J.L. Orthogeriatric Care Models and Outcomes in Hip Fracture Patients: A Systematic Review and Meta-Analysis. *Journal of Orthopaedic Trauma*, Mar, 2014, vol. 28, no. 3. pp. 49 ISSN 1531-2291; 0890-5339; 0890-5339. DOI 10.1097/BOT.0b013e3182a5a045.

306. NORDIN, M. and FRANKEL, V.H. *Basic Biomechanics of the Musculoskeletal System.* Lippincott Williams & Wilkins, 2001.

307. SHEEHAN, S.E., et al. Proximal Femoral Fractures: What the Orthopedic Surgeon Wants to Know. *Radiographics*, 2015, vol. 35, no. 5. pp. 1563-1584 DOI https://doi.org/10.1148/rg.2015140301.

308. EGOL, K.A., KOVAL, K.J., KUMMER, F. and FRANKEL, V.H. Stress Fractures of the Femoral Neck. *Clinical Orthopaedics and Related Research*, Mar, 1998, vol. (348), no. 348. pp. 72-78 ISSN 0009-921X; 0009-921X.

309. SHAH, A.K., EISSLER, J. and RADOMISLI, T. Algorithms for the Treatment of Femoral Neck Fractures. *Clinical Orthopaedics and Related Research®*, 2002, vol. 399. Available from: https://journals.lww.com/clinorthop/fulltext/2002/06000/algorithms_for_the_treatment_of_femoral_neck.5.aspx ISSN 0009-921X.

310. SINGH, J.A. and LEWALLEN, D.G. Patients with Osteoarthritis and Avascular Necrosis have Better Functional Outcomes and those with Avascular Necrosis Worse Pain Outcomes Compared to Rheumatoid Arthritis After Primary Hip Arthroplasty: A Cohort Study. *BMC Medicine*, 2013, vol. 11, no. 1. pp. 210. Available from: https://doi.org/10.1186/1741-7015-11-210 ISSN 1741-7015. DOI 10.1186/1741-7015-11-210.

311. *Cirugía De Reemplazo Parcial Vs. Total De Cadera "¿Es Un Reemplazo Parcial De Cadera Adecuado Para Mí?" - the Leone Center for Orthopedic Care*. -05-13T18:36:31+00:00, 2020 [viewed Feb 15, 2024]. Available from:https://holycrossleonecenter.com/cirugiadereemplazoparcialvstotal.

312. PAGNANO, M.W., MCLAMB, L.A. and TROUSDALE, R.T. Primary and Revision Total Hip Arthroplasty for Patients 90 Years of Age and Older. *Mayo Clinic Proceedings*, 2003, vol. 78, no. 3. pp. 285-288. Available from: https://www.sciencedirect.com/science/article/pii/S0025619611620466 ISSN 0025-6196. DOI 10.4065/78.3.285.

313. RIDZWAN, M., et al. Problem of Stress Shielding and Improvement to the Hip Implant Designs: A Review. *Journal of Medical Sciences*, 2007, vol. 7 DOI 10.3923/jms.2007.460.467.

314. *Osteonecrosis Information | Mount Sinai - New York*. [viewed Feb 16, 2024]. Available from:https://www.mountsinai.org/health-library/diseases-conditions/osteonecrosis.

315. Fractura de cadera - Cirugías [viewed Feb 16, 2024]. Available from: https://drjulianguerra.com/fractura-de-cadera/fractura-de-cadera-2/.

316. KONAN, S., ABDEL, M.P. and HADDAD, F.S. Cemented Versus Uncemented Hip Implant Fixation. *Bone & Joint Research*, 2019, vol. 8, no. 12. pp. 604-607. Available from: https://doi.org/10.1302/2046-3758.812.BJR-2019-0337 DOI 10.1302/2046-3758.812.BJR-2019-0337.

317. GARLAND, A., et al. Risk of Early Mortality After Cemented Compared with Cementless Total Hip Arthroplasty. *The Bone & Joint Journal*, 2017, vol. 99-B, no. 1. pp. 37-43. Available from: https://doi.org/10.1302/0301-620X.99B1.BJJ-2016-0304.R1 DOI 10.1302/0301-620X.99B1.BJJ-2016-0304.R1.

318. MAGGS, J. and WILSON, M. The Relative Merits of Cemented and Uncemented Prostheses in Total Hip Arthroplasty. *Indian Journal of Orthopaedics*, 2017, vol. 51, no. 4. pp. 377-385. Available from: https://doi.org/10.4103/ortho.IJOrtho_405_16 ISSN 1998-3727. DOI 10.4103/ortho.IJOrtho_405_16.

319. GÓMEZ-GARCÍA, F., FERNÁNDEZ-FAIREN, M. and ESPINOSA-MENDOZA, R.L. A Proposal for the Study of Cementless Short-Stem Hip Prostheses. *Acta Ortopedica Mexicana*, 2016, vol. 30, no. 4. pp. 204-215 ISSN 2306-4102; 2306-4102.

320. SORNAY-RENDU, E., BOUTROY, S., MUNOZ, F. and DELMAS, P.D. Alterations of Cortical and Trabecular Architecture are Associated with Fractures in Postmenopausal Women, Partially Independent of Decreased BMD Measured by DXA: The OFELY Study. *Journal of Bone and Mineral Research*, 2007, vol. 22, no. 3. pp. 425-433. Available from: https://doi.org/10.1359/jbmr.061206 ISSN 0884-0431. DOI 10.1359/jbmr.061206.

321. VASHISHTH, D. Collagen Glycation and its Role in Fracture Properties of Bone. *Journal of Musculoskeletal & Neuronal Interactions*, 2005, vol. 5, no. 4. pp. 316 ISSN 1108-7161; 1108-7161.

322. SAITO, M., FUJII, K., SOSHI, S. and TANAKA, T. Reductions in Degree of Mineralization and Enzymatic Collagen Cross-Links and Increases in Glycation-Induced Pentosidine in the Femoral Neck Cortex in Cases of Femoral Neck Fracture. *Osteoporosis International : A Journal Established as Result of Cooperation between the European Foundation for Osteoporosis and the National Osteoporosis Foundation of the USA*, 2006, vol. 17. pp. 986-95 DOI 10.1007/s00198-006-0087-0.

323. TANG, S., ZEENATH, U. and VASHISHTH, D. Effects of Non-Enzymatic Glycation on Cancellous Bone Fragility. *Bone*, 2007, vol. 40. pp. 1144-51 DOI 10.1016/j.bone.2006.12.056.

324. KHEIR, M., DRAYER, N. and CHEN, A. An Update on Cementless Femoral Fixation in Total Hip Arthroplasty. *The Journal of Bone and Joint Surgery*, 2020, vol. Publish Ahead of Print DOI 10.2106/JBJS.19.01397.

325. MCTIGHE, T., et al., 2016 *Short-Stem Designs for Total Hip Arthroplasty: Neck Stabilized Femoral Components*, pp. 823-849 ISBN 978-1-4511-8369-6.

326. GARDEN, R.S. Low-Angle Fixation in Fractures of the Femoral Neck. *The Journal of Bone & Joint Surgery British Volume*, 1961, vol. 43-B, no. 4. pp. 647-663. Available from: https://doi.org/10.1302/0301-620X.43B4.647 DOI 10.1302/0301-620X.43B4.647.

327. SWIONTKOWSKI, M.F., WINQUIST, R.A. and HANSEN, S.T.J. Fractures of the Femoral Neck in Patients between the Ages of Twelve and Forty-Nine Years. *The Journal of Bone and Joint Surgery.American Volume*, Jul, 1984, vol. 66, no. 6. pp. 837-846 ISSN 0021-9355; 0021-9355. DOI 10.2106/00004623-198466060-00003.

328. CAPULLI, M., PAONE, R. and RUCCI, N. Osteoblast and Osteocyte: Games without Frontiers. *Archives of Biochemistry and Biophysics*, 20140514, Nov 1, 2014, vol. 561. pp. 3-12 ISSN 1096-0384; 0003-9861. DOI 10.1016/j.abb.2014.05.003.

329. *Definición De Apoptosis - Diccionario De Cáncer Del NCI - NCI*. 02/02/ - 07:00, 2011 [viewed Feb 19, 2024]. Available from:https://www.cancer.gov/espanol/publicaciones/diccionarios/diccionario-cancer/def/apoptosis.

330. BELLIDO, T., PLOTKIN, L.I. and BRUZZANITI, A. Basic and Applied Bone Biology (Second Edition) D.B. BURR and M.R. ALLEN eds., Academic Press, 2019 *Chapter 3 - Bone*

Cells, pp. 37-55. Available from: https://www.sciencedirect.com/science/article/pii/B9780128132593000038 ISBN 9780128132593. DOI 10.1016/B978-0-12-813259-3.00003-8.

331. BHASKAR, B., ARUN, S., SREEKANTH, P.S. and SUBRAMANI, K., 2016 *Biomaterials in Total Hip Joint Replacements: The Evolution of Basic Concepts, Trends, and Current Limitations – A Review*, pp. 175-210 ISBN 978-981-4613-98-9. DOI 10.1201/b19906-6.

332. RIVIÈRE, C., et al. Long-Term Bone Remodelling Around 'Legendary' Cementless Femoral Stems. *EFORT Open Reviews*, 20180226, Feb 26, 2018, vol. 3, no. 2. pp. 45-57 ISSN 2058-5241; 2058-5241; 2058-5241. DOI 10.1302/2058-5241.3.170024.

333. TAN, C., et al. Additive Manufacturing of Bio-Inspired Multi-Scale Hierarchically Strengthened Lattice Structures. *International Journal of Machine Tools and Manufacture*, 2021, vol. 167. pp. 103764. Available from: https://www.sciencedirect.com/science/article/pii/S0890695521000730 ISSN 0890-6955. DOI 10.1016/j.ijmachtools.2021.103764.

334. ALSHEGHRI, A., et al. Optimization of 3D Network Topology for Bioinspired Design of Stiff and Lightweight Bone-Like Structures. *Materials Science and Engineering: C*, 2021, vol. 123. pp. 112010. Available from: https://www.sciencedirect.com/science/article/pii/S0928493121001491 ISSN 0928-4931. DOI 10.1016/j.msec.2021.112010.

335. TAN, X.P., et al. Metallic Powder-Bed Based 3D Printing of Cellular Scaffolds for Orthopaedic Implants: A State-of-the-Art Review on Manufacturing, Topological Design, Mechanical Properties and Biocompatibility. *Materials Science & Engineering.C, Materials for Biological Applications*, 20170224, Jul 1, 2017, vol. 76. pp. 1328-1343 ISSN 1873-0191; 0928-4931. DOI 10.1016/j.msec.2017.02.094.

336. PARK, J., SUTRADHAR, A., SHAH, J.J. and PAULINO, G.H. Design of Complex Bone Internal Structure using Topology Optimization with Perimeter Control. *Computers in Biology and Medicine*, 20180113, Mar 1, 2018, vol. 94. pp. 74-84 ISSN 1879-0534; 0010-4825. DOI 10.1016/j.compbiomed.2018.01.001.

337. ALMEIDA, H. and BÁRTOLO, P. *Topological Optimisation of Scaffolds for Tissue Engineering.* , 2013 DOI 10.1016/j.proeng.2013.05.125.

338. WU, C., et al. A Time-Dependent Mechanobiology-Based Topology Optimization to Enhance Bone Growth in Tissue Scaffolds. *Journal of Biomechanics*, 20210113, Mar 5, 2021, vol. 117. pp. 110233 ISSN 1873-2380; 0021-9290. DOI 10.1016/j.jbiomech.2021.110233.

339. GYGER, L.S., et al. *Porous Gelcast Ceramics for Bone Repair Implants.* , 2005.

340. KIM, J.H., et al. TBA-Based Freeze/Gel Casting of Porous Hydroxyapatite Scaffolds. *Ceramics International*, 2011, vol. 37, no. 7. pp. 2317-2322. Available from: https://www.sciencedirect.com/science/article/pii/S0272884211001349 ISSN 0272-8842. DOI 10.1016/j.ceramint.2011.03.023.

341. ORIŇÁKOVÁ, R., GOREJOVÁ, R., ORSAGOVA KRALOVA, Z. and ORINAK, A. *Surface Modifications of Biodegradable Metallic Foams for Medical Applications.* , 2020 DOI 10.3390/coatings10090819.

342. CONRAD, T.L. and ROEDER, R.K. Effects of Porogen Morphology on the Architecture, Permeability, and Mechanical Properties of Hydroxyapatite Whisker Reinforced Polyetheretherketone Scaffolds. *Journal of the Mechanical Behavior of Biomedical Materials*, 20200324, Jun, 2020, vol. 106. pp. 103730 ISSN 1878-0180; 1878-0180. DOI 10.1016/j.jmbbm.2020.103730.

343. KHODA, B., AHSAN, A.M.M.N., SHOVON, A.N. and ALAM, A.I. 3D Metal Lattice Structure Manufacturing with Continuous Rods. *Scientific Reports*, 20210111, Jan 11, 2021, vol. 11, no. 1. pp. 434-6 ISSN 2045-2322; 2045-2322. DOI 10.1038/s41598-020-79826-6.

344. LANTADA, A.D. and MORGADO, P.L. Rapid Prototyping for Biomedical Engineering: Current Capabilities and Challenges. *Annual Review of Biomedical Engineering*, 20120418, 2012, vol. 14. pp. 73-96 ISSN 1545-4274; 1523-9829. DOI 10.1146/annurev-bioeng-071811-150112.

345. WANG, X., et al. Topological Design and Additive Manufacturing of Porous Metals for Bone Scaffolds and Orthopaedic Implants: A Review. *Biomaterials*, 2016, vol. 83. pp. 127-141. Available from: https://www.sciencedirect.com/science/article/pii/S0142961216000144 ISSN 0142-9612. DOI 10.1016/j.biomaterials.2016.01.012.

346. C. OFFICE. *3D Matter made to Order (3DMM2O) - Homepage.* Cluster Office. 12.02. 13:51, 2024 [viewed Feb 15, 2024]. Available from:https://www.3dmattermadetoorder.kit.edu.

347. O'BRIEN, F.J. Biomaterials & Scaffolds for Tissue Engineering. *Materials Today*, 2011, vol. 14, no. 3. pp. 88-95. Available from: https://www.sciencedirect.com/science/article/pii/S136970211170058X ISSN 1369-7021. DOI 10.1016/S1369-7021(11)70058-X.

348. WALKER, J., TAHERI ANDANI, M., HABERLAND, C. and ELAHINIA, M. *Additive Manufacturing of Nitinol Shape Memory Alloys to Overcome Challenges in Conventional Nitinol Fabrication.* , 2014 DOI 10.1115/IMECE2014-40432.

349. SEZER, N., EVIS, Z. and KOÇ, M. Additive Manufacturing of Biodegradable Magnesium Implants and Scaffolds: Review of the Recent Advances and Research Trends. *Journal of Magnesium and Alloys*, 2021, vol. 9, no. 2. pp. 392-415. Available from: https://www.sciencedirect.com/science/article/pii/S221395672030205X ISSN 2213-9567. DOI 10.1016/j.jma.2020.09.014.

350. WEN, P., et al. Laser Additive Manufacturing of Zn Porous Scaffolds: Shielding Gas Flow, Surface Quality and Densification. *Journal of Materials Science & Technology*, 2019, vol. 35, no. 2. pp. 368-376. Available from: https://www.sciencedirect.com/science/article/pii/S1005030218302524 ISSN 1005-0302. DOI 10.1016/j.jmst.2018.09.065.

351. SVANBORG, P., ELIASSON, A. and STENPORT, V. Additively Manufactured Titanium and Cobalt-Chromium Implant Frameworks: Fit and Effect of Ceramic Veneering. *The*

International Journal of Oral & Maxillofacial Implants, 2018, vol. 33, no. 3. pp. 590-596 ISSN 1942-4434; 0882-2786. DOI 10.11607/jomi.6028.

352. CHAKKRAVARTHY, V. and JEROME, S. Printability of Multiwalled SS 316L by Wire Arc Additive Manufacturing Route with Tunable Texture. *Materials Letters*, 2020, vol. 260. pp. 126981. Available from: https://www.sciencedirect.com/science/article/pii/S0167577X19316131 ISSN 0167-577X. DOI 10.1016/j.matlet.2019.126981.

353. HONG, D., et al. Binder-Jetting 3D Printing and Alloy Development of New Biodegradable Fe-Mn-Ca/mg Alloys. *Acta Biomaterialia*, 20160822, Nov, 2016, vol. 45. pp. 375-386 ISSN 1878-7568; 1742-7061. DOI 10.1016/j.actbio.2016.08.032.

354. MIRZAALI, M.J., BOBBERT, F., LI, Y. and ZADPOOR, A., 2019 *Additive Manufacturing of Metals using Powder Bed-Based Technologies*, pp. 93-145 ISBN 9780429466236. DOI 10.1201/9780429466236-4.

355. ZADPOOR, A.A. *Meta-Biomaterials.* The Royal Society of Chemistry, 2020 Available from: http://dx.doi.org/10.1039/C9BM01247H ISBN 2047-4830. DOI 10.1039/C9BM01247H.

356. DAVIS, R., et al. A Comprehensive Review on Metallic Implant Biomaterials and their Subtractive Manufacturing. *The International Journal, Advanced Manufacturing Technology*, 20220223, 2022, vol. 120, no. 3-4. pp. 1473-1530 ISSN 0268-3768; 1433-3015; 0268-3768. DOI 10.1007/s00170-022-08770-8.

357. UCHIDA, A., NADE, S.M., MCCARTNEY, E.R. and CHING, W. The use of Ceramics for Bone Replacement. A Comparative Study of Three Different Porous Ceramics. *The Journal of Bone and Joint Surgery.British Volume*, Mar, 1984, vol. 66, no. 2. pp. 269-275 ISSN 0301-620X; 0301-620X. DOI 10.1302/0301-620X.66B2.6323483.

358. HEISE, U., OSBORN, J.F. and DUWE, F. Hydroxyapatite Ceramic as a Bone Substitute. *International Orthopaedics*, 1990, vol. 14, no. 3. pp. 329-338 ISSN 0341-2695; 0341-2695. DOI 10.1007/BF00178768.

359. LAKHDAR, Y., et al. Additive Manufacturing of Advanced Ceramic Materials. *Progress in Materials Science*, 2021, vol. 116. pp. 100736. Available from: https://www.sciencedirect.com/science/article/pii/S0079642520301006 ISSN 0079-6425. DOI 10.1016/j.pmatsci.2020.100736.

360. MITTERAMSKOGLER, G., et al. Light Curing Strategies for Lithography-Based Additive Manufacturing of Customized Ceramics. *Additive Manufacturing*, 2014, vol. 1-4. pp. 110-118. Available from: https://www.sciencedirect.com/science/article/pii/S2214860414000086 ISSN 2214-8604. DOI 10.1016/j.addma.2014.08.003.

361. GATTO, M.L., et al. Lithography-Based Ceramic Manufacturing (LCM) Versus Milled Zirconia Blocks Under Uniaxial Compressive Loading: An in Vitro Comparative Study. *Journal of Dentistry*, 20211108, Jan, 2022, vol. 116. pp. 103886 ISSN 1879-176X; 0300-5712. DOI 10.1016/j.jdent.2021.103886.

362. BAINO, F., et al. DLP Stereolithography of Hydroxyapatite Scaffolds with Bone-like Architecture, Permeability and Mechanical Properties. *Journal of the American Ceramic Society*, 2021, vol. 105 DOI 10.1111/jace.17843.

363. D'ANDREA, L., et al. Mechanical Characterization of Miniaturized 3D-Printed Hydroxyapatite Parts obtained through Vat Photopolymerization: An Experimental Study. *Journal of the Mechanical Behavior of Biomedical Materials*, 20230306, May, 2023, vol. 141. pp. 105760 ISSN 1878-0180; 1878-0180. DOI 10.1016/j.jmbbm.2023.105760.

364. PATERLINI, A., et al. Lithography-Based Manufacturing of Advanced Ceramics for Orthopaedic Applications: A Comparative Tribological Study. *Open Ceramics*, 2021, vol. 8. pp. 100170 DOI 10.1016/j.oceram.2021.100170.

365. DIAZ LANTADA, A., et al. *Monolithic 3D Labs- and Organs-on-Chips obtained by Lithography-Based Ceramic Manufacture.* , 2017 DOI 10.1007/s00170-017-0443-6.

366. RYBICKI, E.F., SIMONEN, F.A. and WEIS, E.B.J. On the Mathematical Analysis of Stress in the Human Femur. *Journal of Biomechanics*, Mar, 1972, vol. 5, no. 2. pp. 203-215 ISSN 0021-9290; 0021-9290. DOI 10.1016/0021-9290(72)90056-5.

367. ZHANG, X., et al. Additive Manufacturing of Cellular Ceramic Structures: From Structure to Structure–function Integration. *Materials & Design*, 2022, vol. 215. pp. 110470. Available from: https://www.sciencedirect.com/science/article/pii/S0264127522000910 ISSN 0264-1275. DOI 10.1016/j.matdes.2022.110470.

368. UÇAR, Y., AYSAN MERIÇ, İ and EKREN, O. Layered Manufacturing of Dental Ceramics: Fracture Mechanics, Microstructure, and Elemental Composition of Lithography-Sintered Ceramic. *Journal of Prosthodontics : Official Journal of the American College of Prosthodontists*, 20180211, Jan, 2019, vol. 28, no. 1. pp. e310-e318 ISSN 1532-849X; 1059-941X. DOI 10.1111/jopr.12748.

369. C. ROCHE, E. BONACCIO and J. FILIPPINI. *Radiology Data from the Cancer Genome Atlas Sarcoma [TCGA-SARC] Collection.* The Cancer Imaging Archive. , 2016 Available from:https://wiki.cancerimagingarchive.net/x/4oUiAQ DOI.org (Datacite). DOI 10.7937/K9/TCIA.2016.CX6YLSUX.

370. RINALDI, G., CAPITANI, D., MASPERO, F. and SCITA, V. Mid-Term Results with a Neck-Preserving Femoral Stem for Total Hip Arthroplasty. *HIP International*, 2018, vol. 28, no. 2. pp. 28-34. Available from: https://doi.org/10.1177/1120700018813216 ISSN 1120-7000. DOI 10.1177/1120700018813216.

371. MORLOCK, M.M., et al. Taper Corrosion: A Complication of Total Hip Arthroplasty. *EFORT Open Reviews*, 2020, vol. 5, no. 11. pp. 776-784. Available from: https://eor.bioscientifica.com/view/journals/eor/5/11/2058-5241.5.200013.xml https://tore.tuhh.de/bitstreams/a7598be3-0397-4da8-8f49-483ee93a2eaa/download DOI.org (Crossref); Taper corrosion. ISSN 2396-7544, 2058-5241. DOI 10.1302/2058-5241.5.200013.

372. ISO, D. Implants for Surgery-Partial and Total Hip Joint Prostheses-Part 4: Determination of Endurance Properties and Performance of Stemmed Femoral Components, 2010.

373. SOLÓRZANO, W., OJEDA, C. and DIAZ LANTADA, A. Biomechanical Study of Proximal Femur for Designing Stems for Total Hip Replacement. *Applied Sciences*, 2020, vol. 10, no. 12. pp. 4208. Available from: https://www.mdpi.com/2076-3417/10/12/4208 https://www.mdpi.com/2076-3417/10/12/4208/pdf DOI.org (Crossref). ISSN 2076-3417. DOI 10.3390/app10124208.

374. WANG, S., et al. On the Design and Properties of Porous Femoral Stems with Adjustable Stiffness Gradient. *Medical Engineering & Physics*, 2020, vol. 81. pp. 30-38. Available from: https://www.sciencedirect.com/science/article/pii/S1350453320300679 ISSN 1350-4533. DOI 10.1016/j.medengphy.2020.05.003.

375. LU, C., et al. Mechanical Behaviors of Multidimensional Gradient Gyroid Structures Under Static and Dynamic Loading: A Numerical and Experimental Study. *Additive Manufacturing*, 2022, vol. 59. pp. 103187. Available from: https://www.sciencedirect.com/science/article/pii/S2214860422005760 ISSN 2214-8604. DOI 10.1016/j.addma.2022.103187.

376. DIXIT, T., et al. High Performance, Microarchitected, Compact Heat Exchanger Enabled by 3D Printing. *Applied Thermal Engineering*, 2022, vol. 210. pp. 118339. Available from: https://www.sciencedirect.com/science/article/pii/S1359431122002976 ISSN 1359-4311. DOI 10.1016/j.applthermaleng.2022.118339.

377. HAYASHI, K., KISHIDA, R., TSUCHIYA, A. and ISHIKAWA, K. Superiority of Triply Periodic Minimal Surface Gyroid Structure to Strut-Based Grid Structure in both Strength and Bone Regeneration. *ACS Applied Materials & Interfaces*, 2023, vol. 15, no. 29. pp. 34570-34577. Available from: https://doi.org/10.1021/acsami.3c06263 ISSN 1944-8244. DOI 10.1021/acsami.3c06263.

378. LI, D., LIAO, W., DAI, N. and XIE, Y.M. Comparison of Mechanical Properties and Energy Absorption of Sheet-Based and Strut-Based Gyroid Cellular Structures with Graded Densities. *Materials*, 2019, vol. 12, no. 13 ISSN 1996-1944. DOI 10.3390/ma12132183.

379. ZHANG, Z., et al. Topological Design of all-Ceramic Dental Bridges for Enhancing Fracture Resistance. *International Journal for Numerical Methods in Biomedical Engineering*, 2016, vol. 32, no. 6. pp. e02749. Available from: https://doi.org/10.1002/cnm.2749 ISSN 2040-7939. DOI 10.1002/cnm.2749.

380. MIKIĆ, B. and CARTER, D.R. Bone Strain Gage Data and Theoretical Models of Functional Adaptation. *Journal of Biomechanics*, 1995, vol. 28, no. 4. pp. 465-469. Available from: https://www.sciencedirect.com/science/article/pii/002192909400085I ISSN 0021-9290. DOI 10.1016/0021-9290(94)00085-I.

381. TURNER, A.W.L., et al. Computational Bone Remodelling Simulations and Comparisons with DEXA Results. *Journal of Orthopaedic Research*, 2005, vol. 23, no. 4. pp. 705-712. Available from: https://doi.org/10.1016/j.orthres.2005.02.002 ISSN 0736-0266. DOI 10.1016/j.orthres.2005.02.002.

382. WEIBULL, W. A Statistical Distribution Function of Wide Applicability. *Journal of Applied Mechanics*, 2021, vol. 18, no. 3 [viewed 2/4/2024]. pp. 293-297. Available from: https://doi.org/10.1115/1.4010337 ISSN 0021-8936. DOI 10.1115/1.4010337.

383. ARAYA, M., et al. Assessing the Compressive and Tensile Properties of TPMS-Gyroid and Stochastic Ti64 Lattice Structures: A Study on Laser Powder Bed Fusion Manufacturing for Biomedical Implants. *Journal of Science: Advanced Materials and Devices*, 2024, vol. 9, no. 1. pp. 100663. Available from: https://www.sciencedirect.com/science/article/pii/S2468217923001326 ISSN 2468-2179. DOI 10.1016/j.jsamd.2023.100663.

384. ALTUN, A.A., et al. Additive Manufacturing of Lunar Regolith Structures. *Open Ceramics*, 2021, vol. 5. pp. 100058. Available from: https://www.sciencedirect.com/science/article/pii/S2666539521000043 ISSN 2666-5395. DOI 10.1016/j.oceram.2021.100058.

385. ZHANG, Y., DU, W., ZHOU, X. and YU, H. Review of Research on the Mechanical Properties of the Human Tooth. *International Journal of Oral Science*, Jun, 2014, vol. 6, no. 2. pp. 61-69 ISSN 1674-2818; 2049-3169; 1674-2818. DOI 10.1038/ijos.2014.21.

386. BUTLER, N., ZHAO, Y., LU, S. and YIN, S. Effects of Light Exposure Intensity and Time on Printing Quality and Compressive Strength of B-TCP Scaffolds Fabricated with Digital Light Processing. *Journal of the European Ceramic Society*, 2024, vol. 44, no. 4. pp. 2581-2589. Available from: https://www.sciencedirect.com/science/article/pii/S0955221923009500 ISSN 0955-2219. DOI 10.1016/j.jeurceramsoc.2023.11.046.